PUCRS

ESCOLA DE CIÊNCIAS
PROGRAMA DE PÓS-GRADUAÇÃO EM ECOLOGIA E EVOLUÇÃO DA BIODIVERSIDADE
DOUTORADO EM ECOLOGIA E EVOLUÇÃO DA BIODIVERSIDADE

FERNANDO JOSÉ MARÍA ROJAS RUNJAIC

SISTEMÁTICA FILOGENÉTICA DOS SAPOS-CUIDADORES *AROMOBATES* E *MANNOPHRYNE* (DENDROBATOIDEA: AROMOBATIDAE: AROMOBATINAE) INFERIDA MEDIANTE EVIDÊNCIA TOTAL

Porto Alegre
2019

PÓS-GRADUAÇÃO - *STRICTO SENSU*

Pontifícia Universidade Católica
do Rio Grande do Sul

PONTIFÍCIA UNIVERSIDADE CATÓLICA DO RIO GRANDE DO SUL

ESCOLA DE CIÊNCIAS

PROGRAMA DE PÓS-GRADUAÇÃO EM ECOLOGIA E EVOLUÇÃO DA BIODIVERSIDADE

SISTEMÁTICA FILOGENÉTICA DOS SAPOS-CUIDADORES *AROMOBATES* E *MANNOPHRYNE* (DENDROBATOIDEA: AROMOBATIDAE: AROMOBATINAE) INFERIDA MEDIANTE EVIDÊNCIA TOTAL

Fernando José María Rojas Runjaic

TESE DE DOUTORADO

PONTIFÍCIA UNIVERSIDADE CATÓLICA DO RIO GRANDE DO SUL

Av. Ipiranga 6681 - Caixa Postal 1429

Fone: (051) 320-3500

CEP 90619-900 Porto Alegre - RS

Brasil

2019

PONTIFÍCIA UNIVERSIDADE CATÓLICA DO RIO GRANDE DO SUL

ESCOLA DE CIÊNCIAS

PROGRAMA DE PÓS-GRADUAÇÃO EM ECOLOGIA E EVOLUÇÃO DA BIODIVERSIDADE

SISTEMÁTICA FILOGENÉTICA DOS SAPOS-CUIDADORES *AROMOBATES* E *MANNOPHRYNE* (DENDROBATOIDEA: AROMOBATIDAE: AROMOBATINAE) INFERIDA MEDIANTE EVIDÊNCIA TOTAL

Fernando José María Rojas Runjaic

Orientador: Dr. Santiago José Castroviejo Fisher

TESE DE DOUTORADO

PORTO ALEGRE - RS - BRASIL

2019

Sumário

A minha esposa, pelo seu amor,
amizade, companhia e apoio
incodicional.

Agradecimentos

Agradeço a Daniel Quihua, Adriana Becerra, José Luis Vieira, Ygrein Roos, Michelle Castellanos, Arnaldo Ferrer, Miguel Matta, Jhorman Piñeiro, Edwin Infante, José Gerardo Espinoza, Pedro Cabello, J. Celsa Señaris, Dennys Mora, Edward Camargo, Wendy Bolaños, Carlos Briceño, David Sierralta, Jesús Adolfo Aguiar, Marcial Quiroga, Jhonathan Miranda, Diego Flores, Oscar Lasso, Daniel Calcaño, Nelson Castro, Andrés Osorio e Marlon Fochler pela colaboração em campo. César L. Barrio-Amorós, Francisco Nava e Enrique La Marca forneceram informação valiosa sobre localidades chave para a busca de algumas espécies de sapos cuidadores. Um grande número de amigos, familiares e colegas brindaram apoio logístico durante o doutorado, entre eles agradeço particularmente a Amanda Delgado, Michelle Castellanos, Arnaldo Ferrer, Olga Herrera, Vicky Malavé, Giuseppe Gagliardi, Moisés Escalona, J. Celsa Señaris, Pedro Cabello, Luis Aular, Franger García, Alfredo Morales, Israel Cañizalez, Enzo La Marca, Odoardo Ravelo, Martín Rondón, Lennys Rondón, Martín Rondón Velásquez, José Martín Rondón, Giselle Runjaic, Bárbara Rojas, Rafael Moreno, Maricarmen Santiago Rondón, Cristobal Burgos, Mariví Burgos, Luis Alberto Terán, José Domingo La Chica e Helga Terzenbach. Enrique La Marca, Aldemar Acevedo, Orlando Armesto, Ada Sánchez Mercado, Lisandro Morán e Miguel Vences gentilmente providenciaram alícoutas de tecidos de algumas espécies analizadas neste estudo. Pelo acesso às coleções e empréstimo de espécimenes, expresso minha gratidão a Enrique La Marca (Colección de Anfibios y Reptiles del Laboratorio de Biogeografía, Universidad de los Andes, Venezuela) Gláucia Funk e Santiago Castroviejo-Fisher (Museu de Ciência e Teconolgia da PUCRS, Brasil), Carmen Ferreira e Mercedes Salazar (Museo de Biología de la Universidad Central de Venezuela), Amelia Díaz de Pascual e Moisés Escalona (Colección de Vertebrados de la Universidad de los Andes, Venezuela), J. Celsa Señaris (Instituto Venezolano de Investigaciones Científicas), Fernando Bird (Universidad de Puerto Rico) e Stephen P. Rogers (Carnegie Museum, EUA). Sou grato a Daniel Quihua, José Luis Vieira, Ignacio de la Riva, Santiago Castroviejo-Fisher, J. Celsa Señaris, Michelle Castellanos, Pedro Cabello, Andrés Jaramillo, César Barrio-Amorós, Tobby Hibbitts, Maël Dewynter, Josua

Mata, Alan Resetar, Courtney Whitcher, Greg Schneider, Aldemar Acevedo, Orlando Armesto, Edwin Infante, Helga Terzenbach, Frank Espinoza, Sebastian Lotzkat, Rafael Morillo, Miguel Matta e Jhonathan Miranda por ter compartilhado comigo suas fotos de espécimes vivos e preservados. Por compartilhar suas gravações de cantos de adevertência de algumas espécies de sapos cuidadores, ou até ir ao campo para gravá-los para mim, agradeço a Santiago Castroviejo-Fisher, Andreas Hertz, Rafael Morillo, Darwin Rangel, Andrés Osorio, Marlon Fochler, J. Celsa Señaris, César L. Barrio-Amorós, Wilmer Díaz, Manuel Centeno e Jesús Bello. The Macaulay Library at the Cornell Lab of Ornithology, forneciou acesso às gravações de cantos de advertência de algumas espécies venezuelanas de *Mannophryne* feitas por Stephen R. Edwards e atualmente tombadas na sua coleção. Agradeço a Pedro Ivo Simões, Lourdes Echevarria e Santiago Castroviejo-Fisher pela revisão do inglês. Também agradeço a Lourdes Alcaraz pela assitencia na amplificação e sequenciação das amostras, Bruno Gonzalez pela assistência no procesamento das gravações de cantos, Lourdes Echevarria e Andrés Jaramillo pela assistência nas análises filogenéticas, Adolpho Agustin e Miriam Souza Vianna (IPR-PUCRS) pela produção dos modelos 3D de esqueletos a partir de microtomografias computadas de alta resolução, usados neste estudo. A Pedro Simões pelas orientações nas análises bioacústicas, Pedro Dias pelas orientações no estudo da morfologia de girinos, Carla Fontana pelo empréstimo de equipos para digitalização de gravações e a David Blackburn pelo acesso aos modelos 3D de Aromobatidae gerados no projeto oVert. Pelo apoio institucional durante o doutorado, sou grato à Fundación La Salle de Ciencias Naturales (Caracas, Venezuela) e ao Programa de Pós-Graduação em Zoologia da PUCRS (agora PPG em Ecologia e Evolução da Biodiversidade). Sou particularmente grato a Santiago Castroviejo-Fisher, não só pela orientação mas também por seu grande apoio, motivação e amizade durante o doutorado. Finalmente, agradeço ao Conselho Nacional de Desenvolvimento Científico e Tecnológico (CNPq) pela bolsa de estudo de doutorado (processo 142444/2014-6).

Resumo. Em conjunto, *Aromobates* e *Mannophryne* reúnem 39 espécies, distribuídas no norte dos Andes e Cordilheira da Costa, na Colômbia, Venezuela e Trinidade e Tobago. Estudos prévios suportaram a monofilia destes gêneros, sua relação como grupos irmãos e elucidaram as relações filogenéticas de algumas de suas espécies; porém, filogenias prévias foram baseadas apenas em amostragens taxonômicas parciais. As relações de parentesco de 41 % dos Aromobatinae ainda não foram elucidadas e a diversidade de espécies dos dois gêneros não foi avaliada apropriadamente. Neste estudo foram reconstruídas as relações evolutivas dos Aromobatinae, incluindo pela primeira vez todas suas espécies reconhecidas. A filogenia inferida baseia-se numa análise de evidência total por parcimônia, de sequências de DNA de 31 genes mitocondriais e nucleares (analisados sob tree-alignment) e 383 caracteres fenotípicos (188 deles são novos) amostrados para 400 terminais de Aromobatinae e do outgroup. O grupo interno esta representado por uma amostragem taxonômica e geográfica abrangente, com 260 terminais representando as 39 espécies reconhecidas e várias novas, de cerca de 100 localidades ao longo das áreas de distribuição de *Aromobates* e *Mannophryne*. Nove espécies de *Aromobates*, *"Colostethus" caribe*, *"Prostherapis" dunni* e *"Phyllobates" mandelorum*, foram incluídos só com base em dados fenotípicos. Foi obtida uma filogenia bem resolvida, com *Aromobates* e *Mannophryne* recuperados como clados irmãos e reciprocamente monofiléticos. Descobriram-se relações filogenéticas novas e inesperadas para *"C." caribe*, *"P." dunni* e *"P." mandelorum* dentro de Aromobatidae. Com base nos resultados obtidos, reconhece-se um quarto grupo de espécies dentro de *Mannophryne* e redefine-se o grupo de *M. collaris*. As 12 espécies de *Aromobates* incluídas pela primeira vez neste estudo, são corroboradas como pertencentes a este gênero. Também foram descobertas numerosas relações intragenéricas novas e pelo menos sete espécies novas. *Aromobates ericksonae* é considerado um sinônimo de *A. mayorgai*. Ademais, descreve-se uma nova espécie de *Mannophryne* com base em evidência morfológica e bioacústica, redelimita-se *M. herminae* e se discute sobre a relevância da evidência bioacústica na delimitação de espécies. Por fim, identifica-se pela primeira vez, numerosas sinapomorfías fenotípicas não ambíguas para todos os táxons supraespecíficos e para os grupos de espécies. Durante o trabalho de campo para colheita de espécimes, três espécies desaparecidas há muitos anos foram redescobertas, entre elas *Mannophryne neblina*, do qual não existiam registros posteriores a sua descoberta há 70 anos. Os resultados ressaltam a importância de incrementar as amostragens taxonômicas nas análises filogenéticas para aprimorar o conhecimento sobre a sistemática e diversidade de espécies. Também destaca a importância das inferências baseadas em evidência total ao permitir a inclusão de espécies só representadas por dados fenotípicos. Com base nos resultados deste estudo, propõe-se uma taxonomia atualizada para Aromobatidae, concordante com as topologias ótimas inferidas.

Palavras chave: Amphibia. Andes. Anura. Colômbia. Neotrópico. Sapos-cuidadores. Parcimônia. Filogenia. Taxonomia. Venezuela.

Phylogenetic systematics of the nurse frogs *Aromobates* and *Mannophryne* (Dendrobatoidea: Aromobatidae: Aromobatinae) inferred through total evidence

Abstract. Together, *Aromobates* and *Mannophryne* (Aromobatinae) include 39 recognized species distributed along the north of the Cordillera de los Andes and Cordillera de la Costa in Colombia, Venezuela, and Trinidad and Tobago. Previous studies supported the monophyly of these genera, their sister relationship, and elucidated the phylogenetic position of some of their species; however, these studies were based in an incomplete taxon sampling. Thus, the phylogenetic relationships of 41 % of the species in Aromobatinae remain unknown and the species diversity within both genera is not properly assessed. Herein we inferred the evolutionary relationships of Aromobatinae including for the first time all their recognized species. The inference was based on a parsimony total evidence analysis of DNA sequences of 31 mitochondrial and nuclear genes (analyzed under tree-alignment) and 383 phenotypic characters (188 of which are novel) sampled for 400 aromobatin and outgroup terminals. The ingroup is represented by a remarkably expanded taxonomic and geographic sampling, which includes 260 terminals representing the 39 recognized species and several putative new species from near 100 localities covering almost the entire geographic ranges of *Aromobates* and *Mannophryne*. Nine *Aromobates* species, as well as *"Colostethus" caribe*, *"Prostherapis" dunni*, and *"Phyllobates" mandelorum*, were included in the analyses only based on phenotypic data. The analyses rendered a well-resolved phylogeny, with *Aromobates* and *Mannophryne* as sister and reciprocally monophyletic. Novel and highly unexpected phylogenetic positions were discovered for *"C." caribe*, *"P." dunni*, and *"P." mandelorum* within Aromobatidae. A fourth species group is recognized within *Mannophryne* and the *M. collaris* group is redefined. The 12 species of *Aromobates* included in this study for the first time are corroborated as part of this genus. Numerous novel intrageneric relationships and at least seven putative new species were also discovered. *Aromobates ericksonae* is considered a junior synonym of *A. mayorgai*. A new species of *Mannophryne* is described based on morphological and bioacoustic evidence, *M. herminae* is redefined, and the importance of bioacoustics evidence in species delimitations is discussed. Finally, we identified for the first time, numerous unambiguously optimized phenotypic synapomorphies for all supraspecific taxa and species groups. In the course of the field work of our study, three long-time missing species were rediscovered, among them, *Mannophryne neblina*, which had not been seen since its discovery 70 years ago. Our results highlight the importance of increasing the taxon sampling in phylogenetic analyses to improve the understanding of the systematics and species diversity. Also demonstrates the relevance of total evidence phylogenetic inference, for example by including species only represented by phenotypic data. According to the results, an updated taxonomy is proposed for Aromobatidae, concordant with our optimal topologies.

Keywords: Amphibia. Andes. Anura. Colombia. Neotropics. Nurse frogs. Parsimony. Phylogeny. Taxonomy. Venezuela.

Apresentação

Em um esforço para superar as limitações dos estudos prévios em melhorar a compreensão da sistemática e a diversidade de espécies dos sapos-cuidadores em *Aromobates* e *Mannophryne*, apresentamos neste estudo uma análise filogenética de evidência total baseada numa amostragem taxonômica e geográfica notavelmente mais abrangente que as de estudos prévios, incluindo a totalidade das espécies descritas, várias espécies novas e numerosos espécimes de populações não determinadas. A partir desta filogenia avaliamos: 1) a monofilia de Aromobatinae, 2) a monofilia de *Aromobates* e *Mannophryne*, 3) as relações filogenéticas intergenéricas, 4) as relações filogenéticas interespecíficas, 5) a posição filogenética de "*Colostethus*" *caribe*, "*Phyllobates*" *mandelorum* e "*Prostherapis*" *dunni*, 6) a ocorrência de novas espécies, e 7) a ocorrência de sinapomorfias fenotípicas não ambíguas para a subfamília, os dois gêneros e os grupos de espécies.

A tese está estruturada em dois artigos escritos em inglês. O primeiro artigo intitula-se: "Phylogenetic systematics of the nurse frogs *Aromobates* and *Mannophryne* (Dendrobatoidea: Aromobatidae: Aromobatinae) inferred through total evidence". Este constitui o artigo principal, abrange os sete objetivos enumerados acima, e pretende-se submetê-lo a consideração para publicação no Bulletin of the American Museum of Natural History. O segundo artigo, intitulado: "Unveiling species diversity in collared frogs through morphological and bioacoustic evidence: a new *Mannophryne* (Amphibia, Aromobatidae) from Sierra de Aroa, northwestern Venezuela, and an amended definition and call description of *M. herminae* (Boettger, 1893)", foi publicado na Zootaxa (volume 4461, de agosto de 2018). Como indicado no título, neste artigo descreve-se

uma nova espécie de *Mannophryne* relacionada com *M. herminae*, mas que possui um canto de advertência marcadamente diferente ao desta última. Adicionalmente, neste estudo redefinimos morfologicamante *M. herminae*, o qual permitirá diagnosticar outras espécies novas ainda por descrever. Já por fim, discutimos o valor dos cantos de anuncio na delimitação de espécies morfologicamente crípticas dentro de *Mannophryne*.

Capítulo 1

Phylogenetic systematics of the nurse frogs *Aromobates* and *Mannophryne* (Dendrobatoidea: Aromobatidae: Aromobatinae) inferred through total evidence

Fernando J.M. Rojas-Runjaic, Enrique la Marca, Ignacio de La Riva & Santiago Castroviejo-Fisher

Phylogenetic systematics of the nurse frogs *Aromobates* and *Mannophryne* (Dendrobatoidea: Aromobatidae: Aromobatinae) inferred through total evidence

FERNANDO J.M. ROJAS-RUNJAIC[1,2,*], ENRIQUE LA MARCA[3], IGNACIO DE LA RIVA[4] & SANTIAGO CASTROVIEJO-FISHER[1,5]

[1] *Laboratory of Vertebrate Systematics. Pontifical Catholic University of Rio Grande do Sul (PUCRS). Av. Ipiranga 6681, Porto Alegre, RS, 90619-900, Brazil*.

[2] *Museo de Historia Natural La Salle, Fundación La Salle de Ciencias Naturales. Apartado Postal 1930, Caracas 1010-A, Distrito Capital, Venezuela.*

[3] *Amphibian and Reptile Collection, Biogeography Lab., Universidad de Los Andes. Mérida 5101, Venezuela.*

[4] *Department of Biodiversity and Evolutionary Biology, Museo Nacional de Ciencias Naturales-CSIC, C/ José Gutiérrez Abascal 2,*
28006, Madrid, Spain

[5] *Department of Herpetology, American Museum of Natural History, Central Park West & 79th St., New York, NY 10024, USA.*

** Corresponding author. E-mail: rojas_runjaic@yahoo.com.*

Abstract. Together, *Aromobates* and *Mannophryne* (Aromobatinae) include 39 recognized species distributed along the north of the Cordillera de los Andes and Cordillera de la Costa in Colombia, Venezuela, and Trinidad and Tobago. Previous studies support the monophyly of these genera, their sister

relationship, and elucidated the phylogenetic position of some of their species; however, these studies were based in an incomplete taxon sampling. Thus, the phylogenetic relationships of 41 % of the species in Aromobatinae remain unknown and the species diversity within both genera is not properly assessed. Herein we inferred the evolutionary relationships of Aromobatinae including for the first time all their recognized species. Our inference was based on a parsimony total evidence analysis of DNA sequences of 31 mitochondrial and nuclear genes (analyzed under tree-alignment) and 383 phenotypic characters (188 of which are novel) sampled for 400 aromobatin and outgroup terminals. The ingroup is represented by a remarkably expanded taxonomic and geographic sampling, which includes 260 terminals representing the 39 recognized species and several putative new species from near 100 localities covering almost the entire geographic ranges of *Aromobates* and *Mannophryne*. Nine *Aromobates* species, as well as *"Colostethus" caribe*, *"Prostherapis" dunni*, and *"Phyllobates" mandelorum*, were included in our analyses based exclusively on phenotypic data. Our analyses rendered a well-resolved phylogeny, with *Aromobates* and *Mannophryne* as sister and reciprocally monophyletic. Novel and highly unexpected phylogenetic positions were discovered for *"C." caribe*, *"P." dunni*, and *"P." mandelorum* within Aromobatidae; we propose new genera for the first two and recognize the latter as *insertae sedis* within Aromobatinae. A fourth species group is recognized within *Mannophryne*, and the *M. collaris* group is redefined. The 12 species of *Aromobates* included in our study for the first time are corroborated as part of this genus. Numerous novel intrageneric relationships and at least seven putative new species were also discovered. *Aromobates ericksonae* is

considered a junior synonym of *A. mayorgai*. Finally, we identified, for the first time, numerous unambiguously optimized phenotypic synapomorphies for all supraspecific taxa and species groups. In the course of the field work of our study, three long-time missing species were rediscovered, among them, *Mannophryne neblina*, which had not been seen since its discovery 70 years ago. Our results highlight the importance of increasing taxon sampling in phylogenetic analyses to improve the undertanding of amphibian systematics and species diversity. They also demonstrate the relevance of total evidence phylogenetic inference, for example by allowing the inclusion of species only represented by phenotypic data. According to our results, we propose an updated taxonomy for Aromobatidae, concordant with our optimal topologies.
Keywords: Amphibia. Andes. Anura. Colombia. *Colostethus caribe*. Cordillera de la Costa. Neotropics. New genus. New species. Nurse frogs. Parsimony. *Phyllobates mandelorum*. Phylogeny. *Prostherapis dunni*. Taxonomy. Venezuela.

Resumen. *Aromobates* y *Mannophryne* (Aromobatinae) agrupan 39 especies distribuidas en el norte de la Cordillera de los Andes y a lo largo de la Cordillera de la Costa en Colombia, Venezuela, Trinidad y Tobago. Estudio previos corroboran la monofilia de ambos géneros y su relación como clados hermanos, además de elucidar la posición filogenética de varias de sus especies; no obstante, estos estudios estuvieron basados en muestreos taxonómicos incompletos. En consecuencia, las relaciones filogenéticas de cerca de 41 % de las especies de Aromobatinae aun son desconocidas y la diversidad de especies dentro de ambos géneros no ha sido evaluada

apropiadamente. En este estudio inferimos las relaciones evolutivas de Aromobatinae, incluyendo por vez primera la totalidad de sus especies reconocidas. Nuestra inferencia está basada en un análisis de evidencia total por parsimonia, de secuencia de ADN de 31 genes mitocondriales y nucleares (analizados bajo tree-alignment), y 383 caracteres fenotípicos (188 de ellos son nuevos) muestreados para 400 terminales de Aromobatinae y del grupo externo. El grupo interno incluye 260 terminales en los que están representadas las 39 especies reconocidas y varias nuevas, de unas 100 localidades a lo largo del área de distribución de *Aromobates* y *Mannophryne*. Nueve especies de *Aromobates*, *"Colostethus" caribe*, *"Prostherapis" dunni*, y *"Phyllobates" mandelorum*, fueron incluidas en los análisis solo con datos fenotípicos. Obtuvimos una filogenia bien resuelta en la que *Aromobates* y *Mannophryne* son clados hermanos y recíprocamente monofiléticos. Descubrimos nuevas e inesperadas relaciones filogenéticas para *"C." caribe*, *"P." dunni* y *"P." mandelorum* dentro de Aromobatidae; en consecuencia, proponemos nuevos géneros para los dos primeros y reconocemos a "*P*." *mandelorum* como *insertae sedis* dentro de Aromobatinae. Reconocemos un cuarto grupo de especies dentro de *Mannophryne* y redefinimos el grupo de *M. collaris*. Las 12 especies de *Aromobates* no estudiadas en estudios previos son corroboradas como pertenecientes a este género. También descubrimos numerosas relaciones intragenéricas nuevas y al menos siete nuevas especies putativas. *Aromobates ericksonae* es considerado como sinónimo de *A. mayorgai*. Finalmente, identificamos por primera vez, numerosas sinapomorfías fenotípicas no ambiguas para todos los taxones supraespecíficos y grupos de especies. En el curso de nuestras expediciones de colecta redescubrimos tres

especies que no habían sido vistas por muchos años, entre ellas *Mannophryne neblina*, la cual no había sido registrada nuevamente desde su descubrimiento, hace 70 años. Nuestros resultados resaltan la importancia del incremento de los muestreos taxonómicos en los análisis filogenéticos para mejorar el conocimiento sobre la sistemática y diversidad de especies. También destacan el valor de las inferencias filogenéticas basadas en evidencia total al permitir la inclusión de especies representadas solo con base en datos fenotípicos. Finalmente, se propone una taxonomía actualizada para Aromobatidae, concordante con nuestras topologías óptimas.

Palabras clave: Amphibia. Andes. Anura. Colombia. *Colostethus caribe*. Cordillera de la Costa. Especie nueva. Filogenia. Género nuevo. Neotrópico. Parsimonia. *Phyllobates mandelorum*. *Prostherapis dunni*. Sapito niñera. Taxonomía. Venezuela.

Introduction

The systematics of the Neotropical superfamily Dendrobatoidea has been assessed by numerous works in the last four decades; the firsts studies were based on phenotypic data, including morphology, bioacoustics, behavior, and alkaloid profiles (e.g., Savage 1968, Edwards 1974, Silverstone 1975, 1976, Myers *et al*. 1978, Zimmermann & Zimmermann 1988, Myers *et al*. 1991, La Marca 1994a, 1995, Coloma 1995, Kaplan 1997), while the most recent ones focused on molecular data (Clough & Summers 2000, Vences *et al*. 2000, 2003, Summers & Clough 2001, Santos *et al*. 2003). Regardles of the type of data, most of these studies addressed questions regarding the diversity of the colorful and aposematic Neotropical poison frogs (mainly of Dendrobatidae). As a

consequence, the understanding of the systematics—at both the species and supraspecific level—of the cryptic colored dendrobatoids (mostly concentrated in Aromobatidae) lagged behind, with relatively limited alpha taxonomy contributions, and questionable monophyly of several aromobatid genera (Kaiser *et al*. 1994, Coloma 1995, Grant & Castro-Herrera 1998).

The situation changed with the work of Grant *et al*. (2006), a milestone in the study of the systematics of dendrobatoids. Grant *et al*. (2006) studied the phylogenetic relationships of 156 described species and many undescribed ones by combining previous and novel phenotypic and genotypic data in an unprecedented total evidence analysis, which included 174 adult and larval phenotypic characters—morphology, behavior, alkaloid profiles—and ~6,100 bp from five mitochondrial and six nuclear gene fragments. The new understanding resulting from this study allowed a taxonomy based on quantitatively inferred monophyletic groups: one superfamily (Dendrobatoidea), with two families (Dendrobatidae and Aromobatidae), six subfamilies (three in each family), and 16 genera. Aromobatidae included five genera, grouped in three subfamilies: *Allobates* in Allobatinae, *Anomaloglossus* and *Rheobates* in Anomaloglossinae, and *Aromobates* and *Mannophryne* in Aromobatinae. All supraspecific taxa were accompanied by new phenotypic definitions.

The decade following Grant *et al*. (2006) witnessed the publication of numerous new studies focusing on key groups of dendrobatoids, expanding the taxon and molecular sampling, and increasing the knowledge about their species diversity and phylogenetic relationships. Yet, most contributions assessed aposematic taxa (e.g., Brown *et al*. 2008, Twomey & Brown 2008, Brown & Twomey 2009, Lötters *et al*. 2009, Santos *et al*. 2009, Páez-Vacas *et*

al. 2010, Pérez-Peña *et al*. 2010, Brown *et al*. 2011, Santos & Cannatella 2011, Vaz-Silva & Maciel 2011, Santos *et al*. 2014, Marin *et al*. 2018). Nonetheless, there were also new research groups publishing on aromobatids, but almost exclusively on *Allobates* (e.g., Simões *et al*. 2010, Melo-Sampaio *et al*. 2018, Simões *et al*. 2019) and *Anomaloglossus* (Vacher *et al*. 2017, Fouquet *et al*. 2018, Kok *et al*. 2018, Fouquet *et al*. 2019). In reference to Aromobatinae, several species were described in the last decade (Manzanilla 2007a, b, Vargas & La Marca 2007, La Marca 2009, Rojas-Runjaic *et al*. 2011, Barrio-Amorós *et al*. 2010a, Barrio-Amorós *et al*. 2011, Barrio-Amorós & Santos 2012, La Marca & Otero 2012, Rojas-Runjaic *et al*. 2018), but only two studies (Manzanilla *et al*. 2009, Barrio-Amorós & Santos 2012) quantitatively addressed the phylogenetics of the subfamily, with focus on *Mannophryne* and *Aromobates*, respectively. Both studies used DNA sequences and included a noticeable increases in taxon sampling with regards to Grant *et al*. (2006). However, results were mainly concordant.

More recently, Grant *et al*. (2017) revisited the systematics of dendrobatoids based in a total evidence analysis. Their phenotypic and genotypic datasets were updated with both data published during the last 11 years and new data generated by them. The new dataset included 189 phenotypic transformation series and 17,208 aligned nucleotides (15 loci) for 564 terminals (495 of the ingroup). Several unexpected relationships were discovered among dendrobatoids and, consequently, some taxonomic rearrangements were proposed. These included two additional dendrobatid genera (*Ectopoglossus* and *Paruwrobates*), the recognition of several species groups within *Colostethus*, *Allobates*, *Ameerega* and *Anomaloglossus*, and the

identification of a number of new unambiguously optimized synapomorphies. Regarding Aromobatinae, the monophyly of the subfamily and that of its two genera (*Aromobates* and *Mannophryne*) was corroborated, with one phenotypic synapomorphy for Aromobatinae and five for *Mannophryne*.

Currently, Aromobatinae harbors 39 described species (19 of them in *Aromobates*, and the remaining 20 in *Mannophryne* [Barrio-Amorós & Santos 2012, Frost 2019]). Frogs in this subfamily are commonly called nurse frogs, due to the peculiar parental care exhibited by the males, which consist of collecting the tadpoles from their nest (hidden in the leaf litter) just after hatching and carrying them on their backs by several days, then releasing them in ponds near streams (La Marca 1989, Jowers & Downie 2005). These frogs inhabit streamside environments, from lowland forests to paramos (La Marca 1994a, 2007) and their diel activity is diurnal, as in other dendrobatoids. The unique exception is *Aromobates nocturnus*, which, as highlighted by its name, is apparently active at night (Myers *et al*. 1991, but see our results). Most aromobatins are small in size, ranging between 20–35 mm of snout-vent length (SVL), with two species noticeably larger: *Aromobates nocturnus* (62 mm SVL) and *Mannophryne riveroi* (42 mm SVL). Dorsal pattern is cryptically colored in all known species of both genera; however, females of *Mannophryne* have the throat—occasionally also the chest and belly—conspicuously bright yellow. This striking ventral coloration is associated to territoriality and emission of agonistic signals by females (Test 1954, Sexton 1960, Durant & Dole 1975, Wells 1980).

Aromobatinae is distributed in the mountain systems of northern Venezuela, with a few species present in Colombia and Trinidad and Tobago. *Aromobates* is distributed from a small area in the northeastern portion of

Cordillera Oriental of the Colombian Andes and through the Tamá massif, Sierra de Perijá and Cordillera de Mérida in the Venezuelan Andes, with a disjunct species distributed in Sierra de Aroa in the western portion of the Cordillera de la Costa. Species of *Mannophryne* are known from the southwestern limit of Cordillera de Mérida in the Venezuelan Andes, the entire Cordillera de la Costa in northern Venezuela, and the islands of Trinidad and Tobago. Most species in both genera have a small geographic distribution (La Marca 2007, Barrio-Amorós & Santos 2012), and many are threatened of extinction (IUCN 2019).

The first supraspecific grouping for the Venezuelan nurse frogs lacking a dark dermal collar was proposed by La Marca (1985), who defined the *Colostethus alboguttatus* group for a cluster of eight species: seven from the Venezuelan Andes (*C*. *alboguttatus*, *C*. *haydeeae*, *C. leopardalis*, *C*. *mayorgai*, *C*. *meridensis*, *C*. *molinarii*, and *C*. *orostoma*) and one (*C. dunni*) from Cordillera de la Costa. This group was defined by the presence of elongated and fang-like maxillary and premaxillary teeth. Rivero (1990) proposed the *Colostethus* Group VIII for the Venezuelan species without dark dermal collar nor pale oblique lateral stripe. This group was similar in species composition to the *C. alboguttatus* group of La Marca (1985), differing only in the inclusion of *C. duranti*, *C. saltuensis*, and *C. serranus* and the exclusion of *C. meridensis* and *C. dunni*. Rivero (1990) did not assign *C. meridensis*, *C. dunni*, and *C. mandelorum* to any species group and considered their relationships uncertain.

Aromobates was described by Myers *et al*. (1991) as a monotypic genus to accommodate *A. nocturnus*, a species morphologically and behaviorally very different from its relatives of the *Colostethus alboguttatus* group of La Marca

(1985) and the *Colostethus* Group VIII of Rivero (1990). It was defined, among other characteristics, by having an *adductor mandibulae externus superficilis* muscle, by the presence of fang-like teeth on the maxillary arch, by releasing a defensive mercaptan-like smell, and by its aquatic and nocturnal habits. La Marca (1993) deduced a close relationship between *A. nocturnus* and the species in the *Colostethus alboguttatus* group and considered the possibility that they were congeneric. However, shortly after, the same author erected *Nephelobates* (La Marca 1994b) to relocate six of the eight species previously included in the *C. alboguttatus* species group, which shared two putative synapomorphies: the presence of large fang-like maxillary and premaxillary teeth and a supracloacal dermal flap. The species transferred were: *C*. *alboguttatus*, *C*. *haydeeae*, *C*. *mayorgai*, *C*. *meridensis*, *C*. *molinarii*, and *C*. *orostoma*. The exclusion of *C*. *dunni* and *C*. *leopardalis* (both in the *C. alboguttatus* group), as well as of *C. capurinensis*, *C. duranti*, *C. saltuensis*, and *C. serranus* (in the Group VIII *sensu* Rivero [1990], and Péfaur [1993]), was not explained. Mijares-Urrutia & La Marca (1997) transferred *C. duranti* and *C. serranus* to *Nephelobates* and mentioned the reduced nasal bones as an additional character shared by all the species in the genus. La Marca (1997) presumed a close relationship between *Aromobates nocturnus* and *C. leopardalis* based on their shared aquatic habits and mercaptan-like smell, but was cautious and not to suggest any nomenclatural changes.

The taxonomic position of *Colostethus mandelorum* and *C. dunni*, both considered part of *Colostethus* (*sensu lato*), remained unknown. Whereas Rivero (1961, 1984a, b, 1990) presumed that *mandelorum* was closely related to the collared nurse frogs of his Group VII (= *Mannophryne*), La Marca (1993)

found resemblances between it and the *C. alboguttatus* group, but those were insufficient to consider it as part of that group. *Colostethus dunni* was considered by Rivero (1961, 1984a, 1990) as not closely related to any Venezuelan species. La Marca (1985) included it in the *C. alboguttatus* group based on its long teeth, but he did not transfer it to *Nephelobates* (La Marca 1994b), and later considered it as not closely related to any dendrobatoid (La Marca 2004).

The taxonomy of the non-collared nurse frogs of the Venezuelan Andes remained unaltered by near a decade until Grant *et al*. (2006) inferred that *Aromobates nocturnus* and *Colostethus "saltuensis"* were nested within *Nephelobates*. Consequently, *Nephelobates* was synonymized with *Aromobates*. Although only *N. molinarii* and two undetermined species were included in the analysis, all the eight species previously assigned to *Nephelobates* by La Marca (1994b) and Mijares-Urrutia & La Marca (1997) were transferred together with *C. capurinensis*, *C. leopardalis* and *C. saltuensis* to *Aromobates*. Additionally, due to the absence of new evidence, Grant *et al*. (2006) followed La Marca (2004) in considering that the phylogenetic relationships of *Colostethus dunni* remained enigmatic. Grant *et al*. (2006) germane contribution was to refer it as Aromobatidae *incertae sedis* (provisionally referred as *"Prostherapis" dunni*). They also relocated *Colostethus mandelorum* to *Allobates* based on morphological similarities.

More recently, six species of *Aromobates* were described: *A. ornatissimus*, *A. tokuko*. *A. walterarpi*, *A. cannatellai*, *A. ericksonae*, and *A. zippeli* (Barrio-Amorós *et al.* 2011, Rojas-Runjaic *et al.* 2011, Barrio-Amorós & Santos 2012, La Marca & Otero 2012), and Barrio-Amorós & Santos (2012)

proposed to reestablish *A. inflexus*, which has been synonymized with *A. alboguttatus* by Rivero (1984b) shortly after its description (Rivero 1980). Barrio-Amorós & Santos (2012) also corroborated the monophyly of *Aromobates*, its sister relationship with *Mannophryne*, and revealed the existence of at least two unnamed species in addition to the three described in their study—their phylogeny included at least nine putative species, including seven of the 19 currently described. Grant *et al*. (2017) again recovered a monophyletic *Aromobates*, with phylogenetic relationships similar to those reported by Barrio-Amorós & Santos (2012). However, there was not an increase in taxon sampling and unambiguous phenotypic synapomorphies for the genus remained elusive.

Mannophryne was described by La Marca (1992) to name a clade that includes the northern Venezuelan nurse frogs possessing dark dermal collar, which was previously referred as *Colostethus collaris* group (La Marca 1989) and as Group VII or *trinitatis* Group by Rivero (1990). The genus was originally composed of *C. collaris*, *C. herminae*, *C. neblina*, *C. oblitteratus*, *C. olmonae*, *C. riveroi*, *C. trinitatis*, and *C. yustizi* and defined by three putative synapomorphies: the presence of a dark dermal collar, a yellow throat in adult females, and elaborate social behavior in females, associated to territoriality and courtship (La Marca 1992, 1994a). In subsequent years, other three species of *Mannophryne* were described: *M. cordilleriana*, *M. caquetio*, and *M. lamarcai* (La Marca 1994a, Mijares-Urritia & Arends 1999a, Mijares-Urrutia & Arends 1999b), and *Colostethus larandinus*, previously assigned to the *C. collaris* group (Yústiz 1991), was transferred to *Mannophryne* by Mijares-Urrutia & Arends (1999b).

Although the validity of *Mannophryne* was questioned for being allegedly erected without identifying reliable synapomorphies (Kaiser *et al*. 1994, Kaiser & Altig 1994, Meinhardt & Parmelee 1996), its monophyly was corroborated by La Marca *et al*. (2002) and Vences *et al*. (2003) in their molecular phylogenetic analyses. However, in both cases, the taxon and molecular sampling were very limited (two species and 547 bp of 16S in the first study; four species and a total of 870 bp of the 12S and 16S genes, in the second). Grant *et al*. (2006) increased the taxon sampling to seven putative species (only three determined), which were represented by 1–10 loci (358–5,708 bp) and up to 124 phenotypic characters. They also corroborated the monophyly of *Mannophryne*, but only the presence of a dark dermal collar was identified as an unambiguous phenotypic synapomorphy for the genus.

Other four species of *Mannophryne* were described in the next years: *M. venezuelensis*, *M. leonardoi*, *M. trujillensis*, and *M. speeri* (La Marca & Vargas 2007, Manzanilla *et al*. 2007a, b, La Marca 2009, respectively). Only *M. venezuelensis* was supported by molecular data in addition to the morphological and bioacoustic evidence (Manzanilla *et al*. 2007a); the phylogenetic relationships of the other three species remained unassessed. Shortly after, Manzanilla *et al*. (2009) studied the phylogenetic relationships of *Mannophyne* based on DNA sequences of two mitochondrial fragments (489 bp of 16S and 751 bp of COI) and expanding the taxon sampling, including 13 of the 15 species described until then. Manzanilla *et al*. (2009) corroborated the monophyly of the genus and defined three clades as species groups: Clade A or *Mannophryne trinitatis* group (Central-Oriental clade) including the species of the central and oriental sections of the Cordillera de la Costa: *M. leonardoi*, *M.*

olmonae, *M. riveroi*, *M. trinitatis*, *M. venezuelensis*, and several unnamed linages. Clade B or *Mannophryne collaris* group (Central-Western clade) including the Andean species *M. collaris*, *M. cordilleriana*, *M. lamarcai*, *M. larandina*, and *M. yustizi*, as well as *M. herminae* and *M. caquetio*, from the central and western portion of Cordillera de la Costa, respectively. Clade C or *Mannophryne oblitterata* group which only included its homonymous species, is also distributed in the central portion of the Cordillera de la Costa. No phenotypic synapomorphy was proposed for these species groups.

Barrio-Amorós *et al*. (2010a) described *Mannophryne orellana*, *M. urticans*, and *M. vulcano*, based only on external morphology and bioacoustics. But later, their phylogenetic relationships were inferred by Santos *et al*. (2014) in a wider study on aposematism, acoustic diversification, and speciation in poison frogs. More recently, Grant *et al*. (2017) included at least 19 species of *Mannophryne* (16 of the 20 species described) in their new phylogeny. In this study no new terminals or sequences were obtained, but for the first time all the species for which molecular data was available, were assessed in the same analysis. Phenotypic data were scored for all named terminals (between 36–141 phenotypic characters) and the molecular dataset varied between 466–10,385 bp. As in all previous studies, the monophyly of the genus was corroborated. Additionally, the three species groups defined by Manzanilla *et al*. (2009) were recovered (*M. trinitatis* group, *M. collaris* group, and *M. oblitterata* group). *Mannophryne orellana* and *M. urticans* were found nested within the *M. collaris* group, and *M. vulcano* within the *M. trinitatis* group. In this study, five unambiguously optimized phenotypic synapomorphies were identified for *Mannophryne*: 1) length of finger II equal to finger III, 2) toe disc I moderately

expanded, 3) toe disc V moderately expanded, 4) webbing on preaxial side of toe IV leaving free three and a half phalanges, and 5) presence of a dark dermal collar.

Finally, Rojas-Runjaic *et al*. (2018) described *Mannophryne molinai*, and redefined *M. herminae*. Both species are morphologically similar, but emit strikingly different advertisement calls. The authors presumed that both species are close relatives, but their phylogenetic relationships remained unassessed.

As noted above, the knowledge about the systematics of *Aromobates* and *Mannophryne* has experienced a remarkable increase in the last thirteen years. However, most previous phylogenetic studies were restricted to a single terminal or a few terminals of a single population per species. This strategy was sufficient to test the monophyly of genera, to corroborate the validity of some species originally delimited based only on phenotypic evidence, and to discover phylogenetic relationships among recognized species. However, it proves limited to discover phenotypically cryptic diversity.

Additionally, the phylogenetic relationships of 12 of the 19 described species of *Aromobates* remain unassessed due to the unavailability of well-preserved or fresh tissue samples for DNA extraction. These are: *Aromobates alboguttatus*, *A. capurinensis*, *A. duranti*, *A. haydeeae*, *A. inflexus*, *A. leopardalis*, *A. mayorgai*, *A. orostoma*, *A. serranus*, *A. tokuko*, *A. walterarpi*, and *A. zippeli*. All of them are currently listed under some IUCN extinction risk category and have not been seen for a decade or more (La Marca & García-Pérez 2004a, b, c, d, 2010a, b, c, d, Barrio-Amorós & Santos 2012, La Marca & Otero 2012, Rojas-Runjaic & Señaris 2015a). We presumed that some of them may be already extinct, at least in their historic localities. This is also the case of

Mannophryne neblina, "*Colostethus*" *caribe*, "*Phyllobates*" *mandelorum*, and "*Prostherapis*" *dunni* (La Marca & Manzanilla 2004, Barrio-Amorós *et al*. 2006a, La Marca *et al*. 2006, La Marca 2015, Rojas-Runjaic & Señaris 2015b, Señaris & Rojas-Runjaic 2015, Rivas *et al*. 2018). The absence of these species from quantitative phylogenetic analyses not only prevents the inference of their phylogenetic relationships, but also hinders species delimitation among several unnamed linages already included in previous phylogenies. Moreover, the absence of *Aromobates alboguttatus*, the type species of *Nephelobates* (La Marca 1994b) from quantitative phylogenetic analyses has prevented to definitively corroborate the status of this last genus as a junior synonym of *Aromobates*. Finally, the absence of phenotypic synapomorphies for *Aromobates* in the two total evidence phylogenies published to date (Grant *et al*. 2006, 2017) has also impeded the evaluation of the position of *A. alboguttatus*.

In an effort to overcome the limitations of previous studies to estimate the species diversity of Aromobatinae and to better understand the systematics of this group, we present a phylogenetic total evidence analysis based on a remarkably expanded taxon and geographic sampling, which includes for the first time: all the species currently recognized in *Aromobates* and *Mannophryne* (some only represented by phenotypic data); specimens from numerous populations covering a large area of the geographic distribution of both genera; and the enigmatic "*Colostethus*" *caribe*, "*Phyllobates*" *mandelorum*, and "*Prostherapis*" *dunni* (all three also only represented by phenotypic data). By quantitatively analyzing the aforementioned data and taxa, we are able to test 1) the monophyly of Aromobatinae, 2) the monophyly of *Aromobates* and

Mannophryne, 3) the phylogenetic relationships among the species of each genera, 4) the relationships of these genera with the others within Aromobatidae, 5) the phylogenetic position of "*Colostethus*" *caribe*, "*Phyllobates*" *mandelorum*, and "*Prostherapis*" *dunni*, 6) the existence of new putative species, and 7) previous and new unambiguous phenotypic synapomorphies for the subfamily, its two genera, and species groups.

Material and methods

Fieldwork and visits to museums for data collection

Over 70 localities were visited in Tamá massif and Cordillera de Mérida in the Venezuelan Andes, and in Cordillera de la Costa of Venezuela, between 2014 and 2019. Localities were selected considering type localities, their vicinities, and unsampled regions within the distributional ranges of *Aromobates* and *Mannophryne*. All specimens were captured manually and transported to improvised laboratories in the field, where they were photographed in life, anesthetized and euthanized with topical benzocaine solution (50 mg/g), fixed in 10 % formalin solution and posteriorly preserved in 70 % ethanol. Tadpoles were preserved in 10 % formalin. Prior to fixation of each specimen, a tissue sample from the muscles of the thigh and/or from the liver was dissected and preserved in 95 % ethanol for molecular analyses. When possible, calling males were recorded *in situ* and collected. All the specimens collected during this study are housed at the herpetological collection of the Museo de Historia Natural La Salle (MHNLS) in Caracas, Venezuela. Biosecurity protocols were

applied during and after field work in each locality, as indicated by Aguirre & Lampo (2006).

Herpetological collections of the MHNLS, Laboratorio de Biogeografía at the Universidad de Los Andes, Mérida, Venezuela (ULABG), and Colección de Vertebrados at the Universidad de los Andes, Mérida, Venezuela (CVULA), were visited to study and loan specimens and tissue samples. Additional loans and photos were obtained from the museum of Estación Biológica Rancho Grande, Maracay, Venezuela (EBRG); University of Puerto Rico, Mayagüez, Puerto Rico (UPR-M); Carnegie Museum of Natural History, Pittsburg, USA (CM); Biodiveristy Research and Teach Collections, Texas A&M University, College Station, Texas, USA (TCWC); University of Michigan, Museum of Zoology, Ann Arbor, Michigan, USA (UMMZ); Field Museum, Division of Amphibians and Reptiles, Chicago, Illinois, USA (FMNH); Museo de Ciencias Naturales de Madrid, Spain (MCNM); herpetological collection of Universidad de Pamplona, Colombia (MCNUP-H); Zoological Institute of the Technical University of Braunschweig, Germany; and from the Spatial Ecology Lab, at the Centro de Estudios Botánicos y Agroforestales, Instituto Venezolano de Investigaciones Científicas, Zulia, Venezuela (IVIC).

Taxon sampling

Our dataset is composed of 400 terminals, of which 260 correspond to ingroup terminals and 140 to outgroup terminals. The ingroup comprises 100 % of the described species of Aromobatinae (19 species of *Aromobates* including *A. inflexus*, and 20 species of *Mannophryne*) and a number of undescribed species in both genera. Given that one of our objectives is to discover cryptic

species diversity, we included terminals from as many localities as possible, for both determined and undetermined specimens of *Aromobates* and *Mannophryne*. Those species of *Aromobates* that seem to have disappeared from their known historical localities and with phylogenetic relationships not yet been analyzed in previous molecular studies due to the absence of tissue samples (i.e., *A. alboguttatus*, *A. capurinensis*, *A. duranti*, *A. haydeeae*, *A. inflexus*, *A. leopardalis*, *A. orostoma*, *A. serranus*, *A. walterarpi*, and *A.* sp. 3) were represented only by phenotypic data and as single terminals.

Outgroups were selected based on the phylogeny of Grant *et al*. (2017) and mostly using data from that study, but also complemented with some terminals of *Anomaloglossus* from Vacher *et al*. (2017). Because *Allobates*, *Anomaloglossus*, and *Rheobates* were recovered together with Aromobatinae forming a monophyletic group (Aromobatidae), we selected two or more terminals per species group or subclade within each of these three aromobatid genera to better sample their phylogenetic diversity. In total, we included 51 terminals representing 46 species of *Allobates*, three terminals/species of *Rheobates*, and 35 terminals representing 28 species of *Anomaloglossus*. Within Dendrobatidae, the sister clade of Aromobatidae, we selected a single terminal for each of its 16 genera (*Adelphobates*, *Ameerega*, *Andinobates*, *Colostethus*, *Dendrobates*, *Ectopoglossus*, *Epipedobates*, *Excidobates*, *Hyloxalus*, *Leucostethus*, *Minyobates*, *Oophaga*, *Paruwrobates*, *Phyllobates*, *Ranitomeya*, and *Silverstoneia*), covering the phylogenetic diversity of that family (Appendix 4).

Since the phylogenetic relationships of the enigmatic *“Prostherapis” dunni*, “*Phyllobates” mandelorum*, and *“Colostethus” caribe* have not been

quantitatively evaluated, there are not available tissue samples, and they have not been found after their discoveries (between 18 and 87 years ago), we included them with phenotypic data only. Finally, we used *Thoropa miliaris*, the sister taxon of Dendrobatoidea (Frost *et al*. 2006, Grant *et al*. 2017) to root all trees in the phylogenetic analyses.

Phenotypic character sampling and coding

As a starting point, we revisited the phenotypic characters of Grant *et al.* (2006), expanded and modified in Grant *et al*. (2017), which consist of 188 characters of adult and larval external morphology, internal organs, musculature, osteology, behavior, bioacoustics, alkaloid profiles, and chromosome number. We also included five osteological characters from Mendelson *et al*. (2000), other six from De Sá *et al*. (2014), and one of larval external morphology from Mijares-Urrutia (1998). Additionally, we scored 188 novel characters, primarily on osteological (n = 150), but also based on external morphology (n = 35), behavior (n = 2), and bioacoustics (n = 1). We scored characteristics for which we observed variation among the different taxa included in this study. For all the new continuous characters included in our matrix, states were delimited based on discontinuities observed in the variation. The phenotypic matrix was constructed in Mesquite 3.5 (Maddison & Maddison 2018) and exported as a SilverStripe file (.ss) to be integrated into the total evidence analyses. Ninety-seven of the 383 phenotypic characters were coded as additive (see Results for details).

For the ingroup (except *Mannophryne olmonae*), characters related to external morphology were coded by direct examination or through high

resolution digital photographs from museum specimens (Appendix 1), and from photographs of live specimens. Osteological characters were mostly scored from virtual 3D models of osteology generated in this study (Appendix 2). Additionally, some osteological characters were scored from cleared-and-stained specimens of *Aromobates duranti*, *Mannophryne yustizi*, and *M. orellana* (Appendix 1). Bioacoustical characters were coded from call recordings obtained during fieldwork or downloaded from the onlline repository at the Macaulay Library (https://www.macaulaylibrary.org/), and from call descriptions in the literature (source of data for each species indicated in parentheses) for *Aromobates cannatellai*, *A. ericksonae*, *A. saltuensis* (Barrio-Amorós & Santos 2012), *A. ornatissimus* (Barrio-Amorós *et al*. 2011), *Mannophryne leonardoi* (Santos *et al.* 2014), *M. trinitatis*, and *M. olmonae* (Lehtinen *et al*. 2010). Character states for *Mannophryne olmonae* were taken from the dataset of Grant *et al*. (2017), and complemented with descriptions from the literature (Hardy 1983, Lehtinen & Hailey 2008) and color photos of live specimens available at Dendrowiki repository (http://www.dendrowiki.org/).

For the outgroup, phenotypic characters codification was taken mostly from the dataset of Grant *et al*. (2017), and completed with data from the literature (source of data for each species indicated in parentheses) for *Allobates algorei* (Barrio-Amorós & Santos 2009), *A. amissibilis* (Kok *et al.* 2013a), *A. bacurau* (Simões 2016), *A. caeruleodactylus* (Lima & Caldwell 2001), *A. chalcopis* (Kaiser *et al*. 1994), *A. conspicuus*, *A. crombiei* (Morales 2002), *A. granti* (Kok *et al*. 2006a), *A. grillisimilis* (Simões *et al*. 2013), *A. hodli* (Simões *et al*. 2010), *A. humilis* (La Marca *et al*. 2002), *A. insperatus* (Morales 2002), *A. juami* (Simões *et al*. 2018), *A. magnussoni* (Lima *et al*. 2014), *A.*

masniger (Morales 2002), *A. nidicola* (Caldwell & Lima 2003), *A. niputidea* (Grant *et al*. 2007), *A. paleovarzensis* (Lima *et al*. 2010), *A. subfolionidificans* (Lima *et al*. 2007), *A. tapajos* (Lima *et al*. 2015) *A. tinae* (Melo-Sampaio *et al*. 2018), *A. trilineatus* (Grant & Rodriguez 2001), *A. undulates* (Myers & Donnelly 2001), *Andinobates bombetes* (Myers & Daly 1980), *Anomaloglossus apiau* (Fouquet *et al*. 2015), *A. beebei* (Kok *et al*. 2006a), *A. blanci*, *A. dewynteri* (Fouquet *et al*. 2018), *A. kaiei* (Kok *et al*. 2006b), *A. meansi* (Kok *et al*. 2018), *A. megacephalus* (Kok *et al*. 2010a), *A. praderioi* (Kok *et al*. 2010b), *A. roraima* (Kok *et al*. 2013b), *A. stepheni* (Martins 1989), *A. tamacuarensis* (Myers & Donnelly 1997), *A. tepuyensis* (Myers & Donnelly 2008), *Colostethus ruthveni* (Kaplan 1997), *Ectopoglossus saxatilis* (Grant *et al*. 2017), *Exidobates captivus* (Myers 1982, Twomey & Brown 2008), *Leucostethus fugax* (Morales & Schulte 1993), *Myniobates steyermarki* (Rivero 1971, Lötters *et al*. 2007), *Oophaga pumilio* (Lötters *et al*. 2007), *Paruwrobates erythromos* (Vigle & Miyata 1980, Lötters *et al*. 2007, Grant *et al*. 2017), "*Prostherapis" dunni* (La Marca 2004), and *Rheobates palmatus* (Jerez & Yara-Contreras 2018, Lüddecke 2000).

Characters of coloration in life were also coded from photos taken during fieldwork and from photos available at the online repositories Dendrobates (https://www.dendrobates.org/), DendroWiki (http://www.dendrowiki.org/), and BioWeb Ecuador (https://bioweb.bio/). Osteological characters were coded from 3D models either generated in this study or from Morphosource (Appendix 2), photos of cleared-and-stained specimens for *"Prostherapis" dunni*, and from a x-rays image available at BioWeb Ecuador (https://bioweb.bio/) for *Paruwrobates erythromos* (Appendix 1).

Following Grant *et al*. (2006), phenotypic data were coded for the species (or population, in those cases where cryptic diversity was suspected) as a whole, and duplicated for each molecular terminal. All the new characters were described and illustrated (see results). Modifications to the characters taken from Mendelson *et al*. (2000), and Grant *et al*. (2006), are explained in detail. Photos of live specimens used to illustrate characters of color in life were taken in situ during fieldwork. Macrophotography used to illustrate characters of external morphology was acquired from preserved specimens with a Leica DMC 2900 digital camera attached to a Leica M205 A stereo microscope at the facilities of the Museu de Ciências e Tecnologia (MCP) of Pontifícia Universidade Católica do Rio Grande do Sul (PUCRS). For this, individual digital images were captured and electronically assembled into a single panfocal image with the software LAS (Leica Application Suite; Leica Microsystems Imaging Solutions Ltd, Cambridge, U.K.). Illustrations of osteology are based on printscreens of virtual 3D osteology reconstructions visualized in the software CTvox 3.2.0 (Bruker microCT®).

Virtual 3D osteology models

High resolution computed microtomography scans from 103 specimens (Appendix 2) were conducted using a Bruker Skyscan 1173 X-ray microCT at the Instituto do Petróleo e dos Recursos Naturais (IPR) facility of PUCRS. Ethanol-preserved specimens were placed inside a polyethylene vessel, which contained a cotton ball impregnated with 70 % ethanol to keep the microatmosphere of the container saturated, avoiding dehydration during scanning. Specimens were scanned in one to three parts, depending on their

size. Scans were conducted at a voltage of 40 kV and current of 50–55 μA; each acquisition was composed of 960–1,200 projections (up to 3600 projections for specimens scanned in three parts), with 800 ms exposure, two frames averaged per projection, and 6–24 μm voxel size. Reconstructions were obtained with NRecon 1.7.1.6 (Bruker microCT®), and visualized with CTvox 3.2.0 (Bruker microCT®). Scanned specimens were mainly adult females; we used males when there were no females for that species, or when it was possible to scan more than one specimen per species. Our micro-CT scans do not render cartilage, therefore characters based on these cartilage structures were not studied from 3D models.

Call recordings and acquisition of bioacustic data

Advertisement calls generated in this study were obtained *in situ* during fieldwork, mainly using an Olympus LS-10 digital recorder at a sampling rate of 44.1 kHz and 16 bits/sample, and a Senheiser K6-ME66 directional microphone. The microphone was positioned about 0.5–5 m away from each calling male. In some cases, calls were recorded in .mp4 format using cell phones, and posteriorly converted to .wav format with enough quality to be analyzed (sampling rate of 44.1 kHz, and 16 bits/sample). Whenever possible, calling males were collected and associated to recordings as voucher specimens; when that was not possible, other syntopic specimens collected were indicated as reference. Calls were analyzed using Raven Pro 1.3 (Bioacoustics Research Program 2008). Call and note envelope, note arrangement, and rate of note emission (notes/s) were determined from oscillograms.

Molecular sampling

A total of 1,747 sequences of 31 genes (18 mitochondrial and 13 nuclear) were compiled in our analysis, corresponding to 1–23 gene fragments, and 382–13,372 unaligned base pairs per terminal. Mitochondrial gene fragments included were: Cytochrome b (cyt-b; 245–1144 bp), Phenylalanine transfer RNA (tRNA-Phe 10–72 bp), 12S ribosomal RNA (12S; 292–936 bp), Valine transfer RNA (tRNA-Val; 60–74 bp), 16S ribosomal RNA (16S; 396–1608 bp), Leucine transfer RNA (tRNA-Leu; 60–74 bp), Reduced nicotinamide adenine dinucleotide (NADH) dehydrogenase, subunit 1 (ND1; 632–796 bp), Isoleucine transfer RNA (tRNA-Ile; 69–71 bp), Glutamine transfer RNA (tRNA-Gln; 70–72 bp), Methionine transfer RNA (tRNA-Met; 69–70 bp), Reduced nicotinamide adenine dinucleotide (NADH) dehydrogenase, subunit 2 (ND2; 1030–1035 bp), Tryptophan transfer RNA (tRNA-Trp; 67–70 bp), Alanine transfer RNA (tRNA-Ala; 67–70 bp), Asparagine transfer RNA (tRNA-Asn; 73 bp), Light Strand Replication Origin (LSRO; 28–31 bp), Cysteine transfer RNA (tRNA-Cys; 62–65 bp), Tyrosine transfer RNA (tRNA-Tyr; 67–73 bp), Cytochrome oxidase I (COI; 573–1545 bp). Nuclear gene fragments were: Rhodopsin (RHO; 316–332 bp), H3 histone family member 3C (H3F3C; 290–328 bp), Tyrosinase (TYR; 419–578 bp), Recombination activating 1 (RAG 1; 406–1397 bp), Seven in absentia homolog 1 (SIAH1; 397 bp), 28S ribosomal RNA (28S rRNA; 756–782 bp), Zinc finger e-box binding homeobox 2 (ZEB2; 924–927 bp), Proopiomelanocortin (POMC; 456–474 bp), Neurotrophin 3 (NT-3; 576–579 bp), Solute carrier family 8 (sodium/calcium exchanger), member 1 (NCX1; 1233–1424 bp), Bone morphogenetic protein 2 (BMP2; 521–576 bp), Brain derived neurotrophic factor

(BDNF; 603–700 bp), and C-X-C motif chemokine receptor 4 (CXCR4; 602–630 bp).

We generate 543 new sequences from 10 genes, for 210 terminals (Appendix 4). From the total of new sequences, 208 correspond to 16S, whereas the remaining 335 sequences correspond to the genes cyt-b (n = 47), tRNA-Phe (n = 30), 12S (n = 30), COI (n = 64), TYR (n = 28), POMC (n = 30), BMP2 (n = 40), BDNF (n = 33), and CXCR4 (n = 33). The molecular dataset was completed with 1,204 sequences downloaded from GenBank (http://www.ncbi.nlm.nih.gov/genbank) prior to December 25, 2018. These sequences correspond to all the genes listed above (except CXCR4), for 177 terminals (Appendix 4). Outgroup terminals were selected among the better represented in terms of molecular data available in GenBank. We created eight chimeric outgroup terminals composed of two different specimens each, to reduce the amount of missing data. In these cases, the divergence of the 16S sequences of the two conspecific specimens was never greater than 1.8 %. Also seven chimeric ingroup terminals were created, but in all cases both specimens came from the same population and their 16S sequences were identical.

The identities of several sequences available in GenBank, that were published previous to September 2017, but not corrected in Grant *et al*. (2017: Appendix S3), or corresponding to species described posteriorly, are updated herein: Sequences first published by Grant *et al*. (2006) as “Manaus 1” MPEG 13826, and posteriorly referred by Grant *et al*. (2017) as *Allobates* sp. Manaus 1 MPEG13826 (DQ502531, DQ502099, DQ503217, DQ502327, DQ503328, DQ503079, DQ502979) were reidentified as pertaining to *Allobates tinae* by

Mello-Sampaio *et al*. (2018). Sequences referred by Grant *et al*. (2017) as *Allobates* sp. “Carajas” (MF614177, MF624180, MF614376, MF624104, MF624150, MF614338, MF614242) and by Simões *et al*. (2018) as *Allobates* sp (Carajás BR) (MG252610, MG 252611) are from the recently described *Allobates carajas* (Simões *et al.* 2019). The specimen originally identified as “Ayangana” 607 by Grant *et al*. (2006) and subsequently referred by Grant *et al*. (2017) and Vacher *et al*. (2017) as *Anomaloglossus* sp. Ayanganna ROM39639 and *A*. sp “Ayanganna”, respectively (DQ502560, DQ502129, DQ502836, DQ503235, DQ502345, DQ503163, DQ503344, DQ503096, DQ502993) was reidentified by Kok *et al*. (2018) as *Anomaloglossus meansi*. Terminals first referred by Vacher *et al*. (2017) as *Anomaloglossus* sp. “Mitaraka” (KY510141, KY510142, KY510145, KY549547, KY549548, KY549508, KY549509, KY549466, KY549467) correspond to the recently described *A. mitaraka* (Fouquet *et al*. 2019). Finally, sequences of the three specimens referred by Grant *et al*. (2006) as *Colostethus fraterdanielli* Cauca isolate 1226, 1227 and 1228 (DQ502175–DQ502177, DQ502372–DQ502374, DQ502611–DQ502613, DQ502878–DQ502880, DQ503013–DQ503015, DQ503256–DQ503258, DQ503371–DQ503373) were reidentified by Marin *et al*. (2018) as *Leucostethus brachistriatus*.

DNA extraction, amplification and sequencing

Genomic DNA was extracted from 99 % ethanol-preserved tissue samples of finger tips, thigh muscle, or liver, using the Wizard® Genomic DNA Purification Kit (Promega Corporation) and following the manufacturer’s protocol. Primers

used to amplify DNA fragments of cyt-b, tRNA-Phe, 12S, 16S, COI, TYR, POMC, BMP2, BDNF, and CXCR4 are listed in Table 1.

Table 1. Primers for the five mitochondrial and five nuclear gene fragments amplified in this study.

Gene fragment	Primer name	Primer sequence (5'–3')	Reference
cyt-b	MVZ 15-L	GAACTAATGGCCCACACWWTACGNAA	Moritz *et al*. (1992)
	H15149	AAACTGCAGCCCCTCAGAAATGATATTTGTCCT CA	Kocher *et al*. (1989)
tRNA-Phe + 12S	t-Phe-frog	ATAGCRCTGAARAYGCTRAGATG	Wiens *et al*. (2005)
	12S-frogR1	TCRATTRYAGGACAGGCTCCTCTAG	Wiens *et al*. (2005)
16S	AR	CGCCTGTTTATCAAAAACAT	Palumbi *et al*. (1991)
	BR	CCGGTCTGAACTCAGATCACGT	Palumbi *et al*. (1991)
COI	AnF1	ACHAAYCAYAAAGAYATYGG	Lyra *et al*. (2017)
	AnR1	CCRAARAATCARAADARRTGTTG	Lyra *et al*. (2017)
TYR	TyrC	GGCAGAGGAWCRTGCCAAGATGT	Bossuyt & Milinkovitch (2000)
	TyrG	TGCTGGCRTCTCTCCARTCCCA	Bossuyt & Milinkovitch (2000)
POMC	POMCF	ATATGTCATGASCCAYTTYCGCTGGA	Wiens *et al*. (2005)
	POMCR1	GGCRTTYTTGAAWAGAGTCATTAGW	Wiens *et al*. (2005)
BMP2	BMP2_F7	AGACTATTGGACACCAGACTGGTACAT CATA	Santos & Cannatella (2011)
	BMP2_R3	CRCAYCCCTCCACRACCATGTCTTGA TA	Santos & Cannatella (2011)
BDNF	BDNF_F1	ACCATCCTTTTCCTKACTATGG	Santos & Cannatella (2011)
	BDNF_R1	CTATCTTCCCCTTTTAATGGTC	Santos & Cannatella (2011)
CXCR4	CXC-F1	TCCAGAACCATGACTGATAAGTA	Castroviejo-Fisher *et al*. (2015)
	CXC-R1	CAAGGCTTCTGTGATGGAGATCC	Castroviejo-Fisher *et al*. (2015)

Polymerase Chain Reaction (PCR) for DNA amplification of fragments was performed at 25 µL volume, using 2 µL extracted DNA, 1.25 µL of each forward and reverse primers, 8 µL of MasterMix, and 12.5 µL H_2O. Standard reaction conditions consisted of an initial denaturing step of 3 min at 94º C, followed by 35–45 cycles of amplification of 1 min at 94º C, 1 min at 45–62º C, and 1 min at 72º C; and a final extension step of of 6 min at 72º C. Aliquots of

the PCR products were mixed with loading buffer, run in 1 % agarose gel electrophoresis, flanked by a DNA ladder, and visualized in a UV lamp, in order to verify their quality and size. Cycle sequencing reactions were performed by Macrogen Labs (Macrogen Inc., Korea). All fragments were sequenced in both forward and reverse directions to check for potential errors. Chromatograms obtained were manually edited and contigs were assembled using Sequencher 4.8 (GeneCodes, Ann Arbor, MI, USA). Finally, we performed BLAST queries (https://blast.ncbi.nlm.nih.gov/Blast.cgi) to verify the identity of each of the new sequences and to discard contamination or mislabeling of the samples.

We tried to extrac ancient DNA and amplify 16S (following the same methods described below) from 56 old museum specimens corresponding to 10 species/populations of *Mannophryne,* and 11 species of *Aromobates,* of which we did not have access to fresh DNA, but all amplification reactions failed.

Phylogenetic analyses

Sequences of each of the 31 gene fragments were independently aligned in Aliview 1.14 (Larsson 2014), using Muscle (Edgar 2004) with default parameters. The resulting multiple sequence alignments were visualized and edited in the same program. Terminals represented by a very short sequence, which Muscle failed to align, were manually placed at the corresponding position within the whole alignment. After alignment, each gene was divided into putatively homologous fragments whose length variation among sequences is only due to insertions and/or deletions of nucleotides, a requisite for tree-alignment analysis in POY (Wheeler *et al*. 2006). Points selected to split the homologous fragments were located in conserved regions (no gaps and few or

none nucleotide substitutions) of the multiple sequence alignments. Finally, for each fragment, gaps implied by the multiple sequences alignment were removed. A total of 138 putatively homologous fragments were generated from the 31 genes. These fragments were saved as .fasta format, and analyzed along with the phenotypic matrix in POY 5.1.1 (Wheeler *et al*. 2015).

Tree-alignment was performed under parsimony with equal weights for all transformations using direct optimization. Tree searches were conducted using the command "search"—which implements an algorithm based on Random Addition Sequence (RAS) Wagner builds, Subtree Pruning and Regrafting (SPR), and Tree Bisection and Reconnection (TBR) branch swapping (see Goloboff 1996, 1999), Parsimony ratcheting (Nixon, 1999) and tree fusing (Goloboff 1999)—running consecutive rounds of searches within a specified run-time, storing the shortest trees of each independent run and performing a final round of tree fusing on the pooled trees. We executed four consecutive searches of 24, 48, 96, and 168 hours (totaling 336 hours); for the three last rounds, we used as starting topology the tree from the previous round. The resulting shortest trees were submitted independently to a final round of swapping using iterative pass optimization (Wheeler 2003a) in POY 4.1.2 (Varón *et al*. 2010). Finally, the optimal implied alignment from iterative pass optimization was converted to a data matrix (Wheeler 2003b) and submitted to driven searches in TNT 1.5 (Goloboff *et al*. 2008, Goloboff & Catalano 2016), with equal cost for all transformations and gaps treated as a fifth state. All the New Technologies algorithms (sectorial search, ratchet, drift, tree fusing) in their default mode were implemented. Search was set for all taxa,

at level 50, with the minimum length tree to be found set to 100 times and random seed = 1.

Once we identified the most parsimonious trees, we used the software YBYRÁ (Machado 2015) to identify and plot unambiguously optimized synapomorphies shared across all optimal trees. This program generates color-coded boxes that indicate if a derived state occurs only in a particular clade (non-homoplastic) or if also is present in other clades (homoplastic), and if the state is shared by all terminals of the clade (unique) or if it is subsequently transformed into one or more different states within the clade (non-unique).

Given the heterogeneity of gene coverage (0–23 loci per terminal) in our data set, we analyzed the potential wildcard behavior of terminals (Simmons 2012a,b, Simmons & Norton 2013, Simmons & Goloboff 2013, Padial *et al*. 2014) for all terminals, also with YBYRÁ (Machado 2015) using all optimal topologies resulting from the parsimony analyses. Briefly, this analysis ranks all terminals according to the number of clades shared by all topologies when one terminal is pruned. Then, it prunes each terminal, one at a time, from all optimal topologies to calculate the average matching split distances among each set of pruned optimal topologies and compares it with the average matching split distance among the original topologies (Bogdanowicz & Giaro 2012, Machado 2015). Jackknife frequencies (JK) were calculated in TNT using the implied alignment for 1,000 pseudoreplicate searches under a Traditional Search analysis with 50 replicates and 50 trees saved per replication, gaps treated as fifth state, and removal probability 0.36 (~e-1) to render bootstrap and JK values comparable (Farris *et al*. 1996). We also estimated uncorrected pairwise

sequence divergences among ingroup terminals using uniform rates and default parameters in MEGA 7.0.14 (Kumar *et al*. 2016).

Analyses in POY were run on two clusters housed at the Laboratório de Alto Desempenho (LAD) of PUCRS. The cluster Amazonia is composed by two HP Proliant BL620c G7 server blades configured to parallel processing. Each server contains two Intel Xeon E7-2850 processors of 2.0 GHz (20 cores and 40 threats each). These two servers are equipped with 512 and 160 Gb of RAM respectively, and are interconnected by four nets of 10 Gigabit-Ethernet. The cluster Atlantica is composed by sixteen Dell PowerEdge R610 servers configured to parallel processing. These servers contain two Intel Xeon E5520 of 2.4 GHz (for three servers) or 2.27 GHz (for thirteen servers), 16 Gb of RAM each, and also are interconnected by four nets of 10 Gigabit-Ethernet. Additionally, two nodes of Atlantica are equipped with four Nvidia Tesla S2050 GPUs of 448 cores (two GPUs by node).

Optimality criteria and nucleotide homology

We chose parsimony as the optimality criterion because it is a non-parametric and evidentially conservative approach of phylogenetic inference that minimizes the assumptions about transformation events required to explain the variation observed in the data, maximizing the explanatory power of the hypothesis (Farris 1983, Kluge & Grant 2006, Grant & Kluge 2009).

Because nucleotides lack developmental and structural complexity required to test their homology separately, nucleotide homology only can be evaluated in reference to a topology (Grant & Kluge 2004). Thus, we applied tree-alignment, which simultaneously optimizes the nucleotide alignment and

the phylogenetic tree under the same optimality criterion (parsimony in this case). In this context, nucleotide correspondences in the resulting alignment directly and explicitly relate to evolutionary transformation events (Padial *et al*. 2014).

Results

Phenotypic characters

We included a total of 383 phenotypic characters in our dataset, including adult and larval external morphology, internal organs, musculature, osteology, behavior, bioacoustics, alkaloid profiles, and chromosome number. Of these, 195 were taken from Grant *et al*. (2017), Mendelson *et al*. (2000), De Sá *et al*. (2014), and Mijares-Urrutia (1998). The remaining 188 corresponded to novel characters, scored for dendrobatoids for the first time. These characters mainly correspond to osteology (n = 150), but also to external morphology (n = 35), behavior (n = 2), and bioacoustics (n = 1). Below we list the 383 characters, describing all new characters, and commenting on modifications and relevant observations.

0. Dorsal skin, texture (Grant *et al*. 2006): 0 = smooth; 1 = posteriorly granular; 2 = strongly granular; 3 = spiculate. Nonadditive.

1. Lateral skin, texture: 0 = smooth to finely granular; 1 = weakly tuberculated; 2 = strongly tuberculated. Nonadditive. (Figure 1).

Lateral skin texture varies in Aromobatinae and frequently differs from dorsal skin texture. However, it is rarely described in detail and independently of dorsal skin. We score the observed variation of lateral skin texture in three states. State 0 includes booth smooth and finely granular textures, because these two conditions are often intergraded at the flanks and finely granulated skin in live specimens can be reduced or erased by preservation, becoming nearly smooth or smooth textures. Our definition of finely granular is equivalent to shagreen texture as defined by Duellman & Lehr (2009) for terraranans: a slightly roughness condition that resembles sandpaper. In state 1, flank skin contains tubercles irregularly scattered; when a pale oblique lateral stripe is present, most of these tubercles (but not all) appear associated with this stripe (e.g., *Mannophryne* spp and most *Aromobates* species). Finally, in state 2, lateral skin appears densely and evenly covered by tubercles of different size (e.g., *Aromobates capurinensis*). Based on the same argument exposed by Grant *et al*. (2006) for dorsal skin texture, in the absence of developmental evidence that suggests that transformations between states 0 and 2 pass through state 1, we treat this character as nonadditive.

2. Dorsolateral ridge: 0 = absent; 1 = weak; 2 = moderate. Additive. (Figure 1)

Dermal ridges (or folds) are linear elevations of skin, in most cases anteroposteriorly oriented. These ridges are variable and can be formed by discontinuous and aligned series of granules or tubercles, or be continuous, either formed by anastomosing granules/tubercles, or smooth without differentiated granules/tubercles. Dermal ridges are present on dorsal and lateral surfaces of the body in several groups of anurans, and are informative at

the species level (e.g., *Leptodactylus* [De Sá *et al*. 2014], and *Pristimantis* [Duellman & Lehr 2009]). As far as we know, the presence of dorsolateral ridges has not been explicitly documented in any species of Aromobatinae nor mentioned in systematic and taxonomic reviews including this group (Edwards 1974, Rivero 1990, Grant *et al*. 2017). We detected the presence of moderately raised dorsolateral ridges (state 2) formed by aligned tubercles in specimens of *Aromobates capurinensis* and *A. inflexus*, and weakly raised dorsolateral ridges in *A. meridensis* and a putative new species of *Aromobates*. Although the presence of dorsolateral ridges in *A. capurinensis* was described by Péfaur (1993) as "…some tubercles on […] dorsolateral stripes areas"; it was not included in the definition and diagnosis, and was consequently ignored in subsequent studies. Rivero (1980) also noted this ridge in *A. inflexus* and described it as the presence of tubercles along the dorsolateral stripes forming elongated bulges, but as in the previous case, this was excluded in the definition and diagnosis and subsequently ignored in following studies. In *A. meridensis*, the presence of weakly raised dorsolateral ridges (state 1) was not reported neither in the original description (Dole & Durant 1974), nor in the redescription of Barrio-Amorós *et al*. (2010b). However, La Marca & Otero (2012) mentioned in their redescription of the holotype the presence of "a line of low dorsolateral tubercles from the level of the shoulders to level of groin".

3. Palmar skin (Grant *et al*. 2017): 0 = taut; 1 = loose.

4. Paired dorsal digital scutes (Grant *et al*. 2006): 0 = absent; 1 = present.

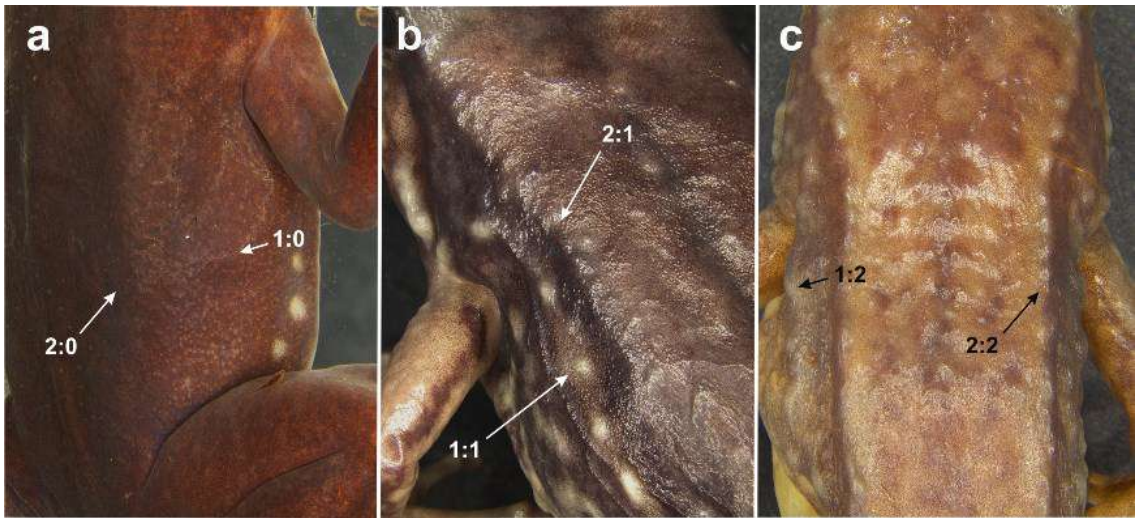

Figure 1. Lateral skin, texture (character 1) smooth (state 0) in *Anomaloglossus rufulus* (**a**), weakly tuberculated (state 1) in *Aromobates meridensis* CVULA 5973 (**b**), and strongly tuberculated (state 2) in *Aromobates capurinensis* CVULA 5938 (**c**). Dorsolateral ridge (character 2) absent (state 0) in *Anomaloglossus rufulus* MHNLS 20609 (**a**), weak (state 1) in *Aromobates meridensis* (**b**), and moderate (state 2) in *Aromobates capurinensis* (**c**).

5. Hand, supernumerary tubercles (Grant *et al*. 2006): 0 = absent; 1 = present. (Figure 2).

Grant *et al*. (2006, 2017) studied this character and confirmed their presence (state 1) only in some non-dendrobatoids used as outgroups. However, we detected the presence of some supernumerary tubercles on the hands of all specimens of *Mannophryne riveroi* examined. These tubercles are irregular in shape, variable in size and thickness, and are located proximal to the basal subarticular tubercles of fingers II–IV, and anterior to the thenar tubercle. Donoso-Barros (1964) and La Marca (1994a) explicitly state that supernumerary tubercles are absent on hands of this species. Barrio-Amorós *et al*. (2010c) do not mention this character, although these dermal structures can be observed in their figure 1A. None of the other specimens of *Mannophryne* studied by us exhibits this condition.

6–8: Fingers III and IV, distal subarticular tubercles (Figure 2)**.**

Fingers III and IV (FIII and FIV) of anurans commonly bear two subarticular tubercles each: a basal tubercle located at the joint between metacarpal and basal phalanx, and a distal tubercle between the basal and middle phalanges. The occurrence of the distal subarticular tubercle of FIV varies between dendrobatoidea and is commonly used as a diagnostic character. It is absent in species with FIV notably short (e.g., some *Allobates*). We followed Grant *et al*. (2006) in scoring the occurrence of this tubercle on FIV (character 7). Distal subarticular tubercles on FIII and FIV typically are circular to elliptical, and rounded in cross-section (state 0). Even though these tubercles were originally described as rounded in *Aromobates leopardalis*, *A. orostoma* (Rivero 1978), and *A. molinarii* (La Marca 1985), we noted that all of the studied specimens of these three species (see Appendix 1) have bilobed (in cross-section) subarticular tubercles on FIII and FIV (state 1; Figure 2b). We do not consider this cooccurrence as evidence of transformational dependence and, as in the other characters coded from FIII and FIV (e.g., finger disc width) that shown to be transformationally independent, we treated the shape of distal subarticular tubercles of each finger as an independent transformation series.

6. Finger III, distal subarticular tubercle, structure: 0 = single, rounded; 1 = bilobate to sagittally divided. (Figure 2).

7. Finger IV, distal subarticular tubercle, occurrence (Grant *et al*. 2006): 0 = absent; 1 = present.

8. Finger IV, distal subarticular tubercle, structure: 0 = single, rounded; 1 = bilobate to sagittally divided. (Figure 2).

Figure 2. Presence of supernumerary tubercles on hand (character 5:1) and rounded distal subarticular tubercles on FIII (character 6:0) and FIV (character 8:0) in *Mannophryne riveroi* MHNLS 15740 (**a**). Palm without supernumerary tubercles (5:0) and with bilobed distal subarticular tubercles on FIII (6:1) and FIV (8:1) in *Aromobates leopardalis* CVULA 464 (**b**).

9. Finger IV, length (Grant *et al*. 2006): 0 = surpassing distal subarticular tubercle of finger III; 1 = reaching distal subarticular tubercle of finger III; 2 = not reaching distal subarticular tubercle of finger III. Additive.

The state 1 of this character was originally described by Grant *et al*. (2006: 64) as "[FIV] reaches the distal half of, but does not surpass, the distal subarticular tubercle". We observed some specimens of *Anomaloglossus wothuja* and *A. rufulus* in which the distal tip of FIV reaches the level of the distal subarticular tubercle of FIII, but without surpassing his proximal half. This condition can be present in one or both hands of the same specimen and varies between

individuals of the same species. To accommodate this newly discovered variation, we relaxed the delimitation of state 1 redefining it as “reaching distal subarticular tubercle”.

10. Fingers I and II, ratio (Grant *et al*. 2006): 0 = I<<II (II 1.2 or more times longer than I); 1 = I<II; 2 = I=II; 3 = I>II. Additive.

Grant *et al*. (2006) quantitatively defined the state 0 as that in which FII is at least 20 % longer than FI; in state 1, FII is less than 15 % longer than FI; in state 2, FI and FII are subequal in length; and in state 3, FI is unambiguously longer than FII. Considering that in Aromobatinae, FI and FII are very small (from *ca*. 3.1 mm in *Aromobates ornatissimus* [Barrio-Amorós *et al*. 2011] to *ca*. 11.0 mm in *A. nocturnus*), differences in length, smaller than 10 %, between these fingers are almost imperceptible to the human eye, even under magnification. Thus, in order to objectively delimit state 2 of this character, we consider FI and FII equal to subequal when their difference in length is 10 % or less (measured following Kaplan [1997] under a stereomicroscope with graduated lenses), and state 3, for those in which FI length overcomes, in more than 10 %, FII length. Grant *et al*. (2017) coded *A. meridensis*, *A. ornatissimus*, and *Mannophryne urticans* as having FI unambiguously longer than FII (state 3), and *A. molinarii*, *A. nocturnus* and *M. trinitatis* as having FI slightly shorter than FII (state 1). Based on our observations and following the definitions provided above, we coded this character in all studied species of *Aromobates* and *Mannophryne* as state 2 (except *M. olmonae* for which we not examined any preserved specimen). In most cases, FII is slightly longer than FI, but does not exceed the length of the latter in more than 10 %. We also observed a few

cases of specimens with both conditions: FI little longer than FII on one hand, and FII little longer than FI on the other hand (e.g, *Mannophryne riveroi*, and *Aromobates* sp1). However, in all cases these differences were less than 10 % and, regardless of the polymorphism, fall within state 2.

11. Digital discs (Grant *et al*. 2006): 0 = absent; 1 = present.

12. Finger I, disc, expansion (Grant *et al*. 2006): 0 = unexpanded; 1 = weakly expanded; 2 = moderately expanded. Additive.

13. Finger II, disc, expansion (Grant *et al*. 2006): 0 = unexpanded; 1 = weakly expanded; 2 = moderately expanded; 3 = greatly expanded. Additive.

14. Finger III, disc, expansion (Grant *et al*. 2006): 0 = unexpanded; 1 = weakly expanded; 2 = moderately expanded; 3 = greatly expanded. Additive.

15. Finger IV, disc, expansion (Grant *et al*. 2006): 0 = unexpanded; 1 = weakly expanded; 2 = moderately expanded; 3 = greatly expanded. Additive.

16. Finger I, preaxial fringe (Grant *et al*. 2006): 0 = absent; 1 = present.

17. Finger I, postaxial fringe (Grant *et al*. 2006, 2017): 0 = absent; 1 = present.

18. Finger II, preaxial fringe (Grant *et al*. 2006): 0 = absent; 1 = present.

19. Finger II, postaxial fringe (Grant *et al*. 2006): 0 = absent; 1 = present.

20. Finger III, preaxial fringe (Grant *et al*. 2006): 0 = absent; 1 = present.

21. Finger III, postaxial fringe (Grant *et al*. 2006): 0 = absent; 1 = present.

22. Finger IV, preaxial fringe (Grant *et al*. 2006): 0 = absent; 1 = present.

23. Finger IV, postaxial fringe (Grant *et al*. 2006): 0 = absent; 1 = present.

24. Metacarpal ridge (Grant *et al*. 2006): 0 = absent; 1 = weak; 2 = strong. Additive.

We added a third state (2 = strong) as part of this transformation series to include the strongly elevated metacarpal ridge observed in *Anomaloglossus dewynteri* (Fouquet *et al*. 2018: Figure 7).

25. Finger III, swelling (Grant *et al*. 2006): 0 = absent; 1 = present.

Within Aromobatinae, the occurrence of glandular swelling on FIII has only been documented in adult males of *Aromobates meridensis* (Barrio-Amorós *et al*. 2010b), and in the holotype of *A. ornatissimus* (Barrio-Amorós *et al*. 2011). Grant *et al*. (2017) qualifies its presence in *A. meridensis* as highly unexpected. However, we confirmed this observation and reported it in other seven species of *Aromobates*.

26. Adult males, finger III, morphology of swollen finger (Grant *et al*. 2006): 0 = pre- and postaxial swelling; 1 = weak preaxial swelling; 2 = strong preaxial swelling; 3 = swelling extending from wrist, mainly preaxial on digit. Nonadditive.

27. Carpal pad (Grant *et al*. 2006): 0 = absent; 1 = present.

28. Male excrescences on thumb (Grant *et al*. 2006): 0 = absent; 1 = present. Grant *et al*. (2006, 2017), scored *Mannophryne oblitterata* as the unique dendrobatoid species in wich males have nuptial excrescences on thumbs (state 1). This statement was based on the observation of “non-cornified swollen structures resembling nuptial pads” on the dorsal surface of first and second fingers of a single adult male (TCWC 61415), first documented by La Marca (1994a), and subsequently illustrated by the same author (La Marca 1995). We examined specimen TCWC 61415 from photos (Figure 3), and confirmed the presence of slightly hypertrophied glandular tissue visible through skin, restricted to dorsal surfaces of fingers I and II (as described by La Marca 1995), but also in lower density on the dorsal surface of the distal portion of fingers III and IV of both hands. Due to the differences we observed in the extension, texture and size of the structures in *M. obiltterata* with regards to nuptial pads as defined by Grant *et al*. (2006; characters 23 and 24), we assumed that they are not part of the same transformation series. Consequently, we recoded nuptial pads in *M. oblitterata* as absent (state 0). Nonetheless, we highlight the need of an appropriate characterization of these glandular structures based on histological analysis. Hypertrophied glandular

structures on fingers were not detected in any of the other adult males examined.

29. Adult males, excrescences on thumb, morphology (Grant *et al*. 2006): 0 = large, cornified spines; 1 = small, uncornified spines; 2 = nonspinous asperities. Additive.

30. Female excrescences on thumb (Grant *et al*. 2006): 0 = absent; 1 = present (large, cornified spines).

31. Thenar tubercle, size (Grant *et al*. 2006): 0 = absent or small, inconspicuous swelling; 1 = large, conspicuous, well-defined tubercle.

Figure 3. Swollen glandular patches (indicated by arrows) on dorsal surface of all fingers of both hands, in the adult male TCWC 61415 of *Mannophryne oblitterata*. Photo: Toby Hibbitts.

32. Palmar tubercle, shape: 0 = distally rounded; 1 = slightly bilobate to bifid distally. (Figure 4).

Sometimes referred in older descriptions as outer metacarpal tubercle or outer palmar tubercle (e.g., Péfaur 1985, Myers *et al*. 1991). This is a well-defined dermal thickness, typically almost circular or subtriangular, located at the proximal and postaxial portion of the palmar surface of hand. No significant variation has been documented for this structure among dendrobatoids, however we observed two discrete states on the distal contour of this tubercle: rounded (state 0), the most common condition, and slightly bilobate to bifid distally (state 1). This last condition was observed in *Prostherapis dunni*, several species of *Anomaloglossus* (*A. beebei*, *A. blanci*, *A. megacephalus*, *A. rufulus*, *A. tepuyensis*, *A. verbeeksnyderorum*, and *A. wothuja*), and *Ectopoglossus saxatilis*. In the latter, the distal contour is slightly bilobate (Grant

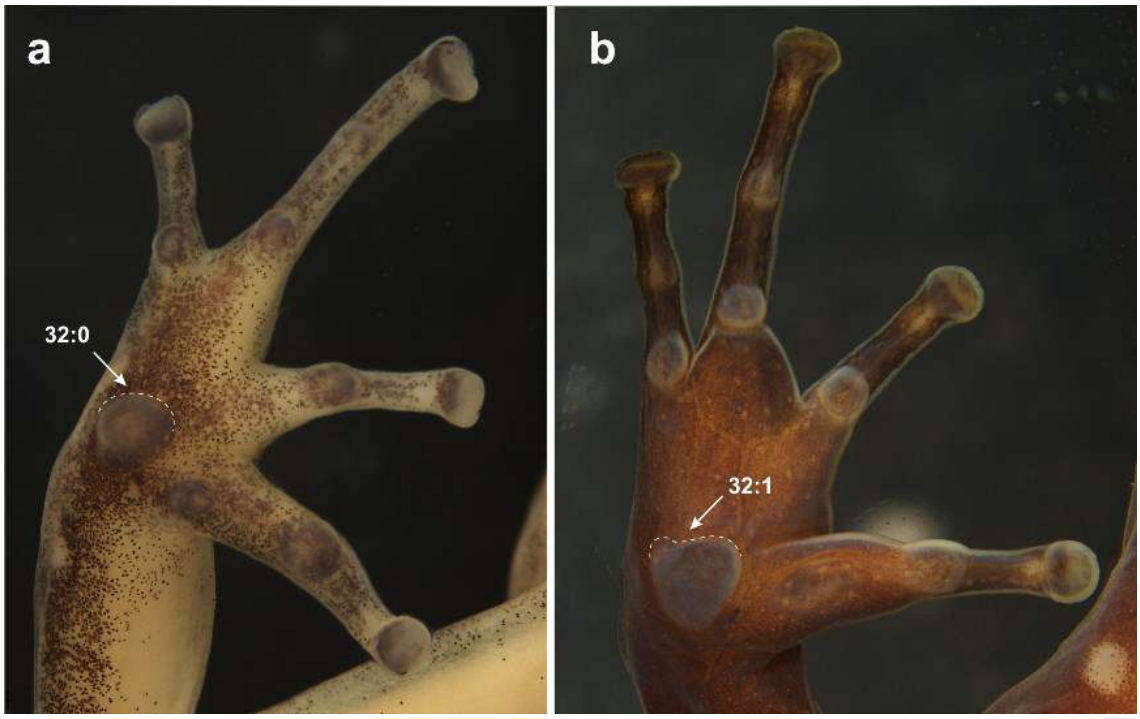

Figure 4. Distal contour of the plamar tubercle (character 32) rounded (state 0) in *Allobates pittieri* MHNLS 21488 (**a**), and slightly bilobate (state 1) in *Anomaloglossus rufulus* MHNLS 20609 (**b**).

et al. 2017: Figure 4a), whereas a bifid distal contour was observed in *A. blanci* (Fouquet *et al*. 2018: Figure 2f). Polymorphism for this character was detected in a population of *Mannophryne* from El Jarillo, related to *M. speeri*.

33. Black arm gland in adult males (Grant *et al*. 2006): 0 = absent; 1 = present.

34. Tarsal keel (Grant *et al*. 2006): 0 = absent; 1 = present.

35. Tarsal keel, development at level of Inner Metatarsal Tubercle (IMT): 0 = absent; 1 = lower than its proximal portion; 2 = as high as its proximal portion . Additive. (Figure 5).

Grant *et al*. (2006) coded the variation of the tarsal keel into four states (see character 36). Based on their coding, all species of *Aromobates* and *Mannophryne* exhibit a straight or very weakly curved tarsal keel, extending proximolaterally from the preaxial edge of IMT (state 0). However, we observed additional and undescribed variation of the tarsal keel, namely the height of the keel at the IMT in reference to that of the keel at its proximal edge. In most *Aromobates* and "*Colostethus" caribe*, the tarsal keel is lower at the level of the IMT. In all species of *Mannophryne*, *Aromobates* sp 1, and "*Prostherapis" dunni*, the tarsal keel is as developed as at the level of the IMT than at the proximal portion of the keel (state 2). State 0 (absence of tarsal keel at the level of IMT) is observed in numerous species of *Allobates* and dendrobatids. It is worth mentioning that state 1 is generally associated with a partial fusion of the keel with the preaxial side of the IMT, while in state 2 the keel is not fused with

this tubercle. However, we have not coded this character (i.e., fusion of keel and IMT), which we considered a different transformation series.

36. Tarsal keel, morphology (Grant *et al*. 2006): 0 = straight or very weakly curved, extending proximolaterad from preaxial edge of inner metatarsal tubercle; 1 = tubercle-like (i.e., enlarged) and strongly curved at proximal end, extending from metatarsal tubercle; 2 = short, tubercle-like, curved or directed transversely across tarsus, not extending from metatarsal tubercle; 3 = weak, short dermal thickening, not extending from metatarsal tubercle. Additive.

37. Tarsal fringe (Grant *et al*. 2006): 0 = absent; 1 = present.

38. Middle metatarsal tubercle: 0 = absent; 1 = present. (Figure 5).

The middle metatarsal tubercle (MMT) is located at the base of the foot, between inner and outer metatarsal tubercles (IMT and OMT, respectively), and slightly more proximal than them. As described by Myers *et al*. (1991) for *Aromobates nocturnus*, the MMT can vary intraspecifically from an inconspicuous calloused patch in some specimens, to a prominent projection in others, but generally it is larger than the OMT, flat and less protuberant than the IMT and OMT. Donoso-Barros (1964), Mijares-Urritia & Arends (1999a, 1999b), and Rojas-Runjaic *et al*. (2018) also documented the occurrence of this tubercle in *Mannophryne riveroi*, *M. caquetio*, *M. lamarcai*, and *M. molinai*, respectively. Rivero (1980) also indicated its presence in *A. mayorgai*. Additionaly, we observed that a MMT is present in most species of *Aromobates*, all species of

Mannophryne, and some *Allobates*, *Anomaloglossus*, and dendrobatids included on our outgroup.

39. Toes, basal subarticular tubercles, shape: 0 = rounded to oval; 1 = elongate. (Figure 5).

Basal subarticular tubercles of feet are typically rounded to oval in dendrobatoids. However, Rivero (1978) noted that these are elongate in *Aromobates leopardalis* and *A. alboguttatus*. The same condition was also documented for *A. mayorgai*, *A. saltuensis* (Rivero 1980), and for *Mannophryne larandina* (Yústiz 1991). We confirmed all the previous observations and additionally detected the occurrence of elongate basal subarticular tubercles in *M. riveroi*, *M. orellana*, *M. yustizi*, *A. nocturnus*, *Anomaloglossus megacephalus*, and in *Aromobates* sp. 3. In state 0 (rounded to oval) basal subarticular tubercles are as long as wide, or slightly longer than wide. In state 1 (elongate) these are twice (or more) as long as wide.

40. Toe I, disc, expansion (Grant *et al*. 2006): 0 = unexpanded; 1 = weakly expanded; 2 = moderately expanded. Additive.

41. Toe II, disc, expansion (Grant *et al*. 2006): 0 = unexpanded; 1 = weakly expanded; 2 = moderately expanded. Additive.

42. Toe III, disc, expansion (Grant *et al*. 2006): 0 = unexpanded; 1 = weakly expanded; 2 = moderately expanded. Additive.

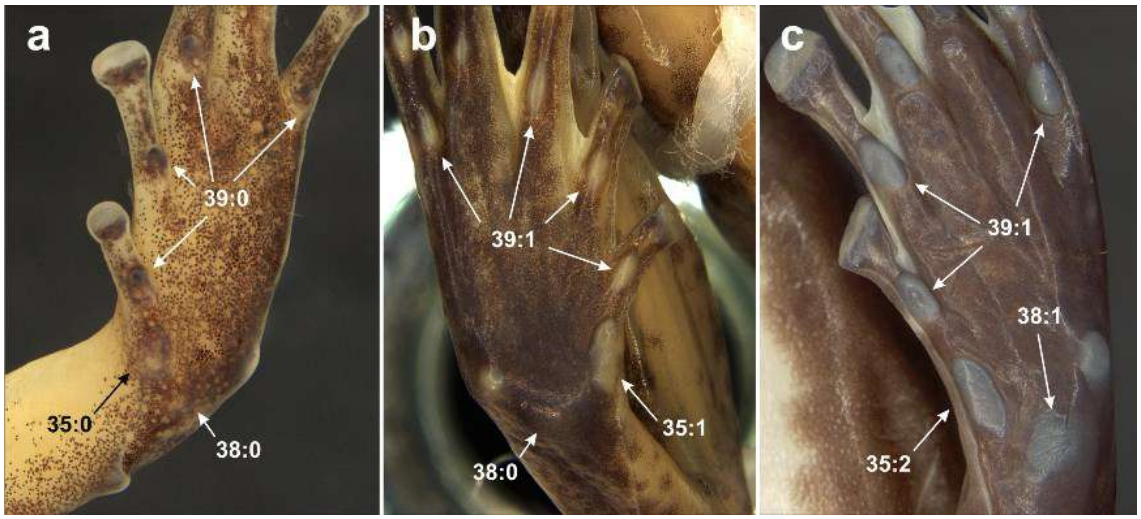

Figure 5. Tarsal keel at the level of the inner metatarsal tubercle (IMT; character 35) absent (state 0) in **a**; lower than the height of proximal edge of the keel (state 1) and fused to the IMT in **b**; equal height of the keel (state 2) and not fused in **c**. Middle metatarsal tubercle (character 38) absent (state 0) in **a**–**b**; present (state 1) in **c**. Basal subarticular tubercles of foot (character 39) rounded to oval (state 0) in **a**; elongated (state 1) in **b**–**c**. *Allobates pittieri* MHNLS 21488 (**a**), *Aromobates leopardalis* CVULA 464 (**b**), *Mannophryne riveroi* MHNLS 17910 (**c**).

43. Toe IV, disc, expansion (Grant *et al*. 2006): 0 = unexpanded; 1 = weakly expanded; 2 = moderately expanded; 3 = greatly expanded. Additive.

We added a fourth state (3 = greatly expanded) to this transformation series, to include the variation observed in *Allobates juami* Simões, Gagliardi-Urrutia, Rojas-Runjaic & Castroviejo-Fisher, 2018, in which toe disc IV is ≥ 3x the width of previous phalanx (Simões *et al*. 2018).

44. Toe V, disc, expansion (Grant *et al*. 2006): 0 = unexpanded; 1 = weakly expanded; 2 = moderately expanded. Additive.

45. Toe I, preaxial webbing, development (Grant *et al*. 2006): 0 = absent; 1 = fringe.

46. Toe I, postaxial webbing, development (Grant *et al*. 2006): 0 = absent; 1 = fringe; 2 = 2; 3 = 1.5; 4 = 1; 5 = 0. Additive.

47. Toe II, preaxial webbing, development (Grant *et al*. 2006): 0 = absent; 1 = 2.5 2 = 2; 3 = 1; 4 = 0. Additive.

48. Toe II, postaxial webbing, development (Grant *et al*. 2006): 0 = absent; 1 = 2 (without fringe); 2 = 2 (with fringe); 3 = 1.5; 4 = 1; 5 = 0. Additive.

49. Toe III, preaxial webbing, development (Grant *et al*. 2006): 0 = absent; 1 = fringe; 2 = 3.5 (without fringe); 3 = 3.5 (with fringe); 4 = 3; 5 = 2.5; 6 = 2; 7 = 1.5; 8 = 1. Additive.

50. Toe II, postaxial webbing, development (Grant *et al*. 2006): 0 = absent; 1 = 3 without fringe; 2 = 3 with fringe; 3 = 2.5; 4 = 2; 5 = 1.5; 6 = 1. Additive.

51. Toe IV, preaxial webbing, development (Grant *et al*. 2006): 0 = absent; 1 = 4 without fringe; 2 = 4 with fringe; 3 = 3.5; 4 = 3; 5 = 2.5; 6 = 2; 7 = 1. Additive.

52. Toe IV, postaxial webbing, development (Grant *et al*. 2006): 0 = absent; 1 = fringe; 2 = 4; 3 = 3.5; 4 = 3; 5 = 2.5; 6 = 2; 7 = 1. Additive.

53. Toe V, preaxial webbing, development (Grant *et al*. 2006): 0 = absent; 1 = fringe; 2 = 2.5 (with fringe); 3 = 2; 4 = 1.5; 5 = 1. Additive.

54. Toe V, webbing, development (Grant *et al*. 2006): 0 = absent; 1 = fringe.

55. Metatarsal fold, development (Grant *et al*. 2006): 0 = absent; 1 = weak; 2 = strong. Additive.

56. Metatarsal fold, length 0 = on the distal third; 1 = on the distal half; 2 = on the two distal thirds; 3 = complete or almost reaching the outer metatarsal tubercle. Additive. (Figure 6).

This dermal linear thickening runs on the postaxial edge of the sole, from the base of toe V and towards the outer metatarsal tubercle. Its protuberance and extension varies notably among species and consequently is often used in species descriptions. Grant *et al*. (2006) scored the variation in protuberance of this fold in dendrobatoids (character 55 in this study). We additionally coded as a different transformation series the variation observed in the extension of this fold. The extension of the metatarsal fold is related to the metatarsus V, which externally corresponds to the distance between the basal subarticular tubercle of toe V and the outer metatarsal tubercle. In the state 0, the extension of the metatarsal fold does not exceed the distal third of the metatarsus V; in state 1, it extends to the distal half of the metatarsus; in state 2, the metatarsal fold does not exceed the two distal thirds; and finally, in state 3, this fold is complete, extending from the basal subarticular tubercle to the level of the outer metatarsal tubercle, or proximally very close to this.

57. Cloacal tubercles (Grant *et al*. 2006): 0 = absent; 1 = present.

58. Nares, orientation: 0 = laterodorsal (visible dorsally); 1 = lateral (not visible dorsally nor ventrally); 2 = lateroventral (visible ventrally). Nonadditive. (Figure 7).

Nares are located lateroposteriorly to the tip of snout. In aromobatids, the orientation of narial openings (in the vertical plane) varies among species, but rarely among conspecifics. This character is not commonly included in species definitions and diagnoses, but recent descriptions typically indicate the view in which narial openings are visible (e.g., Barrio-Amorós *et al*. 2010a, Barrio-Amorós & Santos 2012). Based on our observations, we individuated three character states for this transformation series: narial openings laterodorsally oriented (state 0), when they are visible in dorsal view; narial openings laterally oriented (state 1), when they are visible neither in dorsal nor in ventral views; and narial openings lateroventrally oriented (state 2), when they are only visible in ventral view.

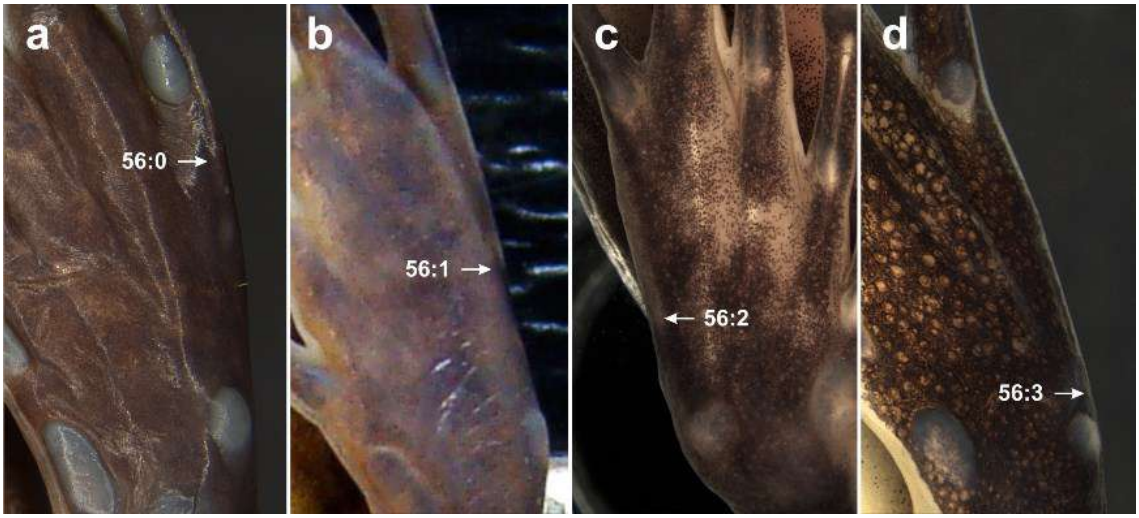

Figure 6. Metatarsal fold length (character 56) extending to the distal third of the metatarsus (state 0) in *Mannophryne riveroi* MHNLS 17910 (**a**); on the distal half (state 1) in *Aromobates* sp 1 EBRG 2206 (**b**); on the two distal thirds (state 2) in *A. alboguttatus* CVULA 1448 (**c**); almost reaching the outer metatarsal tubercle (state 3) in *A. zippeli* MHNLS 22048 (**d**).

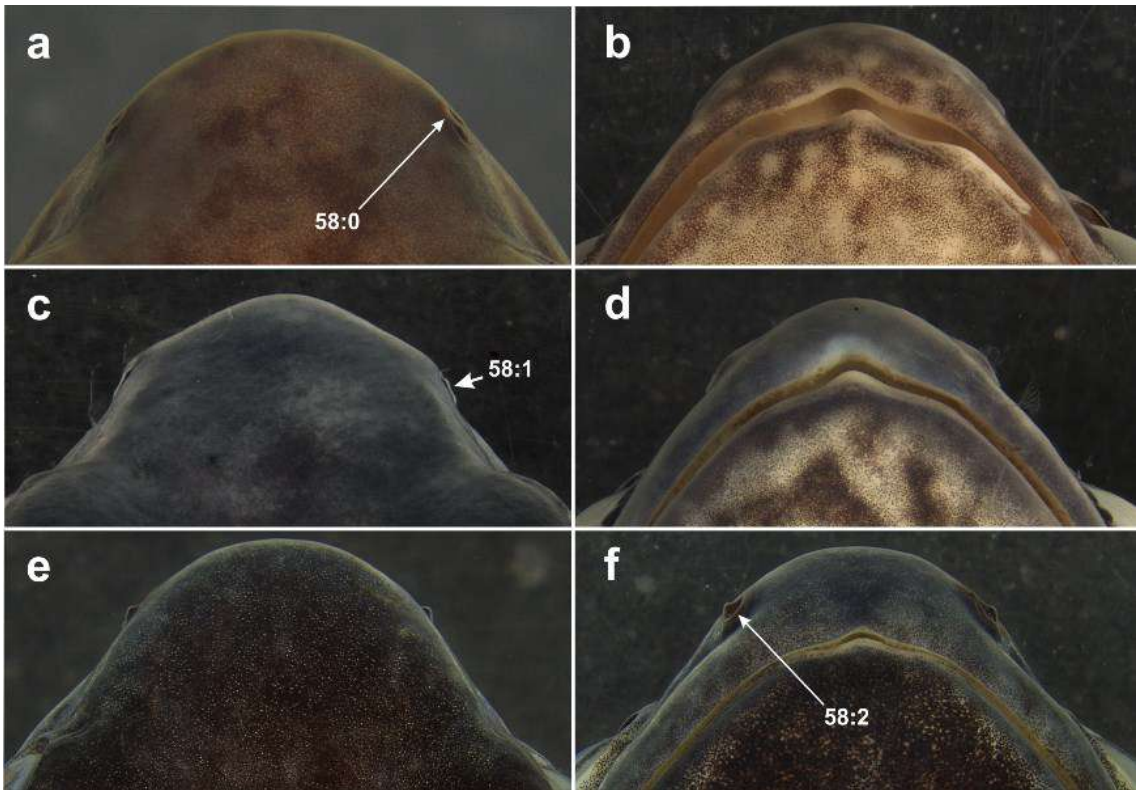

Figure 7. Narial orientation (character 58). Nares laterodorsally oriented (visible dorsally; state 0) in *Aromobates leopardalis* CVULA 464 (**a–b**); laterally oriented (not visible dorsally nor ventrally; state 1) in *A. meridensis* MHNLS 22019 (**c–d**); lateroventrally oriented (visible ventrally; state 2) in *Mannophryne oblitterata* MHNLS 21818 (**e–f**).

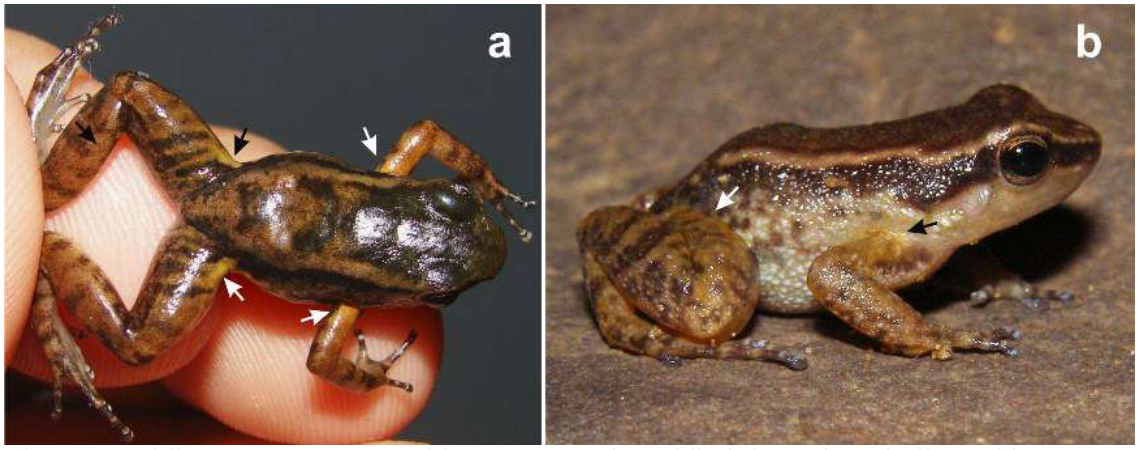

Figure 8. Iridiscent orange or golden spots at dorsal limb insertions indicated by arrows in a *Mannophryne* sp. from Araira, pertaining to the complex of *M*. *vulcano* (**a**) and *Aromobates tokuko* MHNLS 18499 (**b**).

59. Iridescent orange or golden spot at dorsal limb insertions (Grant *et al*. 2006): 0 = absent; 1 = present. (Figure 8).

This character was coded as absent for all species of *Aromobates* and *Mannophryne* included in the studies of Grant *et al*. (2006, 2017). Nonetheless, we noted that this spot is present in most species of these two genera, but it is smaller and less evident than in *Adelphobates quinquevittatus*. In photos of live specimens the iridescent spot is poorly defined but evident and it fades in preserved specimens, so its presence can go unnoticed in the latter.

60. Yellow translucent coloration on hidden parts of hind limbs: 0 = absent; 1 = present. (Figure 9).

In most species of *Aromobates*, hidden parts of the proximal portions of shank, and tarsus are stained in life by translucent yellow coloration; these spots become diffuse at their edges and are commonly restricted to concealed parts, but in some cases the pigments extend to almost the entire ventral surface of hind limbs. Grant *et al*. (2006) noted the presence of this flash bright coloration on the concealed surface of the shanks in *Leucostethus fraterdanieli*, and pointed out that it differs from the calf spot (character 63 of this study) of *Colostethus imbricolus* by not forming a discrete spot. The translucent yellow coloration fades in preserved specimens, so the character can only be coded from living specimens.

61. Pale paracloacal mark (Grant *et al*. 2006): 0 = absent; 1 = present.

62. Thigh, dorsal surface, color pattern (Grant *et al*. 2006): 0 = pale with dark spots (forming reticulum when spots are close together); 1 = solid dark; 2 = dark with pale spots/bands; 3 = solid pale; 4 = brown with dark brown

bands/blotches; 5 = dark with pale longitudinal stripe; 6 = pale background speckled with small dark dots. Nonadditive.

Some specimens of *Aromobates duranti*, *A. orostoma*, and *A. zippeli* exhibit a thigh dorsal color pattern different from those described by Grant *et al*. (2006). This pattern consists on a pale brown background irregularly speckled with small and irregular dark brown dots (Figure 10). We included the new pattern observed as a seventh state for this transformation series. This new pattern (state 6) differs from state 0 (Grant *et al*. 2006: Figure 35a) in the much smaller size and irregular shape of the dark brown spots.

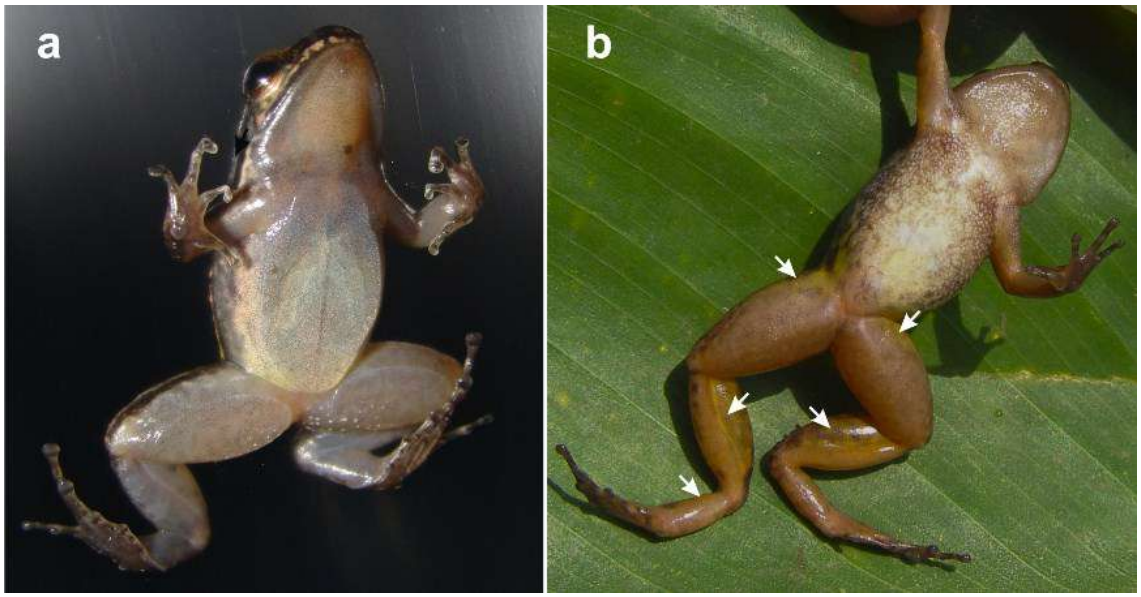

Figure 9. Yellow transluscent coloration on hidden parts of hind limbs (character 60) absent (state 0) in *Mannophryne vulcano* (**a**), and present (state 1; indicated by arrows) in *Aromobates tokuko* MHNLS 18490 (**b**).

63. Discrete pale proximoventral calf spot (Grant *et al*. 2006): 0 = absent; 1 = present.

64. Dorsolateral stripe A (Grant *et al*. 2006, 2017): 0 = absent; 1 = present.

The posterior end of this stripe does not drop to the thigh.

Figure 10. Dorsal surface of the left thigh of *Aromobates zippeli* MHNLS 22052 showing a pale background color, densely speckled with small dark dots (character 62: state 6).

65. Dorsolateral stripe A, length (Grant *et al*. 2006, 2017): 0 = anterior (extending from eye to area above arm insertion); 1 = to midbody (from eye and passing arm insertion but not reaching the level of groin); 2 = complete (extending from eye to the area above groin and distal tip of urostyle). Additive.

Grant *et al*. (2017) scored this transformation series as binary, with the state 0 corresponding to the dorsolateral stripe A (DLSA) reaching no further than the arm insertion, and state 1 including the rest of the variation in the extension of the DLSA between the arm insertion and the posterior end of dorsum. In order to better reflect the variation observed on this transformation series in aromobatids, we divided the state 1 of Grant *et al*. (2017) in two states: to midbody (state 1) in which DLSA reaches any point posterior to the level of the arm insertion, but without surpassing the midbody; and complete (state 2) for

those cases in that DLSA surpass the level of midbody, reaching in some cases the supracloacal dermal flap where it converges with the opposite DLSA.

66. Dorsolateral stripe A, structure (Grant *et al*. 2006, 2017): 0 = series of discrete spots; 1 = solid; 2 = diffuse. Nonadditive.

Grant *et al*. (2017) scored this transformation series in two character states: DLSA formed by a series of discrete spots (state 0), and DLSA solid (state 1). In order to better describe the variation observed in Aromobatinae for this transformation series, we added the condition of DLSA diffuse as a third state. A diffuse DLSA is present in most species of *Mannophryne* and also in some species of *Aromobates* (e.g., *A. ornatissimus* and some specimens of *A. mayorgai*).

67. Dorosolateral stripe A pattern: 0 = straight to nearly straight; 1 = sinuous. (Figure 11).

We individuated this additional transformation series to score the variation observed in the form of DLSA in *Aromobates*, that can be straight to almost straight (state 0) or markedly sinuous (state 1). A sinuous DLSA is present in *A. inflexus*, *A. zippeli* and some specimens of *A. molinarii*.

68. Dorsolateral stripe A ontogeny (Grant *et al*. 2006, 2017): 0 = present in juveniles only (i.e., lost ontogenetically); 1 = present in juveniles and adults.

69. Dorsolateral stripe B (Grant *et al*. 2006): 0 = absent; 1 = present.

The posterior end of this stripe drops to the top of thigh, but not the groin.

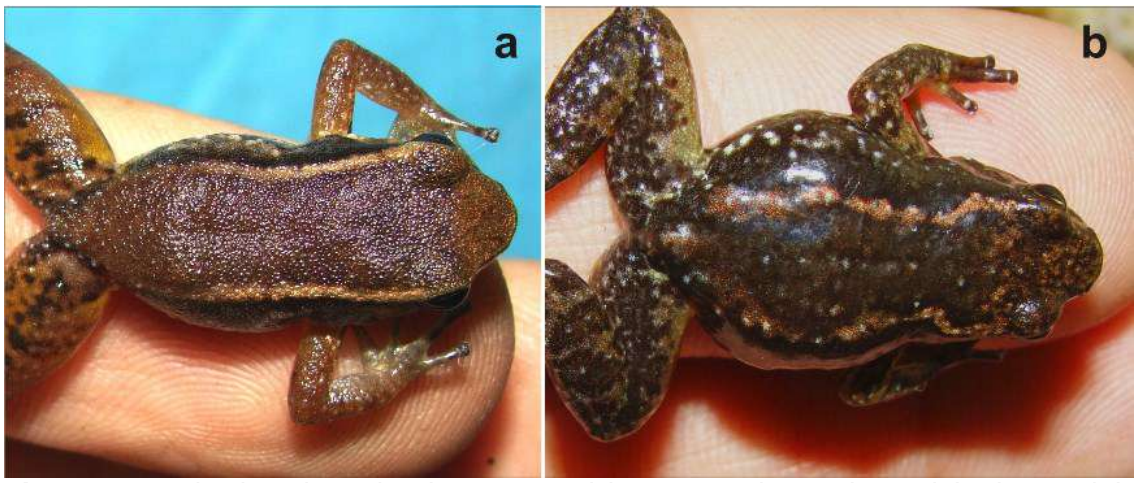

Figure 11. Pale dorsolateral stripe pattern (character 67): nearly straight (state 0) in *Aromobates mayorgai* (**a**), and sinuous (state 1) in *Aromobates zippeli* (**b**).

70–74: Lateral dark band and supratympanic dark stripe.

The lateral dark band has been mentioned in numerous descriptions of *Aromobates* and *Mannophryne*, but rarely considered as a relevant diagnostic character. Péfaur (1985) and La Marca (1994a) described it as a "dark dorsolateral stripe", whereas Barrio-Amorós *et al*. (2010a) refer it as "lateral black band". This band begins at the tip of snout, is interrupted by the eye, and continues posteriorly on the flank of body. Its superior margin is commonly straight, well-defined, and juxtaposed to the lateral margin of the pale dorsolateral stripe (when the latter is present). The inferior margin is more variable; it can be very well-defined and be in contact with the pale ventrolateral stripe (as in numerous *Allobates* species), or it can be diffuse ventrally and not reach the inferior portion of the flank. This band varies in vertical broadness (width) to the midlevel of flank, in its posterior extension, and intensity. In some cases, a thin supratympanic dark stripe is also present, delineating the inferior margin of the lateral dark band between the posterior corner of the eye and the anterodorsal insertion of the arm. This stripe seems to be associated with the lateral dark band in some specimens of *Anomaloglossus rufulus* (Figure 12a)

and *Allobates chalcopis* (Figure 12e), but is present even when the lateral dark band is absent in other specimens of *A. rufulus* (Barrio-Amorós & Santos 2011: Figure 1a). Nonetheless, it is absent in most aromobatids with lateral dark band. Thus, we treated the supratympanic dark stripe as an independent transformation series. Additionally, the lateral dark band was individuated in four transformation series (occurrence, width, extension, and structure).

70. Lateral dark band: 0 = absent; 1 = present. (Figure 12).

71. Supratimpanic dark stripe: 0 = absent; 1 = present. (Figure 12).

72. Lateral dark band, width: 0 = wider at the midbody than in the arm insertion level; 1 = as wide (or almost as wide) at the midbody as at the level of arm insertion; 2 = wider at the arm insertion than in the midbody (restricted to the dorsal portion of flank). Nonadditive. (Figure 12).

73. Lateral dark band, extension: 0 = from posterior border of the eye and extending to the arm insertion or to the midbody; 1 = from posterior border of the eye to the groin. (Figure 12).

74. Lateral dark band, structure: 0 = diffuse; 1 = formed by irregular spots anastomosed; 2 = solid. Nonadditive. (Figure 12).

75. Ventrolateral stripe (Grant *et al*. 2006, 2017): 0 = absent; 1 = present.

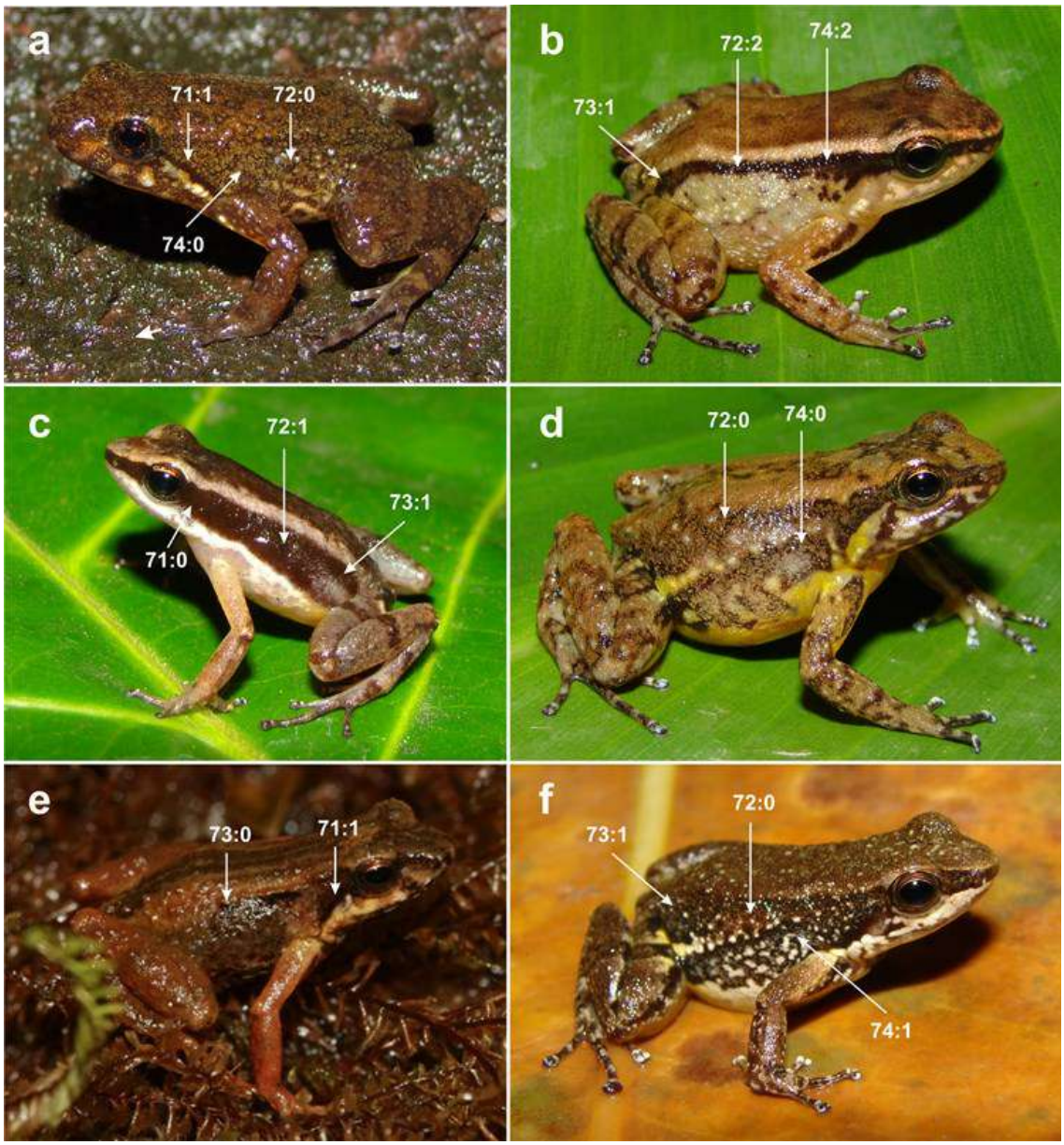

Figure 12. Occurrence of a lateral dark band (character 70:1) in six species of Aromobatidae. Supratimpanic dark stripe (character 71): absent (state 0) in **b**–**d** and **f**; present (state 1) in **a** and **e**. Lateral dark band width (character 72): wider at the midbody (state 0) in **a**, **d** and **f**; as width at the arm insertion as at the midbody (state 1) in **c**; wider at the arm insertion (state 2) in **b** and **e**. Lateral dark band extension (character 73): incomplete, to the arm insertion level or to the midbody (state 0) in **e**; complete, reaching the groin (state 1) in **a**–**d**, and **f**. Lateral dark band structure (character 74): diffuse (state 0) in **a**, **d**, and **e**; formed by irregular spots anastomosed (state 1) in **f**; solid (state 2) in **b**–**c**. **a.** *Anomaloglossus rufulus*; **b.** *Aromobates mayorgai*; **c.** *Allobates pittieri*; **d.** *Aromobates meridensis*; **e.** *Allobates chalcopis* (photo: Maël Dewynter); **f.** *Mannophryne vulcano*.

76. Ventrolateral stripe, structure (Grant *et al*. 2006, 2017): 0 = wavy series of elongate spots; 1 = straight; 2 = series of discrete spots. Nonadditive.

Grant *et al*. (2017) defined this transformation series with two states: “wavy series of elongate spots” (state 0), and “straight” (state 1). This was derived from the multistate character 54 (“ventrolateral stripe”), originally defined by Grant *et al*. (2006). As highlighted by Grant *et al*. (2006), the wavy series of elongate spots often are interconnected, forming an almost continuous irregular stripe (as illustrated in his figure 39a), different to the continuous and at least dorsally straight stripe defined by the other state that composed the series (Grant *et al*. 2006: Figure 39b). None of these two states describe the ventrolateral stripe (VLS) formed by anteroposteriorly aligned, non-elongate, and discrete pale spots observed by us in most of the species of *Aromobates* possessing VLS. To better describe variation in VLS, we add a third state on this transformation series (state 2).

77. Oblique lateral stripe (Grant *et al*. 2006): 0 = absent; 1 = present.

78. Oblique lateral stripe, length (Grant *et al*. 2006): 0 = partial; 1 = complete.

79. Oblique lateral stripe, structure (Grant *et al*. 2006): 0 = solid; 1 = series of spots; 2 = diffuse. Nonadditive.

80–87: Dark dermal collar.

The dark dermal collar is one of the most conspicuous phenotypic synapomophies of *Mannophryne* (La Marca 1992, 1994a, 1995, Grant *et al*. 2006, 2017). A similar type of dark dermal marking is present on the posterior portion of the throat of some species of *Hyloxalus*. In these, the so-called gular-

chest markings vary from two small paramedial spots, as in *Hyloxalus vertebralis* and *H. bocagei*, to a diffuse, transverse, and medially broken bar, as in *H. awa* and *H. shuar* (Coloma *et al*. 1995). Myers *et al*. (1991) considered that the gular-chest markings could be homologous to the dark dermal collar of *Mannophryne*. But Grant *et al*. (2006) treated the gular-chest markings of *Hyloxalus* and the dark dermal collar of *Mannophryne* as different transformation series because the gular-chest markings are always separated medially and do not form a continuous transverse band. However, Barrio-Amorós *et al*. (2010a) documented the occurrence of a medially broken collar—similar to the gular broken band-like marks of some *Hyloxalus*—in some specimens of *Mannophryne vulcano*. We confirmed the occurrence of a broken collar in *M. vulcano* and additionally detected this condition in numerous specimens of *M. herminae*, *M. lamarcai*, *M. urticans*, *M. yustizi, Mannophryne* sp. 3 and *Mannophryne* sp. 4. Thus, and contrary to *Grant et al*. (2006, 2017), we treated the gular-chest markings as homologous to the dark dermal collar. Additionally, and as indicated by La Marca (1995) we observed that part of the variation of the dark dermal collar can be explained by sexual dimorphism and development (Dixon & Rivero-Blanco 1985, La Marca 1995). In an attempt to better reflect the observed variation of the dark dermal collar into homologous transformation series, we separated males and females into different semaphoronts, and individuated four transformations series for each sex: occurrence, structure, continuity, and broadness (Figure 13). Although ontogenetic variation in the dark dermal collar in *Mannophryne* was noted by Dixon & Rivero-Blanco (1985) and La Marca (1995) we coded all transformation series associated with it from adult specimens.

80. Male, dark dermal collar: 0 = absent; 1 = present.

81. Male, dark dermal collar, structure: 0 = diffuse; 1 = solid; 2 = reticulate. Nonadditive.

82. Male, dark dermal collar, continuity: 0 = complete; 1 = medially broken.

83. Male, dark dermal collar, broadness: 0 = narrow (posterior margin of the dark collar does not pass the level of the arm insertion); 1 = broad (posterior margin of the dark collar surpass the level of the arm insertion).

84. Female, dark dermal collar: 0 = absent; 1 = present.

85. Female, dark dermal collar, structure: 0 = diffuse; 1 = solid; 2 = reticulate. Nonadditive.

86. Female, dark dermal collar, continuity: 0 = complete; 1 = medially broken.

87. Female, dark dermal collar, broadness: 0 = narrow (posterior margin of the dark collar does not pass the level of the arm insertion); 1 = broad (posterior margin of the dark collar surpass the level of the arm insertion).

88. Dark lower labial stripe (Grant *et al*. 2006): 0 = absent; 1 = present.

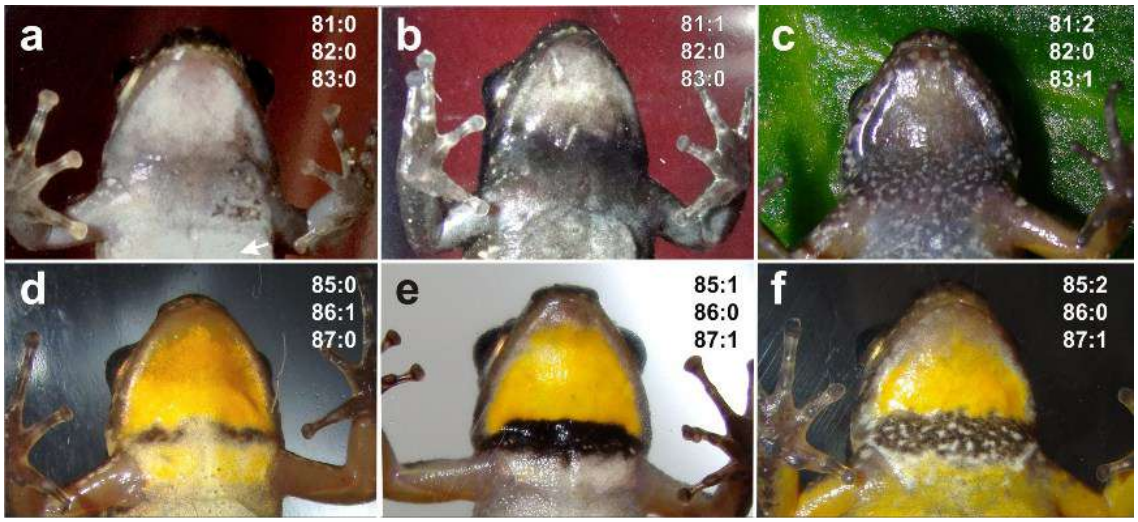

Figure 13. Dark dermal collar in males (**a–c**; character 80:1) and females (**d–f**; character 84:1) of several species of *Mannophryne*. Male collar structure in males (character 81) and females (character 85): diffuse (state 0) in **a** and **d**; solid (state 1) in **b** and **e**; reticulated (state 2) in **c** and **f**. Dark dermal collar continuity in males (character 82) and in females (character 86): complete (state 0) in **a**–**c**, **e**–**f**; medially broken (state 1) in **d**. Dark dermal collar broadness in males (Character 83), and in females (character 87): narrow (state 0) in **a**–**b** and **d**; broad (state 1) in **c**, **e**–**f**. **a.** *M. urticans*; **b.** *M. collaris*; **c.** *M.* aff. *yustizi*; **d.** *M. vulcano*; **e.** *M. herminae*; **f.** *M.* aff. *yustizi*.

89. Dark lower labial stripe, structure 0 = diffuse, poorly defined; 1 = solid or almost solid, well-defined.

A dermal dark stripe formed by aggregation of melanophores on the lower lip, contouring the throat, is present in numerous species of *Aromobates* and *Mannophryne*, but in some cases it is diffuse and poorly defined and different from the conspicuous dark lower labial stripe coded by Grant *et al*. (2006) for *Leucostethus fraterdanieli*. We individuated an additional transformation series to code the variation observed in the definition of this stripe among the species of Aromobatinae.

90. Male, throat, color pattern (Grant *et al*. 2006): 0 = pale, free or almost free of melanophores; 1 = dark, due to the absence of iridophores; 2 = evenly stippled; 3 = pale with discrete dark spotting/reticulation/marbling; 4 = solid

dark; 5 = dark with discrete pale spotting/reticulation/marbling; 6 = irregular (clumped) stippling or faint, diffuse spotting. Nonadditive.

91. Female, throat, color pattern (Grant *et al*. 2006, 2017): 0 = pale, free or almost free of melanophores; 1 = irregular (clumped) stippling or faint, diffuse spotting; 2 = solid dark; 3 = dark with discrete pale spotting/reticulation/marbling; 4 = pale with discrete dark spotting/reticulation/marbling; 5 = dark with pale medial longitudinal stripe; 6 = evenly stippled. Nonadditive.

92–93: Bright yellow spot on female throat in life. (Figure 14)

A solid bright yellow spot is present on the throat of adult females of all known species of *Mannophryne* (figure 14). This spot is exhibited as an antagonistic signal, generally in territorial defense situations against intruder females (Test 1954, Sexton 1960), but also in male rejection during courtship events (Dole & Durant 1974, Durant & Dole 1975). The presence of a bright yellow spot on the throat of the females was proposed as a phenotypic synapomorphy for *Mannophryne* by La Marca (1992, 1994a, 1995), who additionally observed two different conditions for this character: spot restricted to the posterior portion of throat, and spot extensive on throat (La Marca 1995). Grant *et al*. (2006, 2017) did not include this character in their analyses. A similar discrete bright yellow spot is present in several species of the *Ranitomeya vanzolinii* species Group (Brown *et al*. 2011) and in *Exidobates captivus* (Twomey & Brown 2008) but in all these cases the spot is shared by both sexes. Accordingly, we did not consider the later spots homologous to the sexually dimorphic spot exhibited by

adult females of *Mannophryne*. Following La Marca (1995), we individuated two transformation series from this spot. This character can only be coded from living specimens.

92. Bright yellow spot: 0 = absent 1 = present.

93. Bright yellow spot, extension: 0 = restricted to the posterior half; 1 = extending on the entire surface of the throat.

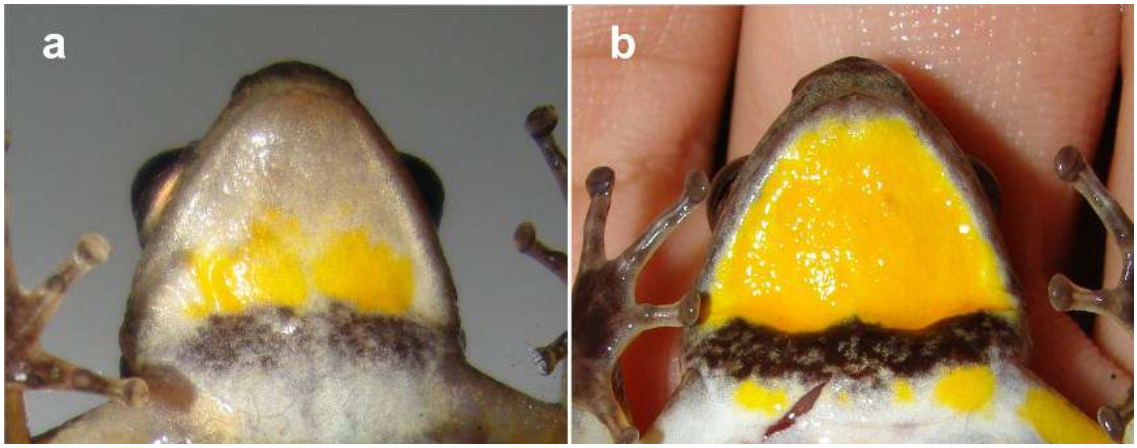

Figure 14. Bright yellow spot extension (character 93): restricted to the posterior half of the throat (state 0) in *Mannophryne lamarcai* (**a**), and extending on the entire surface of the throat (state 1) in *Mannophryne oblitterata* (**b**).

94. Male, abdomen color (Grant *et al*. 2006): 0 = pale free or almost free of melanophores; 1 = pale with discrete dark spotting/reticulation/marbling; 2 = evenly stippled; 3 = dark with discrete pale spotting/reticulation/marbling; 4 = irregular (clumped) stippling or faint, diffuse spotting; 5 = solid dark.

95. Female, abdomen color (Grant *et al*. 2006, 2017): 0 = pale, free or almost free of melanophores; 1 = pale with discrete dark spotting/reticulation/marbling; 2 = solid dark; 3 = dark with discrete pale spotting/reticulation/marbling; 4 =

irregular (clumped) stippling or faint, diffuse spotting; 5 = evenly stippled. Nonadditive.

96. Iris, coloration (similar to Grant *et al*. 2006): 0 = lacking metallic pigmentation; 1 = possessing metallic pigmentation. (Figure 15).

Grant *et al*. (2006) stated that the occurrence of a pupillary ring in dendrobatoids is invariably associated to irises with metallic pigmentation. However, we noted that at least in *Paruwrobates erythromos* its golden iris is not accompanied by a ring around pupil (Figure 15a). Vigle & Miyata (1980) described it as possessing a brown iris and did not mention the presence of a pupillary ring, but based on the inspection of high resolution color photographs of this species (Coloma *et al*. 2018), we observed an iris with metallic pigmentation and lacking a pupillary ring. Based on this observation we treat pupillary ring as independent from iris coloration.

97–102: Pupillary ring, peripheral lobes of pupillary ring, and ocular dark bands. (Figure 15)

The occurrence of a pupillary ring is widespread in anurans, but has been usually ignored in species' descriptions (Myers & Donnelly 2001), with exception on centrolenid systematics where this character has progressively gained relevance (Cisneros-Heredia & McDiarmid 2007, Castroviejo-Fisher *et al*. 2011). As far as we know, a metallic pigmented pupillary ring is common to all aromobatids; however, as in much other anuran groups, this structure has received very little attention. Recently, Fouquet *et al*. (2018) described in detail the pupil ring of four species of *Anomaloglossus*, highlighting the occurrence of

dorsal and ventral breaks on this structure “by transversal black pigmentation” (a vertical black band that divides the eye). Rojas-Runjaic *et al*. (2018) also described in detail the structure of the pupil ring in *Mannophryne molinai*, describing it as unbroken and possessing a lobe on its ventral portion, and compared it with the pupil ring structure of some congeneric species. Rojas-Runjaic *et al*. (2018) also documented the occurrence of a horizontal dark band on the eye of the aforementioned species. We also detected relevant variation in the structure of the pupillary ring through Aromobatidae, including vertical and horizontal breaks of the pupillary ring, presence of lobes (dilatations) on dorsal and ventral portions of the ring, and the occurrence of horizontal and vertical dark bands on the eye. We scored pupillary ring occurrence and variation in four independent transformation series, and two additional characters for the occurrence of horizontal and vertical dark bands on the eye (Figure 15). All these characters become undetectable in preserved specimens.

97. Pupillary ring: 0 = absent; 1 = present.

98. Pupillary ring, structure: 0 = partial (restricted to a small part of dorsal and ventral borders of pupil); 1 = complete; 2 = ventrally broken; 3 = laterally broken; 4 = laterally and ventrally broken; 5 = dorsally and ventrally broken; 6 = ventrally, dorsally, and laterally broken. Nonadditive.

99. Pupillary ring, peripheral lobes : 0 = absent; 1 = present.

100. Pupillary ring, peripheral lobes, position: 0 = dorsal and ventral; 1 = only ventral; 2 = only dorsal.

101. Ocular horizontal dark band: 0 = absent; 1 = present.

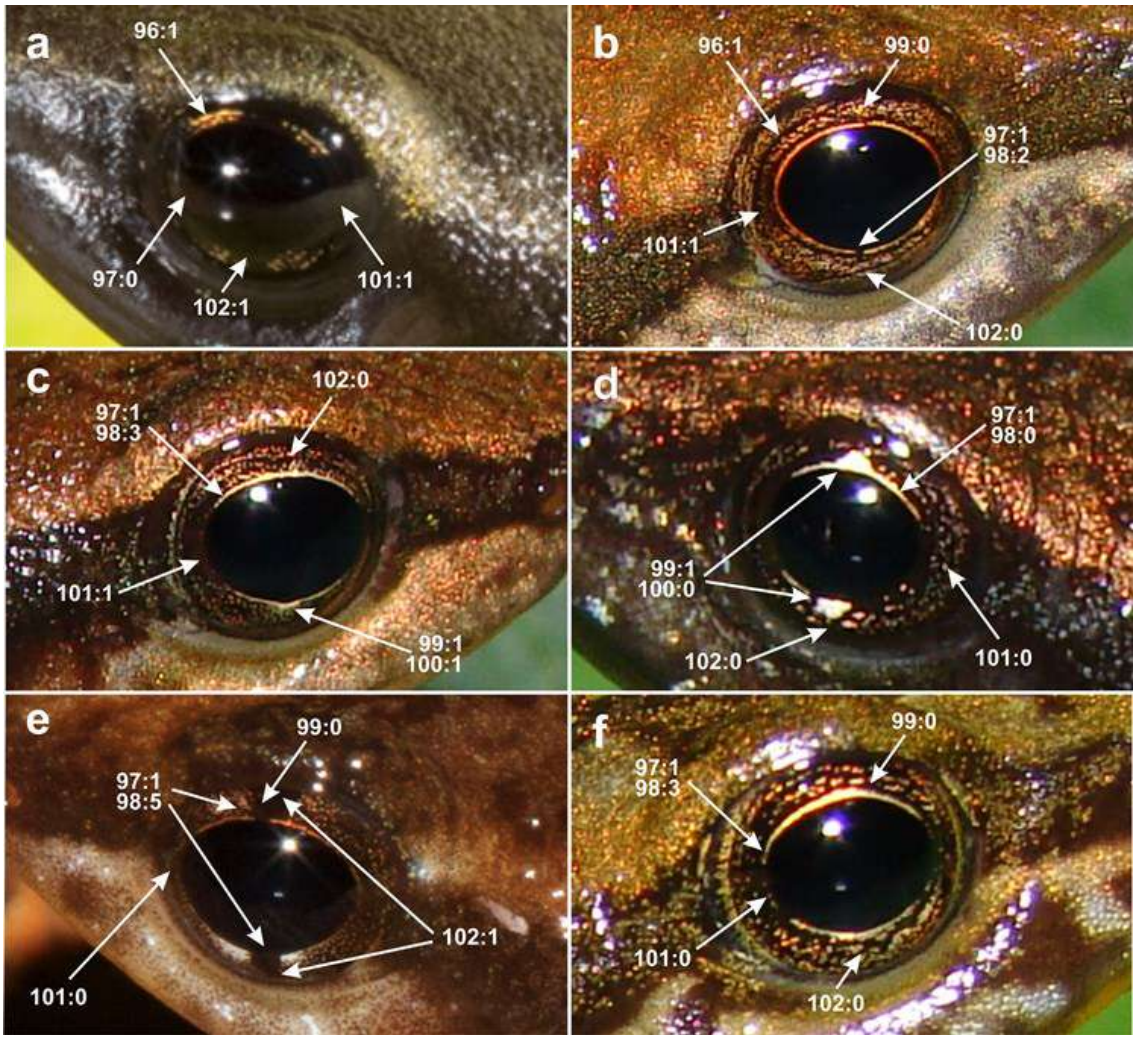

Figure 15. Pupillary ring (character 97) absent (state 0) in **a**; present (state 1) in **b–f**. Structure of the pupillary ring (character 98): partial (state 0) in **d**; ventrally broken (state 2) in **b**; laterally broken (state 3) in **c** and **f**; dorsally and ventrally broken (state 5) in **e**. Peripheral lobes (character 99): absent (state 0) in **b**, **e**–**f**; present (state 1) in **c** and **d**. Position of peripheral lobes (character 100): dorsal and ventral (state 0) in **d**; only ventral (state 1) in **c**. Ocular horizontal dark band (character 101): absent (state 0) in **d**–**f**; present (state 1) in **a**–**c**. Ocular vertical dark band (character 102): absent (state 0) in **b**–**d** and **f**; present (state 1) in **a** and **e**. **a**. *Paruwrobates erythromos* (Photo: Santiago Ron); **b**. *Mannophryne urticans*; **c**. *Aromobates mayorgai*; **d**. *Aromobates zippeli*; **e**. *Anomaloglossus verbeeksnyderorum* (Photo: Santiago Castroviejo-Fisher); **f**. *Aromobates meridensis*.

102. Ocular vertical dark band: 0 = absent; 1 = present.

103. Tongue, color: 0 = unpigmented; 1 = yellowish. (Figure 16).

Very little is known about the tongue color in life of anurans. Researchers rarely examine and include in their field notes the tongue color of live or freshly preserved specimens and the coloration fades shortly after preservation, making it impossible to obtain this information from museum specimens. Based on the observations of Duellman (2015) on tongue color variation in hemiphractids of the genus *Gatrotheca* and in our own observations on aromobatids, we suspected that this can be a useful source of information for delimiting species or to infer evolutionary relationships. Rojas-Runjaic *et al*. (2018) mentioned that both males and females of *Mannophryne molinai* have a mustard yellow colored tongue. Aside from this, no other description of *Mannophryne* report on tongue color. Besides *M. molinai*, we noted yellowish colored tongues in 18 of the 19 species of *Mannophryne* for which we examined live specimens. The only exception noted was for *M. oblitterata*, which has an unpigmented tongue. On the other hand, all the examined live specimens of *Aromobates* and *Allobates* (seven and two species, respectively) have unpigmented tongues. We did not find evidence of sexual dimorphism in this character (i.e., live specimens of the same species consistently show the character state regardless of sex).

A bright yellowish colored tongue is associated to mouth-gaping defensive displays in the hemiphractids *Hemiphractus elioti*, *H. kaylockae*, and *H. panamensis* (Myers 1966, Hill *et al*. 2018), and to the antipredator behavior of thanatosis with tongue protrusion in the hyperoliid *Acanthixalus spinosus*

(Perret 1961, Toledo *et al*. 2011). However, none of the social behaviors described for *Mannophryne* included mouth-gaping nor tongue protrusion (Test 1954, Sexton 1960, Dole & Durant 1974, Durant & Dole 1975).

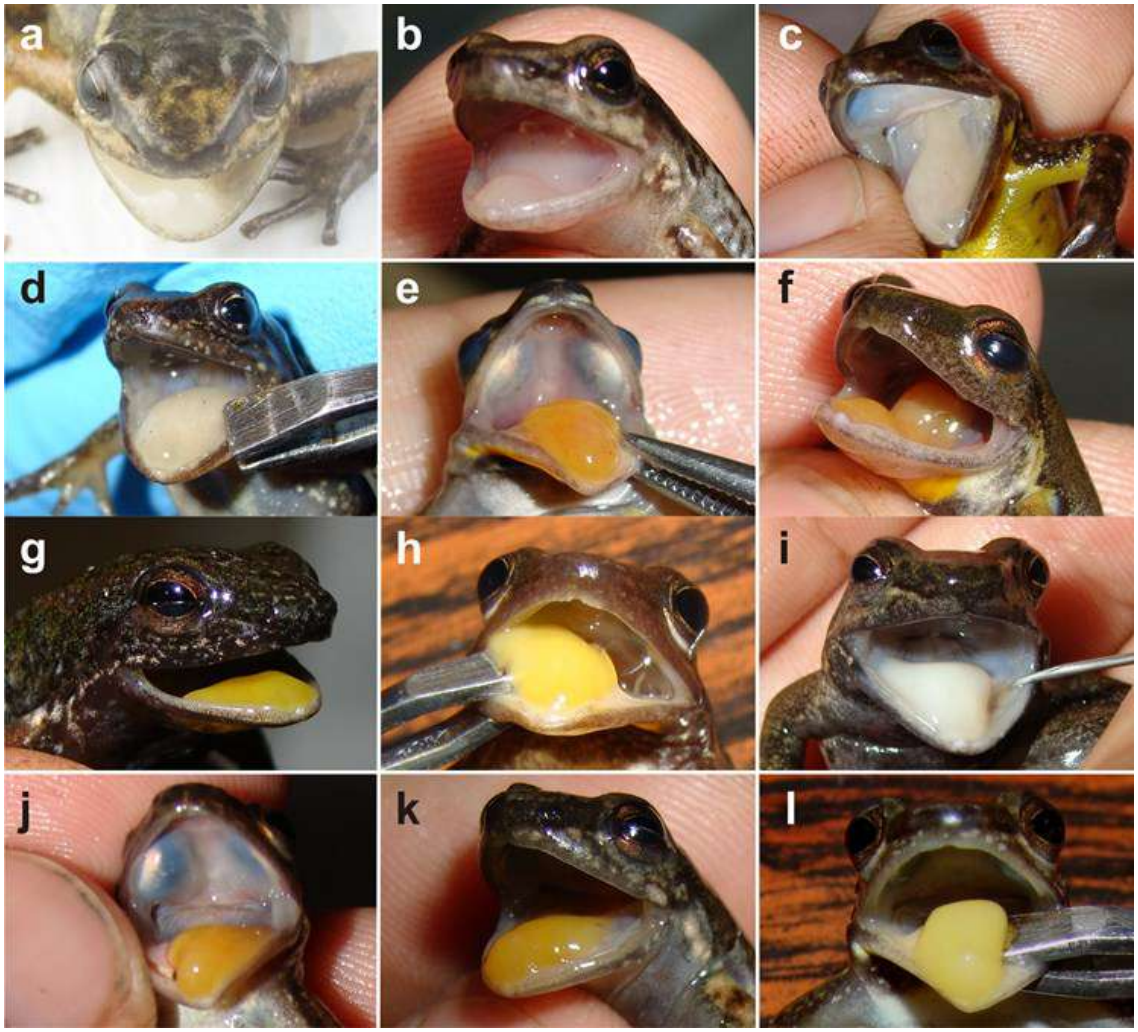

Figure 16. Tongue color (character 103): unpigmented (state 0) in **a**–**d**, and **l**; yellowish pigmented (state 1) in **e**–**h**, **j**–**l**. **a.** *Aromobates cannatellai* (Photo: Daniel Quihua); **b.** *A. mayorgai*; **c.** *A. meridensis*; **d.** *A. zippeli*; **e.** *Mannophryne herminae*; **f.** *M. lamarcai*; **g.** *M. molinai*; **h.** *M. neblina*; **i.** *M. oblitterata*; **j.** *M. trujillensis*; **k.** *M. urticans*; **l.** *Mannophryne* sp. 3.

104. Large intestine, color (Grant *et al*. 2006): 0 = unpigmented; 1 = pigmented anteriorly; = 2 pigmented extensively. Additive.

105. Adult testis (mesorchium), color (Grant *et al*. 2006): 0 = unpigmented; 1 = pigmented medially only; 2 = entirely pigmented. Additive.

106. Mature oocytes, color (Grant *et al*. 2006): 0 = unpigmented (uniformly white or creamy yellow); 1 = pigmented (animal pole brown or black).

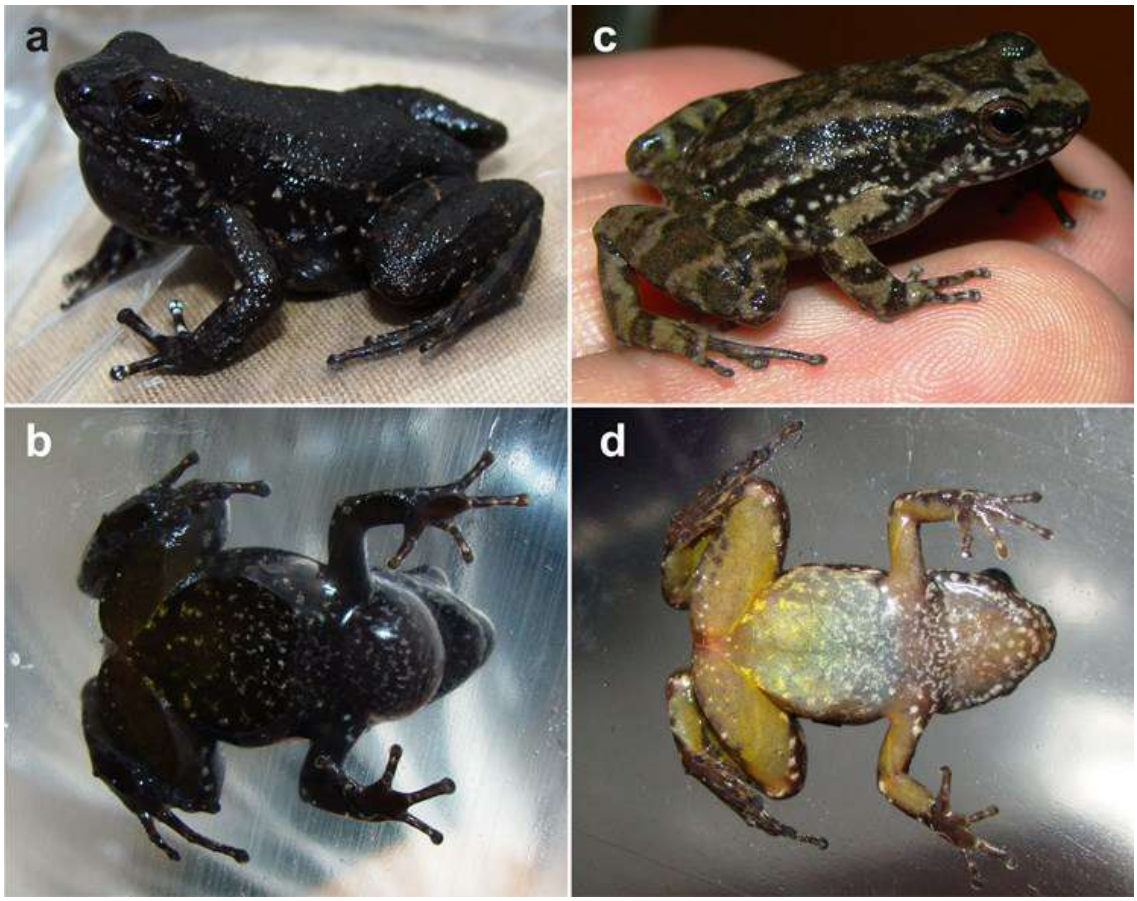

Figure 17. Skin blackening during call activity (character 107: 1) in a male specimen of *Mannophryne* cf. *yustizi* (**a, b**). The same specimen, a few minutes after stopping calling (**c, d**).

107. Skin blackening during calling activity: 0 = absent; 1 = present. (Figure 17).

While calling, adult males of *Mannophryne* quickly become black and when this reproductive behavior stops, they quickly return to their usual light brown color pattern. This behavior, that we link to visual communication, is uncommon among frogs, and constitutes a threat signal against potential reproductive

competitors (other calling males), but is not associated to territoriality (Wells 1980). Skin blackening during calling activity is widespread in *Mannophryne*, and has been documented for *M. collaris* (La Marca 1995), *M. cordilleriana* (La Marca 1994a), *M. herminae* (La Marca 1995) *M. lamarcai* (Mijares-Urrutia & Arends 1999b), *M. larandina* (Yústiz 1991), *M. molinai* (Rojas-Runjaic *et al*. 2018), *M. riveroi* (Barrio-Amorós *et al*. 2010c), *M. trinitatis* (Test 1962, Kenny 1969, Wells 1977, 1980, Manzanilla *et al*. 2007b), *M*. *venezuelensis* (Manzanilla *et al*. 2007b), and *M. vulcano* (Molina 2003). Based on field observations, we confirmed this behavior in almost all the aforementioned species, and also in all the other ten currently recorgnized species. Aside from *Mannophryne*, skin blackening in calling males has only been noted in the anomaloglossin *Rheobates palmatus* (Lüddecke 1976, 2000).

108. Defensive mercaptan-like odor: 0 = absent; 1 = present.

Myers *et al*. (1991) first documented the emission of a defensive, unpleasant, mercaptan-like odor in *Aromobates nocturnus* (feature highlighted in the genus name), although they could not identify the compound responsible by the noxious odor. The emission of this odor was considered by Myers *et al*. (1991) as unique among dendrobatoids and rare among anurans. However, La Marca (1997), and Barrio-Amorós & Santos (2012) affirmed that *A. leopardalis* might also release this mercaptan-like odor, and more recently Rojas-Runjaic *et al*. (2018) detected a mild mercaptan-like odor in all the live specimens of *M. molinai* handled by them. Additionally, we noted a mild mercaptan-like odor in other eight species of *Aromobates* and other thirteen species of *Mannophryne* (particularly strong in *M. urticans*). Thus, and contrary to Myers *et al*. (1991), a

mercaptan-like odor seems to be a widespread trait in Aromobatinae. Despite the lack of knowledge on the chemical nature of this odor, we presume the homology of this trait in aromobatins, based on the similarity of the smell—very different from the one noted in several species of Cophomantini (see Faivovich *et al.* 2013)—, the defensive context in which it is emitted, and the phylogenetic proximity among all species in which this was detected. We did not perceive defensive odors in live specimens of *Allobates pittieri* and *A. juami*.

109. *Musculus semitendinosus*, insertion (Grant *et al*. 2006): 0 = "bufonid type" (ventrad); 1 = "ranid type" (dorsad).

110. *Musculus semitendinosus*, binding tendon (Grant *et al*. 2006): 0 = absent; 1 = present.

111. *Musculus adductor mandibulae externus superficialis*, structure (Grant *et al*. 2006): 0 = undivided (s); 1 = divided (s+e).

112. *Musculus depressor mandibulae*, dorsal flap (Grant *et al*. 2006): 0 = absent; 1 = present.

113. *Musculus depressor mandibulae*, origin posterior to squamosal (Grant *et al*. 2006): 0 = absent; 1 = present.

114. *Musculus depressor mandibulae*, partial origin on *annulus tympanicus* (Grant *et al*. 2006): 0 = absent (no fibers originating from *annulus tympanicus*); 1 = present (some fibers originating from *annulus tympanicus*).

115. Tympanum and *musculus depressor mandibulae*, relation (Grant *et al*. 2006): 0 = tympanum superficial to *musculus depressor mandibulae*; 1 = tympanum covered superficially by *musculus depressor mandibulae*.

116. Vocal sac (Grant *et al*. 2006, 2017): 0 = absent; 1 = present.

117. Vocal sac, structure (Grant *et al*. 2006, 2017): 0 = median, subgular; 1 = paired lateral.

118. *Musculus intermandibularis*, supplementary element (Grant *et al*. 2006): 0 = absent; 1 = present.

119. *Musculus intermandibularis*, supplementary element, orientation (Grant *et al*. 2006): 0 = anterolateral; 1 = anteromedial.

120. Median lingual process (MLP) (Grant *et al*. 2006): 0 = absent; 1 = present.

121. MLP, shape (Grant *et al*. 2006): 0 = short, bumplike; 1 = elongate.

122. MLP, tip (Grant *et al*. 2006): 0 = blunt; 1 = tapering to point.

123. MLP, texture (Grant *et al*. 2006): 0 = smooth; 1 = rugose.

124. MLP, orientation when protruded (Grant *et al*. 2006): 0 = upright; 1 = posteriorly reclined.

125. MLP, retractility (Grant *et al*. 2006): 0 = nonretractile; 1 = retractile.

126. MLP, associated pit (Grant *et al*. 2006): 0 = absent; 1 = present.

127. MLP, epithelium (Grant *et al*. 2006): 0 = glandular; 1 = nonglandular.

128. Larva, caudal coloration (Grant *et al*. 2006): 0 = vertically striped; 1 = scattered melanophores clumped to form diffuse blotches and reticulations; 2 = evenly pigmented. Additive.

129. Larva, oral disc (Grant *et al*. 2006, 2017): 0 = absent; 1 = present.

130. Larva, oral disc, morphology (Grant *et al*. 2006, 2017): 0 = normal; 1 = umbelliform; 2 = suctorial. Nonadditive.

131. Larva, oral disc, lateral indentation (Grant *et al*. 2006): 0 = absent (not emarginate); 1 = present (emarginate).

132. Larva, marginal labial papillae, size (Grant *et al*. 2006): 0 = short; 1 = enlarged; 2 = greatly enlarged. Additive.

133. Larva, oral disc, submarginal papillae (Grant *et al*. 2006): 0 = absent; 1 = present.

134. Larva, lower labium, marginal papillae, median gap (Grant *et al*. 2006): 0 = absent; 1 = present.

135. Larva, anterior keratodont rows, number (Grant *et al*. 2006): 0 = absent; 1 = one; 2 = two. Additive.

136. Larva, posterior keratodont rows, number (Grant *et al*. 2006): 0 = absent; 1 = one; 2 = two; 3 = three. Additive.

137. Larval jaw sheaths (Grant *et al*. 2006): 0 = absent; 1 = lower only, not keratinized; 2 = entire, keratinized. Additive.

138. Larva, upper jaw sheat, shape (Sánchez 2013, Grant *et al*. 2017): 0 = W-shape; 1 = U-shape.

139. Larva, interorbital distance (IoD) and internarial distance (InD), ratio (Mijares-Urrutia 1998): 0 = IoD > InD; 1 = IoD < InD. (Figure 18).

Mijares & La Marca (1997) and Mijares-Urrutia (1998) described this relation as diagnostic between tadpoles of *Aromobates* and *Mannophryne*. They stated

that in tadpoles of *Aromobates* IoD is wider than InD (IoD > InD, our state 0), whereas in *Mannophryne* this relation is inverse (IoD < InD, our state 1). Measurements were taken between inner margins as indicate by Mijares-Urrutia (1998). We observed that tadpoles of *A. serranus* and *A. molinarii* have IoD < InD (state 1). In *Anomaloglossus* and *Allobates* this character was scored only for a few species, but both show a more complex pattern of character-state distribution.

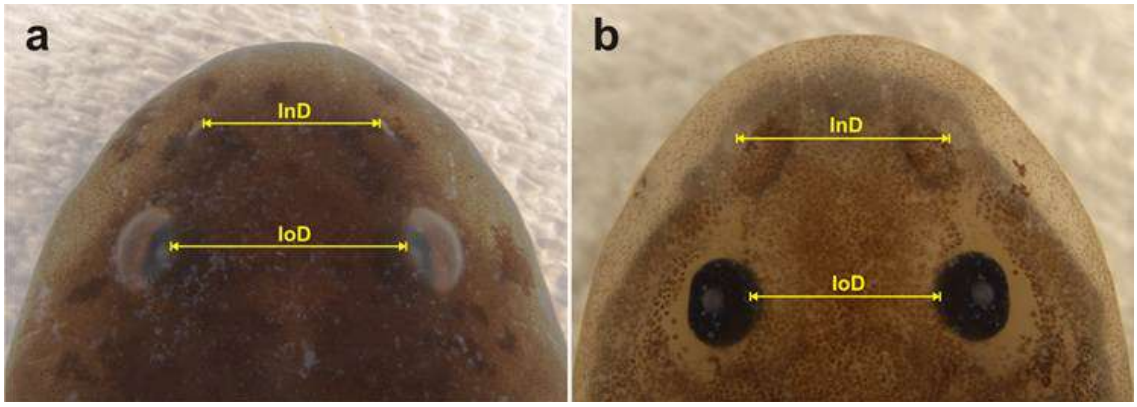

Figure 18. Larval interorrbital distance (IoD) / internarial distance (InD) ratio (character 139): IoD > InD (state 0) in *Aromobates* sp. 2 MHNLS 22093; IoD < InD (state 1) in *Mannophryne urticans* MHNLS 21585.

140. Larva, vent tube, position (Grant *et al*. 2006): 0 = dextral; 1 = median.

141. Spiracle (Grant *et al*. 2006): 0 = absent; 1 = present.

142. Lateral line, stitches (Grant *et al*. 2006): 0 = absent; 1 = present.

143. Larva, gut, morphology (Sánchez 2013, Grant *et al*. 2017): 0 = Long gut concealing other organs (S); 1 = short gut revealing other organs (D).

144. Larva, narial rim, sagital projection (Sánchez 2013, Grant *et al*. 2017): 0 = absent (NP); 1 = present (P).

145. Advertisement calls, structure (Grant *et al*. 2006): 0 = buzz; 1 = chirp; 2 = trill; 3 = retarded trill; 4 = retarded chirp. Nonadditive.

146. Advertisement calls, note arrangement: 0 = single; 1 = duplets; 2 = triplets; 3 = mix of single and duplets; 4 = mix of single and triplets; 5 = mix of singles, duplets and triplets. Nonadditive.

Advertisement calls play a critical role in mate recognition and mate choice (Wells 2007) and generally are species-specific. Consequently, these acoustic signals have been recognized as an important source of evidence in systematic studies of dendrobatoids (e.g., Myer & Daly 1976; Lötter *et al*. 2003; Vacher *et al*. 2017). Grant *et al*. (2006) scored advertisement calls following Lötters *et al*. (2003), which, as they recognized, are composites of temporal and spectral transformation series that should be decomposed in future studies. As in Grant *et al*. (2017), we include in our phenotypic matrix the same transformation series defined by Grant *et al*. (2006) (character 145 in this study), but additionally we individuate a new transformation series based in note arrangement. Except for a few exceptions, note arrangement is an invariable trait within species and consequently useful in species delimitations (e.g., Manzanilla *et al*. 2007b; Rojas-Runjaic *et al*. 2018).

147. Male, courtship, stereotyped strut (Grant *et al*. 2006): 0 = absent; 1 = present.

148. Male, courtship, jumping up and down (Grant *et al*. 2006): 0 = absent; 1 = present.

149. Female, courtship, crouching (Grant *et al*. 2006): 0 = absent; 1 = present.

150. Female, courtship, sliding under male (Grant *et al*. 2006): 0 = absent; 1 = present.

151. Sperm deposition, timing (Grant *et al*. 2006): 0 = after oviposition; 1 = prior to oviposition.

152. Reproductive amplexus (Grant *et al*. 2006, 2017): 0 = absent; 1 = present.

153. Reproductive amplexus, position (Grant *et al*. 2006, 2017): 0 = axillary; 1 = cephalic.

154. Cloaca-cloaca touching (Grant *et al*. 2006): 0 = absent; 1 = present.

155. Egg deposition, site (Grant *et al*. 2006): 0 = aquatic; 1 = terrestrial: leaf litter, soil, on or under stones; 2 = terrestrial: above ground in vegetation (bromeliads, etc). Nonadditive.

156. Egg clutch, attendance (Grant *et al*. 2006, 2017): 0 = absent; 1 = present.

157. Egg clutch, attendance, sex (Grant *et al*. 2006, 2017): 0 = male; 1 = female; 2 = both. Nonadditive.

158. Dorsal tadpole transport (Grant *et al*. 2006): 0 = absent; 1= present.

159. Nurse frog, sex (Grant *et al*. 2006): 0 = male; 1 = female; 2 = both. Nonadditive.

160. Larva, habitat (Grant *et al*. 2006): 0 = pool or stream; 1= phytotelmata; 2 = nidicolous. Nonadditive.

161. Larva, trophic guild (Grant *et al*. 2006, 2017): 0 = exotrophic; 1 = endotrophic.

162. Larva, exotrophic diet (Grant *et al*. 2006, 2017): 0 = detritivorous; 1 = predaceous; 2 = oophagous. Nonadditive.

163. Egg provisioning for larval oophagy, sex (Grant *et al*. 2006): 0 = both sexes involved; 1 = female only.

164. Adult, habitat selection (Grant *et al*. 2006): 0 = aquatic; 1 = riparian (<3 m from water); 2= independent of water (up to ca. 30 m from water 3 = associated to forest ponds (<3 m from water). Nonadditive.

Grant *et al*. (2006) scored the degree of association with water in adult frogs in three groups: aquatic (sate 0), riparian (state 1), and independent of water (state 2). Most dendrobatoids are associated to streams (state 1), whereas only some species are independent of water (state 2), and apparently the only known case of a "fully aquatic" species in this superfamily is represented by *Aromobates nocturnus* (Myers *et al*. 1991).

As defined by Grant *et al*. (2006), the state 1 (riparian) only includes species "…confined to the areas immediately adjacent to streams…" (lotic waters), and does not mention any case of species inhabiting lentic waters. Based on the recently documented and uncommon case of *Aromobates* sp. 1 from El Tigre, Venezuela (Rojas-Runjaic *et al*. in prep) that inhabits borders of forest ponds, we add and additional state (associated to forest ponds) to this transformation series.

In the case of *Aromobates nocturnus*, we follow Myers *et al*. (1991) and Grant *et al*. (2006, 2017) and code it as aquatic, but drawing attention on the fact that *A. nocturnus* is not an truly aquatic species as for example, any pipid frog, but a riparian species, apparently more aquatic than most known dendrobatoids. Myers *et al*. (1991) based their classification of *A. nocturnus* as aquatic on the following observations: 1) none specimen was detected away the stream, 2) most (but not all) specimens were found siting in shallow water or swimming, and 3) they dive and hide under water, but soon return to their original location. Based on our observations, most *Aromobates* species have

their habitat confined to streams; specimens sitting in shallow water were frequently detected by us in a population of *A. mayorgai*, in *A. meridensis* and *Mannophryne oblitterata*, and similar observations to those of Myers *et al*. (1991) were also documented for *A. leopardalis* (La Marca 1997, Rivero 1978), and *M. riveroi* (Barrio-Amorós *et al*. 2010c); and finally, dive and hide under water is an escape behavior widespread in Aromobatinae. Evidently, the degree of aquaticity in riparian dendrobatoids varies and this topic should be object of future studies, but the condition of aquatic awarded to *A. nocturnus* should not be equated to that of truly aquatic frogs. Finally, *Aromobates ornatissimus* was coded by Grant *et al*. (2017) as independent of water. But as stated by Barrio-Amorós *et al*. (2011), the species is associated to mountain creeks and only eventually isolated males were eared calling inside forest, away from the water. Thus, we recoded this species as riparian.

165. Diel activity (Grant *et al*. 2006): 0 = nocturnal; 1 = diurnal.

In the broadest sense, a frog is considered active when is performing any task, such as foraging, dispersing, calling, mating, fighting, or any other than resting (usually hidden) with his eyes closed (Jaeger & Hailman 1981, Graves 1999, Rocha *et al*. 2015). Their diel activity is defined as the period in which they are executing any of these tasks. But, as it is defined, it likely involves a composite of transformation series. Diurnal activity is widespread in dendrobatoids, and *Aromobates nocturnus* apparently is the exception (Myers *et al*. 1991). It was considered as a nocturnal species because all specimens observed were active at night, sitting on exposed sites, walking, foraging, and diving to escape (but never calling), whereas diurnal activity was apparently absent. However, some

nocturnal activity (at least facultative) has been noted in *A. ornatissimus* in nights of full moon (referred as *Colostethus*; Myers *et al*. 1991), in *Hyloxalus bocagei*, *H. nexipus*, and *H. awa* in captivity (Coloma 1995), in *Mannophryne olmonae* (Myers *et al*. 1991, La Marca 1994a), and *M. riveroi* (Donoso-Barros 1964, Barrio-Amorós *et al*. 2010c). Additionally, we observed some nocturnal activity (i.e., sitting in exposed places, foraging, and moving) in *M. herminae*, *M. oblitterata*, and *M. vulcano*. We code *Aromobates* sp. 1 (Rojas-Runjaic *et al*. in prep) as polymorphic because its diel activity (i.e., call activity and exposition in open sites) takes place for a few hours before and after sunrise and sunset, including periods of darkness and daylight. Despite some nocturnal activity in the aforementioned species, they are primarily diurnal, and we code them as that. In the case of *A. nocturnus*, the fact that 1) calling activity was not detected during the night, 2) two of the three nights of field work when the species was discovered were of full moon, and 3) several specimens were observed by the discoverers during the day coming out of the grass into the water at the rivulet edge, makes it likely that this species exhibits both diurnal and nocturnal activity (as noted above for other species of the subfamily). Unfortunately, *A. nocturnus* has not been observed since November 1987, when the type series was collected, and we cannot evaluate its activity pattern.

166. Toe trembling (Grant *et al*. 2006): 0 = absent; 1 = present.

167. Hyale, anterior process (Grant *et al*. 2006): 0 = absent; 1 = present.

168–169: Hyoid plate, posteromedial processes.

This is one of the three pairs of processes that typically bears the hyoid plate of the hyobranchial apparatus in anurans. Posteromedial processes invariably are present; these support the laryngeal apparatus, are long, symmetrical and ossified (Trueb 1993). Although their shape varies slightly, we detected variation among dendrobatoids in the inner contour of the anterior portion of these processes. They can be straight to nearly straight (weakly concave) or noticeably concave (when the inner corner of the anterior tip is noticeably more developed than the outer corner). Additionally, a very small apophysis is present on the medial side of these processes in "*Colostethus*" *caribe*, whereas in *Aromobates leopardalis* the apophysis is strong, but is a polymorphic character inasmuch as it is absent in some specimens.

168. Hyoid plate, posteromedial process, anteromedial contour, form: 0 = straight to nearly straight; 1 = noticeably concave. (Figure 19).

169. Hyoid plate, posteromedial process, medial apophysis: 0 = absent; 1 = present. (Figure 19).

170. Epicoracoid, fusion (Grant *et al*. 2006): 0 = entirely fused (Kaplan E); 1= anteriorly fused, posteriorly free (Kaplan C); 2 = fused at anterior extreme, free posteriorly (Kaplan A). Additive.

171. Epicoracoid, overlap (Grant *et al*. 2006): 0 = no overlap (Kaplan B); 1 = partial overlap (Kaplan E); 2 = partial overlap (Kaplan C); 3 = partial overlap (Kaplan A). Nonadditive.

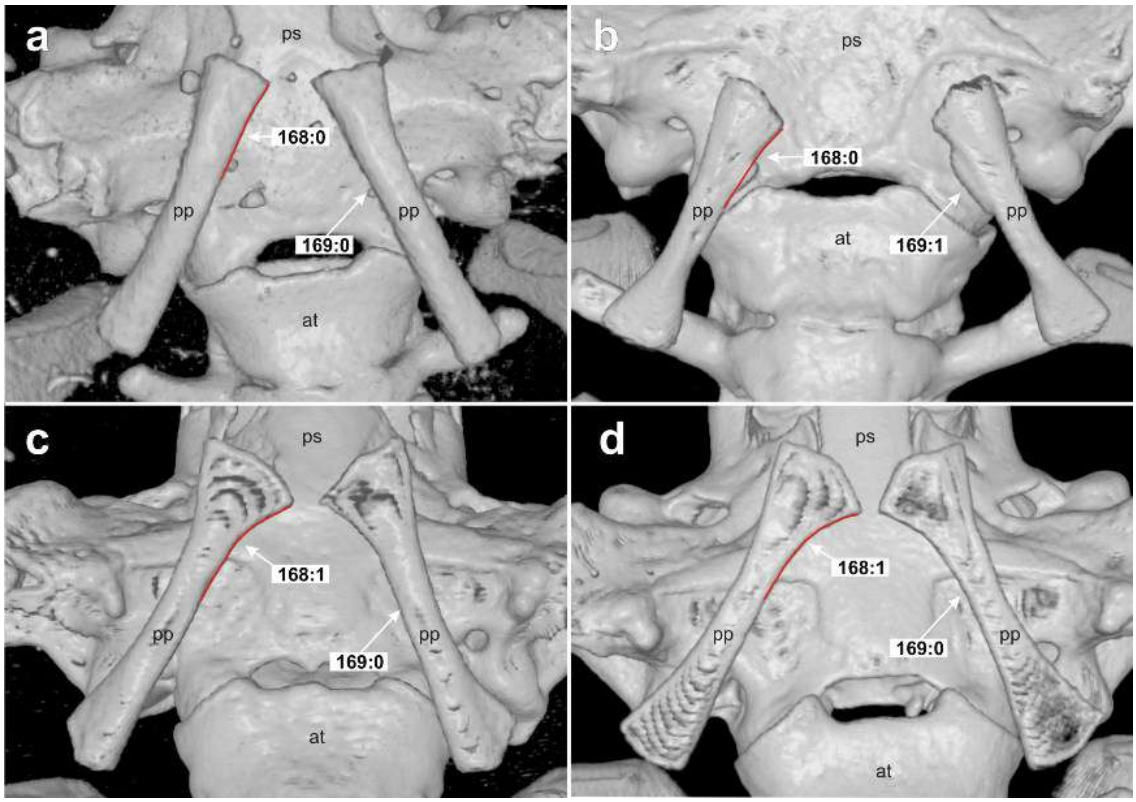

Figure 19. Ventral view of the posterior portion of the skull of *Aromobates haydeeae* CVULA 6047 (**a**), *Aromobates leopardalis* CVULA 5886 (**b**), *Mannophryne caquetio* MHNLS 21220 (**c**), and *Mannophryne* sp. 4 MHNLS 22306 (**d**). Anteromedial contour of the posteromedial process (character 168): straight to nearly straight (state 0) in **a**, and **b**; noticeably concave (state 1) in **c**, and **d** (red lines highlighting the anteromedial contour). Medial apophysis of the posteromedial process (character 169): absent (state 0) in **a**, **c**, and **d**; present (state 1) in **b** (indicated by black arrows). at: atlas; pp: posteromedial process of the hyoid plate; **ps**: parasphenoid.

172–183: Scapula, clavicle and coracoid.

Scapula, clavicle and coracoid are paired bones that constitute the lateral and lateroventral portions of the pectoral girdle. The clavicle is a dermal bone, whereas the scapula and coracoid are endochondral elements (Duellman & Trueb 1994). The scapula is laterally in contact with the suprascapula and medially meets the lateral ends of the clavicle and coracoid to form the glenoid cavity, where the humerus is inserted. Anterior to the glenoid cavity is the acromion process, an anteroventral projection of the scapula, that can be cartilaginous or completely ossified (Grant *et al*. 2006); its anterior extension

and angle with respect to the sagittal plane varies among dendrobatoids. Dorsally to the glenoid cavity is the *pars glenoidalis*, the laminar dorsomedial end of the scapula that forms the roof of the glenoid fossa. On the anterodorsal border of the *pars glenoidalis* can be present a ridge that varies in its development and orientation (anterior or dorsal). The clavicle is styliform and perpendicular to the sagittal plane, its medial end articulates with the epicoracoid cartilage and omosternum, and can be wider or thinner than their mid portion. Bordering the entire posterior edge of the clavicle is the procoracoid cartilage; a longitudinal roof along the posterodorsal surface of the clavicle, where the procoracoid fits. is often present (Myers *et al*. 1991) and, in some cases, a small postclavicular apophysis is also present on the posterolateral corner of the clavicle, delimiting the posterodistal margin of the procoracoid. The coracoid is posterior and parallel to the clavicle, also perpendicular to the sagittal plane, medially expanded, and articulating at its medial end with the epicoracoid cartilage and sternum. Its anteromedial corner may be in touch with the medial end of the clavicle, and the development of this anteromedial corner is very variable, being strongly projected in some species. Variation in the orientation of the clavicle with respect to the sagittal plane, and in the degree of ossification of the acromion process, were coded by Grant *et al*. (2006). In addition to these characters (172 and 178 of this study), we scored 1) variation in the clavicle medial width, 2) clavicle posterodorsal surface development, 3) presence of postclavicular apophysis, 4) relation between the clavicle medial end and the coracoid anteromedial angle, 5) coracoid posteromedial angle development, 6) acromion process orientation and anterior

extension, 7 and 8) anterior ridge of *pars glenoidalis* occurrence and orientation, and 9) thickness of this *pars* as related to the glenoid fossa vertical diameter.

172. Clavicle, angle (Grant *et al*. 2006): 0 = directed laterally, perpendicular to sagittal plane; 1 = directed posteriad; 2 = directed anteriad. Nonadditive.

173. Clavicle, distal width: 0 = distal third narrower than middle third; 1 = distal third as wide as the middle third; 2 = distal third wider than middle third. Additive. (Figure 20).

Clavicle distal width is defined in relation to its middle width, when observed from ventral view.

174. Clavicle, posterodorsal surface, ornamentation: 0 = ungrooved; 1 = weakly grooved; 2 = deeply grooved. Additive. (Figure 21).

175. Postclavicular apophysis: 0 = absent; 1 = present. (Figures 21d–e).

176. Clavicle distal end and anteromedial portion of coracoid, relation: 0 = not in contact; 1 = in contact. (Figure 20).

177. Coracoid, anteromedial angle, form: 0 = without a notorius projection; 1 = weakly projected anterioly; 2 = abruptly projected anteriorly. Additive. (Figure 20).

178. Acromion process, ossification (Grant *et al*. 2006): 0 = cartilaginous, distinct; 1 = fully calcified/ossified, continuous with clavicle and scapula.

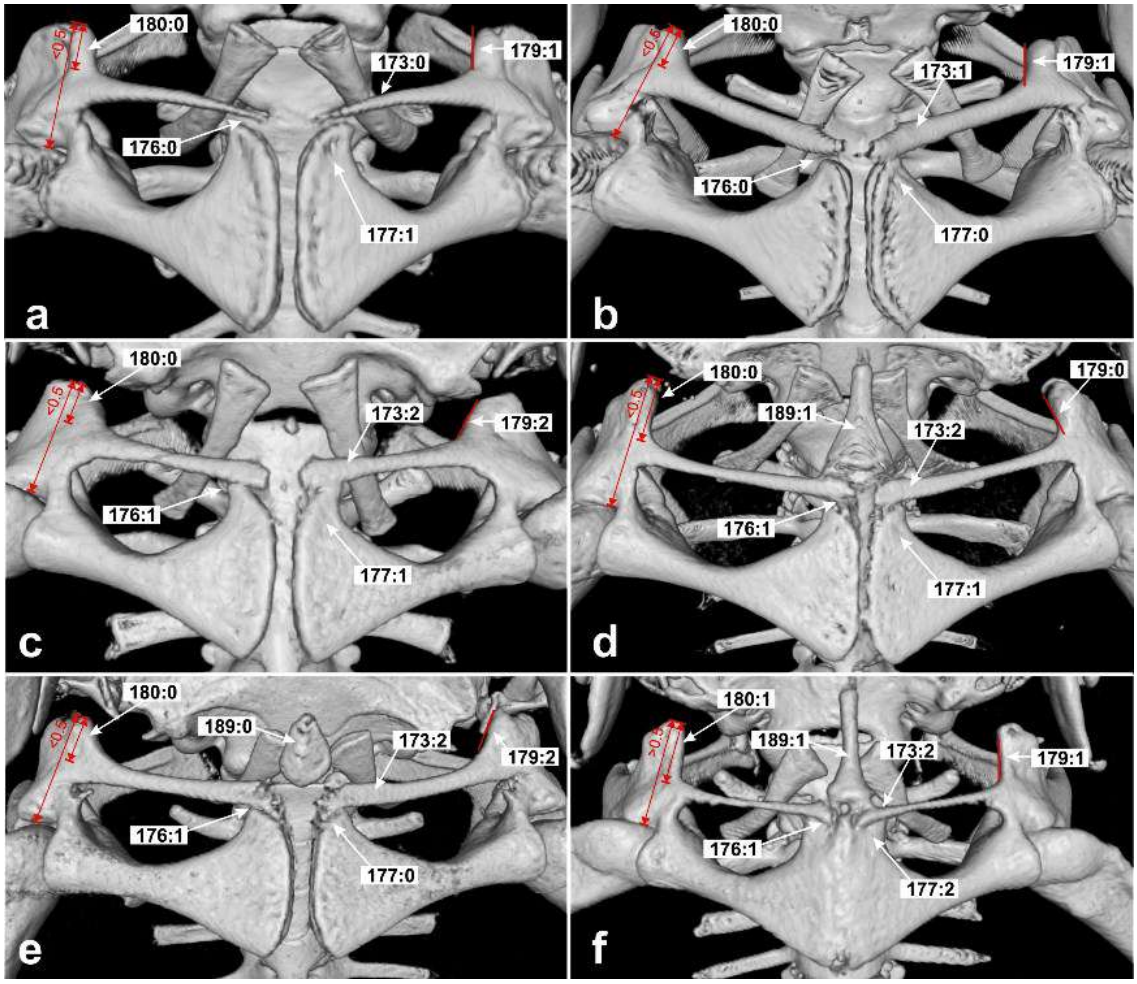

Figure 20. Ventral view of the pectoral girdle of *Aromobates ornatissimus* ULABG 4976 (**a**), *Aromobates nocturnus* ULABG2223 (**b**), *"Colostethus" caribe* MHNLS 17463 (**c**), *Mannophryne* sp. 4 MHNLS 22306 (**d**), *Aromobates molinarii* CVULA 1877 (**e**), and *Allobates pittieri* MHNLS 21488 (**f**). Clavicle, distal width (character 173): narrower than middle third (state 0) in **a**; as wide as the middle third (state 1) in **b**; wider than middle third (state 2) in **c**–**f**. Clavicle distal end and coracoid anteromedial portion, relation (character 176): not in contact (state 0) in **a**–**b**; in contact (state 1) in **c**–**f**. Coracoid, anteromedial angle (character 177): without a notable projection (state 0) in **b** and **e**; weakly projected anteriorly (state 1) in **a**, **c**, and **d**; abruptly projected anteriorly (state 2) in **f**. Acromion process, orientation (character 179; red line on the left acromion highlighting the inclination angle): markedly inward (30–70º) (state 0) in **d**; slightly inward to anterior (71–90º) (state 1) in **a**, **b**, and **f**; slightly outward (>90º) (state 2) in **c** and **e**. Acromion process, extension (d1) in relation to the distance between the glenoid cavity and the acromion tip (d2) (character 180; short and long two-tips red arrows on the right acromion representing d1 and d2, respectively): short, d1/d2 ≤ 0.5 (state 0) in **a**–**e**; long, d1/d2 > 0.5 (state 1) in **f**. Omosternum ossified portion, form (character 189): short, truncate, without an elongate tip (state 0) in **e**; pointed, with an elongate cilindrical tip (state 1) in **d** and **f**.

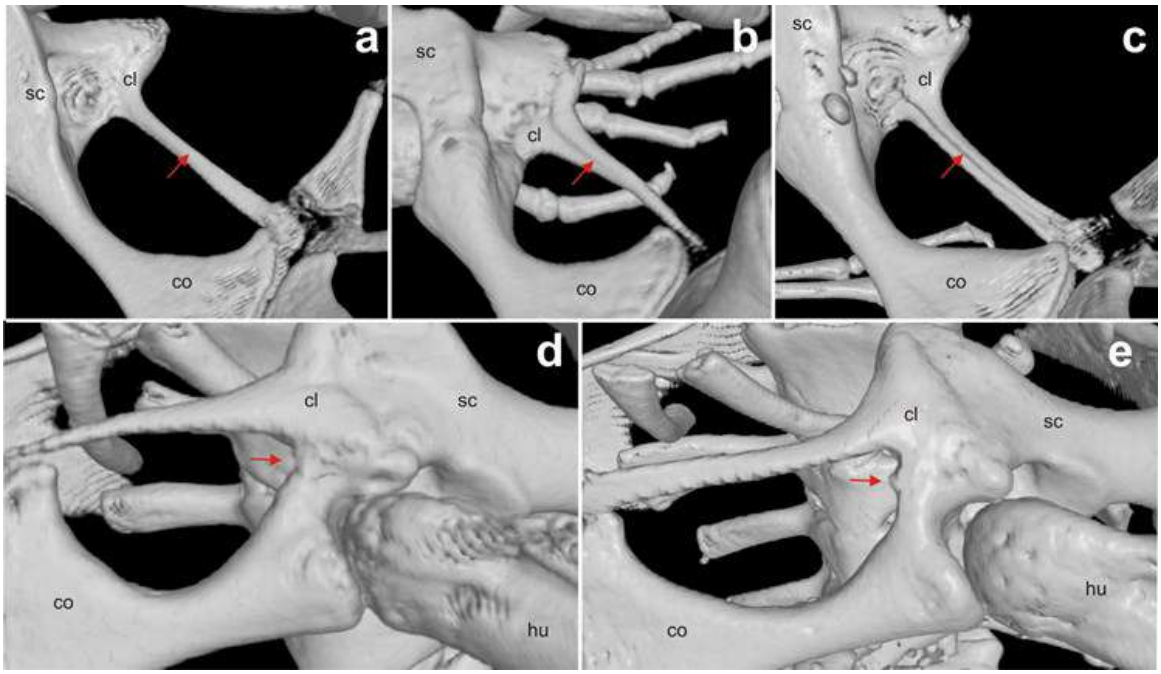

Figure 21. a–c: Dorsal view of the left side of the pectoral girdle of *Mannophryne* sp. 4 MHNLS 22306 (**a**), *Aromobates ornatissimus* ULABG 4976 (**b**), and *Mannophryne neblina* MHNLS 4956 (**c**). Clavicle, posterodorsal surface, ornamentation (character 174): ungrooved (state 0) in **a**; weakly grooved (state 1) in **b**; deeply grooved (state 2) in **c**. **d**–**e**: Lateroventral view of the left side of the pectoral girdle of *Aromobates ornatissimus* ULABG 4976 (**d**) and *Aromobates zippeli* MHNLS 22502 (**e**). Postclavicular apophysis (character 175): absent (state 0) in **a**; present (state 1) in **b**. **cl:** clavicle; **co:** coracoid; **hu:** humerus; **sc:** scapula.

179. Acromion process, orientation: 0 = markedly inward (30–70º); 1 = slightly inward to anterior (71–90º); 2 = slightly outward (>90º). Nonadditive. (Figure 20).

180. Acromion process, extension in relation to the distance between the glenoid cavity and acromion tip: 0 = short (≤ 0.5 x); 1 = long (> 0.5 x). (Figure 20).

This relation is defined by dividing the distance between the acromion process tip and the anterior border of the clavicle (d1), by that between the tip of acromion and the glenoid cavity margin (d2), both measured in ventral view.

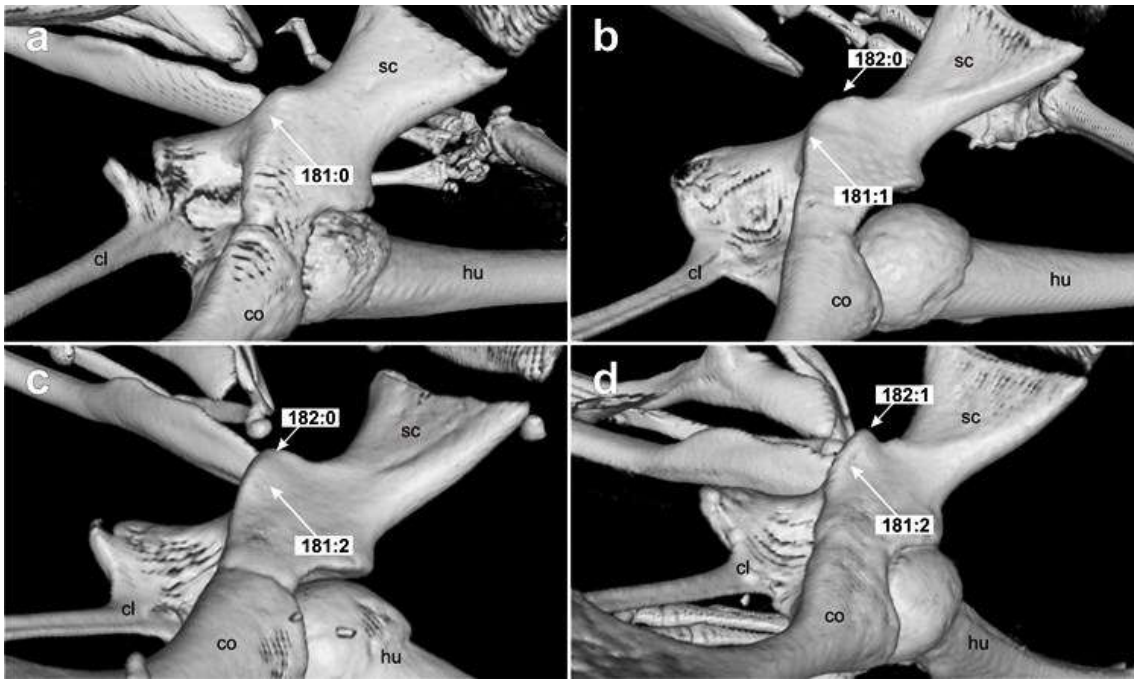

Figure 22. Dorsal view of the right side of the pectoral girdle of *Mannophryne riveroi* MHNLS 17910 (**a**), *Aromobates meridensis* MHNLS 22019 (**b**), *Mannophryne neblina* MHNLS 4956 (**c**), and *Mannophryne molinai* MHNLS 21337 (**d**). *Pars glenoidalis*. anterior ridge, development (character 181): absent (state 0) in **a**; weak (state 1) in **b**; strong (state 2) in **c** and **d**. *Pars glenoidalis*, anterior ridge, orientation (character 182): anterior (state 0) in **b** and **c**; dorsal (state 1) in **d**. **cl:** clavicle; **co:** coracoid; **hu:** humerus; **sc:** scapula.

181. *Pars glenoidalis*, anterior ridge, development: 0 = absent; 1 = weak; 2 = strong. Additive. (Figure 22).

In the cases where the ridge is absent (state 0), the *pars glenoidalis* anterior border is rounded and not projected (figure 22a); in the state 1, the ridge is represented by an angular border weakly projected anteriorly (figure 22b); in the state 2 the anterior ridge appears strongly projected anteriorly (figures 22c–d).

182. *Pars glenoidalis*, anterior ridge, orientation: 0 = anterior; 1 = dorsal. (Figure 22).

183. *Pars glenoidalis* and glenoid fossa, relation in anterior view: 0 = *pars glenoidalis* narrower than glenoid cavity; 1 = *pars glenoidalis* as wide as glenoid cavity; 2 = *pars glenoidalis* wider than glenoid cavity. Nonadditive. (Figure 23).

184. Omosternun (Grant *et al*. 2006): 0 = absent; 1= present.

185. Omosternum, anterior expansion (Grant *et al*. 2006): 0 = not expanded distally, tapering to tip; 1 = weakly expanded, to 2.5 x style at base of cartilage or equivalent; 2 = extensively expanded distally, 3.5 x or greater. Additive.

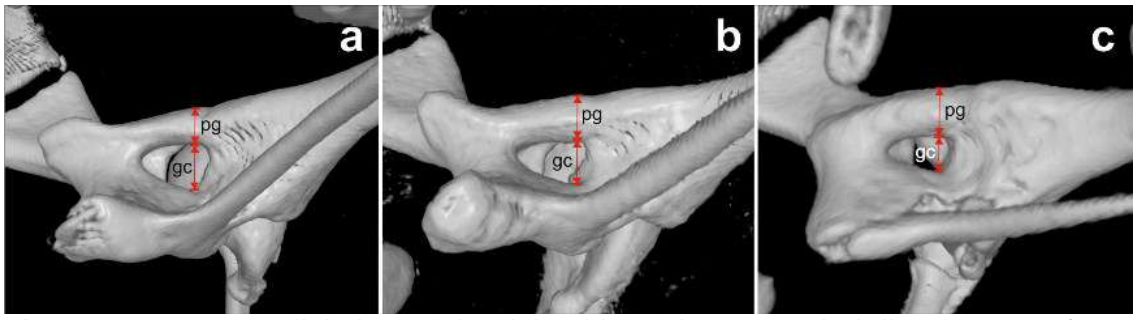

Figure 23. Anteromedial view of the right side of the pectoral girdle of *Mannophryne neblina* MHNLS 4956 (**a**), *Mannophryne molinai* MHNLS 21337 (**b**), and *Aromobates ornatissimus* ULABG 4967 (**c**). *Pars glenoidalis* and glenoid fossa, relation in anterior view (character 183): *pars glenoidalis* narrower than glenoid cavity (state 0) in **a**; *pars glenoidalis* as wide as glenoid cavity (state 1) in **b**; *pars glenoidalis* wider than glenoid cavity (state 2) in **c**. **gc:** glenoid cavity; **pg:** *pars glenoidalis*.

186.Omosternum, anterior terminus, shape (Grant *et al*. 2006): 0 = rounded or irregularly shaped; 1 = distinctly bifid.

187. Omosternum, posterior terminus, shape (Grant *et al*. 2006): 0 = simple; 1 = notched, forming two struts continuous with epicoracoid cartilage.

188. Omosternum, ossification (Grant *et al*. 2006): 0 = entirely cartilaginous; 1 = medially ossified (cartilaginous base and tip); 2 = basally ossified (cartilaginous tip); 3 = entirely ossified. Additive.

189. Omosternum, ossified portion, form: 0 = short, truncate, without an elongate tip; 1 = pointed, with an elongate cilindrical tip; 2 = with an elongate and expanded tip. Additive. (Figure 20).

Myers *et al*. (1991) noted that the cartilaginous omosternum of *Aromobates nocturnus* usually has a small and more or less pentagonal center of calcification, whereas in *Mannophryne* the ossification extends anteriorly to this robust calcified center, forming a well-defined long bony style. We confirm this last condition in almost all species of *Mannophryne*, but also observe that the variation in *Aromobates* is more complex. Additionally, we observe that the tip of the bony style can be cylindrical (most frequently) or distally expanded as in *Mannophryne* sp. n. from Cúpira.

190. Suprascapula, anterior projection, ossification (Grant *et al*. 2006): 0 = cartilaginous; 1 = heavily calcified.

191. Sternum, shape (Grant *et al*. 2006): 0 = simple, ovoid, or irregular; 1 = medially divided, bifid.

192–194. Squamosal.

The squamosal is a paired dermal bone, it is located lateroposteriorly to the neurocranium and is part of the *suspensorium* (a complex of exo- and

endocranial elements that joints the upper jaw to the neurocranium). This bone is triradiate; its ventral ramus invests laterally the quadrate cartilage and typically articulates at the distal tip with the posterodorsal portion of the quadratojugal; the anterodorsal zygomatic ramus is very variable and extends anteriorly forming an incomplete posterior margin to the orbit; and the posterodorsal otic ramus invest the lateral margin of the crista parotica and extends dorsally to the stapes and tympanic *annulus* (Trueb 1993). Variation of squamosal zygomatic ramus in dendrobatoids was scored by Grant *et al*. (2006) in a transformation series composed by nine character states, which combine form, extension and orientation, as observed from a lateral plane (character 193 in this study). We additionally individuate as a different transformation series (character 194) the tip of the zygomatic process horizontal orientation (in dorsal view), which is medially oriented in most Aromobatinae, and directed toward the front or polymorphic only in some species, but laterally oriented in all dendrobatids and *Anomaloglossus*, as well as some *Allobates* examined by us (Figure 25). We also score the the otic ramus posterior end form in lateral view (character 192) as truncated (state 0), when the posterior border is vertical or nearly vertical, and fusiform (state 1), when its is pointed due to its dorsal angle being markedly posterior to the ventral angle (Figure 24).

192. Squamosal, otic ramus, form: 0 = truncated; 1 = fusiform. (Figure 24).

193. Squamosal, zygomatic ramus, form (Grant *et al*. 2006): 0 = elongate, slender, pointed 1 = very long and slender; 2 = robust, truncate, and elongate; 3 = shorter and less robust but still well defined; 4 = well defined, moderate

length, abruptly directed ventrad; 5 = inconspicuous, poorly differentiated; 6 = very small, inconspicuous, hook-like; 7 = miniscule bump; 8 = robust, elongate, in broad contact with the maxilla. Nonadditive.

194. Squamosal, zygomatic ramus, horizontal orientation: 0 = medially oriented; 1 = towards front; 2 = laterally oriented. (Figure 25).

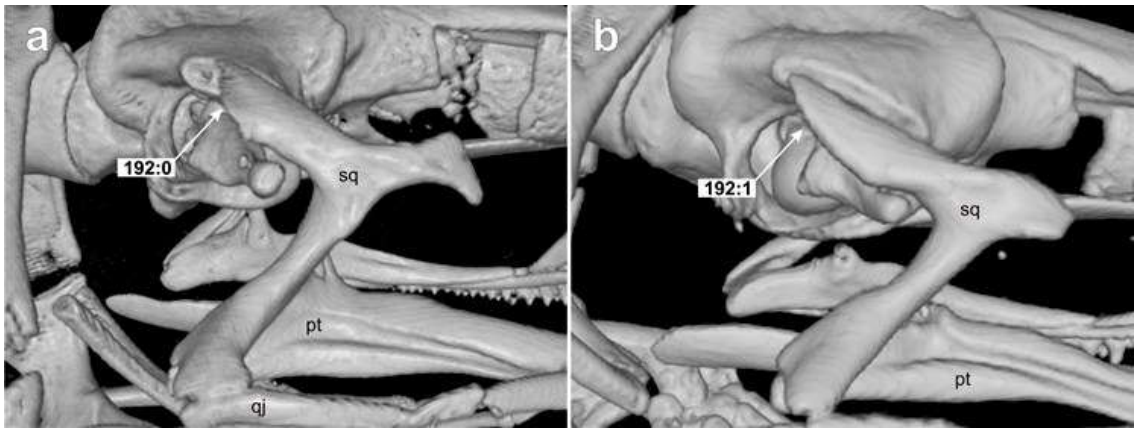

Figure 24. Squamosel, otic ramus, form (character 192): truncated (state 0) in *Mannophryne collaris* MHNLS 21598 (**a**); fusiform in *Aromobates ornatissimus* ULABG 4976 (**b**). **pt:** pterygoid; **qj:** quadratojugal; **sq:** squamosal.

Figure 25. Dorsal view of posterolateral portion of the skull of *Aromobates ornatissimus* ULABG 4976 (**a**), *Mannophryne neblina* MHNLS 4956 (**b**), and *"Colostethus" caribe* MHNLS 17463 (**c**). Squamosal, zygomatic ramus, orientation (character 194): medially oriented (state 1) in **a**; oriented towards front (state 1) in **b**; laterally oriented (state 2) in **c**. Orientation indicated by yellow arrows.

195–202. Pterygoid.

Pterygoid is a paired, triradiate, dermal bone of the *suspensorium*, medial to the squamosal and forming the lateroventral and posteroventral margins of the

orbit. Its anterior ramus is sulcate along the lateral surface and medially invests the pterygoid process of the quadrate cartilage; this ramus articulates anteriorly with the maxilla and extends forward, medially to the latter, reaching in some cases the lateral end of the palatine; its dorsal surface form the ventral *margo orbitalis*. The posterior ramus extends posteriorly to almost converge with the quadratojugal posterior end and the squamosal ventral ramus tip, and invests medially the quadrate cartilage. Finally, the pterygoid medial of ramus invests the quadrate pseudobasal process and, when it is not reduced, articulates with the otic capsule (Trueb 1993, Duellman & Trueb 1994). Variation in the pterygoid bone typically involves the anterior and medial rami extension and development (Trueb 1993). We follow De Sá *et al*. (2014) in coding the posterior ramus length relative to the medial ramus length. Additionally, we score variation in the medial ramus form (character 196), orientation (character 197), and extension (character 198)—all of them observed in ventral view. We also score the medial ramus tip form in anterior view (character 199), the occurrence of middorsal and posterodorsal lobes on the *margo orbitalis* of the anterior ramus (characters 200 and 201), and the continuity of the lateral sulcus on this ramus (character 202).

195. Pterygoid, posterior ramus, length relative to medial ramus (De Sá *et al*. 2014): 0 = posterior ramus almost twice the length of medial ramus; 1 = posterior ramus slightly longer or equal to medial ramus; 2 = posterior ramus shorter than medial ramus. Additive.

196. Pterygoid, medial ramus, form in ventral view: 0 = robust, conical; 1 = slender, styliform. (Figure 26).

197. Pterygoid, medial ramus, orientation in ventral view: 0 = dorsal-anterior; 1 = dorsal-medial; 2 = dorsal-posterior. (Figure 26).

198. Pterygoid, medial ramus, extension in ventral view: 0 = very short (does not reach the level of the lateroventral edge of the otic capsule); 1 = short (it reaches the level of the otic capsule lateroventral edge); 2 = long (surpass the level of the otic capsule lateroventral edge). Additive. (Figure 26).

199. Pterygoid, medial ramus, distal tip in anterolateral view, shape: 0 = pointed; 1 = bulged (laterodistally expanded). (Figure 27).

200. Pterygoid, anterior ramus, *margo orbitalis*, middorsal lobe: 0 = absent; 1 = present. (Figure 28).

201. Pterygoid, anterior ramus, *margo orbitalis*, posterodorsal lobe: 0 = absent; 1 = present. (Figure 28).

202. Pterygoid, anterior ramus, lateral sulcus: 0 = continuous; 1 = discontinuous (interrupted at the midlevel of the ramus); 2 = restricted to the posterior portion. Nonadditive. (Figure 28).

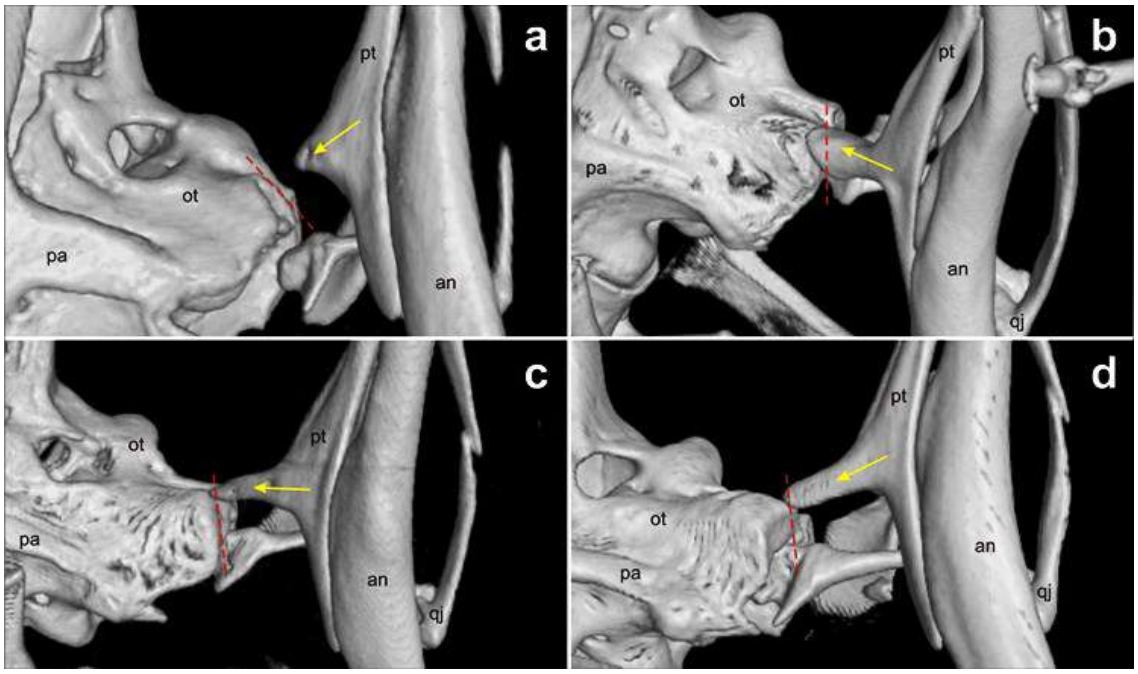

Figure 26. Ventral view of the posterolateral portion of the skull of *Aromobates ornatissimus* ULABG 4976 (**a**), *Aromobates alboguttatus* CVULA 1448 (**b**), *Mannophryne collaris* MHNLS 21598 (**c**), and *Mannophryne neblina* MHNLS 4956 (**d**). Pterygoid, medial ramus, form in ventral view (character 196): robust, conical (state 0) in **a**; slender, styliform (state 1) in **b**–**d**. Pterygoid, medial ramus, orientation in ventral view (character 197; indicated by yellow arrows): dorsal-anterior (state 0) in **b**; dorsal-medial (state 1) in **c**; dorsal-posterior (state 2) in **a**, and **d**. Pterygoid, medial ramus, extension in ventral view (character 198; ventrolateral border of the otic capsule indicated by red dashed lines): very short, does not reach the level of the otic capsule lateroventral edge (state 0) in **a**; short, it reaches the level of the otic capsule lateroventral edge (state 1) in **c** and **d**; long, surpass the level of the otic capsule lateroventral edge (state 2) in **b**. **an:** angulosplenial; **ot:** otoccipital; **pa:** parasphenoid; **pt:** pterygoid; **qj:** quadratojugal.

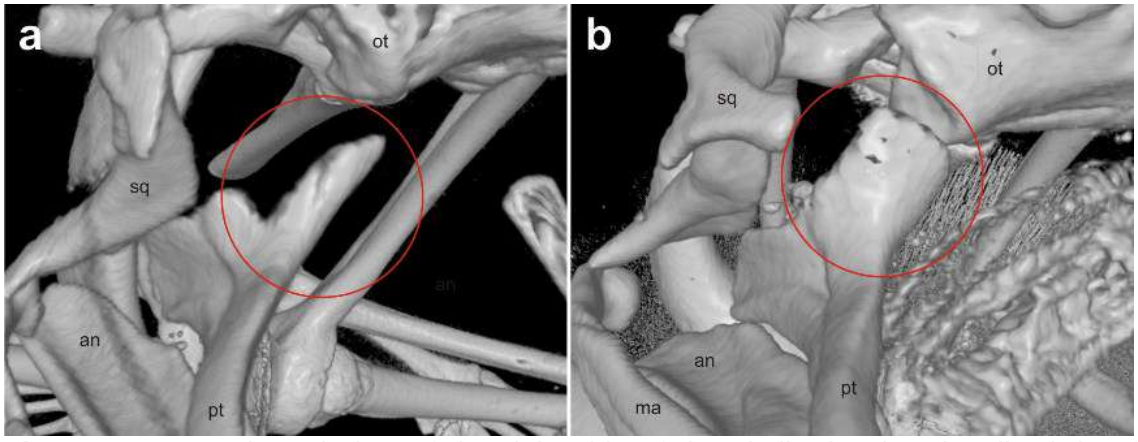

Figure 27. Anterolateral view of the right side of the skull, showing the distal tip of medial ramus of pterygoid (character 199; in the red circle): pointed (state 0) in *Mannophryne collaris* MHNLS 21598 (**a**); bulged, laterodistally expanded (state 1) in *Aromobates nocturnus* ULABG 2223 (**b**). **an:** angulosplenial; **ma:** maxilla; **ot:** otoccipital; **pt:** pterygoid; **sq:** squamosal.

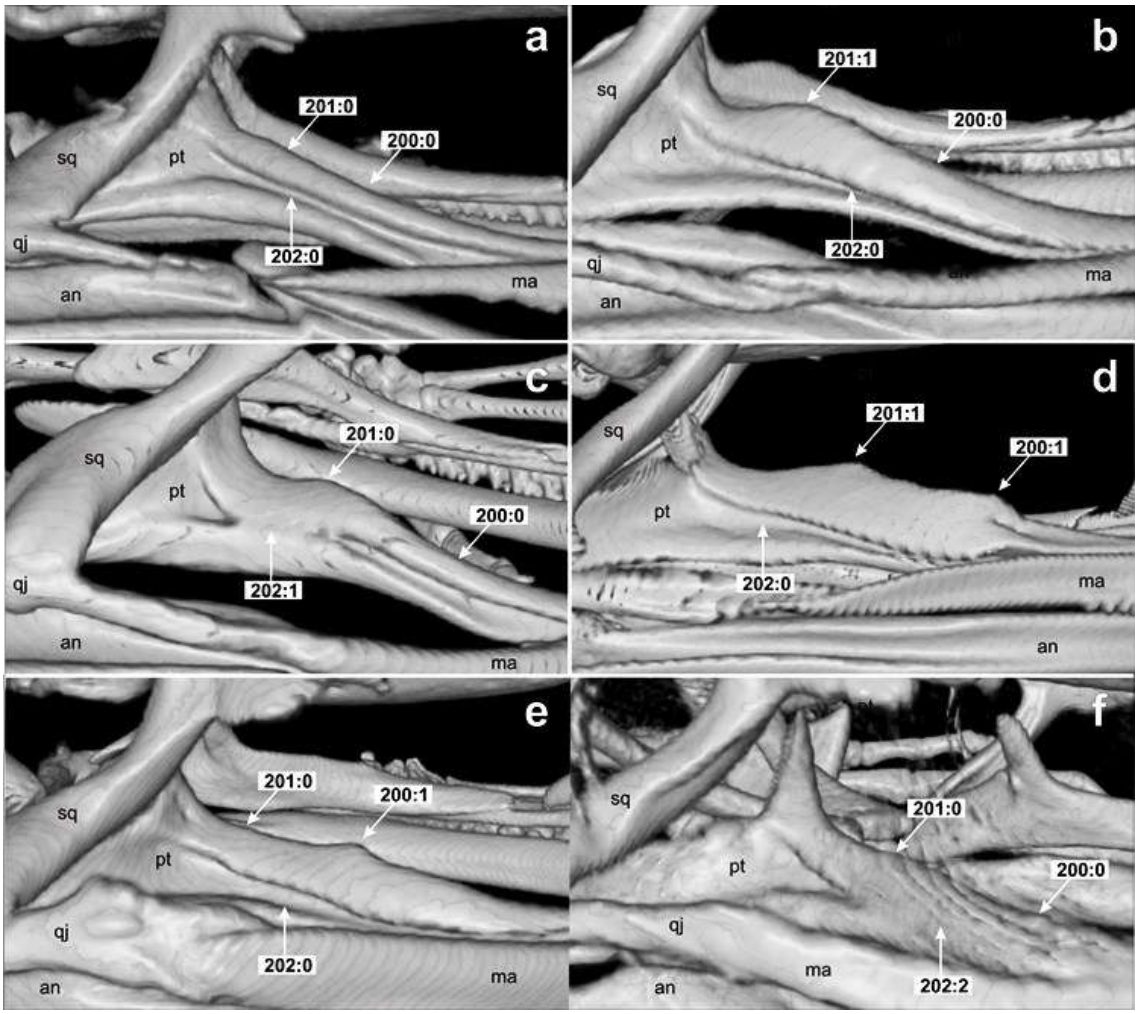

Figure 28. Lateral view of the right side of the skull of *"Colostethus" caribe* MHNLS 17463 (**a**), *Allobates femoralis* MCP 13869 (**b**), *Mannophryne caquetio* MHNLS 21220 (**c**), *Mannophryne oblitterata* MHNLS 21799 (**d**), *Aromobates walterarpi* ULABG 1577 (**e**), and *Aromobates* sp. 4 T10-1(**f**). Pterygoid, anterior ramus, *margo orbitalis*, middorsal lobe (character 200): absent (state 0) in **a**–**c**, and **e**–**f**; present (state 1) in **d**–**e**. Pterygoid, anterior ramus, *margo orbitalis*, posterodorsal lobe (character 201): absent (state 0) in **a**, **e**–**f**; present (state 1) in **b**–**d**. Pterygoid, anterior ramus, lateral sulcus (character 202): continuous (state 0) in **a**–**b**, **d**–**e**; discontinuous, interrupted to the midlevel of the ramus (state 1) in **c**; restricted to the posterior portion (state 2) in **f**. **an:** angulosplenial; **ma:** maxilla; **pt:** pterygoid; **qj:** quadratojugal; **sq:** squamosal.

203–207: Premaxilla.

Premaxyllae are a pair of dermal bones, medially in contact, that form the anterior part of the upper jaw. These bones bear a dorsal alary process each, that support the superior prenasal process of the olfactory capsule. Their horizontal base (*pars dentalis*) can be provided with teeth, and from this base a horizontal palatal shelf (*pars palatina*) is projected posteriorly. The *pars palatina*

of each premaxilla bears a medial process that contacts medially with the opposite, and eventually a lateral process that contacts with the palatal shelf of the maxilla (Trueb 1993). Alary processes of premallixa vary in their orientation, length and form, and an anterolaterally tilted alary process was referred as a synapomorphy of Dendrobatidae by Myers & Ford (1986). Grant *et al*. (2006) scored the orientation of the alary process in dendrobatoids, and De Sá *et al*. (2014) coded their relative width in *Leptodactylus*. *Pars palatina* also exhibits considerable variation among anurans (Trueb 1993) and De Sá *et al*. (2014) scored the relative width of the middle process of this shelf. We follow Grant *et al*. (2006) for the orientation of the alary process and modified the definition of De Sá *et al*. (2014) for the relative width of the alary process and the relative width of the *pars palatina* medial process. Additionally, we score the variation observed in the alary process distal tip contour (character 204), and the posterior border of the *pars palatina* medial process (character 207).

203. Premaxilla, alary process, distal width (modified from De Sá *et al*. 2014): 0 = narrower than base (dw/pw: <1); 1 = unexpanded to weakly expanded (dw/pw: 1.0 to 1.3); 2 = moderately expanded (dw/pw: >1.3). Additive. (Figure 29).

De Sá *et al*. (2014) used the relation between the width at the base and that of the dorsal portion, and defined two states: base narrower or subequal to the dorsal extreme (state 0), and base broader than the dorsal extreme (state 1). We use the distal width with respect to the basal width and define three states: distally narrower than the base (state 0), distally unexpanded to weakly expanded (state 1), and moderately expanded distally (state 2).

204. Pramaxilla, alary process, distal tip, contour : 0 = truncate; 1 = pointed; 2 = bifid (notched); 3 = trifid. Nonadditive. (Figure 29).

205. Premaxilla, alary process, orientation (Grant *et al*. 2006): 0 = tilted anteriorly; 1 = directed dorsally (vertical, not tilted); 2 = tilted posteriorly. Additive.

206. Premaxilla, *Pars palatina*, medial process-lateral process ratio (De Sá *et al*. 2014): 0 = medial process equal to or slightly narrower than lateral process; 1 = medial process clearly narrower than lateral process; 2 = medial process wider than lateral process. Nonadditive. (Figure 30).

207. Premaxilla, *pars palatina*, medial process, posterior contour: 0 = truncate; 1 = pointed (subtriangular to triangular); 2 = rounded. Nonadditive. (Figure 30).

208–211: Palatine.

Palatine is also a dermal paired bone, slender and transversely oriented. It underlays the *planum antorbitale*, usually articulates medially with the sphenethmoid and laterally with the maxilla (Trueb 1993). In dendrobatoids this bone is reduced or absent (Myers & Ford 1986), and its absence in some groups has been considered as synapomorphic (Kaplan 1997, Grant *et al*. 2006). We follow Grant *et al*. (2006) and Mendelson *et al*. (2000) in coding the occurrence of this bone, and the presence/absence of an anteromedial process, respectively. We also score the variation observed in the lateral extension of the

palatine (character 209), and the proximity between the palatine and pterygoid (character 210).

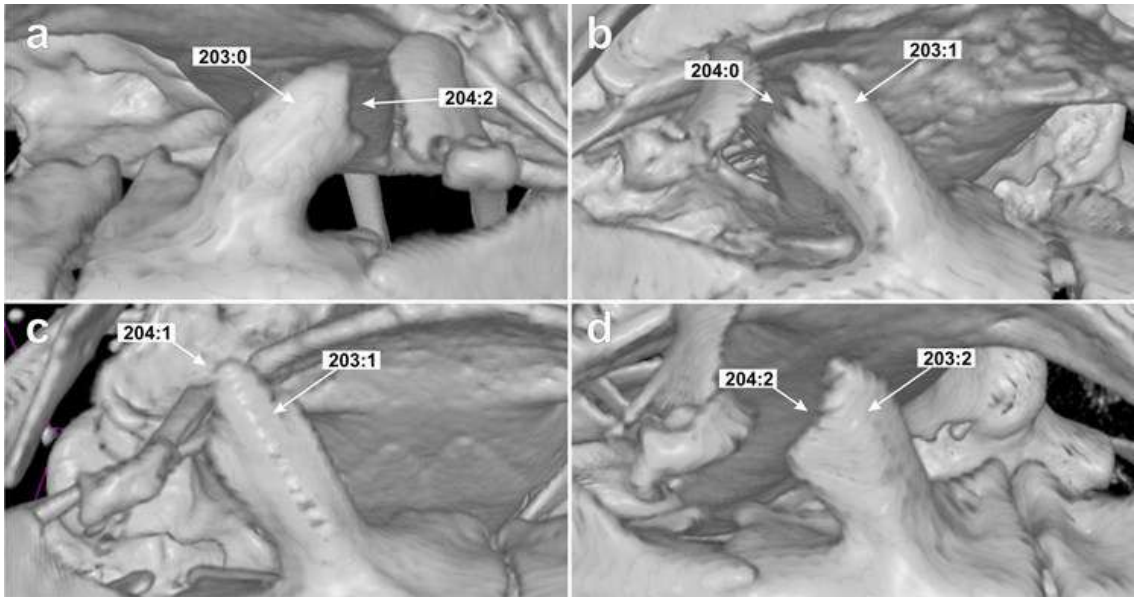

Figure 29. Anterior view of the skull, showing the alary process of the premaxilla in *Aromobates ornatissimus* ULABG 4976 (**a**), *Aromobates serranus* CVULA 7099 (**b**), *Mannophryne larandina* MHNLS 22600 (**c**), and *Mannophryne* sp. 3 MHNLS 22355 (**d**). Premaxilla, alary process, distal width (character 203): narrower than base (state 0) in **a**; unexpanded to weakly expanded (state 1) in **b**–**c**; moderately expanded (state 2) in **d**. Premaxilla, alary process, distal tip, contour (character 204): truncate (state 0) in **b**; pointed (state 1) in **c**; bifid (state 2) in **a** and **c**.

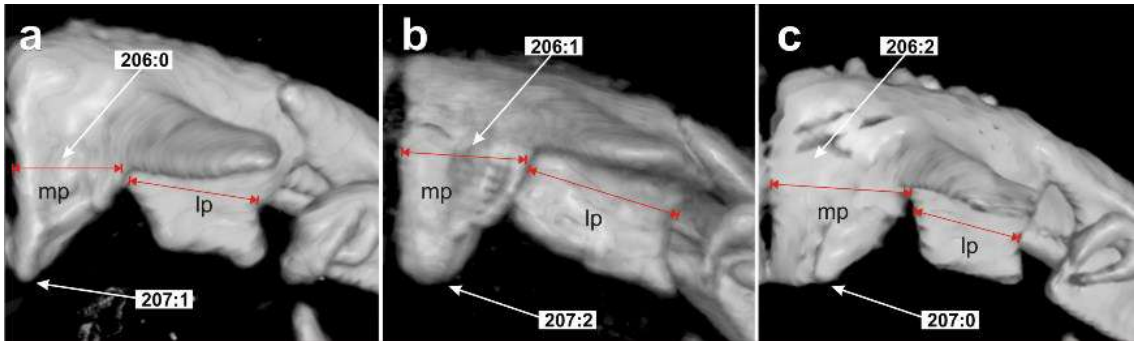

Figure 30. Dorsal view of the right premaxilla of *Mannophryne* sp. 3 MHNLS 22355 (**a**), *Aromobates cannatellai* MHNLS 22625 (**b**), and *Aromobates zippeli* MHNLS 22052 (**c**). Premaxilla*, pars palatina*, medial process-lateral process ratio (character 206): medial process equal to or slightly narrower than lateral process (state 0) in **a**; medial process clearly narrower than lateral process (state 1) in **b**; medial process wider than lateral process (state 2) in **c**. Premaxilla, *pars palatina*, medial process, posterior contour (character 207): truncate (state 0); pointed (state 1); rounded (state 2). **mp:** medial process; **lp:** lateral process.

208. Palatine (Grant *et al*. 2006): 0 = absent; 1 = present. (Figure 31).

209. Palatine, lateral extension: 0 = does not reach the maxilla; 1 = in contact with maxilla. (Figure 31).

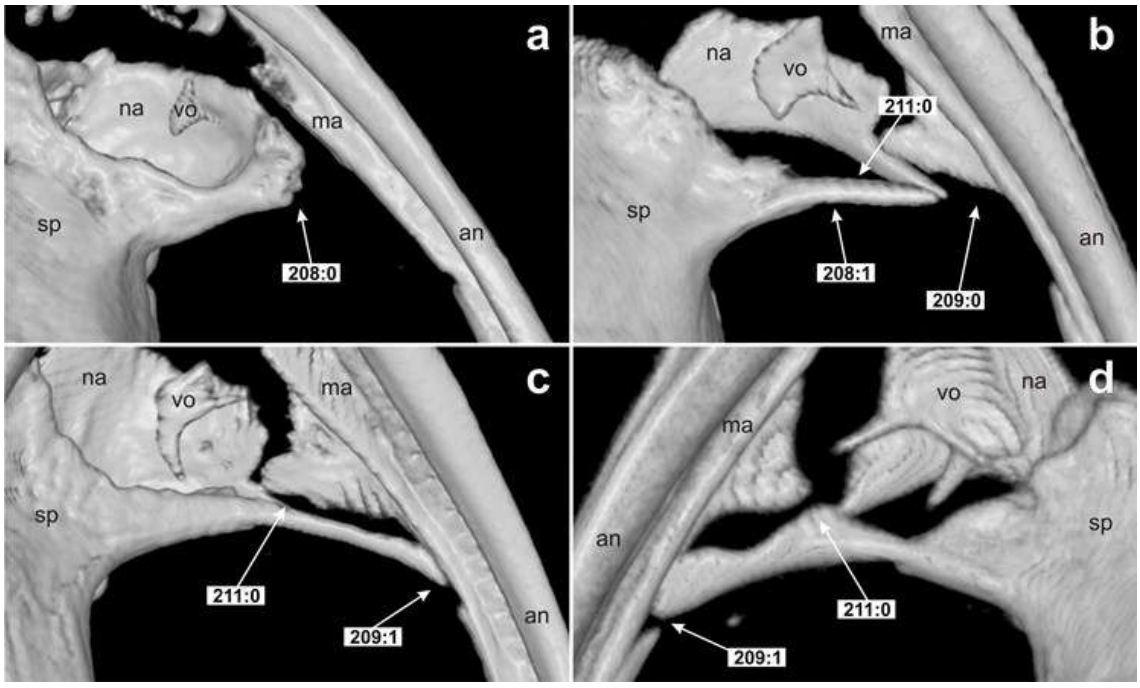

Figure 31. Ventral view of the skull, showing the anterolateral portion in *Ranitomeya toraro* MCP 13107 (**a**), *Aromobates ornatissimus* ULABG 4976 (**b**), *Anomaloglossus wothuja* MHNLS 19992 (**c**), and *Aromobates zippeli* MHNLS 22052 (**d**). Palatine (character 208): absent (state 0) in **a**; present (state 1) in **b**–**d**. Palatine, lateral extension (character 209): does not reach the maxilla (state 0) in **b**; in contact with maxilla (state 1) in **c**–**d**. Palatine, anteromedian process (character 211): absent (state 0) in **b**–**c**; present (state 1) in **d**. **an:** angulosplenial; **ma:** maxilla; **na:** nasal; **sp:** sphenethmoid; **vo:** vomer.

210. Palatine-pterygoid, distance: 0 = widely separated; 1 = sharply separated; 2 = in contact or nearly in contact. Additive. (Figure 32).

In the state 0 the tips of the palatine and the pterygoid anterior ramus are notably separated, the distance between both tips is equal or greater than a third of the orbital diameter; in state 1 the distance between these two tips is

short (less than one third of the orbital diameter) but are evidently separated; and, in state 3 these two bones are in contact or nearly in contact.

211. Palatine, anteromedian process (Mendelson *et al*. 2000): 0 = absent; 1 = present. (Figure 31).

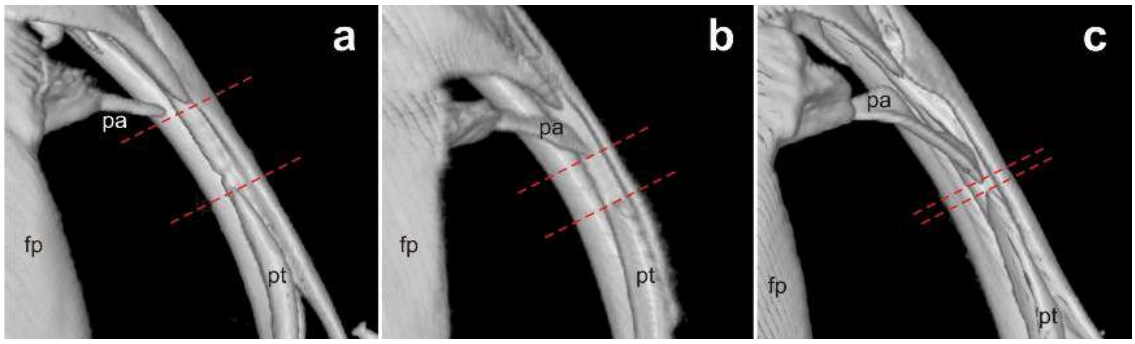

Figure 32. Dorsal view of the skull, showing the anterolater portion in *Aromobates ornatissimus* ULABG 4976 (**a**), *Mannophryne vulcano* MHNLS 21780 (**b**), and *Aromobates zippeli* MHNLS 22052 (**c**). Palatine-pterygoid, distance (character 210): widely separate (state 0) in **a**; sharply separated (state 1) in **b**; in contact or nearly in contact (state 2) in **c**. **fr:** frontoparietal; **pa:** palatine; **pt:** pterygoid. Red dashed lines highlighting the distance between the palatine and pterygoid tips.

212–216: Quadratojugal.

This paired bone, absent in some anurans, and frequently reduced in Neobatrachia (Trueb 1993, Duellman & Trueb 1994), it conforms the posterior portion of the upper jaw, and connects posteriorly to the *suspensorium*. Anteriorly, it articulates with the maxilla, but in some hypo-ossified anurans as dendrobatids, these bones are never in contact and the connection is completed by ligaments (Grant *et al*. 2006). Posteriorly, the quadratojugal is integrated with the pars articularis of the quadrate and posterodorsally articulates with the ventral ramus of the squamosal (Trueb 1993). Grant *et al*. (2006) coded variation in the quadratojugal-maxilla relation (our character 216). We additionally scored variation observed in dendrobatoids in the ossification of

quadratojugal (character 212), its articulation with the squamosal (character 213), the extension of this articulation (character 214), and the quadratojugal anterior expansion (character 215), which is defined as the relation between its anterior and posterior heights (ah and ph, respectively).

212. Quadratojugal, ossification: 0 = cartilaginous; 1 = ossified. (Figure 33).

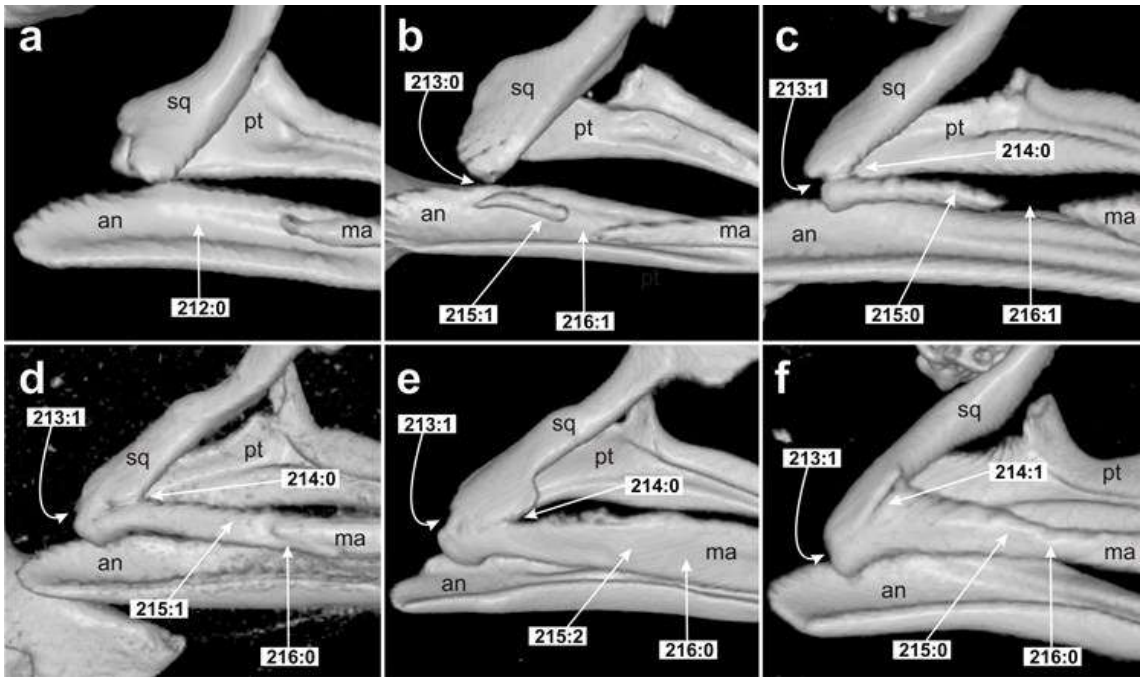

Figure 33. Lateral view of the skull, showing the mandible posterior portion and part of the *suspensorium* in *Ranitomeya toraro* MCP 13107 (**a**), *Adelphobates galactonotus* MCP 2252 (**b**), *Aromobates ornatissimus* ULABG 4976 (**c**), *Aromobates haydeeae* (**d**), *Aromobates meridensis* MHNLS 22019 (**e**), and *Mannophryne trujillensis* MHNLS 22067 (**f**). Quadratojugal, ossification (character 212): cartilaginous (state 0) in **a** (cartilage not recovered in these 3D models; presence confirmed in the skinned specimen); ossified (state 1) in **b**–**f**. Quadratojugal-squamosal, relation (character 213): not in contact (state 0) in **b**; in contact (state 1) in **c**–**f**. Quadratojugal-squamosal articulation, extension (character 214): only with the squamosal ventral surface (state 0) in **c**–**e**; with squamosal ventral and anterior surfaces (state 1) in **f**. Quadratojugal, anterior width (character 215): narrowed to pointed, ah/ph < 1 (state 0) in **c** and **f**; unexpanded, ah/ph = 1–1.4 (state 1) in **b** and **d**; moderately expanded (2.0 or >2) in **e**. Quadratojugal-maxilla relation (character 216): overlapping (state 0) in **d**–**f**; separate (state 1) in **b**–**c**. **an:** angulosplenial; **ma:** maxilla; **pt:** pterygoid; **sq:** squamosal.

213. Quadratojugal-squamosal, relation: 0 = not in contact; 1 = in contact. (Figure 33).

214. Quadratojugal-squamosal articulation, extension: 0 = only with the squamosal ventral surface; 1 = with squamosal ventral and anterior surfaces. (Figure 33).

215. Quadratojugal, anterior width: 0 = narrowed to pointed (ah/ph: < 1); 1 = unexpanded (ah/ph: 1–1.4); 2 = weakly expanded (ah/ph: 1.5–1.9); 3 = moderately expanded (ah/ph: ≥ 2.0). (Figure 33).

216. Quadratojugal-maxilla, relation (Grant *et al*. 2006): 0 = overlapping; 1 = separate. (Figure 33).

217–221: Maxilla.

This paired bone is the most extensive element of the upper jaw and is composed of three parts: the *pars dentalis* that bears the dental ridge; the *pars palatina*, a poorly developed lingual shelf; and, the *pars facialis*, a dorsal flange that at its anterior portion, where it is more elevated, covers the olfactory capsule. The *pars facialis* delimits the orbit ventrally, and can be provided with preorbital and a postorbital process (Trueb 1993, Duellman & Trueb 1994). The *pars facialis* may be in contact with the nasal bone (Grant *et al*. 2006). The maxilla also articulates anteriorly with the premaxilla, medially with the palatine (when the latter is present and complete) and the pterygoid anterior ramus, and posteriorly with the quadratojugal—joined by ligaments in dendrobatids (Grant *et al*. 2006). To score the variation observed in dendrobatoids maxilla, we redefine the preorbital process codification of Mendelson *et al*. (2000) and individuate other four transformation series: *pars facialis* lateral surface

(character 217), posterior height of the *pars facialis* orbital border (character 219), maxilla posterior extension (character 220), and the occurrence of a postorbital process (character 221).

217. Maxilla, *pars fascialis*, lateral surface, ornamentation: 0 = smooth; 1 = anteroposteriorly sulcated. (Figure 34).

218. Maxilla, *pars fascialis*, preorbital process, development in relation with the anterior contour (modified from Mendelson *et al*. 2000): 0 = absent; 1 = weak, barely differentiated; 2 = strong, well-differentiated. Additive.

Mendelson *et al*. (2000) described two states for the maxilla preorbital process: distinct (state 0) and, not distinct from *pars facialis* (state 1). We redefine this transformation series to better describe the variation in the development of this process. Absence of a preorbital process is observed in some individuals of the aromobatid *Rheobates palmatus*, the dendrobatids *Adelphobates galactonotus*, *Ranitomeya toraro*, and the cycloramphid *Thoropa miliaris*. *Mannophryne* sp. from La Sierra is polymorphic for this character. (Figure 34).

219. Maxilla, *pars fascialis*, orbital border, antero-posterior relative height: 0 = lowest posteriorly; 1 = posteriorly as high as anteriorly; 2 = higher posteriroly. Additive. (Figure 34).

220. Maxilla, posterior extension: 0 = does not reach the level of triple point of squamosal; 1 = reaches the level of triple point of squamosal. (Figure 34).

221. Maxilla, postorbital process: 0 = absent; 1 = vestigial. (Figure 34).

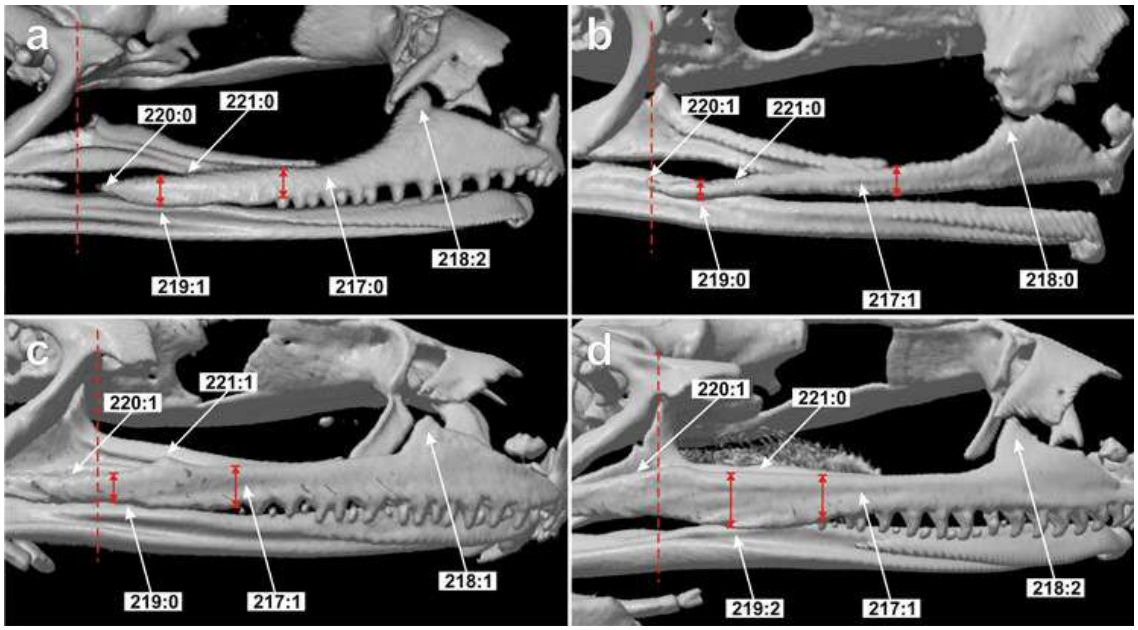

Figure 34. Lateral view of the skull of *Aromobates ornatissimus* ULABG 4976 (**a**), *Ranitomeya toraro* MCP 13107 (**b**), *Aromobates zippeli* MHNLS 22052 (**c**), and *Aromobates nocturnus* ULABG 2223 (**d**). Maxilla, *pars fascialis*, lateral surface, ornamentation (character 217): smooth (state 0) in **a**; anteroposteriorly sulcated (state 1) in **b**–**d**. Maxilla, *pars fascialis*, preorbital process, development in relation with the anterior contour (character 218): absent (state 0) in **b**; weak, barely differentiated (state 1) in **c**; strong, well-differentiated (state 2) in **a** and **d**. Maxilla, *pars fascialis*, orbital border, antero-posterior relative height (character 219; anterior and posterior heighs indicated by two-tip red arrows): lowest posteriorly (state 0) in **b**–**c**; posteriorly as high as anteriorly (state 1) in **a**; higher posteriroly (state 2) in **d**. Maxilla, posterior extension (character 220; level of the base of the squamosal zygomatic process indicated by the red dashed line): does not reach the level of the base of the zygomatic process of squamosal (state 0) in **a**; reaches the level of the base of the zygomatic process (state 1) in **b**–**d**. Maxilla, postorbital process (character 221): absent (state 0) in **a**–**b**, and **d**; vestigial (state 1) in **c**.

222–226: Nasal.

Nasal is a paired, dorsally flat, and slim dermal bone, that lies anterior to the ossified portion of the sphenethmoid, and forms the roof of the olfactory capsule. This bone bears a posterolateral maxillary process that may articulate whit the maxilla. Depending upon cranial ossification, there is considerable variation in the development of the nasal (Trueb 1993, Duellman & Trueb 1994). La Marca (1992, 1994a) defined the moderately large, but widely separate

medially nasals of *Mannophryne* as a diagnostic character to separate it from the closely related *Nephelobates* (= *Aromobates*), which has small nasal bones (La Marca 1994b, Mijares-Urrutia & La Marca 1997). Grant *et al*. (2006) did not test this hypothesis, but scored variation in the nasal-maxilla and nasal-sphenethmoid relations (i.e., presence or absence of contact) in dendrobatoids (our characters 222 and 226, respectively). We code the nasal coverage in dendrobatoids (character 223) to test previous hypotheses of La Marca (1992, 1994a, b) and Mijares-Urrutia & La Marca (1997), and additionally, we score the variation observed in the posterior extension of the maxillary process noted in lateral view (character 224), and the development of the maxillary process lateral crest (character 225).

222. Nasal-maxilla, relation (Grant *et al*. 2006): 0 = separate; 1 = in contact.

223. Nasal, size: 0 = small; 1 = large. (Figure 35)

In state 0 the nasal is small, its medial margin does not reach or barely reaches the level of the lateral process of the premaxilla *pars palatina*, and its dorsal surface is about half of the dorsal surface of sphenethmoid (figure 35a). State 1 correspond to a moderately large nasal, which covers about half of the snout, and is similar in size to sphenethmoid; its medial margin surpass the level of the lateral process of the *pars palatina* of premaxilla (Figure 35b).

224. Nasal, maxillary process tip, posterior extension: 0 = does not reach the level of *planum antorbitale*; 1 = reaches the level of *planum antorbitale*; 2 = surpass the level of *planum antorbitale*. Additive. (Figure 36).

225. Nasal, maxillary process, lateral crest, development: 0 = absent; 1 = weak; 2 = strong. Additive. (Figure 36).

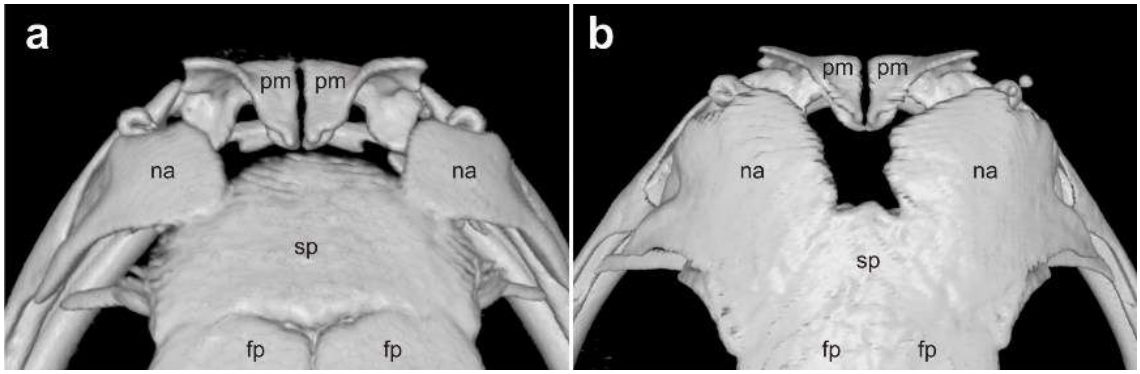

Figure 35. Dorsal view of the anterior portion of the skull of *Aromobates ornatissimus* ULABG 4976 (**a**) and *Mannophryne herminae* MHNLS 22111 (**b**). Nasal, size (character 223): small (state 0) in **a**; large (state 1) in **b**. **fp:** frontoparietal; **na:** nasal; **pm:** premaxilla; **sp:** sphenethmoid.

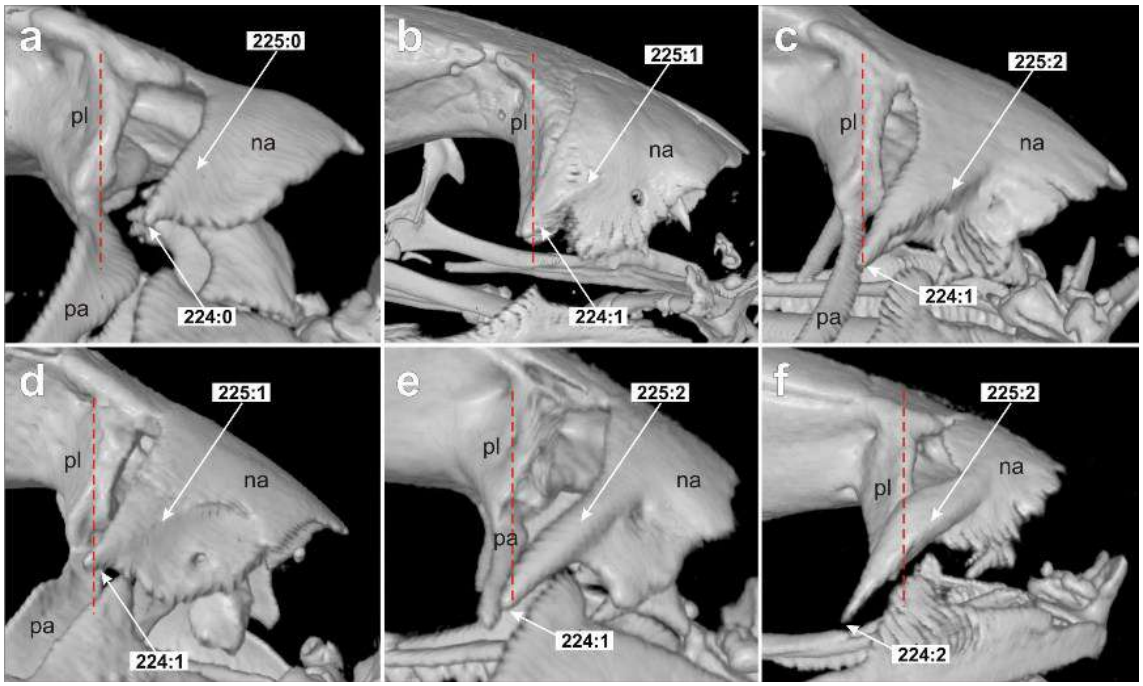

Figure 36. Lateral view of the anterior portion of the skull of *Aromobates zippeli* MHNLS 22052 (**a**), *Adelphobates galactonotus* MCP 2252 (**b**), *Mannophryne herminae* MHNLS 22111 (**c**), *Aromobates meridensis* MHNLS 22019 (**d**), *Aromobates ornatissimus* ULABG 5976 (**e**), and *Allobates pittieri* MHNLS 21488 (**f**). Nasal, maxillary process tip, posterior extension (character 224): does not reach the level of *planum antorbitale* (state 0) in **a**; reaches the level of *planum antorbitale* (state 1) in **b**–**e**; surpass the level of planum antorbitae (state 2) in **f**. Nasal, maxillary process, lateral crest, development (character 225): absent (state 0) in **a**; weak (state 1) in **b** and **d**; strong (state 2) in **c** and **e**. **na:** nasal; **pa:** palatine; **pl:** *planum antorbitale*. Red dashed line highlights the level of the *planum antorbitale*.

226. Nasal-sphenethmoid relation (Grant *et al*. 2006): 0 = separate; 1 = overlapping or fused. (Figure 37).

227–233: Sphenethmoid.

This bone is located anteromedially to the orbit, forms the posteromedial wall of the nasal capsule and the anterior portion of the braincase. In most adult anurans, the two halves of the sphenethmoid are medially fused forming a single element together with the *septum nasi*. The *planum antorbitale* also is fused in adults to the sphenethmoid (Trueb 1994). A pair of ventrolateral processes formed by fusion of the ossified *planum antorbitale* with the sphenethmoid, are more developed in dendrobatoids lacking palatines (Myers *et al*. 1991). Dorsally, the anterolateral margins of the sphenethmoid may be in contact or partially covered by the nasals, and its posterior margin, that usually forms the frontoparietal fenestra posterodorsally, may be overlapped by the frontoparietals; ventrally, articulates anterolaterally with the palatines (if present), and posteromedially with the cultriform process of parasphenoid. The sphenethmoid can extend posterolaterally to the optic foramen and even surround it (Trueb 1993, Myers *et al*. 1991, La Marca 1995). We individuate seven transformation series to score the variation observed in dendrobatoids in the sphenethmoid long-wide relation (character 227), dorsal anterior contour (character 228), ventral anterior contour (character 229), ventral anteromedial surface (character 230), posterior contour of the floor (character 231), posterior extension of the posteroventral margin in relation to the posterolateral margins (character 232), and the lateral projection of the sphenethmoid ventrolateral process (character 233).

227. Sphenethmoid, length-width relation: 0 = l/w: < 0.5; 1 = l/w: 0.5; 2 = l/w: > 0.5. Additive. (Figure 37).

Length (l) measured from the posterior contact with the frontoparietals to the anteriormost edge. Width (w) transversely measured between the posterolateral corners.

228. Sphenethmoid, dorsal anterior contour: 0 = straight to nearly straight; 1 = convex; 2 = bilobed; 3 = trilobed. Nonadditive. (Figure 37).

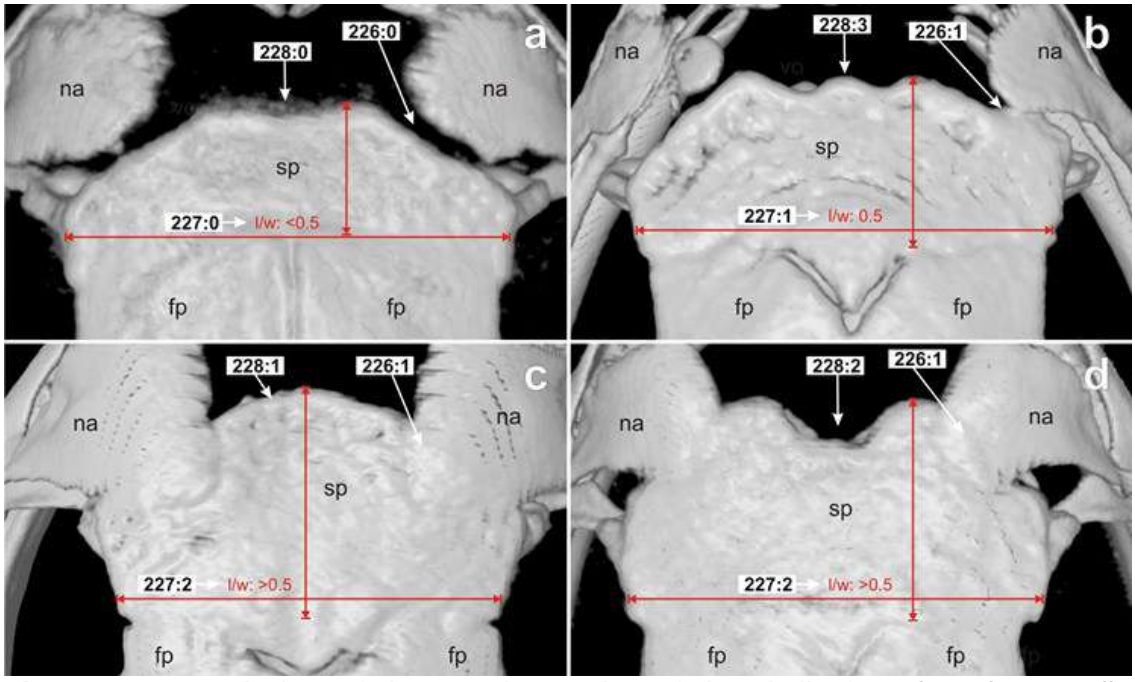

Figure 37. Dorsal view of the anterior portion of the skull of "*Colostethus*" *caribe* MHNLS 17463 (**a**), *Allobates juami* MCP 13288 (**b**), *Aromobates meridensis* MHNLS 22019 (**c**), *Aromobates zippeli* MHNLS 22052 (**d**). Nasal-sphenethmoid relation (character 226): separate (state 0) in **a**; overlapping or fused (state 1) in **b**–**d**. Sphenethmoid, length-width (l and w, respectively) relation (character 227): l/w: < 0.5 (state 0) in **a**; l/w: 0.5 (state 1) in **b**; l/w: > 0.5 (state 2) in **c**–**d**. Sphenethmoid, dorsal anterior contour (character 228): straight to nearly straight (state 0) in **a**; convex (state 1) in **c**; bilobed (state 2) in **d**; trilobed (state 3) in **b**. **fp:** frontoparietal; **na:** nasal; **sp:** sphenethmoid. Red lines indicate the long and width of sphenethmoid.

229. Sphenethmoid, ventral anteromedial surface, shape: 0 = flat; 1 = concave. (Figure 38).

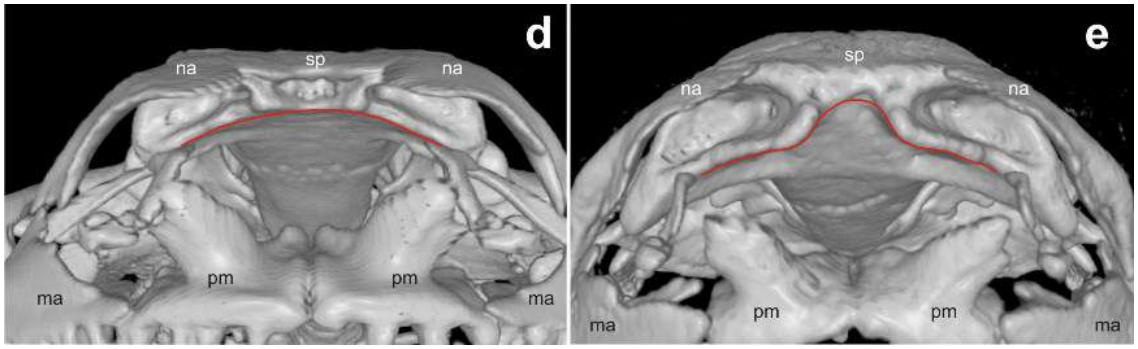

Figure 38. Anterior view of the skull, showing the profile of the ventral surface of the sphenethmoid in *Aromobates nocturnus* ULABG 2223 (**a**), and *Allobates pittieri* MHNLS 21488 (**b**). Sphenethmoid, ventral anteromedial surface, shape (character 229): flat (state 0) in **a**; concave (state 1) in **b**. **ma:** maxilla; **na:** nasal; **pm:** premaxilla; **sp:** sphenethmoid. Red lines highlight the sphenethmoid ventral surface.

230. Sphenethmoid, ventral anterior contour: 0 = medially notched; 1 = straight; 2 = convex. Nonadditive. (Figure 39).

231. Sphenethmoid, floor posterior contour, dorsal to parasphenoid cultriform process: 0 = concave; 1 = straight; 2 = convex. Nonadditive. (Figure 40).

232. Sphenethmoid, posteroventral border, posterior extension in relation to the posterolateral borders: 0 = posteroventral border anterior to lateral ones; 1 = posteroventral border to the level of the lateral ones; 2 = posteroventral border posterior to lateral ones. Additive. (Figure 40).

233. Sphenethmoid, ventrolateral process, extension: 0 = less than 1/3 of the distance between orbitonasal foramen and the maxilla; 1 = 1/3 to 1/2 of the distance; 2 = > 1/2 of the distance. Additive. (Figure 41).

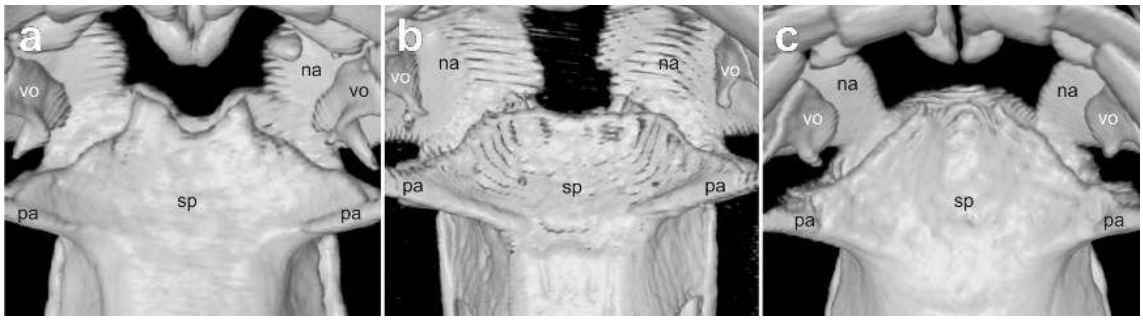

Figure 39. Ventral view of the anterior portion of the skull of *Aromobates nocturnus* ULABG 2223 (**a**), *Aromobates tokuko* MHNLS 18523 (**d**), and *Aromobates ornatissimus* ULABG 4976 (**e**). Sphenethmoid, ventral anterior contour (character 230): medially notched (state 0) in **a**; straight (state 1) in **b**; convex (state 2) in **c**. **na:** nasal; **pa:** palatine; **sp:** sphenethmoid; **vo:** vomer.

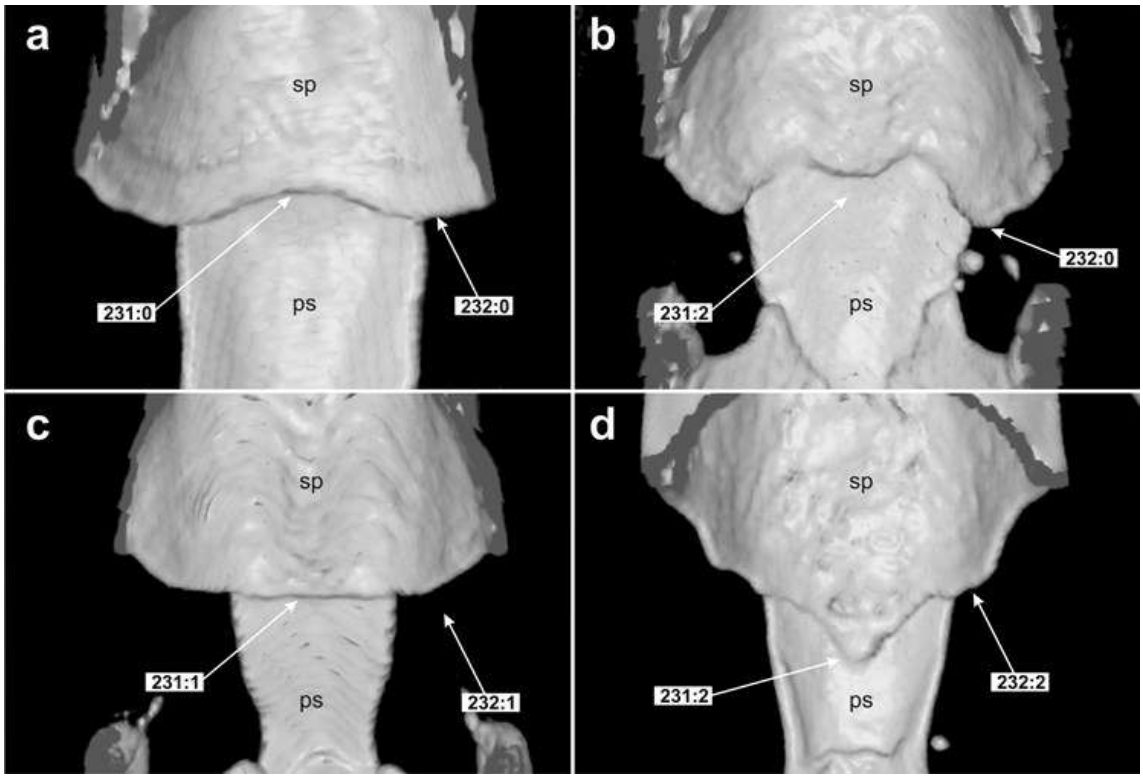

Figure 40. Dorsal view of the floor of the braincase, showing the posteroventral portion of the sphenethmoid in *Aromobates nocturnus* ULABG 2223 (**a**), *Aromobates zippeli* MHNLS 22052 (**b**), *Mannophryne* sp. MHNLS 21831 (**c**), and *Anomaloglossus wothuja* MHNLS 19992 (**d**). Sphenethmoid, floor posterior contour, dorsal to parasphenoid cultriform process (character 231): concave (state 0) in **a**; straight (state 1) in **c**; convex (state 2) in **b** and **d**. Sphenethmoid, posteroventral border, posterior extension in relation to the posterolateral borders (character 232): posteroventral border anterior to lateral ones (state 0) in **a**–**b**; posteroventral border to the level of the lateral ones (state 1) in **c**; posteroventral border posterior to lateral ones (state 2) in **d**. **ps:** parasphenoid; **sp:** sphenethmoid.

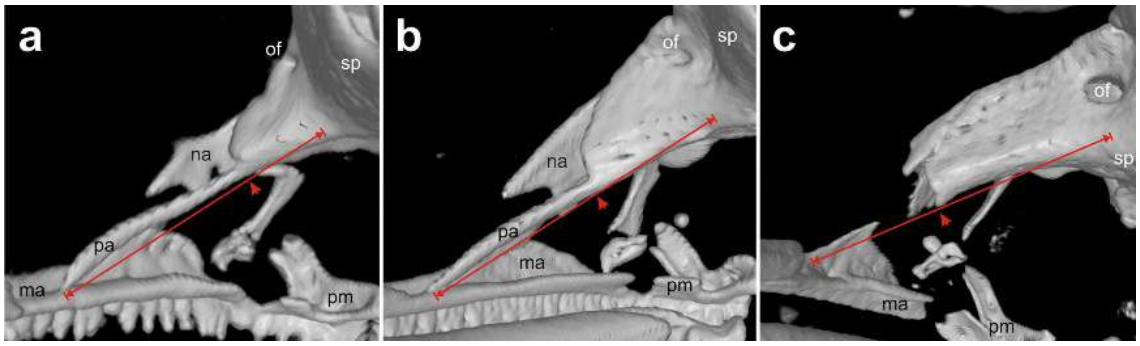

Figure 41. Posteroventral view of the skull, showing the anterolateral portion of the ocular orbit in *Anomaloglossus rufulus* MHNLS 20245 (**a**), *Mannophryne herminae* MHNLS 22111 (**b**), and *Adelophobates galactonotus* MCP 2252 (**c**). Sphenethmoid, ventrolateral process, extension (character 233): less than 1/3 of the distance between orbitonasal foramen and the maxilla (state 0) in **a**; 1/3 to 1/2 of the distance (state 1) in **b**; > 1/2 of the distance (state 2) in **c**.

234–239: Frontoparietal.

Frontoparietal is a paired dermal roofing bone that overlays the dorsal aspect of the braincase, it is usually the largest of the dorsal components of the skull; is located posterior to sphenethmoid, its lateral border forms the inner orbital margin, and posteriorly articulates to the otoccipital. Both frontoparietal are medially in contact, either extensively, or only in their posterior portion when a frontoparietal fenestra is present (Trueb 1993). Grant *et al*. (2006) scored the occurrence and degree of medial fusion of frontoparietals (character 234), and the occurrence of fusion between frontoparietal and otoccipital (character 235) in dendrobatoids. We additionally coded the variation in the ornamentation of the posterolateral corner of frontoparietal (character 236), the relation between its anterior and posterior width (character 237), the occurrence of a frontoparietal-sphenoethmoidal pit (character 238), and the shape of the orbital margin (character 239).

234. Frontoparietal, fusion (Grant *et al*. 2006): 0 = entirely free (articulating, but not fused); 1 = fused posteriorly; 2 = fused along entire length. Additive.

235. Frontoparietal-otoccipital, relation (Grant *et al*. 2006): 0 = free, articulating but not fused; 1 = fused.

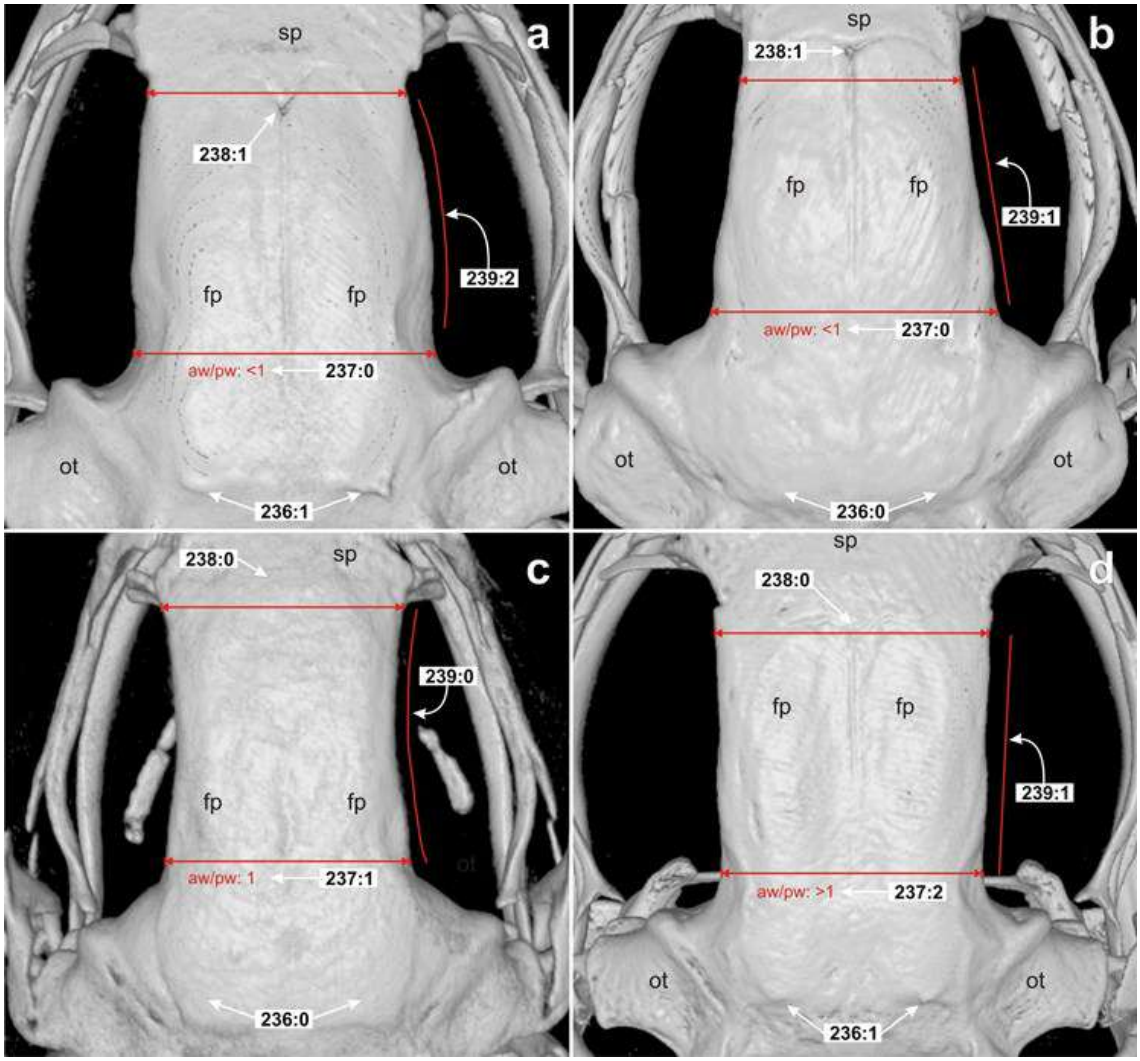

Figure 42. Dorsal view of the skull of *Aromobates zippeli* MHNLS 22052 (**a**), *Anonaloglossus rufulus* MHNLS 20245 (**b**), *Allobates olfersioides* MCP 12698 (**c**), and *Aromobates saltuensis* ULABG 4981 (**d**). Frontoparietal, posterolateral corner, ornamentation (character 236): smooth (state 0) in **b**–**c**; ornamented (weakly crested or with a small tubercles) (state 1) in **a** and **d**. Frontoparietals, anterior-posterior width ratio (character 237; two-tip red arrows indicate the anterios and posterior widths): slightly narrower anteriorly, aw/pw: <1 (state 0) in **a**–**b**; equally wide, aw/pw: 1 (state 1) in **c**; slightly wider anteriorly, aw/pw: >1 (state 2) in **d**. Frontoparietal-sphenoethmoidal pit (character 238): absent (state 0) in **c**–**d**; present (state 1) in **a**–**b**. Frontoparietals, orbital margin, shape (character 239; vertical red line highlights the form of the orbital margin): sligthly concave (state 0) in **c**; straight (state 1) in **b** and **d**; sligthly convex (state 2) in **2**. **fr:** frontoparietal; **ot:** otoccipital; **sp:** sphenethmoid.

236. Frontoparietal, posterolateral corner, ornamentation: 0 = smooth; 1 = ornamented (weakly crested or with small tubercles).

237. Frontoparietal, anterior-posterior width ratio: 0 = slightly narrower anteriorly (aw/pw: < 1); 1 = equally wide (aw/pw: 1); 2 = slightly wider anteriorly (aw/pw: > 1). Additive. (Figure 42).

The anterior width (aw) is measured between the anterolateral corners; the posterior width (pw) is measured at the posterior level of the orbits, previous to their posterolateral extension above the otoccipitals.

238. Frontoparietal-sphenoethmoidal pit: 0 = absent; 1 = present. (Figure 42).

239. Frontoparietals, orbital margin, shape: 0 = sligthly concave; 1 = straight; 2 = sligthly convex. Nonadditive. (Figure 42).

240–248: Otoccipital.

This is a paired bone formed by the fusion of the prootic and exoccipital, and constitutes the posterior part of the neurocranium (Lynch 1971). The portion that corresponds to the prootic lies behind the optic foramen. Dorsally, it forms the posterior margin of the frontoparietal fontanelle, constitutes almost all the posterior portion of the braincase, and covers the otic capsule; posteromedially delimits the orbit, and dorsolaterally forms a *crista parotica* that articulates with the *suspensorium* through the otic ramus of the squamosal. Exoccipital only occupies the posterior wall of the braincase, form the margin of the foramen magnum, and bears the occipital condyle that articulates the skull to the axial skeleton (Trueb 1993). Anterodorsally, otoccipital is covered by the posterior portion of the frontoparietal, whereas ventrally bears attached the

parasaphenoid, and ventrolaterally may be in contact with the medial process of pterygoid (Trueb 1993, Duellman & Trueb 1994). Otoccipital varies mainly in their degree of ossification among anurans, particularly between otoccipital and frontoparietal (Lynch 1971), but also in the dorsomedial and ventromedial articulations between pairs of exoccipitals and otoccipitals (Trueb 1993). Grant *et al*. (2006) coded the variation in the degree of ossification of the dorsal contact of exoccipitals (character 240). We noted that the ossification of the ventral articulation varies independently of the dorsal one, so we coded this as a different transformation series (character 246). Additionally, we coded the occurrence of a medial diagonal crest of the exoccipital (character 241), and scored the variation in the ornamentation of the posterior portion of the semicircular crest (character 242), in the orientation (in ventral view) of the posterior wall of the otic capsule (character 243) and the degree of ossification of the ventral-posterior corner of its capsule (character 244), the ocurrece of otoliths inside the inner ear (character 245), the ventral-medial articulation of the prootics above parasphenoid (character 246), and in the relation between otoccipital and parasphenoid (character 247).

240. Exoccipitals, dorsomedial contact (Grant *et al*. 2006): 0 = free, separate; 1 = fused sagitally.

241. Exoccipitals, medial diagonal crest, development: 0 = absent; 1 = weak; 2 = strong. Additive. (Figure 43).

242. Otoccipital, posterior semicircular crest, dorsal apophysis, development: 0 = absent; 1 = weak; 2 = strong. Additive. (Figure 43).

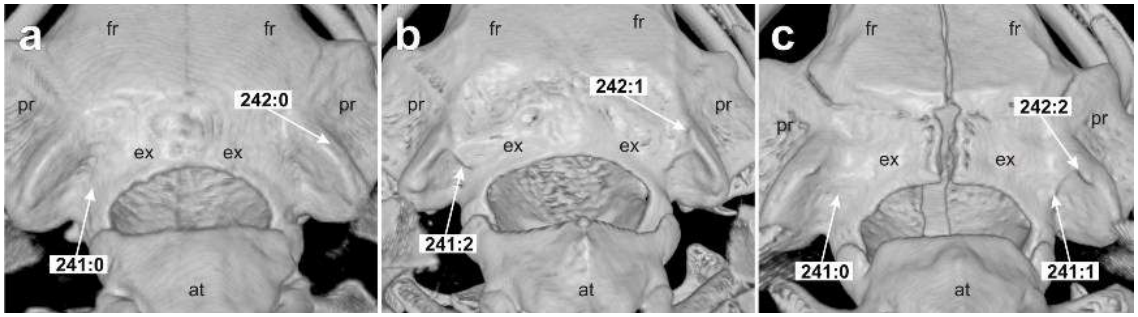

Figure 43. Posterodorosal view of the skull, showing the occipital region in *Mannbophryne volcano* MHNLS 21780 (**a**), *Aromobates saltuensis* ULABG 4981 (**b**), and *Aromobates walterarpi* ULABG 1577 (**c**). Exoccipitals, medial diagonal crest, development (character 241): absent (state 0) in **a** and **c**; weak (state 1) in **c**; strong (state 2) in **b**. Otoccipital, posterior semicircular crest, dorsal apophysis, development (character 242): absent (state 0) in **a**; weak (state 1) in **b**; strong (state 2) in **c**. **at:** atlas; **ex:** exoccipital; **fr:** frontoparietal; **pr:** prootic.

243. Otic capsule, posterior wall, orientation in ventral view: 0 = anteriorly oriented; 1 = laterally oriented; 2 = posteriorly oriented. Nonadditive. (Figure 44).

244. Otic capsule, ventral-posterior corner, development: 0 = open (notched); 1 = closed (not notched or slightly notched). (Figure 44).

245. Otoliths: 0 = absent; 1 = present. (Figure 45).

246. Exoccipitals, ventral-medial contact: 0 = free (not in contact or articulating, but not fused); 1 = fused. (Figure 46).

247. Prootics, ventral-medial contact: 0 = completely separate; 1 = anteriorly separate; 2 = completely fused. Additive. (Figure 46).

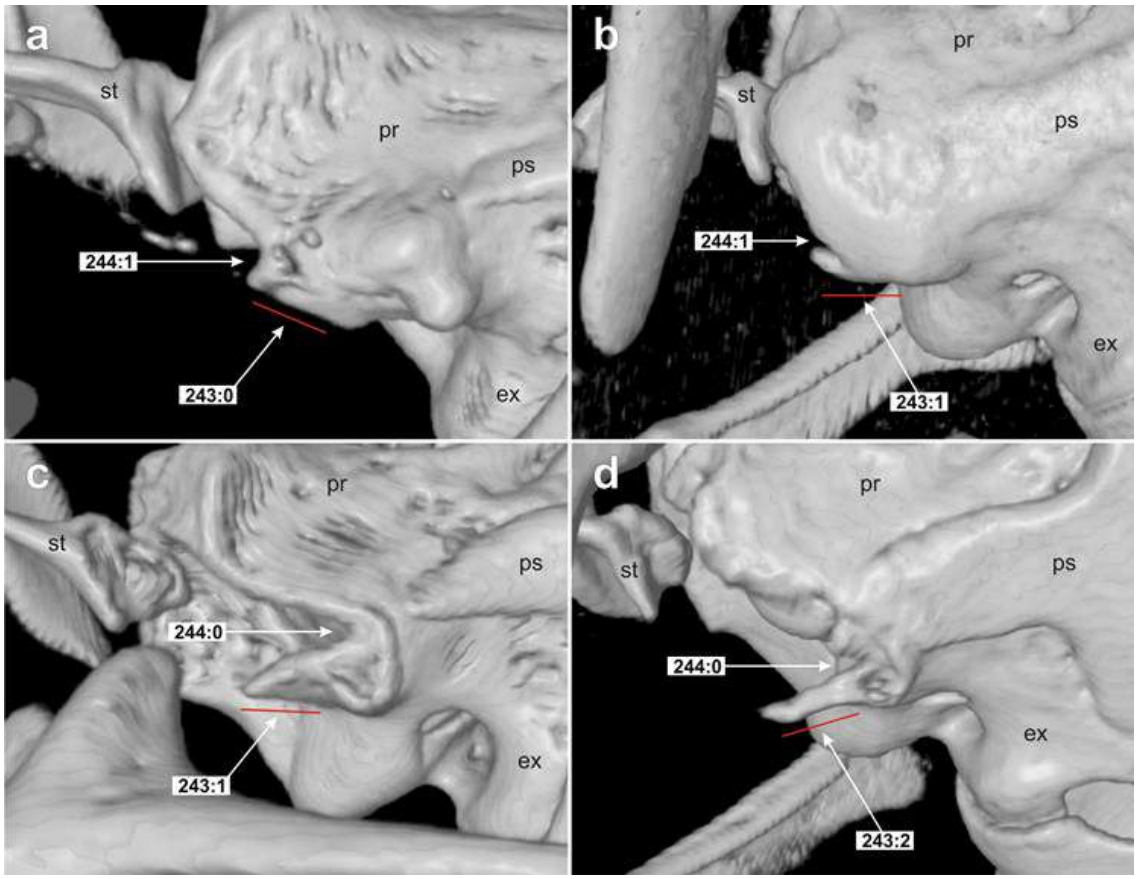

Figura 44. Ventral view of the lateroposterior portion of the skull, showing the otic region in *Mannophryne* sp. 4 MHNLS 22306 (**a**), *Anomaloglossus rufulus* MHNLS 20245 (**b**), *Aromobates walterarpi* ULABG 1577 (**c**), and *Aromobates ornatissimus* ULABG 4976 (**d**). Otic capsule, posterior wall, orientation in ventral view (character 243): oriented anteriad (state 0) in **a**; oriented laterad (state 1) in **b**–**c**; oriented posteriad (state 2) in **d**. Otic capsule, ventral-posterior corner, development (character 244): open (notched) (state 0) in **c**–**d**; closed (not notched or slightly notched) (state 1) in **a**–**b**. **ex:** exoccipital; **pr:** prootic; **ps:** parasphenoid; **st:** stapes (columella).

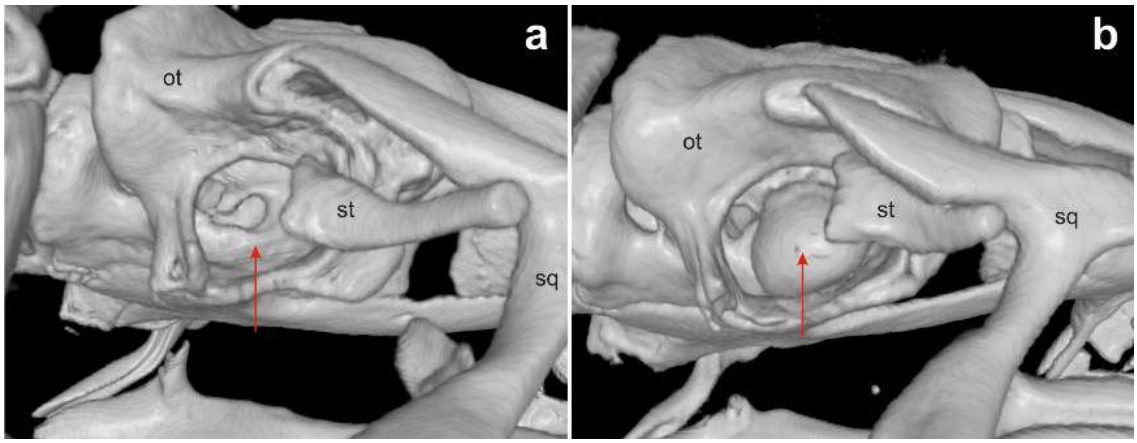

Figure 45. Lateroposterior view of the skull, showing the otic capsule in *Aromobates walterarpi* ULABG 1577 (**a**), and *Aromobates ornatissimus* ULABG 4976 (**b**). Otoliths (character 245): absent (state 0) in **a**; present (state 1) in **b**. **ot:** otoccipital; **sq:** squamosal; **st:** stapes.

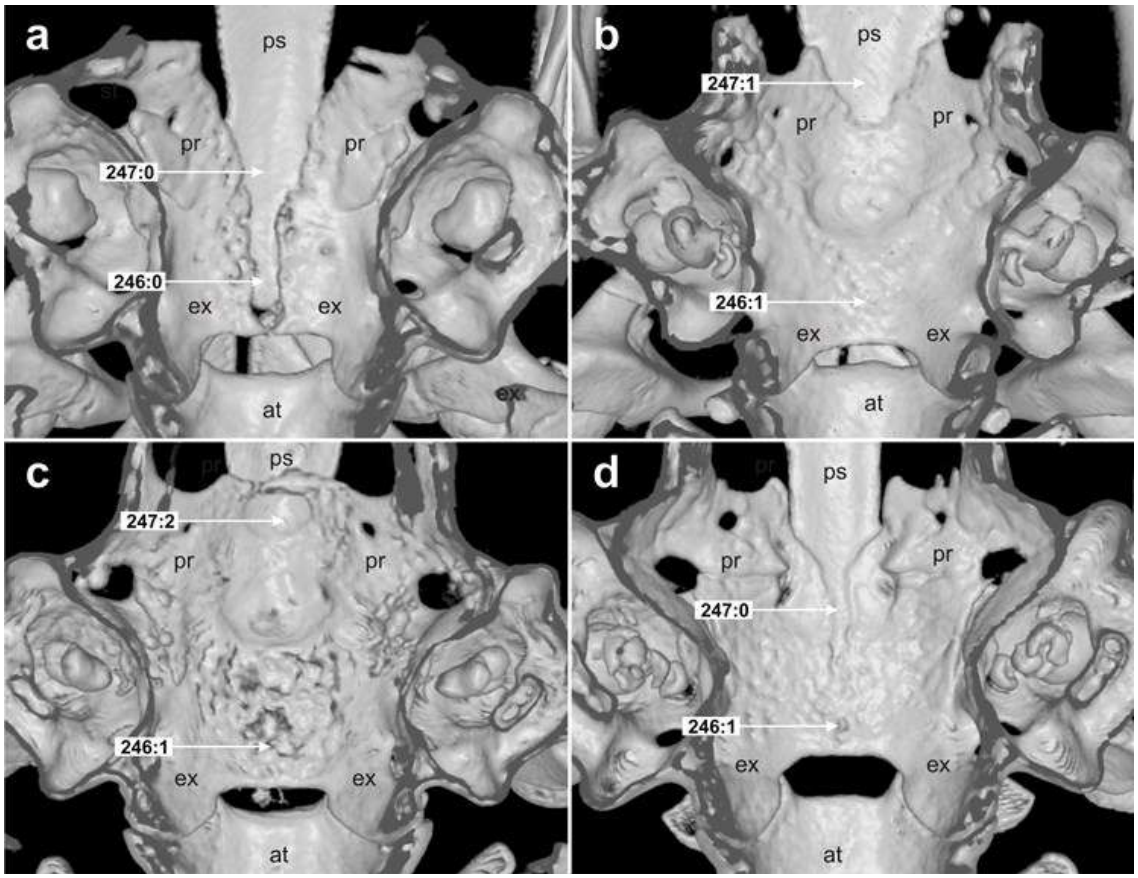

Figure 46. Dorsal view of the posterior portion of the floor of braincase in *Aromobates ornatissimus* ULABG 4976 (**a**), *Aromobates zippeli* MHNLS 22052 (**b**), *Aromobates saltuensis* ULABG 4981 (**c**), and *Mannophryne* sp. 4 MHNLS 22306 (**d**). Exoccipitals, ventral-medial contact (character 246): free (not in contact or articulating, but not fused) (state 0) in **a**; fused (state 1) in **b**–**d**. Prootics, ventral-medial contact (character 247): completely separate (state 0) in **a** and **d**; anteriorly separate (state 1) in **b**; completely fused (state 2) in **c**. **at:** atlas; **ex:** exoccipital; **pr:** prootic; **ps:** parasphenoid.

248. Otoccipital-parasphenoid, articulation: 0 = free (articulating borders defined); 1 = fused posteriorly; 2 = completely fused (limits almost indefined). Additive. (Figure 47).

249–256: Parasphenoid.

This unpaired, flat, and blade-like bone invests ventrally the braincase, and generally bears a pair of posterolateral alae that cover the ventral portion of the otic capsules; its medial portion (cultriform process) extends from the prootic region forward to reach the anterior portion of the neurocranium, which partially

invests the sphenethmoid posteromedial surface (Lynch 1971, Trueb 1993, Duellman & Trueb 1994). Variation in the extension, form, and orientation of the posterolateral alae and in the form and extension of the cultriform process have been scored in systematic studies of several groups of anurans (e.g., Lynch 1971, Mendelson *et al*. 2000). La Marca (1995) characterized the general pattern of the cultriform process in *Mannophryne* and Myers *et al*. (1991) noted differences in the tip of the cultriform process between *Aromobates nocturnus* and some collared frogs. However, this variation was not included in the phenotypic matrices of Grant *et al*. (2006, 2017). We modify the codification of the extension and lateral width of the posterolateral alae and the orientation of the lateral margins of the cultriform process (characters 250, 252, and 253, respectively) from Mendelson *et al*. (2000). Additionally, we score the extension of the parasphenoid posterior process (character 249), the orientation of the lateral alae on the horizontal plane (character 251), the ossification of the optic foramen (character 254), the degree of ossification between the parasphenoid and sphenethmoid (character 255), and the form of the cultriform process tip (character 256).

249. Parasphenoid, posterior process, extension: 0 = reaching the level of the jugular foramina; 1 = surpassing the level of the jugular foramina; 2 = reaching the border of the foramen magnum. Additive. (Figure 47).

250. Parasphenoid, posterolateral alae, extension (modified from Mendelson *et al*. 2000): 0 = does not reach the lateral margin of otic capsule; 1 = reaches the lateral margin of otic capsule. (Figure 47).

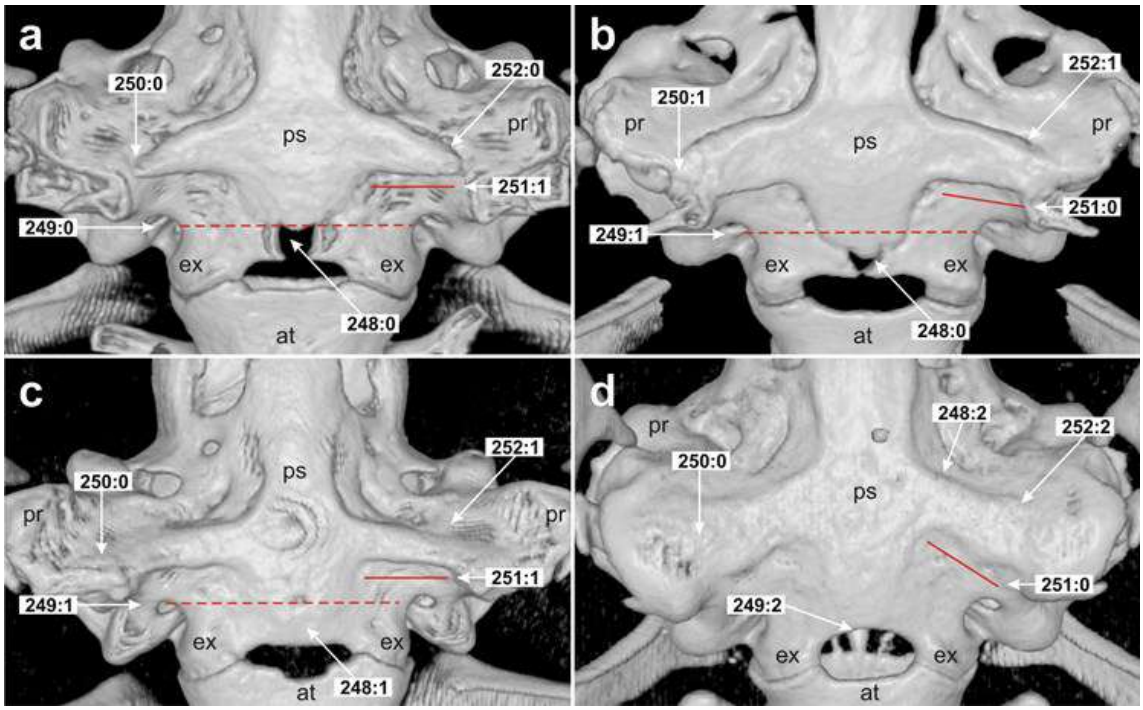

Figure 47. Ventral view of the skull showing the posterior portion of the palatal region in *Aromobates walterarpi* ULABG 1577 (**a**), *Aromobates ornatissimus* ULABG 4976 (**b**), *Mannophryne molinai* MHNLS 21337 (**c**), and *Anomaloglossus rufulus* MHNLS 20245 (**d**). Otoccipital-parasphenoid articulation (character 248): free (articulating borders defined) (state 0) in **a**–**b**; fused posteriorly (state 1) in **c**; completely fused (limits almost indefined) (state 2) in **d**. Parasphenoid, posterior process, extension (character 249): reaching the level of jugular foramina (state 0) in **a**; surpassing the level of jugular foramina (state 1) in **b**–**c**; reaching the border of foramen magnum (state 2) in **d**. Parasphenoid, posterolateral alae, extension (character 250): does not reach the lateral margin of otic capsule (state 0) in **a**, **c**–**d**; reaches the lateral margin of otic capsule (state 1) in **b**. Parasphenoid, posterolateral alae, orientation (character 251): oriented posterolaterally (state 0) in **b** and **d**; perpendicular to axial axis of skull (state 1) in **a** and **c**. Parasphenoid, posterolateral alae, lateral width (character 252): laterally narrower (state 0) in **a**; equally wide (or nearlu equal) laterally (state 1) in **b**–**c**; laterally wider (state 2) in **d**. **at:** atlas; **ex:** exoccipital; **pr:** prootic; **ps:** parasphenoid. Coninuous red line indicates the orientation of the posterolateral alae; red dashed line indicates the level of jugular foramina in a–c.

251. Parasphenoid, posterolateral alae, orientation: 0 = oriented posterolaterally; 1 = perpendicular to axial axis of skull. (Figure 47).

252. Parasphenoid, posterolateral alae, lateral width (modified from Mendelson *et al*. 2000): 0 = laterally narrower; 1 = equally wide (or nearly equal) laterally; 2 = laterally wider. Additive. (Figure 47).

Mendelson *et al*. (2000) coded two states to describe the lateral width of the alae of parasphenoid as related to the width at the the base in hemiphractids: “do not narrow laterally” (state 0), and “narrow laterally” (state 1). We recoded this transformation series in three states to better describe the variation observed in aromobatids.

253. Parasphenoid, cultriform process, lateral margins at the level of optic foramina, orientation (modified from Mendelson *et al*. 2000): 0 = parallel; 1 = anteriorly divergent. (Figure 48).

Character 1 of Mendelson *et al*. (2000) describes variation in the relation of the lateral margins of parasphenoid cultriform process in all its extension. We modified this character by restricting the observation of lateral margins’ relation to the mid-portion of cultriform process, to the level of optic foramina.

254. Optic foramen, contour, ossification: 0 = cartilaginous; 1 = fully ossified. (Figure 48).

255. Parasphenoid-sphenethmoid, articulation: 0 = free to partially fused (articulating borders defined); 1= fused (limits almost indefined). (Figure 48).

256. Parasphenoid, cultriform process, anterior tip, shape: 0 = straight or nearly straight; 1 = rounded to obtuse; 2 = pointed; 3 = bifid; 4 = trifid. Nonadditive. (Figure 48).

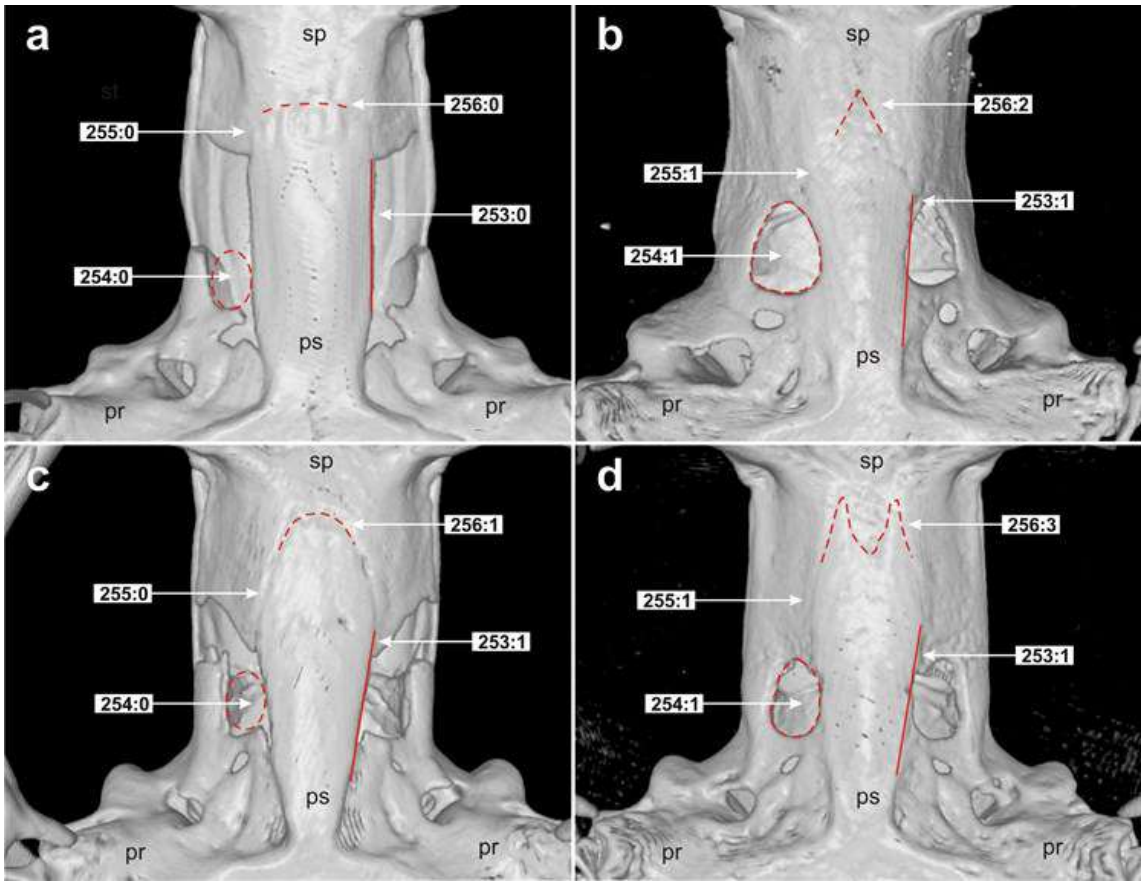

Figure 48. Ventral view of the skull, showing the mid portion of the palatal region in *Aromobates nocturnus* ULABG 2223 (**a**), *Hyloxalus cepedai* AF 49 (**b**), *Aromobates* sp. 1 MHNLS 22128 (**c**), and *Mannophryne venezuelensis* MHNLS 16454 (**d**). Parasphenoid, cultriform process, lateral margins at the level of optic foramina, orientation (character 253; indicated by the vertical red line): parallel (state 0) in **a**; anteriorly divergent (state 1) in **b**–**d**. Optic foramen, contour, pssificatio (character 254; right foramen highlighted by a red dashed line): cartilaginous (state 0) in **b** and **d**; fully ossified (state 1) in **a** and **c**. Parasphenoid-sphenethmoid, articulation (character 255): free to partially fused (articulating borders defined) (state 0) in **a** and **c**; fused (limits almost indefined) (state 1) in **b** and **d**. Parasphenoid, cultriform process, anterior tip, shape (character 256; highlighted by a red dashed line): straight or nearly straight (state 0) in **a**, rounded to obtuse (state 1) in **c**; pointed (state 2) in **b**, bifid (state 3) in **d**. **ps:** parasphenoid; **pr:** prootic; **sp:** sphenethmoid.

257–262: Premaxillary and maxillary teeth.

Dentition on maxillary arcade historically has been considered an important character in dendrobatoid systematics (Grant *et al*. 1997). Its absence was recently inferred as an unambiguous synapomorphy of Dendrobatini, which groups *Adelphobates*, *Andinobates*, *Dendrobates*, *Excidobates*, *Minyobates*, *Oophaga*, and *Ranitomeya* (Grant *et al*. 2017). Teeth morphology has also been considered in systematic studies, inasmuch most amphibians have

pedicellate teeth; but in Dendrobatoidea, as early noted by Myers *et al*. (1991) non-pedicellate teeth are synapomorphic (Grant *et al*. 2006, 2017). The occurrence of enlarged and fang-like teeth (posteromedially recurved) was listed as a diagnostic character of *Aromobates nocturnus* by Myers *et al*. (1991) and posteriorly defined as synapomorphic for *Nephelobates* (= *Aromobates*) by La Marca (1994b) and Mijares-Urrutia & La Marca (1997). La Marca (1992, 1994a, 1995) additionally highlighted the short teeth of *Mannophryne* as a diagnostic character useful to differentiate the species of this genus from its sister *Aromobates* (defined therein as the *Colostethus alboguttatus* group). However, size and shape of maxillary teeth were not included by Grant *et al*. (2006, 2017) in their studies due to difficulties to individuate transformation series related to the absence of a reference point to assess relative tooth size, the variation in tooth size along the maxillary arcade, and the continuous variation observed between species. We include all the tooth characters of Grant *et al*. (2006), and add as new, the number of premaxillary and maxillary teeth (characters 259 and 262, respectively), maxillary teeth length as measured above the preorbital process (character 263), and their shape (character 264).

257. Premaxillary teeth: 0 = absent; 1 = present.

258. Premaxillary tooth, structure: 0 = pedicelate; 1 = nonpedicelate.

259. Premaxillary tooth, number: 0 = < 10; 1 = 10–13; 2 = > 13. Additive.

260. Maxillary teeth (Grant *et al*. 2006): 0 = absent; 1 = present.

261. Maxillary tooth, structure (Grant *et al*. 2006): 0 = pedicelate; 1 = nonpedicelate.

262. Maxillary tooth, number: 0 = ≤ 33; 1 = 34–50; 2 = > 50. Additive.

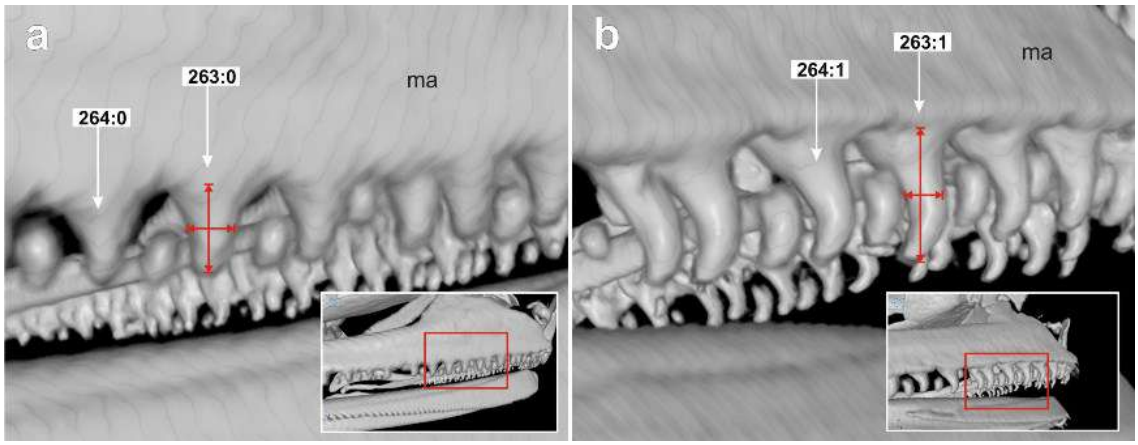

Figure 49. Lateral view of the maxilla, showing teeth at the level of the preorbital process in *Mannophryne neblina* MHNLS 4956 (**a**) and *Aromobates leopardalis* CVULA 5886 (**b**). Teeth, length at the level of preorbital process (character 263): th/tw < 2.0 (state 0) in **a**; th/tw ≥ 2.0 (state 1) in **b**. Maxillary teeth, shape (character 264): conical to almost conical (tip straight to weakly recurved) (state 0) in **a**, fang-like (tip markedly recurved posteromedially) (state 1) in **b**. **ma:** maxilla. Relation th/tw indicated with two-tip red arrows. Red rectangles on the right inferior frames indicate the portion of the maxilla below the preorbital process magnificated in **a** and **b**.

263. Teeth, length at the level of preorbital process: 0 = th/tw < 2.0; 1 = th/tw ≥ 2.0. (Figure 49).

Tooth height (th) is defined as the vertical distance, in straight-line from the tip of teeth to the midpoint of its base, which is delimited by the border of the maxillary bone; tooth width (tw) is measured as the horizontal length at the midlevel of teeth. It is important to note that if tw is measured at the base of teeth, the th/tw ratio hides differences between long and short teeth, because

the width at this level increases in the same proportion than the length of the teeth.

264. Maxillary teeth, shape of: 0 = conical to almost conical (tip weakly recurved); 1 = fang-like (tip markedly recurved posteromedially). (Figure 49).

265. Vomerine teeth (Grant *et al*. 2006): 0 = absent; 1 = present.

266–267: Angulosplenial (mandible).

Angulosplenial is the largest mandible bony component; its posterior portion forms the articular surface, which joins the lower jaw to the skull and extends forward along the lingual surface of the mandible investing the Meckel's cartilage (Trueb 1993, Duellman & Trueb 1994). Posterior to the articular surface extends the retroarticular process, which constitutes a synapomorphy of Dendrobatoidea (Myer & Ford 1986, Ford & Cannatella 1993, Grant *et al*. 2006, 2017). Significant variation in the development of the retroarticular process among dendrobatoids was noted by Myers *et al*. (1991), but Grant *et al*. (2006) only scored its occurrence (character 267) and not the variation in extension due to difficulties to delimit states. Anterior to the articular surface, rises dorsomedially the coronoid process, the point of insertion of the adductor muscles (Haas 2001, Ruiz-Monachesi *et al*. 2016). We score the variation observed in the orientation of the coronoid process in dendrobatoids (character 266).

266. Angulosplenial, coronoid process, orientation in lingual view: 0 = dorsally oriented; 1 = medially oriented. (Figure 50).

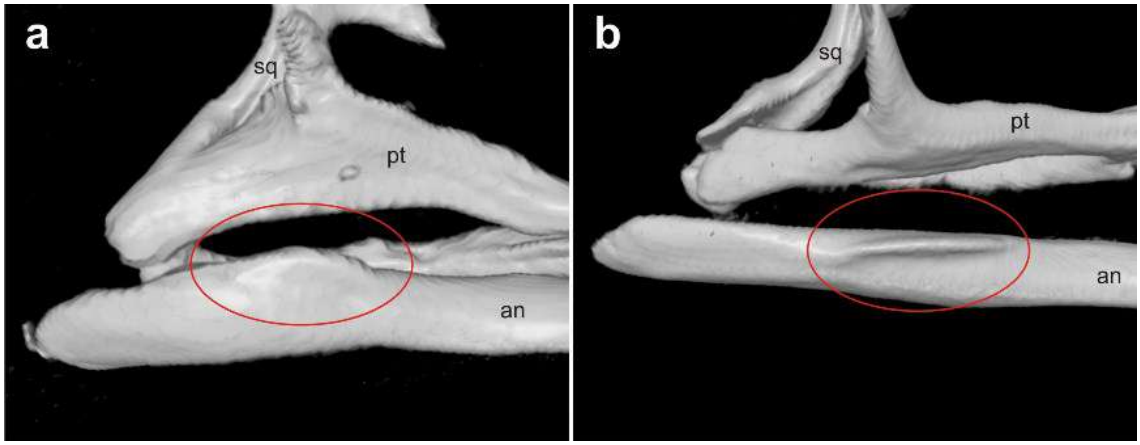

Figure 50. Lingual view of the posterior portion of the mandibular arcade of *Aromobates tokuko* MHNLS 18523 (**a**) and *Aromobates leopardalis* CVULA 5886 (**b**). Angulosplenial, coronoid process, orientation in lingual view (character 266): dorsally oriented (state 0) in **a**; medially oriented (state 1) in **b**. Coronoid process delimited by the red ellipse. **an:** angulosplenial; **pt:** pterygoid; **sq:** squamosal.

267. Mandible, retroarticular process (Grant *et al*. 2006): 0 = absent; 1 = present.

268. Skull proportions (De Sá *et al*. 2014): 0 = wider than long (w/l: > 1.1); 1 = as wide as long (or almost) (w/l: 0.9–1.1); 2 = longer than wide (w/l: < 0.9). Nonadditive.

Following De Sá *et al*. (2014), the width is taken at the wider level between both sides of the maxillary arch; length is measured from the right occipital condyle to the tip of the premaxilla on the same side.

269–315: Vertebrae and urostyle.

The axial skeleton of anurans is divided in three regions: presacral, sacral, and postsacral (Duellman & Trueb 1994). In aromobatids, as in many other anuran

groups, the presacral region consists of eight procoelus vertebrae (Myers *et al*. 1991, La Marca 1995). Vertebral fusion has been documented in some dendrobatids (Noble 1922, Silverstone 1975) and Grant *et al*. (2006) coded fusion between presacrals I–II, II–III and VIII with sacrum (characters 287–289). Presacral I (atlas) lacks transverse processes and bears a pair of atlantal cotyles that articulate to occipital condyles of the skull; presacrals II–VIII bear a pair of pre- and postzygoapophyses on the neural arch and a pair of transverse processes extending laterally from the pedicel; transverse processes of presacrals II–IV are distally expanded, provide muscular attachment for suspension of the pectoral girdle (Duellman & Trueb 1994), and in some cases may bear an ossified vestigial rib. The neural arch of all vertebrae typically is complete in dendrobatoidea and bears a very variable neural crest, usually decreasing posteriorly (La Marca 1995). The sacral region is represented only by the sacrum, a specialized vertebra that supports the pelvic girdle. The sacrum bears a pair of prezygoapophyses that articulate with postzygoapophyses of presacral VIII and posteriorly exhibits a bicondilar articulation with the urostyle; its transverse processes are distally expanded, forming the sacral diaphophyses, which articulates with the anterior tips of the ilia; a sesamoid bone may be present in this articulation. The degree of expansion of the sacral diapophyses has been considered in systematic studies of anurans (e.g., Schaeffer 1949, Lynch 1971) and Grant *et al*. (2006) scored variation on distal expansion of sacral diapophyses in dendrobatoids (character 285). The postsacral region is represented by the urostyle, a rodlike bone that represent the fusion of the postsacral elements; this bone lies between the ilia shafts and is attached to them by muscles (Duellman & Trueb 1994). In

dendrobatoids, the urostyle typically bears an anterodorsal process above the bicondilar articulation, from which a dorsal crest extends posteriorly; the anterolateral portion lacks transverse processes, but a poorly or moderately developed crest, starting from the posterolateral foramina of each side, may be present; the posterior tip of the urostyle may be expanded and circular or elliptical in cross-section. We score the variation observed in the degree of development of the neural crest of vertebrae I–VIII (characters 269–276), the posterior projection of the neural arch of vertebrae II–VIII (characters 277–283), the distal expansion of transverse processes of vertebra II (character 284), the occurrence of sesamiods in the articulation sacrum-ilia (character 285), the contour of the postzygoapophyses of vertebrae II–VIII (characters 290–296), the form of the ventral surface of the centrum of vertebrae III–VIII (character 297), the horizontal orientation of the transverse processes of vertebrae II–VIII (characters 298–304), the occurrence of an anterior and a posterodorsal apophysis on presacral III (characters 305 and 306, respectively), the occurrence of a vestigial ossified rib on the tip of the tranverse process of presacral IV (character 307), and the relative length of the transverse processes of vertebra VI in relation to the width of the neural arch (character 308). We individuate seven additional transformation series related to the urostyle: distal width of the anterodorsal process (character 309), occurrence of anterolateral foramina (character 310) and anterolateral crests (character 311), posterior extension of the neural crest (character 313), form of the posterior end in cross-section (character 314), and posterior expansion (character 315).

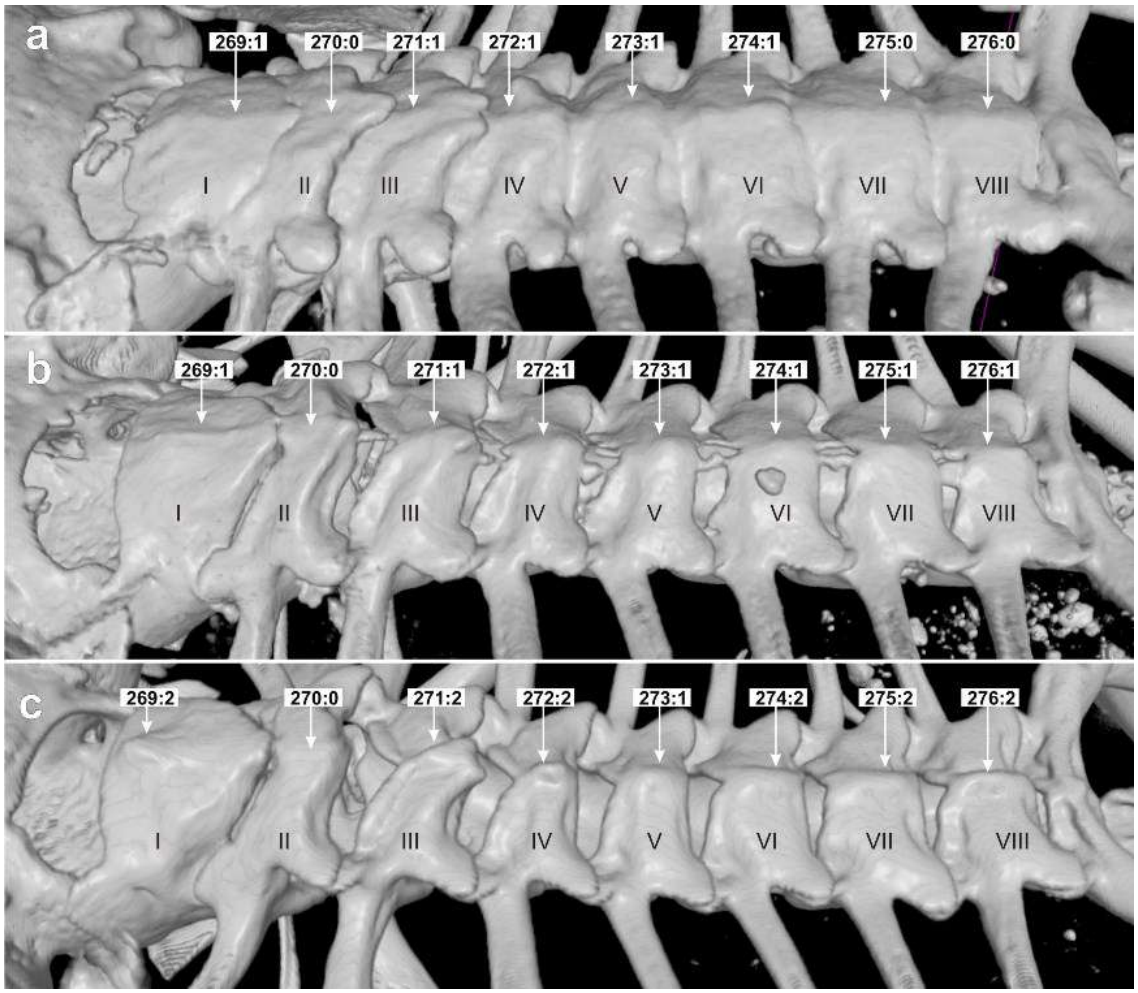

Figure 51. Laterodorsal view of the presacral region of vertebral column, showing the neural arch of all vertebrae in *Allobates pittieri* MHNLS 21488 (**a**), *Mannophryne* sp. 4 MHNLS 22306 (**b**), and *Aromobates capurinensis* CVULA 5920 (**c**). Atlas, neural crest, development (VI) and vertebrae II–VIII, neural crest, development (characters 269 to 276): absent (state 0), weak (state 1), and strong (state 2).

269. Atlas, neural crest, development: 0 = absent; 1 = weak; 2 = strong. Additive. (Figure 51).

270. Vertebra II, neural crest, development: 0 = absent; 1 = weak; 2 = strong. Additive. (Figure 51).

271. Vertebra III, neural crest, development: 0 = absent; 1 = weak; 2 = strong. Additive. (Figure 51).

272. Vertebra IV, neural crest, development: 0 = absent; 1 = weak; 2 = strong. Additive. (Figure 51).

273. Vertebra V, neural crest, development: 0 = absent; 1 = weak; 2 = strong. Additive. (Figure 51).

274. Vertebra VI, neural crest, development: 0 = absent; 1 = weak; 2 = strong. Additive. (Figure 51).

275. Vertebra VII, neural crest, development: 0 = absent; 1 = weak; 2 = strong. Additive. (Figure 51).

276. Vertebra VIII, neural crest, development: 0 = absent; 1 = weak; 2 = strong. Additive. (Figure 51).

277. Vertebra II, neural arch, posterior projection: 0 = anterior to the level of postzygoapophyses; 1 = to the level of postzygoapophyses; 2 = posterior to the level of postzygoapophyses. Additive. (Figure 52).

278. Vertebra III, neural arch, posterior projection: 0 = anterior to the level of postzygoapophyses; 1 = to the level of postzygoapophyses; 2 = posterior to the level of postzygoapophyses. Additive. (Figure 52).

279. Vertebra IV, neural arch, posterior projection: 0 = anterior to the level of the postzygoapophyses; 1 = to the level of the postzygoapophyses; 2 = posterior to the level of the postzygoapophyses. Additive. (Figure 52).

280. Vertebra V, neural arch, posterior projection: 0 = anterior to the level of postzygoapophyses; 1 = to the level of postzygoapophyses; 2 = posterior to the level of postzygoapophyses. Additive. (Figure 52).

281. Vertebra VI, neural arch, posterior projection: 0 = anterior to the level of postzygoapophyses; 1 = to the level of postzygoapophyses; 2 = posterior to the level of postzygoapophyses. Additive. (Figure 52).

282. Vertebra VII, neural arch, posterior projection: 0 = anterior to the level of postzygoapophyses; 1 = to the level of postzygoapophyses; 2 = posterior to the level of postzygoapophyses. Additive. (Figure 52).

283. Vertebra VIII, neural arch, posterior projection: 0 = anterior to the level of postzygoapophyses; 1 = to the level of postzygoapophyses; 2 = posterior to the level of postzygoapophyses. Additive. (Figure 52).

284. Vertebra II, transverse process, distal expansion: 0 = unexpanded (dw/bw: ≤ 1.0); 1 = weakly expanded (dw/bw: 1.1–1.7); 2 = moderately expanded (dw/bw: 1.8–2.4); 3 = greately expanded (dw/bw: > 2.4). Additive. (Figure 53).

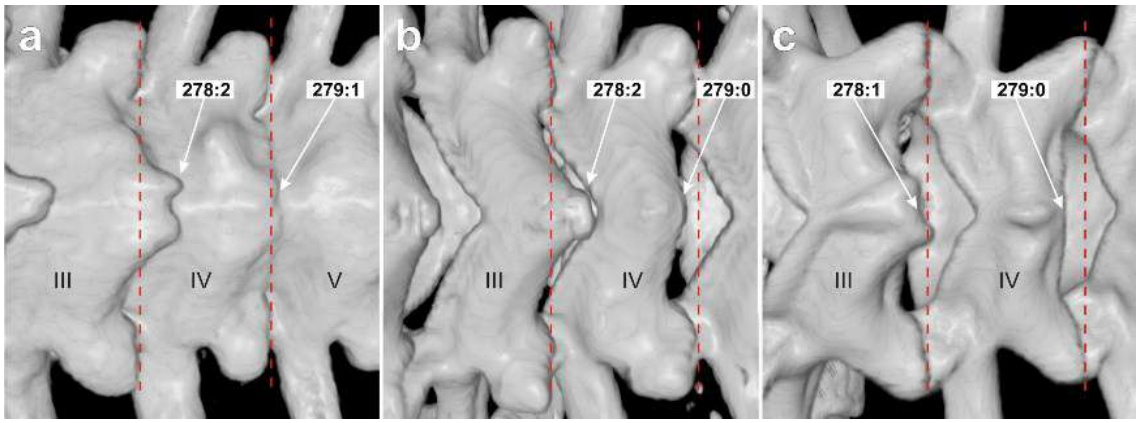

Figure 52. *Allobates pittieri* MHNLS 21488 (**a**), *Mannophryne lamarcai* MHNLS 22091 (**b**), and *Aromobates capurinensis* CVULA 5920 (**c**). Vertebrae II-VIII, neural arch, posterior projection (characters 278 to 283): anterior to the level of postzygoapophyses (state 0); to the level of postzygoapophyses (state 1); posterior to the level of postzygoapophyses (state 2).

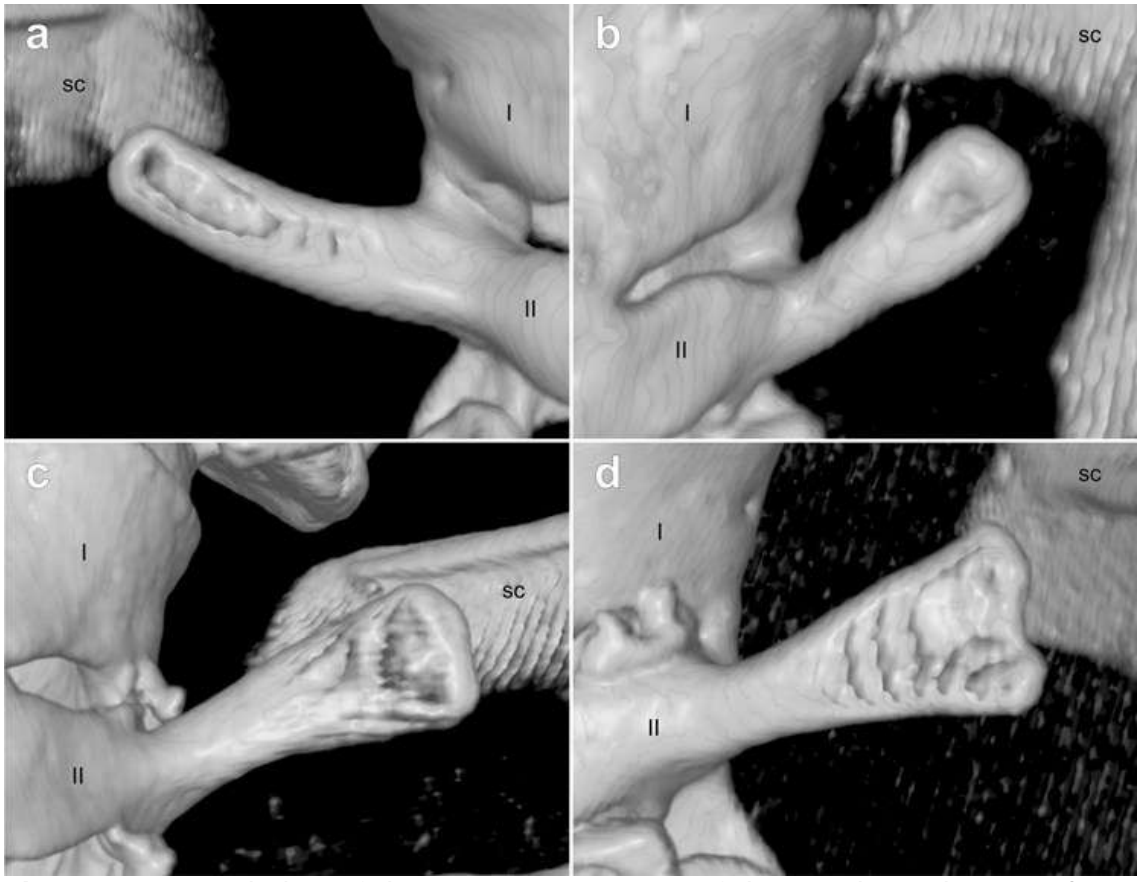

Figure 53. Ventral view of the transverse process of the vertebra II in *Aromobates capurinensis* CVULA 5920 (**a**), *Allobates olfersioides* MCP 12698 (**b**), *Mannophryne* sp. 4 MHNLS 22306 (**c**), and *Mannophryne collaris* MHNLS 21598 (**d**). Vertebra II, transverse process, distal expansion (character 284): unexpanded, dw/bw: up to 1.0 (state 0) in **a**; weakly expanded, dw/bw: 1.1–1.7 (state 1) in **b**; moderately expanded, dw/bw: 1.8–2.4 (state 2) in **c**; greatly expanded, dw/bw: > 2.4 (state 3) in **d**. **I:** centrum of the vertebra I (atlas); **II:** centrum of the vertebra II; **sc:** scapula.

285. Sacral diapophyses, distal expansion (Grant *et al*. 2006): 0 = unexpanded (< 1.5 x); 1 = weakly expanded (1.5–2.5 x); 2 = strongly expanded (> 2.5 x). Additive.

286. Sesamoids in lateral surface of each sacral diapophysis, in the area of iliosacral articulation (De Sá *et al*. 2014): 0 = absent; 1 = present. (Figure 54).

287. Vertebra VIII and sacrum (Grant *et al*. 2006): 0 = free; 1 = fused.

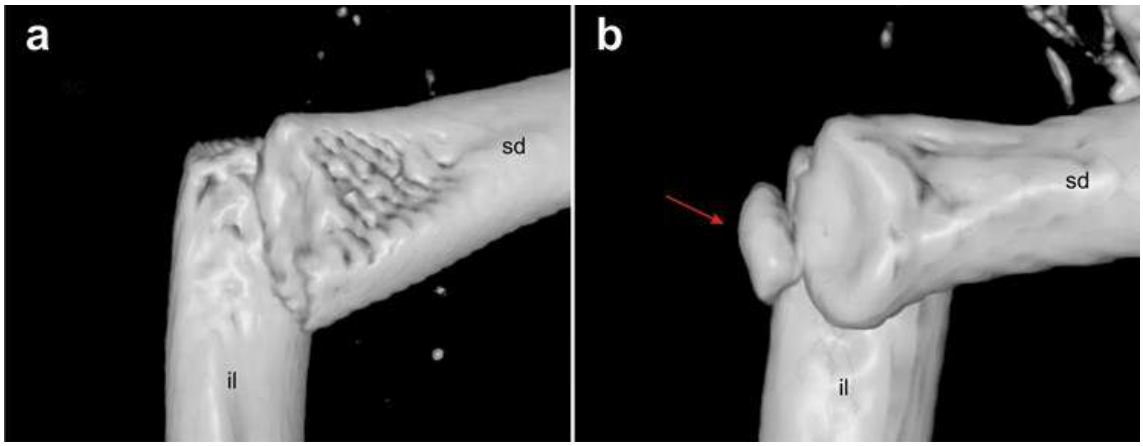

Figure 54. Dorsal view of the distal portions of the sacral diapophysis and ilium in *Aromobates alboguttatus* CVULA 1448, (**a**) and *Anomaloglossus rufulus* MHNLS 20245 (**b**). Sesamoids in lateral surface of each sacral diapophysis, in the area of iliosacral articulation (character 286): absent (state 0) in **a**; present (state 1) in **b**. **il:** ilium; **sd:** sacral diapophysis. Sesamoid bone indicated by the red arrow in **b**.

288. Vertebae I and II (Grant *et al*. 2006): 0 = free; 1 = fused.

289. Vertebae II and III (Grant *et al*. 2006): 0 = free; 1 = fused.

290. Vertebra II, postzygoapophysis, posterior margin, shape: 0 = concave; 1 = straight to nearly straight; 2 = convex. Nonadditive. (Figure 55).

291. Vertebra III, postzygoapophysis, posterior margin, shape: 0 = concave; 1 = straight to nearly straight; 2 = convex. Nonadditive. (Figure 55).

292. Vertebra IV, postzygoapophysis, posterior margin, shape: 0 = concave; 1 = straight to nearly straight; 2 = convex. Nonadditive. (Figure 55).

293. Vertebra V, postzygoapophysis, posterior margin, shape: 0 = concave; 1 = straight to nearly straight; 2 = convex. Nonadditive. (Figure 55).

294. Vertebra VI, postzygoapophysis, posterior margin, shape: 0 = concave; 1 = straight to nearly straight; 2 = convex. Nonadditive. (Figure 55).

295. Vertebra VII, postzygoapophysis, posterior margin, shape: 0 = concave; 1 = straight to nearly straight; 2 = convex. Nonadditive. (Figure 55).

296. Vertebra VIII, postzygoapophysis, posterior margin, shape: 0 = concave; 1 = straight to nearly straight; 2 = convex. Nonadditive. (Figure 55).

297. Vertebrae III–VII, ventral surface: 0 = slightly concave; 1 = flat to convex. (Figure 56).

298. Vertebra II, transverse process, orientation: 0 = directed anteriad; 1 = directed laterad; 2 = directed posteriad. Nonadditive. (Figure 57).

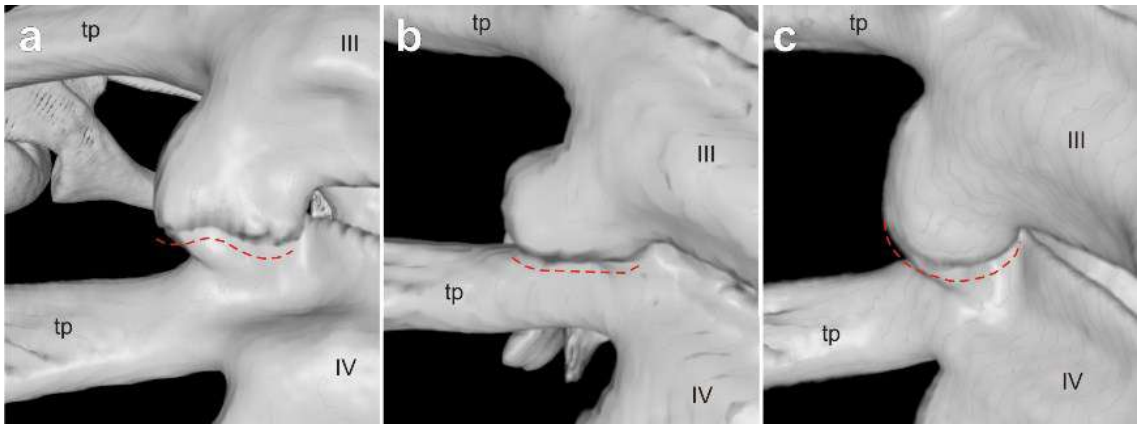

Figure 55. Dorsal view of the left postzygoapophysis of vertebra III in *Aromobates alboguttatus* CVULA 1448 (**a**), *Anomaloglossus rufulus* MHNLS 20245 (**b**), and *Mannophryne* sp. 4 MHNLS 22306 (**c**). Vertebrae II–VIII postzygoapophysis, posterior margin, shape (characters 290–296): concave (state 0) in **a**; straight to nearly straight (state 1) in **b**; convex (state 2) in **c**. **III:** neural arc of the vertebra III; **IV:** neural arc of the vertebra IV; **tp:** tranverse process. Red dashed lines highlight the form of the posterior contour of the postzygoapophysis.

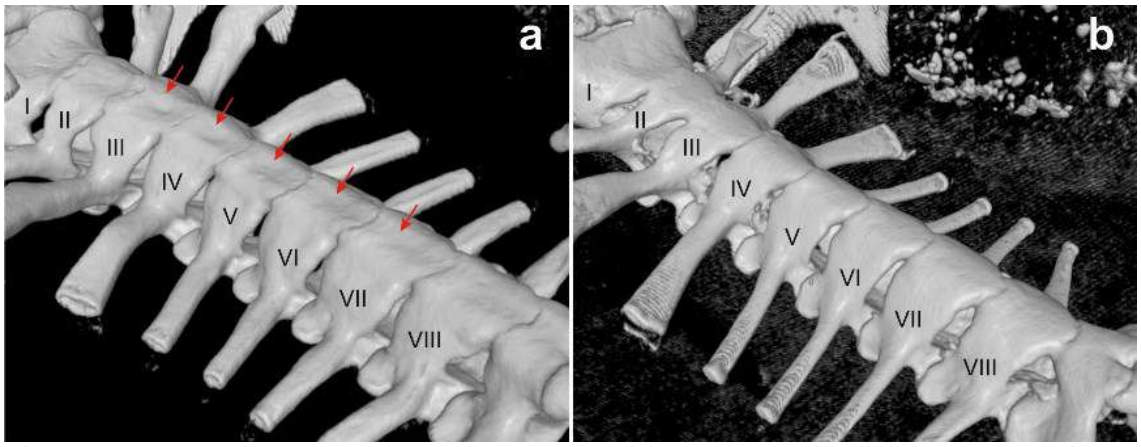

Figure 56. Ventral surface of vertebrae III–VII (character 297): slightly concave (state 0) in *Aromobates leopardalis* CVULA 5886 (**a**); flat to convex (state 1) in *Mannophryne collaris* MHNLS 21598 (**b**).

299. Vertebra III, transverse process, orientation: 0 = directed anteriad; 1 = directed laterad; 2 = directed posteriad. Nonadditive. (Figure 57).

300. Vertebra IV, transverse process, orientation: 0 = directed anteriad; 1 = directed laterad; 2 = directed posteriad. Nonadditive. (Figure 57).

301. Vertebra V, transverse process, orientation: 0 = directed anteriad; 1 = directed laterad; 2 = directed posteriad. Nonadditive. (Figure 57).

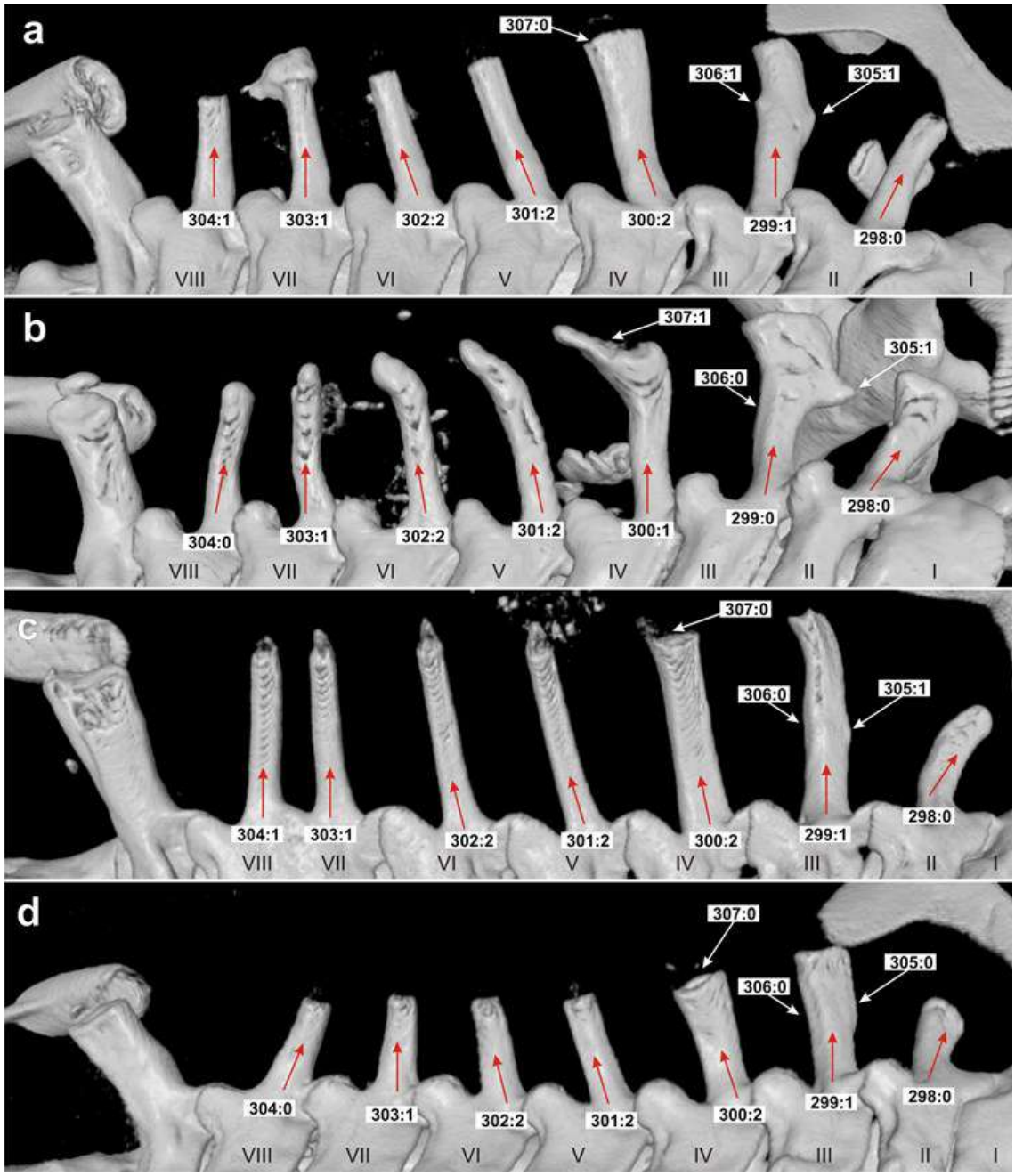

Figure 57. *Aromobates leopardalis* CVULA 5886 (**a**), *Anomaloglossus rufulus* MHNLS 20245 (**b**), *Aromobates orostoma* CVULA 3325 (**c**), and *Aromobates ornatissimus* ULABG 4976 (**d**). Vertebrae II–VIII, transverse process, orientation (characters 298 to 304): directed anteriad (state 0); directed laterad (state 1); directed posteriad (state 2). Anterior apophysis of transverse process of vertebra III (character 305): absent (state 0) in **d**; present (state 1) in **a**–**c**. Posterodorsal apophysis of transverse process of vertebra III (character 306): absent (absent) in **b**–**d**; present (state 1) in **a**. Ossified vestigial rib of vertebra IV (character 307): absent (state 0) in **a**, **c**–**d**; present (state 1) in **b**. Red arrows indicate the horizontal orientation of the transverse processes.

302. Vertebra VI, transverse process, orientation: 0 = directed anteriad; 1 = directed laterad; 2 = directed posteriad. Nonadditive. (Figure 57).

303. Vertebra VII, transverse process, orientation: 0 = directed anteriad; 1 = directed laterad; 2 = directed posteriad. Nonadditive. (Figure 57).

304. Vertebra VIII, transverse process, orientation: 0 = directed anteriad; 1= directed laterad; 2 = directed posteriad. Nonadditive. (Figure 57).

305. Vertebra III, transverse process, anterior apophysis: 0 = absent; 1 = present. (Figure 57).

306. Vertebra III, transverse process, posterodorsal apophysis: 0 = absent; 1 = present. (Figure 57).

307. Vertebra IV, ossified vestigial rib: 0 = absent; 1 = present. (Figure 57).

308. Vertebra VI, transverse process, relative length to neural arch width: 0 = very short (≤ 50 %); 1 = short (51–85 %); 2 = as long as the neural arch width (86–105%); 3 = moderately long (106–125 %); 4 = very long (> 125 %). Additive. (Figure 58).

309. Urostyle, anterodorsal process, shape: 0 = narrower at the tip than at the base; 1 = as wide at the tip as at the base; 2 = wider at the tip than at the base. Additive. (Figure 59).

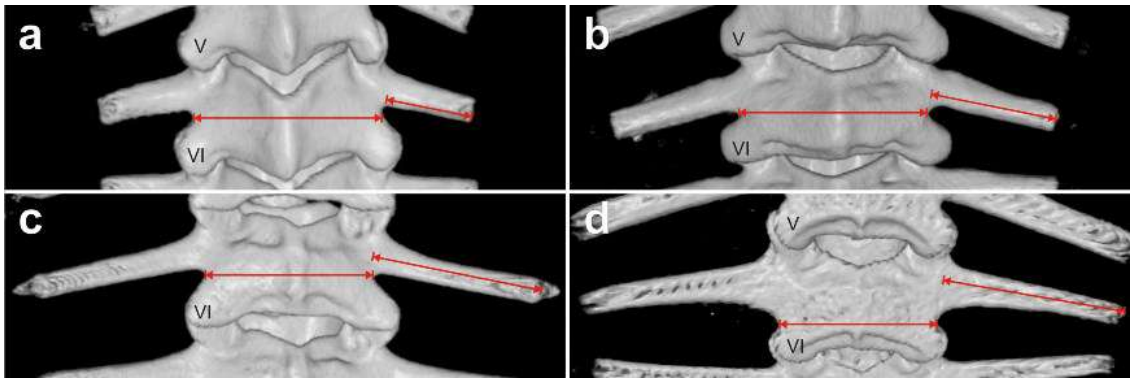

Figure 58. Dorsal view of the vertebra VI in *Aromobates ornatissimus* ULABG 4976 (**a**), *Aromobates leopardalis* CVULA 5886 (**b**), *Aromobates orostoma* CVULA 3325, and *Thoropa miliaris* MCP 12229 (**d**). Vertebra VI, transverse process, relative length to neural arch width (character 308): very short, up to 50% (state 0) in **a**; short, 51–85 % (state 1) in **b**; as long as neural arch wide, 86–105 % (state 2) in **c**; moderately long, 106–125 % (state 3) in **d**.

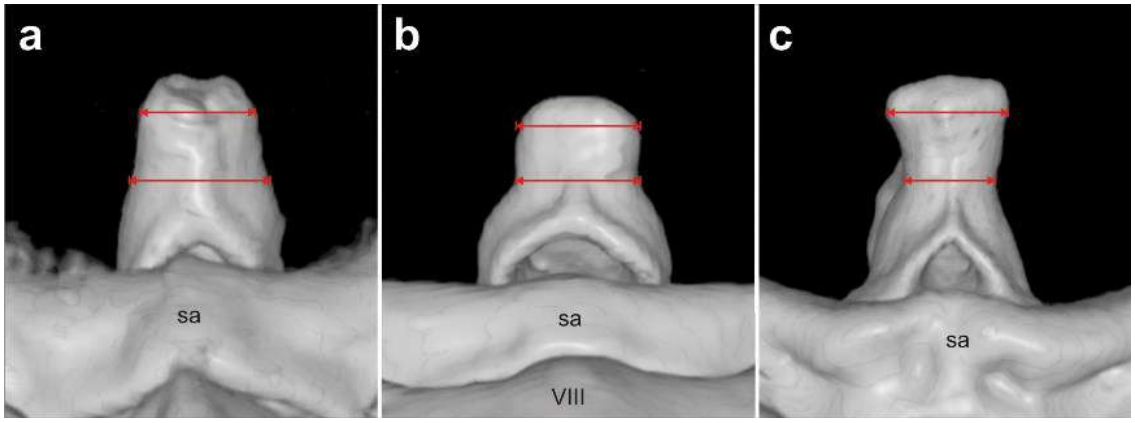

Figure 59. Anterior view of the anterodorsal process of urostyle (character 309): narrower at the tip than at the base (state 0) in *Aromobates ornatissimus* ULABG 4976 (**a**); as wide at the tip as at the base (state 1) in *Mannophryne lamarcai* MHNLS 22091 (**b**); wider at the tip than at the base (state 2) in *Aromobates orostoma* CVULA 3325 (**c**). **sa:** sacrum; **VIII:** vertebra VIII.

310. Urostyle, anterolateral foramina: 0 = absent; 1 = present. (Figure 60).

311. Urostyle, anterolateral crests, development: 0 = absent; 1 = weak; 2 = strong. Additive. (Figure 60).

312. Urostyle, dorsal sulcus, size: 0 = absent; 1 = short; 2 = long. Additive. (Figure 61).

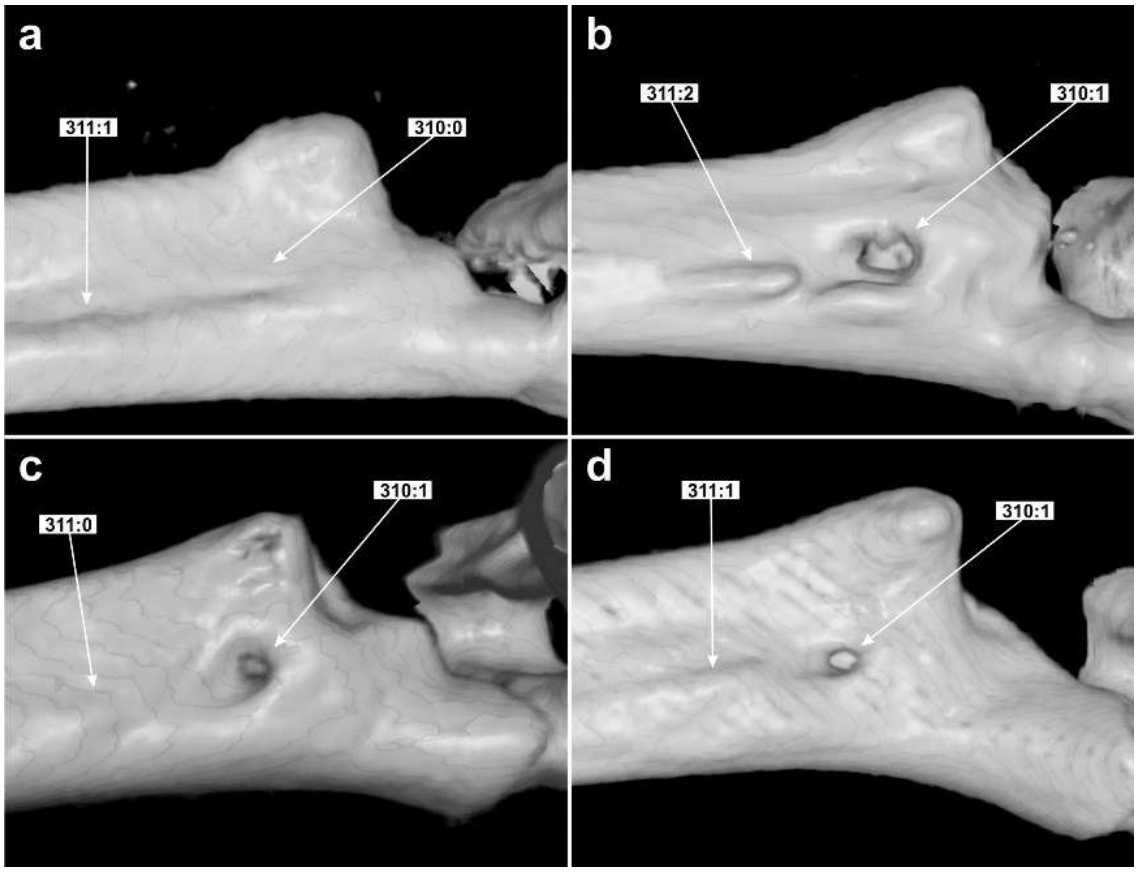

Figure 60. Lateral view of the anterior portion of the urostyle in *Allobates pittieri* MHNLS 21488 (**a**), *Mannophryne lamarcai* MHNLS 22091 (**b**), *Aromobates capurinensis* CVULA 5920 (**c**), and *Aromobates orostoma* CVULA 3325 (**d**). Anterolateral foramina of urostyle (character 310): absent (state 0) in **a**; present (state 1) in **b**–**d**. Anterolateral crests of urostyle (character 311): absent (state 0) in **c**; weak (state 1) in **a**, and **d**; strong (state 2) in **b**.

313. Urostyle, neural crest, extension: 0 = on the anterior half; 1 = on the two anterior thirds; 2 = almost reaching the distal end. Additive. (Figure 61).

314. Urostyle, distal end, shape in cross-section: 0 = circular (w/h: 1.0–1.1); 1 = slightly elliptical (w/h: 1.2–2.4); 2 = strongly ellipitical (w/h: > 2.4). Nonadditive. (Figure 62).

315. Urostyle, distal expansion in dorsal view: 0 = unexpanded (1.0–1.1); 1 = weakly expanded (1.2–1.6); 2 = moderately expanded (> 1.6). Additive. (Figure 61).

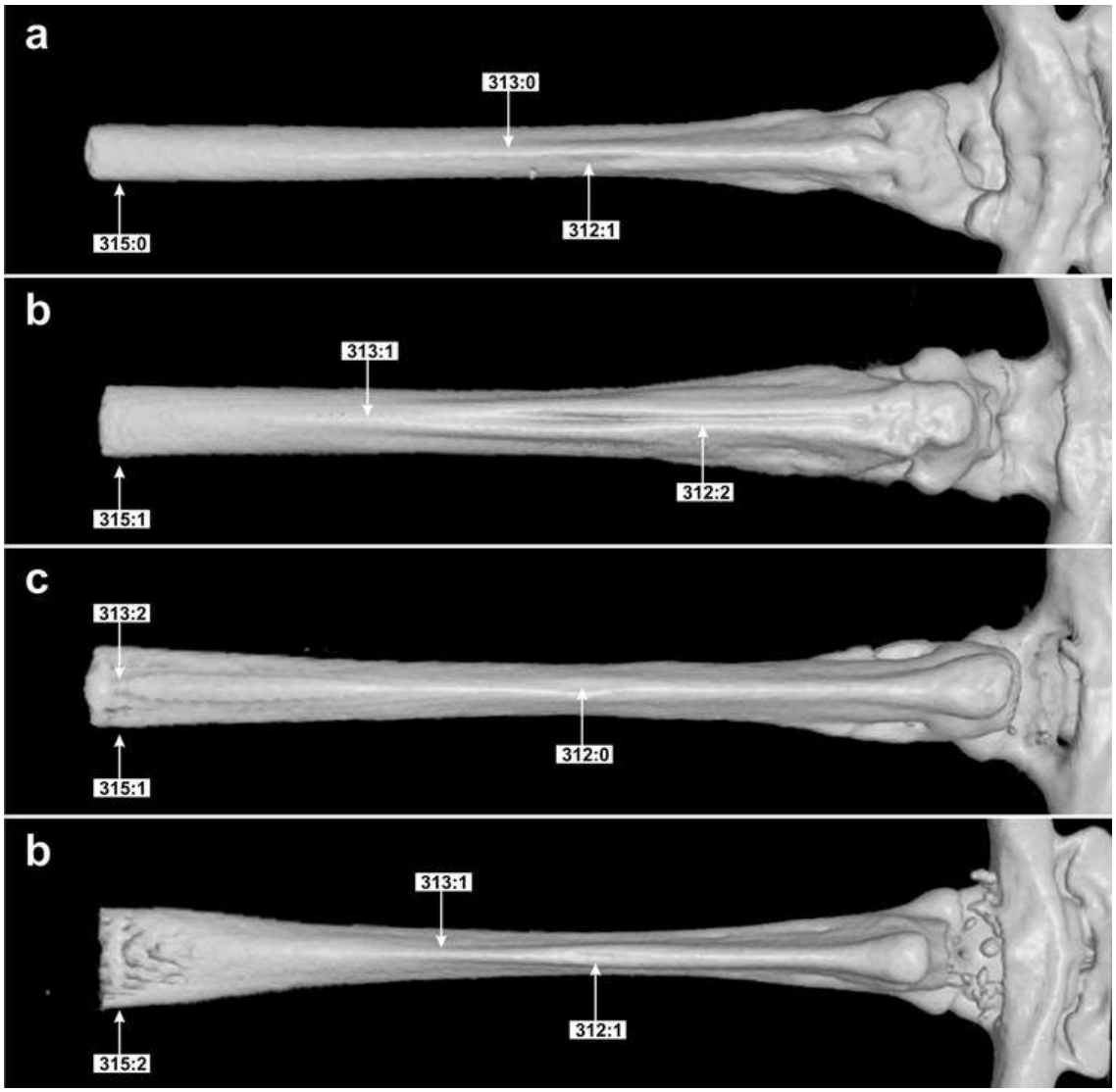

Figure 61. Dorsal view of the postsacral region of *Ranitomeya toraro* MCP 13107 (**a**), *Aromobates leopardalis* CVULA 5886 (**b**), *Mannophryne lamarcai* MHNLS 22091 (**c**), and *Mannophryne* sp. 4 (**d**). Urostyle, dorsal sulcus, size (character 312): absent (state 0) in **c**; short (state 1) in **a**; long (state 2) in **b**. Urostyle, neural crest, extension (character 313): on the anterior half (state 0) in **a**; on the two anterior thirds (state 1) in **b**; almost reaching the distal end (state 2) in **c**. Urostyle, distal expansion in dorsal view (character 315): unexpanded, 1.0–1.1 (state 0) in **a**; weakly expanded, 1.2–1.6 (state 1) in **b**–**c**; moderately expanded, > 1.6 (state 2) in **d**.

316–325: Ilium.

Ilium is the largest of three paired bones that integrate the pelvic girdle. It consists of two main portions: an anterior shaft that articulates with the sacral diapophysis of the sacrum, which may bear a dorsal crest and a posterior expansion that forms the anterior half of the acetabulum. The posterior expansion medially connecs both ilia by a symphysis, articulates

ventroposteriorly with the ischium, and ventroanteriorly with the pubis; the *margo acetabularis* delimits the acetabular fossa and may be dorsally a small supraacetabular fossa. On the anterodorsal surface of the posterior expansion, porterior to the ilial shaft, is the dorsal prominence. This may bear laterally adjoined, a knoblike, dorsal protuberance, and ventrally, a tubercular fossa. The ilium of anurans has been very valuable in taxonomy (particularly in fossil taxa) due to its abundant anatomical features, consistently variable among groups (Lynch 1971, Gómez & Turazzini 2015), but it has not been considered in systematic studies of dendrobatoids (Grant *et al*. 2006, 2017). We score variation observed in the ilial crest—height (character 316), shape of anterior end (character 317), and orientation of anterior portion (character 318)—, the orientation of the anterior tips of ilia (character 319), form of its tip in cross-section (character 320), presence of a tubercular fossa (character 321), development of the dorsal prominence (character 322), and dorsal protuberance (character 323), orientation of dorsal protuberance (character 324), and occurrence of a supraacetabular fossa (character 325).

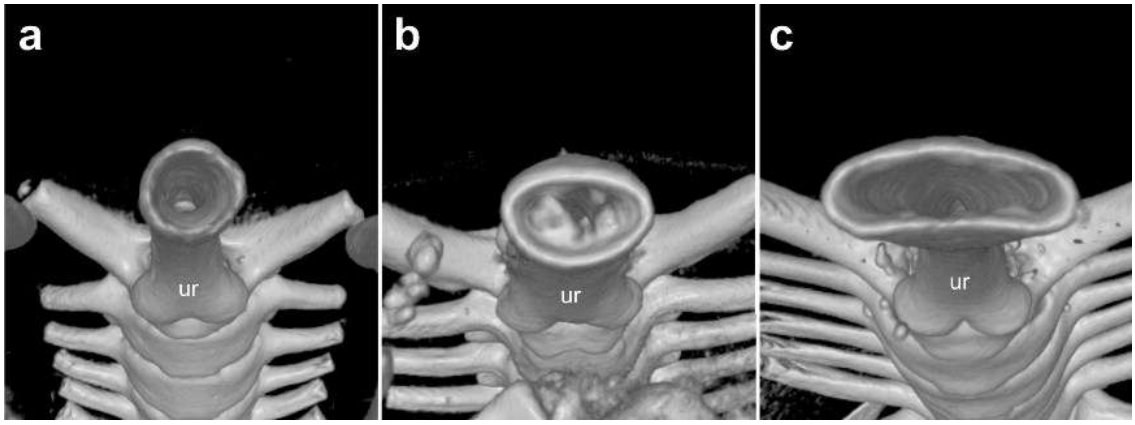

Figure 62. Posterior view of the urostyle of *Aromobates ornatissimus* ULABG 4976 (**a**), *Aromobates leopardalis* CVULA 5886 (**b**), and *Mannophryne* sp. 4 (**c**). Urostyle, distal end, shape in cross-section (character 314): circular, w/h: 1.0–1.1 (state 0) in **a**; slightly elliptical, w/h: 1.2–2.4 (state 1) in **b**; strongly ellipitical, w/h: > 2.4 (state 2) in **c**. **ur:** urostyle.

316. Ilial crest, midlevel of the schaft, height: 0 = absent; 1 = very low (≤ 25 % of the shaft height); 2 = low (26–50 % of the shaft height); 3 = high (51–100 % of the shaft height); 4 = very high (> 100 % of the shaft height). Additive. (Figure 63).

317. Ilial crest, anterior end, shape: 0 = sloped; 1 = stepped. (Figure 63).

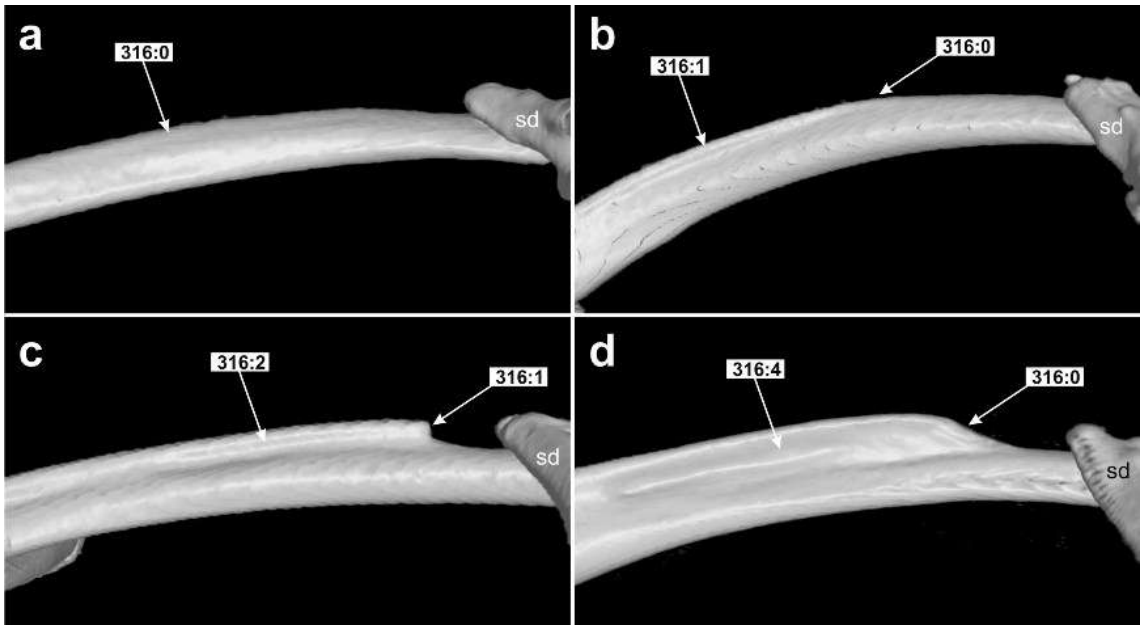

Figure 63. Inner view of the shaft of the ilium in *Ranitomeya toraro* MCP 13107 (**a**), *Aromobates zippeli* MHNLS 22052 (**b**), *Mannophryne lamarcai* MHNLS 22091 (**c**), and *Aromobates tokuko* MHNLS 18523 (**d**). Ilial crest, midlevel of the schaft, height (character 316): absent (state 0) in **a**; very low, ≤ 25 % of the shaft height (state 1) in **b**; low, 26–50 % of the shaft height (state 2) in **c**; very high, > 100 % of the shaft height (state 4) in **d**. Ilial crest, anterior end, shape (character 317): sloped (state 0) in **b** and **d**; stepped (state 1) in **c**. **sd:** sacral diapophysis.

318. Ilial crest, anterior portion, orientation: 0 = medial; 1= dorsal; 2 = lateral. Nonadditive. (Figure 64).

319. Ilium, anterior tip, orientation: 0 = slightly oriented medially; 1 = anterior; 2 = sligthly oriented laterally. Nonadditive. (Figure 65).

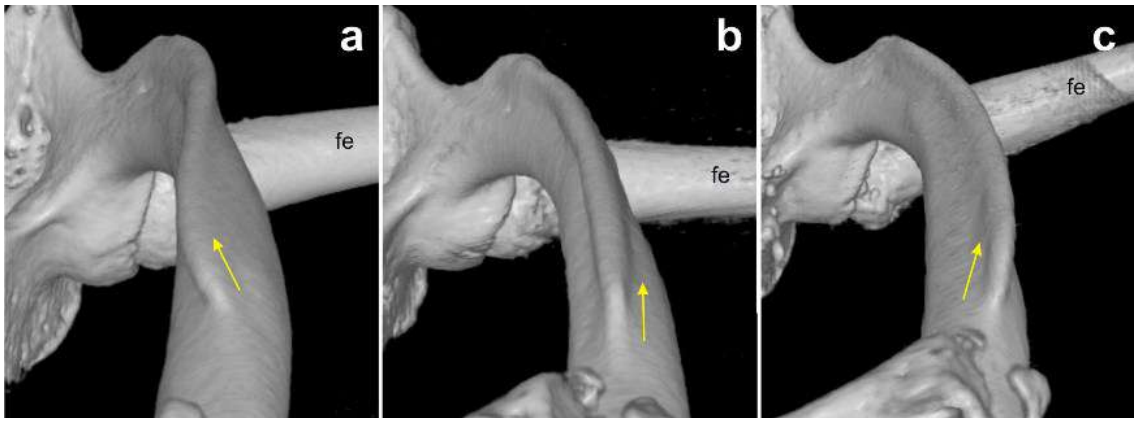

Figure 64. Ilial crest, anterior portion, orientation (character 318; indicated by yellow arrows): medial (state 0) in *Mannophryne collaris* MHNLS 21598 (**a**); dorsal (state 1) in *Mannophryne lamarcai* MHNLS 22091 (**b**); lateral *Mannophryne urticans* MHNLS 21563 (**c**). **fe:** femur.

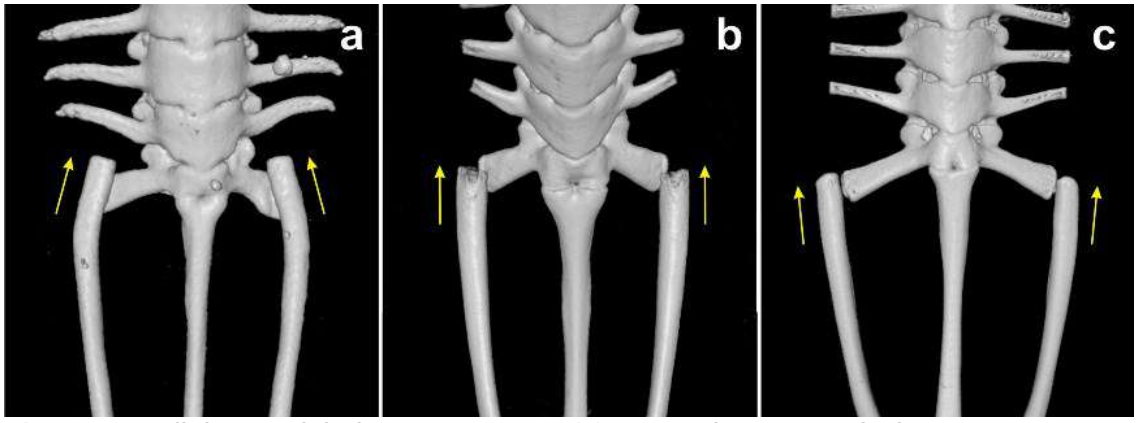

Figure 65. *Allobates pittieri* MHNLS 21488 (**a**), *Aromobates ornatissimus* ULABG 4076 (**b**), and *Mannophryne collaris* MHNLS 21598 (**c**). Ilium, anterior tip, orientation (character 319; indicated by yellow arrows): markedly to slightly oriented medially (state 0) in **a**; anterior (state 1) in **b**; sligthly oriented laterally (state 2) in **c**.

320. Ilium, anterior end, shape in cross-section: 0 = circular; 1 = elliptical; 2 = reniform. Nonadditive. (Figure 66).

321. Ilium, tubercular fossa: 0 = absent; 1 = present. (Figure 67).

322. Ilium, dorsal prominence: 0 = undifferentiated; 1 = weakly differentiated; 2 = well-differentiated. Additive. (Figure 67).

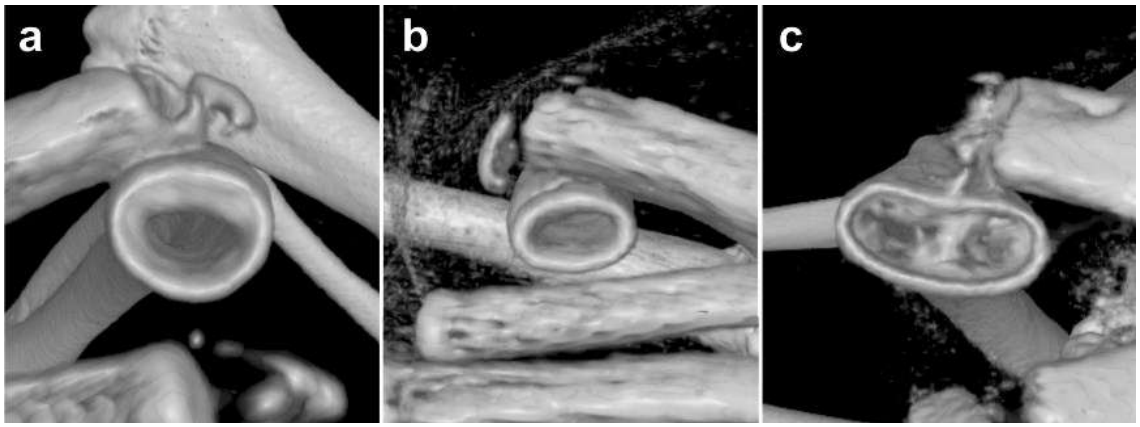

Figure 66. Ilium, anterior end, shape in cross-section (character 320): circular (state 0) in *Mannophryne* sp. 4 MHNLS 22306 (**a**); elliptical (state 1) in *Mannophryne urticans* MHNLS 21563 (**b**); reniform (state 2) in *Aromobates leopardalis* CVULA 5886.

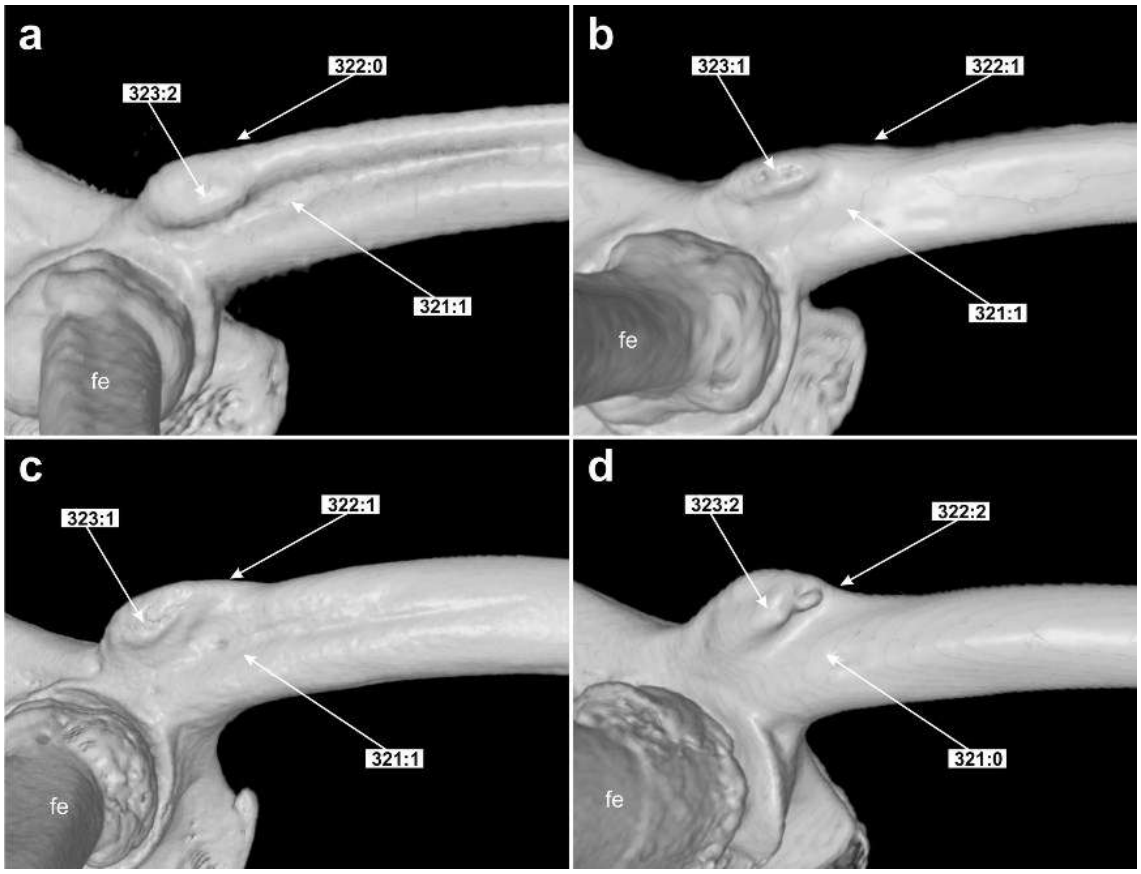

Figure 67. Lateral view of the base of the ilial shaft in *Allobates pittieri* MHNLS 21488 (**a**), *Ranitomeya toraro* MCP 13107 (**b**), *Adelphobates galactonotus* MCP 2252 (**c**), and *Aromobates nocturnus* ULABG 2223 (**d**). Ilium, tubercular fossa (character 321): absent (state 0) in **d**; present (state 1) in **a**–**c**. Ilium, dorsal prominence (character 322): undifferentiated (state 0) in **a**; weakly differentiated (state 1) in **b**–**c**; well-differentiated (state 2) in **d**. Dorsal protuberance of ilium (character 323): weak (state 1) in **b**–**c**; strong (state 2) in **a**, and **d**. **fe:** femur.

323. Ilium, dorsal protuberance: 0 = absent; 1 = weak; 2 = strong. Additive. (Figure 67).

324. Ilium, dorsal protuberance, orientation: 0 = lateral; 1 = anteroventral. (Figure 68).

325. Ilium, supraacetabular fossa: 0 = absent; 1 = present. (Figure 69).

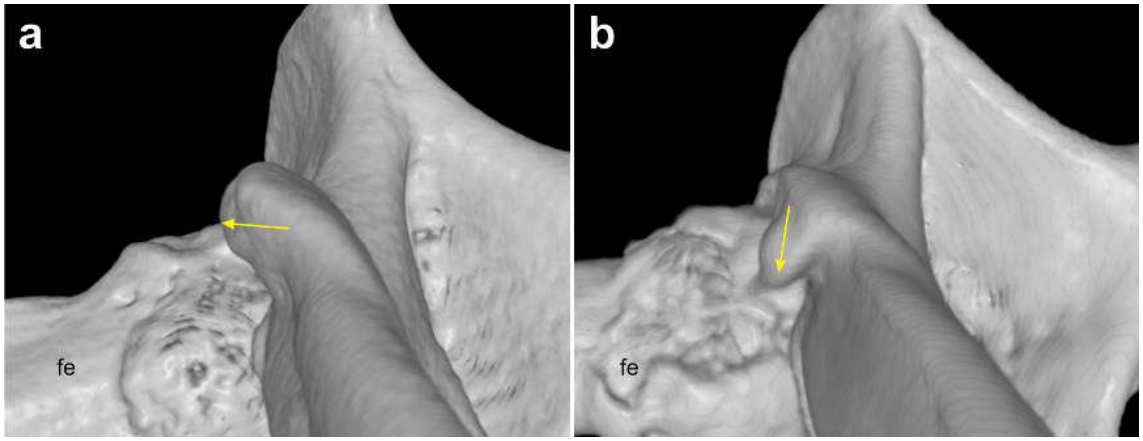

Figure 68. Anterolateral view of the posterior portion of the ilium of *Adelphobates galactonotus* MCP 2252 (**a**) and *Aromobates capurinensis* CVULA5920 (**b**). Ilium, dorsal protuberance, orientation (character 324): lateral (state 0) in **a**; anteroventral in **b**.

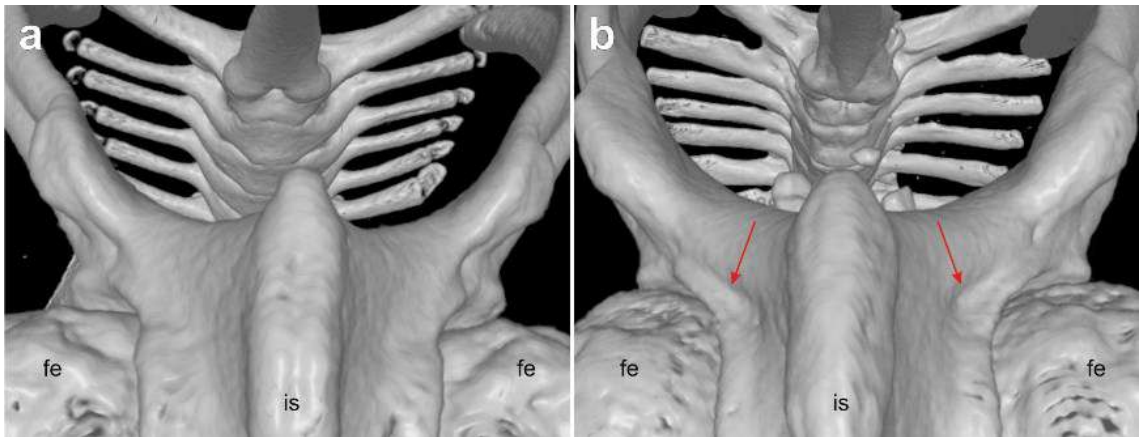

Figura 69. Posterior view of the pelvic girdle in *Lecostethus brachistriatus* MCP 11516 (**a**) and *Adelphobates galactonotus* MCP 2252 (**b**). Supraacetabular fossa of ilium (character 325): absent (state 0) in **a**; present (state 1) in **b**. **fe:** femur; **is:** ischium.

326–330: Humerus.

This bone is the propodial element of the forelimb; ventroproximally bears a *crista ventralis*, poorly elevated in dendrobatoids but variable in distal extension (character 326). The development of this crest constitutes an important character in the systematics of some anurans, such as centrolenids (Cisneros-Heredia & McDiarmid 2007, Guayasamin *et al*. 2009), but, as many other anatomical features of this bone, it has been overlooked in dendrobatoids. An incipient paraventral crest is also present in the humerus of dendrobatoids, and its proximal section varies from undefined to strongly developed, forming a bony bridge to the proximal portion of *crista ventralis* (character 327). Also at the proximal end, a small tubercle—generally a bump, but in some cases strongly developed—may be present (character 328). The *crista medialis* and *crista lateralis* (characters 329 and 330, respectively) are absent in dendrobatoids, but we include them due their strong development in *Thoropa miliaris*.

326. Humerus, *crista ventralis*, distal extension in relation to humerus length: 0 = almost reaching or reaching the anterior third; 1 = surpassing the anterior third but not reaching the anterior half; 2 = reaching to surpassing the anterior half. Additive. (Figure 70).

327. Humerus, paraventral crest, proximal end: 0 = undifferentiated; 1 = weakly raised (forming a small bulge); 2 = strongly raised (forming a well-defined tubercle); 3 = forming a bony bridge to the *crista ventralis*. Additive. (Figure 70).

328. Humerus, medial proximal tubercle: 0 = absent; 1 = weak; 2 = strong. Additive. (Figure 70).

329. Humerus, *crista medialis*: 0 = absent; 1 = present. (Figure 71).

330. Humerus, *crista lateralis*: 0 = absent; 1 = present. (Figure 71).

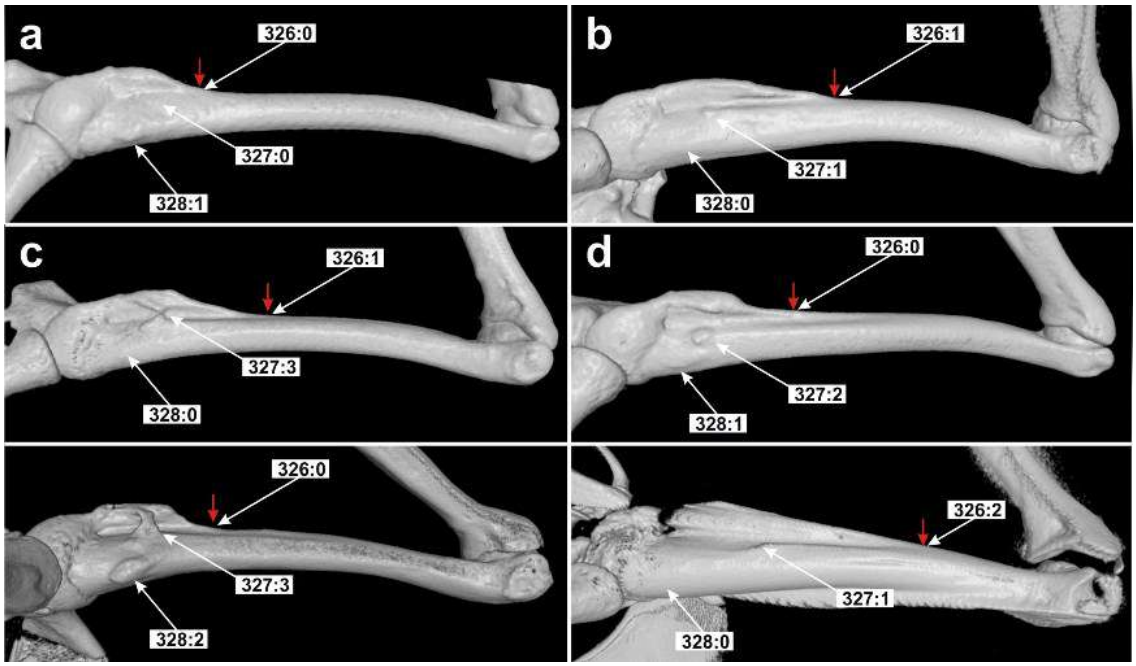

Figure 70. Ventral view of the humerus of *Allobates pittieri* MHNLS 21488 (**a**), *Aromobates* sp. 3 CVULA 239 (**b**), *Mannophryne herminae* MHNLS 22111 (**c**), *Leucostethus brachistriatus* MCP 11516 (**d**), *Adelphobates galactonotus* MCP 2252 (**e**), and *Thoropa miliaris* MCP 12229 (**f**). Humerus, *crista ventralis*, distal extension in relation to humerus length (character 326): almost reaching or reaching the anterior third (state 0) in **a**, **d**–**e**; surpassing the anterior third but not reaching the anterior half (state 1) in **b**–**c**; reaching to surpassing the anterior half (state 2) in **f**. Humerus, paraventral crest, proximal end (character 327): undifferentiated (state 0) in **a**; weakly raised, forming a small bulge (state 1) in **b** and **f**; strongly raised, forming a well-defined tubercle (state 2) in **d**; forming a bony bridge to the *crista ventralis* (state 3) in **c**–**e**. Humerus, medial proximal tubercle (character 328): absent (state 0) in **b**–**c**, and **f**; weak (state 1) in **a** and **d**; strong (state 2) in **e**.

331–332: Femur.

This is the propodial element of the hindlimb, proximally articulates with the acetabulum of the pelvic girdle and distally with the tibiofibula. Usually present

at the proximal portion of the femur of dendrobatoids, are the *crista femoris* posterodorsally, and ventrally, the supplementary ventral crest, in which several short pelvic muscles are anchored. We score the variation in the development of these two crests (characters 331 and 332).

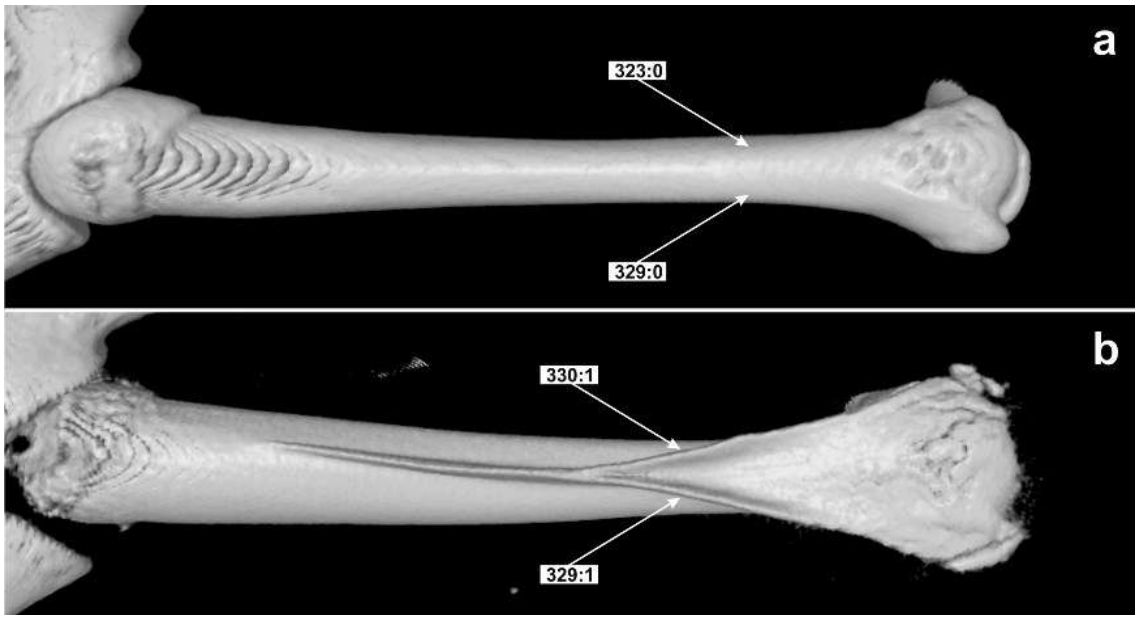

Figure 71. *Mannophryne yustizi* MHNLS 8522 (**a**), and *Thoropa miliaris* MCP 12229 (**b**). Humerus, *crista medialis* (character 329): absent (state 0) in **a**; present (state 1) in **b**. Humerus, *crista lateralis* (character 330): absent (state 0) in **a**; present (state 1) in **b**.

331. Femur, *crista femoris*, development: 0 = absent; 1 = weak; 2 = strong. Additive. (Figure 72).

332. Femur, proximal ventral crest, development: 0 = absent; 1 = weak; 2 = strong. Additive. (Figure 72).

333. Tibia, proximal crest, extension: 0 = short (less than half of its length projected beyond the condyle); 1 = long (half or more of its length projected beyond the condyle).

Tibiofibula in anurans is an epipodial compound element. This bone is poor in anatomical features and usually not mentioned in descriptions of anuran osteology. A small crest is present on the anterior surface of the proximal tibial condyle, extending longitudinally on the condyle and projecting distally. We score variation in the distal extension of this crest beyond the border of the condyle, in relation to its total length. (Figure 73).

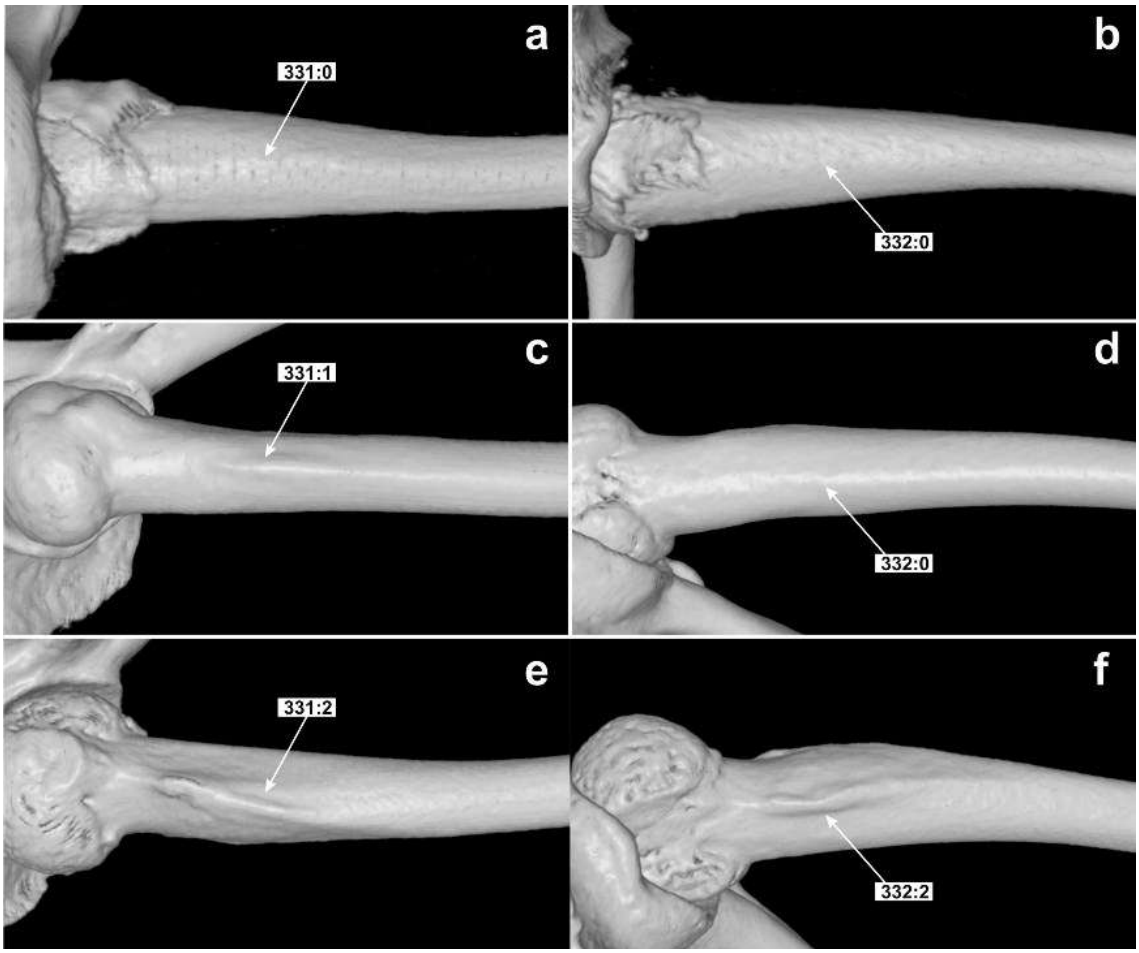

Figure 72. *Aromobates nocturnus* ULABG 2223 (**a**–**b**), *Aromobates alboguttatus* CVULA 1448 (**c**–**d**), and *Adelphobates galactonotus* MCP 2252 (**c**–**d**). *Femur, crista femoris, development* (character 331): absent (state 0) in **a**; weak (state 1) in **c**; strong (state 2) in **e**. Femur, proximal ventral crest, development (character 332): absent (state 0) in **b** and **d**; strong (state 2) in **f**.

334. Hand, prepollical segments, number (De Sá *et al*. 2014): 0 = base + 3 segments; 1 = base + 2 segments; 2 = base + 1 segment. Additive.

Figure 73. Tibia, proximal crest, extension (character 333): short, less than half of its length projected beyond the condyle (state 0) in *Mannophryne herminae* MHNLS 22111 (**a**); long, half of more of its length projected beyond the condyle (state 1) in *Mannophryne yustizi* MHNLS 8522 (**b**).

335–336: Metacarpal IV.

Modifications on anuran metacarpals are generally associated to nuptial structures, such as the nuptial tubercle on metacarpal I in males of some leptodactylids and telmatobids (Lynch 1971). Centrolenids also bear a dilated medial process on the metacarpal III that constitutes a synapomorphy of the family (Hayes & Starret 1980, Guayasamin & Trueb 2007). We score the occurrence of a small dorsal-postaxial process on the metacarpal IV of some dendrobatoids (character 335), and the contour of the postaxial side of the same metacarpal in dorsal view (character 336).

335. Metacarpal IV, dorsal-postaxial process: 0 = absent; 1 = present. (Figure 74).

336. Metacarpal IV, middle portion, postaxial surface, shape: 0 = straight; 1 = slightly convex. (Figure 74).

Figure 74. Dorsal view of the metacarpal IV on the hand in *Aromobates ornatissimus* ULABG 4976 (**a**), *Aromobates capurinensis* CVULA 5920 (**b**), *Allobates pittieri* MHNLS 21488 (**c**), and *Ranitomeya toraro* (**d**). Metacarpal IV, dorsal-postaxial process (character 335; indicated by red arrows): absent (state 0) in **a**–**b**; present (state 1) in **c**–**d**. Metacarpal IV, middle portion, postaxial surface, shape (character 336): slightly concave to straight (state 0) in **a**, **c**–**d**; slightly convex (state 1) in **b**.

337–350: Glide ventral sesamoids on fingers and toes.

These skeletal elements have been usually overlooked in studies of vertebrate osteology. Ponssa *et al*. (2010) characterized their distribution in anurans; highlighted that these elements arise before the differentiation of tendinous tissues and not as consequence of intense mechanical stress; and presume that at least some of them may be useful for phylogenetic analyses. We score the observed variation in the occurrence of paired glide sesamoids on the ventral surfaces of metacarpal-proximal phalanx and proximal-median phalanx articulations of FI–IV (characters 337–342), metatarsal-proximal phalanx articulations of TI–V (character 343–347), and proximal-medial phalanx articulations of TIII–V (characters 348–350). (Figures 75–76).

337. FI, metacarpal-proximal phalanx articulation, sesamoid: 0 = absent; 1 = present. (Figure 75).

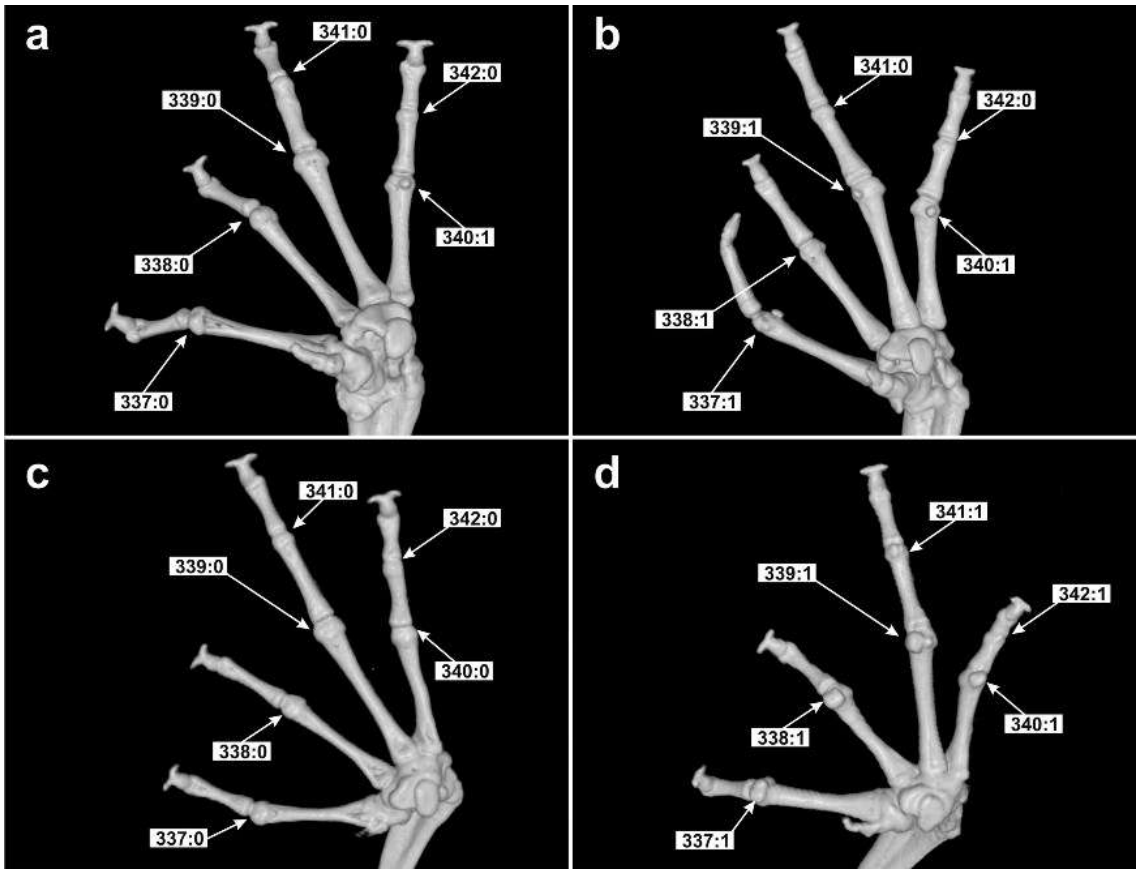

Figure 75. Ventral view of the hand of *Mannophryne herminae* MHNLS 22111 (**a**), *Aromobates ornatissimus* ULABG 4976 (**b**), *Mannophryne volcano* MHNLS 21780 (**c**), and *Allobates pittieri* MHNLS 21488 (**d**). Sesamoids on the articulation of metacarpal and proximal phalanx of FI–FIV (characters 337 to 340), and on the articulation of the proximal and median phalanges of FIII-IV (characters 341 to 342): absent (state 0); present (state 1).

338. FII, metacarpal-proximal phalanx articulation, sesamoid: 0 = absent; 1 = present. (Figure 75).

339. FIII, metacarpal-proximal phalanx articulation, sesamoid: 0 = absent; 1 = present. (Figure 75).

340. FIV, metacarpal-proximal phalanx articulation, sesamoid: 0 = absent; 1 = present. (Figure 75).

341. FIII, proximal-median phalanx articulation, sesamoid: 0 = absent; 1 = present. (Figure 75).

342. FIV, proximal-median phalanx articulation, sesamoid: 0 = absent; 1 = present. (Figure 75).

343. TI, metatarsal-proximal phalanx articulation, sesamoid: 0 = absent; 1 = present. (Figure 76).

344. TII, metatarsal-proximal phalanx articulation, sesamoid: 0 = absent; 1 = present. (Figure 76).

345. TIII, metatarsal-proximal phalanx articulation, sesamoid: 0 = absent; 1 = present. (Figure 76).

346. TIV, metatarsal-proximal phalanx articulation, sesamoid: 0 = absent; 1 = present. (Figure 76).

347. TV, metatarsal-proximal phalanx articulation, sesamoid: 0 = absent; 1 = present. (Figure 76).

348. TIII, proximal-median phalanx articulation, sesamoid: 0 = absent; 1 = present. (Figure 76).

349. TIV, proximal-median phalanx articulation, sesamoid: 0 = absent; 1 = present. (Figure 76).

350. TV, proximal-median phalanx articulation, sesamoid: 0 = absent; 1 = present. (Figure 76).

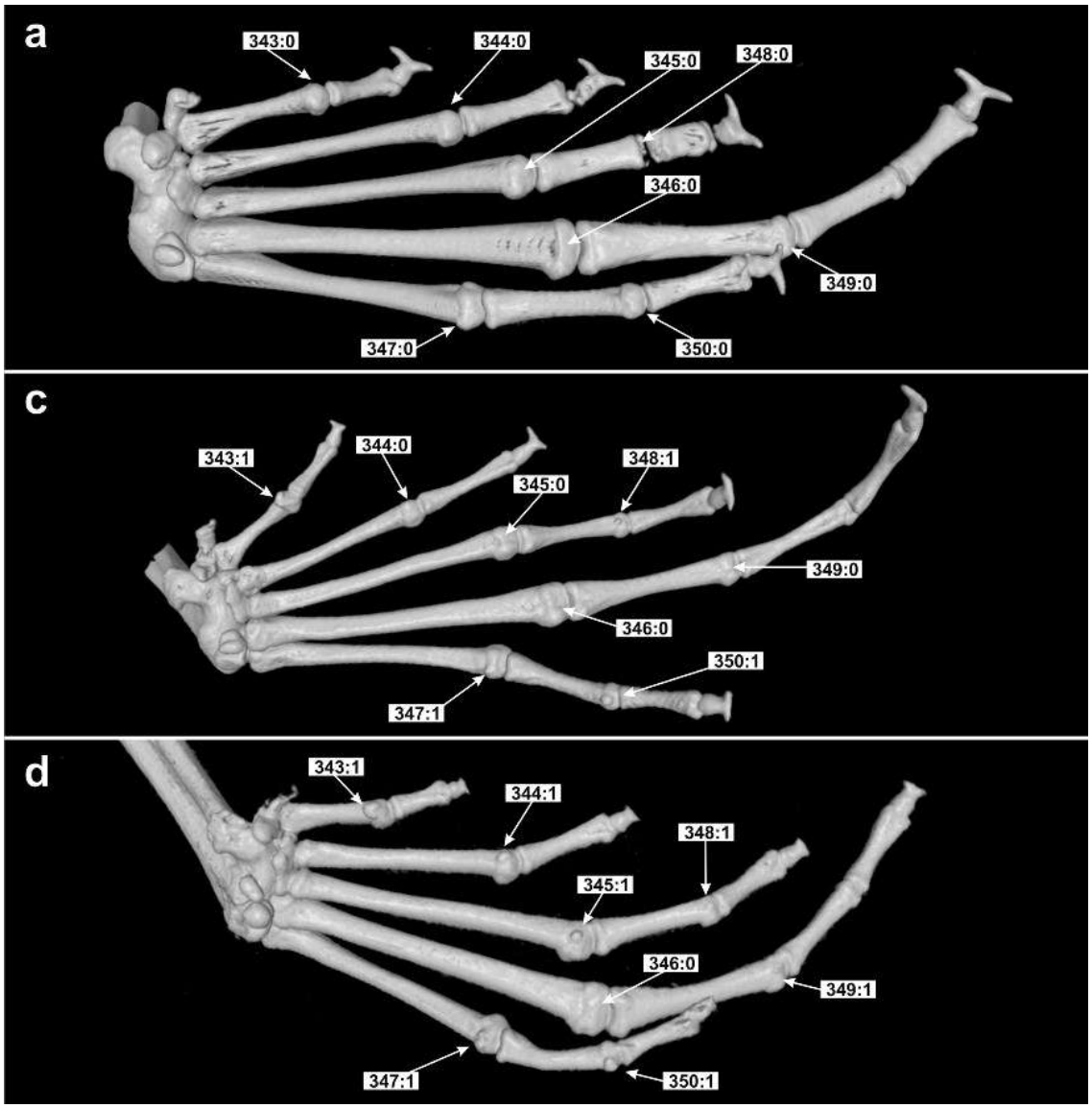

Figure 76. Ventral view of the foot of *Mannophryne oblitterata* MHNLS 21799 (**a**), *Leucostethus brachistriatus* MCP 11516 (**b**), and *Allobates femoralis* MCP 13869 (**c**). Sesamoids on the articulation of the metatarsal and proximal phalanx of TI–TV (characters 343 to 347), and on the articulation of the proximal and median phalanx of TIII-TV (characters 348-350): absent (state 0), present (state 1).

351–353: Terminal phalanges.

The shape of terminal phalanges has been commonly considered as a useful character in amphibian systematics (Boulenger 1882, Noble 1922, Taylor 1951, Lynch 1971). Grant *et al*. (2006) followed Lynch (1971) in coding the form of these phalanges as knobbed when they have a bulge at the tip, or T-shaped when bear a pair of laterodistal processes (character 351 of this study). T-shaped phalanges of dendrobatoids are very variable in their degree of development of their laterodistal processes. We score this variation separately for the terminal phalanges of FIII and TIV, defining the lateral expansion as a relation between the distal width (measured as the the distance between tips of laterodistal processes) and the basal width of the phalanx (characters 352–535).

351. Terminal phalanx, shape (Grant *et al*. 2006): 0 = T-shaped; 1 = knobbed.

352. FIII, terminal phalanx, distal width in relation to basal width: 0 = unexpanded (≤ 1.0); 1 = very weakly expanded (1.1–1.4); 2 = weakly expanded (1.5–2.4); 3 = moderately expanded (2.5–3.0); 4 = strongly expanded (>3.0). Additive. (Figure 77).

353. TIV, terminal phalanx, distal width in relation to basal width: 0 = unexpanded (≤ 1.0); 1 = very weakly expanded (1.1–1.4); 2 = weakly expanded (1.5–2.4); 3 = moderately expanded (2.5–3.0); 4 = strongly expanded (>3.0). Additive.

Figure 77. FIII, terminal phalanx, distal width in relation to basal width (character 352): unexpanded, ≤ 1.0 x (state 0) in *Allobates femoralis* MCP 13869 (**a**); very weakly expanded, 1.1–1.4 x (state 1) in *Aromobates ornatissimus* ULABG 4976 (**b**); weakly expanded, 1.5–2.4 x (state 2) in *Mannophryne neblina* MHNLS 4956 (**c**); moderately expanded, 2.5–3.0 x (state 3) in *Adelphobates galactonotus* MCP 2252 (**d**).

354–381: Alkaloids (Grant *et al*. 2006, 2017).

354. Ability to sequester liophilic alkaloids: 0 = absent; 1 = present.

355. Batrachotoxins (BTX): 0 = absent; 1 = present.

356. Histrionicotoxins (HTX): 0 = absent; 1 = present.

357. Pumiliotoxins (PTX): 0 = absent; 1 = present.

358. Allopumiliotoxins: 0 = absent; 1 = present.

359. Homopumiliotoxins: 0 = absent; 1 = present.

360. Decahydroquinolines (DHQ): 0 = absent; 1 = present.

361. 3,5-Disubstituted pyrrolizidines (3,5-P): 0 = absent; 1 = present.

362. 3,5-Disubstituted indolizidines (3,5-I): 0 = absent; 1 = present.

363. 5,8-Disubstituted indolizidines (5,8-I): 0 = absent; 1 = present.

364. Dehydro-5,8-indolizidines (Dehydro-5,8-I): 0 = absent; 1 = present.

365. 5,6,8-Trisubstituted indolizidines (5,6,8-I): 0 = absent; 1 = present.

366. 4,6-Disubstituted quinolizidines (4,6-Q): 0 = absent; 1 = present.

367. 1,4-Disubstituted quinolizidines (1,4-Q): 0 = absent; 1 = present.

368. Lehmizidines (Lehm): 0 = absent; 1= present.

369. Epiquinamide: 0 = absent; 1 = present.

370. 2,5-Disubstituted pyrrolidines (Pyr): 0 = absent; 1 = present.

371. 2,6-Disubstituted piperidines (Pip): 0 = absent; 1 = present.

372. Gephyrotoxins (GTX): 0 = absent; 1 = present.

373. Coccinelline-like tricyclics (Tricyclic): 0 = absent; 1 = present.

374. Cyclopentylquinolizidines (CPQ): 0 = absent; 1 = present.

375. Spiropyrrolizidines (SpiroP): 0 = absent; 1 = present.

376. Indolic alkaloids: 0 = absent; 1 = present.

377. Epibatidines: 0 = absent; 1 = present.

378. Noranabasamine: 0 = absent; 1 = present.

379. N-methyldecahydroquinolines (N-MeDHQ): 0 = absent; 1 = present.

380. Pumiliotoxin 7-hydroxylase: 0 = absent; 1 = present.

381. Tetrodotoxin (TTX): 0 = absent; 1 = present.

382. Chromosome number (2n): 0 = 18; 1 = 20; 2 = 22; 3 = 24; 4 = 26; 5 = 28; 6 = 30. Additive.

We code this character for *Mannophryne vulcano* based on the study of Rada (1976), which correspond to this species and not to *M. trinitatis* as originally referred by the author. Kaiser *et al*. (2003) noticed relevant differences between the karyotypes of *M. trinitatis* from Trinidad studied by them, and those reported by Rada (1976) for specimens from the valley of Caracas in Venezuela (the type locality of *M. vulcano*).

Phylogenetic analysis

Our searches performed 578 RAS + swapping, 747 rounds of Tree Fusing, and 166 rounds of Ratcheting. This resulted in three different but equally optimal trees of 40,601 steps, all of which converged in the same optimal topology of 40,546 steps after a round of iterative pass optimization. The resulting implied alignment was composed of 18,517 aligned nucleotide characters plus 383 static phenotypic characters. Additional searches of this dataset in TNT did not result in shorter trees, but increased the number of optimal trees to 1,316.

Polytomies and potential wildcards

Despite the heterogeneity of genotypic and phenotypic character sampling in our dataset (0–339 phenotypic characters and 0–23 loci per terminal), the strict consensus of the 1,316 equally optimal topologies obtained is highly resolved. Polytomies in the ingroup are restricted to the clades formed by *Aromobates serranus*, *A. duranti*, and *A. zippeli* (Figure 81); *A. ericksonae* and *A. mayorgai* (Figure 82); *A. saltuensis* complex and *A. tokuko* (Figure 82); the species complexes of *Mannophryne herminae* (Figure 84), and *M. yustizi* (Figure 86). Other polytomies only involved conspecific terminals.

The first 50 terminals listed as potencial wildcars by Ybyrá (Appendix 5), mostly correspond to specimens of *Mannophryne cordilleriana*, *M. vulcano*, *M. collaris*, and *M. herminae*. Those corresponding to the first three species are part of conspecifics polytomies, whereas those of *M. herminae* are part of a politomy that involves other two lineages. However, four terminals included among the first 32, apparently are the responsible for polytomies involving two species complexes: *Mannophryne* sp. MHNLS 22559 of the complex of *M.*

yustizi, in the position 17 of the ranking, and the terminals *Mannophryne* cf. *molinai* MHNLS 21367, 21365, and 21206, in the positions 29, 31, and 32, respectively, all of which are part of *M. herminae* complex.

None of the 13 terminals represented solely by phenotypic data are among the first 200 (first half of the list). Only *Aromobates duranti* and *Aromobates serranus,* positions 227 and 228 respectively, are involved in a tricotomy with *A. zippeli* in the strict consensus. The other 10 terminals are in the positions 217 to 292. Finally, "*Prostherapis*" *dunni* is at the end of the list, in the position 394 (among the 400 terminals included in the analysis).

Phylogenetic relationships and monophyly of supraspecific taxa

In our phylogeny, *Ectopoglossus saxatilis* and *Paruwrobates erythromos* are recovered forming a clade sister to all other Dendrobatoidea (Figure 78); the node that groups these two terminals, and that of the sister clade, composed by Dendrobatidae + Aromobatidae, are poorly supported (JK = 58 % for both). Dendrobatidae (excluding *Ectopoglossus* and *Paruwrobates*) has a JK = 100 % and three unambiguously optimized synapomorphies: 1) Testis entirely pigmented in adults (character 105:2); 2) Posterior margin of the postzygoapohysis of the vertebra VII straight to nearly straight (character 295:1); and, 3) Posterodorsal apophysis of transverse process of vertebra III present (Figure 79).

Aromobatidae and its three subfamilies (Allobatinae, Anomaloglossinae, and Aromobatinae) are monophyletic, with Allobatinae sister to the clade including Anomaloglossinae and Aromobatinae (Figure 78). Aromobatidae (JK = 56 %), is supported by five unambiguous phenotypic synapomorphies (Figure

79): 1) Presence of pale paracloacal marks (character 61:1); 2) Dark lower labial stripe poorly defined (character 89:0); 3) Male throat evenly stippled (character 90:2); 4) Zygomatic ramus of the squamosal short, but well defined (character 193:3); and, 5) Posterior tip of the maxilla not reaching the level of the base of the zygomatic process of the squamosal (character 220:0).

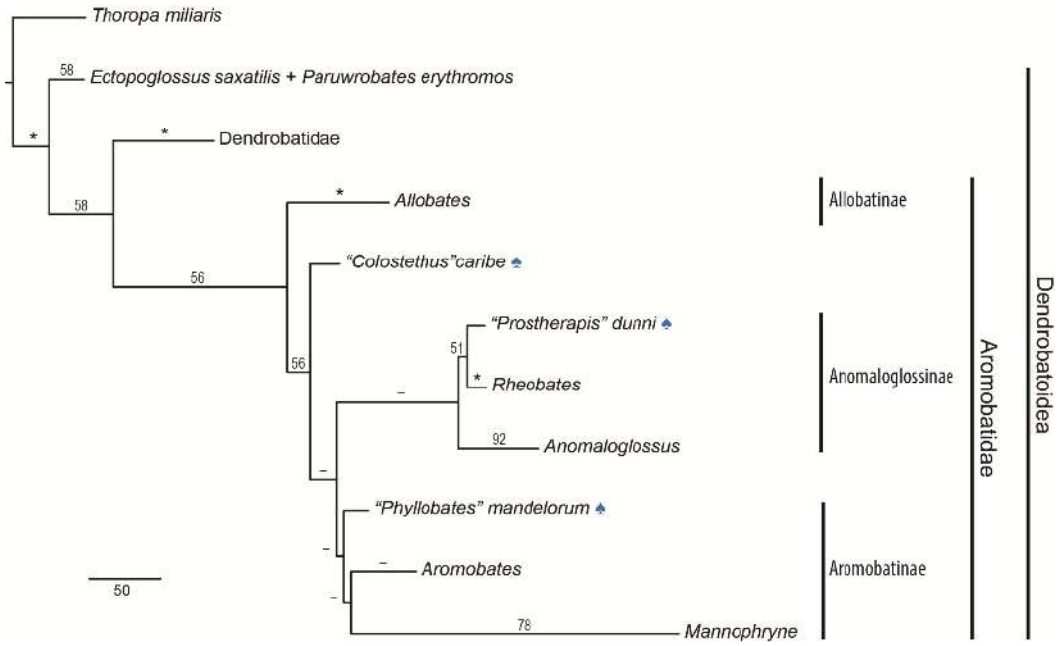

Figure. 78. Optimal hypothesis of the phylogenetic relationships of Aromobatinae and outgroup, inferred from equal weight parsimony analysis of total evidence, with DNA sequences under tree-alignment. This is a pruned topology at the supraspecific level of on of the 1,316 most parsimonious trees (40,546 steps) showing proportional branch lengths. Numbers above the branches represent jackknife proportions (asterisks indicate 100 % jackknife support, and n-dashes indicateJK < 50 %). Blue spades indicate terminals only represented by phenotypic data.

Within Aromobatidae, Allobatinae (= *Allobates*) has a JK = 100 % and 11 unambiguosly optimized phenotypic synapomorphies, all of them unique and homoplastic (Figure 79). *Allobates* is sister to the group composed by *"Colostethus" caribe* and the clade of Anomaloglossinae + Aromobatinae (Figures 78 and 80). This group has a JK = 56 % and is supported by 14 unambiguous phenotypic synapomorphies (Figure 79).

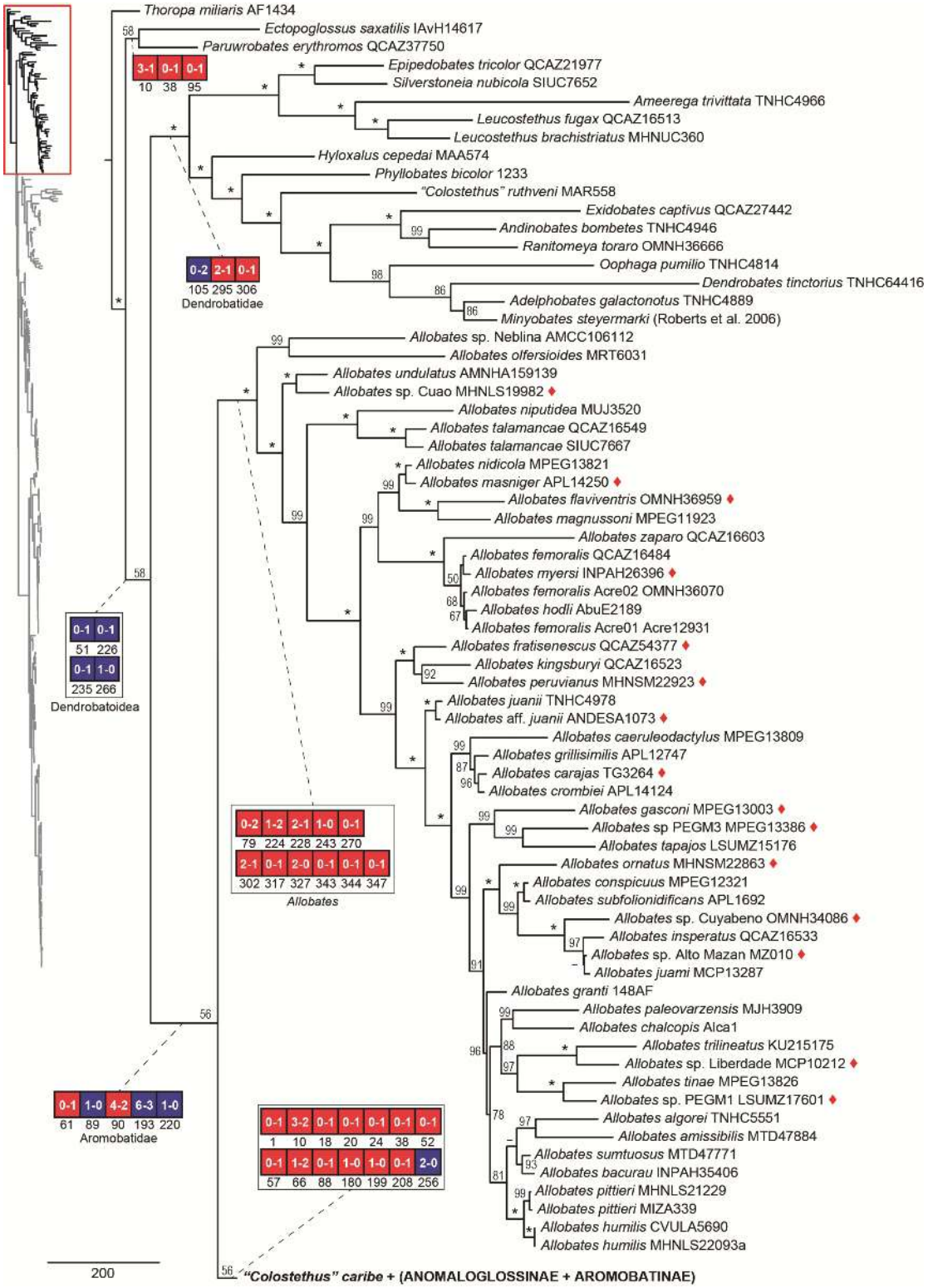

Figure. 79. One of the 1,316 shortest trees (40,546 transformations), with proportional branch lengths, inferred from total evidence parsimony analysis with equal weights and DNA sequences under tree-alignment. The tree shows part of the phylogenetic relationships of the outgroup. Numbers next to the nodes represent jackknife proportions (asterisks = 100 %, n-dashes JK < 50 %). Red diamonds indicate terminals only represented by molecular data. Selected clades are labeled with unambiguously optimized phenotypic synapomorphies (red square = unique, homoplastic; blue square = non-unique, homoplastic; character number below squares; primitive–derived character-states inside squares).

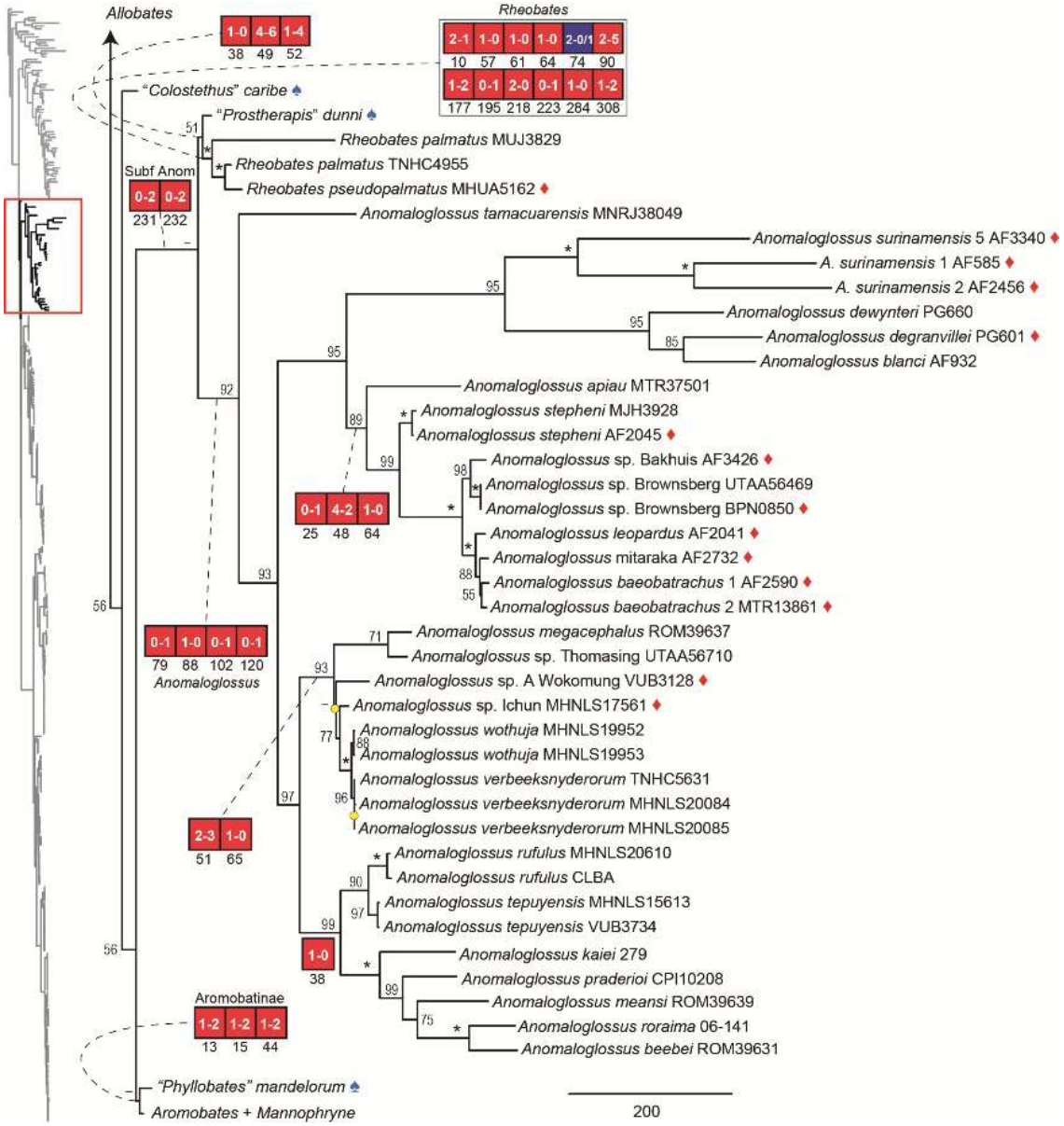

Figure. 80. Continuation of Fig. 79 showing the remaining relationships among the outgroup. Numbers next to the nodes represent jackknife proportions (asterisks = 100 %, n-dashes JK < 50 %). Red diamonds indicate terminals only represented by molecular data, and blue spades for those only represented by phenotypic data. Selected clades are labeled with unambiguously optimized phenotypic synapomorphies (red square = unique, homoplastic; blue square = non-unique, homoplastic; character number below squares; primitive–derived character-states inside squares). Yellow dots on nodes indicate collapsed clades in the strict consensus.

Anomaloglossinae (Figures 78 and 80), although weakly supported (JK < 50 %) is deeply divergent of its sister group (branch length = 85 transformations) and is supported by two unambiguously optimized synapomorphies. This subfamily groups *Anomaloglussus*, *Rheobates*, and *"Prostherapis" dunni*. The latter taxon is represented only by phenotypic data, and is recovered as sister of *Rheobates*; this clade (JK = 51 %) is supported by three unambiguous phenotypic synapomorfies. *Rheobates*, in turn, has JK = 100 % and 12 unambiguous phenotypic synapomorphies. Finally, *Anomaloglossus* (JK = 92 %) has four unambiguous phenotypic synapomorphies.

"*Phyllobates*" *mandelorum*, only represented by phenotypic data, is sister to *Aromobates* + *Mannophryne* (Aromobatinae); the group formed by all of them (JK < 50 %) is sister to Anomaloglossinae (Figure 78) and defined by three phenotypic synapomorfies (Figures 80–81). The clade of *Aromobates* + *Mannophryne* (JK < 50 %) is delimited by five unambigously optimized phenotypic synapomorphies (Figure 81): 1) Quadratojugal anteriorly unexpanded (215:1); 2) Posterior tip of the maxilla reaching the level of the base of the zygomatic process of the squamosal (character 220:1); 3) Anterior tip of the parasphenoid cultriform process bifid (character 256:3); 4 and 5) Neural crest of the vertebrae VI and VII strong (characters 274:2, and 275:2, respectively).

Phylogenetic relationships of skunk frogs (*Aromobates*)

Aromobates is recovered as monophyletic (JK < 50 %) and sister to *Mannophryne* (Figure 78). We identified five unambiguous phenotypic

synamorphies for this genus (Figure 81): 1) Presence of yellow translucent coloration on hidden parts of hind limbs (character 60:1); 2) Ventrolateral pale stripe formed by series of discrete spots (character 76:2); 3) Presence of peripheral lobes on the pupillary ring (character 99:1); 4) Posterolateral corner of the frontoparietal ornamented (character 236:1); and 5) Absence of sesamoids in the iliosacral articulation (character 286:0).

The 10 species of *Aromobates* represented only by phenotypic data (OPD) were recovered within this genus. The subgroups in which they are embedded and their relationships within these subgroups have JK < 65 % and their relationships are fully resolved, except for the clade including *A. duranti*, *A. serranus*, *A. zippeli* (Figures 81–82). *Aromobates alboguttatus* and *A. haydeeae* (both, OPD) are grouped with *A. ornatissimus*; this clade is sister to all other *Aromobates* (except *Aromobates* sp. 1) and is defined by three synapomorphies (Figure 81). *Aromobates walterarpi* (OPD) and *A. nocturnus*, are sister species and supported by nine unambiguous synapomorphies (Figure 81); this clade is sister to other two subgroups including ODP terminals. One of them includes *Aromobates* sp. 3, *A. capurinensis*, *A. orostoma*, *A. inflexus* (all of them ODP), and *A. molinarii*; this subgroup is delimited by three unambiguous synapomorphies. The other subgroup is integrated by *A. serranus*, *A. duranti* (both OPD) and *A. zippeli* and is defined by five unambiguously optimized synapomorphies (Figure 81); the relationships within this clade are unresolved. Finally, *A. leopardalis* (OPD) is sister to *A. meridensis*; this relationship is supported by six synapomorphies (Figure 82).

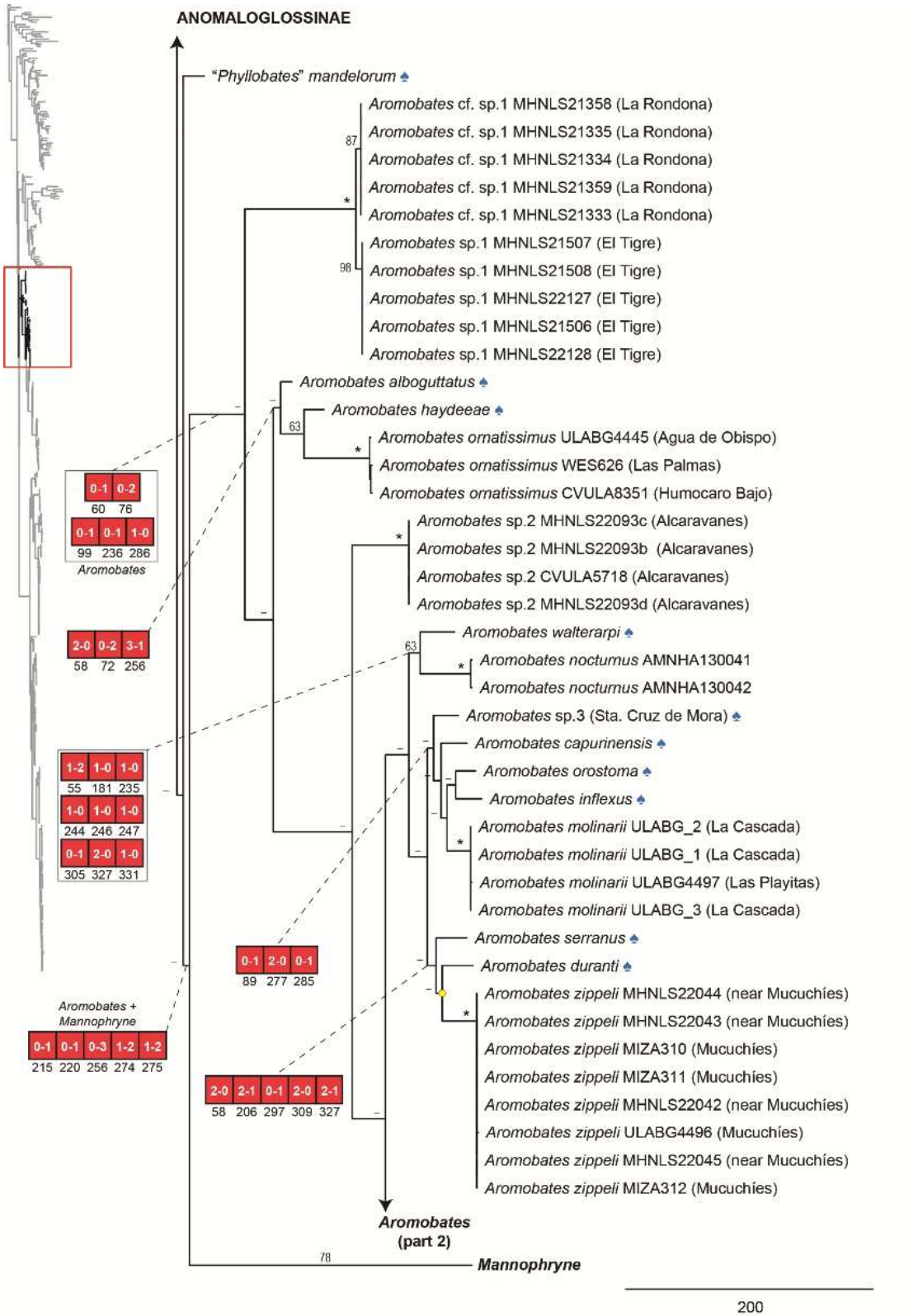

Figure. 81. Continuation of Fig. 80 showing part of the relationships among the ingroup ("*Phyllobates*" *mandelorum* and part of *Aromobates*). Numbers next to the nodes represent jackknife proportions (asterisks = 100 %, n-dashes = JK < 50 %). Blue spades indicate terminals only represented by phenotypic data. Selected clades are labeled with unambiguously optimized phenotypic synapomorphies (red square = unique, homoplastic; character number below squares; primitive–derived character-states inside squares). Yellow dots on nodes indicate collapsed clades in the strict consensus.

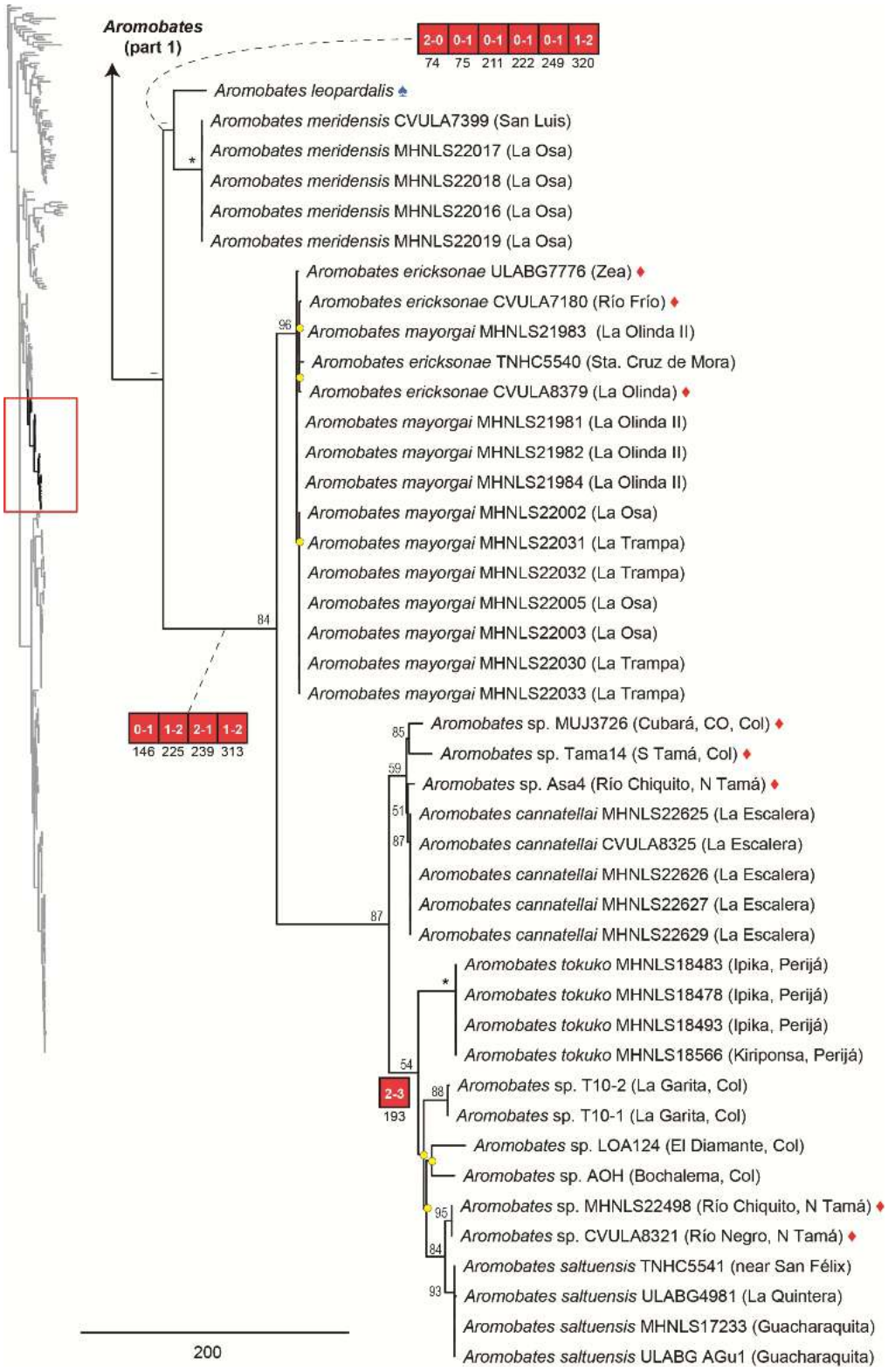

Figure. 82. Continuation of Fig. 81 showing part of the relationships among *Aromobates*. Numbers next to the nodes represent jackknife proportions (asterisks = 100 %, n-dashes = JK < 50 %). Red diamonds indicate terminals only represented by molecular data, and blue spades for those only represented by phenotypic data. Selected clades are labeled with unambiguously optimized phenotypic synapomorphies (red square = unique, homoplastic; character number below squares; primitive–derived character-states inside squares). Yellow dots on nodes indicate collapsed clades in the strict consensus.

Besides the 19 species currently recognized within *Aromobates*, at least other three unnamed putative new species are included in the phylogeny. *Aromobates* sp. 1, is sister and deeply divergent to all other species in the genus, and represented by two reciprocally monophyletic groups corresponding to two nearby populations. Genetic divergence of a fragment of 16S between this species and all other sequenced *Aromobates* is 5.1–8.4 % (Appendix 6). *Aromobates* sp. 2 is sister to a group including almost all other *Aromobates* (except *A.* sp. 1, *A. alboguttatus*, *A. haydeeae* and *A. ornatissimus*); its genetic distance from all other sequenced species of the genus is 3.3–7.3 % for 16S (Appendix 6). *Aromobates* sp. 3, a taxon represented only by phenotypic data, is grouped with *A. capurinensis*, *A. orostoma*, *A. inflexus*, and *A. molinarii*.

The node that groups *Aromobates mayorgai*, *A. ericksonae*, *A. cannatellai*, *A. tokuko*, *A. saltuensis*, and several *Aromobates* sp. (JK = 84 %) is supported by four unambiguous phenotypic synapomorphies (Figure 82). Within it, *A. mayorgai* and *A. ericksonae* form a well-supported clade (JK = 96 %), but the 15 terminals representing both species (four *A. ericksonae* from four different localities and 11 *A. mayorgai* from three localities) are intermixed in a large polytomy, with genetic distances = 0.0 % for both 16S and Cyt-b (Appendices 6–7).

Aromobates cannatellai is grouped (JK = 59 %) with three other terminals from three different and geographically distant populations; the genetic distances (based on 16S) among topotypic samples and those from other populations are 1.3–2.0 % (Appendix 6). The sister clade (JK = 54 %) to *A. cannatellai* and their related terminals, has one unambiguous phenotypic synapomorphy (Figure 82). The interspecific relationships within this clade are

not resolved, but *A. tokuko* and *A. saltuensis* (*sensu stricto*), and *A.* sp from N Tamá are recovered as monophyletic within a polytomy involving additional undetermined samples from other four distant populations. Genetic distances among these three species and other terminals within this subgroup are: 0.9–1.8 % for *A. tokuko*, 0.7–1.8 % for *A. saltuensis*, and 0.6–1.1 % for *Aromobates* sp. from La Garita (Appendix 6).

Phylogenetic relationships of collared frogs (*Mannophryne*)

The monophyly of *Mannophryne* is corroborated in our phylogeny (Figures 78 and 83). This is a clade deeply divergent of *Aromobates* (branch length = 229 transformations), with JK = 78 % and supported by 13 unambiguously optimized phenotypic synapomorphies (Figure 83); these are: 1) metatarsal fold extending on the distal third of the metatarsus V (character 56:0); 2) dark dermal collar present in males (character 80:1); 3) dark dermal collar present in females (character 84:1); 4) presence of a bright yellow spot on the throat of females (character 92:1); 5) tongue yellowish in life (character 103:1); 6) occurrence of skin blackening during calling activity (character 107:1); 7) internarial distance greater than interorbital distance in tadpoles (character 139:1); 8) acromion process markedly oriented inwards (character 179:0); 9) medial ramus of the pterygoid, short (character 198:1); 10) large nasal bone (character 223:1); 11) frontoparietal-otoccipital, free (character 235:0); 12) premaxillary teeth in number of 10 to 13 (character 259:1); and, 13) maxillary teeth conical to almost conical (character 264:0).

The three species groups recognized within *Mannophryne* (i.e., *M. trinitatis*, *M. oblitterata*, and *M. collaris* species groups; Manzanilla *et al*. 2009,

Grant *et al*. 2017) are also recovered as monophyletic. The *Mannophryne trinitatis* species group (JK = 93 %) is sister to all other *Mannophryne* and has a single unambiguous phenotypic synapomorphy: *crista femoris* strongly developed (character 231:2). Within this clade, *M. olmonae* and *M. riveroi* are recovered as reciprocally monophyletic (JK = 99 %) and the pairwise 16S distance between them is 3.8 %. *Mannophryne leonardoi* is deeply divergent and sister to the remaining species in the group. *Mannophryne trinitatis* and *M. venezuelensis* are sister (JK = 99 %) and reciprocally monophyletic and the pairwise 16S distance between them is 1.0–1.7 %; they are sister of the *Mannophryne vulcano* complex (JK = 99 %). The latter is defined by three unambiguous phenotypic synapomorphies (Figure 83) and includes the following lineages: 1) *Mannophryne* sp. 1, a putative new species external to all in the complex, with a remarkable branch length, and pairwise 16S distances of 1.2–2.4 % in relation to the other species in the complex (Appendix 8); 2) an undetermined terminal from Guatopo (TNHC5666) with remarkable branch length and with pairwise 16S distances of 1.4–2.1% in relation to the other terminals in the complex; 3 and 4) *Mannophryne* sp. 2, other putative new species, and *Mannophryne* sp., an undetermined lineage from Araira; both are sister, reciprocally monophyletic, and their clade is delimited by eight unambiguous phenotypic synapomorphies (Figure 83), but with genetic divergence between them for 16S = 0.2–0.5 %; and 5) *M. vulcano*, represented by 21 terminals from 12 localities, forming a large polytomy and with intraspecific pairwise 16S distance = 0.0–0.7 %.

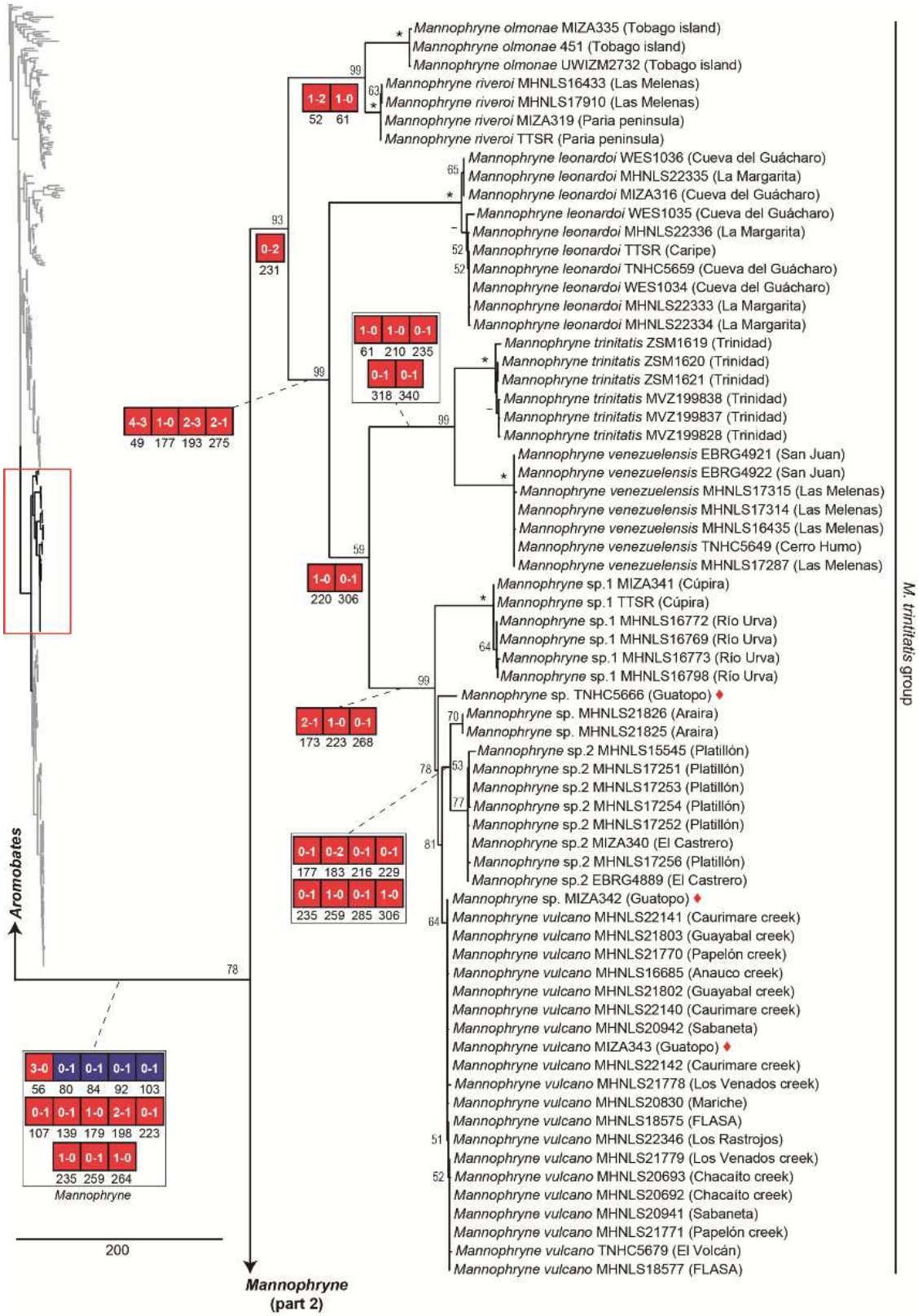

Figure. 83. Continuation of Fig. 82 showing the relationships among species of the *Mannophryne trinitatis* species group. Numbers next to the nodes represent jackknife proportions (asterisks = 100 %, n-dashes < 50 %). Red diamonds indicate terminals only represented by molecular data. Selected clades are labeled with unambiguously optimized phenotypic synapomorphies (red square = unique, homoplastic; blue square = non-unique, homoplastic; character number below squares; primitive–derived character-states inside squares).

The *Mannophryne oblitterata* species group is composed by its homonymous species and *M. neblina*. This group (JK = 56 %) is delimited by two unambiguously optimized phenotypic synapomorfies: 1) anteromedial angle of the coracoid without a notable projection (character 177:0); and, 2) sesamoid present on the metacarpal-proximal phalanx articulation of FII (character 238:1). Genetic pairwise 16S distances between the two species in this group is 4.3 % (Figure 84).

The *Mannophryne collaris* species group as defined by Manzanilla *et al*. (2009) and Grant *et al.* (2017) is the most exclusive clade including *M. caquetio* and *M. speeri*. As such, this species group (JK = 83 %) is delimited by only one unambiguous phenotypic synapomorphy (Fig. 84) and its species diversity is structured into two main clades (Figs. 84–86): one that groups the species of the western portion of the Cordillera de la Costa (JK = 78 %) and the other that includes the Andean species (JK = 85 %).

The Coastal clade (Figure 84) is phenotypically defined by: 1) notched omosternum posterior terminus (character 187:1); 2) frontoparietals fused posteriorly (character 234:1); 3) frontoparietal and occipital articulating but not fused (character 235:1); and, 4) distal portion of the urostyle moderately expanded in dorsal view (character 315:2). This clade is composed by *M. caquetio*, *M. herminae*, *M. molinai*, and at least two putative new species. *Mannophryne caquetio* exhibits filogeographic structure among the three populations sampled from two different mountain ranges; the pairwise 16S distances among them are = 1.0–1.9 %. *Mannophryne caquetio* is recovered as sister to *Mannophryne* sp. 3; they are reciprocally monophyletic and with pairwise 16S distances between 3.6–4.5 %. The clade formed by them (JK =

94) is defined by four morfological synapomorphies (Figure 84) and is sister of the clade that groups the *M. herminae* complex. External to all in the complex of *Mannophryne herminae* is the terminal ULABG5406, represented only by molecular data (specifically by 1,044 bp of 16S) and with pairwise distance of 1.9–3.1 % with other terminals within the complex. *Mannophryne* sp. 4 (JK = 79 %) is represented by terminals from three different populations (16S p-distances = 0.0 %) and is sister to an unresolved clade containing the other terminals.

The node that groups the terminal *Mannophryne* sp. MHNLS 17160 (identified as potencial wildcard) with the clade containing the other three terminals from La Sierra, collapse in the strict consensus. Also collapse in the strict consensus the node that groups *Mannophryne molinai* from the type locality (La Rondona) and from other populations (La Guáquira, Mayorica, Guayabito, and El Abrigo), and other two nodes into the clade of *M. herminae* complex, forming a large multispecific politomy (Figure 84). Genetic pairwise distances for 16S within this complex are low (Appendices 8), ranging between 0.5–1.4 % for *Mannophryne* sp. 4, 0.0–1.2 % for *M. molinai* and *Mannophryne* sp. from La Sierra, and 0.2–1.2 % for *M. herminae* (excluding *Mannophryne* aff. *herminae* ULABG5406, whose 16S p-distances within the complex were commented above).

The Andean clade (Figures 85–86) is composed of *Mannophryne orellana*, *M. cordilleriana*, *M. collaris*, *M. urticans*, *M. lamarcai*, *M. trujillensis*, *M. larandina*, *M. yustizi*, *M. speeri*, and several undetermined terminals, the last three taxa and the undetermined terminals being part of the complex of *M. yustizi* (Figure 86). Phenotypically, the andean clade of the *M*. *collaris* species group is defined by: 1) FII disc weakly expanded (character 13:1); 2) FIV disc

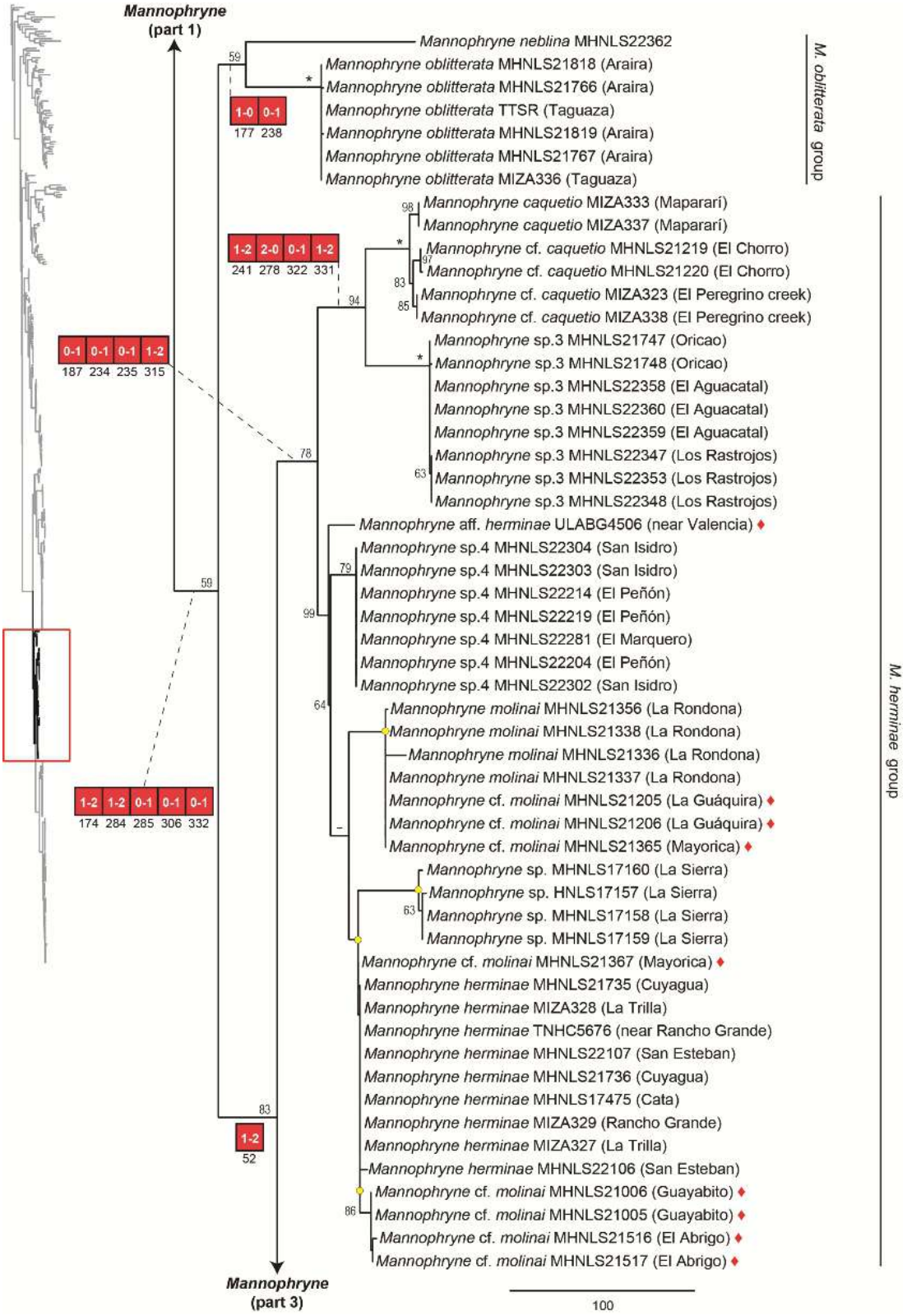

Figure. 84. Continuation of Fig. 83 showing the relationships among species of the *Mannophryne oblitterata* and, the newly proposed, *M. herminae* species groups. Numbers next to the nodes represent jackknife proportions (asterisks = 100 %, n-dashes < 50 %). Red diamonds indicate terminals only represented by molecular data. Selected clades are labeled with unambiguously optimized phenotypic synapomorphies (red square = unique, homoplastic; character number below squares; primitive–derived character-states inside squares). Yellow dots on nodes indicate collapsed clades in the strict consensus.

weakly expanded (character 15:1); 3) TII preaxial webbing leaving two phalanges free (character 47:2); 4) TIV preaxial webbing leaving three and half phalanges free (character 51:3); and, 5) Bright yellow spot on female throat restricted to the posterior half (character 93:0). In this clade, *Mannophryne orellana* and *M. cordilleriana* are sister (JK = 98 %; Figure 85) and reciprocally monophyletic, with four unambiguous phenotypic synapomorphies joining both species. Pairwise 16S distances between them are of 1.0–1.7 %. *Mannophryne collaris* is sister to the remaining species in the group, with 16S genetic distances = 0.5–1.9 % for 16S (Appendix 8). Intraspecific p-distances among terminals of *M. collaris* from five localities are 0.0–0.2 %.

Mannophryne urticans and *M. lamarcai* are recovered as sister and reciprocally monophyletic. The node that groups these two species (JK = 81 %), has six unambiguously optimized phenotypic synapomorphies (Figure 85). Pairwise 16S distances between *M. urticans* and *M. lamarcai* ranges between 0.7–1.4 %. *Mannophryne trujillensis* (JK = 97 %) is sister to the complex of *M. yustizi*; as in most other species, the six conspecific terminals of *M. trujillensis* from three distant populations form a polytomy and lack genetic divergence in 16S (p-distance = 0.0 %). The pairwise 16S distance of *M. trujillensis* with the species of the *M. yustizi* complex is 0.5–0.7 %.

Seven unambiguously optimized phenotypic synapomorphies delimit the *Mannophryne yustizi* complex (Figure 86). In it, *M. larandina* (JK = 57 %) appears as external to the other species and separated by a remarkable total evidence branch length; the terminal CWM1141, represented only by molecular data and identified as *“M. herminae”* is nested within *M. larandina*, with identical 16S and Cyt-b sequences to other samples of *M. larandina*.

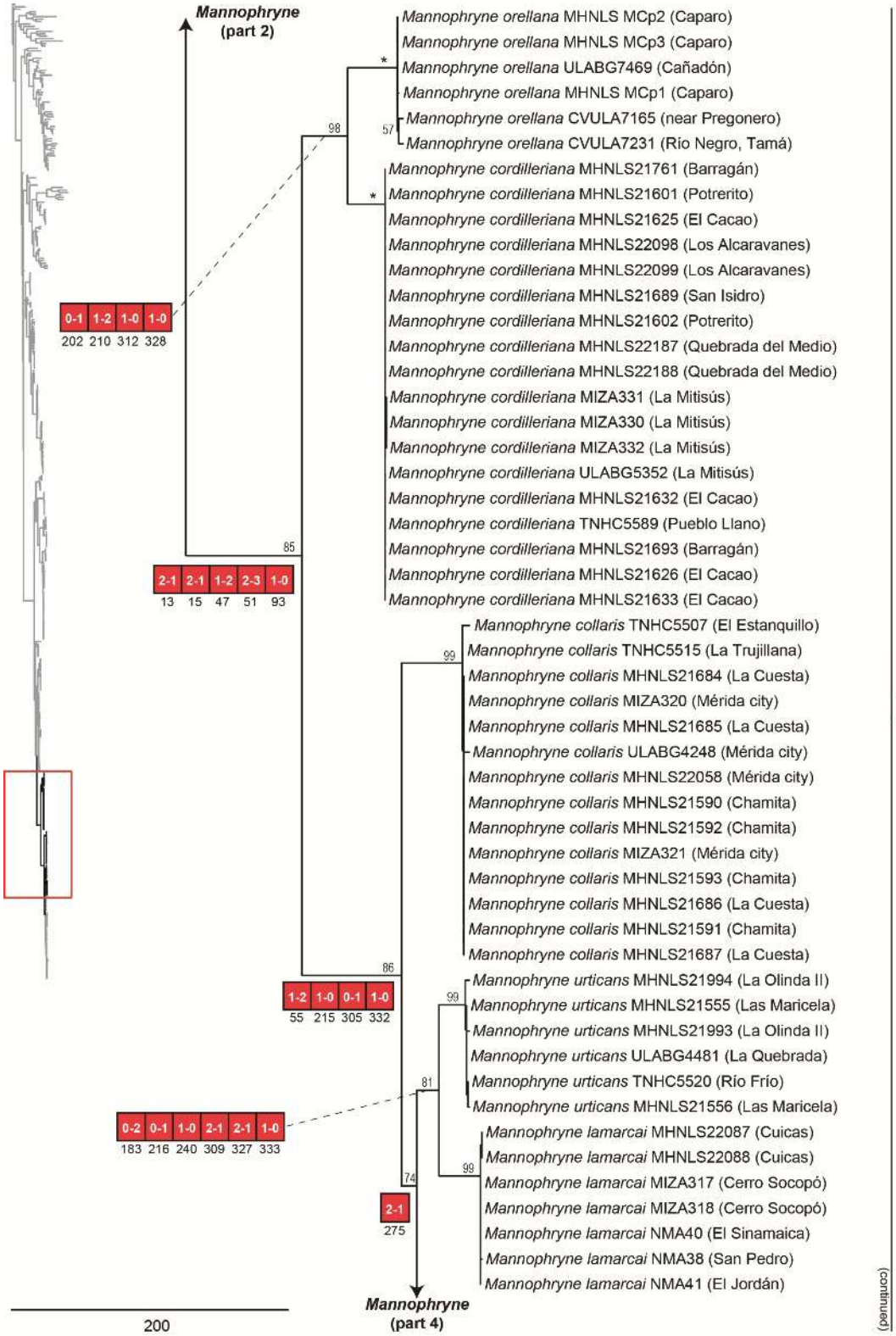

Figure. 85. Continuation of Fig. 84 showing the relationships among part of the *Mannophryne collaris* species groups. Numbers next to the nodes represent jackknife proportions (asterisks = 100 %, n-dashes = < 50 %). Selected clades are labeled with unambiguously optimized phenotypic synapomorphies (red square = unique, homoplastic; character number below squares; primitive–derived character-states inside squares).

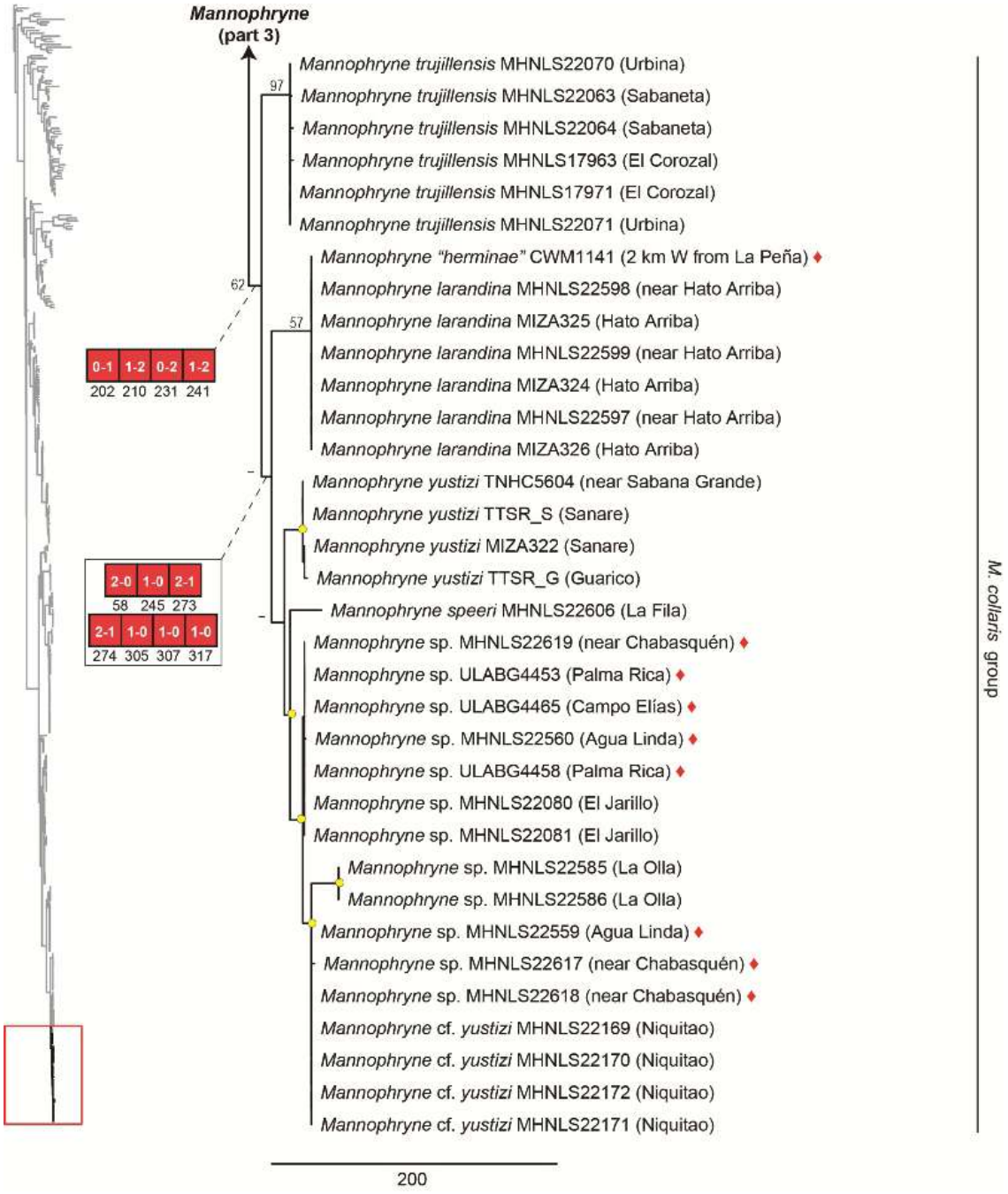

Figure. 86. Continuation of Fig. 85 showing the relationships among part of the *Mannophryne collaris* species group. Numbers next to the nodes represent jackknife proportions(n-dashes = < 50 %). Red diamonds indicate terminals only represented by molecular data. Selected clades are labeled with unambiguously optimized phenotypic synapomorphies (red square = unique, homoplastic; character number below squares; primitive–derived character-states inside squares). Yellow dots on nodes indicate collapsed clades in the strict consensus.

Mannophryne yustizi, *M. speeri*, and several undetermined terminals are part of a polytomy in the strict consensus (Figure 86). Pairwise distances among all terminals in the *M. yustizi* complex ranges between 0.0–0.5 % for 16S (Appendix 8) and between 0.3–2.7 % for Cyt-b (Appendix 9). We highlight that eight terminals in this complex are represented only by short 16S fragments and that at least the terminal *Mannophryne* sp. MHNLS 22559 was identified as a possible wild card (Appendix 5).

Discussion

Phylogenetic relationships of supraspecific taxa and the position of the enigmatic *"Colostethus" caribe*, *"Prostherapis" dunni*, and *"Phyllobates" mandelorum*

Grant *et al*. (2017) is, to date, the most complete quantitative phylogenetic study of dendrobatoids in terms of taxa and characters sampled. As in previous studies (Grant *et al.* 2006, Santos *et al.* 2009), they recovered Dendrobatoidea as monophyletic as well as the two families (Aromobatidae and Dendrobatidae) that group their diversity. Within Aromobatidae, *Aromobates* and *Mannophryne* (Aromobatinae) were recovered by them as reciprocally monophyletic and sister to the clade including *Anomaloglossus* and *Rheobates* (Anomaloglossinae). Finally, *Allobates* (Allobatinae) was inferred as sister to Anomaloglossinae + Aromobatinae. Despite that our study is focused in Aromobatinae and that the taxon sampling of all other dendrobatoids (herein treated as outgroups) represents a subsample of Grant *et al*.'s (2017) study, our results largely agree with their topology regarding relationships among supraspecific taxa (Figure

78); namely, a monophyletic Aromobatidae sister of Dendrobatidae and all five recognized aromobatid genera monophyletic and exhibiting similar relationships. However, we have discovered some remarkable novelties due to the inclusion of additional taxa, such as: 1) the position of "*Colostethus*" *caribe* as sister to the clade containing all aromobatids but *Allobates*; 2) the position of *"Prostherapis" dunni* within Anomaloglossinae, as sister to *Rheobates*; and 3) the position of *"Phyllobates" mandelorum* as sister to Aromobatinae (Figure 78).

"*Colostethus*" *caribe* is only known from its type locality, a cloud forest above 1,000 m asl at the Serranía de Paria, eastern part of the Cordillera de la Costa in northeastern Venezuela. The species is only known by three adult females collected in 2001, and was originally described by Barrio-Amorós *et al*. (2006a) as part of that genus based on alleged morphological similarities with some *Allobates* from northern Venezuela (at the time also placed in *Colostethus*). The description was published almost simultaneously with Grant *et al*. (2006) and its generic allocation was not evaluated by the latter study. Frost (2007) transferred it to *Allobates* by implication of the results of Grant *et al*. (2006), a taxonomy that has been widely accepted (Barrio-Amorós *et al*. 2009, Frost 2019), although remains without quantitative evaluation. As aforementioned, we evaluated this species on the basis of 269 phenotypic characters due to the absence of tissue samples for molecular studies. Its phylogenetic position is an unexpected discovery supported by 14 unambiguously optimized phenotypic synapomorphies (Figure 79). On the other hand, *Allobates*, to which was presumed that *"Colostethus" caribe* belonged, has 11 unique, unambiguously optimized phenotypic synapomorphies (Figure 79). Additionally, *"C." caribe* was not identified as a potential wildcard in our

analysis (Appendix 5). Thus, it seems unlikely that *"C". caribe* is part of *Allobates* or of any of the other recognized aromobatid genera. Consequently, with the evidence at hand, the less disruptive taxonomic change is to create a new genus to accommodate this species.

The phylogenetic position of *"Prostherapis" dunni* is also a remarkable discovery. This species is only know from two nearby localities in the northern slopes of the Caracas valley, in the central part of the Venezuelan Cordillera de la Costa (Barrio-Amorós 1999, La Marca 2004) and has not been seen for several decades (Rojas-Runjaic & Señaris 2015b). Although prior to this study, this species has not been included in a quantitative phylogenetic analysis, Rivero (1961, 1984a, 1990) and La Marca (2004) stated that *"Prostherapis" dunni* does not have any close relative in Venezuela. Grant *et al*. (2006) suspected a close relationship with *Aromobates* or *Rheobates* on the basis of some shared character sates (i.e., feet extensively webbed, zygomatic ramus elongate and robust, and absence of a median lingual process on tongue), but in absence of additional evidence, they just referred it to Aromobatidae as *incertae sedis*. Our finding of *"Prostherapis" dunni* nested deep inside Anomaloglossinae as sister of *Rheobates*, confirms one of the alternative relationships advanced by Grant *et al*. (2006). Despite *"Prostherapis" dunni* being represented in our study only by 166 phenotypic characters and the nodes grouping it with *Rheobates* and into Anomaloglossine have very low jackknife values, it shares with *Rheobates* the absence of a metatarsal tubercle (38: 0), and an the presence of an extensive toe webbing that only leaves free two phalanges on TIII preaxial side (49: 6) and three phalanges on TIV postaxial side (52: 4). Besides these synapomorphies, *"Prostherapis" dunni* also

shares with *Rheobates* the long and fang-like teeth on the maxillary arch, and a low number of premaxillary teeth (< 10). On the other hand, the monophyly of *Rheobates* (JK = 100 %) is supported by 12 unambiguously optimized phenotypic synapomorphies (Figure 80). Based on these evidences, we decided to create a new genus for *"Prostherapis" dunni*.

"Prostherapis" dunni is the only Anomaloglossinae in the Venezuela Cordillera de la Costa and its very restricted geographic distribution is markedly isolated from all other representatives of this subfamily. *Rheobates* is restricted to the Cordillera Central and Cordillera Oriental of the Colombian Andes and is separated from "*Prostherapis" dunni* by at least 700 km and two important mountain ranges (i.e., Cordillera de Mérida and the western half of Cordillera de La Costa), whereas *Anomaloglossus* is distributed in the Guiana region, at least 600 km, and separated by the Llanos and the Orinoco river.

"Phyllobates" mandelorum is only known from a few specimens collected on 1930 and 1932 in two imprecise localities at mount Turimiquire, in the eastern part of the Venezuelan Cordillera de la Costa (Schmidt 1932, La Marca 1993) and it has not been seen ever since (Señaris & Rojas-Runjaic 2015). Rivero (1961, 1984a, b, 1990) presumed that this species is closely related to *Mannophryne* (its Group VII), whereas La Marca (1993) highlighted resemblances between it and *Aromobates* (by then defined as *C. alboguttatus* group), but their relationships remained uncertain. Grant *et al*. (2006) transferred it to *Allobates* on the basis of general morphological similarities. More recently, Dias (2018) in his unpublished thesis on the evolution on larval characters in Dendrobatoidea, recovered *"Phyllobates" mandelorun* nested within *Aromobates*. Our hypothesis corroborates that *"Phyllobates" mandelorum*

is an aromobatid closely related to (but not part of) *Aromobates* and *Mannophryne* as previously suspected by Rivero (1990) and La Marca (2006). Our evidence is incompatible with the proposals of Grant *et al*. (2006) and Dias (2018), and deserves further discusion. Our results reveal that *"Phyllobates" mandelorum* shares with *Aromobates* and *Mannophryne* the presence of moderately expanded discs on FII, FIV and TV as unambiguously optimized synapomorphies (characters 13:2, 15:2, and 44:2, respectively). Furthermore, the clade formed by *Aromobates* and *Mannophryne* (Aromobatinae) is delimited by other five unambiguous synapomorphies, all related to osteology and identified in this study for the first time —Grant *et al*. (2017) only recovered the presence of dorsolateral stripe A (character 64 in this study) as synapomorphy for Aromobatinae, but this was not corroborated by us (Figure 81). Moreover, we identified five new synapomophies for *Aromobates*. We interpreted our results as strong evidence indicating the position of *"Phyllobates" mandelorum* as sister to the clade containing *Aromobates* and *Mannophryne* and not as nested within *Aromobates*. Nonetheless, we refrain from taking nomenclatural actions (e.g., a new genus) in view of the contrasting results of Dias (2018). Both studies substantially differ in the taxon and phenotypic character sampling: whereas we included 383 phenotypic characters, of which almost half corresponds to osteology, Dias (2018) included more than 500 characters, of which 392 derived from larval morphology. As per taxon sampling, we do not know the breath of aromobatins sampled by Dias (2018), but it is likely smaller than ours, which includes all the 39 currently recognized species and a number of putative new species. Differences in both taxon and character sampling can strongly affect the results of phylogenetic analyses (e.g., Castroviejo-Fisher *et*

al. 2015, Grant *et al*. 2017) and although extensive taxon sampling is recognized as one of the most important determinants of phylogenetic estimation (Heat *et al*. 2008) we consider that the relationships of *"Phyllobates" mandelorum* must be evaluated in a new quantitative study based on the combined datasets of both studies before making a taxonomic decision.

Phylogenetic relationships of skunk frogs (*Aromobates*)

The more complete phylogenetic analyses of *Aromobates* to date are those of Barrio-Amorós & Santos (2012) and Grant *et al*. (2017). In Barrio-Amorós & Santos (2012), the taxon sampling was notably expanded in relation to previous studies—they included 10 putative species, although only seven of the 19 currently recognized species were identified. However, they excluded all phenotypic evidence and several loci previously employed in Grant *et al*. (2006) and analyzed mitochondrial and nuclear loci separately. Grant *et al*. (2017) did not include new terminals, but incorporated all previous evidence and some additional phenotypic characters to their total evidence analysis. Despite differences in character sampling and analytical methods, the optimal topologies inferred by both studies are largely congruent. Nonetheless, incomplete taxon sampling—12 (63 %) of the 19 described species—still hampered the understanding of the evolutionary history of *Aromobates*. Our study is the first that analyzes all the 19 species plus some additional putative new species of *Aromobates*. This was only possible by including several terminals as OPD. Our result corroborates the monophyly of *Aromobates* as currently understood, identifies for first time several new unambiguously

optimized phenotypic synapomorphies for the genus, and uncovers several putative new species and new relationships.

The position of *Aromobates* sp. 1 as sister to all other *Aromobates* is a novel relationship. This taxon is a new putative species (Rojas-Runjaic *et al*. in prep.), with some noteworthy characteristics. It inhabits forest ponds, their diel activity includes diurnal and nocturnal periods, males present conspicuous glandular swelling on fingers, and it is the only species in the genus that shows a highly raised metatarsal fold to the level of the inner metatarsal tubercle and not fused to it. Specimens from the two sampled localities were recovered as sister and reciprocally monophyletic (Figure 81). Some morphological differences were detected between them (Figure 87), but they are distanced by short branches (only nine transformations between them) and their genetic 16S and Cyt-b p-distances are 0.0 % and 0.3 % respectively. Thus, we treated then as conspecific but highlighting the necessity of additional interpopulational studies.

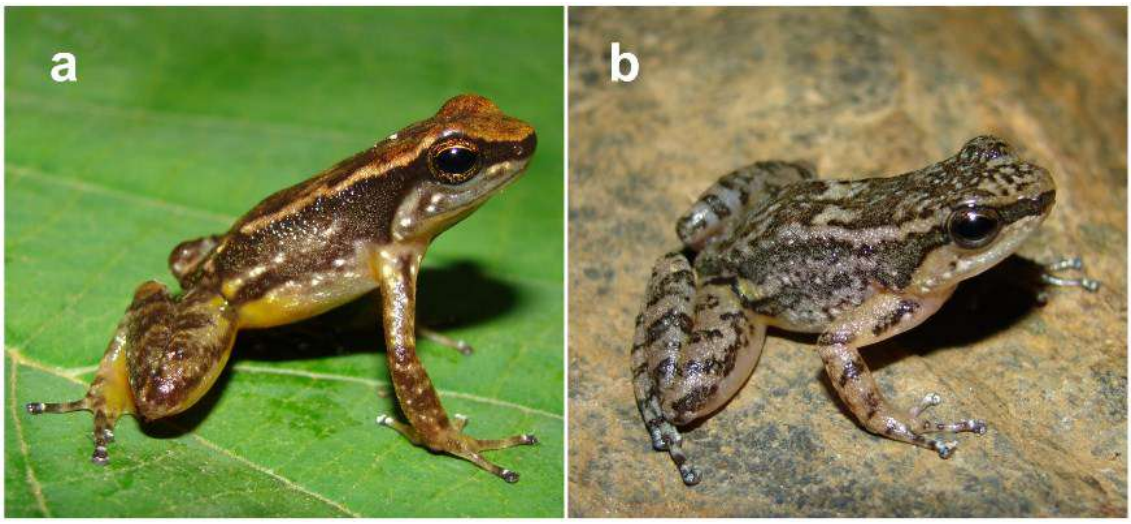

Figure 87. *Aromobates* sp. 1 from Cerro El Tigre (a) and *A.* cf. sp. 1 from La rondona. Both localities are in the Sierra de Aroa and distanced by ~13 km.

Aromobates sp. 1 inhabits the Sierra de Aroa, in the western end of Cordillera de la Costa and is the first *Aromobates* discovered outside of the Andean mountain system. This finding indicates that the Barquisimeto depression, the biogeographic barrier that separates the Andean Cordillera de Mérida and the Cordillera de la Costa, does not limit the distribution of *Aromobates* (Barrio-Amorós & Santos 2012) and generates expectations about the potential discovery of other representatives of this genus in the Cordillera de la Costa.

Different from Barrio-Amorós *et al*. (2012) and Grant *et al*. (2017), who inferred *Aromobates ornatissimus* as sister to all other *Aromobates*, we recovered it nested deep within the genus, in a clade with *A. alboguttatus* and *A. haydeeae*—two OPD taxa, included for the first time in a quantitative phylogenetic study. It seems likely that the topological differences involving *A. ornatissimus* with regards to previous studies are due to our new taxon additions (Figure 81). On the other hand, Rivero (1978) previously suggested a close relationship between *A. alboguttatus* and *A. haydeeae*, although he also discussed a close relationship of these two species with *A. orostoma*, which we do not recover. *Aromobates ornatissimus* exhibits some morphological peculiarities in relation to other *Aromobates* (e.g., reduced finger and toe discs) and its general external aspect differs from that of *A. albogutatus* and *A. haydeeae*, so this new relationship was unexpected. However, the three species share laterodorsally oriented nares (58:0), a lateral dark band wider at the arm insertion than in the midbody (72:2), and a rounded to obtuse cultriform process anterior tip (256:1) as unambiguously optimized phenotypic synapomorphies (Figure 81).

Particularly relevant is the position of *Aromobates alboguttatus*, well-nested within *Aromobates*. This is the type species of *Nephelobates* (La Marca 1994b) and was transferred to *Aromobates* based on general morphological similarities, but in the absence of unambiguous phenotypic synapomorphies (Grant *et al*. 2006). Our results now corroborate *Aromobates alboguttatus* as belonging to *Aromobates* and objectively confirm *Nephelobates* as a junior synonym of *Aromobates*.

Aromobates sp. 2 is recovered herein as a deeply divergent linage (branch length = 46 transformations), sister to a much more inclusive clade (Figure 81) compared with those of Barrio-Amorós & Santos (2012) and Grant *et al*. (2017), where it was inferred as sister to a clade only containing *A. meridensis*, *A. ericksonae*, *A*. *cannatellai*, *A*. *saltuensis*, and an undetermined related terminal. Although *Aromobates* sp. 2 was discovered in 2008 (Barrio-Amorós & Molina 2010) and Barrio-Amorós & Santos (2012) already suspected that it was an undescribed species, this taxon is known only from tadpoles and postmetamorphs and several subsequent searches failed to find adult specimens. Thus, the lack of knowledge on its adult morphology, together with the limited understanding on the phylogenetic relationships among already described species of *Aromobates*, prevented the formal description of this species. Our results strongly corroborate *Aromobates* sp. 2 as a putative new species. This is the only *Aromobates* inhabiting the western (Orinoquian) slope of Cordillera de Mérida (in a cloud forest rivulet, about 1,700 m asl). Its geographically nearest congener is *A. leopardalis*, which is restricted to the páramo of Mucubají (above 3,300 m asl) and they are not sister.

Aromobates walterarpi is also an ODP terminal. Based on morphological resemblances, La Marca & Otero (2012) suggested that this species could be a close relative of *A. meridensis*. However, we recovered it as sister of *A. nocturnus* (Figure 81). This relationship is strongly supported by nine unambiguously optimized phenotypic synapomorphies: 1) weakly developed metatarsal fold (55:1), 2) anterior ridge of the *pars glenoidalis* absent (181:0), 3) frontoparietal-otoccipital articulation free (235:0), 4) ventral-posterior corner of the otic capsule open (244:0), 5) exoccipitals ventral-medially free (246:0), 6) Prooticts completely separated ventral-medially (247:0), 7) anterior apophysis of the vertebra III transverse process absent (305:0), 8) proximal end of humerus paraventral crest undifferentiated (327:0), and 9) *crista femoris* absent (331:0).

Aromobates sp. 3, *A. capurinensis*, *A. orostoma*, *A. inflexus*, and *A. molinarii* (all but *A molinarii* as OPD) conform a clade with a short branch length (5 transformations) and three phenotypic synapomorphies: 1) a well-defined dark lower labial stripe (89:1), 2) a vertebra II neural arch anterior to the level of the postzygoapophyses (277:0), and 3) sacral diapophyses weakly expanded (285:1). *Aromobates* sp. 3 is only known from a few old museum specimens collected in a locality on the western piedmont of Cordillera de Mérida. Its morphology makes us suspect that it corresponds to a linage different from those already described, wich is also supported by its phylogenetic position and branch length (20 transformations).

The sister relationship between *Aromobates orostoma* and *A. inflexus* recovered in our study, agrees with the suggestion of Barrio-Amorós & Santos (2012), who proposed the resurrection of *A. inflexus* from its synonymy with *A. alboguttatus*. *Aromobates inflexus* was considered a junior synonym of *A.*

alboguttatus by Rivero (1984b) who argued for the absence of diagnostic characters between them. Barrio-Amorós & Santos (2012) defended that the geographic distribution of these two species is very restricted, allopatric—as observed in almost all *Aromobates*—and distanced by about 100 km. They also commented on the need to make a proper comparison of *A. inflexus* with *A. orostoma*, which geographically is the closest species. Our results refuted the synonymy of *A. inflexus* in *A. alboguttatus* (they are not even sister of each other) and also support *A. inflexus* as a different linage from *A. orostoma* because there is considerably divergence between them (a total of 37 transformations) and *A. inflexus* exhibit some remarkable differences in relation to *A. orostoma* (character states of the latter in parenthesis), such as the presence of a strong dorsolateral ridge (absent), lack of a middle metatarsal tubercle (present), and absence of a dark lower labial stripe (present).

Our new sequences of *Aromobates zippeli* form a monophyletic group (JK = 100 %) with the sequences originally published by La Marca *et al*. (2002) as *Nephelobates* sp. ULABG 4496 (AJ430677) and by Manzanilla *et al*. (2009) as *Aromobates* sp. MIZA 310 (EU380798, EU380850), *Aromobates* sp. MIZA 311 (EU380799, EU380851), and *Aromobates* sp. MIZA 312 (EU380800, EU380852). They correspond to topotypic specimens and the pairwise 16S distances among them are = 0.0 %. Thus, we identify all these sequences listed above and repeatedly referred as undetermined in previous studies (La Marca *et al*. 2002, Vences *et al*. 2003, Grant *et al*. 2006, Manzanilla *et al*. 2009, Barrio-Amorós *et al*. 2011, Barrio-Amorós & Santos 2012, Grant *et al*. 2017) as belonging to specimens of *A. zippeli*. This species is grouped with *A. duranti* and *A serranus* (both OPD), sharing the following synapomorphies: 1) nares

laterodorsally oriented (58:0), 2) medial process of the premaxilla *pars palatina* narrower than the lateral process (206:1), 3) ventral surface of the vertebrae III-VIII flat to convex (297:1), 4) anterodorsal process of the urostyle narrower at the tip than at the base (309:0), and 5) proximal end of the humerus paraventral crest weakly raised (327:1). Despite the relationships among these three species are unresolved, branch lengths (between 25 and 28 transformations) support them as different species.

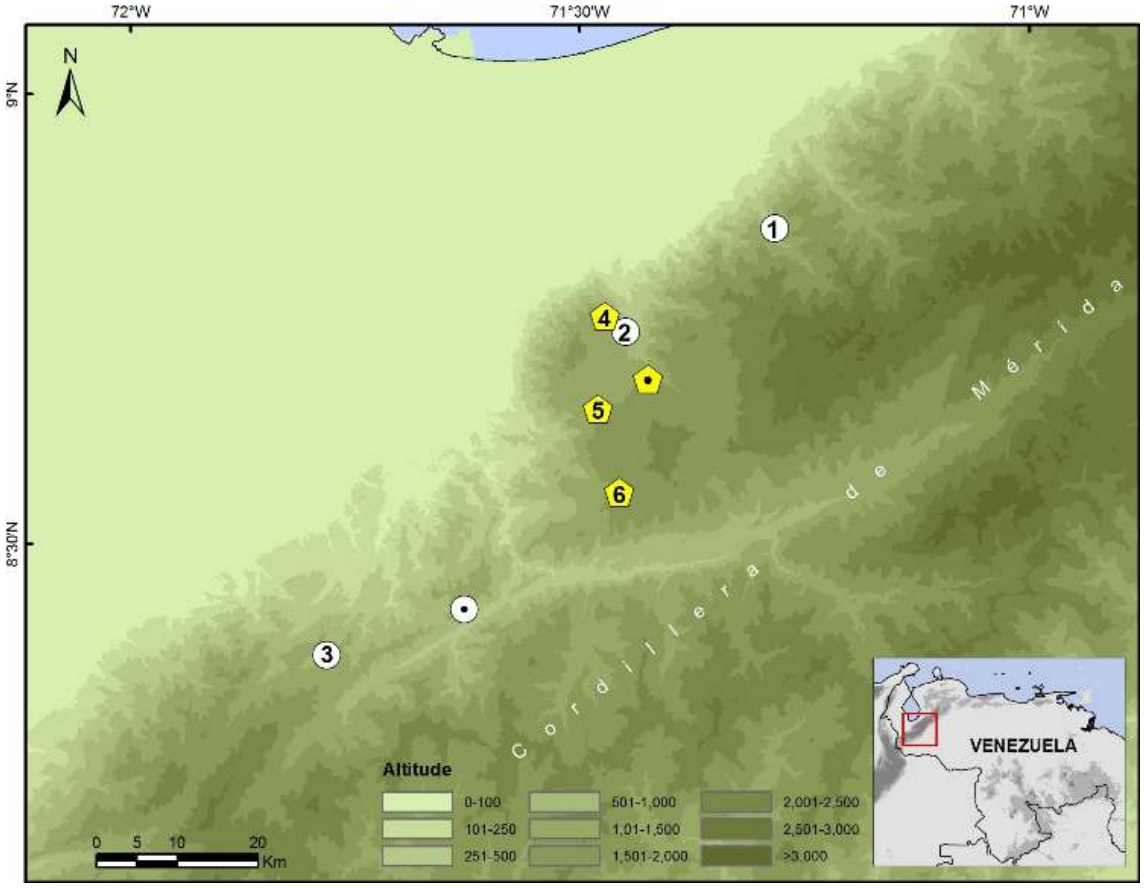

Figure 88. Map of the southwestern part of Cordillera de Mérida in northwestern Venezuela, showing the distribution of *Aromobates ericksonae* (junior synonym of *A. mayorgai*) and *A. mayorgai*. Yellow pentagons: *A. mayorgai* (dotted pentagon: El Chorotal; type locality); white circles: *A. ericksonae* (dotted circle: Los Ranchos, near Santa Cruz de Mora; type locality); 1. Río Frío; 2. La Olinda; 3. Zea; 4. La Olinda II; 5. La Osa; 6. La Trampa.

The sister relation of *Aromobates leopardalis* (an OPD terminal) and *A. meridensis* is also new and unexpected. La Marca (1997) presumed a close

relationship between *A. leopardalis* and *A. nocturnus* (on the basis of their shared extensively webbed feet, aquaticity, and strong smell). On the other hand, La Marca & Otero (2012) considered *A. meridensis* and *A. walterarpi* as closely relatives based on morphological affinities. However, our results recovered *A. leopardalis* and *A. meridensis* more closely related to other species e.g., *A. mayorgai*, *A. tokuko*) than to *A. nocturnus* or *A. walterarpi*. Furthermore, they are recovered as sister species, which is supported by the following unambiguously optimized phenotypic synapomorphies: 1) lateral dark band diffuse (74:0), 2) ventrolateral stripe present (75:1), 3) anteromedian process of the palatine present (211:1), 4) nasal and maxilla in contact (222:1), 5) posterior process of the prasaphenoid surpassing the level of the jugular foramina (249:1), and 6) aterior end of the ilium reniform in cross-section (320:2).

Although Barrio-Amorós & Santos (2012) did not include terminals identified as *Aromobates mayorgai*, they described a new relatively similar species, *A. ericksonae*. This new species was referred from five localities along ~70 km of the western foothills of the Cordillera de Mérida (two of these localities close to La Azulita, which is included into the historical distribution of *A. mayorgai*). The two aforementioned species were morphologically diagnosed on the basis of (characters for *A. mayorgai* in parenthesis): smooth dorsal skin without tubercles in preserved specimens (smooth with a few tubercles posteriorly), FI longer than FII (FI shorter than FII or equal), ventral parts white in females (yellow), dark throat in breeding males (throat, chest and belly dark with a suffusion of small white spots), and oblique lateral stripe formed by small whitish spots (absent). We obtained new samples of *A. mayorgai* from three

populations (Figure 88), two of them (La Osa and La Trampa) ~9 km S of its type locality and the third one (La Olinda II) 5 km W from La Azulita, close to two of the localities referred for *A. ericksonae* by Barrio-Amorós & Santos (2012). We also obtained an additional sample of *A. ericksonae* from a new locality (Zea) 12 km WSW from the type locality of that species. In our phylogeny, we recovered *Aromobates ericksonae* and *A. mayorgai* intermixed in a large polytomy (Figure 82), and despite all of these samples originating from seven localities sparsed through 75 km, they are identical in their 16S and Cyt-b sequences (Appendices 6 and 7). This strongly points to *A. ericksonae* as conspecific with *A. mayorgai*. Furthermore, the alleged morphological differences between both species listed by Barrio-Amorós & Santos (2012) actually represent polymorphism within *A. mayorgai* as per our observations of new and previously available material. Differences in relative size of FI and FII fall within the variation of our state 2 (equal to subequal in size; character 10 in Results: Phenotypic characters). Additionally, no relevant differences were detected in structural, spectral, and temporal parameters between advertisement calls of *A. ericksonae* described by Barrio-Amorós & Santos (2012) and Santos *et al.* (2014), and those of *A. mayorgai* recorded by us (i.e., trills of notes arranged in duplets, with dominant frequency about 3,5–4.3 kHz, duplet duration about 127–153 ms, and time between calls about 1 s). Based on these new results, we considered *A. ericksonae* as a junior synonym of *A. mayorgai*.

Our new topotypic samples of *Aromobates cannatellai* form a monophyletic group with the only previously sequenced sample available for this species (CVULA 8325; Figure 82) and their 16S p-distance is 0.0 %

(Appendix 6). *Aromobates cannatellai* was inferred as sister of an undetermined linage from Cubará, Colombia (Andean Cordillera Oriental, Figure 89), referred as *Aromobates* sp. MUJ 3726 by Barrio-Amorós & Santos (2012), and as *Aromobates saltuensis* MUJ 3726 by Grant *et al*. (2017). However, based on our results, *A. cannatellai* is not sister of *A.* sp MUJ 3726 but of *A.* sp. Asa4 (JK = 51 %), an undetermined linage from Río Chiquito, northern slope of the Tamá massif and south of the Táchira depression in Venezuela (Figure 89). The 16S p-distance between *A. cannatellai* and *A.* sp. Asa4 is 1.3 % (Appendix 6) and the locality of the latter is ~82 km SW from the type locality of *A. cannatellai* (La Escalera, Cordillera de Mérida, north of the Táchira depression; Figure 89). *Aromobates* sp. MUJ 3726, in turn, is sister (JK = 85 %) of another undetermined linage (*Aromobates* sp. Tama14) from the southern slope of the Tamá massif (south of the Táchira depression), also in Colombia. Both localities are separated by ~40 km, in two different river basins (Figure 89), their 16S p-distance is 1.1 %, and there are 27 molecular transformations separating them. Genetic and geographic distance among these two sister linages and *A. cannatellai* is: 1.8 % and 141 km with *A.* sp. MUJ 3726 and 2.0 % and 106 km with *A.* sp. Tama 14. Intraspecific pairwise 16S distances in *Aromobates* typically range between 0.0–0.4 %, whereas interspecific p-distance may be as low as 0.9–1.1 %—as in the case of *A. zippeli* and *A. molinarii*, which are not close relatives. Thus, our evidence—topology, genetic pairwise distances, patristic distances, and biogeography—suggests that, rather than phylogeographic structure of a single species (i.e., *A. cannatellai*), the relationships described in our topology may be representing diversity at the species level. However, we have not been able to examine specimens and

advertisement calls from the three groups related to *A. cannatellai* so we refrain from treating them as putative new species. This group deserves a more detailed study including morphology, bioacoustics, and an improved geographic sampling.

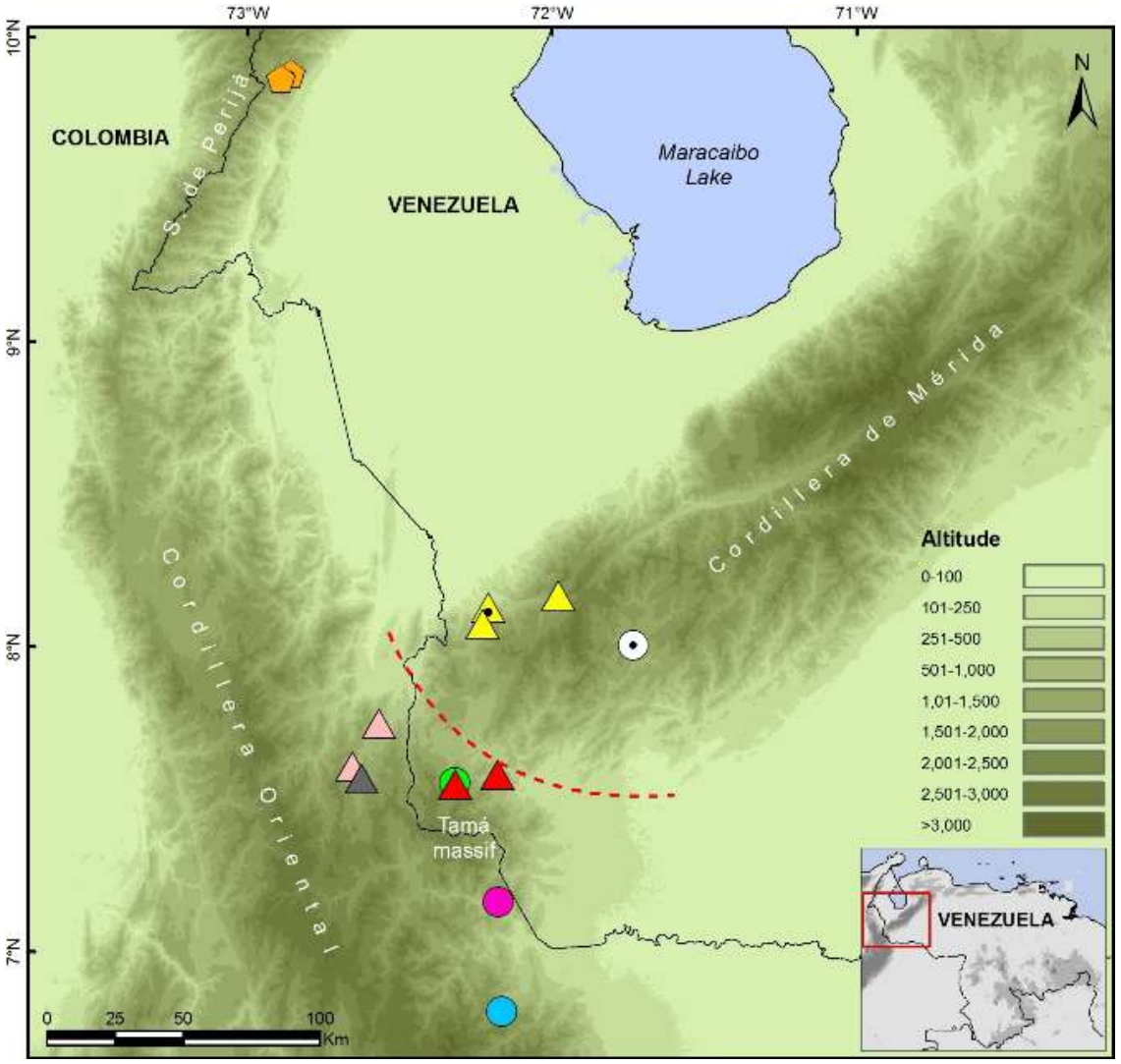

Figure. 89. Map of the northern end of the Andean mountain range showing the Sierra de Perijá, northeastern portion of Cordillera Oriental (CO), Tamá massif, and Cordillera de Mérida. Black line indicates the limits between Colombia and Venezuela. Dashed red line highlights the Táchira depression. Circles correspond to the clade of *Aromobates cannatellai*; black-dotted white circle: *A. cannatellai* (La Escalera, type locality); green circle: *A.* aff. *cannatellai* from Río Chiquito, north of Tamá; fuchsia circle *A.* aff. *cannatellai* from southern slope of Tamá; blue circle: *A.* aff. *cannatellai* from Cubará. Triangles correspond to the complex of *A. saltuensis*; yellow triangles: *A. saltuensis sensu stricto* (dotted triangle indicating the type locality); red triangles: *A.* aff. *saltuensis* from Río Chiquito (left) and Río Negro (right) at the northern slope of Tamá massif; gray triangle: *A.* aff. *saltuensis* from El Diamante, CO; pink triangles: *A.* aff. *saltuensis* from Bochalema (below) and La Garita (above), CO. Orage pentagons: *A. tokuko*.

The position of *Aromobates tokuko* as part of the complex of *A. saltuensis*, which form a polytomy in the strict consensus (Figure 82), also constitutes a new discovery. This species is distributed in the eastern foothills of Sierra de Perijá in Venezuela (Figure 89) and is the unique representative of the genus known from this Andean mountain system. This species was described on the basis of external morphology (Rojas-Runjaic *et al*. 2011) and its relationships remained unknown until now.

Our new samples of *Aromobates saltuensis sensu stricto* from near the type locality (La Quintera, Táchira, Venezuela) and from Guacharaquita (Táchira, Venezuela, ~25 km from the type locality) form a monophyletic group (JK = 93 %) with the only previous sequenced sample available for this species (TNHC 5541, from near san Félix, Táchira, Venezuela, ~7 km from the type locality); 16S p-distances among these samples is 0.0 %. These results corroborate the identity of TNHC 5541 as *A. saltuensis* and confirm its distribution at the three localities north of the Táchira depression.

Aromobates saltuensis is recovered as sister and reciprocally monophyletic to a clade (JK = 95) including two undetermined samples from two different localities (MHNLS 22498 from Río Chiquito and CVULA 8321 from Río Negro, both in Táchira, Venezuela; 16S p-distance = 0.0 %), but both located to south of the Táchira depression (northern slope of the Tamá massif; Figure 89); there are 12 transformations between *A. saltuensis* and this group and the 16S p-distance is 0.7 %. The clade containing *A. saltuensis sensu stricto* and *Aromobates* sp. from the northern slope of the Tamá massif (JK = 84 %) is part of a polytomy with *A. tokuko* from the Sierra de Perijá, and other four undetermined terminals from three different localities of the Cordillera Oriental

of Colombia, all of which with considerable branch length (> 17 transformations) and exhibiting 16S p-distances of 0.4–1.3 % with *A. saltuensis*, *A.* sp from north Tamá (the clade sister of *A. saltuensis*), and *A. tokuko* (Appendix 6). The unresolved relationships within this clade prevent us from making additional taxonomic decisions about the *A. saltuensis* complex, but on the basis of observed geographic distributions and genetic distances, we suggest that *Aromobates saltuensis* is restricted to a small portion of the southwestern slope of the Cordillera de Mérida, north of the Táchira depression, and that specimens from south of the Táchira depression (on the northern slope of the Tamá massif) and the Cordillera Oriental of Colombia, correspond to at least two putative new species (Figure 89). As in the case of the clade of *A. cannatellai*, this group deserves additional study based on an improved molecular and geographic sampling and including bioacoustic evidence, in order to properly define species limits.

Phylogenetic relationships of the collared frogs (*Mannophryne*)

The more complete phylogeny of *Mannophryne* to date also corresponds to Grant *et al*. (2017). Although they did not generate new sequences for this genus, their study included the 13 described species previously analyzed by Manzanilla *et al*. (2009) plus three additional ones sequenced by Santos *et al*. (2014). Our study is the first that includes all the 20 currently recognized species of the genus. Furthermore, we also include several putative new species. Inasmuch as our sampling is also based on a noticeably expanded phenotypic and molecular dataset, including previous and new data, this study represents the largest effort to addres the evolutionary relationships of

Mannophryne and given the total evidence approach, we are in a unique position to evaluate all previous phylogenetic hypotheses.

From the 13 unambiguously optimized phenotypic synapomorphies for *Mannophryne* identified in our study, 11 are new. The other two—related to the dark dermal collar—were already identified by Grant *et al*. (2006, 2017), although as a single transformation series (we scored it for males and females as different semaphoronts). Besides the dark dermal collar, Grant *et al*. (2017) optimized four phenotypic synapomorphies for *Mannophryne*, but none of those were recovered in our analysis. Nonetheless, we found that the length of FI = FII (character state 10:2 in this study), which was recovered as synapomorphic for *Mannophryne* by Grant *et al*. (2017), is a synapomophy for a more inclusive clade that includes all Aromobatidae except *Allobates* (Figure 79). This new optimization probably derives from our modification of states of this character (see character 10 in Results: Phenotypic characters). Following our coding scheme, most sampled aromobatids are now now coded as state 2 (i.e., FI and FII equal to subequal). Finally, the presence of a bright yellow spot on the throat of females (character 92:2) was proposed by La Marca (1992) as a putative synapomorphy, which is herein confirmed for the first time in a quantitative phylogenetic study.

Although we corroborated the monophyly of the genus and the three primary clades (species groups) recovered by Grant *et al*. (2017), some relationships inferred by us differ from those recovered by them, but agree with Manzanilla *et al*. (2007). This is unexpected inasmuch this last study was based on ~1,200 bp of two mitochondrial genes (COI and 16S). We discussed these differences below, as well as the numerous new relationships discovered.

Whereas Grant *et al*. (2017) recovered the *Mannophryne collaris* group as sister to *M. oblitterata* and *M. trinitatis* groups, we recovered the same relationships among species groups inferred by Manzanilla *et al*. (2009), namely, the *M. trinitatis* group sister to *M. oblitterata* and "*M. collaris*" groups. Moreover, we recognize a fourth species group according to our results (Figure 84), which includes species which were previously part of the former *Mannophryne collaris* group (Manzanilla *et al*. 2009). This new species group is sister to the *M. collaris* group (*sensu* this work) and corresponds in our results to the Coastal clade within the *M. collaris* group. Grant *et al*. (2017) did not recover this new species group as monophyletic, because in their phylogeny *M. caquetio* is sister of all species of the *M. collaris* group except *M. herminae*, instead forming a clade with *M. herminae* (as in Manzanilla *et al*. 2009). Herein we formally recognized a fourth species group, the *Mannophryne herminae* group. This new species group is represented in our phylogeny by *M. caquetio*, *M. herminae*, *M. molinai*, and two putative new species. The *Mannophryne herminae* group is defined by four unambiguously phenotypic synapomorphies (Figure 84) and their species are restricted to the western part of the Cordillera de la Costa. The *Mannophryne collaris* group *sensu* this work, is now restricted to the most exclusive clade including *M. orellana* and *M. speeri* and is defined by five unambiguously optimized phenotypic synapomorphies (Figure 85). All their currently known species are restricted to the Venezuelan Andes.

The relationships recovered in our study within the *Mannophryne trinitatis* group differ little from those of Manzanilla *et al*. (2009) and Grant *et al*. (2017). An issue that stands out within this group is the genetic structure and intraspecific pairwise 16S distances (up to 1.2 %) observed within *M. leonardoi*.

All samples included in our phylogeny and attributed to this species come from several localities on a small area (~66 km^2 and maximum distance between localities of ~30 km in straight-line) of the eastern slope of Turimiquire massif and none of them is topotypic. The type locality of *M. leonardoi* (El Toyano) is on the western slope of this massif (Manzanilla *et al*. 2007a), about 96 km W from these localities, and topotypic samples have not been studied to date. On the other hand, intraspecific 16S p-distances in *Mannophryne* are commonly between 0.0–0.5 % (Appendix 8) and genetic structure within species is incipient or absent (Figures 83–86). Thus, we expected greater genetic distances and additional phylogeographic structure within *M. leonardoi* with the inclusion of topotypic samples, which, in turn, could be indicative of cryptic diversity at the species level. Corroboration of the identity of these non-topotypic samples attributed to *M. leonardoi* by us and previous studies (Manzanilla *et al*. 2009, Grant *et al*. 2017) is pending.

Mannophryne sp. 1, and *M.* sp. 2, both putative new species within the complex of *M. vulcano*, are supported by the topology, branch lengths (57 and 17 transformations, respectively), and 16S p-distances (Appendix 8). Samples of these two linages were already included by Manzanilla *et al*. (2009) as unnamed taxa forming a monophyletic group, sister to *M. trinitatis* and *M. venezuelensis,* although it was unclear it they considered them as part of a single or several species. Our results indicate that besides *M. vulcano*, there are two putative new species (*M.* sp. 1, and *M.* sp. 2) closely related. Additionally, we recovered two undetermined linages within the *M. vulcano* complex, one represented by a single terminal from Guatopo (*Mannophryne* sp. TNHC 5566; Figure 90) and the other by two terminals from Araira

(*Mannophryne* sp. MHNLS 21825 and 21826; Figure 90). The first one (TNHC 5566) shows comparatively large 16S p-distances with their relatives within the group (1.4–2.1%; Appendix 8) and is found as sister of all other terminals in the complex, except for *M.* sp. 1; therefore, we suspect that this may correspond to an additional undescribed species. However, in absence of specimens and call recordings from this population we refrain from refer to it as a new putative species.

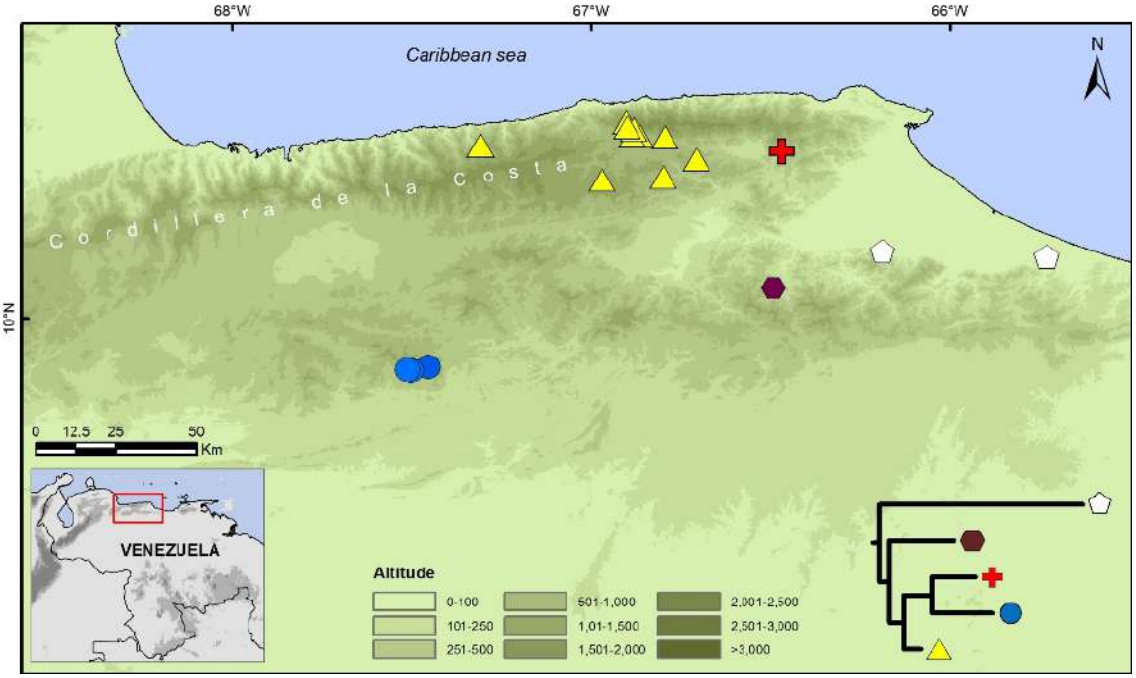

Figure. 90. Map of the central part of Cordillera de la Costa in northern Venezuela showing the distribution of the *Mannophryne vulcano* complex. White pentagons: *Mannophryne* sp. 1; purple hexagon: *Mannophryne* sp. Guatopo (TNHC 5666); red cross: *Mannophryne* sp. from Araira; blue circles: *Mannophryne* sp. 2; yellow triangles: *Mannophryne vulcano*. The topology on the lower right corner depicts the relationships within the complex.

The case of *Mannophryne* sp. Araira, is more complex. It is sister of *M.* sp. 2, and both share eight unambiguously optimized phenotypic synapomorphies (Figure 83). Despite they are geographically distant (~133 km in straight-line; Figure 90) their 16S p-distances are low (0.2–0.5 %). On the other hand, *Mannophryne* sp. Araira is separated from *M. vulcano* by 25

transformations and are not sister linages, but the pairwise 16S distances between both are 0.0–0.5 %. *Mannophryne* sp. Araira and *M. vulcano* differ in some phenotypic characters and in bioacoustic parameters (Table 2). We presume that *M.* sp. Araira may belong to an undescribed species and the absence of genetic distances in 16S between it and some terminals of *M. vulcano*—both parapatric but not sister in our phylogeny—may be due to introgression. However, our study is not designed to properly analyze and interpret this scenario and we refrain from referring to *Mannophryne* sp. Araira as a putative new species.

Table 2. Comparison of some temporal and spectral call parameters between *Mannophryne* sp. from Araira and *M. vulcano* from Caracas valley. Parameter values are presented as minimum-maximum.

Call parameters	***Mannophryne* sp. Araira**	***Mannophryne vulcano***
Note emission rate (notes/s)	4.9–6.3	2.0–4.3
Note duration (s)	0.023–0.037	0.028–0.056
Internote interval (s)	0.023–0.029	0.039–0.056
Duplet duration* (s)	0.078–0.092	0.092–0.126
interduplet time (s)	0.169–0.474	0.282–1.331
Peak frequency (kHz)	4.6–5.0	3.4–4.5
Bandwidth (kHz)	0.3-0.6	0.2–0.7

*The advertisement calls of both liganes are composed by notes arranged in duplets.

The position of *Mannophryne neblina*—herein included by first time in a quantitative phylogenetic study—as sister of *M. oblitterata* is a new discovery and adds a second species to the *M. oblitterata* species group. The two unambiguous phenotypic synapomorphies optimized on the most recent common ancestor of this group (Figure 84) also constitutes a new finding. Previous studies had recovered *M. oblitterata* as the unique representative of their homonymous group and no phenotypic autapomorphy had been identified for it (Manzanilla *et al*. 2009, Grant *et al*. 2017).

The phylogeographic structure (Figure 84) and genetic distances (1.0–1.9 %) observed among three populations of *Mannophryne caquetio* from two different mountain ranges is uncommon among *Mannophryne*. Manzanilla *et al*. (2009) already noted a divergence of 0.8 % between their topotypic samples of *M. caquetio* (from El Macano, Sierra de Churuguara) and those from Quebrada El Peregrino, at the north portion of the same range, but they considered it as intraspecific variation. Several populations of *Mannophryne* from Sierra de San Luis (at least 45 km N from Sierra de Churuguara) were referred by Mijares-Urrutia & Arends (1999a) as belonging to an undescribed species, different to *M. caquetio*. The 16S p-distances observed among the samples from Sierra de Churuguara and those from Sierra de San Luis (Table 3) suggest that the latter correspond to a putative new species. However, if the specimens from the two localities sampled in Sierra de Churuguara are conspecific, as suggested by Manzanilla *et al*. (2009), then our samples from San Luis would render *M. caquetio* paraphyletic (Figure 84). At this point, two alternative scenarios should be considered: 1) *M. caquetio* is widely distributed in both mountain systems and is atypical into the genus by showing remarkable phylogeographic structure and genetic distances; or 2) we are in the presence of three different species, one of which correspond to *M. caquetio*. As noted in this study, intraspecific phylogeographic structure in *Mannophryne* species is, in general, incipient or absent and 16S p-distances among conspecifics from different populations typically are 0.0–0.5 %. Our evidence supports the second scenario; however, we did not have access to any specimen from Sierra de Churuguara nor call recordings from any of the three populations involved. Thus, as in previous cases discussed above, we refrain from considering the specimens from El

Peregrino and El Chorro as two additional putative new species until more data is gathered.

Table 3. Uncorrected pairwise distances (values in %) among six terminals of *Mannophryne caquetio* from three different localities in the Sierra de Churuguara and Sierra de San Luis, based on a similarity alignment of a 467 bp fragment of 16S without gaps and missing data.

Terminals	**1**	**2**	**3**	**4**	**5**	**6**
(1) M. caquetio MIZA333 – Maparará, Churuguara	-					
(2) M. caquetio MIZA337 - Maparará, Churuguara	0.0	-				
(3) M. cf. caquetio MIZA323 - El Peregrino, Churuguara	0.9	0.9	-			
(4) M. cf. caquetio MIZA338 - El Peregrino, Churuguara	0.9	0.9	0.0	-		
(5) M. cf. caquetio MHNLS21219 - El Chorro, San Luis	1.3	1.3	1.1	1.1	-	
(6) M. cf. caquetio MHNLS21220 - El Chorro, San Luis	1.7	1.7	1.4	1.4	0.2	-

Mannophryne sp. 3 is a putative new species also included for the first time in a quantitative phylogenetic study. It is herein represented by samples from three localities, all from the northern slope of the central Cordillera de la Costa and distanced 5–13 km among them. *Mannophryne* sp. 3 was previously studied by Edwards (1974) but erroneously identified as *Colostethus* (= *Prostherapis*) *dunni*. Rivero (1984a) noted that this was a misidentification of Edwards (1974) and that these specimens corresponded to a putative new species sharply different from *Colostethus* (= *Mannophryne*) *trinitatis*—numerous populations from Cordillera de la Costa were referred as belonging to *M. trinitatis* until Kaiser *et al.* (2003), Barrio-Amorós *et al*. (2006b), and Manzanilla *et al*. (2007b), restricted it to Trinidad island. Nevertheless, Rivero (1984a) did not described it because the available name *Colostethus* (= *Mannophryne*) *herminae*—also from Cordillera de la Costa—could be applied to these frogs. Finally, La Marca (1994) referred to the specimens collected by Edwards (1974) as *M. herminae*, which was considered a morphologically very variable species, particularly in its feet webbing extension. Our results corroborate that *Mannophryne* sp. 3 is a putative new species belonging to the

M. herminae species group but not sister of *M. herminae*. Instead it is sister of the geographically distant *Mannophryne caquetio* (*sensu latto*).

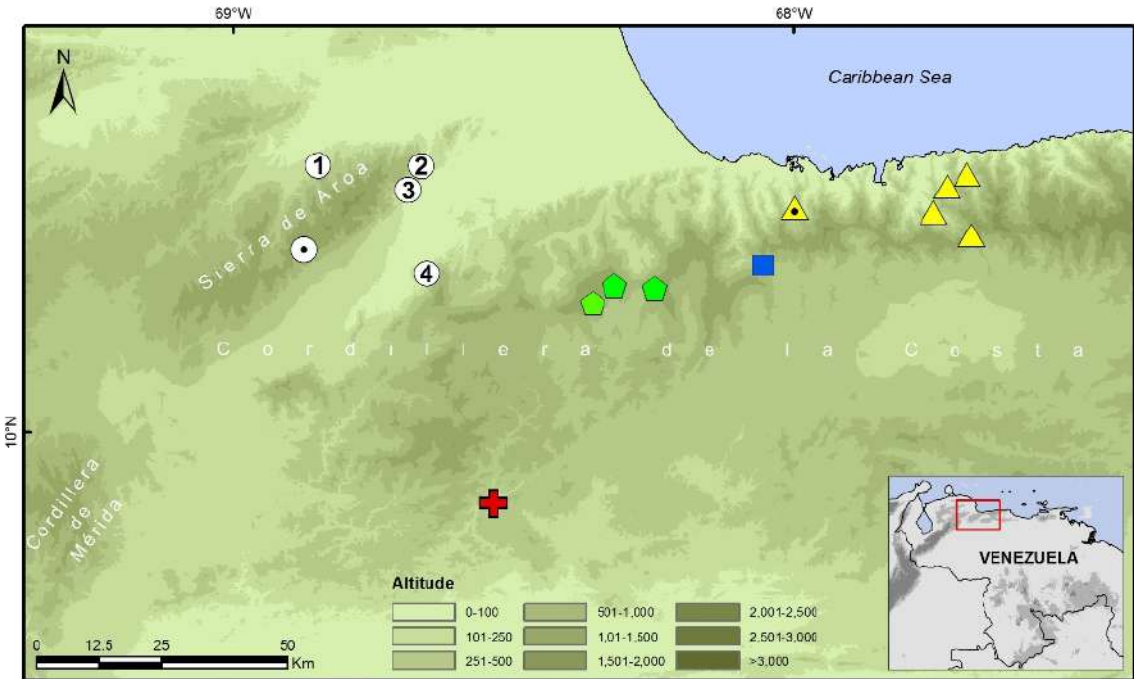

Figure. 91. Map of the western part of Cordillera de la Costa in northern Venezuela showing the distribution of the *Mannophryne herminae* complex. Yellow triangles: *Mannophryne herminae* (dotted triangle: type locality); blue square: *Mannophryne* aff. *herminae* from La Entrada, near Valencia (ULABG 4506); green pentagons: *Mannophryne* sp. 4; red cross: *Mannophryne* sp. from La Sierra; white circles: *Mannophryne molinai* and *M.* cf. *molinai*. Dotted circle: La Rondona, type locality. 1. El Abrigo; 2. Guayabito; 3. Mayorica; 4. La Guáquira.

Within the *Mannophryne herminae* complex, the terminal referred as *M*. aff. *herminae* ULABG 5406 from La Entrada, near Valencia, Carabobo state (Figure 91) is recovered as sister to all other terminals of the *M. herminae* complex (Figure 84) and with 16S p-distances of 1.9–3.1 % in relation to them (Appendix 8). This seems to be a strong indication of a different species. However, this sample is represented in our phylogeny only by two fragments (a total of 1,044 bp) of 16S obtained from GenBank (Vences *et al*. 2003). New sequences from syntopic specimens and also morphological and bioacoustic

evidence will be needed in order to properly assess the taxonomic status of the *Mannophryne* sp from La Entrada.

Mannophryne sp. 4 seem to be restricted to the Montalbán valley in Carabobo state (Figure 91). Although their 16S p-distances with *M. molinai*, *M. herminae* and *M.* sp. from la Sierra are low (0.5–1.4 %), it is sister to a clade containing all of them and there are 24 transformations separating them (Figure 84). This putative new species differs from *M. herminae* and *M. molinai* in some characters of the female dark dermal collar, female abdomen color pattern, and pupillary ring. It also differs notably from *M. herminae* in its advertisement call, which consist of a series of single notes (a series of notes arranged in duplets in *M. herminae*; Figures 92a-b).

Mannophryne sp. from La Sierra, *M. molinai*, and *M. herminae* collapse in a large polytomy and their 16S p-distances are low (Appendix 8). At first glance it seems to be indicative of conspecificity, but as demonstrated by Rojas-Runjaic *et al*. (2018) at least *M. molinai* and *M. herminae*, two geographically distant species (Figure 91), differ in some morphological characters (particularly in female dark dermal collar structure and width) and both emit strikingly different advertisement calls. Whereas *M. molinai* emits trills of single notes, *M. herminae* is unique within the complex by its advertisement call composed by notes arranged in duplets (Figure 92). Additionally, their advertisement calls notably differ in several temporal and spectral parameters (Rojas-Runjaic *et al*. 2018). Ventral coloration (including dark dermal collar) in *Mannophryne* is related to species recognition and social interactions (Test 1954, Sexton 1960, Dole & Durant 1974, Durant & Dole 1975, Wells 1980) and it has proven to be useful in delimiting species (e.g., La Marca 1992; Manzanilla *et al*. 2007a,

Barrio-Amorós *et al*. 2010a). Additionally, acoustic signals play a critical role in mate recognition and mate choice (Wells 2007), often are species-specific, and consequently act as a prezygotic mechanism of reproductive isolation; hence, advertisement call differentiation between specimens, constitutes strong evidence of speciation (e.g., Angulo & Reichle 2008, Padial *et al*. 2008). Thus, despite the low 16S p-distances and unresolved relationships between *M. molinai* and *M. herminae*, we consider both as different linages. Unresolved relationships within the complex can be indicative of recent speciation and incomplete linage sorting, or introgression—similar situation was observed between closely related species in the group of *Rhinella granulosa* by Pereyra *et al*. (2016). However, given the nature of analyses and results, we cannot test if the relationships within the *M. herminae* complex depicted in our phylogeny are consequence of the occurrence of any of these events. On the other hand, multiple terminals poorly represented in terms of molecular and phenotypic characters—eight terminals of *M.* cf. *molinai* lacks phenotypic data, and most of the terminals in the complex are represented only by a little variable 556 bp fragment of 16S—also may be contributing to the polytomy within the group. Furthermore, the terminals referred as *M.* cf. *molinai* MHNLS 21365 and 21367 (from Mayorica) and *M.* cf. *molinai* MHNLS 21306 (from La Guáquira) were listed in the positions 29, 31 and 32 as potential wildcards (among the 400 terminals included in our study). The case of *M.* sp. from La Sierra seems to be similar to the aforementioned one. Those specimens are from a geographically distant locality (Figure 91) and despite exhibiting low 16S p-distances with the others terminals of the *M. herminae* complex, it shows several phenotypic

peculiarities. Nevertheless, we do not have recordings of the calls of *M.* sp. from La Sierra; hence, we prefer not to label them as part of a putative new species.

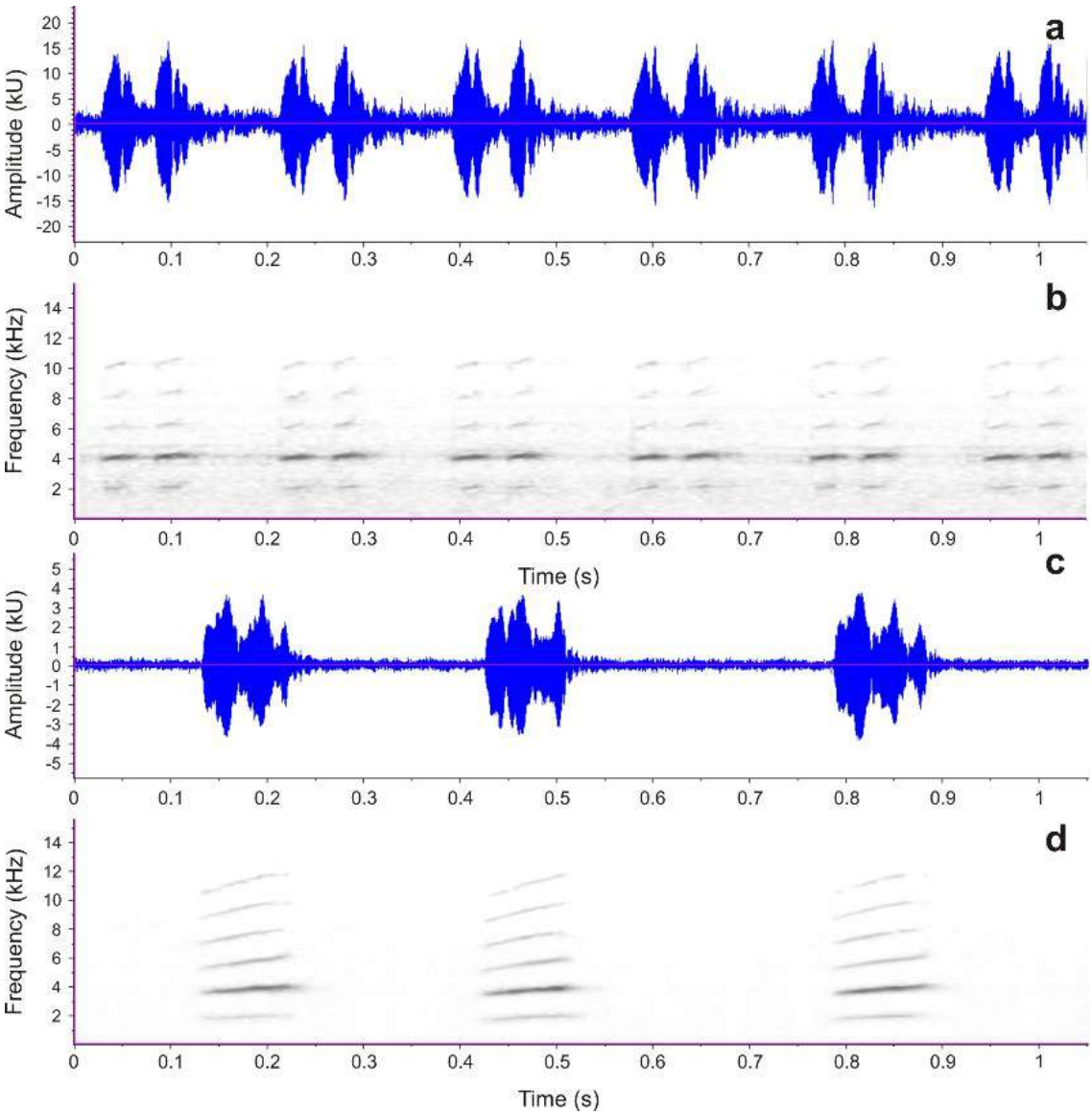

Figure 92. Comparison of the advertisement calls of *Mannophryne herminae* (a–b) and *M. molinai* (c–d). Oscillograms (a–c) and spectrograms (b–d) of a 1 s section of the recordings. Note that the calls of *M. herminae* are composed by fast series of short notes arranged in duplets, whereas those of *M. molinai* consist of series of large single notes.

The relationships recovered within the *Mannophryne collaris* group (*sensu* this work) are similar to those of Grant *et al*. (2017), being the main difference the position of *M. collaris*, which in our study is sister to all terminals

of the group but *M. cordilleriana* and *M. urticans*—in Grant *et al*. (2017), this species is part of a more exclusive clade as sister of *M. larandina* and *M. yustizi*. Other differences correspond to the novel relationships discovered with the inclusion, for the first time in a phylogenetic analysis, of *M. trujillensis* and *M. speeri*. Grant *et al*. (2017) did not recover phenotypic synapomorphies for the species groups of *Mannophryne*. Thus, the five unambiguously optimized phenotypic synapomorphies identified for this group also correspond to new discoveries. Although all the species in this group (but *M. speeri*) are represented by multiple terminals from several localities, their interspecific 16S p-distances are 0.0–0.7 % (Appendix 8) and lack phylogeographic structure, or if present, it is incipient (Figures 85–86) which seems to be a common pattern among aromobatin species.

The identity of the terminal referred as *Mannophryne herminae* 1141 by Grant *et al*. (2006) and as *Mannophryne herminae* CWM by Grant *et al*. (2017) (DQ502595, DQ502160) has been uncertain since first published. Grant *et al*. (2017) recovered it in a polytomy with *M. larandina* and *M. yustizi* instead of more closely related to other terminals of *M. herminae*. The putative locality of collection of this sample is "Venezuela: Trujillo, about 2 km (airline) W La Pena, 1920 m", we suspected that it may correspond to *M. trujillensis* (Rojas-Runjaic, in litt. To Grant, 12 June 2017; Grant *et al*. 2017), with type locality in that region. However, in this study we recovered the terminal CWM 1141 nested within *M. larandina* and not within *M. trujillensis*. In fact, CWM 1141 16S sequence is identical to that of the six sampled terminals of *M. larandina* (Appendix 8), which clearly points that specimen CWM 1141 is, most likely, part of *M. larandina*. The geographic distribution of all known species of

Mannophryne is very restricted; as far as we know *M. trujillensis* is the only species inhabiting La Peña and vicinities of Trujillo city (Trujillo state), whereas *M. larandina* is restricted to Hato Arriba and surrounding areas (Lara state). Both localities are separate by ~67 km. The acronym CWM associated to the specimen corresponds to the field series of Charles W. Myers, who visit the region where *M. larandina* is distributed in November of 1987 (Myers *et al*. 1991). Thus, we presume that the specimen CWM 1141 was collected near the type locality of *M. larandina* and that the locality indicated by Grant *et al*. (2006): "Venezuela: Trujillo, about 2 km (airline) W La Pena, 1920 m" may represent an error.

Another sequence of unknown identity is the one referred by Vences *et al*. (2003) as *Mannophryne* sp. n. B from “Near La Quebrada, [Trujillo state] Venezuela” (AY263223) and as *Mannophryne* sp ULABG4481 by Grant *et al*. (2006). This sequence was excluded from subsequent studies (Manzanilla *et al*. 2009, Grant *et al*. 2017) and its identity remains undetermined. In our phylogeny this sample is nested within *M. urticans*, despite its locality is distanced 86 km NE from the type locality (Río Frío, Mérida) and 109 km NE from the southernmost locality of *M. urticans* (La Olinda II, Mérida state; MHNLS 21993–21994), its 16S p-distances is 0.0–0.7 % to other *M. urticans* and the clade containing the six putatively conspecific samples does not exhibit phylogeographic structure. Thus, although we did not have access to the voucher specimen, its phylogenetic position and p-distances indicate that this sequence corresponds to *M. urticans*.

Manzanilla *et al*. (2009) recovered *Mannophryne larandina* and *M. yustizi* as sister and reciprocally monophyletic. Nonetheless, on the basis of the very

low 16S p-distances (0.2 %) observed between both species and their geographical proximity (Figure 93), these authors suggested that these two names may be corresponding to a single species. Grant *et al*. (2017) found *M. larandina* and *M. yustizi* in a polytomy but did not comment on this result. We found *Mannophryne larandina* as part of the *M. yustizi* complex, which is defined by seven new unambiguous phenotypic synapomorphies (Figure 86). Within this complex, *M. larandina* is sister and reciprocally monophyletic to a large clade containing topotypic samples of *M. yustizi*, *M. speeri*, and a number of undetermined specimens from seven localities along 153 km of the western (Orinoquian) slope of the Cordillera de Mérida (Figure 93). Although we also observed very low 16S p-distances between *M. larandina* and all other terminals in the *M. yustizi* complex (0.2–0.4 %; Table 4), its phylogenetic position, the patristic distance (total branch length = 37 transformations), and their morphological differences (Yústiz 1991, Rojas-Runjaic *et al*. 2018) support it as a different linage.

Table 4. Uncorrected pairwise distances (values in %) among terminals of *Mannophryne yustizi* complex, including *M. larandina*, *M. speeri*, *M. yustizi*, and undetermined specimens from six localities along eastern slope of Cordillera de Mérida, based on a similarity alignment of a 466 bp fragment of 16S without gaps and missing data.

	1	**2**	**3**	**4**	**5**	**6**	**7**	**8**	**9**
(1) *M. larandina* (n = 7)	0.0								
(2) *M. yustizi* (n = 4)	0.2	0.0							
(3) *M. speeri* MHNLS22606	0.4	0.2	-						
(4) *M*. sp. Agua Linda (n = 2)	0.2-0.4	0.0-0.2	0.2-0.4	0.2					
(5) *M*. sp. Chabasquén (n = 3)	0.2-0.4	0.0-0.2	0.2-0.4	0.0-0.2	0.0-0.2				
(6) *M*. sp. Palma Rica (n = 2)	0.4	0.2	0.4	0.0-0.2	0.0-0.2	0.0			
(7) *M*. sp. Campo Elías	0.4	0.2	0.4	0.0-0.2	0.0-0.2	0.0	-		
(8) *M*. sp. El Jarillo (n = 2)	0.4	0.2	0.4	0.0-0.2	0.0-0.2	0.0	0.0		
(9) *M*. sp. Niquitao (n = 4)	0.2	0.0	0.2	0.0-0.2	0.0-0.2	0.2	0.2	0.2	0.0

The relationships among *Mannophryne yustizi*, *M speeri*, and the remaining terminals are unresolved (Figure 86). *Mannophryne speeri* exhibits 16S p-distance values of 0.2–0.4 % with other terminals within the complex—although very low, these values are similar to that of *M. larandina* (Table 4)—, whereas all the undetermined terminals from six different localities show pairwise 16S distances of 0.0–0.2 % among them and with topotypic terminals of *M. yustizi* (Table 4). This suggests that *M. yustizi* is a widely distributed species on the eastern slope of Cordillera de Mérida and that *M. speeri* may be conspecific. However, we consider that a more detailed study involving an improved geographic and molecular sampling, as well as bioacoustics evidence, will be required in order to properly resolve the taxonomic status of *M. speeri*.

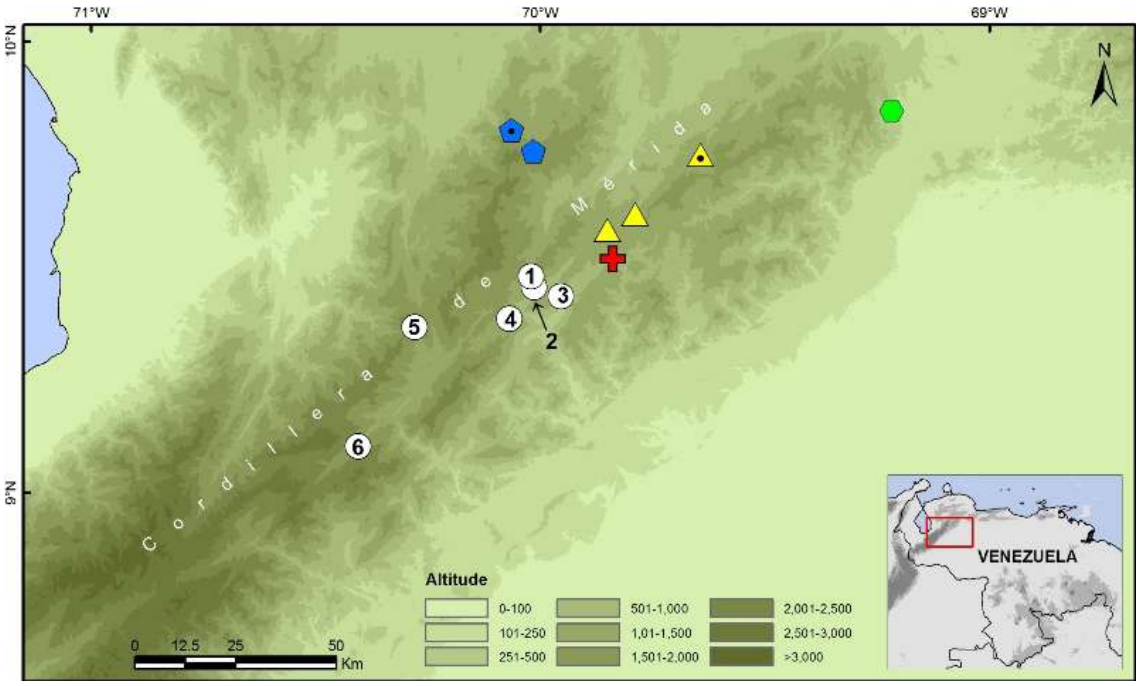

Figure. 93. Map of the northern part of Cordillera de Mérida in northwestern Venezuela showing the distribution of the *Mannophryne yustizi* complex. Yellow triangles: *Mannophryne yustizi* (dotted triangle: type locality); blue pentagons: *Mannophryne larandina* (dotted rhomb: type locality); green hexagon: *Mannophryne* sp. from La Olla; red cross: *Mannophryne speeri*; white circles: *Mannophryne* sp. (probably belonging to *M. yustizi*). 1. Agua Linda; 2. Palma Rica; 3. Chabasquén; 4. Campo Elías; 5. El Jarillo; 6. Niquitao.

As in the case of the *Mannophryne herminae* complex, we suspect the occurrence of recent speciation or introgression within this group as possible causes of the very low genetic variability observed in 16S and the unresolved relationships within the clade. Additionally, multiple terminals poorly represented in the molecular dataset and/or lacking phenotypic data, may also contribute to the polytomy within the *M. yustizi* complex. Furthermore, the terminal *Mannophryne* sp. MHNLS 22559 was identified as a potential wildcard within this complex (listed in the position 17 of the ranking; Appendix 5).

Finally, based on a detailed inspection of a series of specimens of *Mannophryne* sp. from La Olla (Figure 93), we obtained morphological evidence indicating that these may correspond to a putative new species belonging to the *M. yustizi* complex. These specimens markedly differ from *M. yustizi sensu stricto* in the female dark dermal collar pattern, webbing extension, and body size. Furthermore, their pairwise Cyt-b distances in relation to *M. larandina*, *M. speeri*, and some undetermined terminals of the *M. yustizi* complex are 1.4–1.7 %—as reference, Cyt-b p-distances between the sister species *M. urticans* and *M. lamarcai* are 1.0–1.4 %. However, the two samples from this population included in our phylogeny were recovered as part of the polytomy of *M. yustizi* and their closely relatives (Figure 86). These two samples are only represented by a 382 bp fragment of Cyt-b—only another five terminals within the complex were sampled for this marker—and by morphological data. We presume that their unresolved relationships can be affected by our limited character sampling. At this point, we have not enough evidence to refer these specimens as part of a species different from *M. yustizi*, although their inclusion in *M. yustizi* is more

conservative, it is also uncertain. Further molecular data (e.g., 16S sequences) will be required to resolve this taxonomic problem.

Species rediscoveries raise hope about potential findings of other missing aromobatids

Important populational declines have been documented in several Venezuelan aromobatid species and a number of them seem to be extinct, at least in their historical localities (La Marca 2007). Emerging diseases, pollution, habitat fragmentation, and invasive species (e.g., trouts and American bullfrogs) are among the factors suspected as responsibles—either individually or synergically—by these declines and local extinctions (La Marca & Reinthaler 1991, La Marca 2007, Díaz de Pascual & Guerrero 2008, Lampo *et al*. 2008, Sánchez *et al*. 2008, Barrio-Amorós *et al*. 2010b, Nava-González *et al*. 2017). *Aromobates mayorgai*, *A. meridensis*, and *Mannophryne neblina* are three of the at least 17 aromobatid species inhabiting mountain systems from northern Venezuela that have been apparently lost.

Aromobates mayorgai and *A. meridensis* are sympatrical along their distributions (La Marca & Otero 2012) and based on the numerous specimens deposited in museum collections, we presumed that both were common species at their type locality (El Chorotal, Mérida, Venezuela) and vicinities on the road to La Azulita. However, they vanished from all these historical localities more than a decade ago. Exhaustive surveys carried out in their historical localities between 2003 and 2007 failed to find any specimen of *A. mayorgai*, but resulted in the discovery in 2006 of two nearby populations of *A. meridensis*, located 5 km W of El Chorotal (Barrio-Amorós *et al*. 2010b). Since then, no new

observations have been documented for any of these species. During our field work expeditions, we searched for specimens of *A. mayorgai* and *A. meridensis* at their historical localities without success. Nevertheless, we performed additional surveys to several creeks along a nearby valley located 7–14 km W and SW from El Chorotal, that resulted in the discovery of six new populations of *A. meridensis* and three of *A. mayorgai*. Additionally, inasmuch our phylogenetic analysis revealed that *A. ericksonae* is a junior synonym of *A. mayorgai*, we now know that these populations recently discovered by Barrio-Amorós & Santos (2012) and referred as *A. ericksonae*, actually correspond to remnant populations of *A. mayorgai* persisting on the species range periphery, along the western versant of Cordillera de Mérida (Figure 88).

Mannophryne neblina was until now known only by a series of 33 type specimens collected in 1951 from a single locality (Rancho Grande, Aragua state) at the central Cordillera de la Costa (Test 1956). Despite numerous searches for this species carried out at the same locality and vicinities, no new specimens have been recorded, which suggests that it may be extinct at least locally (La Marca & Manzanilla 2004). During a revision of undetermined aromobatids housed at MHNLS we found an additional series of specimens of *M. neblina*, which were collected in 1970—19 years after the type series—from El Limón, a new locality for the species, 47 km E from the type locality. A subsequent visit to this locality in 2016 allowed us to obtain one new specimen of this species after 70 years and to corroborate that *M. neblina* still persists.

As can be noted, a pattern of rediscoveries, as illustrated by *Aromobates mayorgai*, *A. meridensis*, and *Mannophryne neblina*, seems to emerge: all cases correspond to remnant populations persisting on suitable habitat at the

periphery of their historical distributions. This pattern agrees with the hypothesis of decline trajectory termed as range eclipse (Hemerik *et al*. 2006) according to which, anthropogenic threats (e.g., habitat loss and invasive species) spread across species ranges in a contagion-like manner, pushing the declining species to the border of its distribution area. This hypothesis predicts that rediscoveries are more likely to occur closer to the periphery rather than to historical localities toward the core of the species range. Fisher (2010) analyzing data of 67 mammal species affected by habitat loss and long-time disappeared, noted that their rediscoveries were consistent with a range eclipse. The same pattern was observed in New Zealand herpetofauna by Town & Daugherty (1994) and more recently for the rediscoveries of *Atelopus cruciger* in Venezuela (Rodríguez-Contreras *et al*. 2008), *Craugastor taurus* in Costa Rica (Chávez *et al*. 2014), and *Atelopus subornatus* in Colombia (Enciso-Calle *et al*. 2017). The threats identified for most of the disappeared Venezuelan aromobatids are mainly anthropogenic (La Marca 2007) and, as commented above, the three rediscovered species come from remnant populations at the edge of their distributions. Thus, we suspect that range eclipse can be a common explanation in most missing aromobatids and that new searches focused on peripheral areas will likely result in new rediscoveries.

Taxonomy

Although our study is focused in the subfamily Aromobatinae, we provide, on the basis of our results, an updated taxonomy for the family Aromobatidae. We recognized the three subfamilies previously defined (Grant *et al*. 2006, 2017), seven genera (two new), four species groups within *Mannophryne* (one new),

and four species groups of *Anomaloglossus* (Grant *et al*. 2017, Vacher *et al*. 2017). Despite we do not recovered as monophyletic one of the four species groups of *Allobates* inferred by Grant *et al*. (2017), the 22-chromosome group, we maintain their taxonomy. Our study was not designed to test the relationships within *Allobates* and we suspect that topological differences in relation to Grant *et al*. (2017) may be due to our limited taxon sampling within this genus.

Unambiguous phenotypic synapomorfies for Aromobatidae, its subfamilies, genera, and the species groups of *Mannophryne*, are listed in this section. Numerous phenotypic characters that we analyzed were not scored for a significant number of outgroups in *Allobates* and *Anomaloglossus*. In consequence, the phenotypic synapomorphies identified for these genera should be tested in future studies based on more complete phenotypic and taxonomic datasets.

Family: Aromobatidae Grant, Frost, Caldwell, Gagliardo, Haddad, Kok, Means, Noonan, Schargel & Wheeler, 2006

Type genus: *Aromobates* Myers, Paolillo & Daly, 1991

Immediately more inclusive taxon: Dendrobatoidea Cope, 1865

Sister group: Dendrobatidae Cope, 1865

Content: Three subfamilies and a subfamily unranked genus: Allobatinae Grant, Frost, Caldwell, Gagliardo, Haddad, Kok, Means, Noonan, Schargel & Wheeler, 2006; Anomaloglossinae Grant, Frost, Caldwell, Gagliardo, Haddad, Kok, Means, Noonan, Schargel & Wheeler, 2006; Aromobatinae Grant, Frost,

Caldwell, Gagliardo, Haddad, Kok, Means, Noonan, Schargel & Wheeler, 2006; *Genus* 1 **gen. nov.**

Support: branch length: 121 transformations; Jackknife support: 56 %; five unambiguously optimized phenotypic synapomorphies.

Phenotypic synapomorphies: 1) Pale paracloacal mark present (61, 0 → 1); **2)** Dark lower labial stripe diffuse, poorly defined (89, 1 → 0); **3)** Male throat evenly stippled (90, 4 → 2); **4)** Zygomatic ramus of the squamosal short and little robust but well defined (193, 6 → 3); **5)** Maxilla posteriorly reaching the level of the triple point of the squamosal (220, 0 → 1).

Genus: *Genus* 1 **gen. nov.**

Type species: *"Colostethus" caribe* Barrio-Amorós, Rivas & Kaiser, 2006

Immediately more inclusive taxon: Aromobatidae Grant, Frost, Caldwell, Gagliardo, Haddad, Kok, Means, Noonan, Schargel & Wheeler, 2006

Sister group: Unnamed clade composed by Anomaloglossinae Grant, Frost, Caldwell, Gagliardo, Haddad, Kok, Means, Noonan, Schargel & Wheeler, 2006; and Aromobatinae Grant, Frost, Caldwell, Gagliardo, Haddad, Kok, Means, Noonan, Schargel & Wheeler, 2006

Content: "*Colostethus" caribe* Barrio-Amorós, Rivas & Kaiser, 2006

Support: branch length: 21 transformations; 19 unambiguously optimized phenotypic apomorphies.

Phenotypic apomorphies: This is a monotypic genus and consequently we cannot distinguish between autapomorphies and synapomorphies. However, we report the apomorphic states as a definition for this taxon. **1)** Medial apophysis of the hyoid plate posteromedial process, present (169, 0 → 1); **2)** Omosternum

entirely cartilaginous (188, 1 → 0); **3)** Pterygoid posterior ramus slightly longer or equal to medial ramus (195, 0 → 1); **4)** lateral crest of the maxillary process of nasal, weak (225, 2 → 1); **5)** Nasal and sphenethmoid not in contact (226, 1 → 0); **6)** Dorsal apophysis of the posterior semicircular crest of the occipital, weak (242, 0 → 1); **7)** 10–13 premaxillary teeth (259, 0 → 1); **8)** Neural crest of vertebra VI strongly developed (274, 1 → 2); **9)** Neural crest of vertebra VII strongly developed (275, 1 → 2); **10)** Posterior projection of the neural arch of vertebra IV surpassing the level of the postzygoapophyses (279, 0 → 2); **11)** Sesamoids on the lateral surface of the iliosacral articulation, absent (286, 1 → 0); **12)** Posterior margin of the postzygoapophyses of the vertebra II, convex (290, 0 → 2); **13)** Anterolateral foramina of the urostyle, absent (310, 1 → 0); **14)** Anterolateral crest of the urostyle, absent (311, 1 → 0); **15)** Dorsal sulcus of the urostyle, absent (312, 1 → 0); **16)** Distal tip of the urostyle moderately expanded in dorsal view (315, 1 → 2); **17)** Anterior tip of the ilium slightly oriented medially (319, 1 → 0); **18)** Tubercular fossa of the ilium, absent (321, 1 → 0); **19)** Proximal end of the paraventral crest of the humerus, weakly raised (327, 2 → 1).

Subfamily: Allobatinae Grant, Frost, Caldwell, Gagliardo, Haddad, Kok, Means, Noonan, Schargel & Wheeler, 2006

Type genus: *Allobates* Zimmermann & Zimmermann, 1988

Immediately more inclusive taxon: Aromobatidae Grant, Frost, Caldwell, Gagliardo, Haddad, Kok, Means, Noonan, Schargel & Wheeler, 2006

Content: *Allobates* Zimmermann & Zimmermann, 1988

Remarks: This taxon is redundant with *Allobates*. See its phylogenetic relationships, support and synapomorphies under *Allobates*, below.

Genus: *Allobates* Zimmermann & Zimmermann, 1988

Type species: *Prostherapis femoralis* Boulenger, 1884

Immediately more inclusive taxon: Allobatinae Grant, Frost, Caldwell, Gagliardo, Haddad, Kok, Means, Noonan, Schargel & Wheeler, 2006

Sister group: Unnamed clade composed by *"Colostethus" caribe* Barrio-Amorós, Rivas & Kaiser, 2006; Anomaloglossinae Grant, Frost, Caldwell, Gagliardo, Haddad, Kok, Means, Noonan, Schargel & Wheeler, 2006; and Aromobatinae Grant, Frost, Caldwell, Gagliardo, Haddad, Kok, Means, Noonan, Schargel & Wheeler, 2006.

Content: 52 species (Frost 2019).

Support: branch length: 71 transformations; Jackknife support: 100 %; 11 unambiguously optimized phenotypic synapomorphies.

Phenotypic synapomorphies: 1) Oblique lateral stripe formed by a series of spots (79, 0 → 2); **2)** Posterior extension of the maxillary process of the nasal surpassing the level of the *planum antorbitale* (224, 1 → 2); **3)** Dorsal-anterior contour of the sphenethmoid, convex (228, 2 → 1); **4)** Posterior wall of the otic capsule anteriorly oriented in ventral view (243, 1 → 0); **5)** Neural crest of the vertebra II weakly developed (270, 0 → 1); **6)** Transverse process of the vertebra VI laterally oriented (302, 2 → 1); **7)** Anterior end of the ilial crest, stepped (317, 0 → 1); **8)** Proximal end of the paraventral crest of the humerus, undifferentiated (327, 2 → 0); **9)** Sesamoid present on the metatarsal-proximal phalanx articulation of TI (343, 0 → 1); **10)** Sesamoid present on the metatarsal-

proximal phalanx articulation of TII (344, 0 → 1); **11)** Sesamoid present on the metatarsal-proximal phalanx articulation of TV (347, 0 → 1).

Remarks: Grant *et al*. (2017) recognized four species groups: Atlantic Forest group, trans-Andean Group, *A. femoralis* group, and 22-chromosome group. Some species, although included in phylogenetically analyses, remain unassigned to species groups. "*Colostethus*" *caribe* and "*Phyllobates*" *mandelorum* do not belong to this genus as previously suggested (Grant *et al*. 2006 and Frost 2007, respectively).

Subfamily: Anomaloglossinae Grant, Frost, Caldwell, Gagliardo, Haddad, Kok, Means, Noonan, Schargel & Wheeler, 2006

Type genus: *Anomaloglossus* Grant, Frost, Caldwell, Gagliardo, Haddad, Kok, Means, Noonan, Schargel & Wheeler, 2006

Immediately more inclusive taxon: Aromobatidae Grant, Frost, Caldwell, Gagliardo, Haddad, Kok, Means, Noonan, Schargel & Wheeler, 2006

Sister group: Aromobatinae Grant, Frost, Caldwell, Gagliardo, Haddad, Kok, Means, Noonan, Schargel & Wheeler, 2006

Content: *Anomaloglossus* Grant, Frost, Caldwell, Gagliardo, Haddad, Kok, Means, Noonan, Schargel & Wheeler, 2006; *Rheobates* Grant, Frost, Caldwell, Gagliardo, Haddad, Kok, Means, Noonan, Schargel & Wheeler, 2006; *Genus* 2 **gen. nov.**

Support: branch length: 85 transformations; Jackknife support: < 50 %; two unambiguously optimized phenotypic synapomorphies.

Phenotypic synapomorphies: 1) Posterior contour of the floor of the sphenethmoid, convex (231, 0 → 2); **2)** Posteroventral border of the sphenethmoid posterior to the posterolateral borders (232, 0 → 2).

Genus: *Genus* 2 **gen. nov.**

Type species: *Prostherapis dunni* Rivero, 1961

Immediately more inclusive taxon: Anomaloglossinae Grant, Frost, Caldwell, Gagliardo, Haddad, Kok, Means, Noonan, Schargel & Wheeler, 2006

Sister group: *Rheobates* Grant, Frost, Caldwell, Gagliardo, Haddad, Kok, Means, Noonan, Schargel & Wheeler, 2006

Content: "*Prostherapis" dunni* Rivero, 1961

Support: branch length: 12 transformations; nine unambiguously optimized phenotypic apomorphies.

Phenotypic apomorphies: This is a monotypic genus and consequently we cannot distinguish between autapomorphies and synapomorphies. However, we report the apomorphic states as a definition for this taxon. **1)** FII disc moderately expanded (13, 1 → 2); **2)** FIV disc moderately expanded (15, 1 → 2); **3)** Palmar tubercle slightly bilobate to bifid distally (32, 0 → 1); **4)** TI postaxial webbing = 0 (fully webbed) (46, 4 → 5); **5)** TII postaxial webbing = 0 (fully webbed) (48, 4 → 5); **6)** Ossified portion of the omosternum short, truncate, without an elongate tip (189, 1 → 0); **7)** Zygomatic ramus of the squamosal short and little robust but well defined (193, 2 → 3); **8)** Palatine and pterygoid in contact or nearly in contact (210, 1 → 2); **9)** Sphenethmoid length-width relation = 0.5 (227, 0 → 1); **10)** Posterodorsal apophysis of the transverse process of vertebra III, present (306, 0 → 1).

Remarks: *"Prostherapis" dunni* shares three phenotypic synapomorphies with *Rheobates* and both are sister. However, *Rheobates* has 12 unambiguous phenotypic synapomorphies (Figure 80), which are obviously absent from *"P." dunni*, while *"P." dunni* has nine unambiguous phenotypic apomorphies. Additionally, *"P." dunni*, is restricted to central Cordillera de la Costa in Venezuela, which is markedly isolated from the distribution range of *Rheobates* (at least 700 km in straight line and separated by two large mountain ranges). Considering this situation, we prefer to create a new genus for *"Prostherapis" dunni* because it is easily diagnosable from its sister taxon *Rheobates* and because both occupy allopatric and distinct biogeographic areas.

Genus: *Rheobates* Grant, Frost, Caldwell, Gagliardo, Haddad, Kok, Means, Noonan, Schargel & Wheeler, 2006

Type species: *Phyllobates palmatus* Werner, 1899

Immediately more inclusive taxon: Anomaloglossinae Grant, Frost, Caldwell, Gagliardo, Haddad, Kok, Means, Noonan, Schargel & Wheeler, 2006

Sister group: *Genus* 2 **gen. nov.**

Content: 2 species: *Rheobates palmatus* (Werner, 1899) and *Rheobates pseudopalmatus* (Rivero & Serna, 2000).

Support: branch length: 13 transformations; Jackknife support: 100 %; 12 unambiguously optimized phenotypic synapomorphies.

Phenotypic synapomorphies: 1) FI < FII (10, 2 → 1); **2)** Cloacal tubercles absent (57, 1 → 0); **3)** Paracloacal mark absent (61, 1 → 0); **4)** Dorsolateral stripe A, absent (64, 1 → 0); **5)** Lateral dark band diffuse/solid (74, 2 → 0/1); **6)**

Male throat dark with discrete pale spotting/reticulation/marbling (90, 2 → 5); **7)** Vocal sac paired lateral (117, 1 → 2); **8)** Posterior ramus of the pterygoid slightly longer or equal to the medial ramus (195, 0 → 1); **9)** Preorbital process of the maxilla, absent (218, 2 → 0); **10)** Large nasal (223, 0 → 1); **11)** Tranverse process of the vertebra II unexpanded (284, 1 → 0) ; **12)** Transverse process of the vertebra VI as long as the neural arch width (308, 1 → 2).

Genus: *Anomaloglossus* Grant, Frost, Caldwell, Gagliardo, Haddad, Kok, Means, Noonan, Schargel & Wheeler, 2006

Type species: *Colostethus beebei* Noble, 1923

Immediately more inclusive taxon: Anomaloglossinae Grant, Frost, Caldwell, Gagliardo, Haddad, Kok, Means, Noonan, Schargel & Wheeler, 2006

Sister group: Unnamed clade composed by *Genus* 2 **gen. nov.** and *Rheobates* Grant, Frost, Caldwell, Gagliardo, Haddad, Kok, Means, Noonan, Schargel & Wheeler, 2006

Content: 30 species belonging to four species groups: *Anomaloglossus degranvillei* group, *Anomaloglossus stepheni* group, *Anomaloglossus megacephalus* group, and *Anomaloglossus beebei* group (Grant *et al*. 2017, Vacher *et al*. 2017).

Support: branch length: 56 transformations; Jackknife support: 92 %; four unambiguously optimized phenotypic synapomorphies.

Phenotypic synapomorphies: 1) Oblique lateral stripe formed by a series of spots (79, 0 → 1); **2)** Dark lower labial stripe absent (88, 1 → 0); **3)** Ocular vertical dark band present (102, 0 → 1); **4)** Median lingual process present (120, 0 → 1).

Remarks: Ten species of *Anomaloglossus* remains unassigned to species groups due to their unknown phylogenetic position. Nine of them are from the Venezuelan Guayana shield and one from Brazil. They are: *A. ayarzaguenai* (La Marca, 1997), *A. breweri* (Barrio-Amorós, 2006), *A. guanayensis* (La Marca, 1997), *A. moffetti* Barrio-Amorós & Brewer-Carias, 2008, *A. murisipanensis* (La Marca, 1997), *A. parimae* (La Marca, 1997), *A. parkerae* (Meinhardt & Parmalee, 1996), *A. shrevei* (Rivero, 1961), *A. tepequem* Fouquet, Souza, Nunes, Kok, Curcio, Carvalho, Grant & Rodrigues, 2015, and *A. triunfo* (Barrio-Amorós, Fuentes-Ramos & Rivas-Fuenmayor, 2004). Among the species analyzed in quantitative phylogenetic studies only *Anomaloglossus tamacuarensis* (Myers & Donnelly, 1997) remains unassigned to species group.

Species group: *Anomaloglossus degranvillei* group

Immediately more inclusive taxon: *Anomaloglossus* Grant, Frost, Caldwell, Gagliardo, Haddad, Kok, Means, Noonan, Schargel & Wheeler, 2006

Sister group: *Anomaloglossus stepheni* group

Content: four species: *Anomaloglossus blanci* Fouquet, Vacher, Courtois, Villette, Reizine, Gaucher, Jairam, Ouboter & Kok, 2018, *A. degranvillei* (Lescure, 1975), *A. dewinteri* Fouquet, Vacher, Courtois, Villette, Reizine, Gaucher, Jairam, Ouboter & Kok, 2018, and *A. surinamensis* Ouboter & Jairam, 2012.

Support: branch length: 217 transformations; Jackknife support: 95 %; four unambiguously optimized phenotypic synapomorphies.

Phenotypic synapomorphies: No unambiguous phenotypic synapomorphies optimized for this group.

Remarks: Vacher *et al*. (2017) found cryptic diversity in this species group. At least two of these putative new species are included in our phylogeny.

Species group: *Anomaloglossus stepheni* group

Immediately more inclusive taxon: *Anomaloglossus* Grant, Frost, Caldwell, Gagliardo, Haddad, Kok, Means, Noonan, Schargel & Wheeler, 2006

Sister group: *Anomaloglossus degranvillei* group

Content: five species: *Anomaloglossus apiau* Fouquet, Souza, Nunes, Kok, Curcio, Carvalho, Grant & Rodrigues, 2015, *A. baeobatrachus* (Boistel & Massary, 1999), *A. leopardus* Ouboter & Jairam, 2012, *A. mitaraka* Fouquet, Vacher, Courtois, Deschamps, Ouboter, Jairam, Gaucher, Dubois & Kok, 2019, and *A. stepheni* (Martins, 1989).

Support: branch length: 28 transformations; Jackknife support: 89 %; three unambiguously optimized phenotypic synapomorphies.

Phenotypic synapomorphies: 1) FIII swelling present (25, 0 → 1); **2)** TII postaxial webbing = 2 (two free phalanges, with fringe) (48, 4 → 2); **3)** Dorsolateral stripe A absent (64, 1 → 0).

Remarks: Vacher *et al*. (2017) reported on cryptic diversity in this species group. At least three of these putative new species are included in our phylogeny.

Species group: *Anomaloglossus megacephalus* group

Immediately more inclusive taxon: *Anomaloglossus* Grant, Frost, Caldwell, Gagliardo, Haddad, Kok, Means, Noonan, Schargel & Wheeler, 2006

Sister group: *Anomaloglossus beebei* group

Content: Three species: *Anomaloglossus megacephalus* Kok, MacCulloch, Lathrop, Willaert, & Bossuyt, 2010, *A. verbeeksnyderorum* Barrio-Amorós, Santos & Jovanovic, 2010, and *A. wothuja* (Barrio-Amorós, Fuentes-Ramos & Rivas-Fuenmayor, 2004).

Support: branch length: 47 transformations; Jackknife support: 93 %; two unambiguously optimized phenotypic synapomorphies.

Phenotypic synapomorphies: 1) IIV preaxial webbing = 3.5 (three and half free phalanges) (51, 2 → 3); **2)** Dorsolateral stripe A, anterior (extending from eye to area above arm insertion) (65, 1 → 0).

Remarks: At least three putative new species are part of this group according to the results of Grant *et al*. (2017). We included an additional new species (*Anomaloglossus* sp. Ichún MHNLS 17561) of this group.

Species group: *Anomaloglossus beebei* group

Immediately more inclusive taxon: *Anomaloglossus* Grant, Frost, Caldwell, Gagliardo, Haddad, Kok, Means, Noonan, Schargel & Wheeler, 2006

Sister group: *Anomaloglossus megacephalus* group

Content: seven species: *Anomaloglossus beebei* (Noble, 1923), *A. kaiei* (Kok, Sambhu, Roopsind, Lenglet & Bourne, 2006), *A. meansi* Kok, Nicolaï, Lathrop & MacCulloch, 2018, *A. praderioi* (La Marca, 1997), *A. roraima* (La Marca, 1997), *A. rufulus* (Gorzula, 1990), and *A. tepuyensis* (La Marca, 1997).

Support: branch length: 56 transformations; Jackknife support: 99 %; one unambiguously optimized phenotypic synapomorphy.

Phenotypic synapomorphies: 1) Middle metatarsal tubercle absent (38, 1 → 0).

Remarks: Grant *et al*. (2017) recovered *Anomaloglossus tepuyensis* as sister to all other *Anomaloglosus* but *A. tamacuarensis*, whereas Vacher *et al*. (2017) found it as sister of *A*. *rufulus*. Our results agree with Vacher *et al*. (2017) and we corroborate *A. tepuyensis* as part of the *Anomaloglossus beebei* group.

Subfamily: Aromobatinae Grant, Frost, Caldwell, Gagliardo, Haddad, Kok, Means, Noonan, Schargel & Wheeler, 2006

Type genus: *Aromobates* Myers, Paolillo & Daly, 1991

Immediately more inclusive taxon: Aromobatidae Grant, Frost, Caldwell, Gagliardo, Haddad, Kok, Means, Noonan, Schargel & Wheeler, 2006

Sister group: Anomaloglossinae Grant, Frost, Caldwell, Gagliardo, Haddad, Kok, Means, Noonan, Schargel & Wheeler, 2006

Content: *Aromobates* Myers, Paolillo & Daly, 1991, *Mannophryne* La Marca, 1992, *"Phyllobates" mandelorum* Schmidt, 1932

Support: branch length: 85 transformations; Jackknife support: < 50 %; three unambiguously optimized phenotypic synapomorphies.

Phenotypic synapomorphies: 1) FII disc moderately expanded (13, 1 → 2); **2)** FIV disc moderately expanded (15, 1 → 2); **3)** TV disc moderately expanded (44, 1 → 2).

Remarks: We recognize *"Phyllobates" mandelorum* Schmidt, 1932 as *insertae sedis* within Aromobatinae, pending for further studies.

Genus: *Aromobates* Myers, Paolillo & Daly, 1991

Type species: *Aromobates nocturnus* Myers, Paolillo & Daly, 1991

Immediately more inclusive taxon: Aromobatinae Grant, Frost, Caldwell, Gagliardo, Haddad, Kok, Means, Noonan, Schargel & Wheeler, 2006

Sister group: *Mannophryne* La Marca, 1992

Content: 18 species: *Aromobates alboguttatus* (Boulenger, 1903), *A. cannatellai* Barrio-Amorós & Santos, 2012, *A. capurinensis* (Péfaur, 1993), *A. duranti* (Péfaur, 1985), *A. haydeeae* (Rivero, 1978), *A. leopardalis* (Rivero, 1978), *A. mayorgai* (Rivero, 1980), *A. meridensis* (Dole & Durant, 1972), *A. molinarii* (La Marca, 1985), *A. nocturnus* Myers, Paolillo & Daly, 1991, *A. ornatissimus* Barrio-Amorós, Rivero & Santos, 2011, *A. orostoma* (Rivero, 1978), *A. saltuensis* (Rivero, 1980), *A. serranus* (Péfaur, 1985), *A. tokuko* Rojas-Runjaic, Infante-Rivero & Barrio-Amorós, 2011, *A. walterarpi* La Marca & Otero-López, 2012, and *A. zippeli* Barrio-Amorós & Santos, 2012.

Support: branch length: 45 transformations; Jackknife support: < 50 %; five unambiguously optimized phenotypic synapomorphies.

Phenotypic synapomorphies: 1) Yellow translucent coloration on hidden parts of hind limbs, present (60, 0 → 1); **2)** Ventrolateral stripe formed by a series of discrete spots (76, 0 → 2); **3)** Peripheral lobes of the pupillary ring present (99, 0 → 1); **4)** Posterolateral corner of the frontoparietal, ornamented (236, 0 → 1); **5)** Sesamoid absent on the iliosacral articulation (286, 1 → 0).

Remarks: *Aromobates ericksonae* Barrio-Amorós & Santos, 2012 is a junior synonym of *A. mayorgai* (Rivero, 1980). Three putative new species are identified in this study and at least other six undetermined linages may represent undescribed taxa.

Genus: *Mannophryne* La Marca, 1992

Type species: *Colostethus yustizi* La Marca, 1989

Immediately more inclusive taxon: Aromobatinae Grant, Frost, Caldwell, Gagliardo, Haddad, Kok, Means, Noonan, Schargel & Wheeler, 2006

Sister group: *Aromobates* Myers, Paolillo & Daly, 1991

Content: 20 species belonging to four species groups: *Mannophryne trinitatis* group, *Mannophryne oblitterata* group, *Mannoprhyne herminae* group, and *Mannophryne collaris* group (Manzanilla *et al*. 2009, Grant *et al*. 2017, this study).

Support: branch length: 229 transformations; Jackknife support: 78 %; 13 unambiguously optimized phenotypic synapomorphies.

Phenotypic synapomorphies: 1) Metatarsal fold extending on the distal third of the metatarsus V (56, 3 → 0); **2)** Dark dermal collar present in males (80, 0 → 1); **3)** Dark dermal collar present in females (84, 0 → 1); **4)** Bright yellow spot on the female throat present (92, 0 → 1); **5)** Tongue yellowish pigmented in life (103, 1 → 0); **6)** Occurrence of skin blackening during calling activity (107, 0 → 1); **7)** Internarial distance greater than interorbital distance in tadpoles (139, 0 → 1); **8)** Acromion process markedly oriented inwards (179, 1 → 0); **9)** Medial ramus of the pterygoid, short (198, 2 → 1); **10)** Large nasal bone (223, 0 → 1); **11)** Frontoparietal-otoccipital, free (235, 1 → 0); **12)** 10–13 premaxillary teeth (259, 0 → 1); **13)** Maxillary teeth conical to almost conical (264, 1 → 0).

Species group: *Mannophryne trinitatis* group

Immediately more inclusive taxon: *Mannophryne* La Marca, 1992

Sister group: Unnamed clade composed by *M. oblitterata* group, *M. herminae* group, and *M. collaris* group.

Content: Six species: *Mannophryne leonardoi* Manzanilla, La Marca, Jowers, Sánchez & García-París, 2007, *M. olmonae* (Hardy, 1983), *M. riveroi* (Donoso-Barros, 1965), *M. trinitatis* (Garman, 1888), *M. venezuelensis* Manzanilla, Jowers, La Marca & García-París, 2007, and *M. vulcano* Barrio-Amorós, Santos & Molina, 2010.

Support: branch length: 37 transformations; Jackknife support: 93 %; one unambiguously optimized phenotypic synapomorphy.

Phenotypic synapomorphies: 1) Posterior contour of the floor of the sphenethmoid, convex (231, 0 → 2).

Remarks: Two putative new species are identified in this study and other two undetermined linages may represent undescribed taxa.

Species group: *Mannophryne oblitterata* group

Immediately more inclusive taxon: *Mannophryne* La Marca, 1992

Sister group: Unnamed clade composed by *M. herminae* group and *M. collaris* group.

Content: Two species: *Mannophryne neblina* (Test, 1956) and *M. oblitterata* (Rivero, 1984).

Support: branch length: 15 transformations; Jackknife support: 59 %; two unambiguously optimized phenotypic synapomorphies.

Phenotypic synapomorphies: 1) Anteromedial angle of the coracoid weakly projected anterioly (177, 0 → 1); **2)** Frontoparietal-sphenoethmoidal pit present (238, 0 → 1).

Species group: *Mannophryne herminae* group

Immediately more inclusive taxon: *Mannophryne* La Marca, 1992

Sister group: *Mannophryne collaris* group.

Content: Three species: *Mannophryne caquetio* Mijares-Urrutia & Arends, 1999, *M. herminae* (Boettger, 1893), and *M. molinai* Rojas-Runjaic, Matta-Pereira & La Marca, 2018.

Support: branch length: 22 transformations; Jackknife support: 78 %; four unambiguously optimized phenotypic synapomorphies.

Phenotypic synapomorphies: 1) Omosternum posterior terminus, notched (187, 0 → 1); **2)** Frontoparietals fused posteriorly (234, 0 → 1); **3)** Frontoparietal and occipital articulating but not fused (235, 0 → 1); **4)** Distal portion of the urostyle moderately expanded in dorsal view (315, 1 → 2).

Remarks: Two putative new species are identified in this study. Additionally other four undetermined linages (two related to *M. herminae* and other two provisionally identified as *M. caquetio*) may represent undescribed taxa.

Species group: *Mannophryne collaris* group

Immediately more inclusive taxon: *Mannophryne* La Marca, 1992

Sister group: *Mannophryne herminae* group

Content: Nine species:

Support: branch length: 84 transformations; Jackknife support: 85 %; five unambiguously optimized phenotypic synapomorphies.

Phenotypic synapomorphies: 1) FII disc weakly expanded (13, 2 → 1); **2)** FIV disc weakly expanded (15, 2 → 1); **3)** TII preaxial webbing = 2 (two free falanges) (47, 1 → 2); **4)** TIV preaxial webbing = 3.5 (three and half free

phalanges) (51, 2 → 3); **5)** Bright yellow spot on female throat restricted to the posterior half (93, 1 → 0).

Remarks: One undetermined linage within the complex of *M. yustizi* may represent an undescribed taxon.

Acknowledgements

We thank to Daniel Quihua, Adriana Becerra, José Luis Vieira, Ygrein Roos, Michelle Castellanos, Arnaldo Ferrer, Miguel Matta, Jhorman Piñeiro, Edwin Infante, José Gerardo Espinoza, Pedro Cabello, J. Celsa Señaris, Dennys Mora, Edward Camargo, Wendy Bolaños, Carlos Briceño, David Sierralta, Jesús Adolfo Aguiar, Marcial Quiroga, Jhonathan Miranda, Diego Flores, Oscar Lasso, Daniel Calcaño, Nelson Castro, Andrés Osorio, and Marlon Fochler by field collaboration. César L. Barrio-Amorós and Francisco Nava provided valuable information on localities to search for specimens during field work. For logistic support we thank to Luis Aular, Franger García, Alfredo Morales Faillace, Israel Cañizalez, Enzo La Marca, Odoardo Ravelo, Martín Rondón, Lenny Rondón, Martín Rondón Velásquez, José Martín Rondón, Maricarmen Santiago Rondón, Cristobal Burgos, Mariví Burgos, Luis Alberto Terán, José Domingo La Chica, and Helga Terzenbach. For tissue loans we thank Aldemar Acevedo, Orlando Armesto, Ada Sánchez Mercado, Lisandro Morán, and Miguel Vences. For access to collections and institutional specimen loans we also thank Gláucia Funk (MCP), Carmen Ferreira and Mercedes Salazar (MBUCV), Amelia Díaz de Pascual and Moisés Escalona (CVULA), J. Celsa Señaris (Instituto Venezolano de Investigaciones Científicas), Fernando Bird (UPR-M), and Stephen P. Rogers (CM). We are indebted to Daniel Quihua,

José Luis Vieira, J. Celsa Señaris, Michelle Castellanos, Pedro Cabello, Andrés Jaramillo, César Barrio-Amorós, Tobby Hibbitts, Maël Dewynter, Josua Mata, Alan Resetar, Courtney Whitcher, Greg Schneider, Aldemar Acevedo, Orlando Armesto, Edwin Infante, Helga Terzenbach, Frank Espinoza, Sebastian Lotzkat, Rafael Morillo, Miguel Matta, and Jhonathan Miranda, who kindly shared with us photographs of live and preserved specimens. For providing access to advertisement call recordings we also thank Andreas Hertz, Rafael Morillo, Darwin Rangel, Andrés Osorio, Marlon Fochler, J. Celsa Señaris, César L. Barrio-Amorós, and Wilmer Diaz. *Mannophryne* call recordings from Stephen R. Edwards were provided by The Macaulay Library at the Cornell Lab of Ornithology. Special thank to Bruno Gonzalez by its assitance in processing call recordings, to Lourdes Echevarria and Andrés Jaramillo by assistance in phylogenetic analyses, and to Adolpho Agustin and Miriam Souza Vianna from IPR-PUCRS by generating high resolution computed microtomography scans for this study. FJMRR acknowledges the institutional support received from Fundación La Salle de Ciencias Naturales and from the Postgraduate Program in Zoology of PUCRS during the development of its PhD from wich derived this study. Venezuelan permits for collecting (#361, #1445, #941, and #1758) were issued to FRR by the Ministerio del Poder Popular para el Ambiente. FRR was supported by a PhD scholarship from Brazilian Conselho Nacional de Desenvolvimento Científico e Tecnológico (CNPq, process 142444/2014-6).

References

Aguirre, A.A. & M. Lampo. 2006. Protocolo de bioseguridad y cuarentena para prevenir la transmisión de enfermedades en anfibios. *In:* Angulo, A., J.V.

Rueda-Almonacid, J.V. Rodríguez-Mahecha & E. La Marca (eds), *Técnicas de inventario y monitoreo para los anfibios de la region tropical andina*. Conservación Internacionla. Serie Manuales de Campo para la Conservación, No. 2. Panamericana Formas e Impresos S.A., Bogotá D.C. Pp: 73–91.

Angulo, A. & S. Reichle. 2008. Acoustic signals, species diagnosis, and species concepts: the case of a new cryptic species of *Leptodactylus* (Amphibia, Anura, Leptodactylidae) from the Chapare region, Bolivia. *Zoological Journal of the Linnean Society*, 152: 59–77. https://doi.org/10.1111/j.1096-3642.2007.00338.x

Barrio-Amorós, C.L. 1999 “1998”. Sistemática y biogeografía de los anfibios (Amphibia) de Venezuela. *Acta Biologica Venezuelica*, 18(2): 1–93.

Barrio-Amorós, C.L. & C. Molina R. 2010. Herpetofauna del Ramal de Calderas, Andes de Venezuela. *In:* A. Rial B., J.C. Señaris, C.A. Lasso & A. Flores (eds), *Evaluación Rápida de la Biodiversidad y Aspectos Socioecosistémicos del Ramal de Calderas. Andes de Venezuela*. *RAP Bulletin of Biological Assesment*, No. 56. Conservation International, Arlington, VA. Pp: 74–80.

Barrio-Amorós, C.L. & J.C. Santos. 2009. Description of a new *Allobates* (Anura, Dendrobatidae) from the eastern Andean piedmont, Venezuela. *Phyllomedusa*, 8(2): 89–104.

Barrio-Amorós, C.L. & J.C. Santos. 2011. Redescription and generic assignation of *Dendrobates rufulus* Gorzula, 1990 (Anura: Dendrobatidae) from the Chimantá Massif, Venezuela. *Salamandra*, 47(3): 155–160.

Barrio-Amorós, C.L. & J.C. Santos. 2012. A phylogeny for *Aromobates* (Anura: Dendrobatidae) with description of three new species from the Andes of Venezuela, taxonomic comments on *Aromobates saltuensis*, *A. inflexus*, and notes on the conservation status of the genus. *Zootaxa*, 3422: 1–31.

Barrio-Amorós, C.L., G. Rivas & H. Kaiser. 2006a. New species of *Colostethus* (Anura, Dendrobatidae) from the Península de Paria. *Journal of Herpetology*, 40(3): 371–377. https://doi.org/10.1670/0022-1511(2006)40[371:NSOCAD]2.0.CO;2

Barrio-Amorós, C.L, G. Rivas, C. Molina & Kaiser 2006b. *Mannophryne trinitatis* (Anura: Dendrobatidae) a Trinidadian single-island endemic. *Herpetologica Review*, 37(3): 298–299.

Barrio-Amorós, C.L., F.J.M. Rojas-Runjaic & J.C. Señaris. 2009. Anexo 1. Listado de los anfibios de Venezuela. Pp. 29–39. *In*: C. Molina, , J.C. Señaris, M. Lampo & A. Rial (eds.). *Anfibios de Venezuela. Estado del conocimiento y recomendaciones para su conservación*. Conservación Internacional Venezuela – Instituto de Zoología y Ecología Tropical – Fundación La Salle de Ciencias Naturales – Instituto Venezolano de Investigaciones Científicas – Gold Reserves Inc. Caracas, Venezuela.

Barrio-Amorós, C.L., J.C. Santos & C.R Molina. 2010a. An addition to the diversity of dendrobatid frogs in Venezuela: description of three new collared frogs (Anura: Dendrobatidae: *Mannophryne*). *Phyllomedusa*, 9(1): 3–35.

Barrio-Amorós, C.L., E. Romero & E. Infante. 2010b. The critically endangered Venezuelan dendrobatid frog *Aromobates meridensis* (Amphibia: Anura):

redescription, natural history and conservation. *Revista de Ecología Latinoamericana*, 15(1): 1–12.

Barrio-Amorós, C.L., G.A. Rivas, C. Molina, J.C. Santos & H. Kaiser. 2010c. Intraspecific variation in the endangered *Mannophryne riveroi* (Anura, Dendrobatidae, Aromobatinae), with comments on coloration and natural history. *Herpetology Notes*, 3: 151–160.

Barrio-Amorós, C.L., R. Rivero & J.C. Santos. 2011. A new striking dendrobatid frog (Dendrobatidae: Aromobatinae, *Aromobates*) from the Venezuelan Andes. *Zootaxa*, 3063: 39–52.

Bogdanowicz, D. & K. Giaro. 2012. Matching split distance for unrooted binary phylogenetic trees. *IEEE/ACM Transactions on Computational Biology and Bioinformatics*, 9(1): 150–60. https://doi.org/10.1109/TCBB.2011.48.

Bossuyt, F., & M.C. Milinkovitch. 2000. Convergent adaptive radiations in Madagascan and Asian ranid frogs reveal covariation between larval and adult traits. *Proceedings of the National Academy of Science of the United States of America*, 97(12): 6585–9590. https://doi.org/10.1073/pnas.97.12.6585

Boulenger, G.A. 1882. Catalogue of the Batrachia Salientia s. Ecaudata in the collection of the British Museum. 2nd Edition. Taylor and Francis, London, viii + 127 pp. https://doi.org/10.5962/bhl.title.20903

Brown J.L. & E. Twomey. 2009. Complicated histories: three new species of poison frogs of the genus *Ameerega* (Anura: Dendrobatidae) from north-central Peru. *Zootaxa*, 2049: 1–38.

Brown J.L., E. Twomey, M. Pepper, M. Sanchez R. 2008. Revision of the *Ranitomeya fantastica* species complex with description of two new species from central Peru (Anura: Dendrobatidae). *Zootaxa*, 1823: 1–24.

Brown, J.L., E. Twomey, A. Amézquita, M.B. de Souza, J.P. Caldwell, S. Lötters, R. von May, P.R. Melo-Sampaio, D. Mejía-Vargas, P. Perez-Peña, M. Pepper, E.H. Poelman, M. Sanchez-Rodriguez & K. Summers. 2011. A taxonomic revision of the Neotropical poison frog genus *Ranitomeya* (Amphibia: Dendrobatidae). *Zootaxa*, 3083: 1–120.

Caldwell, J. P. & A. P. Lima. 2003. A new Amazonian species of *Colostethus* (Anura: Dendrobatidae) with a nidicolous tadpole. *Herpetologica*, 59: 219–234. https://doi.org/10.1655/0018-0831(2003)059[0219:ANASOC]2.0.CO;2

Castroviejo-Fisher, S., C. Vilà, J. Ayarzagüena, M. Blanc & R. Ernst. 2011. Species diversity of *Hyalinobatrachium glassfrogs* (Amphibia: Centrolenidae) from the Guiana Shield, with the description of two new species. *Zootaxa*, 3132: 1–55.

Castroviejo-Fisher, S., J.M. Padial, I. de la Riva, J.P. Pombal Jr., H.R. da Silva, F.J.M. Rojas-Runjaic, E. Medina-Méndez & D.R. Frost. 2015. Phylogenetic systematics of egg-brooding frogs (Anura: Hemiphractidae) and the evolution of direct development. *Zootaxa*, 4004(1): 1–75. http://doi.org/10.11646/zootaxa.4004.1.1

Chaves, G., H. Zumbado-Ulate, A. García-Rodríguez, E. Gómez, V. Thomas V. & M.J. Ryan. 2014. Rediscovery of the critically endangered streamside frog, *Craugastor taurus* (Craugastoridae), in Costa Rica. *Tropical Conservation Science*, 7(4): 628–638.

https://doi.org/10.1177/194008291400700404

Cisneros-Heredia, D.F. & R.W. McDiarmid. 2007. Revision of the characters of Centrolenidae (Amphibia: Anura: Athesphatanura), with comments on its taxonomy and the description of new taxa of glassfrogs. *Zootaxa*, 1572: 1–82.

Clough, M. & K. Summers 2000. Phylogenetic systematics and biogeography of the poison frogs: evidence from mitochondrial DNA sequences. *Biological Journal of the Linnean Society*, 70(3): 515–540 https://doi.org/10.1111/j.1095-8312.2000.tb01236.x

Coloma, L.A. 1995. Ecuadorina frogs of the genus *Colostethus* (Anura: Dendrobatidae). *Miscellaneous Publication, Natural History Museum, University of Kansas,* 87: 1–72. https://doi.org/10.5962/bhl.title.16171

Coloma, L.A., D.A. Ortiz, C. Frenkel, C. Félix-Novoa & A. Quiguango-Ubillús. 2018. *Paruwrobates erythromos*. *In*: Ron, S.R., A. Merino-Viteri & D.A. Ortiz. (eds). Anfibios del Ecuador. Version 2019.0. Museo de Zoología, Pontificia Universidad Católica del Ecuador. Accessible from: https://bioweb.bio/faunaweb/amphibiaweb/FichaEspecie/Paruwrobates%20erythromos (accesed February 5, 2019).

De Sá, R., T. Grant, A. Camargo, W.R. Heyer, M.L. Ponssa & E. Stanley. 2014. Systematics of the Neotropical genus *Leptodactylus* Fitzinger, 1826 (Anura: Leptodactylidae): Phylogeny, the relevance of non-molecular evidence, and species accounts. *South American Journal of Herpetology*, 9(Special Issue 1), 2014: 1–128. http://doi.org/10.2994/SAJH-D-13-00022.1

Dias, P.E.S. 2018. Evolution of larval characteres in Dendrobatoidea Cope, 1865 (Amphibia; Anura; Dendrobatidae & Aromobatidae). PhD. Thesis. Instituto de Biociências, Universidade de São Paulo (USP). São Paulo, Brazil.
http://doi.org/ 10.11606/T.41.2018.tde-20082018-141408

Díaz de Pascual, A. & C. Guerrero. 2008. Diet composition of bullfrogs, *Rana catesbeiana* (Anura: Ranidae) introduced into the Venezuelan Andes. *Herpetological Review*, 39(4): 425–427.

Dixon, J.R. & C. River-Blanco. 1985. A new dendrobatid frog (*Colostethus*) from Venezuela with notes on its natural history and that of related species. *Journal of Herpetology*, 19(2): 177–184.
https://www.doi.org/10.2307/1564170

Dole, J.W., & P. Durant. 1972. A new species of *Colostethus* (Amphibia: Salientia) from the Merida Andes, Venezuela. *Caribbean Journal of Science*, 12(3–4): 191–193.

Dole, J.W. & P. Durant. 1974. Courtship behavior in *Colostethus collaris* (Dendrobatidae). *Copeia*, 1974(4): 988–990.
https://doi.org/10.2307/1442607

Donoso-Barros, R. 1964. A new Dendrobatidae frog, *Prostherapis riveroi* from Venezuela. *Caribean Journal of Science*, 4(4): 485–489.

Duellman, W.E. 2015. Marsupial frogs. *Gastrotheca* & allied genera. Johns Hopkins University Press. Baltimore. 407 pp.

Duellman, W.E., & E. Lehr. 2009. *Terrestrial breeding frogs (Strabomantidae) in Peru*. Nature und Tier Verlag. Münster, Germany. 382 pp.

Duellman, W.E. & L. Trueb. 1994. *Biology of amphibians*. The Johns Hopkins University Press. Baltimore and London.

Durant, P. & J.W. Dole. 1975. Aggressive behavior in *Colostethus* (=*Prostherapis*) *collaris* (Anura: Dendrobatidae). *Herpetologica*, 31(1): 23–26. https://www.jstor.org/stable/3891981

Edgar, R.C. MUSCLE: multiple sequence alignment with high accuracy and high throughput. *Nucleic Acids Research*, 32(5): 1792–1797. https://doi.org/10.1093/nar/gkh340

Edwards, S.R. 1974. A phenetic analysis of the genus *Colostethus* (Anura: Dendrobatidae). Ph.D. dissertation. University of Kansas, Lawrence. 419 pp.

Enciso-Calle, M.P., A. Viuche-Lozano, M. Anganoy-Criollo & M.H. Bernal. 2017. Rediscovery of *Atelopus subornatus* Werner, 1899 (Anura: Bufonidae), with a redescription of the tadpole. *Zootaxa*, 4344(1): 160–162. https://doi.org/10.11646/zootaxa.4344.1.7

Faivovich, J., R.W. McDiarmid & C.W. Myers. 2013. Two new species of *Myersiohyla* (Anura: Hylidae) from Cerro de la Neblina, Venezuela, with comments on other species of the genus. *American Museum Novitates*, 3792: 1–63. https://doi.org/10.1206/3792.1

Farris, J.S. 1983. The logical basis of phylogenetic analysis. *In*: Platnick, N.I. & Funk, V.A. (eds), Advances in Cladistics: Proceedings of the Third Meeting of the Willi Hennig Society 2. Columbia University Press, New York, USA, pp. 7–36.

Farris, J.S., V.A. Albert, M. Källersjö, D. Lipscomb, & A.G. Kluge. 1996. Parsimony jackknifing outperforms neighbor-joining. *Cladistics*, 12(2): 99–124. https://doi.org/10.1111/j.1096-0031.1996.tb00196.x

Fisher, D.O. 2011. Trajectories from extinction: where are missing mammals rediscovered? *Global Ecology and Biogeography*, 20(3): 415–425. https://doi.org/10.1111/j.1466-8238.2010.00624.x

Ford, L.S. & D.C. Cannatella. 1993. The major clades of frogs. *Herpetological Monographs*, 7: 94–117. https://doi.org/10.2307/1466954

Fouquet, A., S.M. Souza, P.M.S. Nunes, P.J.R. Kok, F.F. Curcio, C.M. de Carvalho, T. Grant & M.T. Rodrigues. 2015. Two new endangered species of *Anomaloglossus* (Anura: Aromobatidae) from Roraima State, northern Brazil. *Zootaxa*, 3926: 191–210. http://dx.doi.org/10.11646/zootaxa.3926.2.2

Fouquet, A., J.-P. Vacher, E.A. Courtois, B. Villette, H. Reizine, P. Gaucher, R. Jairam, P.E. Ouboter & P.J.R. Kok. 2018. On the brink of extinction: two new species of *Anomaloglossus* from French Guiana and amended definitions of *Anomaloglossus degranvillei* and *A. surinamensis* (Anura: Aromobatidae). *Zootaxa*, 4379: 1–23. https://doi.org/10.11646/zootaxa.4379.1.1

Fouquet, A., J-P. Vacher, E.A. Courtois, C. Deschamps, P. Ouboter, R. Jairam, P. Gaucher, A. Dubois & P.J.R. Kok. 2019. A new species of *Anomaloglossus* (Anura: Aromobatidae) of the *stepheni* group with the redescription of *A. baeobatrachus* (Boistel and de Massary, 1999), and

an amended definition of *A. leopardus* Ouboter and Jairam, 2012. *Zootaxa*, 4576 (3): 439–460. https://doi.org/10.11646/zootaxa.4576.3.2

Frost, D. R. 2007. Amphibian Species of the World: An Online Reference. Version 5.0. Electronic Database. American Museum of Natural History, New York, USA.

Frost, D.R. 2019. *Amphibian Species of the World: an Online Reference. Version 6.0*. Electronic Database. American Museum of Natural History, New York, USA. Available at: http://research.amnh.org/herpetology/amphibia/index.html. Accessed on June 14, 2019.

Frost, D.R.; T. Grant, J. Faivovich, R.H. Bain, A. Haas, C.F.B. Haddad, R.O. de Sá, A. Channing, M. Wilkinson, S.C Donnellan, C.J. Raxworthy, J.A. Campbell, B.L. Blotto, P. Moler, R.C. Drewes, R.A. Nussbaum, J.D. Lynch, M. David & W.C. Wheeler. 2006. The amphibian tree of life. *Bulletin of the American Museum of Natural History*, 297: 1–370. http://hdl.handle.net/2246/5781

Goloboff, P.A. 1996. Methods for faster parsimony analysis. *Cladistics*, 12(3): 199–220. https://doi.org/10.1111/j.1096-0031.1996.tb00009.x

Goloboff, P.A. 1999. Analyzing large data sets in reasonable times: solutions for composite optima. *Cladistics*, 15(4): 415–428. https://doi.org/10.1111/j.1096-0031.1999.tb00278.x

Goloboff, P.A. & S.A. Catalano. 2016. TNT, version 1.5, with a full implementation of phylogenetic morphometrics. *Cladistics*, 32(3): 221–238.

https://doi.org/10.1111/cla.12160

Goloboff, P.A., J.S. Farris & K.C. Nixon. 2008. TNT, a free program for phylogenetic analysis. *Cladistics*, 24(5): 774–786. https://doi.org/10.1111/j.1096-0031.2008.00217.x

Gómez, R.O. & G.F. Turazzini. 2015. An overview of the ilium of anurans (Lissamphibia, Salientia), with a critical appraisal of the terminology and primary homology of main ilial features. *Journal of Vertebrate Paleontology*, 36(1): 1–12 (e1030023). https://doi.org/10.1080/02724634.2015.1030023

Grant, T. & F. Castro-Herrera. 1998. The cloud forest *Colostethus* (Anura, Dendrobatidae) of a region of the Cordillera Occidental of Colombia. *Journal of Herpetology*, 32(3): 378–392. http://doi.org/10.2307/1565452

Grant, T. & A.G. Kluge. 2004. Transformation series as an ideographic character concept. *Cladistics*, 20(1): 23–31. http://doi.org/10.1111/j.1096-0031.2004.00003.x

Grant, T. & A.G. Kluge. 2009. Perspective: parsimony, explanatory power, and dynamic homology testing. *Systematics and Biodiversity*, 7(4): 357–363. http://doi.org/10.1017/S147720000999017X

Grant, T., & L.O. Rodríguez. 2001. Two new species of frogs of the genus *Colostethus* (Dendrobatidae) from Peru and a redescription of *C. trilineatus* (Boulenger, 1883). *American Museum Novitates*, 3355: 1–24. https://doi.org/10.1206/0003-0082(2001)355<0001:TNSOFO>2.0.CO;2

Grant, T., E.C. Humphrey & C.W. Myers. 1997. The median lingual process of frogs: a bizarre character of Old World ranoids discovered in South American dendrobatids. *American Museum Novitates*, 3212: 1–40. http://hdl.handle.net/2246/3611

Grant, T., D.R. Frost, J.P. Caldwell, R. Gagliardo, C.F.B. Haddad, P.J.R. Kok, B.D. Means, B.P. Noonan, W.E. Schargel & W.C. Wheeler. 2006. Phylogenetic systematics of dart-poison frogs and their relatives (Amphibia: Athesphatanura: Dendrobatidae). *Bulletin of American Museum of Natural History*, 299: 1–262. https://doi.org/10.1206/0003-0090(2006)299[1:PSODFA]2.0.CO;2

Grant, T., A.R. Acosta-Galvis & M. Rada. 2007. A name for the species of *Allobates* (Anura: Dendrobatoidea: Aromobatidae) from the Magdalena Valley of Colombia. *Copeia*, 2007: 844–854. https://doi.org/10.1643/0045-8511(2007)7[844:ANFTSO]2.0.CO;2

Grant, T., M. Rada, M.A. Anganoy-Criollo, A. Batista, P.H. dos S. Dias, A.M. Jeckel, D.J. Machado & J.V. Rueda-Almonacid. 2017. Phylogenetic systematics of dart-poison frogs and their relatives revisited (Anura: Dendrobatoidea). *South American Journal of Herpetology*, 12(SI): 1–90. https://doi.org/10.2994/SAJH-D-17-00017.1

Graves, B.M. 1999. Diel activity patterns of the sympatric Poison Dart Frogs, *Dendrobates auratus* and *D. pumilio*, in Costa Rica. *Journal of Herpetology*, 33(3): 375–381. https://doi.org/10.2307/1565634

Guayasamin, J.M. & L. Trueb. 2007. A new species of glassfrog (Anura: Centrolenidae) from the lowlands of northwestern Ecuador, with comments on centrolenid osteology. *Zootaxa*, 27–45.

Guayasamin, J.M., S. Castroviejo-Fisher, L. Trueb, J. Ayarzagüena, M. Rada & C. Vilà. 2009. Phylogenetic systematics of Glassfrogs (Amphibia: Centrolenidae) and their sister taxon *Allophryne ruthveni*. *Zootaxa*, 2100: 1–97.

Haas, A. 2001. Mandibular arch musculature of anuran tadpoles, with comments on homologies of amphibian jaw muscles. *Journal of Morphology*, 247(1): 1–33. https://doi.org/10.1002/1097-4687(200101)247:1<1::AID-JMOR1000>3.0.CO;2-3

Hayes, M.P. & P.H. Starrett. 1980. Notes on a collection of centrolenid frogs from the Colombian Chocó. *Bulletin of the Southern California Academy of Science*, 79(3), 89–96. http://direct.biostor.org/reference/101954

Heath, T.A., S.M. Hedtke & D.M. Hillis. 2008. Taxon sampling and the accuracy of phylogenetic analyses. *Journal of Systematics and Evolution*, 46(3): 239–257. https://doi.org/10.3724/SP.J.1002.2008.08016

Hemerik, L., R. Hengeveld & E. Lippe. 2006. The eclipse of species ranges. *Acta Biotheoretica*, 54(4): 255–266. https://doi.org/10.1007/s10441-007-9001-1

Hill, R.L., K.G. Martin, E. Stanley & J.R. Mendelson III. 2018. A taxonomic review of the genus *Hemiphractus* (Anura: Hemiphractidae) in Panama:

description of two new species, resurrection of *Hemiphractus panamensis* (Stejneger, 1917), and discussion of *Hemiphractus fasciatus* Peters, 1862. *Zootaxa*, 4429(3): 495–512. https://doi.org/10.11646/zootaxa.4429.3.3

IUCN 2019. *The IUCN Red List of Threatened Species. Version 2019-1*. Available at: https://www.iucnredlist.org. Accessed on June 05, 2019.

Jaeger, R.G. & J.P. Hailman. 1981. Activity of Neotropical frogs in relation to ambient light. *Biotropica*, 13(1): 59–65. https://doi.org/10.2307/2387871

Jerez, A. & C. Yara-Contreras. 2018. *Rheobates palmatus*. *Catálogo de Anfibios y Reptiles de Colombia*, 4(1): 68–78.

Jowers, M.J. & J.R. Downie. 2005. Tadpole deposition behaviour in male stream frogs *Mannophryne trinitatis* (Anura: Dendrobatidae). *Journal of Natural History*, 39(32): 3013–3027. https://doi.org/10.1080/00222930500221239

Kaiser, H. & R. Altig. 1994. The atypical tadpole of the dendrobatid frog, *Colostethus chalcopis*, from Martinique, French Antilles. *Journal of Herpetology*, 28(3): 374–378. https://doi.org/10.2307/1564539

Kaiser, H., L.A. Coloma & H.M. Gray. 1994. A new species of Colostethus (Anura: Dendrobatidae) from Martinique, French Antilles. Herpetologica, 50(1): 23–32. https://www.jstor.org/stable/3892871

Kaiser, H., L.A. Coloma & H.M. Gray. 1994. A new species of *Colostethus* (Anura: Dendrobatidae) from Martinique, French Antilles. *Herpetologica*, 50(1): 23–32.
https://www.jstor.org/stable/3892871

Kaiser, H., C. Steinlein, W. Feichtinger & M. Schmid. 2003. Chromosome banding of six dendrobatid frogs (*Colostethus*, *Mannophryne*). *Herpetologica*, 59(2): 203–218.
https://doi.org/10.1655/0018-0831(2003)059[0203:CBOSDF]2.0.CO;2

Kaplan, M. 1997. A new species of *Colostethus* from the Sierra Nevada de Santa Marta (Colombia) with comments on intergeneric relationships within the Dendrobatidae. *Journal of Herpetology*, 31(3): 369–375.
https://doi.org/10.2307/1565665

Kenny, J.S. 1969. The Amphibia of Trinidad. *Studies on the Fauna of Curaçao and other Caribbean Islands*, 29(1): 1–78.
http://www.repository.naturalis.nl/document/549896

Kluge, A.G. & T. Grant. 2006. From conviction to anti-superfluity: old and new justifications for parsimony in phylogenetic inference. *Cladistics*, 22(3): 276–288.
http:// doi.org/10.1111/j.1096-0031.2006.00100.x

Kocher, T.D., W.K. Thomas, A. Meyer, S.V. Edwards, S. Pääbo, F.X. Villablanca & A.C. Wilson. 1989. Dynamics of mitochondrial DNA evolution in animals: amplification and sequencing with conserved primers. *Proceedings of the National Academy of Sciences*, 86(16): 6196–6200.
https://doi.org/10.1073/pnas.86.16.6196

Kok, P.J.R., R.D. MacCulloch, P. Gaucher, E.H. Poelman, G.R. Bourne, A. Lathrop & G.L. Lenglet. 2006a. A new species of *Colostethus* (Anura, Dendrobatidae) from French Guiana with a redescription of *Colostethus beebei* (Noble, 1923) from its type locality. *Phyllomedusa*, 5(1): 43–66.

Kok, P.J.R., H. Sambhu, I. Roopsind, G.L. Lenglet & G.R. Bourne. 2006b. A new species of *Colostethus* (Anura: Dendrobatidae) with maternal care from Kaieteur National Park, Guyana. *Zootaxa*, 1238: 35–61.

Kok, P.J.R., R.D. MacCulloch, A. Lathrop, B. Willaert & F. Bossuyt. 2010a. A new species of *Anomaloglossus* (Anura: Aromobatidae) from the Pakaraima Mountains of Guyana. *Zootaxa*, 2660: 18–32.

Kok, P.J.R. 2010. A redescription of *Anomaloglossus praderioi* (La Marca, 1998) (Anura: Aromobatidae: Anomaloglossinae), with description of its tadpole and call. *Papéis Avulsos de Zoologia*, 50(4): 51–68.

Kok, P.J.R., M. Hölting & R. Ernst. 2013a. A third microendemic to the Iwokrama Mountains of central Guyana: a new “cryptic” species of *Allobates* Zimmerman and Zimmerman, 1988 (Anura: Aromobatidae). *Organisms, Diversity and Evolution*, 13: 621-638. https://doi.org/10.1007/s13127-013-0144-4

Kok, P. J. R., B. Willaert & D. B. Means. 2013. A new diagnosis and description of Anomaloglossus roraima (La Marca, 1998) (Anura: Aromobatidae: Anomaloglossinae), with description of its tadpole and call. *South American Journal of Herpetology*, 8: 29-45. https://doi.org/10.2994/SAJH-D-12-00021.1

Kok, P.J.R., M.P.J. Nicolaï, A. Lathrop, & R.D. MacCulloch. 2018. *Anomaloglossus meansi* sp. n., a new Pantepui species of the

Anomaloglossus beebei group (Anura, Aromobatidae). *ZooKeys*, 759: 99–116. https://doi.org/10.3897/zookeys.759.24742

Kumar, S., G. Stecher & K. Tamura. 2016. MEGA7: Molecular Evolutionary Genetics Analysis version 7.0 for bigger datasets. *Molecular Biology and Evolution*, 33: 1870–1874. https://doi.org/10.1093/molbev/msw054

La Marca, E. 1985. A new species of *Colostethus* (Anura: Dendrobatidae) from the Cordillera de Merida, northern Andes, South America. *Occasional Papers of the Museum of Zoology, University of Michigan*, 710: 1–10. http://hdl.handle.net/2027.42/57146

La Marca E. 1992. Catálogo taxonómico, biogeográfico y bibliográfico de las ranas de Venezuela. *Cuadernos Geográficos*, 9: 1–297.

La Marca, E. 1993. Phyllogenetic relationships and taxonomy of *Colostethus mandelorum* (Anura: Dendrobatidae), with notes on coloration, natural history, and description of the tadpole. *Bulletin of the Maryland Herpetological Society*, 29(1): 4–19.

La Marca, E. 1994a. Taxonomy of the frogs of the genus *Mannophryne* (Amphibia: Anura: Dendrobatidae). *Publicaciones de la Asociación de Amigos de Doñana*, 4: 1–75.

La Marca, E. 1994b “1991”. Descripción de un género nuevo de ranas (Amphibia: Dendrobatidae) de la cordillera de Mérida, Venezuela. Anuario de Investigación 1991, Instituto de Geografía, Universidad de Los Andes. Pp. 39–41.

La Marca, E. 1995. Biological and systematic synopsis of a genus of frogs from northern mountains of South America (Anura: Dendrobatidae: *Mannophryne*). *Bulletin of the Maryland Herpetological Society*, 31(2): 40–77. https://www.biodiversitylibrary.org/item/238929#page/283/mode/1up

La Marca, E. 1997 “1996”. Ranas del género *Colostethus* (Amphibia: Anura: Dendrobatidae) de la Guayana venezolana con la descripción de siete especies nuevas. *Publicaciones de la Asociación de Amigos de Doñana*, 9: 1–64.

La Marca, E. 2004. Systematic status of an enigmatic and possibly endangered dendrobatid frog (*Colostethus dunni*) from the valley of Caracas, northern Venezuela. *Herpetotropicos*, 1(3): 19–28.

La Marca, E. 2007 “2005”. Estatus de poblaciones de ranas de la familia Dendrobatidae (Amphibia: Anura) en sus localidades tipo en Los Andes de Venezuela. *Herpetotropicos*, 2(2): 73–86.

La Marca, E. 2009. A frog survivor (Amphibia: Anura: Aromobatidae: *Mannophryne*) of the traditional coffee belt in the Venezuelan Andes. *Herpetotropicos*, 5(1): 49–54.

La Marca, E. 2015. Sapito acollarado de Rancho Grande, *Mannophryne neblina*. *In*: J.P. Rodríguez, A. García-Rawlins & F. Rojas-Suárez (eds.) *Libro Rojo de la Fauna Venezolana*. Fourth edition. Provita and Fundación Empresas Polar, Caracas, Venezuela. Available at: http://animalesamenazados.provita.org.ve/content/sapito-acollarado-de-rancho-grande. Accessed on June 05, 2019.

La Marca, E. & A. Mijares-Urrutia. 1989. Description of the tadpole of *Colostethus mayorgai* (Anura: Dendrobatidae) with preliminary data on the reproductive biology of the species. *Bulletin of the Maryland Herpetological Society*, 24(3): 47–57.

La Marca, E. & H.P. Reinthaler. 1991. Population changes in *Atelopus* species of the Cordillera de Mérida, Venezuela. *Herpetological Review*, 22(4): 125–128.

La Marca, E. & J. Manzanilla 2004. *Mannophryne neblina*. The IUCN Red List of Threatened Species 2004: e.T55247A11280265. http://dx.doi.org/10.2305/IUCN.UK.2004.RLTS.T55247A11280265.en.

La Marca, E., & J.E. García-Pérez. 2004a. *Aromobates capurinensis*. The IUCN Red List of Threatened Species 2004: e.T55062A11234301. http://dx.doi.org/10.2305/IUCN.UK.2004.RLTS.T55062A11234301.en.

La Marca, E., & J.E. García-Pérez. 2004b. *Aromobates duranti*. The IUCN Red List of Threatened Species 2004: e.T55254A11281790. http://dx.doi.org/10.2305/IUCN.UK.2004.RLTS.T55254A11281790.en.

La Marca, E., & J.E. García-Pérez. 2004c. *Aromobates haydeeae*. The IUCN Red List of Threatened Species 2004: e.T55255A11281918. http://dx.doi.org/10.2305/IUCN.UK.2004.RLTS.T55255A11281918.en.

La Marca, E., & J.E. García-Pérez. 2004d. *Aromobates serranus*. The IUCN Red List of Threatened Species 2004: e.T55260A11265129. http://dx.doi.org/10.2305/IUCN.UK.2004.RLTS.T55260A11265129.en.

La Marca, E., & J.E. García-Pérez. 2010a. *Aromobates alboguttatus*. The IUCN Red List of Threatened Species 2010: e.T55253A11281658. http://dx.doi.org/10.2305/IUCN.UK.2010-2.RLTS.T55253A11281658.en.

La Marca, E., & J.E. García-Pérez. 2010b. *Aromobates leopardalis*. The IUCN Red List of Threatened Species 2010: e.T55104A11250110. http://dx.doi.org/10.2305/IUCN.UK.2010-2.RLTS.T55104A11250110.en.

La Marca, E., & J.E. García-Pérez. 2010c. *Aromobates mayorgai*. The IUCN Red List of Threatened Species 2010: e.T55256A11282171. http://dx.doi.org/10.2305/IUCN.UK.2010-2.RLTS.T55256A11282171.en.

La Marca, E., & J.E. García-Pérez. 2010d. *Aromobates orostoma*. The IUCN Red List of Threatened Species 2010: e.T55259A11264820. http://dx.doi.org/10.2305/IUCN.UK.2010-2.RLTS.T55259A11264820.en.

La Marca, E. & L.M. Otero L. 2012. Rediscovery of the types of *Colostethus meridensis*, with description of a related new species and redescription of *Aromobates mayorgai* (Amphibia: Anura: Dendrobatidae). *Herpetotropicos*, 7(1–2): 55–74.

La Marca, E., M. Vences & S. Lötters. 2002. Rediscovery and mitochondrial relationships of the Dendrobatid frog *Colostethus humilis* suggest parallel colonization of the Venezuelan Andes by poison frogs. *Studies on Neotropical Fauna and Environment*, 37(3): 233–240. http://doi.org/10.1076/snfe.37.3.233.8566

La Marca, E., J. Manzanilla & C. Señaris. 2006. *Prostherapis dunni*. The IUCN Red List of Threatened Species 2006: e.T55072A11248293. http://dx.doi.org/10.2305/IUCN.UK.2006.RLTS.T55072A11248293.en.

Lampo, M., D. Sánchez, A. Nicolás, M. Márquez, F. Nava-González, C.Z. García, M. Rinaldi, A. Rodríguez-Contreras, F. León, B.A. Han & A. Chacón-Ortiz. 2008. *Batrachochytrium dendrobatidis* in Venezuela. *Herpetological Review*, 39(4), 449–454.

Larsson, A. 2014. AliView: a fast and lightweight alignment viewer and editor for large datasets. *Bioinformatics*, 30(22): 3276–3278. https://doi.org/10.1093/bioinformatics/btu531

Lehtinen, R.M., E.A. Wojtowicz & A. Hailey. 2010. Male vocalizations, female discrimination and molecular phylogeny: multiple perspectives on the taxonomic status of a critically endangered Caribbean frog. *Journal of Zoology*, 283(2): 117–125. http://doi:10.1111/j.1469-7998.2010.00752.x

Lima, A.P., & J.P. Caldwell. 2001. A new Amazonian species of *Colostethus* with sky blue digits. *Herpetologica*, 57(2): 133–138. https://www.jstor.org/stable/3893182

Lima, A.P., D.E.A. Sanchez & J.R.D. Souza. 2007. A new amazonian species of the frog genus *Colostethus* (Dendrobatidae) that lays its eggs on the undersides of leaves. *Copeia*, 2007: 114–122. https://doi.org/10.1643/0045-8511(2007)7[114:ANASOT]2.0.CO;2

Lima, A.P., J.P. Caldwell, G. Biavati & A. Montanarin. 2010. A new species of *Allobates* (Anura: Aromobatidae) from Paleovárzea Forest in Amazonas, Brazil. *Zootaxa*, 2337: 1–17.

Lima, A. P., P.I. Simões & I.L. Kaefer. 2014. A new species of *Allobates* (Anura: Aromobatidae) from the Tapajós River basin, Pará State, Brazil. *Zootaxa*, 3889: 355–387. http:/ /dx.doi.org/10.11646/zootaxa.3889.3.2

Lima, A.P., P.I. Simões & Í.L. Kaefer. 2015. A new species of *Allobates* (Anura: Aromobatidae) from Parque Nacional da Amazônia, Pará State, Brazil. *Zootaxa*, 3980: 501–525.

http://dx.doi.org/10.11646/zootaxa.3980.4.3

Lötters, S., S. Reichle & K.-H. Jungfer. 2003. Advertisement calls of Neotropical poison frogs (Amphibia: Dendrobatidae) of the genera *Colostethus*, *Dendrobates* and *Epipedobates*, with notes on dendrobatid call classification. *Journal of Natural History*, 37(15): 1899–1911. http://doi.org/10.1080/00222930110089157

Lötters, S., K.-H. Jungfer, F.W. Henkel & W. Schmidt. 2007. *Poison Frogs. Biology, Species Captive Maintenance*. Frankfurt am Main: Edition Chimaira. 668 pp.

Lötters S., A. Schmitz, S. Reichle, D. Rödder & V. Quennet. 2009. Another case of cryptic diversity in poison frogs (Dendrobatidae: *Ameerega*)—description of a new species from Bolivia. *Zootaxa*, 2028: 20–30.

Lüddecke, H. 1976. Einige Ergebnisse aus Feldbeobachtungen an *Phyllobates palmatus* (Amphibia, Ranidae) in Kolumbien. *Mitteilungen aus dem Instituto Colombo-Alemán de Investigaciones Científicas Punta de Betín*, 8: 157–163. http://hdl.handle.net/1834/3272

Lüddecke, H. 2000 “1999”. Behavioral aspects of the reproductive biology of the Andean frog *Colostethus palmatus* (Amphibia: Dendrobatidae). *Revista de la Academia Colombiana de Ciencias Exactas Fisicas y Naturales*, 23 (Suplemento Especial): 303–316. http://www.accefyn.com/revista/Vol_23/supl/303-316.pdf

Lynch, J.D. 1971. Evolution, relationships, osteology, and zoogeography of leptodactyloid frogs. *Miscellaneous Publication, Natural History Museum, University of Kansas,* 53: 1–238. https://www.biodiversitylibrary.org/page/3662221

Lyra, M.L., C.F.B. Haddad & A.M.L. de Azeredo-Espin. 2017. Meeting the challenge of DNA barcoding Neotropical amphibians: polymerase chain reaction optimization and new COI primers. *Molecular Ecology Resources*, 17(5): 966–980. https://doi.org/10.1111/1755-0998.12648

Machado, D.J., 2015. YBYRÁ facilitates comparison of large phylogenetic trees. *BMC Bioinformatics*, 16: 204. https://doi.org/10.1186/s12859-015-0642-9

Maddison, W. P. & D.R. Maddison. 2018. *Mesquite: a modular system for evolutionary analysis. Version 3.51*. http://www.mesquiteproject.org

Manzanilla, J., E. La Marca, M. Jowers, D. Sánchez & M. García-Paris. 2007a "2005". Un Nuevo *Mannophryne* (Amphibia: Anura: Dendrobatidae) del macizo del Turimiquire, noroeste de Venezuela. *Herpetotropicos*, 2(2): 105–113.

Manzanilla, J., M.J. Jowers, E. La Marca & M. García-París. 2007b. Taxonomic reassessment of *Mannophryne trinitatis* (Anura: Dendrobatidae) with a description of a new species from Venezuela. *Herpetological Journal*, 17(1): 31–42.

Manzanilla J., E. La Marca & M. García-París. 2009. Phylogenetic patterns of diversification in a clade of Neotropical frogs (Anura: Aromobatidae:

Mannophryne). *Biological Journal of the Linnean Society*, 97(1): 185–199.
https://doi.org/10.1111/j.1095-8312.2009.01074.x

Marin, C.M., C. Molina-Zuluaga, A. Restrepo, E. Cano & J.M. Daza. 2018. A new species of *Leucostethus* (Anura: Dendrobatidae) from the eastern versant of the Central Cordillera of Colombia and the phylogenetic status of *Colostethus fraterdanieli*. *Zootaxa*, 4461(3): 359–380.
https://doi.org/10.11646/zootaxa.4461.3.3

Martins, M. 1989. Nova espécie de *Colostethus* da Amazonia central (Amphibia: Dendrobatidae). *Revista Brasileira de Biologia*, 49: 1009–1012.

Meinhardt, D.J. & J.R. Parmelee. 1996. A new species of *Colostethus* (Anura: Dendrobatidae) from Venezuela. *Herpetologica*, 52(1): 70–77.
https://www.jstor.org/stable/3892958

Melo-Sampaio, P.R., R.M. De Oliveira, & I. Prates. 2018. A new nurse frog from Brazil (Aromobatidae: *Allobates*), with data on the distribution and phenotypic variation of Western Amazonian species. *South American Journal of Herpetology*, 13(2): 131–149.
http://doi.org/10.2994/SAJH-D-17-00098.1

Mendelson III, J.R., H.R. da Silva & A.M. Maglia. 2000. Phylogenetic relationships among marsupial frog genera (Anura: Hylidae: Hemiphractinae) based on evidence from morphology and natural history. *Zoological Joumal of the Linnean Society*, 128: 125–148.
https://doi.org/10.1006/zjls.1998.0229

Mijares-Urrutia, A. 1998. Los renacuajos de los anuros (Amphibia) altoandinos de Venezuela: morfología externa y claves. *Revista de Biología Tropical*, 46(1): 119–143.

Mijares-Urrutia, A. & E. La Marca. 1997. Tadpoles of the genus *Nephelobates* La Marca 1994 (Amphibia Anura Dendrobatidae), from Venezuela. *Tropical Zoology*, 10(1): 133–142. https://doi.org/10.1080/03946975.1997.10539331

Mijares-Urrutia, A. & A. Arends R. 1999a. Un nuevo *Mannophryne* (Anura: Dendrobatidae) del Estado Falcón, con comentarios sobre la conservación del género en el noroeste de Venezuela. *Caribbean Journal of Science*, 35(3–4): 231–237.

Mijares-Urrutia, A. & A. Arends R. 1999b. A new *Mannophryne* (Anura: Dendrobatidae) from western Venezuela, with comments on the generic allocation of *Colostethus larandinus*. *Herpetologica*, 55(1): 106–114. http://www.jstor.org/stable/3893069

Molina, C.R. 2003. Ecología de *Mannophryne herminae* (Boettger, 1893) (Anura: Dendrobatidae) en la Cordillera de la Costa, Venezuela. PhD Thesis. Universidad Central de Venezuela. Caracas, Venezuela. 261 pp.

Myers, C.W. 1966. The distribution and behavior of a Tropical Horned Frog, *Cerathyla panamensis* Stejneger. *Herpetologica*, 22(1): 68–71. https://www.jstor.org/stable/3890729

Morales, V.R. 2002 “2000”. Sistematica y biogeografía del grupo *trilineatus* (Amphibia, Anura, Dendrobatidae, *Colostethus*), con descripción de once nuevas especies. *Publicaciones de la Asociación de Amigos de Doñana*, 13: 1–59.

Morales, V.R. & R. Schulte. 1993. Dos especies nuevas de *Colostethus* (Anura, Dendrobatidae) en las vertientes de la Cordillera Oriental del Perú y del Ecuador. *Alytes*, 11: 97–106.

Moritz, C., C.J. Schneider & D.B. Wake. 1992. Evolutionary relationships within the *Ensatina eschscholtzii* complex confirm the ring species interpretation. *Systematic Biology*, 41(3): 273–291. https://doi.org/10.1093/sysbio/41.3.273

Myers, C.W. 1982. Spotted poison frogs: Descriptions of three new *Dendrobates* from western Amazonia, and resurrection of a lost species from “Chiriqui”. *American Museum Novitates*, 2721: 1–23. http://hdl.handle.net/2246/5336

Myers, C.W. & J. Daly. 1976. Preliminary evaluation of skin toxins and vocalizations in taxonomic and evolutionary studies of poison-dart frogs (Dendrobatidae). *Bulletin of the American Museum of Natural History*, 157: 173–262. http://hdl.handle.net/2246/622

Myers, C. W. & J. W. Daly. 1980. Taxonomy and ecology of *Dendrobates bombetes*, a new Andean poison frog with new skin toxins. *American Museum Novitates*, 2692: 1–23. http://hdl.handle.net/2246/5435

Myers, C.W. & L.S. Ford. 1986. On *Atopophrynus*, a recently described frog wrongly assigned to the Dendrobatidae. *American Museum Novitates*, 2843: 1–15. http://hdl.handle.net/2246/3578

Myers, C.W. & M.A. Donnelly. 1997. A tepui herpetofauna on a granitic mountain (Tamacuari) in the borderland between Venezuela and Brazil: Report from the Phipps Tapirapecó Expedition. *American Museum Novitates*, 3213: 1–71.
http://hdl.handle.net/2246/3610

Myers, C.W. & M. Donnelly. 2001. Herpetofauna of the Yutajé-Corocoro massif, Venezuela: second report from the Robert G. Goelet American Museum-Terramar expedition to the northwestern tepuis. *Bulletin of the American Museum of Natural History*, 261: 1–85.
https://doi.org/10.1206/0003-0090(2001)261<0001:HOTYCM>2.0.CO;2

Myers, C.W. & M.A. Donnelly. 2008. The summit herpetofauna of Auyantepui, Venezuela: report from the Robert G. Goelet American Museum–Terramar Expedition. *Bulletin of the American Museum of Natural History*, 308: 1–147.
http://hdl.handle.net/2246/5896

Myers, C.W., J.W. Daly & B. Malkin. 1978. A dangerously toxic new frog (*Phyllobates*) used by embera indians of western colombia, with discussion of blowgun fabrication and dart poisoning. *Bulletin of the American Museum of Natural History*, 161: 307–366.
http://hdl.handle.net/2246/1286

Myers, C.W., A. Paolillo & J.W. Daly. 1991. Discovery of a defensively malodorous and nocturnal frog in the family Dendrobatidae: Phylogenetic significance of a new genus and species from the Venezuelan Andes. *American Museum Novitates*, 3002: 1–33.
http://hdl.handle.net/2246/5084

Nava-González, F., D. Sánchez, M. Márquez, G. Velásquez, J. Valera-Leal & L. Díaz. 2017. Dispersión de la rana toro, *Lithobates catesbeianus* (Shaw 1802) (Anura: Ranidae), en el estado Mérida, Venezuela, entre 2005-2013. *Saber*, 29: 240–248.

Nixon, K.C. 1999. The parsimony ratchet, a new method for rapid parsimony analysis. *Cladistics*, 15(4): 407–414. https://doi.org/10.1111/j.1096-0031.1999.tb00277.x

Noble, G.K. 1922. The phylogeny of the Salientia I. The osteology and the thigh musculature; their bearing on classification and phylogeny. *Bulletin of the American Museum of Natural History*, 46: 1–87. http://hdl.handle.net/2246/1138

Páez-Vacas, M.I., L.A. Coloma & J.C. Santos. 2010. Systematics of the *Hyloxalus bocagei* complex (Anura: Dendrobatidae), description of two new cryptic species, and recognition of *H. maculosus*. *Zootaxa*, 2711: 1–75.

Padial, J.M, J. Köhler, A. Muñoz & I. de la Riva. 2008. Assessing the taxonomic status of tropical frogs through bioacoustics: geographical variation in the advertisement calls in the *Eleutherodactylus discoidalis* species group (Anura). *Zoological Journal of the Linnean Society*, 152: 353–365. https://doi.org/10.1111/j.1096-3642.2007.00341.x

Padial, J.M., T. Grant & D.R. Frost. 2014. Molecular systematics of terraranas (Anura: Brachycephaloidea) with an assessment of the effects of alignment and optimality criteria. *Zootaxa*, 3825(1): 1–132. http://doi.org/10.11646/zootaxa.3825.1.1

Palumbi, S.R., A. Martin, S. Romano, W.O. McMillan, L. Stice & G. Grabawski. 1991. *The Simple Fool's Guide to PCR, Version 2.0*. Privately published, compiled by S. Palumbi, University of Hawaii: Honolulu.

Péfaur, J.E. 1985. New species of Venezuelan *Colostethus* (Dendrobatidae). *Journal of Herpetology*, 19(3): 321–327. http://doi.org/10.2307/1564261

Péfaur, J.E. 1993. Description of a new *Colostethus* (Dendrobatidae) with some natural history comments on the genus in Venezuela. *Alytes*, 11(3): 88–96.

Pereyra, M.O., D. Baldo, B.L. Blotto, P.P. Iglesias, M.T.C. Thomé, C.F.B. Haddad, C. Barrio-Amorós, R. Ibáñez & J. Faivovich. 2016. Phylogenetic relationships of toads of the *Rhinella granulosa* group (Anura: Bufonidae): a molecular perspective with comments on hybridization and introgression. *Cladistics*, 32(1): 36–53. https://doi.org/10.1111/cla.12110

Pérez-Peña, P.E., G. Chavez, E. Twomey & J.L. Brown. 2010. Two new species of *Ranitomeya* (Anura: Dendrobatidae) from eastern Amazonian Peru. *Zootaxa*, 2439: 1–23.

Perret, J.L. 1961. La biologie d'*Acanthixalus spinosus* (Amphibia salientia). *Recherches et Études Camerounaises*, 1(4): 90–101. http://www.documentation.ird.fr/hor/fdi:02511

Ponssa, M.L., J. Goldberg & V. Abdala. 2010. Sesamoids in anurans: new data, old issues. *The Anatomical Record*, 293(10): 1646–1668. https://doi.org/10.1002/ar.21212

Rada de M., D. 1976. Cariotipo de *Colostethus trinitatis* (Amphibia: Dendrobatidae). *Acta Biologica Venezuelica*, 9: 213–220.

Rivas, G., M. De Freitas, H. Kaiser, C.L. Barrio-Arnorós & T.R. Barros. 2018. *Amphibians of the Peninsula de Paria: a pocket field guide*. Chimaira Buchhandels GmbH, Frankfurt am Main, Germany. 20 pp.

Rivero, J.A. 1961. Salientia of Venezuela. *Bulletin of the Museum of Comparative Zoology*, 126(1): 1–209.

Rivero, J.A. 1971. Un nuevo e interesante *Dendrobates* (Amphibia, Salientia) de Cerro Yapacana de Venezuela. *Kasmera*, 3: 389–396.

Rivero, J.A. 1978 “1976”. Notas sobre los anfibios de Venezuela II. Sobre los *Colostethus* de los Andes venezolanos. *Memoria de la Sociedad de Ciencias Naturales La Salle*, 35(105): 327–344.

Rivero, J.A. 1980 “1978”. Notas sobre los anfibios de Venezuela III. Nuevos *Colostethus* de los Andes venezolanos. *Memoria de la Sociedad de Ciencias Naturales La Salle*, 38(109): 95–111.

Rivero, J.A. 1984a. Una nueva especie de *Colostethus* (Amphibia, Dendrobatidae) de la Cordillera de la Costa, con anotaciones sobre otros *Colostethus* de Venezuela. *Brenesia*, 1984(22): 51–56.

Rivero, J.A. 1984b "1982". Sobre el *Colostethus mandelorum* (Schmidt) y el *Colostethus inflexus* Rivero (Amphibia, Dendrobatidae). *Memoria de la Sociedad de Ciencias Naturales La Salle*, 42: 9–16.

Rivero, J.A. 1990 “1988”. Sobre las relaciones de las especies del género *Colostethus* (Amphibia, Dendrobatidae). *Memoria de la Sociedad de Ciencias Naturales La Salle*, 48(129): 3–32.

Rocha, C.F.D., C.C. Siqueira, C.V. Ariani, D. Vrcibradic, D.M. Guedes, M.C. Kiefer, M. Almeida-Gomes, P. Goyannes-Araújo, V.N.T. Borges-Júnior & M. Van Sluys. 2015. Differential success in sampling of Atlantic Forest amphibians among different periods of the day. *Brazilian Journal of Biology*, 75(2): 261–267. https://dx.doi.org/10.1590/1519-6984.19412

Rodríguez-Contreras, A., J.C. Señaris, M. Lampo & R. Rivero. 2008. Rediscovery of Atelopus cruciger (Anura: Bufonidae): current status in the Cordillera de La Costa, Venezuela. Oryx, 42(2): 1–4. https://dx.doi.org/10.1017/S0030605308000082

Rojas-Runjaic, F.J.M., E.E. Infante-Rivero & C.L. Barrio-Amorós. 2011. A new frog of the genus *Aromobates* (Anura, Dendrobatidae) from Sierra de Perijá, Venezuela. *Zootaxa*, 2919: 37–50.

Rojas-Runjaic, F.J.M. & J.C. Señaris. 2015a. Sapito niñera de Perijá, *Aromobates tokuko*. *In*: J.P. Rodríguez, A. García-Rawlins & F. Rojas-Suárez (eds.) *Libro Rojo de la Fauna Venezolana*. Fourth edition. Provita y Fundación Empresas Polar, Caracas, Venezuela. Available at: http://animalesamenazados.provita.org.ve/content/sapito-ninera-de-perija. Accessed on June 05, 2019.

Rojas-Runjaic, F.J.M. & J.C. Señaris. 2015b. Sapito niñera de Dunn, *Prostherapis dunni*. *In*: J.P. Rodríguez, A. García-Rawlins & F. Rojas-Suárez (eds.) *Libro Rojo de la Fauna Venezolana*. Fourth edition. Provita and Fundación Empresas Polar, Caracas, Venezuela. Available at: http://animalesamenazados.provita.org.ve/content/sapito-ninera-de-dunn. Accessed on: June 05, 2019.

Rojas-Runjaic, F.J.M., M.E. Matta-Pereira & E. La Marca. 2018. Unveiling species diversity in collared frogs through morphological and bioacoustic evidence: a new *Mannophryne* (Amphibia, Aromobatidae) from Sierra de Aroa, northwestern Venezuela, and an amended definition and call description of *M. herminae* (Boettger, 1893). *Zootaxa*, 4461(4): 451–476. https://doi.org/10.11646/zootaxa.4461.4.1

Rojas-Runjaic, F.J.M., W. Bolaños, E. Camargo & S. Castroviejo-Fisher. (in press). A new species of skunk frog (Anura, Aromobatidae, *Aromobates*) from Sierra de Aroa, northwestern Venezuela, with comments on the occurrence of glandular swelling on male's fingers in the genus. *Zootaxa*

Ruiz-Monachesi, M.R., E.O. Lavilla & R. Montero. 2016. The skull of *Phyllomedusa sauvagii* (Anura, Hylidae). *The Anatomical Record*, 299(5): 557–572. http://doi.org/10.1002/ar.23331

Sánchez, D.A. 2013. Larval morphology of Dart-Poison Frogs (Anura: Dendrobatoidea: Aromobatidae and Dendrobatidae). *Zootaxa*, 3637(5): 569–591. http://doi.org/10.11646/zootaxa.3637.5.5

Sánchez, D., A. Chacón-Ortiz, F. León, B.A. Han & M. Lampo. 2008. Widespread occurrence of an emerging pathogen in amphibian communities of the Venezuelan Andes. *Biological Conservation*, 141(11): 2898–2905. https://doi.org/10.1016/j.biocon.2008.08.009

Santos, J.C. & D.C. Cannatella. 2011. Phenotypic integration emerges from aposematism and scale in poison frogs. *Proceedings of the National*

Academy of Sciences of the United States of America, 108(15): 6175–6180.

https://doi.org/10.1073/pnas.1010952108

Santos, J.C., L.A. Coloma & D.C. Cannatella. 2003. Multiple, recurring origins of aposematism and diet specialization in poison frogs. *Proceedings of the National Academy of Sciences of the United States of America*, 100(22): 12792–12797.

http://doi.org/10.1073/pnas.2133521100

Santos, J.C., L.A. Coloma, K. Summers, J.P. Caldwell, R. Ree & D.C. Cannatella. 2009. Amazonian amphibian diversity is primarily derived from Late Miocene Andean lineages. *PLOS Biology*, 7(3): 1–14.

https://doi.org/10.1371/journal.pbio.1000056

Santos, J.C., M. Baquero, C. Barrio-Amorós, L.A. Coloma, L.K. Erdtmann, A.P. Lima & D.C. Cannatella. 2014. Aposematism increases acoustic diversification and speciation in poison frogs. *Proceedings of the Royal Society B*, 281: 20141761.

http://doi.org/10.1098/rspb.2014.1761

Savage, J.M. 1968. The dendrobatid frogs of Central America. *Copeia*, 1968(4): 745–776.

https://doi.org/10.2307/1441845

Schaeffer, B. 1949. Anurans from the early tertiary of Patagonia. *Bulletin of the American Museum of Natural History*, 93: 41–68.

http://hdl.handle.net/2246/404

Schmidt, K.P. 1932. Reptiles and amphibians of the Mandel Venezuelan expedition. *Field Museum of Natural History Publication. Zoological Series*, 18(7): 159–163. https://doi.org/10.5962/bhl.title.2974

Señaris, J.C. & F.J.M. Rojas-Runjaic. 2015. Sapito niñera Oriental, *Allobates mandelorum*. *In*: J.P. Rodríguez, A. García-Rawlins & F. Rojas-Suárez (eds.) *Libro Rojo de la Fauna Venezolana*. Fourth edition. Provita and Fundación Empresas Polar, Caracas, Venezuela. Available at: http:animalesamenazados.provita.org.ve/content/sapito-ninera-oriental. Accessed on June 05, 2019.

Sexton, O.J. 1960. Some aspects of the behavior and of the territory of a dendrobatid frog, *Prostherapis tinitatis*. *Ecology*, 41(1): 107–115. https://doi.org/10.2307/1931944

Silverstone, P.A. 1975. A revision of the poison-arrow frogs of the genus *Dendrobates* Wagler. *Science Bulletin. Natural History Museum of Los Angeles County*, 21: 1–55.

Silverstone, P.A. 1976. A revision of the poison-arrow frogs of the genus *Phyllobates* Bibron *in* Sagra (family Dendrobatidae). *Science Bulletin. Natural History Museum of Los Angeles County*, 27: 1–53.

Simões, P.I. 2016. A new species of nurse-frog (Aromobatidae, *Allobates*) from the Madeira River basin with a small geographic range. *Zootaxa*, 4083: 501–525.

Simões, P.I., A.P. Lima & I.P. Farias. 2010. The description of a cryptic species related to the pan-Amazonian frog *Allobates femoralis* (Boulenger 1883) (Anura: Aromobatidae). *Zootaxa*, 2406: 1–28.

Simões, P.I., M.J. Sturaro, P.L.V. Peloso & A.P. Lima. 2013. A new diminutive species of *Allobates* Zimmermann and Zimmermann, 1988 (Anura, Aromobatidae) from the northwestern Rio Madeira—Rio Tapajós interfluve, Amazonas, Brazil. *Zootaxa*, 3609: 251–273. http://dx.doi.org/10.11646/zootaxa.3609.3.1

Simões, P.I., G. Gagliardi-Urrutia, F.J.M. Rojas-Runjaic & S. Castroviejo-Fisher. 2018. A new species of nurse-frog (Aromobatidae, *Allobates*) from the Juami River basin, northwestern Brazilian Amazonia. *Zootaxa*, 4387(1): 109-133. https://doi.org/10.11646/zootaxa.4387.1.5

Simões, P.I., D. Rojas & A.P. Lima. 2019. A name for the nurse-frog (*Allobates*, Aromobatidae) of Floresta Nacional de Carajás, Eastern Brazilian Amazonia. *Zootaxa*, 4550(1): 71–100. https://doi.org/10.11646/zootaxa.4550.1.3

Simmons, M.P. 2012a. Misleading results of likelihood-based phylogenetic analyses in the presence of missing data. *Cladistics*, 28(2): 208–222. https://doi.org/10.1111/j.1096-0031.2011.00375.x

Simmons, M.P. 2012b. Radical instability and spurious branch support by likelihood when applied to matrices with non-random distributions of missing data. *Molecular Phylogenetics and Evolution*, 62(1): 472–484. https://doi.org/10.1016/j.ympev.2011.10.017

Simmons, M.P. & P.A. Goloboff. 2013. An artifact caused by undersampling optimal trees in supermatrix analyses of locally sampled characters. *Molecular Phylogenetics and Evolution*, 69(1): 265–275. https://doi.org/10.1016/j.ympev.2013.06.001

Simmons, M.P. & A.P. Norton. 2013. Quantification and relative severity of inflated branch-support values generated by alternative methods: and empirical example. *Molecular Phylogenetics and Evolution*, 67(1): 277–296.
https://doi.org/10.1016/j.ympev.2013.01.020

Summers, K. & M.E. Clough. 2001. The evolution of coloration and toxicity in the poison frog family (Dendrobatidae). *Proceedings of the National Academy of Sciences*, 98(11): 6227–6232.
https://doi.org/10.1073/pnas.101134898

Taylor, E.H. 1951. Two new genera and a new family of tropical American frogs. *Proceedings of the Biological Society of Washington*, 64: 33–40.

Test, F.H. 1954. Social aggressiveness in an amphibian. *Science*, 120(3108): 140–141.
https://doi.org/10.1126/science.120.3108.140

Test, F.H. 1956. Two new dendrobatid frogs from northern Venezuela. Occasional Papers of the Museum of Zoology, University of Michigan, 577: 1–9.
http://hdl.handle.net/2027.42/57015

Test, F.H. 1962. The highly developed courtship of the frog, *Prostherapis trinitatis*. *American Zoologist*, 2(3): 452.
https://www.jstor.org/stable/3881227

Toledo, L.F., I. Sazima, C.F.B. Haddad. 2011. Behavioural defences of anurans: an overview. *Ethology Ecology & Evolution*, 23(1): 11–25.
https://doi.org/10.1080/03949370.2010.534321

Towns, D.R. & C.H. Daugherty. 1994. Patterns of range contractions and extinctions in the New Zealand herpetofauna following human colonisation. *New Zealand Journal of Zoology*, 21(4): 325–339. https://doi.org/10.1080/03014223.1994.9518003

Trueb, L. 1993. Patterns of cranial diversity among the Lissamphibia. *In*: J. Hanken, & B.K. Hall. The skull. Volume 2. Patterns of structural and systematic diversity. University of Chicago Press, Chicago and London. Pp. 255–343.

Twomey, E. & J.L. Brown. 2008. Spotted poison frogs: rediscovery of a lost species and a new genus (Anura: Dendrobatidae) from northwestern Peru. *Herpetologica*, 64(1): 121–137. https://doi.org/10.1655/07-009.1

Vacher, J-P., P.J.R. Kok, M.T. Rodrigues, J.D. Lima, A. Lorenzini, Q. Martinez, M. Fallet, E.A. Courtois, M. Blanc, P. Gaucher, M. Dewynter, R. Jairam, P. Ouboter, C. Thébaud & A. Fouquet. 2017. Cryptic diversity in Amazonian frogs: integrative taxonomy of the genus *Anomaloglossus* (Amphibia: Anura: Aromobatidae) reveals a unique case of diversification within the Guiana Shield. *Molecular Phylogenetics and Evolution*, 112: 158–173. http://doi.org/10.1016/j.ympev.2017.04.017

Vargas G., J.Y. & E. La Marca. 2007 “2006”. A new species of collared frog (Amphibia: Anura: Aromobatidae: *Mannophryne*) from the Andes of Trujillo state. *Herpetotropicos*, 3(1): 51–57.

Varón, A., L.S Vinh & W.C. Wheeler. 2010. POY version 4: phylogenetic analysis using dynamic homologies. *Cladistics*, 26(1): 72–85.

https://doi.org/10.1111/j.1096-0031.2009.00282.x

Vaz-Silva, W. & N.M. Maciel. 2011. A new cryptic species of *Ameerega* (Anura: Dendrobatidae) from Brazilian Cerrado. *Zootaxa*, 2826: 57–68.

Vences, M., J. Kosuch, S. Lötters, A. Widmer, K-H. Jungfer, J. Köhler & M. Veith. 2000. Phylogeny and classification of poison frogs (Amphibia: Dendrobatidae), based on mitochondrial 16S and 12S ribosomal RNA gene sequences. *Molecular Phylogenetics and Evolution*, 15(1): 34–40. https://doi.org/10.1006/mpev.1999.0738

Vences, M., J. Kosuch, R. Boistel, C.F.B. Haddad, E. La Marca, S. Lötters & M. Veith. 2003. Convergent evolution of aposematic coloration in Neotropical poison frogs: a molecular phylogenetic perspective. *Organisms Diversity & Evolution*, 3: 215-226. https://doi.org/10.1078/1439-6092-00076

Vigle, G.O. & K. Miyata. 1980. A new species of *Dendrobates* (Anura: Dendrobatidae) from the lowland rain forests of western Ecuador. *Breviora*, 459: 1–7. https://www.biodiversitylibrary.org/part/235

Wells, K.D. 1977. The courtship of frogs. *In*: Taylor, D.H. & Guttman, S.I. (eds.), *The Reproductive Biology of the Amphibians*. Plenum Publishing Corp, New York, pp. 233–262. https://doi.org/10.1007/978-1-4757-6781-0_7

Wells. K.D. 1980. Social behavior and communication of a dendrobatid frog (*Colostethus trinitatis*). *Herpetologica*, 36(2): 189–199. http://www.jstor.org/stable/3891485

Wells, K.D. 2007. *The Ecology and Behavior of Amphibians*. The University of Chicago Press, Chicago, 1148 pp. https://doi.org/10.7208/chicago/9780226893334.001.0001

Wheeler, W.C. 2003a. Iterative pass optimization of sequence data. *Cladistics*, 19(3): 254–260. https://doi.org/10.1111/j.1096-0031.2003.tb00368.x

Wheeler, W.C. 2003b. Implied alignment, a synapomorphy-based multiple-sequence alignment method and its use in cladogram search. *Cladistics*, 19(3): 261–268. https://doi.org/10.1111/j.1096-0031.2003.tb00369.x

Wheeler, W.C. 2006. Dynamic homology and the likelihood criterion. *Cladistics*, 22(2): 157–170. https://doi.org/10.1111/j.1096-0031.2006.00096.x

Wheeler, W.C., N. Lucaroni, L. Hong, L.M. Crowley & A. Varón. 2015. POY version 5: phylogenetic analysis using dynamic homologies under multiple optimality criteria. *Cladistics*, 31(2): 189–196. https://doi.org/10.1111/cla.12083

Wiens, J.J., J.W. Fetzner, C.L. Parkinson & T.W. Reeder. 2005. Hylid frog phylogeny and sampling strategies for speciose clades. *Systematic Biology*, 54: 719–748. https://doi.org/10.1080/10635150500234625

Yústiz, E. 1991. Un nuevo *Colostethus* (Amphibia: Dendrobatidae) en Ia Sierra de Barbacoas, Estado Lara, Venezuela. *Bioagro*, 3(4): 145–150.

Zimmermann, H. & E. Zimmermann. 1988. Etho-Taxonomie und zoogeographische Artengruppenbildung bei Pfeilgiftfröschen (Anura: Dendrobatidae). *Salamandra*, 24(2–3): 125–160.

Appendix 1. Specimens examined for phenotipic character sampling. Specimens examined by photo are indicated by an asterisk.

Adelphobates galactonotus.— BRAZIL: Pará: Santarem, MCP 2252, 2380.

Allobates femoralis.— BRAZIL: Amazonas: ESEC Juami-Japurá, trilha do canal da Inveja, MCP 13869.

Allobates juami.— BRAZIL: Amazonas: East bank of the Juami river, within Estação Ecológica Juami-Japurá, MCP 13288–13293 (paratypes).

Allobates olfersioides.— BRAZIL: Bahia: North zone, Ilhéus, MCP 12698–12699.

Allobates pittieri.— VENEZUELA: Aragua: Ocumare de la Costa de Oro municipality, Río Cuyagua, MHNLS 21488, 21490.

Ameerega trivittata.— BRAZIL: Acre: Cruzeiro do Sul, MCP 10078–10079, 10080 (skinned carcass); Amazonas: Carauari, MCP 13084; VENEZUELA: Delta Amacuro: Río Grande Forestal Reserve, MHNLS 20160*.

Anomaloglossus rufulus.— VENEZUELA: Bolívar: Churi-tepui, Chimantá massif, Canaima National Park, MHNLS 20245; Eruoda-tepui, Chimantá massif, Canaima National Park, MHNLS 20609.

Anomaloglossus wothuja.— VENEZUELA: Amazonas: Camp next to the turbines, Raudal de Danto, Cuao river, MHNLS 19992–19993.

Aromobates alboguttatus.— VENEZUELA: Mérida: Monte Zerpa, CVULA 103, 282, 1448, 2364, 3190, 3238.

Aromobates cannatellai.— VENEZUELA: Táchira: Las Escaleras park, Pregonero, road to Mesa de Pérez, MHNLS 22625–22629.

Aromobates capurinensis.— VENEZUELA: Mérida: road to Canaguá, CVULA 1703, 1708; Canagua, CVULA 5920, 5923, 5937–5938.

Aromobates duranti.— VENEZUELA: Mérida: Paramo of La Culata, CVULA 846, 849-850, 853; Truchicultura Monterrey, 8 km NE of the city of Mérida, ULABG 621 (cleared and stained); El Valle, above truchicultura Monterrey, ULABG 1405.

Aromobates haydeeae.— VENEZUELA: Táchira: 3 km O from checkpoint of El Zumbador, CVULA 1854; between paramo El Zumbador and Mesa de Aura, CVULA 6042, 6047; El Vivero, between paramo El Zumbador and Mesa de Aura, UPR-M 4706* (holotype).

Aromobates inflexus.— VENEZUELA: Táchira: El Almogral, between Boca de Monte and the crossroads La Grita-Bailadores, UPR-M 4696* (holotype); Portachuelo-Boca de Monte, MHNLS 3730–3731, 3955.

Aromobates leopardalis.— VENEZUELA: Mérida: Paramo of Mucubají, CVULA 464; La Corcovada, paramo of Mucubají, CVULA 1863; La Victoria lake, paramo of Mucubají, CVULA 3084–3086; La Victoria refuge, paramo of Mucubají, CVULA 5886, 5889.

Aromobates mayorgai.— VENEZUELA: Mérida: La Olinda II, 5 km NNO from La Azulita, MHNLS 21983, 21987, 21992; Road between Las Adjuntas and La Osa, MHNLS 22001–22002, 22004; 1.8 km N of La Trampa, road La Azulita-Lagunillas, MHNLS 22029–22030, 22033.

Aromobates meridensis.— VENEZUELA: Mérida: La Osa, road La Azulita-Lagunillas, MHNLS 22017–22019, 22574 (tadpoles); La Carbonera, CVULA 355; Road La Azulita-Mérida, CVULA 1427, 1438, 2328–2329,

3214; El Chorotal, road to La Azulita, CVULA 5050, 5058; La Azulita, CVULA 5973, 5981, 5982.

Aromobates molinarii.— VENEZUELA: Mérida: Las Playitas, near Bailadores, ULABG 2820* (holotype); La Cascada, Bailadores, CVULA 1876–1877.

Aromobates nocturnus.— VENEZUELA: Trujillo: about 2 km airline ESSE from Agua de Obispo, ULABG 4253 (paratype ex-EBRG 2223).

Aromobates ornatissimus.— VENEZUELA: Trujillo: Near to Agua de Obispo, ca. 600 m from the intersection with the road to La Peña, ULABG 4976.

Aromobates orostoma.— VENEZUELA: Táchira: Boca de Monte, roda to Pregonero, UPR-M 4509* (holotype); km 597, road Bailadores-Pregonero, CVULA 1881–1882, 1907; road Pregonero-Bailadores, CVULA 3323–3325, 3327; km 590, road Bailadores-paramo La Negra, CVULA 3531; 3 km N from Boca de Monte, CVULA 3578; road to Pregonero, CVULA 6887.

Aromobates saltuensis.— VENEZUELA: Táchira: La Quintera, 11 km SSE from La Fría, CVULA 4981; road between La Fría and Michelena, UPR-M 5147* (holotype).

***Aromobates* sp. (aff. *saltuensis*)**.— COLOMBIA: Norte de Santander: El Diamante farm, LOA 124.

***Aromobates* sp. (aff. *saltuensis*)**.— COLOMBIA: Norte de Santander: Bochalema, AOH (froglet), R1–R5 (tadpoles).

***Aromobates* sp. (aff. *saltuensis*)**.— COLOMBIA: Norte de Santander: Vereda La Garita, T10 1–T10 2.

Aromobates serranus.— VENEZUELA: Mérida: La Mucuy, Sierra Nevada National Park, MHNLS 7089–7092; Road Mérida-El Morro, km 10, MHNLS 7096–7099; Truchicultura La Mucuy, ULABG 1769.

Aromobates tokuko.— VENEZUELA: Zulia: surroundings of Ipika, Yukpa indigenous community, Río Tokuko basin, Sierra de Perijá, MHNLS 18520, 18522–18523 (paratypes).

Aromobates walterarpi.— VENEZUELA: Mérida: stream at about 500 m away from "Plaza Bolívar" of Piñango, close to the cemetery, on the road from Piñango to Pico El Águila, 2325 m (9º01'59.8''N 70º53'02.5''W), ULABG 1577 (paratype).

Aromobates zippeli.— VENEZUELA: Mérida: Curves of San Román, transandean highway (troncal 7), MHNLS 22042-22043, 22052-22053.

***Aromobates* sp 1**.— VENEZUELA: Yaracuy: El Tigre peak, Sierra de Aroa, EBRG 2206, MHNLS 21505–21509, 22127–22128 (type series).

***Aromobates* cf. sp 1**.— VENEZUELA: Yaracuy: La Rondona creek, Sierra de Aroa, MHNLS 21284–21286, 21333–21335, 21358–21359.

***Aromobates* sp 2**.— VENEZUELA: Barinas: Los Alcaravanes, MHNLS 22191–22192 (froglets), 22093 (tadpoles).

***Aromobates* sp 3**.— VENEZUELA: Mérida: Santa Cruz de Mora, CVULA 220, 223, 225, 239.

"*Colostethus*" *caribe*.— VENEZUELA: Sucre: southern slope of Cerro El Humo, Paria península, MHNLS 17463 (paratype).

Hyloxalus cepedai.— COLOMBIA: Meta: Reserva La Vanguardia, AFJ 47, 49–52.

Leucostethus brachistriatus.— COLOMBIA: Cauca: Vereda Cenegueta, Cajibio, MCP 11512, 11514–11521.

Leucostethus fugax.— ECUADOR: Pastaza: headwaters of Bobonaza river, USNM-H 2828231* (https://bioweb.bio/galeria/Foto/Leucostethus%20fugax/Tipo/253810).

Mannophryne caquetio.— VENEZUELA: Falcón: Curimagua, Sierra de San Luis, MHNLS 1521; El Chorro, road to La Chapa, Sierra de San Luis, MHNLS 21219–21220; Las Filipinas farm, Cumbres de Urea sector, Sierra de San Luis, MHNLS 21665 (tadpoles).

Mannophryne collaris.— VENEZUELA: Mérida: Urb. Santa María, Mérida city, CVULA 1464, 1468; creek at Los Malabares street, 2.6 km WSW from Chamita sector, MHNLS 21591, 21593, 21595, 21598.

Mannophryne cordilleriana.— VENEZUELA: Barinas: Potrerito, MHNLS 21601–21607, 21612, 21624 (tadpoles); creek with aqueduct, El Cacao sector, MHNLS 21625–21628.

Mannophryne herminae.— VENEZUELA: Carabobo: Puerto Cabello, SMF 7286* (lectotype), 7316–7319*, 54898–54899* (paralectotypes); La Quiguas, San Esteban, MHNLS 1974, 1979; San Esteban, MHNLS 4071–4074; Creek affluent fot the San Esteban river, 300 m upstream of the dike, San Esteban National Park, MHNLS 22104–22105, 22110–22111, 22114 (tadpoles); Los Campamentos, Patanemo, MHNLS 6634, 6639–6640, 6647, 6651, 6664, 6670–6671; Aragua: Rancho Grande, Henri Pittier National Park, MHNLS 4022–4024, 4027; Road Choroní-Maracay, MHNLS 5749–5750, 5754–5755; low basin of cata river, Henri Pittier National Park, MHNLS 17078, 17477, 17651–17652.

Mannophryne larandina.— VENEZUELA: Lara: near Hato Arriba, road El Tocuyo-Barbacoas, MHNLS 22597–22600.

Mannophryne lamarcai.— VENEZUELA: Trujillo: Cuicas, creek to 1.8 km N from Plaza Bolívar of the town, MHNLS 22087–22088; Cuicas, creek to 2.6 km N from Plaza Bolívar of the town, MHNLS 22090–22191, 22092 (tadpoles).

Mannophryne leonardoi.— VENEZUELA: Monagas: Caripe, Cueva del Guácharo, MHNLS 1387a–d; Caripe, La Margarita, MHNLS 22332–22336.

Mannophryne molinai.— VENEZUELA: Yaracuy: La Rondona creek, Sierra de Aroa, MHNLS 21535-21537 (paratypes), 21355 (holotype), 22138 (tadpoles), 21338–21339, 21356, 21536-21537, 21540 (paratypes), 21542–21544.

Mannophryne* cf. *molinai.— VENEZUELA: Yaracuy: El Abrigo, Sierra de Aroa, MHNLS 21516–21518.

Mannophryne neblina.— VENEZUELA: Vargas: Hacienda El Limón, Las Llanadas, MHNLS 4955–4957, 4961–4964; Hacienda El Limón, El Aguacatal, MHNLS 22362.

Mannophryne oblitterata.— VENEZUELA: Miranda: Panaquire, El Sapo village, MHNLS 7608; La culebra creek, km 33 of the road Caucagua-Santa Teresa, Guatopo National Park, MHNLS 16793, 16796; creek affluent of Araira river, road Capayita-Los Limones, MHNLS 21799; creek affluent on the right margin of the lagoon of Araira river, MHNLS 21818–21819, 21822 (tadpoles).

Mannophryne orellana.— VENEZUELA: Mérida: near Canaguá, ULABG 504 (cleared and stained); Táchira: road Pregonero-La Trampa, CVULA 7161 (paratype).

Mannophryne trinitatis.— TRINIDAD AND TOBAGO: Trinidad: Arima-Blanchisseuse road, near Asa Wright Nature Center, Arima valley, MHNLS 17461.

Mannophryne trujillensis.— VENEZUELA: Trujillo: Hacienda El Corozal, km 5 of the road Flor de Patria-Boconó, MHNLS 17965–17966, 17969–17970; 1.4 km NE from Sabaneta, MHNLS 22059 (tadpoles); 3.2 km NE from Sabaneta, MHNLS 22063, 22065, 22067.

Mannophryne riveroi.— VENEZUELA: Sucre: trail from the ranger post of Las Melenas to Cerro Humo, Paria peninsula, MHNLS 15740; Las melenas, trail to Cerro humo, Paria peninsula, MHNLS 16433; trail Macuro-Los Chorros (toward Uquire), Paria peninsula, MHNLS 16458; Las Melenas, first creek on the trail to Cerro Humo, Paria peninsula, MHNLS 17456; Las Melenas, Paria peninsula, MHNLS 17910.

Mannophryne speeri.— VENEZUELA: Portuguesa: La Fila, road Chabasquén-Villa Nueva, MHNLS 22606–22607, 22609–22610, 22616 (tadpoles).

Mannophryne urticans.— VENEZUELA: Mérida: La Azulita, CVULA 5967; Río Frío, northwestern slope of of the Cordilllera de Mérida, CVULA 7227 (paratype); Las Maricelas sector, Pan-American highway, MHNLS 21556-21563; La Olinda II, 5 km NNO from La Azulita, MHNLS 21993–21994.

Mannophryne venezuelensis.— VENEZUELA: Sucre: trail Macuro-Los Chorros (toward Uquire), Paria peninsula, MHNLS 16454; Macuro, Paria peninsula, MHNLS 20832–20833.

Mannophryne vulcano.— VENEZUELA: Capital District: Papelón creek, Cerro El Ávila, MHNLS 21772, 21774; Los Venados creek, Cerro El Ávila, MHNLS 21780–21781; Miranda: El Encanto, MHNLS 5809–5810, 5813, 5820–5821; Chacaíto creek, Cerro El Ávila, MHNLS 20694–20695, 20698–20699,Guayabal creek, IVIC, Altos de Pipe, MHNLS 21804, 21808; Vargas: La Conchita, Hacienda El Limón, MHNLS 5130, 5136; creek 2 km NO from El Limón village, road to Los Rastrojos, MHNLS 22346.

Mannophryne yustizi.— VENEZUELA: Lara: road Sanare-Yacambú National Park, ULABG 812 (paratype; skull cleared and stained); Yacambú National Park, CVULA 7928; La Pastora, 11 km SSO from Sanare, MHNLS 8506–8509, 8520–8523; El Blanquito, Yacambú Natinal Park, MHNLS 21280–21282.

Mannophryne* cf. *yustizi.— VENEZUELA: Trujillo: Laguneta sector, Niquitao, MHNLS 22171, 22173-22174, 22176, 22178, 22179 (tadpoles), 22180.

***Mannophryne* sp 1**.— VENEZUELA: Miranda: Urva river, above the waterfall, Tuy river basin, MHNLS 16768–16769, 16784–16785.

***Mannophryne* sp 2**.— VENEZUELA: Guárico: Hacienda El Picachito, eastern versant of Monumento Natural Cerro Platillón, MHNLS 15545–15547.

***Mannophryne* sp 3**.— VENEZUELA: Vargas: Hacienda El Limón, La Cochinera, MHNLS 4463–4464; Hacienda El Limón, Las Conchitas, MHNLS 5134–5135, 5137–5139; Club Oricao, MHNLS 21747–21751,

21752 (tadpoles); creek 2 km NO from El Limón village, road to Los Rastrojos, MHNLS 22347–22348, 22353–2355; Hacienda El Limón, El Aguacatal, 22359–22360.

***Mannophryne* sp 4**.— VENEZUELA: Carabobo: Montalbán, El Peñón creek, near the base camp, El Peñón sector, MHNLS 22205, 22213, 22219; Montalbán, creek near to the base camp, El Marquero sector, MHNLS 22277, 22280; Montalbán, creek in the San Isidro sector, MHNLS 22306.

***Mannophryne* sp**.— VENEZUELA: Trujillo: El Jarillo, old road Trujillo-Boconó, MHNLS 22081–22083.

***Mannophryne* sp**.— VENEZUELA: Miranda: creek affluent to the left margin of Araira river, above Capayita, MHNLS 21823–21824, 21830–21831, 21833.

***Mannophryne* sp**.— VENEZUELA: Cojedes: Fila La Blanquera, Cerro Azul, MHNLS 8169, 8171, 8174–8177, 8239–8242.

***Mannophryne* sp**.— VENEZUELA: Lara: La Olla, Chupa La Flor sector, MHNLS 22585–22590.

Minyobates steyermarki.— VENEZUELA: Amazonas: Cerro Yapacana, MHNLS 15112* (holotype; ex-UPR-M 3399).

Paruwrobates erythromos.— ECUADOR: Santo Domingo de Tsáchilas: Centro Cientifico Río Palenque (CCRP) - km 43 on the road Santo Domimgo-Quevedo-Estero Sherd, QCAZ 389094 (x-rays: https://bioweb.bio/galeria/Foto/Paruwrobates%20erythromos/Rayos%20X/246570), 37750* (https://bioweb.bio/galeria/Fotos/Paruwrobates%20erythromos/Registros%20fotográficos).

“*Phyllobates*” *mandelorum*.— VENEZUELA: Sucre: Elvecia, CM 9133, 9135, 9137, 9140, 9152, 9153, 9158, 9161, 9165.

“*Prostherapis*” *dunni*.— VENEZUELA: Capital District: Above Caracas, FMNH 35987* (holotype), 67379*–67380*, 67385* (paratypes); Coffee finca Los Venados, in Avila range above N. of Caracas, UMMZ 167131* (cleared and stained), 167132*, 167133* (cleared and stained), 167134*.

Ranitomeya toraro.— BRAZIL: Amazonas: Carauari, MCP 13095, 13106–13107; Eirunepé, MCP 13507 (skinned carcass).

Rheobates palmatus.— COLOMBIA: Cundinamarca: Monte Redondo, USNM-H 137777**

Thoropa miliaris.— BRAZIL: Rio de Janeiro: Corõa Grande, Itaguaí, MCP 12204, 12206, 12229–12230.

Appendix 2. Virtual 3D skeleton models from high resolution computed microtomography scans, generated in this study and from Morphosource (https://www.morphosource.org/).

Species	Catalog number	Sex	Projections	Scans (parts)	Voltage (kV)	Current (µA)	Voxel size (µm)	Source
Adelphobates galactonotus	MCP 2252	female	2400	2	40	50	13.049783	This study
Allobates femoralis	MCP 13869	female	2400	2	40	50	13.049783	This study
Allobates juami	MCP 13288	female	1200	1	40	50	13.049783	This study
Allobates olfersioides	MCP 12698	female	1200	1	40	50	13.049783	This study
Allobates pittieri	MHNLS 21488	female	2400	2	40	50	13.049783	This study
Allobates pittieri	MHNLS 21490	male	1043	1	40	50	13.049783	This study
Ameerega trivittata	MCP 10079	male	3600	3	40	50	13.049783	This study
Anomaloglossus rufulus	MHNLS 20245	male	2400	2	40	50	13.049783	This study
Anomaloglossus rufulus	MHNLS 20609	male	1200	1	40	50	13.049783	This study
Anomaloglossus wothuja	MHNLS 19992	female	2400	2	40	50	13.049783	This study
Aromobates alboguttatus	CVULA 282	male	1142	1	40	50	12.345439	This study
Aromobates alboguttatus	CVULA 1448	female	2400	2	40	50	13.050000	This study
Aromobates alboguttatus	CVULA 3238	female	2400	2	40	50	13.049783	This study
Aromobates cannatellai	MHNLS 22625	female	2400	2	40	50	13.049783	This study
Aromobates cannatellai	MHNLS 22626	male	2400	2	40	50	13.049783	This study
Aromobates capurinensis	CVULA 5920	female	2400	2	40	50	13.050000	This study
Aromobates capurinensis	CVULA 5923	male	2284	2	40	50	13.049783	This study
Aromobates duranti	CVULA 846	female	2400	2	40	50	13.050000	This study
Aromobates duranti	CVULA 853	male	1200	1	40	50	13.049783	This study
Aromobates haydeeae	CVULA 6042	male	1200	1	40	50	13.049783	This study
Aromobates haydeeae	CVULA 6047	female	2400	2	40	50	13.049783	This study
Aromobates inflexus	MHNLS 4320	female	2400	2	40	50	13.049783	This study

Species	Catalog number	Sex	Projections	Scans (parts)	Voltage (kV)	Current (µA)	Voxel size (µm)	Source
Aromobates inflexus	MHNLS 4321	female	2400	2	40	50	13.049783	This study
Aromobates leopardalis	CVULA 3084	female	2400	2	40	50	13.049783	This study
Aromobates leopardalis	CVULA 3085	female	2400	2	40	50	13.049780	This study
Aromobates leopardalis	CVULA 5886	male	3600	3	40	50	13.050000	This study
Aromobates mayorgai	MHNLS 21983	male	1142	1	40	50	11.992423	This study
Aromobates mayorgai	MHNLS 21992	female	1090	1	40	50	14.108832	This study
Aromobates mayorgai	MHNLS 22002	female	2400	2	40	50	13.049783	This study
Aromobates mayorgai	MHNLS 22004	Male	1200	1	40	50	13.049783	This study
Aromobates mayorgai	MHNLS 22030	female	2400	2	40	50	13.049783	This study
Aromobates meridensis	CVULA 5981	male	2400	2	40	50	13.049783	This study
Aromobates meridensis	MHNLS 22019	female	2400	2	40	50	13.049783	This study
Aromobates molinarii	CVULA 1876	female	2400	2	40	50	13.049783	This study
Aromobates molinarii	CVULA 1877	female	2400	2	40	50	13.049783	This study
Aromobates nocturnus	ULABG 2223	male	2400	2	40	50	22.925796	This study
Aromobates ornatissimus	ULABG 4976	female	2400	2	40	50	13.050000	This study
Aromobates orostoma	CVULA 3325	female	2400	2	40	50	11.992423	This study
Aromobates orostoma	CVULA 3327	female	2400	2	40	50	13.049783	This study
Aromobates saltuensis	ULABG 4981	female	2400	2	40	50	13.049783	This study
Aromobates sp. (aff. *saltuensis* 4)	T10-1	female	1920	2	40	50	13.049783	This study
Aromobates sp. (aff. *saltuensis* 4)	T10-2	male	1200	1	40	50	13.049783	This study
Aromobates sp. (aff. *saltuensis* 2)	LOA 124	male	1200	1	40	50	13.049783	This study
Aromobates sp. (aff. *saltuensis* 3)	AOH	? (juvenile)	3600	3	40	50	6.349228	This study
Aromobates serranus	MHNLS 7098	female	2400	2	40	50	13.049783	This study
Aromobates serranus	MHNLS 7099	male	2400	2	40	50	13.049783	This study
Aromobates tokuko	MHNLS 18520	male	1200	1	40	50	13.402799	This study

Species	Catalog number	Sex	Projections	Scans (parts)	Voltage (kV)	Current (µA)	Voxel size (µm)	Source
Aromobates tokuko	MHNLS 18523	female	2400	2	40	50	13.050000	This study
Aromobates walterarpi	ULABG 1577	female	2400	2	40	50	13.050000	This study
Aromobates zippeli	MHNLS 22052	female	2400	2	40	55	13.050000	This study
Aromobates zippeli	MHNLS 22053	male	1200	1	40	50	13.049783	This study
Aromobates sp. 1	MHNLS 21528	male	2400	2	40	50	13.049783	This study
Aromobates sp. 1	MHNLS 22128	male	2400	2	40	50	13.049783	This study
Aromobates sp. 1	MZUC 2206	male	2400	2	40	50	13.049783	This study
Aromobates cf. sp. 1	MHNLS 21285	male	1200	1	40	50	13.049783	This study
Aromobates cf. sp. 1	MHNLS 21286	male	2400	2	40	50	13.049783	This study
Aromobates sp. 2	MHNLS 22191	? (juvenile)	2400	2	40	50	6.349228	This study
Aromobates sp. 3	CVULA 239	female	2400	2	40	50	13.049783	This study
Aromobates sp.	CVULA 886	female	3600	3	40	50	13.050000	This study
"Colostethus" caribe	MHNLS 17463	female	1200	1	40	50	13.049783	This study
Hyloxalus cepedai	AFJ 49	female	1920	2	40	50	8.112621	This study
Leucostethus brachistriatus	MCP 11516	female	2400	2	40	50	13.049783	This study
Mannophryne caquetio	MHNLS 21220	female	2400	2	40	50	13.049783	This study
Mannophryne collaris	MHNLS 21598	female	3600	3	40	50	13.050000	This study
Mannophryne cordilleriana	MHNLS 21603	female	2400	2	40	50	13.049783	This study
Mannophryne herminae	MHNLS 22111	female	2400	2	40	50	13.049783	This study
Mannophryne lamarcai	MHNLS 22091	female	2400	2	40	50	13.049783	This study
Mannophryne larandina	MHNLS 22599	male	2400	2	40	50	13.049783	This study
Mannophryne larandina	MHNLS 22600	female	2400	2	40	50	13.049783	This study
Mannophryne leonardoi	MHNLS 1387c	female	1200	1	40	50	13.049783	This study
Mannophryne molinai	MHNLS 21337	female	2400	2	40	50	13.049783	This study
Mannophryne neblina	MHNLS 4956	female	3600	3	40	50	13.049783	This study

Species	Catalog number	Sex	Projections	Scans (parts)	Voltage (kV)	Current (µA)	Voxel size (µm)	Source
Mannophryne neblina	MHNLS 22362	female	1920	2	40	50	13.049783	This study
Mannophryne oblitterata	MHNLS 21799	female	3600	3	40	50	13.049783	This study
Mannophryne orellana	CVULA 7161	male	2400	2	40	50	13.050000	This study
Mannophryne riveroi	MHNLS 17910	female	1200	1	40	50	23.983156	This study
Mannophryne sp. (*yustizi* complex)	MHNLS 22081	female	2400	2	40	50	13.049783	This study
Mannophryne cf. *yustizi*	MHNLS 22174	female	1200	1	40	50	13.049783	This study
Mannophryne sp. 1	MHNLS 16768	female	1200	1	40	50	13.049783	This study
Mannophryne sp. (cf. vulcano)	MHNLS 21824	male	2400	2	40	50	13.049783	This study
Mannophryne sp. (cf. vulcano)	MHNLS 21831	female	2400	2	40	50	12.345439	This study
Mannophryne sp. 2	MHNLS 15547	male	1200	1	40	50	13.049783	This study
Mannophryne sp. 3	MHNLS 22355	female	2400	2	40	50	13.049783	This study
Mannophryne sp. 4	MHNLS 22306	female	2400	2	40	50	13.049783	This study
Mannophryne sp. (aff. *herminae*)	MHNLS 8242	female	2400	2	40	50	13.402799	This study
Mannophryne sp. (aff. *yustizi*)	MHNLS 22588	female	2400	2	40	50	13.049783	This study
Mannophryne sp. (aff. *yustizi*)	MHNLS 22589	female	2400	2	40	50	13.049783	This study
Mannophryne speeri	MHNLS 22607	male	1200	1	40	50	13.049783	This study
Mannophryne speeri	MHNLS 22610	female	1043	1	40	50	13.049783	This study
Mannophryne trinitatis	MHNLS 17461	female	2400	2	40	50	13.050000	This study
Mannophryne trujillensis	MHNLS 22063	male	2400	2	40	50	13.049783	This study
Mannophryne trujillensis	MHNLS 22067	female	2400	2	40	50	13.049783	This study
Mannophryne urticans	MHNLS 21563	female	2400	2	40	50	13.049783	This study
Mannophryne venezuelensis	MHNLS 16454	male	2400	2	40	50	13.049783	This study
Mannophryne vulcano	MHNLS 20695	male	2400	2	40	50	13.049783	This study
Mannophryne vulcano	MHNLS 21780	female	2400	2	40	50	13.049783	This study
Mannophryne yustizi	MHNLS 7928	female	2400	2	40	50	13.049783	This study

Species	Catalog number	Sex	Projections	Scans (parts)	Voltage (kV)	Current (µA)	Voxel size (µm)	Source
Mannophryne yustizi	MHNLS 8522	female	2400	2	40	50	13.049783	This study
Oophaga pumilio	UF 80874	?	-	-	100	200	2.032547	Morphosource (id: 15470)
Phyllobates bicolor	UF 71742	?	1600	-	100	200	3.305334	Morphosource (id: 15469)
"Phyllobates" mandelorum	CM 9137	female	2400	2	40	55	13.050000	This study
"Phyllobates" mandelorum	CM 9161	female	2400	2	40	50	13.049783	This study
"Phyllobates" mandelorum	CM 9165	male	1200	1	40	50	13.049783	This study
Ranitomeya toraro	MCP 13107	?	1200	1	40	50	13.049783	This study
Rheobates palmatus	USNM-H 137777	?	2200	2	100	200	2.42504	Morphosource (id: 18705)
Thoropa miliaris	MCP 12229	male	2400	2	40	50	13.049783	This study
Thoropa miliaris	CM 68357	?	1200	1	140	250	5.734944	Morphosource (id: 13923)

Appendix 3. Call recordings analyzed in this study for coding bioacoustical characters. Recordings with prefix ML in the code were downloaded from Macaulay Library (https://www.macaulaylibrary.org/).

Species	Locality	Recording code	Author
Allobates humilis	Venezuela: Trujillo: El Jarillo, old road Trujillo-Boconó	LS110068	Fernando J.M. Rojas-Runjaic
Aromobates cannatellai	Venezuela: Táchira: Uribante, Parque Cascada de la Escalera, Mesa de Pérez	-	César Barrio-Amorós
Aromobates mayorgai	Venezuela: Mérida: La Olinda II, 5 km NNO from La Azulita	LS110057	Fernando J.M. Rojas-Runjaic
Aromobates mayorgai	Venezuela: Mérida: La Olinda II, 5 km NNO from La Azulita	LS110058	Fernando J.M. Rojas-Runjaic
Aromobates mayorgai	Venezuela: Mérida: La Olinda II, 5 km NNO from La Azulita	LS110059	Fernando J.M. Rojas-Runjaic
Aromobates mayorgai	Venezuela: Mérida: road between Las Adjuntas and La Osa	LS110060	Fernando J.M. Rojas-Runjaic
Aromobates mayorgai	Venezuela: Mérida: road between Las Adjuntas and La Osa	LS110061	Fernando J.M. Rojas-Runjaic
Aromobates mayorgai	Venezuela: Mérida: 1.8 km N from La Trampa	LS110064	Fernando J.M. Rojas-Runjaic
Aromobates meridensis	Venezuela: Mérida: La Osa, road La Azulita-Lagunillas	LS110063	Fernando J.M. Rojas-Runjaic
Aromobates meridensis	Venezuela: Merida: Altos de San Luis, near La Azulita	-	César Barrio-Amorós
Aromobates saltuensis	Venezuela: Táchira: Quebrada Guacharaquita, road from Sabana Grande to La Grita	Santi 1-V3-04	Santiago Castroviejo-Fisher
Aromobates saltuensis	Venezuela: Táchira: road between San Félix and San Juan de Colón	-	César Barrio-Amorós
Aromobates zippeli	Venezuela: Mérida: Troncal 7, near Mucuchíes	LS110065	Fernando J.M. Rojas-Runjaic
Aromobates zippeli	Venezuela: Mérida: Troncal 7, near Mucuchíes	LS110066	Fernando J.M. Rojas-Runjaic
Aromobates sp. 1	Venezuela: Yaracuy: Sierra de Aroa, Pico El Tigre	LS110072	Fernando J.M. Rojas-Runjaic
Aromobates cf. sp. 1	Venezuela: Yaracuy: Sierra de Aroa, Quebrada La Rondona	LS110024	Fernando J.M. Rojas-Runjaic
Mannophryne collaris	Venezuela: Mérida: 2.6 WSW from El Chamita	LS110041	Fernando J.M. Rojas-Runjaic
Mannophryne collaris	Venezuela: Mérida: El Estanquillo	-	César Barrio-Amorós
Mannophryne cordilleriana	Venezuela: Barinas: El Cacao, Quebrada Los Panches	LS110044	Fernando J.M. Rojas-Runjaic
Mannophryne cordilleriana	Venezuela: Barinas: El Cacao, Quebrada Los Panches	LS110045	Fernando J.M. Rojas-Runjaic
Mannophryne cordilleriana	Venezuela: Barinas: El Cacao, Quebrada La Toma	LS110046	Fernando J.M. Rojas-Runjaic
Mannophryne cordilleriana	Venezuela: Barinas: Potrerito	LS110042	Fernando J.M. Rojas-Runjaic

Species	Locality	Recording code	Author
Mannophryne cordilleriana	Venezuela: Barinas: Potrerito	LS110043	Fernando J.M. Rojas-Runjaic
Mannophryne cordilleriana	Venezuela: Barinas: Agua Blanca sector, road to Mucuposada Los Alcaravanes	-	César Barrio-Amorós
Mannophryne herminae	Venezuela: Carabobo: stream tributary of Río San Esteban	LS110071	Fernando J.M. Rojas-Runjaic
Mannophryne herminae	Venezuela: Aragua: near Estación Biológica Rancho Grande	-	Andreas Hertz
Mannophryne herminae	Venezuela: Aragua: Estación Biológica Rancho Grande	ML 194496	Stephen R. Edwards
Mannophryne herminae	Venezuela: Aragua: Estación Biológica Rancho Grande	ML 194497	Stephen R. Edwards
Mannophryne herminae	Venezuela: Aragua: Estación Biológica Rancho Grande	ML 194498	Stephen R. Edwards
Mannophryne lamarcai	Venezuela: Trujillo: Cuicas, stream to 1.8 km N of the town	LS110070	Fernando J.M. Rojas-Runjaic
Mannophryne lamarcai	Venezuela: Zulia: Serranía de Ziruma, vía a El Jordán	AC-AS	Arlene Cardozo Urdaneta
Mannophryne larandina	Venezuela: Lara: road between Hato Arriba and Barbacoas	-	Enrique La Marca
Mannophryne leonardoi	Venezuela: Monagas: Cueva El Guácharo	-	Darwin Rangel
Mannophryne molinai	Venezuela: Yaracuy: Sierra de Aroa, Quebrada La Rondona	LS110025	Fernando J.M. Rojas-Runjaic
Mannophryne cf. *molinai*	Venezuela: Yaracuy: Guayabito Recreational Park	LS110013	Fernando J.M. Rojas-Runjaic
Mannophryne cf. *molinai*	Venezuela: Yaracuy: Guayabito Recreational Park	LS110014	Fernando J.M. Rojas-Runjaic
Mannophryne cf. *molinai*	Venezuela: Yaracuy: Cerro Zapatero	-	Andreas Hertz
Mannophryne oblitterata	Venezuela: Miranda: stream on the right bank of the Araira river	LS110051	Fernando J.M. Rojas-Runjaic
Mannophryne oblitterata	Venezuela: Miranda: stream tributary of Araira river	LS110054	Fernando J.M. Rojas-Runjaic
Mannophryne oblitterata	Venezuela: Miranda: stream on the right bank of the Araira river	LS110056	Fernando J.M. Rojas-Runjaic
Mannophryne orellana	Venezuela: Táchira: stream along the road from Pregonero to La Trampa	-	César Barrio-Amorós
Mannophryne riveroi	Venezuela: Sucre: 10.0 km N of Macuro	ML 194488	Stephen R. Edwards
Mannophryne riveroi	Venezuela: Sucre: 10.0 km N of Macuro	ML 194489	Stephen R. Edwards
Mannophryne riveroi	Venezuela: Sucre: 10.0 km N of Macuro	ML 194490	Stephen R. Edwards
Mannophryne riveroi	Venezuela: Sucre: 10.0 km N of Macuro	ML 194491	Stephen R. Edwards
Mannophryne riveroi	Venezuela: Sucre: 10.0 km N of Macuro	ML 194492	Stephen R. Edwards
Mannophryne riveroi	Venezuela: Sucre: 10.0 km N of Macuro	ML 194493	Stephen R. Edwards
Mannophryne riveroi	Venezuela: Sucre: 10.0 km N of Macuro	ML 194494	Stephen R. Edwards

Species	Locality	Recording code	Author
Mannophryne urticans	Venezuela: Mérida: Las Maricelas	LS110038	Fernando J.M. Rojas-Runjaic
Mannophryne urticans	Venezuela: Mérida: Las Maricelas	LS110039	Fernando J.M. Rojas-Runjaic
Mannophryne urticans	Venezuela: Mérida: Las Maricelas	LS110040	Fernando J.M. Rojas-Runjaic
Mannophryne urticans	Venezuela: Mérida: Río Frío	-	César Barrio-Amorós
Mannophryne venezuelensis	Venezuela: Sucre: 10.0 km N of Macuro	ML 194488	Stephen R. Edwards
Mannophryne venezuelensis	Venezuela: Sucre: 10.0 km N of Macuro	ML 194489	Stephen R. Edwards
Mannophryne venezuelensis	Venezuela: Sucre: 10.0 km N of Macuro	ML 194490	Stephen R. Edwards
Mannophryne venezuelensis	Venezuela: Sucre: 10.0 km N of Macuro	ML 194491	Stephen R. Edwards
Mannophryne venezuelensis	Venezuela: Sucre: 10.0 km N of Macuro	ML 194492	Stephen R. Edwards
Mannophryne venezuelensis	Venezuela: Sucre: 10.0 km N of Macuro	ML 194493	Stephen R. Edwards
Mannophryne venezuelensis	Venezuela: Sucre: 10.0 km N of Macuro	ML 194494	Stephen R. Edwards
Mannophryne venezuelensis	Venezuela: Sucre: 10.0 km N of Macuro	ML 194495	Stephen R. Edwards
Mannophryne vulcano	Venezuela: Miranda: Sabaneta de Cañaveral, Santa María Ecological Farm	LS110008	Fernando J.M. Rojas-Runjaic
Mannophryne vulcano	Venezuela: Miranda: Sabaneta de Cañaveral, Santa María Ecological Farm	LS110009	Fernando J.M. Rojas-Runjaic
Mannophryne vulcano	Venezuela: Miranda: Sabaneta de Cañaveral, Santa María Ecological Farm	LS110010	Fernando J.M. Rojas-Runjaic
Mannophryne vulcano	Venezuela: Miranda: Altos de Pipe, IVIC, Quebrada Guayabal	LS110048	Fernando J.M. Rojas-Runjaic
Mannophryne vulcano	Venezuela: Miranda: Altos de Pipe, IVIC, Quebrada Guayabal	LS110049	Fernando J.M. Rojas-Runjaic
Mannophryne vulcano	Venezuela: Miranda: Cerro El Ávila, Quebrada Papelón	LS110047	Fernando J.M. Rojas-Runjaic
Mannophryne vulcano	Venezuela: Miranda: Caracas, Quebrada Caurimare	LS110073	Fernando J.M. Rojas-Runjaic
Mannophryne vulcano	Venezuela: Miranda: Caracas, Quebrada Caurimare	LS110074	Fernando J.M. Rojas-Runjaic
Mannophryne vulcano	Venezuela: Miranda: Northern slope of Cerro El Volcán	-	César Barrio-Amorós
Mannophryne vulcano	Venezuela: Miranda: Caracas, El Ávila	-	César Barrio-Amorós
Mannophrye cf. *vulcano*	Venezuela: Vargas: 3.0 km S of El Limón, road to Colonia Tovar	ML 194499	Stephen R. Edwards
Mannophrye cf. *vulcano*	Venezuela: Vargas: 3.0 km S of El Limón, road to Colonia Tovar	ML 194500	Stephen R. Edwards
Mannophrye cf. *vulcano*	Venezuela: Vargas: 3.0 km S of El Limón, road to Colonia Tovar	ML 194501	Stephen R. Edwards
Mannophryne yustizi	Venezuela: Lara: El Blanquito	-	Enrique La Marca

Species	Locality	Recording code	Author
Mannophryne cf. *yustizi*	Venezuela: Trujillo: Niquitao, Laguneta sector	LS110076	Fernando J.M. Rojas-Runjaic
Mannophryne sp. (*yustizi* complex)	Venezuela: Trujillo: El Jarillo, old road Trujillo-Boconó	LS110069	Fernando J.M. Rojas-Runjaic
Mannophryne sp. (*yustizi* complex)	Venezuela: Trujillo: 3.0 km NE of Boconó	ML 194505	Stephen R. Edwards
Mannophryne sp. (*yustizi* complex)	Venezuela: Trujillo: 3.0 km NE of Boconó	ML 194506	Stephen R. Edwards
Mannophyrne sp. (cf. *vulcano*)	Venezuela: Miranda: stream tributary of Araira river	LS110054	Fernando J.M. Rojas-Runjaic
Mannophryne sp. (cf. *vulcano*)	Venezuela: Miranda: stream tributary of Araira river	LS110050	Fernando J.M. Rojas-Runjaic
Mannophryne sp. (cf. *vulcano*)	Venezuela: Miranda: stream tributary of Araira river	LS110052	Fernando J.M. Rojas-Runjaic
Mannophryne sp. nov. 2	Venezuela: Guárico: Cerro Platillón	Santi 8-V3-04	Santiago Castroviejo-Fisher
Mannophryne sp. nov. 2	Venezuela: Guárico: Cerro Platillón	Santi 9-V3-04	Santiago Castroviejo-Fisher
Mannophryne sp. nov. 2	Venezuela: Guárico: Cerro Platillón	Santi 10-V3-04	Santiago Castroviejo-Fisher
Mannophryne sp. nov. 2	Venezuela: Guárico: Cerro Platillón	-	Andreas Hertz
Mannophryne sp. nov. 2	Venezuela: Guárico: Santa Rosa	-	Andreas Hertz
Mannophryne sp. nov. 3	Venezuela: Vargas: Los Rastrojos, road to Puerto Cruz	LS110077	Fernando J.M. Rojas-Runjaic
Mannophryne sp. nov. 3	Venezuela: Vargas: El Aguacatal, road to Puerto Cruz	LS110078	Fernando J.M. Rojas-Runjaic
Mannophryne sp. nov. 3	Venezuela: Vargas: 3.0 km S of El Limón, road to Colonia Tovar	ML 194502	Stephen R. Edwards
Mannophryne sp. nov. 3	Venezuela: Vargas: 3.0 km S of El Limón, road to Colonia Tovar	ML 194503	Stephen R. Edwards
Mannophryne sp. nov. 3	Venezuela: Vargas: 3.0 km S of El Limón, road to Colonia Tovar	ML 194504	Stephen R. Edwards
Mannophryne sp. nov. 4	Venezuela: Carabobo: Montalbán, El Peñón	-	Andrés E. Osorio, Marlon Fochler
Mannophryne sp. nov. 6	Venezuela: Lara: La Olla	180311-001	Rafael Morillo
Mannophryne sp. nov. 6	Venezuela: Lara: La Olla	180311-002	Rafael Morillo
Mannophryne sp. nov. 6	Venezuela: Lara: La Olla	180315-001	Rafael Morillo

Appendix 4. Terminals, voucher codes, and GenBank accession numbers of DNA sequences used in this study. Acronyms follow Frost (2019). New sequences in bold.

Species	Voucher	Locality	Cyt-b	tRNA-Phe	12S	tRNA-Val
Aromobates cannatellai	CVULA 8325	Venezuela: Táchira: Uribante, Parque Cascada de la Escalera, Mesa de Pérez (8.003100N, -71.731600W; 1,140 m)	-	-	JX035995	JX035995
Aromobates cannatellai	MHNLS 22625	Venezuela: Táchira: Parque Las Escaleras, near Pregonero (8.003103N, -71.731533W; 1,178 m)	-	-	-	-
Aromobates cannatellai	MHNLS 22626	Venezuela: Táchira: Parque Las Escaleras, near Pregonero (8.003103N, -71.731533W; 1,178 m)	-	-	-	-
Aromobates cannatellai	MHNLS 22627	Venezuela: Táchira: Parque Las Escaleras, near Pregonero (8.003103N, -71.731533W; 1,178 m)	-	-	-	-
Aromobates cannatellai	MHNLS 22629	Venezuela: Táchira: Parque Las Escaleras, near Pregonero (8.003103N, -71.731533W; 1,178 m)	-	-	-	-
Aromobates sp. (aff. *cannatellai*)	Asa4	Venezuela: Táchira: Hacienda El Progreso, between Río Chiquito and San Vicente de la Revancha (7.552292N, -72.319539W; 1,471 m)	-	-	-	-
Aromobates sp. (aff. *cannatellai*)	MUJ 3726	Colombia: Boyacá: Cubará, Fátima, Quebrada Gralanday (6.800000N, -72.166667W; 1,576 m)	DQ502705	-	DQ502274	DQ502274
Aromobates sp. (aff. *cannatellai*)	Tama14	Colombia: Norte de Santander: southern slope of Tamá massif (7.161127N, -72.177713W; 760)	-	-	-	-
Aromobates ericksonae	TNHC 5540	Venezuela: Merida: Santa Cruz de Mora, via Los Ranchos (8.426500N, -71.628100W; 861 m)	HQ290533	-	HQ290953	HQ290953
Aromobates ericksonae	CVULA 7180	Venezuela: Mérida: Río Frío (8.850000N, -71.283300W; 1,105 m)	-	-	JX035993	JX035993
Aromobates ericksonae	CVULA8379	Venezuela: Mérida: La Olinda (8.734678N, -71.448667W; 916 m)	-	-	JX035994	JX035994
Aromobates ericksonae	ULABG 7776	Venezuela: Mérida: Zea (8.375457N, -71.781410W; 925 m)	-	-	-	-
Aromobates mayorgai	MHNLS 21981	Venezuela: Mérida: La Olinda II, 5 km NNO from La Azulita (8.751944N, -71.472028W; 1,206 m)	-	-	-	-
Aromobates mayorgai	MHNLS 21982	Venezuela: Mérida: La Olinda II, 5 km NNO from La Azulita (8.751944N, -71.472028W; 1,206 m)	-	-	-	-
Aromobates mayorgai	MHNLS 21983	Venezuela: Mérida: La Olinda II, 5 km NNO from La Azulita (8.751944N, -71.472028W; 1,206 m)	-	-	-	-
Aromobates mayorgai	MHNLS 21984	Venezuela: Mérida: La Olinda II, 5 km NNO from La Azulita (8.751944N, -71.472028W; 1,206 m)	-	-	-	-
Aromobates mayorgai	MHNLS 22002	Venezuela: Mérida: road between Las Adjuntas and La Osa (8.649083N, -71.479472W; 1,551 m)	-	-	-	-
Aromobates mayorgai	MHNLS 22003	Venezuela: Mérida: road between Las Adjuntas and La Osa (8.649083N, -71.479472W; 1,551 m)	**Ama2**	**Ama2**	**Ama2**	-
Aromobates mayorgai	MHNLS 22005	Venezuela: Mérida: road between Las Adjuntas and La Osa (8.649083N, -71.479472W; 1,551 m)	-	-	-	-

Species	Voucher	Locality	Cyt-b	tRNA-Phe	12S	tRNA-Val
Aromobates mayorgai	MHNLS 22030	Venezuela: Mérida: 1.8 km N from La Trampa (8.556861N, -71.455778W; 1,701 m)	-	-	-	-
Aromobates mayorgai	MHNLS 22031	Venezuela: Mérida: 1.8 km N from La Trampa (8.556861N, -71.455778W; 1,701 m)	-	-	-	-
Aromobates mayorgai	MHNLS22032	Venezuela: Mérida: 1.8 km N from La Trampa (8.556861N, -71.455778W; 1,701 m)	-	-	-	-
Aromobates mayorgai	MHNLS 22033	Venezuela: Mérida: 1.8 km N from La Trampa (8.556861N, -71.455778W; 1,701 m)	-	-	-	-
Aromobates meridensis	CVULA7399	Venezuela: Merida: Altos de San Luis, near La Azulita (8.690367N, -71.493396W; 1,555 m)	-	-	JX035992	JX035992
Aromobates meridensis	MHNLS22016	Venezuela: Mérida: La Osa, road La Azulita-Lagunillas (8.630917N, -71.475500W; 1,832 m)	**Ame1**	-	-	-
Aromobates meridensis	MHNLS 22017	Venezuela: Mérida: La Osa, road La Azulita-Lagunillas (8.630917N, -71.475500W; 1,832 m)	-	-	-	-
Aromobates meridensis	MHNLS 22018	Venezuela: Mérida: La Osa, road La Azulita-Lagunillas (8.630917N, -71.475500W; 1,832 m)	-	-	-	-
Aromobates meridensis	MHNLS 22019	Venezuela: Mérida: La Osa, road La Azulita-Lagunillas (8.630917N, -71.475500W; 1,832 m)	-	-	-	-
Aromobates molinarii	ULABG 4497	Venezuela: Mérida: Las Playitas, near Bailadores (8.266337N, -71.843621W; 2,270 m)	-	-	AY263216	-
Aromobates molinarii	ULABG sn1	Venezuela: Mérida: Las Playitas, near Bailadores (8.266337N, -71.843621W; 2,270 m)	-	-	-	-
Aromobates molinarii	ULABG sn2	Venezuela: Mérida: Las Playitas, near Bailadores (8.266337N, -71.843621W; 2,270 m)	-	-	-	-
Aromobates molinarii	ULABG sn3	Venezuela: Mérida: Las Playitas, near Bailadores (8.266337N, -71.843621W; 2,270 m)	-	-	-	-
Aromobates nocturnus	AMNHA 130041	Venezuela:Trujillo: About 2 km ESE Agua de Obispos (9.693627N, -70.083038W; 2,280 m)	DQ502590	-	DQ502154	DQ502154
Aromobates nocturnus	AMNHA 130042	Venezuela:Trujillo: About 2 km ESE Agua de Obispos (9.693627N, -70.083038W; 2,280 m)	DQ502592	-	DQ502156	DQ502156
Aromobates ornatissimus	ULABG 4445	Venezuela: Trujillo: Agua de Obispos (9.801235N, -70.150709W; 1,138 m)	-	-	-	-
Aromobates ornatissimus	CVULA 8351	Venezuela: Trujillo: Carache, Las Palmas (9.696389N, -70.140000W; 2,304 m)	-	JN584174	JN584174	JN584174
Aromobates ornatissimus	WES 626	Venezuela: Estado Trujillo: road Humocaro Bajo-Agua de Obispos (2,400 m)	DQ502674	-	DQ502242	DQ502242
Aromobates saltuensis	ULABG 4981	Venezuela: Táchira: La Quintera, 11 km SSE from La Fría (8.126667N, -72.210556W; 659 m)	-	-	-	-
Aromobates saltuensis	TNHC 5541	Venezuela: Táchira: road between San Félix and San Juan de Colón (8.073600N, -72.229300W; 727 m)	HQ290548	-	HQ290970	HQ290970
Aromobates saltuensis	ULABG AGu1	Venezuela: Táchira: Quebrada Guacharaquita, road from Sabana Grande to La Grita (8.167444N, -71.978944W; 1,706 m)	-	-	-	-

Species	Voucher	Locality	Cyt-b	tRNA-Phe	12S	tRNA-Val
Aromobates saltuensis	MHNLS 17233	Venezuela: Táchira: Quebrada Guacharaquita, road from Sabana Grande to La Grita (8.167444N, -71.978944W; 1,706 m)	**Asa5**	**Asa5**	**Asa5**	-
Aromobates sp. (aff. *saltuensis* 1)	CVULA 8321	Venezuela: Táchira: El Tamá National Park, Río Negro (7.578700N, -72.179000; 491 m)	-	-	JX035996	JX035996
Aromobates sp. (aff. *saltuensis* 1)	MHNLS 22498	Venezuela: Táchira: Hacienda El Progreso, between Río Chiquito and San Vicente de la Revancha (7.547131N, -72.317769W; 1,540 m)	**Asa3**	**Asa3**	**Asa3**	-
Aromobates sp. (aff. *saltuensis* 3)	AOH	Colombia: Norte de Santander: Bochalema (7.606277N, -72.656150W; 1,185 m)	**ACo1**	-	-	-
Aromobates sp. (aff. *saltuensis* 2)	LOA 124	Colombia: Norte de Santander: Finca El Diamante, UFPS (7.564758N, -72.625766W; 1,300 m)	**ACo2**	-	-	-
Aromobates sp. (aff. *saltuensis* 4)	T10_1	Colombia: Norte de Santander: La Garita (7.746989N, -72.569343W; 681 m)	-	-	-	-
Aromobates sp. (aff. *saltuensis* 4)	T10_2	Colombia: Norte de Santander: La Garita (7.746989N, -72.569343W; 681 m)	-	-	-	-
Aromobates tokuko	MHNLS 18478	Venezuela: Zulia: Sierra de Perijá, Río Tokuko, near Ipika (9.881667N, -72.859167W; 558 m)	**Ato1**	**Ato1**	**Ato1**	-
Aromobates tokuko	MHNLS 18483	Venezuela: Zulia: Sierra de Perijá, Río Tokuko, near Ipika (9.881667N, -72.859167W; 558 m)	-	-	-	-
Aromobates tokuko	MHNLS 18493	Venezuela: Zulia: Sierra de Perijá, Río Tokuko, near Ipika (9.881667N, -72.859167W; 558 m)	-	-	-	-
Aromobates tokuko	MHNLS 18566	Venezuela: Zulia: Sierra de Perijá, Río Tokuko basin, Kiriponsa (9.862848N, -72.891369W; 1,005 m)	-	-	-	-
Aromobates zippeli	MHNLS 22042	Venezuela: Mérida: Troncal 7, near Mucuchíes (8.732833N, -70.953444W; 2,708 m)	-	**Azi1**	**Azi1**	-
Aromobates zippeli	MHNLS 22043	Venezuela: Mérida: Troncal 7, near Mucuchíes (8.732833N, -70.953444W; 2,708 m)	-	-	-	-
Aromobates zippeli	MHNLS 22044	Venezuela: Mérida: Troncal 7, near Mucuchíes (8.732833N, -70.953444W; 2,708 m)	-	-	-	-
Aromobates zippeli	MHNLS 22045	Venezuela: Mérida: Troncal 7, near Mucuchíes (8.732833N, -70.953444W; 2,708 m)	-	-	-	-
Aromobates zippeli	MIZA 310	Venezuela: Mérida: Troncal 7, near Mucuchíes (8.732833N, -70.953444W; 2,708 m)	-	-	-	-
Aromobates zippeli	MIZA 311	Venezuela: Mérida: Troncal 7, near Mucuchíes (8.732833N, -70.953444W; 2,708 m)	-	-	-	-
Aromobates zippeli	MIZA 312	Venezuela: Mérida: Troncal 7, near Mucuchíes (8.732833N, -70.953444W; 2,708 m)	-	-	-	-
Aromobates zippeli	ULABG 4496	Venezuela: Mérida: Troncal 7, near Mucuchíes (8.732833N, -70.953444W; 2,708 m)	-	-	-	-
Aromobates sp. 1	MHNLS 21506	Venezuela: Yaracuy: Sierra de Aroa, Pico El Tigre (10.404306N, -68.800306W; 1,948 m)	**ATi1**	**ATi1**	**ATi1**	-
Aromobates sp. 1	MHNLS 21507	Venezuela: Yaracuy: Sierra de Aroa, Pico El Tigre (10.404306N, -68.800306W; 1,948 m)	-	-	-	-

Species	Voucher	Locality	Cyt-b	tRNA-Phe	12S	tRNA-Val
Aromobates sp. 1	MHNLS 21508	Venezuela: Yaracuy: Sierra de Aroa, Pico El Tigre (10.404306N, -68.800306W; 1,948 m)	-	-	-	-
Aromobates sp. 1	MHNLS 22127	Venezuela: Yaracuy: Sierra de Aroa, Pico El Tigre (10.404306N, -68.800306W; 1,948 m)	-	-	-	-
Aromobates sp. 1	MHNLS 22128	Venezuela: Yaracuy: Sierra de Aroa, Pico El Tigre (10.404306N, -68.800306W; 1,948 m)	-	-	-	-
Aromobates cf. sp. 1	MHNLS 21333	Venezuela: Yaracuy: Sierra de Aroa, Quebrada La Rondona (10.324444N, -68.873333W; 1,180 m)	-	-	-	-
Aromobates cf. sp. 1	MHNLS 21334	Venezuela: Yaracuy: Sierra de Aroa, Quebrada La Rondona (10.324444N, -68.873333W; 1,180 m)	-	-	-	-
Aromobates cf. sp. 1	MHNLS 21335	Venezuela: Yaracuy: Sierra de Aroa, Quebrada La Rondona (10.324444N, -68.873333W; 1,180 m)	-	-	-	-
Aromobates cf. sp. 1	MHNLS 21358	Venezuela: Yaracuy: Sierra de Aroa, Quebrada La Rondona (10.324444N, -68.873333W; 1,180 m)	**ARo4**	**ARo4**	**ARo4**	-
Aromobates cf. sp. 1	MHNLS 21359	Venezuela: Yaracuy: Sierra de Aroa, Quebrada La Rondona (10.324444N, -68.873333W; 1,180 m)	-	-	-	-
Aromobates sp. 2	CVULA 5718	Venezuela: Barinas: Los Alcaravanes, Agua Blanca sector (8.957167N, -70.428250W; 1,725 m)	-	-	JX035991	JX035991
Aromobates sp. 2	MHNLS 22093b	Venezuela: Barinas: Los Alcaravanes, Agua Blanca sector (8.957167N, -70.428250W; 1,725 m)	**AAl2**	-	-	-
Aromobates sp. 2	MHNLS 22093c	Venezuela: Barinas: Los Alcaravanes, Agua Blanca sector (8.957167N, -70.428250W; 1,725 m)	-	-	-	-
Aromobates sp. 2	MHNLS 22093d	Venezuela: Barinas: Los Alcaravanes, Agua Blanca sector (8.957167N, -70.428250W; 1,725 m)	-	-	-	-
Mannophryne caquetio	MIZA 333	Venezuela: Falcón: Sierra de Churuguara, Mapararí, El Macano (10.793219N, -69.421352W; 752 m)	-	-	-	-
Mannophryne caquetio	MIZA 337	Venezuela: Falcón: Sierra de Churuguara, Mapararí, El Macano (10.793219N, -69.421352W; 752 m)	-	-	-	-
Mannophryne caquetio	MIZA 323	Venezuela: Falcón: Sierra de Churuguara: Quebrada El Peregrino	-	-	-	-
Mannophryne caquetio	MIZA 338	Venezuela: Falcón: Sierra de Churuguara: Quebrada El Peregrino	-	-	-	-
Mannophryne caquetio	MHNLS 21219	Venezuela: Falcón: Sierra de San Luis, El Chorro sector, road to La Chapa (11.228689N, -69.601892W; 1,326 m)	**MCh1**	**MCh1**	**MCh1**	-
Mannophryne caquetio	MHNLS 21220	Venezuela: Falcón: Sierra de San Luis, El Chorro sector, road to La Chapa (11.228689N, -69.601892W; 1,326 m)	-	-	-	-
Mannophryne collaris	TNHC 5515	Venezuela: Mérida: stream along the autopista El Vigía to Mérida, near sector Trujillana (8.543683N, -71.583030W; 222 m)	-	KJ940466	KJ940466	KJ940466
Mannophryne collaris	TNHC 5507	Venezuela: Mérida: El Estanquillo (8.51915N, -71.341239W; 1,120 m)	HQ290581	-	HQ291004	HQ291004
Mannophryne collaris	MIZA 320	Venezuela: Mérida: Mérida city (8.620714N, -71.143761W; 1,783 m)	-	-	-	-
Mannophryne collaris	MIZA 321	Venezuela: Mérida: Mérida city (8.620714N, -71.143761W; 1,783 m)	-	-	-	-

Species	Voucher	Locality	Cyt-b	tRNA-Phe	12S	tRNA-Val
Mannophryne collaris	ULABG 4248	Venezuela: Mérida: Mérida city (8.620714N, -71.143761W; 1,783 m)	-	-	-	-
Mannophryne collaris	MHNLS 21590	Venezuela: Mérida: 2.6 WSW from El Chamita (8.547139N, -71.200611W; 1,244 m)	-	-	-	-
Mannophryne collaris	MHNLS 21591	Venezuela: Mérida: 2.6 WSW from El Chamita (8.547139N, -71.200611W; 1,244 m)	-	-	-	-
Mannophryne collaris	MHNLS 21592	Venezuela: Mérida: 2.6 WSW from El Chamita (8.547139N, -71.200611W; 1,244 m)	-	-	-	-
Mannophryne collaris	MHNLS 21593	Venezuela: Mérida: 2.6 WSW from El Chamita (8.547139N, -71.200611W; 1,244 m)	-	-	-	-
Mannophryne collaris	MHNLS 22058	Venezuela: Mérida: Campo Claro, Mérida city (8.561186N, -71.211944W; 1,224 m)	-	-	-	-
Mannophryne collaris	MHNLS 21684	Venezuela: La Cuesta sector, Mérida city (8.566878N, -71.168746W; 1,295 m)	-	-	-	-
Mannophryne collaris	MHNLS 21685	Venezuela: La Cuesta sector, Mérida city (8.566878N, -71.168746W; 1,295 m)	-	-	-	-
Mannophryne collaris	MHNLS 21686	Venezuela: La Cuesta sector, Mérida city (8.566878N, -71.168746W; 1,295 m)	-	-	-	-
Mannophryne collaris	MHNLS 21687	Venezuela: La Cuesta sector, Mérida city (8.566878N, -71.168746W; 1,295 m)	-	-	-	-
Mannophryne cordilleriana	TNHC 5589	Venezuela: Mérida: stream near the road to Pueblo Llano (8.878350N, -70.654820W; 1,676 m)	-	KJ940460	KJ940460	KJ940460
Mannophryne cordilleriana	MIZA 330	Venezuela: Mérida: La Mitisús (8.883361N, -70.647957W; 1,642 m)	-	-	-	-
Mannophryne cordilleriana	MIZA 331	Venezuela: Mérida: La Mitisús (8.883361N, -70.647957W; 1,642 m)	-	-	-	-
Mannophryne cordilleriana	MIZA 332	Venezuela: Mérida: La Mitisús (8.883361N, -70.647957W; 1,642 m)	-	-	-	-
Mannophryne cordilleriana	MHNLS 22098	Venezuela: Barinas: Agua Blanca sector, road to Mucuposada Los Alcaravanes (8.946806N, -70.431250W; 1,464 m)	-	-	-	-
Mannophryne cordilleriana	MHNLS 22099	Venezuela: Barinas: Agua Blanca sector, road to Mucuposada Los Alcaravanes (8.946806N, -70.431250W; 1,464 m)	-	-	-	-
Mannophryne cordilleriana	MHNLS 21693	Venezuela: Barinas: Barinitas, Barragán sector, stream tributary of Río Santo Domingo (8.789672N, -70.453873W; 462 m)	-	-	-	-
Mannophryne cordilleriana	MHNLS 21761	Venezuela: Barinas: Barinitas, Barragán sector, stream tributary of Río Santo Domingo (8.789672N, -70.453873W; 462 m)	-	-	-	-
Mannophryne cordilleriana	MHNLS 21625	Venezuela: Barinas: El Cacao, Quebrada La Toma (8.768417N, -70.447861W; 907 m)	-	-	-	-
Mannophryne cordilleriana	MHNLS 21626	Venezuela: Barinas: El Cacao, Quebrada La Toma (8.768417N, -70.447861W; 907 m)	-	-	-	-
Mannophryne cordilleriana	ULABG 5352	Venezuela: Mérida: La Mitisús (8.883361N, -70.647957W; 1,642 m)	**Mcd1**	-	-	-
Mannophryne cordilleriana	MHNLS 21632	Venezuela: Barinas: El Cacao, Quebrada Los Panches (8.762972N, -70.461278W; 837 m)	-	-	-	-

Species	Voucher	Locality	Cyt-b	tRNA-Phe	12S	tRNA-Val
Mannophryne cordilleriana	MHNLS 21633	Venezuela: Barinas: El Cacao, Quebrada Los Panches (8.762972N, -70.461278W; 837 m)	-	-	-	-
Mannophryne cordilleriana	MHNLS 21601	Venezuela: Barinas: Potrerito (8.842722N, -70.508861W; 1,020 m)	-	-	-	-
Mannophryne cordilleriana	MHNLS 21602	Venezuela: Barinas: Potrerito (8.842722N, -70.508861W; 1,020 m)	-	-	-	-
Mannophryne cordilleriana	MHNLS 22187	Venezuela: Barinas: Qda del Medio, near Barrio Escondido, ramal de Calderas (8.942583N, -70.420583W; 1,125 m)	-	-	-	-
Mannophryne cordilleriana	MHNLS 22188	Venezuela: Barinas: Qda del Medio, near Barrio Escondido, ramal de Calderas (8.942583N, -70.420583W; 1,125 m)	-	-	-	-
Mannophryne cordilleriana	MHNLS 21689	Venezuela: Barinas: San Isidro (8.836080N, -70.568344W; 1,191 m)	-	-	-	-
Mannophryne herminae	TNHC 5676	Venezuela: Aragua: near Estación Biológica Rancho Grande (10.350712N, -67.681593W; 1,145 m)	-	KJ940461	KJ940461	KJ940461
Mannophryne herminae	MIZA 329	Venezuela: Aragua: near Estación Biológica Rancho Grande (10.350712N, -67.681593W; 1,145 m)	-	-	-	-
Mannophryne herminae	MIZA 328	Venezuela: Aragua: La Trilla (10.391200N, -67.749748W; 127 m)	-	-	-	-
Mannophryne herminae	MIZA 327	Venezuela: Aragua: La Trilla (10.391200N, -67.749748W; 127 m)	-	-	-	-
Mannophryne herminae	MHNLS 17475	Venezuela: Aragua: Cata River (10.437111N, -67.724611W; 96 m)	-	-	-	-
Mannophryne herminae	MHNLS 21735	Venezuela: Aragua: Cuyagua River (10.458111N, -67.690000W; 130 m)	-	-	-	-
Mannophryne herminae	MHNLS 21736	Venezuela: Aragua: Cuyagua River (10.458111N, -67.690000W; 130 m)	-	-	-	-
Mannophryne herminae	MHNLS 22106	Venezuela: Carabobo: stream tributary of San Esteban River (10.397917N, -67.997417W; 170 m)	**Mhe6**	-	-	-
Mannophryne herminae	MHNLS 22107	Venezuela: Carabobo: stream tributary of San Esteban River (10.397917N, -67.997417W; 170 m)	-	-	-	-
Mannophryne aff. *herminae*	ULABG 4506	Venezuela: Carabobo: La Entrada, near Valencia (10.296950N, -68.053739W; 641 m)	-	-	-	-
Mannophryne lamarcai	MIZA 317	Venezuela: Falcon: Cerro Socopó 30.0 km (by road) SW from Guajiro (10.492318N, -70.801131W; 1,248 m)	-	-	-	-
Mannophryne lamarcai	MIZA 318	Venezuela: Falcon: Cerro Socopó 30.0 km (by road) SW from Guajiro (10.492318N, -70.801131W; 1,248 m)	-	-	-	-
Mannophryne lamarcai	NMA 38	Venezuela: Zulia: near San Pedro del Páramo (10.206292N, -70.703808W; 1,334 m)	-	-	-	-
Mannophryne lamarcai	NMA 40	Venezuela: Zulia: Serranía de Ziruma, vía a El Jordán (10.343650N, -70.764622W; 1,460 m)	**Mla2**	**Mla2**	**Mla2**	-
Mannophryne lamarcai	NMA 41	Venezuela: Zulia: Serranía de Ziruma, vía a El Jordán (10.343650N, -70.764622W; 1,460 m)	-	-	-	-
Mannophryne lamarcai	MHNLS 22087	Venezuela: Trujillo: Cuicas, stream to 1.8 km N of the town (9.717028N, -70.303972W; 1,098 m)	**MCu1**	**MCu1**	**MCu1**	-

Species	Voucher	Locality	Cyt-b	tRNA-Phe	12S	tRNA-Val
Mannophryne lamarcai	MHNLS 22088	Venezuela: Trujillo: Cuicas, stream to 1.8 km N of the town (9.717028N, -70.303972W; 1,098 m)	-	-	-	-
Mannophryne larandina	MIZA 324	Venezuela: Lara: road between Hato Arriba and Barbacoas (9.803108N, -70.062672W; 1,606 m)	-	-	-	-
Mannophryne larandina	MIZA 325	Venezuela: Lara: road between Hato Arriba and Barbacoas (9.803108N, -70.062672W; 1,606 m)	-	-	-	-
Mannophryne larandina	MIZA 326	Venezuela: Lara: road between Hato Arriba and Barbacoas (9.803108N, -70.062672W; 1,606 m)	-	-	-	-
Mannophryne larandina	MHNLS 22597	Venezuela: Lara: near Hato Arriba, road from Barbacoas to El Tocuyo (9.754990N, -70.014150W; 1,983 m)	**Mlr1**	**Mlr1**	**Mlr1**	-
Mannophryne larandina	MHNLS 22598	Venezuela: Lara: near Hato Arriba, road from Barbacoas to El Tocuyo (9.754990N, -70.014150W; 1,983 m)	-	-	-	-
Mannophryne larandina	MHNLS 22599	Venezuela: Lara: near Hato Arriba, road from Barbacoas to El Tocuyo (9.754990N, -70.014150W; 1,983 m)	-	-	-	-
Mannophryne "herminae"	CWM 1141	Venezuela: Trujillo: about 2 km (airline) W La Peña, 1920 m (apparently wrong location)	DQ502595	-	DQ502160	DQ502160
Mannophryne leonardoi	TNHC 5659	Venezuela: Monagas: near the Cueva del Guácharo, proximity to Caripe River (10.170880N, -63.553600W; 1,120 m)	-	KJ940463	KJ940463	KJ940463
Mannophryne leonardoi	TTSR	Venezuela: Monagas: Caripe (10.167069N, -63.515677W; 867 m)	-	-	-	-
Mannophryne leonardoi	MIZA 316	Venezuela: Monagas: Cueva del Guácharo (10.200000N, -63.639722W; 1,280 m)	-	-	-	-
Mannophryne leonardoi	WES 1034	Venezuela: Monagas: stream near Cueva del Guácharo (10.201841N, -63.637513W; 1,400 m)	DQ502675	-	DQ502243	DQ502243
Mannophryne leonardoi	WES 1035	Venezuela: Monagas: stream near Cueva del Guácharo (10.201841N, -63.637513W; 1,400 m)	DQ502676	-	DQ502244	DQ502244
Mannophryne leonardoi	WES 1036	Venezuela: Monagas: stream near Cueva del Guácharo (10.201841N, -63.637513W; 1,400 m)	DQ502677	-	DQ502245	DQ502245
Mannophryne leonardoi	MHNLS 22333	Venezuela: Monagas: La Margarita, Caripe (10.206117N, -63.361400W; 910 m)	-	-	-	-
Mannophryne leonardoi	MHNLS 22334	Venezuela: Monagas: La Margarita, Caripe (10.206117N, -63.361400W; 910 m)	-	-	-	-
Mannophryne leonardoi	MHNLS 22335	Venezuela: Monagas: La Margarita, Caripe (10.206117N, -63.361400W; 910 m)	-	-	-	-
Mannophryne leonardoi	MHNLS 22336	Venezuela: Monagas: La Margarita, Caripe (10.206117N, -63.361400W; 910 m)	-	-	-	-
Mannophryne molinai	MHNLS 21336	Venezuela: Yaracuy: Sierra de Aroa, Quebrada La Rondona (10.324444N, -68.873333W; 1,217 m)	**MRo1**	**MRo1**	**MRo1**	-
Mannophryne molinai	MHNLS 21337	Venezuela: Yaracuy: Sierra de Aroa, Quebrada La Rondona (10.324444N, -68.873333W; 1,217 m)	**MRo2**	-	-	-
Mannophryne molinai	MHNLS 21338	Venezuela: Yaracuy: Sierra de Aroa, Quebrada La Rondona (10.324444N, -68.873333W; 1,217 m)	-	-	-	-
Mannophryne molinai	MHNLS 21356	Venezuela: Yaracuy: Sierra de Aroa, Quebrada La Rondona	-	-	-	-

Species	Voucher	Locality	Cyt-b	tRNA-Phe	12S	tRNA-Val
		(10.324444N, -68.873333W; 1,217 m)				
Mannophryne cf. *molinai*	MHNLS 21005	Venezuela: Yaracuy: Guayabito Recreational Park (10.472917N, -68.664083W; 143 m)	**MPg1**	-	-	-
Mannophryne cf. *molinai*	MHNLS 21006	Venezuela: Yaracuy: Guayabito Recreational Park (10.472917N, -68.664083W; 143 m)	**MPg2**	-	-	-
Mannophryne cf. *molinai*	MHNLS 21365	Venezuela: Yaracuy: Mayorica sector, Mayorica River (10.430306N, -68.688333W; 178 m)	-	-	-	-
Mannophryne cf. *molinai*	MHNLS 21367	Venezuela: Yaracuy: Mayorica sector, Mayorica River (10.430306N, -68.688333W; 178 m)	-	-	-	-
Mannophryne cf. *molinai*	MHNLS 21205	Venezuela: Yaracuy: Hacienda La Guáquira, Quebrada La Herrera (10.281917N, -68.654056W; 153 m)	**MQh1**	**MQh1**	**MQh1**	-
Mannophryne cf. *molinai*	MHNLS 21206	Venezuela: Yaracuy: Hacienda La Guáquira, Quebrada La Herrera (10.281917N, -68.654056W; 153 m)	-	-	-	-
Mannophryne cf. *molinai*	MHNLS 21516	Venezuela: Yaracuy: Sierra de Aroa: El Abrigo (10.473750N, -68.849028W; 464 m)	**MAb1**	-	-	-
Mannophryne cf. *molinai*	MHNLS 21517	Venezuela: Yaracuy: Sierra de Aroa: El Abrigo (10.473750N, -68.849028W; 464 m)	**MAb2**	-	-	-
Mannophryne neblina	MHNLS 22362	Venezuela: Vargas: El Aguacatal, road to Puerto Cruz (10.456750N, -67.267778W; 954 m)	**Mne3**	**Mne3**	**Mne3**	-
Mannophryne oblitterata	TTSR	Venezuela: Miranda: Taguaza (10.179730N, -66.435901W; 201 m)	-	-	-	-
Mannophryne oblitterata	MIZA 336	Venezuela: Miranda: Taguaza (10.179730N, -66.435901W; 201 m)	-	-	-	-
Mannophryne oblitterata	MHNLS 21766	Venezuela: Miranda: Araira River (10.502339N, -66.457217W; 683 m)	-	-	-	-
Mannophryne oblitterata	MHNLS 21767	Venezuela: Miranda: Araira River (10.502339N, -66.457217W; 683 m)	-	-	-	-
Mannophryne oblitterata	MHNLS 21818	Venezuela: Miranda: stream on the right bank of the Araira river (10.489153N, -66.462889W; 556 m)	**Mob4**	**Mob4**	**Mob4**	-
Mannophryne oblitterata	MHNLS 21819	Venezuela: Miranda: stream on the right bank of the Araira river (10.489153N, -66.462889W; 556 m)	-	-	-	-
Mannophryne olmonae	MIZA 334 / isolate 451	Trinidad and Tobago: North Tobago	DQ341161	-	AY206717	-
Mannophryne olmonae	MIZA335 / isolate 452	Trinidad and Tobago: Tobago Island	DQ341160	-	AY255850	-
Mannophryne olmonae	UWIZM 2732 / ZSM 1622	Trinidad and Tobago: Tobago Island: Charlotteville (11.317283N, -60.553567W; 99 m)	MF614228	-	MF624237	MF624237
Mannophryne orellana	CVULA 7165	Venezuela: Táchira: stream along the road from Pregonero to La Trampa (8.032520N, -71.727700W; 1,181 m)	-	KJ940464	KJ940464	KJ940464
Mannophryne orellana	CVULA 7231	Venezuela: Táchira: stream tributary of Río Negro, near El Tamá National Park (7.578720N, -72.178980W; 491 m)	-	KJ940465	KJ940465	KJ940465
Mannophryne orellana	ULABG 7469	Venezuela: Táchira: El Cañadón (8.013694N, -71.537722W; 1,727 m)	**Mor1**	-	-	-

Species	Voucher	Locality	Cyt-b	tRNA-Phe	12S	tRNA-Val
Mannophryne orellana	MHNLS MCp1	Venezuela: Mérida: Uribante-Caparo dam (7.941217N, -71.301672W; 319 m)	-	-	-	-
Mannophryne orellana	MHNLS MCp2	Venezuela: Mérida: Uribante-Caparo dam (7.941217N, -71.301672W; 319 m)	-	-	-	-
Mannophryne orellana	MHNLS MCp3	Venezuela: Mérida: Uribante-Caparo dam (7.941217N, -71.301672W; 319 m)	-	-	-	-
Mannophryne riveroi	MIZA 319	Venezuela: Sucre: Paria península	-	-	-	-
Mannophryne riveroi	TTSR	Venezuela: Sucre: Paria península	-	-	-	-
Mannophryne riveroi	MHNLS16433 / TNHC 5644	Venezuela: Sucre: Paria peninsula, Las Melenas (10.684444N, -62.616667W; 637 m)	**Mri1**	-	EU342503	EU342503
Mannophryne riveroi	MHNLS 17910	Venezuela: Sucre: Paria peninsula, Las Melenas (10.684444N, -62.616667W; 637 m)	-	-	-	-
Mannophryne speeri	MHNLS 22606	Venezuela: Lara: Sector La Fila sector, road from Chabasquén to Villa Nueva (9.516300N, -69.837100W; 1,232 m)	**Msp1**	**Msp1**	**Msp1**	-
Mannophryne trinitatis	MVZ 199837	Trinidad and Tobago: Trinidad island: Tamana Cave (10.468933N, -61.190383W; 284 m)	JX564878	EU342504	JX564878	JX564878
Mannophryne trinitatis	MVZ199838 / isolate 405	Trinidad and Tobago: Trinidad island: Tamana Cave (10.468933N, -61.190383W; 284 m)	DQ341141	-	DQ283071	DQ283071
Mannophryne trinitatis	MVZ 199828	Trinidad and Tobago: Trinidad island: Nariva Parish, Charuma Ward, Tamana Cave (10.468933N, -61.190383W; 284)	DQ502562	-	DQ502131	DQ502131
Mannophryne trinitatis	ZSM 1619	Trinidad and Tobago: Trinidad island: Pax Guest House (Mount St. Benedikt) (10.663000N, -61.395000; 186 m)	-	-	-	-
Mannophryne trinitatis	ZSM 1620	Trinidad and Tobago: Trinidad island: Pax Guest House (Mount St. Benedikt) (10.663000N, -61.395000; 186 m)	-	-	-	-
Mannophryne trinitatis	ZSM 1621	Trinidad and Tobago: Trinidad island: Maracas waterfalls (10.728873N, -61.404887W; 390 m)	-	-	-	-
Mannophryne trujillensis	MHNLS 17963	Venezuela: Trujillo: Hacienda El Corozal (9.475833N, -70.435917W; 573 m)	-	-	-	-
Mannophryne trujillensis	MHNLS 17971	Venezuela: Trujillo: Hacienda El Corozal (9.475833N, -70.435917W; 573 m)	-	-	-	-
Mannophryne trujillensis	MHNLS 22070	Venezuela: Trujillo: Urbina, old road Trujillo-Boconó (9.330889N, -70.398500W; 1,762 m)	-	-	-	-
Mannophryne trujillensis	MHNLS 22071	Venezuela: Trujillo: Urbina, old road Trujillo-Boconó (9.330889N, -70.398500W; 1,762 m)	-	-	-	-
Mannophryne trujillensis	MHNLS 22063	Venezuela: Trujillo: 3.2 NE from Sabaneta (9.329722N, -70.470833W; 1,378 m)	-	-	-	-
Mannophryne trujillensis	MHNLS 22064	Venezuela: Trujillo: 3.2 NE from Sabaneta (9.329722N, -70.470833W; 1,378 m)	**Mtr4**	**Mtr4**	**Mtr4**	-
Mannophryne urticans	TNHC 5520	Venezuela: Mérida: Río Frío (8.858674N, -71.294185W; 676 m)	-	KJ940467	KJ940467	KJ940467
Mannophryne urticans	ULABG 4481	Venezuela: Trujillo: 1.3 from La Quebrada, on the road to Cabimbú (9.157501N, -70.56765W; 1583 m)	-	-	-	-

Species	Voucher	Locality	Cyt-b	tRNA-Phe	12S	tRNA-Val
Mannophryne urticans	MHNLS 21555	Venezuela: Mérida: Las Maricelas (8.886861N, -71.319667W; 270 m)	**Mur2**	-	-	-
Mannophryne urticans	MHNLS 21556	Venezuela: Mérida: Las Maricelas (8.886861N, -71.319667W; 270 m)	-	-	-	-
Mannophryne urticans	MHNLS 21994	Venezuela: Mérida: La Olinda II, 5 km NNO from La Azulita (8.751944N, -71.472028W; 1,206 m)	-	-	-	-
Mannophryne urticans	MHNLS 21993	Venezuela: Mérida: La Olinda II, 5 km NNO from La Azulita (8.751944N, -71.472028W; 1,206 m)	-	-	-	-
Mannophryne venezuelensis	EBRG 4921 / isolate 469	Venezuela: Sucre: Paria peninsula: 4 km E from San Juan de las Galdonas (10.717728N, -62.799345W; 180 m)	DQ341122	-	DQ343209	-
Mannophryne venezuelensis	EBRG 4922 / isolate 555 / isoalte 470	Venezuela: Sucre: Paria peninsula: 4 km E from San Juan de las Galdonas (10.717728N, -62.799345W; 180 m)	DQ341123	-	DQ343210	-
Mannophryne venezuelensis	MHNLS 16435	Venezuela: Sucre: Paria peninsula: Las Melenas (10.684444N, -62.616667W; 637 m)	-	**Mve1**	**Mve1**	-
Mannophryne venezuelensis	MHNLS 17287	Venezuela: Sucre: Paria peninsula: Las Melenas (10.684444N, -62.616667W; 637 m)	-	-	-	-
Mannophryne venezuelensis	MHNLS 17314	Venezuela: Sucre: Paria peninsula: Las Melenas (10.684444N, -62.616667W; 637 m)	-	-	-	-
Mannophryne venezuelensis	MHNLS 17315	Venezuela: Sucre: Paria peninsula: Las Melenas (10.684444N, -62.616667W; 637 m)	-	-	-	-
Mannophryne venezuelensis	TNHC 5649	Venezuela: Sucre: Península de Paria National Park, Cerro Humo (10.689920N, -62.610230W; 859 m)	-	KJ940468	KJ940468	KJ940468
Mannophryne vulcano	TNHC 5679	Venezuela: Miranda: Northern slope of Cerro El Volcán (10.423170N, -66.857820W; 1,183 m)	-	KJ940469	KJ940469	KJ940469
Mannophryne vulcano	MIZA 342	Venezuela: Miranda: Guatopo	-	-	-	-
Mannophryne vulcano	MIZA 343	Venezuela: Miranda: Guatopo	-	-	-	-
Mannophryne vulcano	MHNLS 16685	Venezuela: Distrito Capital: Boca de Tigre sector, headwaters of Quebrada Anauco (10.548133N, -66.900213W; 1,880 m)	-	-	-	-
Mannophryne vulcano	MHNLS 22140	Venezuela: Miranda: Caracas, Quebrada Caurimare (10.507167N, -66.793750W; 1,134 m)	**Mvu36**	-	-	-
Mannophryne vulcano	MHNLS 22141	Venezuela: Miranda: Caracas, Quebrada Caurimare (10.507167N, -66.793750W; 1,134 m)	-	-	-	-
Mannophryne vulcano	MHNLS 22142	Venezuela: Miranda: Caracas, Quebrada Caurimare (10.507167N, -66.793750W; 1,134 m)	-	-	-	-
Mannophryne vulcano	MHNLS 20692	Venezuela: Miranda: Caracas, Quebrada Chacaíto (10.510194N, -66.862056W; 978 m)	-	-	-	-
Mannophryne vulcano	MHNLS 20693	Venezuela: Miranda: Caracas, Quebrada Chacaíto (10.510194N, -66.862056W; 978 m)	-	-	-	-
Mannophryne vulcano	MHNLS 18575	Venezuela: Distrito Capital: basement of the building FLASA (10.511473N, -66.884106W; 988 m)	-	-	-	-
Mannophryne vulcano	MHNLS 18577	Venezuela: Distrito Capital: basement of the building FLASA (10.511473N, -66.884106W; 988 m)	-	-	-	-

Species	Voucher	Locality	Cyt-b	tRNA-Phe	12S	tRNA-Val
Mannophryne vulcano	MHNLS 21802	Venezuela: Miranda: Altos de Pipe, IVIC, Quebrada Guayabal (10.387667N, -66.968972W; 1,393 m)	-	-	-	-
Mannophryne vulcano	MHNLS 21803	Venezuela: Miranda: Altos de Pipe, IVIC, Quebrada Guayabal (10.387667N, -66.968972W; 1,393 m)	-	-	-	-
Mannophryne vulcano	MHNLS 20830	Venezuela: Miranda: Filas de Mariche, Villa Dolores (10.444167N, -66.705556W; 946 m)	-	-	-	-
Mannophryne vulcano	MHNLS 21770	Venezuela: Miranda: Cerro El Ávila, Quebrada Papelón (10.528667N, -66.880028W; 1,669 m)	-	-	-	-
Mannophryne vulcano	MHNLS 21771	Venezuela: Miranda: Cerro El Ávila, Quebrada Papelón (10.528667N, -66.880028W; 1,669 m)	-	-	-	-
Mannophryne vulcano	MHNLS 22346	Venezuela: Vargas: Los Rastrojos, road to Puerto Cruz (10.483556N, -67.308361W; 702 m)	-	-	-	-
Mannophryne vulcano	MHNLS 20941	Venezuela: Miranda: Sabaneta de Cañaveral, Santa María Ecological Farm (10.395083N, -66.796889W; 813 m)	-	-	-	-
Mannophryne vulcano	MHNLS 20942	Venezuela: Miranda: Sabaneta de Cañaveral, Santa María Ecological Farm (10.395083N, -66.796889W; 813 m)	-	-	-	-
Mannophryne vulcano	MHNLS 21778	Venezuela: Distrito Capital: Cerro El Ávila, Los Venados (10.534306N, -66.898500W; 1,408 m)	-	-	-	-
Mannophryne vulcano	MHNLS 21779	Venezuela: Distrito Capital: Cerro El Ávila, Los Venados (10.534306N, -66.898500W; 1,408 m)	-	-	-	-
Mannophryne yustizi	TTSR_G	Venezuela: Lara: Guarico (9.616820N, -69.788138W; 1,181 m)	-	-	-	-
Mannophryne yustizi	TNHC 5604	Venezuela: Lara: stream along the road to Guarico, near Sabana Grande (9.582280N, -69.849800W; 1,485 m)	-	KJ940470	KJ940470	KJ940470
Mannophryne yustizi	TTSR_S	Venezuela: Lara: Sanare (9.748147N, -69.641482W; 1,242 m)	-	-	-	-
Mannophryne yustizi	MIZA 322	Venezuela: Lara: Sanare (9.748147N, -69.641482W; 1,242 m)	-	-	-	-
Mannophryne sp. 1	TTSR	Venezuela: Miranda: Cúpira (10.171821N, -65.727270W; 53 m)	-	-	-	-
Mannophryne sp. 1	MIZA 341	Venezuela: Miranda: Cúpira (10.171821N, -65.727270W; 53 m)	-	-	-	-
Mannophryne sp. 1	MHNLS 16769	Venezuela: Miranda: Urva River (10.186000N, -66.186111W; 174 m)	-	-	-	-
Mannophryne sp. 1	MHNLS 16772	Venezuela: Miranda: Urva River (10.186000N, -66.186111W; 174 m)	**MRu1**	**MRu1**	**MRu1**	-
Mannophryne sp. 1	MHNLS 16773	Venezuela: Miranda: Urva River (10.186000N, -66.186111W; 174 m)	-	-	-	-
Mannophryne sp. 1	MHNLS 16798	Venezuela: Miranda: Urva River (10.186000N, -66.186111W; 174 m)	-	-	-	-
Mannophryne sp. (cf. *vulcano*)	MHNLS 21825	Venezuela: Miranda: stream tributary of Araira river (10.465667N, -66.467250W; 500 m)	-	-	-	-
Mannophryne sp. (cf. *vulcano*)	MHNLS 21826	Venezuela: Miranda: stream tributary of Araira river (10.465667N, -66.467250W; 500 m)	-	-	-	-

Species	Voucher	Locality	Cyt-b	tRNA-Phe	12S	tRNA-Val
Mannophryne sp. 2	MIZA 340	Venezuela: Guárico: El Castrero (9.864787N, -67.453707W; 703 m)	-	-	-	-
Mannophryne sp. 2	EBRG 4889	Venezuela: Guárico: El Castrero (9.864787N, -67.453707W; 703 m)	-	-	-	-
Mannophryne sp. 2	MHNLS 17251	Venezuela: Guárico: Cerro Platillón (9.856000N, -67.503000W; 1,102 m)	-	-	-	-
Mannophryne sp. 2	MHNLS 17252	Venezuela: Guárico: Cerro Platillón (9.856000N, -67.503000W; 1,102 m)	-	-	-	-
Mannophryne sp. 2	MHNLS 17253	Venezuela: Guárico: Cerro Platillón (9.856000N, -67.503000W; 1,102 m)	**MPl1**	**MPl1**	**MPl1**	-
Mannophryne sp. 2	MHNLS 17254	Venezuela: Guárico: Cerro Platillón (9.856000N, -67.503000W; 1,102 m)	-	-	-	-
Mannophryne sp. 2	MHNLS 17256	Venezuela: Guárico: Cerro Platillón (9.856000N, -67.503000W; 1,102 m)	-	-	-	-
Mannophryne sp. 2	MHNLS 15545	Venezuela: Guárico: Cerro Platillón, Hacienda El Picachito (9.856667N, -67.512222W; 1319 m)	**MPi1**	**MPi1**	**MPi1**	-
Mannophryne sp. 3	MHNLS 22358	Venezuela: Vargas: El Aguacatal, road to Puerto Cruz (10.456750N, -67.267778W; 954 m)	-	-	-	-
Mannophryne sp. 3	MHNLS 22359	Venezuela: Vargas: El Aguacatal, road to Puerto Cruz (10.456750N, -67.267778W; 954 m)	-	-	-	-
Mannophryne sp. 3	MHNLS 22360	Venezuela: Vargas: El Aguacatal, road to Puerto Cruz (10.456750N, -67.267778W; 954 m)	**MAg3**	**MAg3**	**MAg3**	-
Mannophryne sp. 3	MHNLS 22347	Venezuela: Vargas: Los Rastrojos, road to Puerto Cruz (10.483556N, -67.308361W; 702 m)	-	-	-	-
Mannophryne sp. 3	MHNLS 22348	Venezuela: Vargas: Los Rastrojos, road to Puerto Cruz (10.483556N, -67.308361W; 702 m)	-	-	-	-
Mannophryne sp. 3	MHNLS 22353	Venezuela: Vargas: Los Rastrojos, road to Puerto Cruz (10.483556N, -67.308361W; 702 m)	-	-	-	-
Mannophryne sp. 3	MHNLS 21747	Venezuela: Vargas: stream in front of the Oricao club (10.547524N, -67.184115W; 69 m)	-	-	-	-
Mannophryne sp. 3	MHNLS 21748	Venezuela: Vargas: stream in front of the Oricao club (10.547524N, -67.184115W; 69 m)	-	-	-	-
Mannophryne sp. 4	MHNLS 22204	Venezuela: Carabobo: Montalbán: El Peñón (10.228306N, -68.357583W; 1,304 m)	**MMo1**	**MMo1**	**MMo1**	-
Mannophryne sp. 4	MHNLS 22214	Venezuela: Carabobo: Montalbán: El Peñón (10.228306N, -68.357583W; 1,304 m)	-	-	-	-
Mannophryne sp. 4	MHNLS 22219	Venezuela: Carabobo: Montalbán: El Peñón (10.228306N, -68.357583W; 1,304 m)	-	-	-	-
Mannophryne sp. 4	MHNLS 22281	Venezuela: Carabobo: Montalbán: Sector El Marquero (10.259861N, -68.319556W; 1,162 m)	-	-	-	-
Mannophryne sp. 4	MHNLS 22302	Venezuela: Carabobo: Montalbán: Sector San Isidro (10.255056N, -68.246722W; 1,234 m)	-	-	-	-

Species	Voucher	Locality	Cyt-b	tRNA-Phe	12S	tRNA-Val
Mannophryne sp. 4	MHNLS 22303	Venezuela: Carabobo: Montalbán: Sector San Isidro (10.255056N, -68.246722W; 1,234 m)	-	-	-	-
Mannophryne sp. 4	MHNLS 22304	Venezuela: Carabobo: Montalbán: Sector San Isidro (10.255056N, -68.246722W; 1,234 m)	-	-	-	-
Mannophryne sp. (aff. *herminae*)	MHNLS 17157	Venezuela: Cojedes: road from Manrique to La Sierra, bridge over the San Carlos river (9.873000N, -68.535000W; 506 m)	**MSi1**	**MSi1**	**MSi1**	-
Mannophryne sp. (aff. *herminae*)	MHNLS 17158	Venezuela: Cojedes: road from Manrique to La Sierra, bridge over the San Carlos river (9.873000N, -68.535000W; 506 m)	-	-	-	-
Mannophryne sp. (aff. *herminae*)	MHNLS 17159	Venezuela: Cojedes: road from Manrique to La Sierra, bridge over the San Carlos river (9.873000N, -68.535000W; 506 m)	-	-	-	-
Mannophryne sp. (aff. *herminae*)	MHNLS 17160	Venezuela: Cojedes: road from Manrique to La Sierra, bridge over the San Carlos river (9.873000N, -68.535000W; 506 m)	-	-	-	-
Mannophryne sp. (*yustizi* complex)	MHNLS 22585	Venezuela: Lara: La Olla (9.844303N, -69.215564; 565 m)	**MN01**	-	-	-
Mannophryne sp. (*yustizi* complex)	MHNLS 22586	Venezuela: Lara: La Olla (9.844303N, -69.215564; 565 m)	**MN02**	-	-	-
Mannophryne sp. (aff. *vulcano*)	TNHC 5666	Venezuela: Miranda: Guatopo National Park, road to Altagracia de Orituco (10.084950N, -66.489080W; 413 m)	-	KJ940462	KJ940462	KJ940462
Mannophryne sp. (*yustizi* complex)	ULABG 4465	Venezuela: Portuguesa: Campo Elías (9.383776N, -70.068402W; 1,272 m)	-	-	-	-
Mannophryne sp. (*yustizi* complex)	ULABG 4453	Venezuela: Lara: Palma Rica (9.453889N, -70.013333W; 1,306 m)	-	-	-	-
Mannophryne sp. (*yustizi* complex)	ULABG 4458	Venezuela: Lara: Palma Rica (9.453889N, -70.013333W; 1,306 m)	-	-	-	-
Mannophryne sp. (*yustizi* complex)	MHNLS 22080	Venezuela: Trujillo: El Jarillo, old road Trujillo-Boconó (9.365306N, -70.279528W; 2,149 m)	**MJa1**	**MJa1**	**MJa1**	-
Mannophryne sp. (*yustizi* complex)	MHNLS 22081	Venezuela: Trujillo: El Jarillo, old road Trujillo-Boconó (9.365306N, -70.279528W; 2,149 m)	-	-	-	-
Mannophryne sp. (*yustizi* complex)	MHNLS 22617	Venezuela: Portuguesa: near Chabasquén (9.434097N, -69.952967W; 667 m)	**Msp6**	-	-	-
Mannophryne sp. (cf. *speeri-yustizi*)	MHNLS 22618	Venezuela: Portuguesa: near Chabasquén (9.434097N, -69.952967W; 667 m)	**Msp7**	-	-	-
Mannophryne sp. (*yustizi* complex)	MHNLS 22619	Venezuela: Portuguesa: near Chabasquén (9.434097N, -69.952967W; 667 m)	-	-	-	-
Mannophryne sp. (cf. *speeri-yustizi*)	MHNLS 22169	Venezuela: Trujillo: Niquitao, Laguneta sector (9.101778N, -70.405472W; 2,010 m)	**MNi1**	**MNi1**	**MNi1**	-
Mannophryne sp. (*yustizi* complex)	MHNLS 22170	Venezuela: Trujillo: Niquitao, Laguneta sector (9.101778N, -70.405472W; 2,010 m)	-	-	-	-
Mannophryne sp. (*yustizi* complex)	MHNLS 22171	Venezuela: Trujillo: Niquitao, Laguneta sector (9.101778N, -70.405472W; 2,010 m)	-	-	-	-
Mannophryne sp. (*yustizi* complex)	MHNLS 22172	Venezuela: Trujillo: Niquitao, Laguneta sector (9.101778N, -70.405472W; 2,010 m)	-	-	-	-
Mannophryne sp. (*yustizi* complex)	MHNLS 22559	Venezuela: Lara: Agua Linda sector, road from Humocaro alto to Chabasquen (9.478170N, -70.020180W; 2,099 m)	-	-	-	-

Species	Voucher	Locality	Cyt-b	tRNA-Phe	12S	tRNA-Val
Mannophryne sp. (*yustizi* complex)	MHNLS 22560	Venezuela: Lara: Agua Linda sector, road from Humocaro alto to Chabasquen (9.478170N, -70.020180W; 2,099 m)	**Myu3**	**Myu3**	**Myu3**	-
Andinobates bombetes	TNHC 4946 / MAR 1265	Colombia: Quindío: Barbas, Finlandia, Hacienda Lusitania (1,958 m)	HQ290558	-	HQ290981	HQ290981
Adelphobates galactonotus	TNHC 4889 / MTR 5088	No data (captive bred)	HQ290561	-	HQ290984	HQ290984
Allobates aff. *juanii*	ANDESA 1073	Colombia: Antioquia: Sabanalarga (-4.773000S, -73.038000W; 320 m)	-	-	-	-
Allobates algorei	TNHC 5551	Venezuela: Táchira: road from San Cristobal to Río Negro vía el Piñal (529 m)	HQ290530	-	HQ290950	HQ290950
Allobates amissibilis	MTD 47884	Guyana: Iwokrama	KC520691	-	KC520679	-
Allobates bacurau	INPAH 35406	Brazil: Estrada do Miriti, Manicore, Amazonas	-	-	-	-
Allobates caeruleodactylus	MPEG 13809	Brazil: Amazonas: Castanho: ca. 40 km S Manaus, at km 12 on road to Autazes (-3.619556S, -60.455111W)	DQ502532	-	DQ502100	DQ502100
Allobates chalcopis	Alca1	Martinique: Montagne Pelee	-	-	KC520675	KC520675
Allobates conspicuus	MPEG 12321	Brazil: Acre: Porto Walter (-8.258667S, -72.776972W)	DQ502566	-	DQ502134	DQ502134
Allobates crombiei	APL 14124	Brazil: Pará: Fazenda Raio de Sol	-	-	-	-
Allobates femoralis (Acre01)	Acre 12931	Brazil: Acre: Basilia	-	-	-	-
Allobates femoralis (Acre02)	OMNH 36070	Brazil: Acre: Porto Walter (-8.258667S, -72.776972W)	DQ502524	-	DQ502092	DQ502092
Allobates femoralis	QCAZ 16484	Francisco de Orellana: Parque Nacional Yasuní-Estación PUCE, 230 m	HQ290531	-	HQ290951	HQ290951
Allobates flaviventris	OMNH 36959	Brazil: Rondônia: Parque Estadual Guajará-Mirim (-10.321444N, -64.563306W)	DQ502620	-	DQ502184	DQ502184
Allobates fratisenescus	QCAZ 54377	Ecuador: Morona Santiago: Comunidad Jempekat, riachuelo	MF614174	-	-	-
Allobates gasconi	MPEG 13003	Brazil: Amazonas: Rio Ituxi: Scheffer Madeireira (-8.479389S, -65.716556W)	DQ502483	-	DQ502052	DQ502052
Allobates granti	148 AF	Suriname: Brownsberg Natural Park (4.941944N, -55.175833W)	-	-	-	-
Allobates grillisimilis	APL 12747	Brazil: Amazonas: Borba	-	-	-	-
Allobates hodli	AbuE 2189	Brazil: Rondônia: Abuanú	-	-	-	-
Allobates humilis	CVULA 5690	Venezuela: Barinas: On the road to San Ramón, Calderas	-	KJ940454	KJ940454	KJ940454
Allobates humilis	MHNLS22093a	Venezuela: Barinas: Los Alcaravanes, Agua Blanca sector (8.957167N, -70.428250W; 1,725 m)	-	-	-	-
Allobates insperatus	QCAZ1 6533	Ecuador: Francisco de Orellana: Parque Nacional Yasuní-Estación PUCE (230 m)	HQ290539	-	HQ290959	HQ290959
Allobates juami	MCP 13287	Brazil: Amazonas, Japura, Estação Ecologica Juami-Japura (-	-	-	-	-

Species	Voucher	Locality	Cyt-b	tRNA-Phe	12S	tRNA-Val
		1.964550S, 67.935790W; 87 m)				
Allobates juanii	TNHC 4978	Meta: Villavicencio, Villavicencio-Restrepo road (411 m)	HQ290540	-	HQ290960	HQ290960
Allobates kingsburyi	QCAZ 16523	Ecuador: Zamora Chinchipe: Río Chicaña (1,085 m)	HQ290541	-	HQ290963	HQ290963
Allobates magnussoni	MPEG 11923	Brazil: Pará: 101 km S and 15 km E Santarém (near Rio Curuà-una) (-3.150000S, -54.833333W)	DQ502564	-	DQ502132	DQ502132
Allobates masniger	APL 14250	Brazil: Pará: Jacareanga (-6.248750S, -57.974583W)	-	-	-	-
Allobates myersi	INPAH 26396	Brazil: Sao Gabriel da Cachoeira, Amazonas	-	-	-	-
Allobates nidicola	MPEG 13821	Brazil: Amazonas: Castanho: ca. 40 km S Manaus, at km 12 on road to Autazes (-3.619556S, -60.455111W)	DQ502533	-	DQ502101	DQ502101
Allobates niputidea	MUJ 3520	Colombia: Caldas: La Dorada: San Roque, Reserva Natural Privada Riomanso (5.666667N, -74.766667W; 280 m)	DQ502703	-	DQ502272	DQ502272
Allobates olfersioides	MRT 6031	Brazil: Bahia: São José da Vitória, Fazenda Unacau (-15.150000S, -39.300000W)	DQ502557	-	DQ502126	DQ502126
Allobates ornatus	MHNSM 22863	Peru: San Martin: 17km W from Tarapoto to Moyobamba	-	EU342550	EU342550	EU342550
Allobates paleovarzensis	MJH 3909	Brazil: Amazonas: Facenda São Francisco, 2 km N km 49 on Manaus-Manacapuru road	DQ502541	-	DQ502109	DQ502109
Allobates peruvianus	MHNSM 22923	Peru: San Martin: Road to San Jose de Sisa (-6.633944S, -76.624944W)	-	EU342524	EU342524	EU342524
Allobates pittieri	MIZA 339	Venezuela: Aragua: La Trilla (10.391200N, -67.749748W; 127 m)	-	-	-	-
Allobates pittieri	MHNLS 21229	Venezuela: Falcón: Sierra de San Luis, Hacienda Las Filipinas (11.226269N, -69.615781; 1,386 m)	**Lpi1**	**Lpi1**	**Lpi1**	-
Allobates subfolionidificans	APL 1692	Brazil: Acre: Rio Branco (-9.950000S, -67.950000W)	-	-	-	-
Allobates sumtuosus	MTD 47771	Guyana: Mabura Hill Forest Reserve	KC520692	-	KC520681	-
Allobates talamancae	QCAZ 16549	Ecuador: Carchi, Rio Baboso near Lita (534 m)	HQ290552	-	HQ290974	HQ290974
Allobates talamancae	SIUC 7667	Panama: Coclé: El Copé, Parque Nacional General de División "Omar Torrijos Herrera"	DQ502601	-	DQ502166	DQ502166
Allobates tapajos	LSUMZ 15176	Brazil: Pará: 101 km S and 15 km E Santarém (near Rio Curuá-una) (-3.150000S, -54.833333W)	DQ502477	-	DQ502046	DQ502046
Allobates tinae	MPEG 13826	Brazil: Amazonas: Castanho: ca. 40 km S Manaus, at km 12 on road to Autazes (-3.619556S, -60.455111W)	DQ502531	-	DQ502099	DQ502099
Allobates trilineatus	KU 215175	Peru: Madre de Dios: Cusco Amazónico, 15 km E Puerto Maldonado (200 m)	DQ502423	-	DQ501998	DQ501998
Allobates undulatus	AMNHA 159139	Venezuela: Amazonas: Cerro Yutajé (5.766667N, -66.133333W; 1,700 m)	DQ502459	-	DQ283044	DQ283044
Allobates zaparo	QCAZ 16603	Ecuador: Napo: Jatun Sacha, vía Ahuano (390 m)	HQ290580	-	HQ291003	HQ291003

Species	Voucher	Locality	Cyt-b	tRNA-Phe	12S	tRNA-Val
Allobates sp. (Alto Mazan)	MZ 010	Peru: Loreto: Alto Mazan (-2.586111S, -74.492222W)	-	-	MF624185	MF624185
Allobates sp. (Carajas)	TG 3264	Brazil: Pará: Paraupebas, Floresta Nacional de Carajás, Igarapé Bahia, area around tunnel at Galeria do Alemão	MF614177	-	-	MF624180
Allobates sp. (Cuao)	MHNLS 19982	Venezuela: Amazonas: near Tobogán del Cuao (5.104056N, -67.507917W; 100 m)	-	-	-	-
Allobates sp. (Cuyabeno)	OMNH 34086	Ecuador: Sucumbíos: Estación Científica de Universidad Católica near Reserva Faunística Cuyabeno (-0.000000S, -76.166667; 220 m)	DQ502472	-	DQ502041	DQ502041
Allobates sp. (Liberdade)	MCP 10212	Brazil: Acre: Cruzeiro do Sul, Reserva Extrativista Riozinho Liberdade, near Igarap_ Esperan □a	MF614180	-	MF624184	MF624184
Allobates sp. (Neblina)	AMCC 106112	Venezuela: Amazonas: Rio Negro: Neblina Base Camp on Rio Mawarinuma (0.833333N, -66.166667W; 140 m)	DQ502505	-	DQ502074	DQ502074
Allobates sp. (PEGM1)	LSUMZ 17601	Brazil: Rondônia: Parque Estadual Guajarà-Mirim (-10.321444S, -64.563306W)	DQ502568	-	DQ502136	DQ502136
Allobates sp. (PEGM3)	MPEG 13386	Brazil: Rondônia: Parque Estadual Guajará-Mirim (-10.321444S, -64.563306W)	DQ502571	-	DQ502139	DQ502139
Ameerega trivittata	TNHC 4966 / MPEG 12504	Colombia: Amazonas: Leticia, Cerca Viva (83 m)	HQ290579	-	HQ291002	HQ291002
Anomaloglossus apiau	MTR 37501	Brazil: Roraima: Serra do Apiau (580 m)	MF614192	-	MF624198	MF624198
Anomaloglossus baeobatrachus 1	AF 2590	French Guiana: Saint-Elie, crique Saint Eugene	KU958559	KU958559	KU958559	KU958559
Anomaloglossus baeobatrachus 2	MTR 13861	Brazil: Amapá: Lourenço	-	-	-	-
Anomaloglossus beebei	ROM 39631	Guyana: Mount Ayanganna, northeast plateau (5.400000N, -59.950000W; 1,490 m)	DQ502558	-	DQ502127	DQ502127
Anomaloglossus blanci	AF 932	French Guiana: montagne de Kaw, Crique Patawa	MG264895	MG264895	MG264895	MG264895
Anomaloglossus degranvillei	PG 601	French Guiana: Mounts Atachi-Bakka, alt. 650m	MG264892	MG264892	MG264892	MG264892
Anomaloglossus dewynteri	PG 660	French Guiana: Mount Itoupe	MG264891	MG264891	MG264891	MG264891
Anomaloglossus kaiei	279	Guyana: Mereme Mountains	DQ502446	-	DQ502020	DQ502020
Anomaloglossus leopardus	AF 2041	Suriname: Sipaliwini (2.178100N, -56.085200W)	-	-	-	-
Anomaloglossus meansi	ROM 39639	Guyana: Mount Ayanganna, northeast plateau (5.400000N, -59.950000W; 1,490 m)	DQ502560	-	DQ502129	DQ502129
Anomaloglossus megacephalus	ROM 39637	Guyana: Mount Ayanganna, northeast plateau (5.400000N, -59.950000W; 1,490 m)	DQ502559	-	DQ502128	DQ502128
Anomaloglossus praderioi	CPI 10208	Guyana: Mazaruni-Potoro: Mt. Roraima (1,310 m)	DQ502688	-	DQ502256	DQ502256
Anomaloglossus roraima	06-141	Guyana: Maringma Tepui	MF614240	-	MF624249	MF624249
Anomaloglossus rufulus	MHNLS 20610	Venezuela: Bolívar: Chimanta massif, summit of Eruoda-tepui (5.375444N, -62.094528W; 2,638 m)	**Nru2**	**Nru2**	**Nru2**	-

Species	Voucher	Locality	Cyt-b	tRNA-Phe	12S	tRNA-Val
Anomaloglossus rufulus	CLBA / voucher 214 (Vacher et al)	Venezuela: Bolívar: summit of Churi-tepui (5.300000N, -62.166700W)	-	KJ940456	KJ940456	KJ940456
Anomaloglossus mitaraka	AF 2732	French Guiana: Mitaraka (2.235700N, -54.449200W)	-	-	-	-
Anomaloglossus stepheni	AF 2045	Suriname: Sipaliwini	-	-	-	-
Anomaloglossus stepheni	MJH 3928	Brazil: Amazonas: Reserva Florestal Adolfo Ducke	DQ502539	-	DQ502107	DQ502107
Anomaloglossus surinamensis 1	AF 585	French Guiana: Saint-Elie, piste Saint-Elie	MG264890	MG264890	MG264890	MG264890
Anomaloglossus surinamensis 2	AF 2456	Suriname: Nassau mountain	MG264894	MG264894	MG264894	MG264894
Anomaloglossus surinamensis 5	AF 3340	Suriname: Bakhuis mountains	MG264893	MG264893	MG264893	MG264893
Anomaloglossus tamacuarensis	MNRJ 38049	Brazil: Amazonas: Barcelos, Serra do Tapirapecó, base camp at southern versant of Pico Tamacuari (1.207222N, -64.788333W; 350 m)	MF614193	-	MF624199	MF624199
Anomaloglossus tepuyensis	MHNLS 15613	Venezuela: Bolívar: Purumay-vena, Cucurital (5.880000N, -62.756111W; 430 m)	**Nte1**	**Nte1**	**Nte1**	-
Anomaloglossus tepuyensis	VUB 3734	Venezuela: Bolívar: Auyán-tepui (5.766667N, -62.550000W; 2,100 m)	-	-	-	-
Anomaloglossus verbeeksnyderorum	MHNLS 20084	Venezuela: Amazonas: Tobogán de la selva (5.468611N, -67.613361W; 148 m)	-	-	-	-
Anomaloglossus verbeeksnyderorum	MHNLS 20085	Venezuela: Amazonas: Tobogán de la selva (5.468611N, -67.613361W; 148 m)	-	-	-	-
Anomaloglossus verbeeksnyderorum	TNHC5631	Venezuela: Amazonas: Tobogán de la Selva (5.468611N, -67.613361W; 148 m)	HQ290532	-	HQ290952	HQ290952
Anomaloglossus wothuja	MHNLS 19952 / VUB 3735	Venezuela: Amazonas: Tobogán del Cuao (5.098500N, -67.494556W; 144 m)	-	-	-	-
Anomaloglossus wothuja	MHNLS 19953 / VUB 3736	Venezuela: Amazonas: Tobogán del Cuao (5.098500N, -67.494556W; 144 m)	-	-	-	-
Anomaloglossus sp. (Brownsberg)	UTAA 56469	Suriname: Brokopondo: Brownsberg Nature Park	DQ502681	-	DQ502249	DQ502249
Anomaloglossus sp. A (Wokomung)	VUB 3128	Guyana: Wokomung Massif (5.109722N, -59.810278W; 700 m)	-	-	-	-
Anomaloglossus sp. (Bakhuis)	AF 3426	Suriname: Bakhuis (5.232800N, -55.804600W)	-	-	-	-
Anomaloglossus sp. (Brownsberg)	BPN 0850	Suriname: Brownsberg	-	-	JN690359	-
Anomaloglossus sp. (Ichún)	MHNLS 17561	Venezuela: Bolívar: Salto Ichún (4.767778N, -63.465833W)	-	-	-	-
Anomaloglossus sp. (Thomasing)	UTAA 56710	Guyana: Mazaruni-Potaro: Mt. Thomasing (~2 km N Imbaimadai) (5.739667N, -60.297583W)	DQ502686	-	DQ502254	DQ502254
Rheobates pseudopalmatus	MHUA 5162	Colombia: Antioquia, Anori, Quebrada 2	-	-	-	-
Rheobates palmatus	MUJ 3829	Colombia: Meta: Villavicencio, Vereda El Carmen, Caño Blanco (900 m)	MF614234	-	MF624243	MF624243

Species	Voucher	Locality	Cyt-b	tRNA-Phe	12S	tRNA-Val
Rheobates palmatus	TNHC 4955	Colombia: Boyacá: Villa de Leiva (2118 m)	HQ290545	-	HQ290967	HQ290967
Hyloxalus cepedai	MAA 574	Colombia: Meta: Villavicencio, Barrio Vanguardia, carretera Vieja Villavicencio-Restrepo, km 2 (550 m)	MF614220	-	-	MF624226
Leucostethus fugax	QCAZ 16513	Ecuador: Morona Santiago: 2 km E Santiago (495 m)	HQ290538	-	HQ290958	HQ290958
Leucostethus brachistriatus	MHNUC 360	Colombia: Cauca: Popayán, Hacienda La Paz (2.478400N, -76.604280W; 1,740 m)	DQ502611	-	DQ502175	DQ502175
Silverstoneia nubicola	SIUC 7652	Panama: Coclé: El Copé, Parque Nacional General de División "Omar Torrijos Herrera"	DQ502596	-	DQ502161	DQ502161
Epipedobates tricolor	QCAZ 21977	Ecuador: Cotopaxi: Corazón-Moraspungo (1,250 m)	HQ290578	-	HQ291001	HQ291001
Ectopoglossus saxatilis	IAvH 14617	Colombia: Chocó: Unguña, Balboa, small tributary of the headwaters of the Rio Tanelita, NW flank of Cerro Tacarcuna, Serranía del Darién (8.233694N, -77.281000W; 1,100 m)	MF614214	-	MF624220	MF624220
Paruwrobates erythromos	QCAZ 37750	Ecuador: Los Rios: Centro Científico Rio Palenque (CCRP) (-0.583300S, -79.350000)	-	KJ940458	KJ940458	KJ940458
Phyllobates bicolor	1233	Colombia: No data (captive bred)	DQ502617	-	DQ502181	DQ502181
"Colostethus" ruthveni	MAR 558	Colombia: Magdalena: cuchilla de San Lorenzo, abajo de la Estación Experimental San Lorenzo, borde de carretera (1,600 m)	MF614195	-	MF624201	MF624201
Minyobates steyermarki	Roberts et al. / Vences et al.	Venezuela: Amazonas: Cerro Yapacana	DQ371340	-	DQ371310	-
Oophaga pumilio	TNHC 4814	Panama: Bocas del Toro: Isla Colón, Bocas del Drago (Dragomar) (11 m)	HQ290565	-	HQ290988	HQ290988
Dendrobates tinctorius	TNHC64416 / UTA 56495	Surinam: captivity breed	HQ290568	-	HQ290991	HQ290991
Exidobates captivus	QCAZ 27442	Ecuador: Zamora Chinchipe: near Panguitza (870 m)	HQ290559	-	HQ290982	HQ290982
Ranitomeya toraro	OMNH 36666	Brazil: Amazonas: Rio Ituxi: Scheffer Madeireira (-8.479389S, -65.716556W)	DQ502502	-	DQ502071	DQ502071
Thoropa miliaris	AF 1434	Brazil: São Paulo: Santos	JX298411	-	KF214095	-

Continued (part 2)…

Species	Voucher	16S	tRNA-Leu	ND1	tRNA-Ile	tRNA-Gln	tRNA-Met	ND2	tRNA-Trp	tRNA-Ala
Aromobates cannatellai	CVULA 8325	JX035995	-	-	-	-	-	-	-	-
Aromobates cannatellai	MHNLS 22625	**Acn1**	-	-	-	-	-	-	-	-
Aromobates cannatellai	MHNLS 22626	**Acn2**	-	-	-	-	-	-	-	-
Aromobates cannatellai	MHNLS 22627	**Acn3**	-	-	-	-	-	-	-	-
Aromobates cannatellai	MHNLS 22629	**Acn4**	-	-	-	-	-	-	-	-
Aromobates sp. (aff. *cannatellai*)	Asa4	**Asa4**	-	-	-	-	-	-	-	-
Aromobates sp. (aff. *cannatellai*)	MUJ 3726	DQ502274	-	-	-	-	-	-	-	-
Aromobates sp. (aff. *cannatellai*)	Tama14	**14**	-	-	-	-	-	-	-	-
Aromobates ericksonae	TNHC 5540	HQ290953	HQ290953	HQ290953	HQ290953	HQ290953	HQ290953	HQ290953	HQ290953	HQ290953
Aromobates ericksonae	CVULA 7180	JX035993	-	-	-	-	-	-	-	-
Aromobates ericksonae	CVULA8379	JX035994	-	-	-	-	-	-	-	-
Aromobates ericksonae	ULABG 7776	**Aer1**	-	-	-	-	-	-	-	-
Aromobates mayorgai	MHNLS 21981	**Aer2**	-	-	-	-	-	-	-	-
Aromobates mayorgai	MHNLS 21982	**Aer3**	-	-	-	-	-	-	-	-
Aromobates mayorgai	MHNLS 21983	**Aer4**	-	-	-	-	-	-	-	-
Aromobates mayorgai	MHNLS 21984	**Aer5**	-	-	-	-	-	-	-	-
Aromobates mayorgai	MHNLS 22002	**Ama1**	-	-	-	-	-	-	-	-
Aromobates mayorgai	MHNLS 22003	**Ama2**	-	-	-	-	-	-	-	-
Aromobates mayorgai	MHNLS 22005	**Ama4**	-	-	-	-	-	-	-	-
Aromobates mayorgai	MHNLS 22030	**Ama5**	-	-	-	-	-	-	-	-
Aromobates mayorgai	MHNLS 22031	**Ama6**	-	-	-	-	-	-	-	-
Aromobates mayorgai	MHNLS22032	**Ama7**	-	-	-	-	-	-	-	-
Aromobates mayorgai	MHNLS 22033	**Ama8**	-	-	-	-	-	-	-	-
Aromobates meridensis	CVULA7399	JX035992	-	-	-	-	-	-	-	-
Aromobates meridensis	MHNLS22016	**Ame1**	-	-	-	-	-	-	-	-

Species	Voucher	16S	tRNA-Leu	ND1	tRNA-Ile	tRNA-Gln	tRNA-Met	ND2	tRNA-Trp	tRNA-Ala
Aromobates meridensis	MHNLS 22017	**Ame2**	-	-	-	-	-	-	-	-
Aromobates meridensis	MHNLS 22018	**Ame3**	-	-	-	-	-	-	-	-
Aromobates meridensis	MHNLS 22019	**Ame4**	-	-	-	-	-	-	-	-
Aromobates molinarii	ULABG 4497	AY263263, AJ430678	-	-	-	-	-	-	-	-
Aromobates molinarii	ULABG sn1	**Amo3**	-	-	-	-	-	-	-	-
Aromobates molinarii	ULABG sn2	**Amo4**	-	-	-	-	-	-	-	-
Aromobates molinarii	ULABG sn3	**Amo5**	-	-	-	-	-	-	-	-
Aromobates nocturnus	AMNHA 130041	DQ502154	-	-	-	-	-	-	-	-
Aromobates nocturnus	AMNHA 130042	DQ502156	-	-	-	-	-	-	-	-
Aromobates ornatissimus	ULABG 4445	AY263229	-	-	-	-	-	-	-	-
Aromobates ornatissimus	CVULA 8351	JN584174	-	-	-	-	-	-	-	-
Aromobates ornatissimus	WES 626	DQ502242	-	-	-	-	-	-	-	-
Aromobates saltuensis	ULABG 4981	**Asa1**	-	-	-	-	-	-	-	-
Aromobates saltuensis	TNHC 5541	HQ290970	HQ290970	HQ290970	HQ290970	HQ290970	HQ290970	HQ290970	HQ290970	HQ290970
Aromobates saltuensis	ULABG AGu1	**AGu1**	-	-	-	-	-	-	-	-
Aromobates saltuensis	MHNLS 17233	**Asa5**	-	-	-	-	-	-	-	-
Aromobates sp. (aff. *saltuensis* 1)	CVULA 8321	JX035996	-	-	-	-	-	-	-	-
Aromobates sp. (aff. *saltuensis* 1)	MHNLS 22498	**Asa3**	-	-	-	-	-	-	-	-
Aromobates sp. (aff. *saltuensis* 3)	AOH	**ACo1**	-	-	-	-	-	-	-	-
Aromobates sp. (aff. *saltuensis* 2)	LOA 124	**ACo2**	-	-	-	-	-	-	-	-
Aromobates sp. (aff. *saltuensis* 4)	T10_1	**ACo3**	-	-	-	-	-	-	-	-
Aromobates sp. (aff. *saltuensis* 4)	T10_2	**ACo4**	-	-	-	-	-	-	-	-
Aromobates tokuko	MHNLS 18478	**Ato1**	-	-	-	-	-	-	-	-
Aromobates tokuko	MHNLS 18483	**Ato2**	-	-	-	-	-	-	-	-
Aromobates tokuko	MHNLS 18493	**Ato3**	-	-	-	-	-	-	-	-
Aromobates tokuko	MHNLS 18566	**Ato4**	-	-	-	-	-	-	-	-

Species	Voucher	16S	tRNA-Leu	ND1	tRNA-Ile	tRNA-Gln	tRNA-Met	ND2	tRNA-Trp	tRNA-Ala
Aromobates zippeli	MHNLS 22042	**Azi1**	-	-	-	-	-	-	-	-
Aromobates zippeli	MHNLS 22043	**Azi2**	-	-	-	-	-	-	-	-
Aromobates zippeli	MHNLS 22044	**Azi3**	-	-	-	-	-	-	-	-
Aromobates zippeli	MHNLS 22045	**Azi4**	-	-	-	-	-	-	-	-
Aromobates zippeli	MIZA 310	EU380798	-	-	-	-	-	-	-	-
Aromobates zippeli	MIZA 311	EU380799	-	-	-	-	-	-	-	-
Aromobates zippeli	MIZA 312	EU380800	-	-	-	-	-	-	-	-
Aromobates zippeli	ULABG 4496	AJ430677	-	-	-	-	-	-	-	-
Aromobates sp. 1	MHNLS 21506	**ATi1**	-	-	-	-	-	-	-	-
Aromobates sp. 1	MHNLS 21507	**ATi2**	-	-	-	-	-	-	-	-
Aromobates sp. 1	MHNLS 21508	**ATi3**	-	-	-	-	-	-	-	-
Aromobates sp. 1	MHNLS 22127	**ATi4**	-	-	-	-	-	-	-	-
Aromobates sp. 1	MHNLS 22128	**ATi5**	-	-	-	-	-	-	-	-
Aromobates cf. sp. 1	MHNLS 21333	**ARo1**	-	-	-	-	-	-	-	-
Aromobates cf. sp. 1	MHNLS 21334	**ARo2**	-	-	-	-	-	-	-	-
Aromobates cf. sp. 1	MHNLS 21335	**ARo3**	-	-	-	-	-	-	-	-
Aromobates cf. sp. 1	MHNLS 21358	**ARo4**	-	-	-	-	-	-	-	-
Aromobates cf. sp. 1	MHNLS 21359	**ARo5**	-	-	-	-	-	-	-	-
Aromobates sp. 2	CVULA 5718	JX035991	-	-	-	-	-	-	-	-
Aromobates sp. 2	MHNLS 22093b	**AAl2**	-	-	-	-	-	-	-	-
Aromobates sp. 2	MHNLS 22093c	**AAl3**	-	-	-	-	-	-	-	-
Aromobates sp. 2	MHNLS 22093d	**AAl4**	-	-	-	-	-	-	-	-
Mannophryne caquetio	MIZA 333	EU380835	-	-	-	-	-	-	-	-
Mannophryne caquetio	MIZA 337	EU380836	-	-	-	-	-	-	-	-
Mannophryne caquetio	MIZA 323	EU380837	-	-	-	-	-	-	-	-
Mannophryne caquetio	MIZA 338	EU380838	-	-	-	-	-	-	-	-

Species	Voucher	16S	tRNA-Leu	ND1	tRNA-Ile	tRNA-Gln	tRNA-Met	ND2	tRNA-Trp	tRNA-Ala
Mannophryne caquetio	MHNLS 21219	**MCh1**	-	-	-	-	-	-	-	-
Mannophryne caquetio	MHNLS 21220	**MCh2**	-	-	-	-	-	-	-	-
Mannophryne collaris	TNHC 5515	KJ940466	-	-	-	-	-	-	-	-
Mannophryne collaris	TNHC 5507	HQ291004	HQ291004	HQ291004	HQ291004	HQ291004	HQ291004	HQ291004	-	-
Mannophryne collaris	MIZA 320	EU380833	-	-	-	-	-	-	-	-
Mannophryne collaris	MIZA 321	EU380834	-	-	-	-	-	-	-	-
Mannophryne collaris	ULABG 4248	AJ430675	-	-	-	-	-	-	-	-
Mannophryne collaris	MHNLS 21590	**Mco5**	-	-	-	-	-	-	-	-
Mannophryne collaris	MHNLS 21591	**Mco6**	-	-	-	-	-	-	-	-
Mannophryne collaris	MHNLS 21592	**Mco7**	-	-	-	-	-	-	-	-
Mannophryne collaris	MHNLS 21593	**Mco8**	-	-	-	-	-	-	-	-
Mannophryne collaris	MHNLS 22058	**Mco11**	-	-	-	-	-	-	-	-
Mannophryne collaris	MHNLS 21684	**Mco1**	-	-	-	-	-	-	-	-
Mannophryne collaris	MHNLS 21685	**Mco2**	-	-	-	-	-	-	-	-
Mannophryne collaris	MHNLS 21686	**Mco3**	-	-	-	-	-	-	-	-
Mannophryne collaris	MHNLS 21687	**Mco4**	-	-	-	-	-	-	-	-
Mannophryne cordilleriana	TNHC 5589	KJ940460	-	-	-	-	-	-	-	-
Mannophryne cordilleriana	MIZA 330	EU380828	-	-	-	-	-	-	-	-
Mannophryne cordilleriana	MIZA 331	EU380829	-	-	-	-	-	-	-	-
Mannophryne cordilleriana	MIZA 332	EU380830	-	-	-	-	-	-	-	-
Mannophryne cordilleriana	MHNLS 22098	**Mcd36**	-	-	-	-	-	-	-	-
Mannophryne cordilleriana	MHNLS 22099	**Mcd37**	-	-	-	-	-	-	-	-
Mannophryne cordilleriana	MHNLS 21693	**Mcd27**	-	-	-	-	-	-	-	-
Mannophryne cordilleriana	MHNLS 21761	**Mcd26**	-	-	-	-	-	-	-	-
Mannophryne cordilleriana	MHNLS 21625	**Mcd9**	-	-	-	-	-	-	-	-
Mannophryne cordilleriana	MHNLS 21626	**Mcd10**	-	-	-	-	-	-	-	-

Species	Voucher	16S	tRNA-Leu	ND1	tRNA-Ile	tRNA-Gln	tRNA-Met	ND2	tRNA-Trp	tRNA-Ala
Mannophryne cordilleriana	ULABG 5352	**Mcd1**	-	-	-	-	-	-	-	-
Mannophryne cordilleriana	MHNLS 21632	**Mcd15**	-	-	-	-	-	-	-	-
Mannophryne cordilleriana	MHNLS 21633	**Mcd16**	-	-	-	-	-	-	-	-
Mannophryne cordilleriana	MHNLS 21601	**Mcd3**	-	-	-	-	-	-	-	-
Mannophryne cordilleriana	MHNLS 21602	**Mcd4**	-	-	-	-	-	-	-	-
Mannophryne cordilleriana	MHNLS 22187	**Mcd38**	-	-	-	-	-	-	-	-
Mannophryne cordilleriana	MHNLS 22188	**Mcd39**	-	-	-	-	-	-	-	-
Mannophryne cordilleriana	MHNLS 21689	**Mcd22**	-	-	-	-	-	-	-	-
Mannophryne herminae	TNHC 5676	KJ940461	-	-	-	-	-	-	-	-
Mannophryne herminae	MIZA 329	EU380849	-	-	-	-	-	-	-	-
Mannophryne herminae	MIZA 328	EU380848	-	-	-	-	-	-	-	-
Mannophryne herminae	MIZA 327	EU380847	-	-	-	-	-	-	-	-
Mannophryne herminae	MHNLS 17475	**Mhe1**	-	-	-	-	-	-	-	-
Mannophryne herminae	MHNLS 21735	**Mhe2**	-	-	-	-	-	-	-	-
Mannophryne herminae	MHNLS 21736	**Mhe3**	-	-	-	-	-	-	-	-
Mannophryne herminae	MHNLS 22106	**Mhe6**	-	-	-	-	-	-	-	-
Mannophryne herminae	MHNLS 22107	**Mhe7**	-	-	-	-	-	-	-	-
Mannophryne aff. *herminae*	ULABG 4506	AY263269, AJ430676	-	-	-	-	-	-	-	-
Mannophryne lamarcai	MIZA 317	EU380845	-	-	-	-	-	-	-	-
Mannophryne lamarcai	MIZA 318	EU380846	-	-	-	-	-	-	-	-
Mannophryne lamarcai	NMA 38	**Mla1**	-	-	-	-	-	-	-	-
Mannophryne lamarcai	NMA 40	**Mla2**	-	-	-	-	-	-	-	-
Mannophryne lamarcai	NMA 41	**Mla3**	-	-	-	-	-	-	-	-
Mannophryne lamarcai	MHNLS 22087	**MCu1**	-	-	-	-	-	-	-	-
Mannophryne lamarcai	MHNLS 22088	**MCu2**	-	-	-	-	-	-	-	-
Mannophryne larandina	MIZA 324	EU380839	-	-	-	-	-	-	-	-

Species	Voucher	16S	tRNA-Leu	ND1	tRNA-Ile	tRNA-Gln	tRNA-Met	ND2	tRNA-Trp	tRNA-Ala
Mannophryne larandina	MIZA 325	EU380840	-	-	-	-	-	-	-	-
Mannophryne larandina	MIZA 326	EU380841	-	-	-	-	-	-	-	-
Mannophryne larandina	MHNLS 22597	**Mlr1**	-	-	-	-	-	-	-	-
Mannophryne larandina	MHNLS 22598	**Mlr2**	-	-	-	-	-	-	-	-
Mannophryne larandina	MHNLS 22599	**Mlr3**	-	-	-	-	-	-	-	-
Mannophryne "herminae"	CWM 1141	DQ502160	-	-	-	-	-	-	-	-
Mannophryne leonardoi	TNHC 5659	KJ940463	-	-	-	-	-	-	-	-
Mannophryne leonardoi	TTSR	EU380817	-	-	-	-	-	-	-	-
Mannophryne leonardoi	MIZA 316	EU380816	-	-	-	-	-	-	-	-
Mannophryne leonardoi	WES 1034	DQ502243	-	-	-	-	-	-	-	-
Mannophryne leonardoi	WES 1035	DQ502244	-	-	-	-	-	-	-	-
Mannophryne leonardoi	WES 1036	DQ502245	-	-	-	-	-	-	-	-
Mannophryne leonardoi	MHNLS 22333	**Mle2**	-	-	-	-	-	-	-	-
Mannophryne leonardoi	MHNLS 22334	**Mle3**	-	-	-	-	-	-	-	-
Mannophryne leonardoi	MHNLS 22335	**Mle4**	-	-	-	-	-	-	-	-
Mannophryne leonardoi	MHNLS 22336	**Mle5**	-	-	-	-	-	-	-	-
Mannophryne molinai	MHNLS 21336	**MRo1**	-	-	-	-	-	-	-	-
Mannophryne molinai	MHNLS 21337	**MRo2**	-	-	-	-	-	-	-	-
Mannophryne molinai	MHNLS 21338	**MRo3**	-	-	-	-	-	-	-	-
Mannophryne molinai	MHNLS 21356	**MRo6**	-	-	-	-	-	-	-	-
Mannophryne cf. *molinai*	MHNLS 21005	**MPg1**	-	-	-	-	-	-	-	-
Mannophryne cf. *molinai*	MHNLS 21006	**MPg2**	-	-	-	-	-	-	-	-
Mannophryne cf. *molinai*	MHNLS 21365	**MMa1**	-	-	-	-	-	-	-	-
Mannophryne cf. *molinai*	MHNLS 21367	**MMa3**	-	-	-	-	-	-	-	-
Mannophryne cf. *molinai*	MHNLS 21205	**MQh1**	-	-	-	-	-	-	-	-
Mannophryne cf. *molinai*	MHNLS 21206	**MQh2**	-	-	-	-	-	-	-	-

Species	Voucher	16S	tRNA-Leu	ND1	tRNA-Ile	tRNA-Gln	tRNA-Met	ND2	tRNA-Trp	tRNA-Ala
Mannophryne cf. *molinai*	MHNLS 21516	**MAb1**	-	-	-	-	-	-	-	-
Mannophryne cf. *molinai*	MHNLS 21517	**MAb2**	-	-	-	-	-	-	-	-
Mannophryne neblina	MHNLS 22362	**Mne3**	-	-	-	-	-	-	-	-
Mannophryne oblitterata	TTSR	EU380832	-	-	-	-	-	-	-	-
Mannophryne oblitterata	MIZA 336	EU380831	-	-	-	-	-	-	-	-
Mannophryne oblitterata	MHNLS 21766	**Mob1**	-	-	-	-	-	-	-	-
Mannophryne oblitterata	MHNLS 21767	**Mob2**	-	-	-	-	-	-	-	-
Mannophryne oblitterata	MHNLS 21818	**Mob4**	-	-	-	-	-	-	-	-
Mannophryne oblitterata	MHNLS 21819	**Mob5**	-	-	-	-	-	-	-	-
Mannophryne olmonae	MIZA 334 / isolate 451	AY191230	-	-	-	-	-	-	-	-
Mannophryne olmonae	MIZA335 / isolate 452	EU380825	-	-	-	-	-	-	-	-
Mannophryne olmonae	UWIZM 2732 / ZSM 1622	MF624237	-	-	-	-	-	-	-	-
Mannophryne orellana	CVULA 7165	KJ940464	-	-	-	-	-	-	-	-
Mannophryne orellana	CVULA 7231	KJ940465	-	-	-	-	-	-	-	-
Mannophryne orellana	ULABG 7469	**Mor1**	-	-	-	-	-	-	-	-
Mannophryne orellana	MHNLS MCp1	**MCp1**	-	-	-	-	-	-	-	-
Mannophryne orellana	MHNLS MCp2	**MCp2**	-	-	-	-	-	-	-	-
Mannophryne orellana	MHNLS MCp3	**MCp3**	-	-	-	-	-	-	-	-
Mannophryne riveroi	MIZA 319	EU380827	-	-	-	-	-	-	-	-
Mannophryne riveroi	TTSR	EU380826	-	-	-	-	-	-	-	-
Mannophryne riveroi	MHNLS16433 / TNHC 5644	**Mri1**, EU342503	-	-	-	-	-	-	-	-
Mannophryne riveroi	MHNLS 17910	**Mri3**	-	-	-	-	-	-	-	-
Mannophryne speeri	MHNLS 22606	**Msp1**	-	-	-	-	-	-	-	-
Mannophryne trinitatis	MVZ 199837	EU342504	JX564878	JX564878	JX564878	JX564878	JX564878	JX564878	JX564878	JX564878
Mannophryne trinitatis	MVZ199838 / isolate 405	DQ283071	-	-	-	-	-	-	-	-
Mannophryne trinitatis	MVZ 199828	DQ502131	-	-	-	-	-	-	-	-

Species	Voucher	16S	tRNA-Leu	ND1	tRNA-Ile	tRNA-Gln	tRNA-Met	ND2	tRNA-Trp	tRNA-Ala
Mannophryne trinitatis	ZSM 1619	**ZSM1619**	-	-	-	-	-	-	-	-
Mannophryne trinitatis	ZSM 1620	**ZSM1620**	-	-	-	-	-	-	-	-
Mannophryne trinitatis	ZSM 1621	**ZSM1621**	-	-	-	-	-	-	-	-
Mannophryne trujillensis	MHNLS 17963	**Mtr1**	-	-	-	-	-	-	-	-
Mannophryne trujillensis	MHNLS 17971	**Mtr2**	-	-	-	-	-	-	-	-
Mannophryne trujillensis	MHNLS 22070	**Mtr7**	-	-	-	-	-	-	-	-
Mannophryne trujillensis	MHNLS 22071	**Mtr8**	-	-	-	-	-	-	-	-
Mannophryne trujillensis	MHNLS 22063	**Mtr3**	-	-	-	-	-	-	-	-
Mannophryne trujillensis	MHNLS 22064	**Mtr4**	-	-	-	-	-	-	-	-
Mannophryne urticans	TNHC 5520	KJ940467	-	-	-	-	-	-	-	-
Mannophryne urticans	ULABG 4481	AY263223	-	-	-	-	-	-	-	-
Mannophryne urticans	MHNLS 21555	**Mur2**	-	-	-	-	-	-	-	-
Mannophryne urticans	MHNLS 21556	**Mur3**	-	-	-	-	-	-	-	-
Mannophryne urticans	MHNLS 21994	**MLo2**	-	-	-	-	-	-	-	-
Mannophryne urticans	MHNLS 21993	**MLo1**	-	-	-	-	-	-	-	-
Mannophryne venezuelensis	EBRG 4921 / isolate 469	EU380812	-	-	-	-	-	-	-	-
Mannophryne venezuelensis	EBRG 4922 / isolate 555 / isoalte 470	EU380813	-	-	-	-	-	-	-	-
Mannophryne venezuelensis	MHNLS 16435	**MHNLS 16435**	-	-	-	-	-	-	-	-
Mannophryne venezuelensis	MHNLS 17287	**MHNLS 17287**	-	-	-	-	-	-	-	-
Mannophryne venezuelensis	MHNLS 17314	**MHNL S17314**	-	-	-	-	-	-	-	-
Mannophryne venezuelensis	MHNLS 17315	**MHNLS 17315**	-	-	-	-	-	-	-	-
Mannophryne venezuelensis	TNHC 5649	KJ940468	-	-	-	-	-	-	-	-
Mannophryne vulcano	TNHC 5679	KJ940469	-	-	-	-	-	-	-	-
Mannophryne vulcano	MIZA 342	EU380820	-	-	-	-	-	-	-	-
Mannophryne vulcano	MIZA 343	EU380821	-	-	-	-	-	-	-	-

Species	Voucher	16S	tRNA-Leu	ND1	tRNA-Ile	tRNA-Gln	tRNA-Met	ND2	tRNA-Trp	tRNA-Ala
Mannophryne vulcano	MHNLS 16685	**Mvu1**	-	-	-	-	-	-	-	-
Mannophryne vulcano	MHNLS 22140	**Mvu36**	-	-	-	-	-	-	-	-
Mannophryne vulcano	MHNLS 22141	**Mvu37**	-	-	-	-	-	-	-	-
Mannophryne vulcano	MHNLS 22142	**Mvu38**	-	-	-	-	-	-	-	-
Mannophryne vulcano	MHNLS 20692	**Mvu4**	-	-	-	-	-	-	-	-
Mannophryne vulcano	MHNLS 20693	**Mvu5**	-	-	-	-	-	-	-	-
Mannophryne vulcano	MHNLS 18575	**Mvu2**	-	-	-	-	-	-	-	-
Mannophryne vulcano	MHNLS 18577	**Mvu3**	-	-	-	-	-	-	-	-
Mannophryne vulcano	MHNLS 21802	**Mvu30**	-	-	-	-	-	-	-	-
Mannophryne vulcano	MHNLS 21803	**Mvu31**	-	-	-	-	-	-	-	-
Mannophryne vulcano	MHNLS 20830	**Mvu10**	-	-	-	-	-	-	-	-
Mannophryne vulcano	MHNLS 21770	**Mvu22**	-	-	-	-	-	-	-	-
Mannophryne vulcano	MHNLS 21771	**Mvu23**	-	-	-	-	-	-	-	-
Mannophryne vulcano	MHNLS 22346	**MLr1**	-	-	-	-	-	-	-	-
Mannophryne vulcano	MHNLS 20941	**Mvu11**	-	-	-	-	-	-	-	-
Mannophryne vulcano	MHNLS 20942	**Mvu12**	-	-	-	-	-	-	-	-
Mannophryne vulcano	MHNLS 21778	**Mvu26**	-	-	-	-	-	-	-	-
Mannophryne vulcano	MHNLS 21779	**Mvu27**	-	-	-	-	-	-	-	-
Mannophryne yustizi	TTSR_G	EU380844	-	-	-	-	-	-	-	-
Mannophryne yustizi	TNHC 5604	KJ940470	-	-	-	-	-	-	-	-
Mannophryne yustizi	TTSR_S	EU380842	-	-	-	-	-	-	-	-
Mannophryne yustizi	MIZA 322	EU380843	-	-	-	-	-	-	-	-
Mannophryne sp. 1	TTSR	EU380819	-	-	-	-	-	-	-	-
Mannophryne sp. 1	MIZA 341	EU380818	-	-	-	-	-	-	-	-
Mannophryne sp. 1	MHNLS 16769	**MHNLS 16769**	-	-	-	-	-	-	-	-
Mannophryne sp. 1	MHNLS 16772	**MHNLS**	-	-	-	-	-	-	-	-

Species	Voucher	16S	tRNA-Leu	ND1	tRNA-Ile	tRNA-Gln	tRNA-Met	ND2	tRNA-Trp	tRNA-Ala
		16772								
Mannophryne sp. 1	MHNLS 16773	**MHNLS 16773**	-	-	-	-	-	-	-	-
Mannophryne sp. 1	MHNLS 16798	**MHNLS 16798**	-	-	-	-	-	-	-	-
Mannophryne sp. (cf. *vulcano*)	MHNLS 21825	**MRa2**	-	-	-	-	-	-	-	-
Mannophryne sp. (cf. *vulcano*)	MHNLS 21826	**MRa3**	-	-	-	-	-	-	-	-
Mannophryne sp. 2	MIZA 340	EU380823	-	-	-	-	-	-	-	-
Mannophryne sp. 2	EBRG 4889	EU380822	-	-	-	-	-	-	-	-
Mannophryne sp. 2	MHNLS 17251	**MHNLS 17251**	-	-	-	-	-	-	-	-
Mannophryne sp. 2	MHNLS 17252	**MHNLS 17252**	-	-	-	-	-	-	-	-
Mannophryne sp. 2	MHNLS 17253	**MHNLS 17253**	-	-	-	-	-	-	-	-
Mannophryne sp. 2	MHNLS 17254	**MHNLS 17254**	-	-	-	-	-	-	-	-
Mannophryne sp. 2	MHNLS 17256	**MHNLS 17256**	-	-	-	-	-	-	-	-
Mannophryne sp. 2	MHNLS 15545	**MHNLS 15545**	-	-	-	-	-	-	-	-
Mannophryne sp. 3	MHNLS 22358	**MAg1**	-	-	-	-	-	-	-	-
Mannophryne sp. 3	MHNLS 22359	**MAg2**	-	-	-	-	-	-	-	-
Mannophryne sp. 3	MHNLS 22360	**MAg3**	-	-	-	-	-	-	-	-
Mannophryne sp. 3	MHNLS 22347	**MLr2**	-	-	-	-	-	-	-	-
Mannophryne sp. 3	MHNLS 22348	**MLr3**	-	-	-	-	-	-	-	-
Mannophryne sp. 3	MHNLS 22353	**MLr4**	-	-	-	-	-	-	-	-
Mannophryne sp. 3	MHNLS 21747	**MQo1**	-	-	-	-	-	-	-	-
Mannophryne sp. 3	MHNLS 21748	**MQo2**	-	-	-	-	-	-	-	-
Mannophryne sp. 4	MHNLS 22204	**MMo1**	-	-	-	-	-	-	-	-
Mannophryne sp. 4	MHNLS 22214	**MMo3**	-	-	-	-	-	-	-	-
Mannophryne sp. 4	MHNLS 22219	**MMo4**	-	-	-	-	-	-	-	-

Species	Voucher	16S	tRNA-Leu	ND1	tRNA-Ile	tRNA-Gln	tRNA-Met	ND2	tRNA-Trp	tRNA-Ala
Mannophryne sp. 4	MHNLS 22281	**MMo5**	-	-	-	-	-	-	-	-
Mannophryne sp. 4	MHNLS 22302	**MMo6**	-	-	-	-	-	-	-	-
Mannophryne sp. 4	MHNLS 22303	**MMo7**	-	-	-	-	-	-	-	-
Mannophryne sp. 4	MHNLS 22304	**MMo8**	-	-	-	-	-	-	-	-
Mannophryne sp. (aff. *herminae*)	MHNLS 17157	**MHNLS 17157**	-	-	-	-	-	-	-	-
Mannophryne sp. (aff. *herminae*)	MHNLS 17158	**MHNLS 17158**	-	-	-	-	-	-	-	-
Mannophryne sp. (aff. *herminae*)	MHNLS 17159	**MHNLS 17159**	-	-	-	-	-	-	-	-
Mannophryne sp. (aff. *herminae*)	MHNLS 17160	**MHNLS 17160**	-	-	-	-	-	-	-	-
Mannophryne sp. (*yustizi* complex)	MHNLS 22585	-	-	-	-	-	-	-	-	-
Mannophryne sp. (*yustizi* complex)	MHNLS 22586	-	-	-	-	-	-	-	-	-
Mannophryne sp. (aff. *vulcano*)	TNHC 5666	KJ940462	-	-	-	-	-	-	-	-
Mannophryne sp. (*yustizi* complex)	ULABG 4465	AY263222	-	-	-	-	-	-	-	-
Mannophryne sp. (*yustizi* complex)	ULABG 4453	AY263221	-	-	-	-	-	-	-	-
Mannophryne sp. (*yustizi* complex)	ULABG 4458	AY263224	-	-	-	-	-	-	-	-
Mannophryne sp. (*yustizi* complex)	MHNLS 22080	**MJa1**	-	-	-	-	-	-	-	-
Mannophryne sp. (*yustizi* complex)	MHNLS 22081	**MJa2**	-	-	-	-	-	-	-	-
Mannophryne sp. (*yustizi* complex)	MHNLS 22617	**Msp6**	-	-	-	-	-	-	-	-
Mannophryne sp. (cf. *speeri-yustizi*)	MHNLS 22618	**Msp7**	-	-	-	-	-	-	-	-
Mannophryne sp. (*yustizi* complex)	MHNLS 22619	**Msp8**	-	-	-	-	-	-	-	-
Mannophryne sp. (cf. *speeri-yustizi*)	MHNLS 22169	**MNi1**	-	-	-	-	-	-	-	-
Mannophryne sp. (*yustizi* complex)	MHNLS 22170	**MNi2**	-	-	-	-	-	-	-	-
Mannophryne sp. (*yustizi* complex)	MHNLS 22171	**MNi3**	-	-	-	-	-	-	-	-
Mannophryne sp. (*yustizi* complex)	MHNLS 22172	**MNi4**	-	-	-	-	-	-	-	-
Mannophryne sp. (*yustizi* complex)	MHNLS 22559	**Myu4**	-	-	-	-	-	-	-	-
Mannophryne sp. (*yustizi* complex)	MHNLS 22560	**Myu3**	-	-	-	-	-	-	-	-

Species	Voucher	16S	tRNA-Leu	ND1	tRNA-Ile	tRNA-Gln	tRNA-Met	ND2	tRNA-Trp	tRNA-Ala
Andinobates bombetes	TNHC 4946 / MAR 1265	HQ290981	HQ290981	HQ290981	HQ290981	HQ290981	HQ290981	HQ290981	-	-
Adelphobates galactonotus	TNHC 4889 / MTR 5088	HQ290984	HQ290984	HQ290984	HQ290984	HQ290984	HQ290984	HQ290984	-	-
Allobates aff. *juanii*	ANDESA 1073	KJ130697	-	-	-	-	-	-	-	-
Allobates algorei	TNHC 5551	HQ290950	HQ290950	HQ290950	HQ290950	HQ290950	HQ290950	HQ290950	-	-
Allobates amissibilis	MTD 47884	KC520680	-	-	-	-	-	-	-	-
Allobates bacurau	INPAH 35406	KU195698	-	-	-	-	-	-	-	-
Allobates caeruleodactylus	MPEG 13809	DQ502100	-	-	-	-	-	-	-	-
Allobates chalcopis	Alca1	KC520675, KC520676	-	-	-	-	-	-	-	-
Allobates conspicuus	MPEG 12321	DQ502134	-	-	-	-	-	-	-	-
Allobates crombiei	APL 14124	KJ747346	-	-	-	-	-	-	-	-
Allobates femoralis (Acre01)	Acre 12931	GU017463	-	-	-	-	-	-	-	-
Allobates femoralis (Acre02)	OMNH 36070	DQ502092	-	-	-	-	-	-	-	-
Allobates femoralis	QCAZ 16484	HQ290951	HQ290951	HQ290951	HQ290951	HQ290951	HQ290951	HQ290951	-	-
Allobates flaviventris	OMNH 36959	DQ502184	-	-	-	-	-	-	-	-
Allobates fratisenescus	QCAZ 54377	MF624172	-	-	-	-	-	-	-	-
Allobates gasconi	MPEG 13003	DQ502052	-	-	-	-	-	-	-	-
Allobates granti	148 AF	JN690181	-	-	-	-	-	-	-	-
Allobates grillisimilis	APL 12747	KF250504	-	-	-	-	-	-	-	-
Allobates hodli	AbuE 2189	GU017423	-	-	-	-	-	-	-	-
Allobates humilis	CVULA 5690	KJ940454	-	-	-	-	-	-	-	-
Allobates humilis	MHNLS22093a	**Lhu1**	-	-	-	-	-	-	-	-
Allobates insperatus	QCAZ1 6533	HQ290959	HQ290959	HQ290959	HQ290959	HQ290959	HQ290959	HQ290959	-	-
Allobates juami	MCP 13287	MG243349	-	-	-	-	-	-	-	-
Allobates juanii	TNHC 4978	HQ290960	HQ290960	-	-	-	-	-	-	-
Allobates kingsburyi	QCAZ 16523	HQ290963	HQ290963	HQ290963	HQ290963	HQ290963	HQ290963	HQ290963	-	-
Allobates magnussoni	MPEG 11923	DQ502132	-	-	-	-	-	-	-	-

Species	Voucher	16S	tRNA-Leu	ND1	tRNA-Ile	tRNA-Gln	tRNA-Met	ND2	tRNA-Trp	tRNA-Ala
Allobates masniger	APL 14250	JQ966886	-	-	-	-	-	-	-	-
Allobates myersi	INPAH 26396	MG252614	-	-	-	-	-	-	-	-
Allobates nidicola	MPEG 13821	DQ502101	-	-	-	-	-	-	-	-
Allobates niputidea	MUJ 3520	DQ502272	-	-	-	-	-	-	-	-
Allobates olfersioides	MRT 6031	DQ502126	-	-	-	-	-	-	-	-
Allobates ornatus	MHNSM 22863	EU342550	-	-	-	-	-	-	-	-
Allobates paleovarzensis	MJH 3909	DQ502109	-	-	-	-	-	-	-	-
Allobates peruvianus	MHNSM 22923	EU342524	-	-	-	-	-	-	-	-
Allobates pittieri	MIZA 339	EU380803	-	-	-	-	-	-	-	-
Allobates pittieri	MHNLS 21229	**Lpi1**	-	-	-	-	-	-	-	-
Allobates subfolionidificans	APL 1692	KF250493	-	-	-	-	-	-	-	-
Allobates sumtuosus	MTD 47771	KC520682	-	-	-	-	-	-	-	-
Allobates talamancae	QCAZ 16549	HQ290974	HQ290974	HQ290974	HQ290974	HQ290974	HQ290974	HQ290974	HQ290974	HQ290974
Allobates talamancae	SIUC 7667	DQ502166	-	-	-	-	-	-	-	-
Allobates tapajos	LSUMZ 15176	DQ502046	-	-	-	-	-	-	-	-
Allobates tinae	MPEG 13826	DQ502099	-	-	-	-	-	-	-	-
Allobates trilineatus	KU 215175	DQ501998	-	-	-	-	-	-	-	-
Allobates undulatus	AMNHA 159139	DQ283044	-	-	-	-	-	-	-	-
Allobates zaparo	QCAZ 16603	HQ291003	HQ291003	HQ291003	HQ291003	HQ291003	HQ291003	HQ291003	-	-
Allobates sp. (Alto Mazan)	MZ 010	MF624185	-	-	-	-	-	-	-	-
Allobates sp. (Carajas)	TG 3264	MF624180	-	-	-	-	-	-	-	-
Allobates sp. (Cuao)	MHNLS 19982	**AJC3036**	-	-	-	-	-	-	-	-
Allobates sp. (Cuyabeno)	OMNH 34086	DQ502041	-	-	-	-	-	-	-	-
Allobates sp. (Liberdade)	MCP 10212	MF624184	-	-	-	-	-	-	-	-
Allobates sp. (Neblina)	AMCC 106112	DQ502074	-	-	-	-	-	-	-	-
Allobates sp. (PEGM1)	LSUMZ 17601	DQ502136	-	-	-	-	-	-	-	-

Species	Voucher	16S	tRNA-Leu	ND1	tRNA-Ile	tRNA-Gln	tRNA-Met	ND2	tRNA-Trp	tRNA-Ala
Allobates sp. (PEGM3)	MPEG 13386	DQ502139	-	-	-	-	-	-	-	-
Ameerega trivittata	TNHC 4966 / MPEG 12504	HQ291002	HQ291002	HQ291002	HQ291002	HQ291002	HQ291002	HQ291002	-	-
Anomaloglossus apiau	MTR 37501	MF624198	-	-	-	-	-	-	-	-
Anomaloglossus baeobatrachus 1	AF 2590	KU958559	KU958559	KU958559	KU958559	KU958559	KU958559	KU958559	KU958559	KU958559
Anomaloglossus baeobatrachus 2	MTR 13861	JN691025	-	-	-	-	-	-	-	-
Anomaloglossus beebei	ROM 39631	DQ502127	-	-	-	-	-	-	-	-
Anomaloglossus blanci	AF 932	MG264895	MG264895	MG264895	MG264895	MG264895	MG264895	MG264895	MG264895	MG264895
Anomaloglossus degranvillei	PG 601	MG264892	MG264892	MG264892	MG264892	MG264892	MG264892	MG264892	MG264892	MG264892
Anomaloglossus dewynteri	PG 660	MG264891	MG264891	MG264891	MG264891	MG264891	MG264891	MG264891	MG264891	MG264891
Anomaloglossus kaiei	279	DQ502020	-	-	-	-	-	-	-	-
Anomaloglossus leopardus	AF 2041	KY510108	-	-	-	-	-	-	-	-
Anomaloglossus meansi	ROM 39639	DQ502129	-	-	-	-	-	-	-	-
Anomaloglossus megacephalus	ROM 39637	DQ502128	-	-	-	-	-	-	-	-
Anomaloglossus praderioi	CPI 10208	DQ502256	-	-	-	-	-	-	-	-
Anomaloglossus roraima	06-141	MF624249	-	-	-	-	-	-	-	-
Anomaloglossus rufulus	MHNLS 20610	**Nru2**	-	-	-	-	-	-	-	-
Anomaloglossus rufulus	CLBA / voucher 214 (Vacher et al)	KJ940456	-	-	-	-	-	-	-	-
Anomaloglossus mitaraka	AF 2732	KY510141	-	-	-	-	-	-	-	-
Anomaloglossus stepheni	AF 2045	KY510111	-	-	-	-	-	-	-	-
Anomaloglossus stepheni	MJH 3928	DQ502107	-	-	-	-	-	-	-	-
Anomaloglossus surinamensis 1	AF 585	MG264890	MG264890	MG264890	MG264890	MG264890	MG264890	MG264890	MG264890	MG264890
Anomaloglossus surinamensis 2	AF 2456	MG264894	MG264894	MG264894	MG264894	MG264894	MG264894	MG264894	MG264894	MG264894
Anomaloglossus surinamensis 5	AF 3340	MG264893	MG264893	MG264893	MG264893	MG264893	MG264893	MG264893	MG264893	MG264893
Anomaloglossus tamacuarensis	MNRJ 38049	MF624199	-	-	-	-	-	-	-	-
Anomaloglossus tepuyensis	MHNLS 15613	**Nte1**	-	-	-	-	-	-	-	-
Anomaloglossus tepuyensis	VUB 3734	JQ742104	-	-	-	-	-	-	-	-

Species	Voucher	16S	tRNA-Leu	ND1	tRNA-Ile	tRNA-Gln	tRNA-Met	ND2	tRNA-Trp	tRNA-Ala
Anomaloglossus verbeeksnyderorum	MHNLS 20084	**Nve1**	-	-	-	-	-	-	-	-
Anomaloglossus verbeeksnyderorum	MHNLS 20085	**Nve2**	-	-	-	-	-	-	-	-
Anomaloglossus verbeeksnyderorum	TNHC5631	HQ290952	HQ290952	HQ290952	HQ290952	HQ290952	HQ290952	HQ290952	HQ290952	HQ290952
Anomaloglossus wothuja	MHNLS 19952 / VUB 3735	**Nwo1**	-	JQ742283	-	-	-	-	-	-
Anomaloglossus wothuja	MHNLS 19953 / VUB 3736	**Nwo2**	-	JQ742284	-	-	-	-	-	-
Anomaloglossus sp. (Brownsberg)	UTAA 56469	DQ502249	-	-	-	-	-	-	-	-
Anomaloglossus sp. A (Wokomung)	VUB 3128	JQ742119	-	JQ742296	-	-	-	-	-	-
Anomaloglossus sp. (Bakhuis)	AF 3426	KY510165	-	-	-	-	-	-	-	-
Anomaloglossus sp. (Brownsberg)	BPN 0850	JN691039	-	-	-	-	-	-	-	-
Anomaloglossus sp. (Ichún)	MHNLS 17561	**NIc1**	-	-	-	-	-	-	-	-
Anomaloglossus sp. (Thomasing)	UTAA 56710	DQ502254	-	-	-	-	-	-	-	-
Rheobates pseudopalmatus	MHUA 5162	KJ130727	-	-	-	-	-	-	-	-
Rheobates palmatus	MUJ 3829	MF624243	-	-	-	-	-	-	-	-
Rheobates palmatus	TNHC 4955	HQ290967	HQ290967	HQ290967	HQ290967	HQ290967	HQ290967	HQ290967	-	-
Hyloxalus cepedai	MAA 574	MF624226	-	-	-	-	-	-	-	-
Leucostethus fugax	QCAZ 16513	HQ290958	HQ290958	HQ290958	HQ290958	HQ290958	HQ290958	HQ290958	-	-
Leucostethus brachistriatus	MHNUC 360	DQ502175	-	-	-	-	-	-	-	-
Silverstoneia nubicola	SIUC 7652	DQ502161	-	-	-	-	-	-	-	-
Epipedobates tricolor	QCAZ 21977	HQ291001	HQ291001	HQ291001	HQ291001	HQ291001	HQ291001	HQ291001	-	-
Ectopoglossus saxatilis	IAvH 14617	MF624220	-	-	-	-	-	-	-	-
Paruwrobates erythromos	QCAZ 37750	KJ940458	-	-	-	-	-	-	-	-
Phyllobates bicolor	1233	DQ502181	-	-	-	-	-	-	-	-
"Colostethus" ruthveni	MAR 558	MF624201	-	-	-	-	-	-	-	-
Minyobates steyermarki	Roberts et al. / Vences et al.	AY263244	-	-	-	-	-	-	-	-
Oophaga pumilio	TNHC 4814	HQ290988	HQ290988	HQ290988	HQ290988	HQ290988	HQ290988	HQ290988	HQ290988	HQ290988
Dendrobates tinctorius	TNHC64416 / UTA 56495	HQ290991	HQ290991	HQ290991	HQ290991	HQ290991	HQ290991	HQ290991	-	-

Species	Voucher	16S	tRNA-Leu	ND1	tRNA-Ile	tRNA-Gln	tRNA-Met	ND2	tRNA-Trp	tRNA-Ala
Exidobates captivus	QCAZ 27442	HQ290982	HQ290982	HQ290982	HQ290982	HQ290982	HQ290982	HQ290982	HQ290982	HQ290982
Ranitomeya toraro	OMNH 36666	DQ502071	-	-	-	-	-	-	-	-
Thoropa miliaris	AF 1434	GQ174532	-	-	-	-	-	GQ174934	GQ174934	GQ174934

Continued (part 3)…

Species	Voucher	tRNA-Asn	LSRO	tRNA-Cys	tRNA-Tyr	COI	RHO	H3F3C	TYR	RAG1
Aromobates cannatellai	CVULA 8325	-	-	-	-	-	-	-	-	-
Aromobates cannatellai	MHNLS 22625	-	-	-	-	-	-	-	-	-
Aromobates cannatellai	MHNLS 22626	-	-	-	-	-	-	-	-	-
Aromobates cannatellai	MHNLS 22627	-	-	-	-	-	-	-	-	-
Aromobates cannatellai	MHNLS 22629	-	-	-	-	-	-	-	-	-
Aromobates sp. (aff. *cannatellai*)	Asa4	-	-	-	-	-	-	-	-	-
Aromobates sp. (aff. *cannatellai*)	MUJ 3726	-	-	-	-	DQ502935	DQ503280	DQ502404	-	DQ503406
Aromobates sp. (aff. *cannatellai*)	Tama14	-	-	-	-	**14**	-	-	-	-
Aromobates ericksonae	TNHC 5540	HQ290953	HQ290953	HQ290953	HQ290953	-	-	-	HQ290893	-
Aromobates ericksonae	CVULA 7180	-	-	-	-	-	-	-	-	-
Aromobates ericksonae	CVULA8379	-	-	-	-	-	-	-	-	-
Aromobates ericksonae	ULABG 7776	-	-	-	-	-	-	-	-	-
Aromobates mayorgai	MHNLS 21981	-	-	-	-	**Aer2**	-	-	-	-
Aromobates mayorgai	MHNLS 21982	-	-	-	-	-	-	-	-	-
Aromobates mayorgai	MHNLS 21983	-	-	-	-	-	-	-	-	-
Aromobates mayorgai	MHNLS 21984	-	-	-	-	-	-	-	-	-
Aromobates mayorgai	MHNLS 22002	-	-	-	-	-	-	-	-	-
Aromobates mayorgai	MHNLS 22003	-	-	-	-	**Ama2**	-	-	**Ama2**	-
Aromobates mayorgai	MHNLS 22005	-	-	-	-	-	-	-	-	-
Aromobates mayorgai	MHNLS 22030	-	-	-	-	-	-	-	-	-
Aromobates mayorgai	MHNLS 22031	-	-	-	-	-	-	-	-	-
Aromobates mayorgai	MHNLS22032	-	-	-	-	-	-	-	-	-
Aromobates mayorgai	MHNLS 22033	-	-	-	-	-	-	-	-	-
Aromobates meridensis	CVULA7399	-	-	-	-	-	-	-	-	-
Aromobates meridensis	MHNLS22016	-	-	-	-	**Ame1**	-	-	**Ame1**	-

Species	Voucher	tRNA-Asn	LSRO	tRNA-Cys	tRNA-Tyr	COI	RHO	H3F3C	TYR	RAG1
Aromobates meridensis	MHNLS 22017	-	-	-	-	-	-	-	-	-
Aromobates meridensis	MHNLS 22018	-	-	-	-	-	-	-	-	-
Aromobates meridensis	MHNLS 22019	-	-	-	-	-	-	-	-	-
Aromobates molinarii	ULABG 4497	-	-	-	-	-	-	-	-	-
Aromobates molinarii	ULABG sn1	-	-	-	-	-	-	-	-	-
Aromobates molinarii	ULABG sn2	-	-	-	-	-	-	-	-	-
Aromobates molinarii	ULABG sn3	-	-	-	-	-	-	-	-	-
Aromobates nocturnus	AMNHA 130041	-	-	-	-	DQ502859	DQ503243	DQ502357	-	-
Aromobates nocturnus	AMNHA 130042	-	-	-	-	DQ502860	-	DQ502359	-	-
Aromobates ornatissimus	ULABG 4445	-	-	-	-	-	-	-	-	-
Aromobates ornatissimus	CVULA 8351	-	-	-	-	-	-	-	-	-
Aromobates ornatissimus	WES 626	-	-	-	-	-	-	DQ502379	-	DQ503381
Aromobates saltuensis	ULABG 4981	-	-	-	-	**Asa1**	-	-	-	-
Aromobates saltuensis	TNHC 5541	HQ290970	HQ290970	HQ290970	HQ290970	-	-	-	HQ290908	-
Aromobates saltuensis	ULABG AGu1	-	-	-	-	-	-	-	-	-
Aromobates saltuensis	MHNLS 17233	-	-	-	-	**Asa5**	-	-	-	-
Aromobates sp. (aff. *saltuensis* 1)	CVULA 8321	-	-	-	-	-	-	-	-	-
Aromobates sp. (aff. *saltuensis* 1)	MHNLS 22498	-	-	-	-	**Asa3**	-	-	-	-
Aromobates sp. (aff. *saltuensis* 3)	AOH	-	-	-	-	**ACo1**	-	-	-	-
Aromobates sp. (aff. *saltuensis* 2)	LOA 124	-	-	-	-	**ACo2**	-	-	-	-
Aromobates sp. (aff. *saltuensis* 4)	T10_1	-	-	-	-	-	-	-	-	-
Aromobates sp. (aff. *saltuensis* 4)	T10_2	-	-	-	-	-	-	-	-	-
Aromobates tokuko	MHNLS 18478	-	-	-	-	**Ato1**	-	-	**Ato1**	-
Aromobates tokuko	MHNLS 18483	-	-	-	-	-	-	-	-	-
Aromobates tokuko	MHNLS 18493	-	-	-	-	-	-	-	-	-
Aromobates tokuko	MHNLS 18566	-	-	-	-	-	-	-	-	-

Species	Voucher	tRNA-Asn	LSRO	tRNA-Cys	tRNA-Tyr	COI	RHO	H3F3C	TYR	RAG1
Aromobates zippeli	MHNLS 22042	-	-	-	-	-	-	-	**Azi1**	-
Aromobates zippeli	MHNLS 22043	-	-	-	-	-	-	-	-	-
Aromobates zippeli	MHNLS 22044	-	-	-	-	-	-	-	-	-
Aromobates zippeli	MHNLS 22045	-	-	-	-	-	-	-	-	-
Aromobates zippeli	MIZA 310	-	-	-	-	EU380850	-	-	-	-
Aromobates zippeli	MIZA 311	-	-	-	-	EU380851	-	-	-	-
Aromobates zippeli	MIZA 312	-	-	-	-	EU380852	-	-	-	-
Aromobates zippeli	ULABG 4496	-	-	-	-	-	-	-	-	-
Aromobates sp. 1	MHNLS 21506	-	-	-	-	**ATi1**	-	-	**ATi1**	-
Aromobates sp. 1	MHNLS 21507	-	-	-	-	-	-	-	-	-
Aromobates sp. 1	MHNLS 21508	-	-	-	-	-	-	-	-	-
Aromobates sp. 1	MHNLS 22127	-	-	-	-	-	-	-	-	-
Aromobates sp. 1	MHNLS 22128	-	-	-	-	-	-	-	-	-
Aromobates cf. sp. 1	MHNLS 21333	-	-	-	-	-	-	-	-	-
Aromobates cf. sp. 1	MHNLS 21334	-	-	-	-	-	-	-	-	-
Aromobates cf. sp. 1	MHNLS 21335	-	-	-	-	-	-	-	-	-
Aromobates cf. sp. 1	MHNLS 21358	-	-	-	-	-	-	-	**ARo4**	-
Aromobates cf. sp. 1	MHNLS 21359	-	-	-	-	-	-	-	-	-
Aromobates sp. 2	CVULA 5718	-	-	-	-	-	-	-	-	-
Aromobates sp. 2	MHNLS 22093b	-	-	-	-	-	-	-	**AAl2**	-
Aromobates sp. 2	MHNLS 22093c	-	-	-	-	-	-	-	-	-
Aromobates sp. 2	MHNLS 22093d	-	-	-	-	-	-	-	-	-
Mannophryne caquetio	MIZA 333	-	-	-	-	EU380887	-	-	-	-
Mannophryne caquetio	MIZA 337	-	-	-	-	EU380888	-	-	-	-
Mannophryne caquetio	MIZA 323	-	-	-	-	EU380889	-	-	-	-
Mannophryne caquetio	MIZA 338	-	-	-	-	EU380890	-	-	-	-

Species	Voucher	tRNA-Asn	LSRO	tRNA-Cys	tRNA-Tyr	COI	RHO	H3F3C	TYR	RAG1
Mannophryne caquetio	MHNLS 21219	-	-	-	-	**MCh1**	-	-	**MCh1**	-
Mannophryne caquetio	MHNLS 21220	-	-	-	-	-	-	-	-	-
Mannophryne collaris	TNHC 5515	-	-	-	-	-	-	-	-	-
Mannophryne collaris	TNHC 5507	-	-	-	-	-	-	-	HQ290941	-
Mannophryne collaris	MIZA 320	-	-	-	-	EU380885	-	-	-	-
Mannophryne collaris	MIZA 321	-	-	-	-	EU380886	-	-	-	-
Mannophryne collaris	ULABG 4248	-	-	-	-	-	-	-	-	-
Mannophryne collaris	MHNLS 21590	-	-	-	-	-	-	-	-	-
Mannophryne collaris	MHNLS 21591	-	-	-	-	-	-	-	-	-
Mannophryne collaris	MHNLS 21592	-	-	-	-	-	-	-	-	-
Mannophryne collaris	MHNLS 21593	-	-	-	-	-	-	-	-	-
Mannophryne collaris	MHNLS 22058	-	-	-	-	-	-	-	-	-
Mannophryne collaris	MHNLS 21684	-	-	-	-	-	-	-	-	-
Mannophryne collaris	MHNLS 21685	-	-	-	-	-	-	-	-	-
Mannophryne collaris	MHNLS 21686	-	-	-	-	-	-	-	-	-
Mannophryne collaris	MHNLS 21687	-	-	-	-	-	-	-	-	-
Mannophryne cordilleriana	TNHC 5589	-	-	-	-	-	-	-	-	-
Mannophryne cordilleriana	MIZA 330	-	-	-	-	EU380880	-	-	-	-
Mannophryne cordilleriana	MIZA 331	-	-	-	-	EU380881	-	-	-	-
Mannophryne cordilleriana	MIZA 332	-	-	-	-	EU380882	-	-	-	-
Mannophryne cordilleriana	MHNLS 22098	-	-	-	-	-	-	-	-	-
Mannophryne cordilleriana	MHNLS 22099	-	-	-	-	-	-	-	-	-
Mannophryne cordilleriana	MHNLS 21693	-	-	-	-	-	-	-	-	-
Mannophryne cordilleriana	MHNLS 21761	-	-	-	-	-	-	-	-	-
Mannophryne cordilleriana	MHNLS 21625	-	-	-	-	-	-	-	-	-
Mannophryne cordilleriana	MHNLS 21626	-	-	-	-	-	-	-	-	-

Species	Voucher	tRNA-Asn	LSRO	tRNA-Cys	tRNA-Tyr	COI	RHO	H3F3C	TYR	RAG1
Mannophryne cordilleriana	ULABG 5352	-	-	-	-	-	-	-	**Mcd1**	-
Mannophryne cordilleriana	MHNLS 21632	-	-	-	-	-	-	-	-	-
Mannophryne cordilleriana	MHNLS 21633	-	-	-	-	-	-	-	-	-
Mannophryne cordilleriana	MHNLS 21601	-	-	-	-	-	-	-	-	-
Mannophryne cordilleriana	MHNLS 21602	-	-	-	-	-	-	-	-	-
Mannophryne cordilleriana	MHNLS 22187	-	-	-	-	-	-	-	-	-
Mannophryne cordilleriana	MHNLS 22188	-	-	-	-	-	-	-	-	-
Mannophryne cordilleriana	MHNLS 21689	-	-	-	-	-	-	-	-	-
Mannophryne herminae	TNHC 5676	-	-	-	-	-	-	-	-	-
Mannophryne herminae	MIZA 329	-	-	-	-	EU380901	-	-	-	-
Mannophryne herminae	MIZA 328	-	-	-	-	EU380900	-	-	-	-
Mannophryne herminae	MIZA 327	-	-	-	-	EU380899	-	-	-	-
Mannophryne herminae	MHNLS 17475	-	-	-	-	**MHNLS 17475**	-	-	-	-
Mannophryne herminae	MHNLS 21735	-	-	-	-	-	-	-	-	-
Mannophryne herminae	MHNLS 21736	-	-	-	-	-	-	-	-	-
Mannophryne herminae	MHNLS 22106	-	-	-	-	-	-	-	**Mhe6**	-
Mannophryne herminae	MHNLS 22107	-	-	-	-	-	-	-	-	-
Mannophryne aff. *herminae*	ULABG 4506	-	-	-	-	-	-	-	-	-
Mannophryne lamarcai	MIZA 317	-	-	-	-	EU380897	-	-	-	-
Mannophryne lamarcai	MIZA 318	-	-	-	-	EU380898	-	-	-	-
Mannophryne lamarcai	NMA 38	-	-	-	-	-	-	-	-	-
Mannophryne lamarcai	NMA 40	-	-	-	-	-	-	-	**Mla2**	-
Mannophryne lamarcai	NMA 41	-	-	-	-	-	-	-	-	-
Mannophryne lamarcai	MHNLS 22087	-	-	-	-	**MCu1**	-	-	**MCu1**	-
Mannophryne lamarcai	MHNLS 22088	-	-	-	-	-	-	-	-	-
Mannophryne larandina	MIZA 324	-	-	-	-	EU380891	-	-	-	-

Species	Voucher	tRNA-Asn	LSRO	tRNA-Cys	tRNA-Tyr	COI	RHO	H3F3C	TYR	RAG1
Mannophryne larandina	MIZA 325	-	-	-	-	EU380892	-	-	-	-
Mannophryne larandina	MIZA 326	-	-	-	-	EU380893	-	-	-	-
Mannophryne larandina	MHNLS 22597	-	-	-	-	**Mlr1**	-	-	-	-
Mannophryne larandina	MHNLS 22598	-	-	-	-	-	-	-	-	-
Mannophryne larandina	MHNLS 22599	-	-	-	-	-	-	-	-	-
Mannophryne "herminae"	CWM 1141	-	-	-	-	-	-	-	-	-
Mannophryne leonardoi	TNHC 5659	-	-	-	-	-	-	-	-	-
Mannophryne leonardoi	TTSR	-	-	-	-	EU380869	-	-	-	-
Mannophryne leonardoi	MIZA 316	-	-	-	-	EU380868	-	-	-	-
Mannophryne leonardoi	WES 1034	-	-	-	-	DQ502913	DQ503263	DQ502380	-	DQ503382
Mannophryne leonardoi	WES 1035	-	-	-	-	DQ502914	-	DQ502381	-	DQ503383
Mannophryne leonardoi	WES 1036	-	-	-	-	DQ502915	-	DQ502382	-	DQ503384
Mannophryne leonardoi	MHNLS 22333	-	-	-	-	-	-	-	-	-
Mannophryne leonardoi	MHNLS 22334	-	-	-	-	-	-	-	-	-
Mannophryne leonardoi	MHNLS 22335	-	-	-	-	-	-	-	-	-
Mannophryne leonardoi	MHNLS 22336	-	-	-	-	-	-	-	-	-
Mannophryne molinai	MHNLS 21336	-	-	-	-	**MRo1**	-	-	**MRo1**	-
Mannophryne molinai	MHNLS 21337	-	-	-	-	-	-	-	-	-
Mannophryne molinai	MHNLS 21338	-	-	-	-	-	-	-	-	-
Mannophryne molinai	MHNLS 21356	-	-	-	-	-	-	-	-	-
Mannophryne cf. *molinai*	MHNLS 21005	-	-	-	-	**MPg1**	-	-	-	-
Mannophryne cf. *molinai*	MHNLS 21006	-	-	-	-	**MPg2**	-	-	-	-
Mannophryne cf. *molinai*	MHNLS 21365	-	-	-	-	-	-	-	-	-
Mannophryne cf. *molinai*	MHNLS 21367	-	-	-	-	-	-	-	-	-
Mannophryne cf. *molinai*	MHNLS 21205	-	-	-	-	**MQh1**	-	-	**MQh1**	-
Mannophryne cf. *molinai*	MHNLS 21206	-	-	-	-	-	-	-	-	-

Species	Voucher	tRNA-Asn	LSRO	tRNA-Cys	tRNA-Tyr	COI	RHO	H3F3C	TYR	RAG1
Mannophryne cf. *molinai*	MHNLS 21516	-	-	-	-	**MAb1**	-	-	-	-
Mannophryne cf. *molinai*	MHNLS 21517	-	-	-	-	**MAb2**	-	-	-	-
Mannophryne neblina	MHNLS 22362	-	-	-	-	**Mne3**	-	-	**Mne3**	-
Mannophryne oblitterata	TTSR	-	-	-	-	EU380884	-	-	-	-
Mannophryne oblitterata	MIZA 336	-	-	-	-	EU380883	-	-	-	-
Mannophryne oblitterata	MHNLS 21766	-	-	-	-	-	-	-	-	-
Mannophryne oblitterata	MHNLS 21767	-	-	-	-	-	-	-	-	-
Mannophryne oblitterata	MHNLS 21818	-	-	-	-	-	-	-	-	-
Mannophryne oblitterata	MHNLS 21819	-	-	-	-	-	-	-	-	-
Mannophryne olmonae	MIZA 334 / isolate 451	-	-	-	-	EU380876	-	-	-	-
Mannophryne olmonae	MIZA335 / isolate 452	-	-	-	-	EU380877	-	-	-	-
Mannophryne olmonae	UWIZM 2732 / ZSM 1622	-	-	-	-	MF614326	MF614420	-	MF624165	MF614368
Mannophryne orellana	CVULA 7165	-	-	-	-	-	-	-	-	-
Mannophryne orellana	CVULA 7231	-	-	-	-	-	-	-	-	-
Mannophryne orellana	ULABG 7469	-	-	-	-	**Mor1**	-	-	**Mor1**	-
Mannophryne orellana	MHNLS MCp1	-	-	-	-	-	-	-	-	-
Mannophryne orellana	MHNLS MCp2	-	-	-	-	-	-	-	-	-
Mannophryne orellana	MHNLS MCp3	-	-	-	-	-	-	-	-	-
Mannophryne riveroi	MIZA 319	-	-	-	-	EU380879	-	-	-	-
Mannophryne riveroi	TTSR	-	-	-	-	EU380878	-	-	-	-
Mannophryne riveroi	MHNLS16433 / TNHC 5644	-	-	-	-	**Mri1**	-	-	**Mri1**	-
Mannophryne riveroi	MHNLS 17910	-	-	-	-	-	-	-	-	-
Mannophryne speeri	MHNLS 22606	-	-	-	-	**Msp1**	-	-	-	-
Mannophryne trinitatis	MVZ 199837	JX564878	JX564878	JX564878	JX564878	JX564878	-	-	-	-
Mannophryne trinitatis	MVZ199838 / isolate 405	-	-	-	-	-	DQ283796	DQ284108	-	-
Mannophryne trinitatis	MVZ 199828	-	-	-	-	DQ502838	DQ503236	DQ502347	-	DQ503345

Species	Voucher	tRNA-Asn	LSRO	tRNA-Cys	tRNA-Tyr	COI	RHO	H3F3C	TYR	RAG1
Mannophryne trinitatis	ZSM 1619	-	-	-	-	**ZSM1619**	-	-	-	-
Mannophryne trinitatis	ZSM 1620	-	-	-	-	**ZSM1620**	-	-	-	-
Mannophryne trinitatis	ZSM 1621	-	-	-	-	**ZSM1621**	-	-	-	-
Mannophryne trujillensis	MHNLS 17963	-	-	-	-	**MHNLS 17963**	-	-	-	-
Mannophryne trujillensis	MHNLS 17971	-	-	-	-	**MHNLS 17971**	-	-	-	-
Mannophryne trujillensis	MHNLS 22070	-	-	-	-	-	-	-	-	-
Mannophryne trujillensis	MHNLS 22071	-	-	-	-	-	-	-	-	-
Mannophryne trujillensis	MHNLS 22063	-	-	-	-	-	-	-	-	-
Mannophryne trujillensis	MHNLS 22064	-	-	-	-	**Mtr4**	-	-	**Mtr4**	-
Mannophryne urticans	TNHC 5520	-	-	-	-	-	-	-	-	-
Mannophryne urticans	ULABG 4481	-	-	-	-	-	-	-	-	-
Mannophryne urticans	MHNLS 21555	-	-	-	-	**Mur2**	-	-	**Mur2**	-
Mannophryne urticans	MHNLS 21556	-	-	-	-	-	-	-	-	-
Mannophryne urticans	MHNLS 21994	-	-	-	-	-	-	-	-	-
Mannophryne urticans	MHNLS 21993	-	-	-	-	-	-	-	-	-
Mannophryne venezuelensis	EBRG 4921 / isolate 469	-	-	-	-	EU380864	-	-	-	-
Mannophryne venezuelensis	EBRG 4922 / isolate 555 / isoalte 470	-	-	-	-	EU380865	-	-	-	-
Mannophryne venezuelensis	MHNLS 16435	-	-	-	-	**MHNLS 16435**	-	-	**Mve1**	-
Mannophryne venezuelensis	MHNLS 17287	-	-	-	-	-	-	-	-	-
Mannophryne venezuelensis	MHNLS 17314	-	-	-	-	**MHNLS 17314**	-	-	-	-
Mannophryne venezuelensis	MHNLS 17315	-	-	-	-	**MHNLS 17315**	-	-	-	-
Mannophryne venezuelensis	TNHC 5649	-	-	-	-	-	-	-	-	-
Mannophryne vulcano	TNHC 5679	-	-	-	-	-	-	-	-	-
Mannophryne vulcano	MIZA 342	-	-	-	-	EU380872	-	-	-	-
Mannophryne vulcano	MIZA 343	-	-	-	-	EU380873	-	-	-	-

Species	Voucher	tRNA-Asn	LSRO	tRNA-Cys	tRNA-Tyr	COI	RHO	H3F3C	TYR	RAG1
Mannophryne vulcano	MHNLS 16685	-	-	-	-	**MHNLS 16685**	-	-	-	-
Mannophryne vulcano	MHNLS 22140	-	-	-	-	**Mvu36**	-	-	**Mvu36**	-
Mannophryne vulcano	MHNLS 22141	-	-	-	-	-	-	-	-	-
Mannophryne vulcano	MHNLS 22142	-	-	-	-	-	-	-	-	-
Mannophryne vulcano	MHNLS 20692	-	-	-	-	-	-	-	-	-
Mannophryne vulcano	MHNLS 20693	-	-	-	-	-	-	-	-	-
Mannophryne vulcano	MHNLS 18575	-	-	-	-	-	-	-	-	-
Mannophryne vulcano	MHNLS 18577	-	-	-	-	-	-	-	-	-
Mannophryne vulcano	MHNLS 21802	-	-	-	-	-	-	-	-	-
Mannophryne vulcano	MHNLS 21803	-	-	-	-	-	-	-	-	-
Mannophryne vulcano	MHNLS 20830	-	-	-	-	-	-	-	-	-
Mannophryne vulcano	MHNLS 21770	-	-	-	-	-	-	-	-	-
Mannophryne vulcano	MHNLS 21771	-	-	-	-	-	-	-	-	-
Mannophryne vulcano	MHNLS 22346	-	-	-	-	-	-	-	-	-
Mannophryne vulcano	MHNLS 20941	-	-	-	-	-	-	-	-	-
Mannophryne vulcano	MHNLS 20942	-	-	-	-	-	-	-	-	-
Mannophryne vulcano	MHNLS 21778	-	-	-	-	-	-	-	-	-
Mannophryne vulcano	MHNLS 21779	-	-	-	-	-	-	-	-	-
Mannophryne yustizi	TTSR_G	-	-	-	-	EU380896	-	-	-	-
Mannophryne yustizi	TNHC 5604	-	-	-	-	-	-	-	-	-
Mannophryne yustizi	TTSR_S	-	-	-	-	EU380894	-	-	-	-
Mannophryne yustizi	MIZA 322	-	-	-	-	EU380895	-	-	-	-
Mannophryne sp. 1	TTSR	-	-	-	-	EU380871	-	-	-	-
Mannophryne sp. 1	MIZA 341	-	-	-	-	EU380870	-	-	-	-
Mannophryne sp. 1	MHNLS 16769	-	-	-	-	-	-	-	-	-
Mannophryne sp. 1	MHNLS 16772	-	-	-	-	**MRu1**	-	-	**MRu1**	-

Species	Voucher	tRNA-Asn	LSRO	tRNA-Cys	tRNA-Tyr	COI	RHO	H3F3C	TYR	RAG1
Mannophryne sp. 1	MHNLS 16773	-	-	-	-	**MHNLS 16773**	-	-	-	-
Mannophryne sp. 1	MHNLS 16798	-	-	-	-	**MHNLS 16798**	-	-	-	-
Mannophryne sp. (cf. *vulcano*)	MHNLS 21825	-	-	-	-	-	-	-	-	-
Mannophryne sp. (cf. *vulcano*)	MHNLS 21826	-	-	-	-	-	-	-	-	-
Mannophryne sp. 2	MIZA 340	-	-	-	-	EU380875	-	-	-	-
Mannophryne sp. 2	EBRG 4889	-	-	-	-	EU380874	-	-	-	-
Mannophryne sp. 2	MHNLS 17251	-	-	-	-	**MHNLS 17251**	-	-	-	-
Mannophryne sp. 2	MHNLS 17252	-	-	-	-	**MHNLS 17252**	-	-	-	-
Mannophryne sp. 2	MHNLS 17253	-	-	-	-	**MHNLS 17253**	-	-	-	-
Mannophryne sp. 2	MHNLS 17254	-	-	-	-	**MHNLS 17254**	-	-	-	-
Mannophryne sp. 2	MHNLS 17256	-	-	-	-	**MHNLS 17256**	-	-	-	-
Mannophryne sp. 2	MHNLS 15545	-	-	-	-	**MPi1**	-	-	-	-
Mannophryne sp. 3	MHNLS 22358	-	-	-	-	-	-	-	-	-
Mannophryne sp. 3	MHNLS 22359	-	-	-	-	-	-	-	-	-
Mannophryne sp. 3	MHNLS 22360	-	-	-	-	**MAg3**	-	-	**MAg3**	-
Mannophryne sp. 3	MHNLS 22347	-	-	-	-	-	-	-	-	-
Mannophryne sp. 3	MHNLS 22348	-	-	-	-	-	-	-	-	-
Mannophryne sp. 3	MHNLS 22353	-	-	-	-	-	-	-	-	-
Mannophryne sp. 3	MHNLS 21747	-	-	-	-	-	-	-	-	-
Mannophryne sp. 3	MHNLS 21748	-	-	-	-	-	-	-	-	-
Mannophryne sp. 4	MHNLS 22204	-	-	-	-	**MMo1**	-	-	-	-
Mannophryne sp. 4	MHNLS 22214	-	-	-	-	-	-	-	-	-
Mannophryne sp. 4	MHNLS 22219	-	-	-	-	-	-	-	-	-
Mannophryne sp. 4	MHNLS 22281	-	-	-	-	-	-	-	-	-

Species	Voucher	tRNA-Asn	LSRO	tRNA-Cys	tRNA-Tyr	COI	RHO	H3F3C	TYR	RAG1
Mannophryne sp. 4	MHNLS 22302	-	-	-	-	-	-	-	-	-
Mannophryne sp. 4	MHNLS 22303	-	-	-	-	-	-	-	-	-
Mannophryne sp. 4	MHNLS 22304	-	-	-	-	-	-	-	-	-
Mannophryne sp. (aff. *herminae*)	MHNLS 17157	-	-	-	-	**MHNLS 17157**	-	-	-	-
Mannophryne sp. (aff. *herminae*)	MHNLS 17158	-	-	-	-	**MHNLS 17158**	-	-	-	-
Mannophryne sp. (aff. *herminae*)	MHNLS 17159	-	-	-	-	-	-	-	-	-
Mannophryne sp. (aff. *herminae*)	MHNLS 17160	-	-	-	-	**MHNLS 17160**	-	-	-	-
Mannophryne sp. (*yustizi* complex)	MHNLS 22585	-	-	-	-	-	-	-	-	-
Mannophryne sp. (*yustizi* complex)	MHNLS 22586	-	-	-	-	-	-	-	-	-
Mannophryne sp. (aff. *vulcano*)	TNHC 5666	-	-	-	-	-	-	-	-	-
Mannophryne sp. (*yustizi* complex)	ULABG 4465	-	-	-	-	-	-	-	-	-
Mannophryne sp. (*yustizi* complex)	ULABG 4453	-	-	-	-	-	-	-	-	-
Mannophryne sp. (*yustizi* complex)	ULABG 4458	-	-	-	-	-	-	-	-	-
Mannophryne sp. (*yustizi* complex)	MHNLS 22080	-	-	-	-	**MJa1**	-	-	**MJa1**	-
Mannophryne sp. (*yustizi* complex)	MHNLS 22081	-	-	-	-	-	-	-	-	-
Mannophryne sp. (*yustizi* complex)	MHNLS 22617	-	-	-	-	**Msp6**	-	-	-	-
Mannophryne sp. (cf. *speeri-yustizi*)	MHNLS 22618	-	-	-	-	**Msp7**	-	-	-	-
Mannophryne sp. (*yustizi* complex)	MHNLS 22619	-	-	-	-	-	-	-	-	-
Mannophryne sp. (cf. *speeri-yustizi*)	MHNLS 22169	-	-	-	-	**MNi1**	-	-	**MNi1**	-
Mannophryne sp. (*yustizi* complex)	MHNLS 22170	-	-	-	-	-	-	-	-	-
Mannophryne sp. (*yustizi* complex)	MHNLS 22171	-	-	-	-	-	-	-	-	-
Mannophryne sp. (*yustizi* complex)	MHNLS 22172	-	-	-	-	-	-	-	-	-
Mannophryne sp. (*yustizi* complex)	MHNLS 22559	-	-	-	-	-	-	-	-	-
Mannophryne sp. (*yustizi* complex)	MHNLS 22560	-	-	-	-	**Myu3**	-	-	-	-
Andinobates bombetes	TNHC 4946 / MAR 1265	-	-	-	-	-	MF614380	MF624106	HQ290918	MF614342

Species	Voucher	tRNA-Asn	LSRO	tRNA-Cys	tRNA-Tyr	COI	RHO	H3F3C	TYR	RAG1
Adelphobates galactonotus	TNHC 4889 / MTR 5088	-	-	-	-	-	DQ503227	DQ502337	HQ290921	-
Allobates aff. *juanii*	ANDESA 1073	-	-	-	-	KJ130661	-	-	-	-
Allobates algorei	TNHC 5551	-	-	-	-	-	-	-	HQ290890	-
Allobates amissibilis	MTD 47884	-	-	-	-	KC520687	-	-	KC520696	-
Allobates bacurau	INPAH 35406	-	-	-	-	-	-	-	-	-
Allobates caeruleodactylus	MPEG 13809	-	-	-	-	DQ502814	DQ503218	DQ502328	-	DQ503329
Allobates chalcopis	Alca1	-	-	-	-	KC520685	-	-	KC520695	-
Allobates conspicuus	MPEG 12321	-	-	-	-	DQ502841	DQ503238	DQ502349	-	DQ503348
Allobates crombiei	APL 14124	-	-	-	-	-	-	-	-	-
Allobates femoralis (Acre01)	Acre 12931	-	-	-	-	-	-	-	-	-
Allobates femoralis (Acre02)	OMNH 36070	-	-	-	-	DQ502811	DQ503215	DQ502325	DQ503156	DQ503327
Allobates femoralis	QCAZ 16484	-	-	-	-	-	-	-	HQ290891	-
Allobates flaviventris	OMNH 36959	-	-	-	-	-	DQ503262	-	DQ503169	DQ503379
Allobates fratisenescus	QCAZ 54377	-	-	-	-	-	-	-	-	-
Allobates gasconi	MPEG 13003	-	-	-	-	DQ502777	-	-	-	-
Allobates granti	148 AF	-	-	-	-	-	-	-	JN691577	-
Allobates grillisimilis	APL 12747	-	-	-	-	-	-	-	-	-
Allobates hodli	AbuE 2189	-	-	-	-	-	-	-	-	-
Allobates humilis	CVULA 5690	-	-	-	-	-	-	-	-	-
Allobates humilis	MHNLS22093a	-	-	-	-	-	-	-	-	-
Allobates insperatus	QCAZ1 6533	-	-	-	-	-	-	-	HQ290899	-
Allobates juami	MCP 13287	-	-	-	-	-	-	-	-	-
Allobates juanii	TNHC 4978	-	-	-	-	-	-	-	HQ290900	-
Allobates kingsburyi	QCAZ 16523	-	-	-	-	-	-	-	HQ290901	-
Allobates magnussoni	MPEG 11923	-	-	-	-	-	DQ503237	DQ502348	-	DQ503347
Allobates masniger	APL 14250	-	-	-	-	-	-	-	-	-

Species	Voucher	tRNA-Asn	LSRO	tRNA-Cys	tRNA-Tyr	COI	RHO	H3F3C	TYR	RAG1
Allobates myersi	INPAH 26396	-	-	-	-	-	-	-	-	-
Allobates nidicola	MPEG 13821	-	-	-	-	-	DQ503219	DQ502329	-	DQ503330
Allobates niputidea	MUJ 3520	-	-	-	-	DQ502934	DQ503278	DQ502402	-	DQ503404
Allobates olfersioides	MRT 6031	-	-	-	-	DQ502833	DQ503232	DQ502342	-	-
Allobates ornatus	MHNSM 22863	-	-	-	-	-	-	-	-	-
Allobates paleovarzensis	MJH 3909	-	-	-	-	-	-	-	-	-
Allobates peruvianus	MHNSM 22923	-	-	-	-	-	-	-	-	-
Allobates pittieri	MIZA 339	-	-	-	-	EU380855	-	-	-	-
Allobates pittieri	MHNLS 21229	-	-	-	-	**Lpi1**	-	-	**Lpi1**	-
Allobates subfolionidificans	APL 1692	-	-	-	-	-	-	-	-	-
Allobates sumtuosus	MTD 47771	-	-	-	-	KC520688	-	-	KC520697	-
Allobates talamancae	QCAZ 16549	HQ290974	HQ290974	HQ290974	HQ290974	-	-	-	HQ290912	-
Allobates talamancae	SIUC 7667	-	-	-	-	DQ502868	DQ503250	DQ502364	-	DQ503363
Allobates tapajos	LSUMZ 15176	-	-	-	-	DQ502772	DQ503201	DQ502310	-	DQ503316
Allobates tinae	MPEG 13826	-	-	-	-	-	DQ503217	DQ502327	-	DQ503328
Allobates trilineatus	KU 215175	-	-	-	-	DQ502720	DQ503184	DQ502287	-	DQ503290
Allobates undulatus	AMNHA 159139	-	-	-	-	DQ502756	DQ283773	DQ284073	-	DQ503308
Allobates zaparo	QCAZ 16603	-	-	-	-	-	-	-	HQ290940	-
Allobates sp. (Alto Mazan)	MZ 010	-	-	-	-	MF614291	MF614378	-	-	MF614341
Allobates sp. (Carajas)	TG 3264	-	-	-	-	-	MF614376	MF624104	MF624150	MF614338
Allobates sp. (Cuao)	MHNLS 19982	-	-	-	-	**MHNLS 19982**	-	-	-	-
Allobates sp. (Cuyabeno)	OMNH 34086	-	-	-	-	DQ502767	DQ503200	DQ502309	-	DQ503315
Allobates sp. (Liberdade)	MCP 10212	-	-	-	-	MF614290	-	-	-	MF614340
Allobates sp. (Neblina)	AMCC 106112	-	-	-	-	DQ502795	DQ503207	DQ502317	DQ503149	DQ503321
Allobates sp. (PEGM1)	LSUMZ 17601	-	-	-	-	DQ502843	-	DQ502350	-	DQ503349
Allobates sp. (PEGM3)	MPEG 13386	-	-	-	-	DQ502844	DQ503240	DQ502352	DQ503164	DQ503351

Species	Voucher	tRNA-Asn	LSRO	tRNA-Cys	tRNA-Tyr	COI	RHO	H3F3C	TYR	RAG1
Ameerega trivittata	TNHC 4966 / MPEG 12504	-	-	-	-	DQ502799	DQ503211	DQ502321	HQ290939	DQ503324
Anomaloglossus apiau	MTR 37501	-	-	-	-	MF614300	-	MF624115	MF624153	MF614349
Anomaloglossus baeobatrachus 1	AF 2590	KU958559	KU958559	KU958559	KU958559	KU958559	-	-	KY549544	KY549462
Anomaloglossus baeobatrachus 2	MTR 13861	-	-	-	-	-	-	-	JN691653	KY549478
Anomaloglossus beebei	ROM 39631	-	-	-	-	DQ502834	DQ503233	DQ502343	-	DQ503342
Anomaloglossus blanci	AF 932	MG264895	MG264895	MG264895	MG264895	MG264895	-	-	-	-
Anomaloglossus degranvillei	PG 601	MG264892	MG264892	MG264892	MG264892	MG264892	-	-	KY549557	KY549485
Anomaloglossus dewynteri	PG 660	MG264891	MG264891	MG264891	MG264891	MG264891	-	-	-	-
Anomaloglossus kaiei	279	-	-	-	-	DQ502741	DQ503189	DQ502297	-	DQ503300
Anomaloglossus leopardus	AF 2041	-	-	-	-	-	-	-	KY549534	KY549452
Anomaloglossus meansi	ROM 39639	-	-	-	-	DQ502836	DQ503235	DQ502345	DQ503163	DQ503344
Anomaloglossus megacephalus	ROM 39637	-	-	-	-	DQ502835	DQ503234	DQ502344	DQ503162	DQ503343
Anomaloglossus praderioi	CPI 10208	-	-	-	-	DQ502923	-	DQ502390	-	DQ503392
Anomaloglossus roraima	06-141	-	-	-	-	MF614336	-	MF624149	MF624171	MF614374
Anomaloglossus rufulus	MHNLS 20610	-	-	-	-	**Nru2**	-	-	**Nru2**	-
Anomaloglossus rufulus	CLBA / voucher 214 (Vacher et al)	-	-	-	-	-	-	-	-	KY549447
Anomaloglossus mitaraka	AF 2732	-	-	-	-	-	-	-	KY549547	KY549466
Anomaloglossus stepheni	AF 2045	-	-	-	-	-	-	-	KY549535	KY549453
Anomaloglossus stepheni	MJH 3928	-	-	-	-	DQ502818	DQ503223	DQ502333	-	DQ503334
Anomaloglossus surinamensis 1	AF 585	MG264890	MG264890	MG264890	MG264890	MG264890	-	-	-	-
Anomaloglossus surinamensis 2	AF 2456	MG264894	MG264894	MG264894	MG264894	MG264894	-	-	-	-
Anomaloglossus surinamensis 5	AF 3340	MG264893	MG264893	MG264893	MG264893	MG264893	-	-	KY549550	KY549469
Anomaloglossus tamacuarensis	MNRJ 38049	-	-	-	-	-	MF614390	MF624116	MF624154	-
Anomaloglossus tepuyensis	MHNLS 15613	-	-	-	-	**Nte1**	-	-	**Nte1**	-
Anomaloglossus tepuyensis	VUB 3734	-	-	-	-	-	-	-	-	-
Anomaloglossus verbeeksnyderorum	MHNLS 20084	-	-	-	-	**MHNLS**	-	-	-	-

Species	Voucher	tRNA-Asn	LSRO	tRNA-Cys	tRNA-Tyr	COI	RHO	H3F3C	TYR	RAG1
						20084				
Anomaloglossus verbeeksnyderorum	MHNLS 20085	-	-	-	-	**MHNLS 20085**	-	-	-	-
Anomaloglossus verbeeksnyderorum	TNHC5631	HQ290952	HQ290952	HQ290952	HQ290952	-	-	-	HQ290892	-
Anomaloglossus wothuja	MHNLS 19952 / VUB 3735	-	-	-	-	**MHNLS 19952**	-	-	-	-
Anomaloglossus wothuja	MHNLS 19953 / VUB 3736	-	-	-	-	**MHNLS 19953**	-	-	-	-
Anomaloglossus sp. (Brownsberg)	UTAA 56469	-	-	-	-	DQ502919	DQ503267	DQ502385	-	-
Anomaloglossus sp. A (Wokomung)	VUB 3128	-	-	-	-	-	-	-	-	-
Anomaloglossus sp. (Bakhuis)	AF 3426	-	-	-	-	-	-	-	KY549552	KY549471
Anomaloglossus sp. (Brownsberg)	BPN 0850	-	-	-	-	-	-	-	JN691716	KY549472
Anomaloglossus sp. (Ichún)	MHNLS 17561	-	-	-	-	-	-	-	-	-
Anomaloglossus sp. (Thomasing)	UTAA 56710	-	-	-	-	-	-	DQ502389	-	DQ503390
Rheobates pseudopalmatus	MHUA 5162	-	-	-	-	KJ130694	-	-	-	-
Rheobates palmatus	MUJ 3829	-	-	-	-	MF614330	MF614424	-	-	-
Rheobates palmatus	TNHC 4955	-	-	-	-	-	-	-	HQ290905	-
Hyloxalus cepedai	MAA 574	-	-	-	-	-	MF614413	MF624132	-	MF614361
Leucostethus fugax	QCAZ 16513	-	-	-	-	-	-	-	HQ290898	-
Leucostethus brachistriatus	MHNUC 360	-	-	-	-	DQ502878	DQ503256	DQ502372	-	DQ503371
Silverstoneia nubicola	SIUC 7652	-	-	-	-	DQ502863	DQ503245	-	-	DQ503359
Epipedobates tricolor	QCAZ 21977	-	-	-	-	-	-	-	HQ290938	-
Ectopoglossus saxatilis	IAvH 14617	-	-	-	-	MF614316	MF614408	MF624130	MF624162	MF614357
Paruwrobates erythromos	QCAZ 37750	-	-	-	-	-	-	-	-	-
Phyllobates bicolor	1233	-	-	-	-	DQ502884	-	DQ502377	-	DQ503377
"Colostethus" ruthveni	MAR 558	-	-	-	-	MF614302	MF614391	MF624118	-	MF614351
Minyobates steyermarki	Roberts et al. / Vences et al.	-	-	-	-	-	-	-	-	-
Oophaga pumilio	TNHC 4814	HQ290988	HQ290988	HQ290988	HQ290988	-	-	-	HQ290925	-

Species	Voucher	tRNA-Asn	LSRO	tRNA-Cys	tRNA-Tyr	COI	RHO	H3F3C	TYR	RAG1
Dendrobates tinctorius	TNHC64416 / UTA 56495	-	-	-	-	DQ502918	DQ503266	DQ502384	HQ290928	DQ503387
Exidobates captivus	QCAZ 27442	HQ290982	HQ290982	HQ290982	HQ290982	-	-	-	HQ290919	-
Ranitomeya toraro	OMNH 36666	-	-	-	-	DQ502793	DQ503206	DQ502316	DQ503148	DQ503320
Thoropa miliaris	AF 1434	GQ174934	GQ174934	GQ174934	-	-	KF214197	-	JX298241	FJ685702

Continued (part 4)…

Species	Voucher	SIAH1	28S	ZEB2	POMC	NT3	NCX1	BMP2	BDNF	CXCR4
Aromobates cannatellai	CVULA 8325	-	-	-	JX036008	-	JX036002	-	-	-
Aromobates cannatellai	MHNLS 22625	-	-	-	-	-	-	-	-	-
Aromobates cannatellai	MHNLS 22626	-	-	-	-	-	-	-	-	-
Aromobates cannatellai	MHNLS 22627	-	-	-	-	-	-	-	-	-
Aromobates cannatellai	MHNLS 22629	-	-	-	-	-	-	-	-	-
Aromobates sp. (aff. *cannatellai*)	Asa4	-	-	-	-	-	-	-	-	-
Aromobates sp. (aff. *cannatellai*)	MUJ 3726	-	-	-	-	-	-	-	-	-
Aromobates sp. (aff. *cannatellai*)	Tama14	-	-	-	-	-	-	-	-	-
Aromobates ericksonae	TNHC 5540	-	-	HQ290653	HQ290833	HQ290773	HQ290713	HQ291016	HQ290593	-
Aromobates ericksonae	CVULA 7180	-	-	-	JX036007	-	JX036001	-	-	-
Aromobates ericksonae	CVULA8379	-	-	-	-	-	-	-	-	-
Aromobates ericksonae	ULABG 7776	-	-	-	-	-	-	-	-	-
Aromobates mayorgai	MHNLS 21981	-	-	-	-	-	-	-	-	-
Aromobates mayorgai	MHNLS 21982	-	-	-	-	-	-	-	-	-
Aromobates mayorgai	MHNLS 21983	-	-	-	-	-	-	-	-	-
Aromobates mayorgai	MHNLS 21984	-	-	-	-	-	-	-	-	-
Aromobates mayorgai	MHNLS 22002	-	-	-	-	-	-	-	-	-
Aromobates mayorgai	MHNLS 22003	-	-	-	**Ama2**	-	-	**Ama2**	**Ama2**	**Ama2**
Aromobates mayorgai	MHNLS 22005	-	-	-	-	-	-	-	-	-
Aromobates mayorgai	MHNLS 22030	-	-	-	-	-	-	-	-	-
Aromobates mayorgai	MHNLS 22031	-	-	-	-	-	-	-	-	-
Aromobates mayorgai	MHNLS22032	-	-	-	-	-	-	-	-	-
Aromobates mayorgai	MHNLS 22033	-	-	-	-	-	-	-	-	-
Aromobates meridensis	CVULA7399	-	-	-	JX036006	-	JX036000	-	-	-
Aromobates meridensis	MHNLS22016	-	-	-	-	-	-	**Ame1**	**Ame1**	-

Species	Voucher	SIAH1	28S	ZEB2	POMC	NT3	NCX1	BMP2	BDNF	CXCR4
Aromobates meridensis	MHNLS 22017	-	-	-	-	-	-	-	-	-
Aromobates meridensis	MHNLS 22018	-	-	-	-	-	-	-	-	-
Aromobates meridensis	MHNLS 22019	-	-	-	-	-	-	-	-	-
Aromobates molinarii	ULABG 4497	-	-	-	-	-	-	-	-	-
Aromobates molinarii	ULABG sn1	-	-	-	-	-	-	-	-	-
Aromobates molinarii	ULABG sn2	-	-	-	-	-	-	-	-	-
Aromobates molinarii	ULABG sn3	-	-	-	-	-	-	-	-	-
Aromobates nocturnus	AMNHA 130041	DQ503107	DQ502996	-	-	-	-	-	-	-
Aromobates nocturnus	AMNHA 130042	DQ503109	DQ502998	-	-	-	-	-	-	-
Aromobates ornatissimus	ULABG 4445	-	-	-	-	-	-	-	-	-
Aromobates ornatissimus	CVULA 8351	-	-	-	-	-	-	-	-	-
Aromobates ornatissimus	WES 626	DQ503127	DQ503023	-	-	-	-	-	-	-
Aromobates saltuensis	ULABG 4981	-	-	-	-	-	-	-	-	-
Aromobates saltuensis	TNHC 5541	-	-	HQ290668	HQ290848	HQ290788	HQ290728	HQ291031	HQ290608	-
Aromobates saltuensis	ULABG AGu1	-	-	-	-	-	-	-	-	-
Aromobates saltuensis	MHNLS 17233	-	-	-	-	-	-	**Asa5**	-	-
Aromobates sp. (aff. *saltuensis* 1)	CVULA 8321	-	-	-	-	-	-	-	-	-
Aromobates sp. (aff. *saltuensis* 1)	MHNLS 22498	-	-	-	**Asa3**	-	-	**Asa3**	**Asa3**	**Asa3**
Aromobates sp. (aff. *saltuensis* 3)	AOH	-	-	-	-	-	-	-	-	-
Aromobates sp. (aff. *saltuensis* 2)	LOA 124	-	-	-	-	-	-	-	-	-
Aromobates sp. (aff. *saltuensis* 4)	T10_1	-	-	-	-	-	-	-	-	-
Aromobates sp. (aff. *saltuensis* 4)	T10_2	-	-	-	-	-	-	-	-	-
Aromobates tokuko	MHNLS 18478	-	-	-	**Ato1**	-	-	**Ato1**	**Ato1**	**Ato1**
Aromobates tokuko	MHNLS 18483	-	-	-	-	-	-	-	-	-
Aromobates tokuko	MHNLS 18493	-	-	-	-	-	-	-	-	-
Aromobates tokuko	MHNLS 18566	-	-	-	-	-	-	-	-	-

Species	Voucher	SIAH1	28S	ZEB2	POMC	NT3	NCX1	BMP2	BDNF	CXCR4
Aromobates zippeli	MHNLS 22042	-	-	-	**Azi1**	-	-	**Azi1**	**Azi1**	**Azi1**
Aromobates zippeli	MHNLS 22043	-	-	-	-	-	-	-	-	-
Aromobates zippeli	MHNLS 22044	-	-	-	-	-	-	-	-	-
Aromobates zippeli	MHNLS 22045	-	-	-	-	-	-	-	-	-
Aromobates zippeli	MIZA 310	-	-	-	-	-	-	-	-	-
Aromobates zippeli	MIZA 311	-	-	-	-	-	-	-	-	-
Aromobates zippeli	MIZA 312	-	-	-	-	-	-	-	-	-
Aromobates zippeli	ULABG 4496	-	-	-	-	-	-	-	-	-
Aromobates sp. 1	MHNLS 21506	-	-	-	**ATi1**	-	-	**ATi1**	**ATi1**	**ATi1**
Aromobates sp. 1	MHNLS 21507	-	-	-	-	-	-	-	-	-
Aromobates sp. 1	MHNLS 21508	-	-	-	-	-	-	-	-	-
Aromobates sp. 1	MHNLS 22127	-	-	-	-	-	-	-	-	-
Aromobates sp. 1	MHNLS 22128	-	-	-	-	-	-	-	-	-
Aromobates cf. sp. 1	MHNLS 21333	-	-	-	-	-	-	-	-	-
Aromobates cf. sp. 1	MHNLS 21334	-	-	-	-	-	-	-	-	-
Aromobates cf. sp. 1	MHNLS 21335	-	-	-	-	-	-	-	-	-
Aromobates cf. sp. 1	MHNLS 21358	-	-	-	**ARo4**	-	-	**ARo4**	**ARo4**	**ARo4**
Aromobates cf. sp. 1	MHNLS 21359	-	-	-	-	-	-	-	-	-
Aromobates sp. 2	CVULA 5718	-	-	-	JX036005	-	JX035999	-	-	-
Aromobates sp. 2	MHNLS 22093b	-	-	-	-	-	-	**AAl2**	**AAl2**	-
Aromobates sp. 2	MHNLS 22093c	-	-	-	-	-	-	-	-	-
Aromobates sp. 2	MHNLS 22093d	-	-	-	-	-	-	-	-	-
Mannophryne caquetio	MIZA 333	-	-	-	-	-	-	-	-	-
Mannophryne caquetio	MIZA 337	-	-	-	-	-	-	-	-	-
Mannophryne caquetio	MIZA 323	-	-	-	-	-	-	-	-	-
Mannophryne caquetio	MIZA 338	-	-	-	-	-	-	-	-	-

Species	Voucher	SIAH1	28S	ZEB2	POMC	NT3	NCX1	BMP2	BDNF	CXCR4
Mannophryne caquetio	MHNLS 21219	-	-	-	**MCh1**	-	-	**MCh1**	**MCh1**	**MCh1**
Mannophryne caquetio	MHNLS 21220	-	-	-	-	-	-	-	-	-
Mannophryne collaris	TNHC 5515	-	-	-	-	-	-	-	-	-
Mannophryne collaris	TNHC 5507	-	-	HQ290701	HQ290881	HQ290821	HQ290761	HQ291064	HQ290641	-
Mannophryne collaris	MIZA 320	-	-	-	-	-	-	-	-	-
Mannophryne collaris	MIZA 321	-	-	-	-	-	-	-	-	-
Mannophryne collaris	ULABG 4248	-	-	-	-	-	-	-	-	-
Mannophryne collaris	MHNLS 21590	-	-	-	-	-	-	-	-	-
Mannophryne collaris	MHNLS 21591	-	-	-	-	-	-	-	-	-
Mannophryne collaris	MHNLS 21592	-	-	-	-	-	-	-	-	-
Mannophryne collaris	MHNLS 21593	-	-	-	-	-	-	-	-	-
Mannophryne collaris	MHNLS 22058	-	-	-	-	-	-	-	-	-
Mannophryne collaris	MHNLS 21684	-	-	-	-	-	-	-	-	-
Mannophryne collaris	MHNLS 21685	-	-	-	-	-	-	-	-	-
Mannophryne collaris	MHNLS 21686	-	-	-	-	-	-	-	-	-
Mannophryne collaris	MHNLS 21687	-	-	-	-	-	-	-	-	-
Mannophryne cordilleriana	TNHC 5589	-	-	-	-	-	-	-	-	-
Mannophryne cordilleriana	MIZA 330	-	-	-	-	-	-	-	-	-
Mannophryne cordilleriana	MIZA 331	-	-	-	-	-	-	-	-	-
Mannophryne cordilleriana	MIZA 332	-	-	-	-	-	-	-	-	-
Mannophryne cordilleriana	MHNLS 22098	-	-	-	-	-	-	-	-	-
Mannophryne cordilleriana	MHNLS 22099	-	-	-	-	-	-	-	-	-
Mannophryne cordilleriana	MHNLS 21693	-	-	-	-	-	-	-	-	-
Mannophryne cordilleriana	MHNLS 21761	-	-	-	-	-	-	-	-	-
Mannophryne cordilleriana	MHNLS 21625	-	-	-	-	-	-	-	-	-
Mannophryne cordilleriana	MHNLS 21626	-	-	-	-	-	-	-	-	-

Species	Voucher	SIAH1	28S	ZEB2	POMC	NT3	NCX1	BMP2	BDNF	CXCR4
Mannophryne cordilleriana	ULABG 5352	-	-	-	-	-	-	**Mcd1**	**Mcd1**	**Mcd1**
Mannophryne cordilleriana	MHNLS 21632	-	-	-	-	-	-	-	-	-
Mannophryne cordilleriana	MHNLS 21633	-	-	-	-	-	-	-	-	-
Mannophryne cordilleriana	MHNLS 21601	-	-	-	-	-	-	-	-	-
Mannophryne cordilleriana	MHNLS 21602	-	-	-	-	-	-	-	-	-
Mannophryne cordilleriana	MHNLS 22187	-	-	-	-	-	-	-	-	-
Mannophryne cordilleriana	MHNLS 22188	-	-	-	-	-	-	-	-	-
Mannophryne cordilleriana	MHNLS 21689	-	-	-	-	-	-	-	-	-
Mannophryne herminae	TNHC 5676	-	-	-	-	-	-	-	-	-
Mannophryne herminae	MIZA 329	-	-	-	-	-	-	-	-	-
Mannophryne herminae	MIZA 328	-	-	-	-	-	-	-	-	-
Mannophryne herminae	MIZA 327	-	-	-	-	-	-	-	-	-
Mannophryne herminae	MHNLS 17475	-	-	-	-	-	-	-	-	-
Mannophryne herminae	MHNLS 21735	-	-	-	-	-	-	-	-	-
Mannophryne herminae	MHNLS 21736	-	-	-	-	-	-	-	-	-
Mannophryne herminae	MHNLS 22106	-	-	-	**Mhe6**	-	-	**Mhe6**	**Mhe6**	**Mhe6**
Mannophryne herminae	MHNLS 22107	-	-	-	-	-	-	-	-	-
Mannophryne aff. *herminae*	ULABG 4506	-	-	-	-	-	-	-	-	-
Mannophryne lamarcai	MIZA 317	-	-	-	-	-	-	-	-	-
Mannophryne lamarcai	MIZA 318	-	-	-	-	-	-	-	-	-
Mannophryne lamarcai	NMA 38	-	-	-	-	-	-	-	-	-
Mannophryne lamarcai	NMA 40	-	-	-	**Mla2**	-	-	**Mla2**	**Mla2**	**Mla2**
Mannophryne lamarcai	NMA 41	-	-	-	-	-	-	-	-	-
Mannophryne lamarcai	MHNLS 22087	-	-	-	**MCu1**	-	-	**MCu1**	**MCu1**	**MCu1**
Mannophryne lamarcai	MHNLS 22088	-	-	-	-	-	-	-	-	-
Mannophryne larandina	MIZA 324	-	-	-	-	-	-	-	-	-

Species	Voucher	SIAH1	28S	ZEB2	POMC	NT3	NCX1	BMP2	BDNF	CXCR4
Mannophryne larandina	MIZA 325	-	-	-	-	-	-	-	-	-
Mannophryne larandina	MIZA 326	-	-	-	-	-	-	-	-	-
Mannophryne larandina	MHNLS 22597	-	-	-	-	-	-	-	-	-
Mannophryne larandina	MHNLS 22598	-	-	-	-	-	-	-	-	-
Mannophryne larandina	MHNLS 22599	-	-	-	-	-	-	-	-	-
Mannophryne "herminae"	CWM 1141	-	-	-	-	-	-	-	-	-
Mannophryne leonardoi	TNHC 5659	-	-	-	-	-	-	-	-	-
Mannophryne leonardoi	TTSR	-	-	-	-	-	-	-	-	-
Mannophryne leonardoi	MIZA 316	-	-	-	-	-	-	-	-	-
Mannophryne leonardoi	WES 1034	DQ503128	DQ503024	-	-	-	-	-	-	-
Mannophryne leonardoi	WES 1035	DQ503129	DQ503025	-	-	-	-	-	-	-
Mannophryne leonardoi	WES 1036	DQ503130	DQ503026	-	-	-	-	-	-	-
Mannophryne leonardoi	MHNLS 22333	-	-	-	-	-	-	-	-	-
Mannophryne leonardoi	MHNLS 22334	-	-	-	-	-	-	-	-	-
Mannophryne leonardoi	MHNLS 22335	-	-	-	-	-	-	**Mle4**	-	**Mle4**
Mannophryne leonardoi	MHNLS 22336	-	-	-	-	-	-	-	-	-
Mannophryne molinai	MHNLS 21336	-	-	-	**MRo1**	-	-	**MRo1**	**MRo1**	**MRo1**
Mannophryne molinai	MHNLS 21337	-	-	-	-	-	-	-	-	-
Mannophryne molinai	MHNLS 21338	-	-	-	-	-	-	-	-	-
Mannophryne molinai	MHNLS 21356	-	-	-	-	-	-	-	-	-
Mannophryne cf. *molinai*	MHNLS 21005	-	-	-	-	-	-	-	-	-
Mannophryne cf. *molinai*	MHNLS 21006	-	-	-	-	-	-	-	-	-
Mannophryne cf. *molinai*	MHNLS 21365	-	-	-	-	-	-	-	-	-
Mannophryne cf. *molinai*	MHNLS 21367	-	-	-	-	-	-	-	-	-
Mannophryne cf. *molinai*	MHNLS 21205	-	-	-	**MQh1**	-	-	**MQh1**	**MQh1**	**MQh1**
Mannophryne cf. *molinai*	MHNLS 21206	-	-	-	-	-	-	-	-	-

Species	Voucher	SIAH1	28S	ZEB2	POMC	NT3	NCX1	BMP2	BDNF	CXCR4
Mannophryne cf. *molinai*	MHNLS 21516	-	-	-	-	-	-	-	-	-
Mannophryne cf. *molinai*	MHNLS 21517	-	-	-	-	-	-	-	-	-
Mannophryne neblina	MHNLS 22362	-	-	-	**Mne3**	-	-	**Mne3**	**Mne3**	**Mne3**
Mannophryne oblitterata	TTSR	-	-	-	-	-	-	-	-	-
Mannophryne oblitterata	MIZA 336	-	-	-	-	-	-	-	-	-
Mannophryne oblitterata	MHNLS 21766	-	-	-	-	-	-	-	-	-
Mannophryne oblitterata	MHNLS 21767	-	-	-	-	-	-	-	-	-
Mannophryne oblitterata	MHNLS 21818	-	-	-	**Mob4**	-	-	**Mob4**	**Mob4**	**Mob4**
Mannophryne oblitterata	MHNLS 21819	-	-	-	-	-	-	-	-	-
Mannophryne olmonae	MIZA 334 / isolate 451	-	-	-	-	-	-	-	-	-
Mannophryne olmonae	MIZA335 / isolate 452	-	-	-	-	-	-	-	-	-
Mannophryne olmonae	UWIZM 2732 / ZSM 1622	MF624096	MF614278	-	**Mol1**	-	-	**Mol1**	**Mol1**	**Mol1**
Mannophryne orellana	CVULA 7165	-	-	-	-	-	-	-	-	-
Mannophryne orellana	CVULA 7231	-	-	-	-	-	-	-	-	-
Mannophryne orellana	ULABG 7469	-	-	-	-	-	-	**Mor1**	-	**Mor1**
Mannophryne orellana	MHNLS MCp1	-	-	-	-	-	-	-	-	-
Mannophryne orellana	MHNLS MCp2	-	-	-	-	-	-	-	-	-
Mannophryne orellana	MHNLS MCp3	-	-	-	-	-	-	-	-	-
Mannophryne riveroi	MIZA 319	-	-	-	-	-	-	-	-	-
Mannophryne riveroi	TTSR	-	-	-	-	-	-	-	-	-
Mannophryne riveroi	MHNLS16433 / TNHC 5644	-	-	-	JX036004	-	JX035997	**Mri1**	**Mri1**	-
Mannophryne riveroi	MHNLS 17910	-	-	-	-	-	-	-	-	-
Mannophryne speeri	MHNLS 22606	-	-	-	**Msp1**	-	-	**Msp1**	**Msp1**	**Msp1**
Mannophryne trinitatis	MVZ 199837	-	-	-	JX036003	-	JX035998	-	-	-
Mannophryne trinitatis	MVZ199838 / isolate 405	-	-	-	-	-	-	-	-	-
Mannophryne trinitatis	MVZ 199828	DQ503097	-	-	-	-	-	-	-	-

Species	Voucher	SIAH1	28S	ZEB2	POMC	NT3	NCX1	BMP2	BDNF	CXCR4
Mannophryne trinitatis	ZSM 1619	-	-	-	-	-	-	-	-	-
Mannophryne trinitatis	ZSM 1620	-	-	-	-	-	-	**Mtn1**	**Mtn1**	-
Mannophryne trinitatis	ZSM 1621	-	-	-	-	-	-	-	-	-
Mannophryne trujillensis	MHNLS 17963	-	-	-	-	-	-	-	-	-
Mannophryne trujillensis	MHNLS 17971	-	-	-	-	-	-	-	-	-
Mannophryne trujillensis	MHNLS 22070	-	-	-	-	-	-	-	-	-
Mannophryne trujillensis	MHNLS 22071	-	-	-	-	-	-	-	-	-
Mannophryne trujillensis	MHNLS 22063	-	-	-	-	-	-	-	-	-
Mannophryne trujillensis	MHNLS 22064	-	-	-	**Mtr4**	-	-	**Mtr4**	**Mtr4**	**Mtr4**
Mannophryne urticans	TNHC 5520	-	-	-	-	-	-	-	-	-
Mannophryne urticans	ULABG 4481	-	-	-	-	-	-	-	-	-
Mannophryne urticans	MHNLS 21555	-	-	-	**Mur2**	-	-	**Mur2**	**Mur2**	**Mur2**
Mannophryne urticans	MHNLS 21556	-	-	-	-	-	-	-	-	-
Mannophryne urticans	MHNLS 21994	-	-	-	-	-	-	-	-	-
Mannophryne urticans	MHNLS 21993	-	-	-	-	-	-	-	-	-
Mannophryne venezuelensis	EBRG 4921 / isolate 469	-	-	-	-	-	-	-	-	-
Mannophryne venezuelensis	EBRG 4922 / isolate 555 / isoalte 470	-	-	-	-	-	-	-	-	-
Mannophryne venezuelensis	MHNLS 16435	-	-	-	**Mve1**	-	-	**Mve1**	**Mve1**	**Mve1**
Mannophryne venezuelensis	MHNLS 17287	-	-	-	-	-	-	-	-	-
Mannophryne venezuelensis	MHNLS 17314	-	-	-	-	-	-	-	-	-
Mannophryne venezuelensis	MHNLS 17315	-	-	-	-	-	-	-	-	-
Mannophryne venezuelensis	TNHC 5649	-	-	-	-	-	-	-	-	-
Mannophryne vulcano	TNHC 5679	-	-	-	-	-	-	-	-	-
Mannophryne vulcano	MIZA 342	-	-	-	-	-	-	-	-	-
Mannophryne vulcano	MIZA 343	-	-	-	-	-	-	-	-	-
Mannophryne vulcano	MHNLS 16685	-	-	-	-	-	-	-	-	-

Species	Voucher	SIAH1	28S	ZEB2	POMC	NT3	NCX1	BMP2	BDNF	CXCR4
Mannophryne vulcano	MHNLS 22140	-	-	-	**Mvu36**	-	-	**Mvu36**	-	**Mvu36**
Mannophryne vulcano	MHNLS 22141	-	-	-	-	-	-	-	-	-
Mannophryne vulcano	MHNLS 22142	-	-	-	-	-	-	-	-	-
Mannophryne vulcano	MHNLS 20692	-	-	-	-	-	-	-	-	-
Mannophryne vulcano	MHNLS 20693	-	-	-	-	-	-	-	-	-
Mannophryne vulcano	MHNLS 18575	-	-	-	-	-	-	-	-	-
Mannophryne vulcano	MHNLS 18577	-	-	-	-	-	-	-	-	-
Mannophryne vulcano	MHNLS 21802	-	-	-	-	-	-	-	-	-
Mannophryne vulcano	MHNLS 21803	-	-	-	-	-	-	-	-	-
Mannophryne vulcano	MHNLS 20830	-	-	-	-	-	-	-	-	-
Mannophryne vulcano	MHNLS 21770	-	-	-	-	-	-	-	-	-
Mannophryne vulcano	MHNLS 21771	-	-	-	-	-	-	-	-	-
Mannophryne vulcano	MHNLS 22346	-	-	-	-	-	-	-	-	-
Mannophryne vulcano	MHNLS 20941	-	-	-	-	-	-	-	-	-
Mannophryne vulcano	MHNLS 20942	-	-	-	-	-	-	-	-	-
Mannophryne vulcano	MHNLS 21778	-	-	-	-	-	-	-	-	-
Mannophryne vulcano	MHNLS 21779	-	-	-	-	-	-	-	-	-
Mannophryne yustizi	TTSR_G	-	-	-	-	-	-	-	-	-
Mannophryne yustizi	TNHC 5604	-	-	-	-	-	-	-	-	-
Mannophryne yustizi	TTSR_S	-	-	-	-	-	-	-	-	-
Mannophryne yustizi	MIZA 322	-	-	-	-	-	-	-	-	-
Mannophryne sp. 1	TTSR	-	-	-	-	-	-	-	-	-
Mannophryne sp. 1	MIZA 341	-	-	-	-	-	-	-	-	-
Mannophryne sp. 1	MHNLS 16769	-	-	-	-	-	-	-	-	-
Mannophryne sp. 1	MHNLS 16772	-	-	-	**MRu1**	-	-	**MRu1**	**MRu1**	**MRu1**
Mannophryne sp. 1	MHNLS 16773	-	-	-	-	-	-	-	-	-

Species	Voucher	SIAH1	28S	ZEB2	POMC	NT3	NCX1	BMP2	BDNF	CXCR4
Mannophryne sp. 1	MHNLS 16798	-	-	-	-	-	-	-	-	-
Mannophryne sp. (cf. *vulcano*)	MHNLS 21825	-	-	-	-	-	-	-	-	-
Mannophryne sp. (cf. *vulcano*)	MHNLS 21826	-	-	-	-	-	-	-	-	-
Mannophryne sp. 2	MIZA 340	-	-	-	-	-	-	-	-	-
Mannophryne sp. 2	EBRG 4889	-	-	-	-	-	-	-	-	-
Mannophryne sp. 2	MHNLS 17251	-	-	-	-	-	-	-	-	-
Mannophryne sp. 2	MHNLS 17252	-	-	-	-	-	-	-	-	-
Mannophryne sp. 2	MHNLS 17253	-	-	-	-	-	-	**MPl1**	-	-
Mannophryne sp. 2	MHNLS 17254	-	-	-	-	-	-	-	-	-
Mannophryne sp. 2	MHNLS 17256	-	-	-	-	-	-	-	-	-
Mannophryne sp. 2	MHNLS 15545	-	-	-	**MPi1**	-	-	**MPi1**	**MPi1**	**MPi1**
Mannophryne sp. 3	MHNLS 22358	-	-	-	-	-	-	-	-	-
Mannophryne sp. 3	MHNLS 22359	-	-	-	-	-	-	-	-	-
Mannophryne sp. 3	MHNLS 22360	-	-	-	**MAg3**	-	-	**MAg3**	**MAg3**	**MAg3**
Mannophryne sp. 3	MHNLS 22347	-	-	-	-	-	-	-	-	-
Mannophryne sp. 3	MHNLS 22348	-	-	-	-	-	-	-	-	-
Mannophryne sp. 3	MHNLS 22353	-	-	-	-	-	-	-	-	-
Mannophryne sp. 3	MHNLS 21747	-	-	-	-	-	-	-	-	-
Mannophryne sp. 3	MHNLS 21748	-	-	-	-	-	-	-	-	-
Mannophryne sp. 4	MHNLS 22204	-	-	-	-	-	-	**MMo1**	-	**MMo1**
Mannophryne sp. 4	MHNLS 22214	-	-	-	-	-	-	-	-	-
Mannophryne sp. 4	MHNLS 22219	-	-	-	-	-	-	-	-	-
Mannophryne sp. 4	MHNLS 22281	-	-	-	-	-	-	-	-	-
Mannophryne sp. 4	MHNLS 22302	-	-	-	-	-	-	-	-	-
Mannophryne sp. 4	MHNLS 22303	-	-	-	-	-	-	-	-	-
Mannophryne sp. 4	MHNLS 22304	-	-	-	-	-	-	-	-	-

Species	Voucher	SIAH1	28S	ZEB2	POMC	NT3	NCX1	BMP2	BDNF	CXCR4
Mannophryne sp. (aff. *herminae*)	MHNLS 17157	-	-	-	**MSi1**	-	-	**MSi1**	**MSi1**	**MSi1**
Mannophryne sp. (aff. *herminae*)	MHNLS 17158	-	-	-	-	-	-	-	-	-
Mannophryne sp. (aff. *herminae*)	MHNLS 17159	-	-	-	-	-	-	-	-	-
Mannophryne sp. (aff. *herminae*)	MHNLS 17160	-	-	-	-	-	-	-	-	-
Mannophryne sp. (*yustizi* complex)	MHNLS 22585	-	-	-	-	-	-	-	-	-
Mannophryne sp. (*yustizi* complex)	MHNLS 22586	-	-	-	-	-	-	-	-	-
Mannophryne sp. (aff. *vulcano*)	TNHC 5666	-	-	-	-	-	-	-	-	-
Mannophryne sp. (*yustizi* complex)	ULABG 4465	-	-	-	-	-	-	-	-	-
Mannophryne sp. (*yustizi* complex)	ULABG 4453	-	-	-	-	-	-	-	-	-
Mannophryne sp. (*yustizi* complex)	ULABG 4458	-	-	-	-	-	-	-	-	-
Mannophryne sp. (*yustizi* complex)	MHNLS 22080	-	-	-	**MJa1**	-	-	**MJa1**	**MJa1**	**MJa1**
Mannophryne sp. (*yustizi* complex)	MHNLS 22081	-	-	-	-	-	-	-	-	-
Mannophryne sp. (*yustizi* complex)	MHNLS 22617	-	-	-	-	-	-	-	-	-
Mannophryne sp. (cf. *speeri-yustizi*)	MHNLS 22618	-	-	-	-	-	-	-	-	-
Mannophryne sp. (*yustizi* complex)	MHNLS 22619	-	-	-	-	-	-	-	-	-
Mannophryne sp. (cf. *speeri-yustizi*)	MHNLS 22169	-	-	-	**MNi1**	-	-	**MNi1**	**MNi1**	**MNi1**
Mannophryne sp. (*yustizi* complex)	MHNLS 22170	-	-	-	-	-	-	-	-	-
Mannophryne sp. (*yustizi* complex)	MHNLS 22171	-	-	-	-	-	-	-	-	-
Mannophryne sp. (*yustizi* complex)	MHNLS 22172	-	-	-	-	-	-	-	-	-
Mannophryne sp. (*yustizi* complex)	MHNLS 22559	-	-	-	-	-	-	-	-	-
Mannophryne sp. (*yustizi* complex)	MHNLS 22560	-	-	-	**Myu3**	-	-	**Myu3**	-	-
Andinobates bombetes	TNHC 4946 / MAR 1265	MF624072	MF614246	HQ290678	HQ290858	HQ290798	HQ290738	HQ291041	HQ290618	-
Adelphobates galactonotus	TNHC 4889 / MTR 5088	DQ503088	DQ502988	HQ290681	HQ290861	HQ290801	HQ290741	HQ291044	HQ290621	-
Allobates aff. *juanii*	ANDESA 1073	-	-	-	-	-	-	-	-	-
Allobates algorei	TNHC 5551	-	-	HQ290650	HQ290830	HQ290770	HQ290710	HQ291013	HQ290590	-
Allobates amissibilis	MTD 47884	-	-	-	-	-	-	-	-	-

Species	Voucher	SIAH1	28S	ZEB2	POMC	NT3	NCX1	BMP2	BDNF	CXCR4
Allobates bacurau	INPAH 35406	-	-	-	-	-	-	-	-	-
Allobates caeruleodactylus	MPEG 13809	DQ503080	-	-	-	-	-	-	-	-
Allobates chalcopis	Alca1	-	-	-	-	-	-	-	-	-
Allobates conspicuus	MPEG 12321	DQ503099	DQ502995	-	-	-	-	-	-	-
Allobates crombiei	APL 14124	-	-	-	-	-	-	-	-	-
Allobates femoralis (Acre01)	Acre 12931	-	-	-	-	-	-	-	-	-
Allobates femoralis (Acre02)	OMNH 36070	DQ503077	-	-	-	-	-	-	-	-
Allobates femoralis	QCAZ 16484	-	-	HQ290651	HQ290831	HQ290771	HQ290711	HQ291014	HQ290591	-
Allobates flaviventris	OMNH 36959	DQ503126	DQ503022	-	-	-	-	-	-	-
Allobates fratisenescus	QCAZ 54377	MF624069	-	-	-	-	-	-	-	-
Allobates gasconi	MPEG 13003	-	-	-	-	-	-	-	-	-
Allobates granti	148 AF	-	-	-	-	-	-	-	-	-
Allobates grillisimilis	APL 12747	-	-	-	-	-	-	-	-	-
Allobates hodli	AbuE 2189	-	-	-	-	-	-	-	-	-
Allobates humilis	CVULA 5690	-	-	-	-	-	-	-	-	-
Allobates humilis	MHNLS22093a	-	-	-	-	-	-	-	-	-
Allobates insperatus	QCAZ1 6533	-	-	HQ290659	HQ290839	HQ290779	HQ290719	HQ291022	HQ290599	-
Allobates juami	MCP 13287	-	-	-	-	-	-	-	-	-
Allobates juanii	TNHC 4978	-	-	HQ290660	HQ290840	HQ290780	HQ290720	HQ291023	HQ290600	-
Allobates kingsburyi	QCAZ 16523	-	-	HQ290661	HQ290841	HQ290781	HQ290721	HQ291024	HQ290601	-
Allobates magnussoni	MPEG 11923	DQ503098	DQ502994	-	-	-	-	-	-	-
Allobates masniger	APL 14250	-	-	-	-	-	-	-	-	-
Allobates myersi	INPAH 26396	-	-	-	-	-	-	-	-	-
Allobates nidicola	MPEG 13821	DQ503081	DQ502980	-	-	-	-	-	-	-
Allobates niputidea	MUJ 3520	-	-	-	-	-	-	-	-	-
Allobates olfersioides	MRT 6031	DQ503093	-	-	-	-	-	-	-	-

Species	Voucher	SIAH1	28S	ZEB2	POMC	NT3	NCX1	BMP2	BDNF	CXCR4
Allobates ornatus	MHNSM 22863	-	-	-	-	-	-	-	-	-
Allobates paleovarzensis	MJH 3909	-	-	-	-	-	-	-	-	-
Allobates peruvianus	MHNSM 22923	-	-	-	-	-	-	-	-	-
Allobates pittieri	MIZA 339	-	-	-	-	-	-	-	-	-
Allobates pittieri	MHNLS 21229	-	-	-	**Lpi1**	-	-	**Lpi1**	**Lpi1**	**Lpi1**
Allobates subfolionidificans	APL 1692	-	-	-	-	-	-	-	-	-
Allobates sumtuosus	MTD 47771	-	-	-	-	-	-	-	-	-
Allobates talamancae	QCAZ 16549	-	-	HQ290672	HQ290852	HQ290792	HQ290732	HQ291035	HQ290612	-
Allobates talamancae	SIUC 7667	DQ503114	DQ503004	-	-	-	-	-	-	-
Allobates tapajos	LSUMZ 15176	DQ503064	DQ502963	-	-	-	-	-	-	-
Allobates tinae	MPEG 13826	DQ503079	DQ502979	-	-	-	-	-	-	-
Allobates trilineatus	KU 215175	DQ503045	DQ502944	-	-	-	-	-	-	-
Allobates undulatus	AMNHA 159139	DQ282656	DQ283464	-	-	-	-	-	-	-
Allobates zaparo	QCAZ 16603	-	-	HQ290700	HQ290880	HQ290820	HQ290760	HQ291063	HQ290640	-
Allobates sp. (Alto Mazan)	MZ 010	-	-	-	-	-	-	-	-	-
Allobates sp. (Carajas)	TG 3264	-	MF614242	-	-	-	-	-	-	-
Allobates sp. (Cuao)	MHNLS 19982	-	-	-	-	-	-	-	-	-
Allobates sp. (Cuyabeno)	OMNH 34086	DQ503063	DQ502962	-	-	-	-	-	-	-
Allobates sp. (Liberdade)	MCP 10212	-	MF614245	-	-	-	-	-	-	-
Allobates sp. (Neblina)	AMCC 106112	DQ503069	DQ502970	-	-	-	-	-	-	-
Allobates sp. (PEGM1)	LSUMZ 17601	DQ503100	-	-	-	-	-	-	-	-
Allobates sp. (PEGM3)	MPEG 13386	-	-	-	-	-	-	-	-	-
Ameerega trivittata	TNHC 4966 / MPEG 12504	DQ503073	DQ502974	HQ290699	HQ290879	HQ290819	HQ290759	HQ291062	HQ290639	-
Anomaloglossus apiau	MTR 37501	MF624077	MF614251	-	-	-	-	-	-	-
Anomaloglossus baeobatrachus 1	AF 2590	-	-	-	KY549504	-	-	-	-	-
Anomaloglossus baeobatrachus 2	MTR 13861	-	-	-	KY549520	-	-	-	-	-

Species	Voucher	SIAH1	28S	ZEB2	POMC	NT3	NCX1	BMP2	BDNF	CXCR4
Anomaloglossus beebei	ROM 39631	DQ503094	DQ502991	-	-	-	-	-	-	-
Anomaloglossus blanci	AF 932	-	-	-	-	-	-	-	-	-
Anomaloglossus degranvillei	PG 601	-	-	-	KY549526	-	-	-	-	-
Anomaloglossus dewynteri	PG 660	-	-	-	-	-	-	-	-	-
Anomaloglossus kaiei	279	DQ503052	DQ502952	-	-	-	-	-	-	-
Anomaloglossus leopardus	AF 2041	-	-	-	-	-	-	-	-	-
Anomaloglossus meansi	ROM 39639	DQ503096	DQ502993	-	-	-	-	-	-	-
Anomaloglossus megacephalus	ROM 39637	DQ503095	DQ502992	-	-	-	-	-	-	-
Anomaloglossus praderioi	CPI 10208	DQ503137	DQ503036	-	-	-	-	-	-	-
Anomaloglossus roraima	06-141	MF624102	MF614288	-	-	-	-	-	-	-
Anomaloglossus rufulus	MHNLS 20610	-	-	-	**Nru2**	-	-	**Nru2**	**Nru2**	**Nru2**
Anomaloglossus rufulus	CLBA / voucher 214 (Vacher et al)	-	-	-	KY549491	-	-	-	-	-
Anomaloglossus mitaraka	AF 2732	-	-	-	KY549508	-	-	-	-	-
Anomaloglossus stepheni	AF 2045	-	-	-	KY549495	-	-	-	-	-
Anomaloglossus stepheni	MJH 3928	DQ503085	DQ502984	-	-	-	-	-	-	-
Anomaloglossus surinamensis 1	AF 585	-	-	-	-	-	-	-	-	-
Anomaloglossus surinamensis 2	AF 2456	-	-	-	-	-	-	-	-	-
Anomaloglossus surinamensis 5	AF 3340	-	-	-	KY549511	-	-	-	-	-
Anomaloglossus tamacuarensis	MNRJ 38049	MF624078	MF614252	-	-	-	-	-	-	-
Anomaloglossus tepuyensis	MHNLS 15613	-	-	-	**Nte1**	-	-	**Nte1**	**Nte1**	**Nte1**
Anomaloglossus tepuyensis	VUB 3734	-	-	-	-	-	-	-	-	-
Anomaloglossus verbeeksnyderorum	MHNLS 20084	-	-	-	-	-	-	-	-	-
Anomaloglossus verbeeksnyderorum	MHNLS 20085	-	-	-	-	-	-	-	-	-
Anomaloglossus verbeeksnyderorum	TNHC5631	-	-	HQ290652	HQ290832	HQ290772	HQ290712	HQ291015	HQ290592	-
Anomaloglossus wothuja	MHNLS 19952 / VUB 3735	-	-	-	-	-	-	-	-	-
Anomaloglossus wothuja	MHNLS 19953 / VUB 3736	-	-	-	-	-	-	-	-	-

Species	Voucher	SIAH1	28S	ZEB2	POMC	NT3	NCX1	BMP2	BDNF	CXCR4
Anomaloglossus sp. (Brownsberg)	UTAA 56469	DQ503134	DQ503029	-	-	-	-	-	-	-
Anomaloglossus sp. A (Wokomung)	VUB 3128	-	-	-	-	-	-	-	-	-
Anomaloglossus sp. (Bakhuis)	AF 3426	-	-	-	KY549513	-	-	-	-	-
Anomaloglossus sp. (Brownsberg)	BPN 0850	-	-	-	KY549514	-	-	-	-	-
Anomaloglossus sp. (Ichún)	MHNLS 17561	-	-	-	-	-	-	-	-	-
Anomaloglossus sp. (Thomasing)	UTAA 56710	DQ503136	DQ503034	-	-	-	-	-	-	-
Rheobates pseudopalmatus	MHUA 5162	-	-	-	KJ130747	-	-	-	-	-
Rheobates palmatus	MUJ 3829	-	MF614283	-	-	-	-	-	-	-
Rheobates palmatus	TNHC 4955	-	-	HQ290665	HQ290845	HQ290785	HQ290725	HQ291028	HQ290605	-
Hyloxalus cepedai	MAA 574	MF624087	MF614267	-	-	-	-	-	-	-
Leucostethus fugax	QCAZ 16513	-	-	HQ290658	HQ290838	HQ290778	HQ290718	HQ291021	HQ290598	-
Leucostethus brachistriatus	MHNUC 360	-	DQ503013	-	-	-	-	-	-	-
Silverstoneia nubicola	SIUC 7652	DQ503111	DQ503000	-	-	-	-	-	-	-
Epipedobates tricolor	QCAZ 21977	-	-	HQ290698	HQ290878	HQ290818	HQ290758	HQ291061	HQ290638	-
Ectopoglossus saxatilis	IAvH 14617	MF624085	MF614264	-	-	-	-	-	-	-
Paruwrobates erythromos	QCAZ 37750	-	-	-	-	-	-	-	-	-
Phyllobates bicolor	1233	-	DQ503019	-	-	-	-	-	-	-
"Colostethus" ruthveni	MAR 558	MF624079	MF614253	-	-	-	-	-	-	-
Minyobates steyermarki	Roberts et al. / Vences et al.	-	-	-	-	-	-	-	-	-
Oophaga pumilio	TNHC 4814	-	-	HQ290685	HQ290865	HQ290805	HQ290745	HQ291048	HQ290625	-
Dendrobates tinctorius	TNHC64416 / UTA 56495	DQ503133	DQ503028	HQ290688	HQ290868	HQ290808	HQ290748	HQ291051	HQ290628	-
Exidobates captivus	QCAZ 27442	-	-	HQ290679	HQ290859	HQ290799	HQ290739	HQ291042	HQ290619	-
Ranitomeya toraro	OMNH 36666	DQ503068	DQ502969	-	-	-	-	-	-	-
Thoropa miliaris	AF 1434	-	-	-	-	-	-	-	-	-

Appendix 5. Ordered list of wildcard candidates identified by YBYRÁ (Machado 2015). Terminals that result in the smallest values of match split distance average when excluded from the primary topologies, are considered potencial wildcards (first positioned in the list).

Position	Teminal name	Average distances
1	*Mannophryne cordilleriana* MHNLS21601	564.745336297
2	*Mannophryne cordilleriana* MHNLS21626	564.806149649
3	*Mannophryne cordilleriana* MHNLS21632	564.85358868
4	*Mannophryne cordilleriana* MHNLS21633	564.854518767
5	*Mannophryne cordilleriana* MHNLS21602	564.871742678
6	*Mannophryne cordilleriana* MHNLS22187	564.872755849
7	*Mannophryne cordilleriana* MHNLS22188	564.887083336
8	*Mannophryne cordilleriana* MHNLS21625	564.897741251
9	*Mannophryne cordilleriana* MHNLS22099	564.906298971
10	*Mannophryne cordilleriana* MHNLS21693	564.907819882
11	*Mannophryne cordilleriana* MHNLS21761	564.909232321
12	*Mannophryne cordilleriana* MHNLS22098	564.917907744
13	*Mannophryne cordilleriana* TNHC5589	564.934432359
14	*Mannophryne cordilleriana* MHNLS21689	564.961007909
15	*Mannophryne cordilleriana* ULABG5352	565.128432723
16	*Mannophryne vulcano* MHNLS22141	565.497104731
17	*Mannophryne* sp. (*yustizi* complex) MHNLS22559	565.663082487
18	*Mannophryne vulcano* MHNLS21770	565.67796618
19	*Mannophryne vulcano* MHNLS21802	565.692349057
20	*Mannophryne vulcano* MHNLS22142	565.71845841
21	*Mannophryne vulcano* MHNLS16685	565.756019599
22	*Mannophryne vulcano* MHNLS21778	565.772262649
23	*Mannophryne vulcano* MHNLS21803	565.83147893
24	*Mannophryne vulcano* MHNLS20942	565.89703734
25	*Mannophryne vulcano* MHNLS22140	565.961287166
26	*Mannophryne vulcano* MHNLS20830	566.032587649
27	*Mannophryne vulcano* MIZA343	566.432654116
28	*Mannophryne vulcano* MIZA342	566.657815843
29	*Mannophryne* cf. *molinai* MHNLS21367	567.541361157
30	*Aromobates ericksonae* ULABG7776	567.741795967
31	*Mannophryne* cf. *molinai* MHNLS21365	567.846863439
32	*Mannophryne* cf. *molinai* MHNLS21206	567.8769447
33	*Mannophryne collaris* MHNLS21593	567.879031048
34	*Mannophryne collaris* MHNLS21591	567.879984214
35	*Mannophryne collaris* MIZA321	567.889982068
36	*Mannophryne collaris* MHNLS22058	567.895516429
37	*Mannophryne collaris* MHNLS21592	567.895908773
38	*Mannophryne collaris* MHNLS21687	567.910665531
39	*Mannophryne collaris* MIZA320	567.917672337

Position	Teminal name	Average distances
40	*Mannophryne collaris* MHNLS21686	567.929029548
41	*Mannophryne collaris* ULABG4248	567.938475812
42	*Mannophryne collaris* MHNLS21684	567.948986021
43	*Mannophryne collaris* MHNLS21685	567.962189558
44	*Mannophryne collaris* MHNLS21590	567.994031752
45	*Mannophryne herminae* MIZA327	568.276971934
46	*Mannophryne herminae* MHNLS21736	568.292792637
47	*Mannophryne herminae* TNHC5676	568.312783728
48	*Mannophryne herminae* MIZA329	568.349781787
49	*Mannophryne herminae* MIZA328	568.354778406
50	*Mannophryne herminae* MHNLS21735	568.369380535
51	*Mannophryne herminae* MHNLS17475	568.38583822
52	*Mannophryne herminae* MHNLS22106	568.430048489
53	*Mannophryne herminae* MHNLS22107	568.493287452
54	*Mannophryne vulcano* MHNLS20693	569.243354958
55	*Mannophryne vulcano* MHNLS21779	569.257758607
56	*Mannophryne vulcano* MHNLS18577	569.264329218
57	*Mannophryne vulcano* MHNLS20941	569.272019165
58	*Mannophryne vulcano* MHNLS20692	569.276351107
59	*Aromobates mayorgai* MHNLS21981	569.281723914
60	*Mannophryne vulcano* MHNLS21771	569.283921042
61	*Aromobates mayorgai* MHNLS21982	569.29395813
62	*Mannophryne vulcano* TNHC5679	569.295723679
63	*Aromobates mayorgai* MHNLS21983	569.34592989
64	*Aromobates mayorgai* MHNLS21984	569.382951029
65	*Mannophryne* sp. (*yustizi* complex) MHNLS22618	569.436866047
66	*Mannophryne* sp. (*yustizi* complex) MHNLS22617	569.510924478
67	*Aromobates mayorgai* MHNLS22002	570.236061972
68	*Aromobates mayorgai* MHNLS22032	570.283168664
69	*Aromobates mayorgai* MHNLS22033	570.288183746
70	*Aromobates mayorgai* MHNLS22005	570.310600448
71	*Aromobates mayorgai* MHNLS22031	570.313683812
72	*Aromobates mayorgai* MHNLS22003	570.319162784
73	*Aromobates mayorgai* MHNLS22030	570.320983722
74	*Mannophryne cordilleriana* MIZA330	570.473268666
75	*Mannophryne cordilleriana* MIZA331	570.473268666
76	*Mannophryne cordilleriana* MIZA332	570.473268666
77	*Aromobates zippeli* MIZA312	570.523966461
78	*Aromobates zippeli* MHNLS22045	570.527532178
79	*Aromobates zippeli* MIZA310	570.542999772
80	*Aromobates zippeli* MHNLS22043	570.548926477
81	*Aromobates zippeli* ULABG4496	570.555637871
82	*Aromobates zippeli* MHNLS22044	570.572243263
83	*Aromobates zippeli* MIZA311	570.573233355

Position	Teminal name	Average distances
84	*Aromobates zippeli* MHNLS22042	570.57971165
85	*Mannophryne molinai* MHNLS21337	570.848785925
86	*Mannophryne molinai* MHNLS21356	570.851640807
87	*Mannophryne molinai* MHNLS21338	570.88813805
88	*Mannophryne molinai* MHNLS21336	570.897708941
89	*Mannophryne* sp. 2 MHNLS17256	570.905295031
90	*Aromobates* sp. (aff. *saltuensis* 3) AOH	570.912904201
91	*Aromobates* sp. (cf. *saltuensis* 2) LOA124	570.912904201
92	*Mannophryne* cf. *molinai* MHNLS21205	570.922502787
93	*Mannophryne vulcano* MHNLS18575	570.962168786
94	*Mannophryne vulcano* MHNLS22346	570.962168786
95	*Mannophryne* sp. (*yustizi* complex) ULABG4453	571.01459982
96	*Mannophryne* sp. (*yustizi* complex) ULABG4458	571.067086244
97	*Mannophryne* sp. (*yustizi* complex) MHNLS22619	571.067614755
98	*Mannophryne* sp. (*yustizi* complex) ULABG4465	571.069754185
99	*Mannophryne* sp. (*yustizi* complex) MHNLS22560	571.147196008
100	*Mannophryne* sp. (*yustizi* complex) MHNLS20080	571.160334923
101	*Mannophryne* sp. (*yustizi* complex) MHNLS20081	571.163129799
102	*Mannophryne venezuelensis* MHNLS17287	571.219181939
103	*Mannophryne venezuelensis* MHNLS16435	571.259851879
104	*Mannophryne* sp. 4 MHNLS22304	571.260061898
105	*Mannophryne larandina* MIZA326	571.260140367
106	*Mannophryne venezuelensis* MHNLS17315	571.269351224
107	*Mannophryne venezuelensis* MHNLS17314	571.272907709
108	*Mannophryne venezuelensis* TNHC5649	571.284721886
109	*Mannophryne* sp. 4 MHNLS22281	571.290173162
110	*Mannophryne venezuelensis* EBRG4922	571.290842455
111	*Mannophryne venezuelensis* EBRG4921	571.299898683
112	*Mannophryne* sp. 4 MHNLS22302	571.310228875
113	*Mannophryne larandina* MIZA324	571.312691412
114	*Mannophryne* sp. 4 MHNLS22204	571.315975564
115	*Mannophryne larandina* MIZA325	571.320102102
116	*Mannophryne* sp. 4 MHNLS22219	571.328722135
117	*Mannophryne larandina* MHNLS22598	571.333619514
118	*Mannophryne* sp. 4 MHNLS22303	571.333626438
119	*Mannophryne larandina* MHNLS22597	571.340028572
120	*Mannophryne larandina* MHNLS22599	571.350017194
121	*Mannophryne* sp. 4 MHNLS22214	571.351180379
122	*Mannophryne* sp. 3 MHNLS22359	571.408037979
123	*Anomaloglossus* sp. A VUB3128	571.408215688
124	*Mannophryne* sp. 3 MHNLS22358	571.425670389
125	*Mannophryne* sp. 3 MHNLS21747	571.444897564
126	*Mannophryne* sp. 3 MHNLS21748	571.455181598
127	*Mannophryne* sp. 3 MHNLS22360	571.501397438

Position	Teminal name	Average distances
128	*Mannophryne* "*herminae*" CWM1141	571.503384546
129	*Aromobates ericksonae* CVULA7180	571.553440743
130	*Mannophryne* cf. *molinai* MHNLS21005	571.564128661
131	*Mannophryne* cf. *molinai* MHNLS21006	571.564128661
132	*Mannophryne* cf. *yustizi* MHNLS22169	571.579923978
133	*Mannophryne* cf. *yustizi* MHNLS22171	571.593113667
134	*Mannophryne* cf. *yustizi* MHNLS22170	571.605241719
135	*Aromobates ericksonae* TNHC5540	571.61464644
136	*Mannophryne* cf. *yustizi* MHNLS22172	571.621034727
137	*Mannophryne lamarcai* NMA38	571.628941617
138	*Mannophryne lamarcai* NMA41	571.655985673
139	*Mannophryne lamarcai* MIZA318	571.663966415
140	*Aromobates ericksonae* CVULA8379	571.667185946
141	*Mannophryne lamarcai* MIZA317	571.681910393
142	*Mannophryne lamarcai* NMA40	571.688494852
143	*Mannophryne oblitterata* TTSR	571.930603541
144	*Mannophryne trujillensis* MHNLS22063	571.949851486
145	*Mannophryne oblitterata* MIZA336	571.968545534
146	*Mannophryne oblitterata* MHNLS21766	571.979249607
147	*Mannophryne trujillensis* MHNLS22071	571.981015156
148	*Mannophryne oblitterata* MHNLS21767	571.9877704
149	*Mannophryne* sp. 2 EBRG4889	571.999649198
150	*Mannophryne trujillensis* MHNLS22070	572.003877284
151	*Mannophryne oblitterata* MHNLS21818	572.005181251
152	*Mannophryne oblitterata* MHNLS21819	572.005610522
153	*Mannophryne trujillensis* MHNLS17963	572.016118423
154	*Mannophryne trujillensis* MHNLS17971	572.016896188
155	*Mannophryne* sp. 2 MHNLS17252	572.01739008
156	*Mannophryne trujillensis* MHNLS22064	572.020048789
157	*Mannophryne* sp. 2 MIZA340	572.058154644
158	*Mannophryne orellana* MHNLS_MCp3	572.309340331
159	*Mannophryne orellana* MHNLS_MCp1	572.328636742
160	*Mannophryne orellana* MHNLS_MCp2	572.352142776
161	*Mannophryne* sp. 2 MHNLS17254	572.357054003
162	*Mannophryne* sp. 2 MHNLS15545	572.358417976
163	*Aromobates tokuko* MHNLS18478	572.376481965
164	*Aromobates tokuko* MHNLS18483	572.376784301
165	*Aromobates tokuko* MHNLS18493	572.376823535
166	*Aromobates tokuko* MHNLS18566	572.377534371
167	*Mannophryne orellana* ULABG7469	572.382344049
168	*Mannophryne* sp. 2 MHNLS17251	572.384430397
169	*Mannophryne* sp. 2 MHNLS17253	572.389265462
170	*Mannophryne* cf. *molinai* MHNLS21516	572.422554715
171	*Mannophryne* cf. *molinai* MHNLS21517	572.422554715

Position	Teminal name	Average distances
172	*Mannophryne urticans* MHNLS21993	572.582421133
173	*Aromobates meridensis* MHNLS22019	572.62980939
174	*Aromobates meridensis* MHNLS22017	572.633852843
175	*Aromobates cannatellai* MHNLS22629	572.639354894
176	*Aromobates meridensis* MHNLS22016	572.645597783
177	*Aromobates* sp. 1 MHNLS21507	572.649807405
178	*Aromobates meridensis* MHNLS22018	572.650622096
179	*Aromobates cannatellai* MHNLS22627	572.651256771
180	*Aromobates meridensis* CVULA7399	572.655288685
181	*Aromobates cannatellai* MHNLS22626	572.659177508
182	*Mannophryne leonardoi* TTSR	572.660271456
183	*Aromobates cannatellai* CVULA8325	572.662500894
184	*Mannophryne leonardoi* MHNLS22333	572.664024113
185	*Aromobates cannatellai* MHNLS22625	572.665819665
186	*Aromobates* sp. 1 MHNLS22128	572.672690304
187	*Aromobates* sp. 1 MHNLS22127	572.676523738
188	*Aromobates* sp. 1 MHNLS21508	572.681485738
189	*Mannophryne leonardoi* MHNLS22334	572.693743033
190	*Mannophryne leonardoi* TNHC5659	572.719420808
191	*Aromobates* sp. 1 MHNLS21506	572.72064169
192	*Mannophryne leonardoi* WES1034	572.740549697
193	*Aromobates* cf. sp. 1 MHNLS21358	572.756462717
194	*Aromobates* cf. sp. 1 MHNLS21335	572.763137184
195	*Aromobates* cf. sp. 1 MHNLS21334	572.769537011
196	*Aromobates* cf. sp. 1 MHNLS21359	572.778235513
197	*Aromobates* cf. sp. 1 MHNLS21333	572.782228192
198	*Mannophryne* sp. 1 MHNLS16769	572.799809828
199	*Mannophryne yustizi* TNHC5604	572.803484017
200	*Mannophryne urticans* ULABG4481	572.807178976
201	*Mannophryne urticans* MHNLS21555	572.843516974
202	*Mannophryne collaris* TNHC5507	572.973537537
203	*Mannophryne collaris* TNHC5515	572.973537537
204	*Mannophryne* sp. 1 MIZA341	572.99940456
205	*Mannophryne* sp. 1 TTSR	572.99940456
206	*Mannophryne* sp. 3 MHNLS22347	573.040028341
207	*Mannophryne* sp. 3 MHNLS22348	573.040028341
208	*Mannophryne* sp. 3 MHNLS22353	573.040028341
209	*Mannophryne* sp. (aff. *herminae*) MHNLS17157	573.083832418
210	*Mannophryne* sp. (aff. *herminae*) MHNLS17158	573.083832418
211	*Mannophryne* sp. (aff. *herminae*) MHNLS17159	573.083832418
212	*Mannophryne yustizi* TTSR_G	573.13093911
213	*Aromobates saltuensis* ULABG4981	573.16444069
214	*Aromobates saltuensis* ULABG_AGu1	573.166503959
215	*Aromobates saltuensis* MHNLS17233	573.166596275

Position	Teminal name	Average distances
216	*Aromobates saltuensis* TNHC5541	573.173861567
217	*Mannophryne yustizi* TTSR_S	573.175290162
218	*Mannophryne yustizi* MIZA322	573.229482129
219	*Aromobates molinarii* ULABGsn3	573.311350518
220	*Aromobates molinarii* ULABG4497	573.311426679
221	*Aromobates molinarii* ULABGsn1	573.311805176
222	*Aromobates molinarii* ULABGsn2	573.312938358
223	*Aromobates* sp. 2 MHNLS22093b	573.378907575
224	*Aromobates* sp. 2 CVULA5718	573.379408391
225	*Aromobates* sp. 2 MHNLS22093c	573.380700819
226	*Aromobates* sp. 2 MHNLS22093d	573.380901607
227	*Aromobates duranti*	573.40725329
228	*Aromobates serranus*	573.40725329
229	*Anomaloglossus verbeeksnyderorum* MHNLS20084	573.561961536
230	*Anomaloglossus verbeeksnyderorum* MHNLS20085	573.561961536
231	*Anomaloglossus verbeeksnyderorum* TNHC5631	573.561961536
232	*Mannophryne riveroi* MIZA319	573.624995096
233	*Mannophryne riveroi* TTSR	573.624995096
234	*Mannophryne* sp. (aff. *herminae*) MHNLS17160	573.685808448
235	*Mannophryne urticans* MHNLS21994	573.854828026
236	*Mannophryne* sp. 1 MHNLS16772	573.91781312
237	*Mannophryne lamarcai* MHNLS22087	573.95079542
238	*Mannophryne lamarcai* MHNLS22088	573.95079542
239	*Mannophryne* sp. 1 MHNLS16773	574.027891058
240	*Mannophryne* sp. 1 MHNLS16798	574.027891058
241	*Mannophryne olmonae* 451	574.065136063
242	*Mannophryne olmonae* MIZA335	574.065136063
243	*Mannophryne olmonae* UWIZM2732	574.065136063
244	*Mannophryne leonardoi* MHNLS22335	574.065865361
245	*Mannophryne leonardoi* MIZA316	574.065865361
246	*Mannophryne leonardoi* WES1036	574.065865361
247	*Mannophryne trinitatis* MVZ199828	574.065874593
248	*Mannophryne trinitatis* MVZ199837	574.065874593
249	*Mannophryne trinitatis* MVZ199838	574.065874593
250	*Mannophryne orellana* CVULA7165	574.241215529
251	*Mannophryne orellana* CVULA7231	574.241215529
252	*Mannophryne* sp. (*yustizi* complex) MHNLS22585	574.266953309
253	*Mannophryne* sp. (*yustizi* complex) MHNLS22586	574.266953309
254	*Mannophryne urticans* MHNLS21556	574.500608134
255	*Mannophryne urticans* TNHC5520	574.500608134
256	*Aromobates* sp. (aff. *saltuensis* 4) T10-1	574.517543556
257	*Aromobates* sp. (aff. *saltuensis* 4) T10-2	574.517543556
258	*Mannophryne speeri* MHNLS22606	574.529016162
259	*Anomaloglossus* sp. MHNLS17561	574.892370751

Position	Teminal name	Average distances
260	*Anomaloglossus wothuja* MHNLS19952	574.892370751
261	*Anomaloglossus wothuja* MHNLS19953	574.892370751
262	*Anomaloglossus megacephalus* ROM39637	574.892486147
263	*Anomaloglossus* sp. UTAA56710	574.892486147
264	*Mannophryne riveroi* MHNLS16433	574.955734341
265	*Mannophryne riveroi* MHNLS17910	574.955734341
266	*Aromobates* sp. (aff. *saltuensis* 1) MHNLS22498	575.014851382
267	*Aromobates* sp. (aff. *saltuensis* 1) CVULA8321	575.014851382
268	*Aromobates* sp. (aff. *cannatellai*) Asa4	575.389923216
269	*Aromobates* sp. (aff. *cannatellai*) MUJ3726	575.389923216
270	*Aromobates* sp. (aff. *cannatellai*) Tama14	575.389923216
271	*Aromobates alboguttatus*	575.389923216
272	*Aromobates capurinensis*	575.389923216
273	*Aromobates* sp. 3	575.389923216
274	*Aromobates haydeeae*	575.389923216
275	*Aromobates inflexus*	575.389923216
276	*Aromobates leopardalis*	575.389923216
277	"*Phyllobates*" *mandelorum*	575.389923216
278	*Aromobates nocturnus* AMNHA130041	575.389923216
279	*Aromobates nocturnus* AMNHA130042	575.389923216
280	*Aromobates ornatissimus* CVULA8351	575.389923216
281	*Aromobates ornatissimus* ULABG4445	575.389923216
282	*Aromobates ornatissimus* WES626	575.389923216
283	*Aromobates orostoma*	575.389923216
284	*Aromobates walterarpi*	575.389923216
285	*Andinobates bombetes* TNHC4946	575.389923216
286	*Adelphobates galactonotus* TNHC4889	575.389923216
287	*Allobates* aff. *juanii* ANDESA1073	575.389923216
288	*Allobates algorei* TNHC5551	575.389923216
289	*Allobates amissibilis* MTD47884	575.389923216
290	*Allobates bacurau* INPAH35406	575.389923216
291	*Allobates caeruleodactylus* MPEG13809	575.389923216
292	"*Colostethus*" *caribe*	575.389923216
293	*Allobates chalcopis* Alca1	575.389923216
294	*Allobates conspicuus* MPEG12321	575.389923216
295	*Allobates crombiei* APL14124	575.389923216
296	*Allobates femoralis* Acre01 Acre12931	575.389923216
297	*Allobates femoralis* Acre02 OMNH36070	575.389923216
298	*Allobates femoralis* QCAZ16484	575.389923216
299	*Allobates flaviventris* OMNH36959	575.389923216
300	*Allobates fratisenescus* QCAZ54377	575.389923216
301	*Allobates gasconi* MPEG13003	575.389923216
302	*Allobates granti* 148AF	575.389923216
303	*Allobates grillisimilis* APL12747	575.389923216

Position	Teminal name	Average distances
304	*Allobates hodli* AbuE2189	575.389923216
305	*Allobates humilis* CVULA5690	575.389923216
306	*Allobates humilis* MHNLS22093a	575.389923216
307	*Allobates insperatus* QCAZ16533	575.389923216
308	*Allobates juami* MCP13287	575.389923216
309	*Allobates juanii* TNHC4978	575.389923216
310	*Allobates kingsburyi* QCAZ16523	575.389923216
311	*Allobates magnussoni* MPEG11923	575.389923216
312	*Allobates masniger* APL14250	575.389923216
313	*Allobates myersi* INPAH26396	575.389923216
314	*Allobates nidicola* MPEG13821	575.389923216
315	*Allobates niputidea* MUJ3520	575.389923216
316	*Allobates olfersioides* MRT6031	575.389923216
317	*Allobates ornatus* MHNSM22863	575.389923216
318	*Allobates paleovarzensis* MJH3909	575.389923216
319	*Allobates peruvianus* MHNSM22923	575.389923216
320	*Allobates pittieri* MHNLS21229	575.389923216
321	*Allobates pittieri* MIZA339	575.389923216
322	*Allobates* sp. Alto Mazan MZ010	575.389923216
323	*Allobates carajas* TG3264	575.389923216
324	*Allobates* sp. Cuao MHNLS19982	575.389923216
325	*Allobates* sp. Cuyabeno OMNH34086	575.389923216
326	*Allobates* sp. Liberdade MCP10212	575.389923216
327	*Allobates* sp. Neblina AMCC106112	575.389923216
328	*Allobates* sp. PEGM1 LSUMZ17601	575.389923216
329	*Allobates* sp. PEGM3 MPEG13386	575.389923216
330	*Allobates subfolionidificans* APL1692	575.389923216
331	*Allobates sumtuosus* MTD47771	575.389923216
332	*Allobates talamancae* QCAZ16549	575.389923216
333	*Allobates talamancae* SIUC7667	575.389923216
334	*Allobates tapajos* LSUMZ15176	575.389923216
335	*Allobates tinae* MPEG13826	575.389923216
336	*Allobates trilineatus* KU215175	575.389923216
337	*Allobates undulatus* AMNHA159139	575.389923216
338	*Allobates zaparo* QCAZ16603	575.389923216
339	*Ameerega trivittata* TNHC4966	575.389923216
340	*Anomaloglossus* sp. UTAA56469	575.389923216
341	*Anomaloglossus apiau* MTR37501	575.389923216
342	*Anomaloglossus baeobatrachus* 1 AF2590	575.389923216
343	*Anomaloglossus baeobatrachus* 2 MTR13861	575.389923216
344	*Anomaloglossus beebei* ROM39631	575.389923216
345	*Anomaloglossus blanci* AF932	575.389923216
346	*Anomaloglossus degranvillei* PG601	575.389923216
347	*Anomaloglossus dewynteri* PG660	575.389923216

Position	Teminal name	Average distances
348	*Anomaloglossus kaiei* 279	575.389923216
349	*Anomaloglossus leopardus* AF2041	575.389923216
350	*Anomaloglossus meansi* ROM39639	575.389923216
351	*Anomaloglossus praderioi* CPI10208	575.389923216
352	*Anomaloglossus roraima* 06-141	575.389923216
353	*Anomaloglossus rufulus* CLBA	575.389923216
354	*Anomaloglossus rufulus* MHNLS20610	575.389923216
355	*Anomaloglossus* sp. AF3426	575.389923216
356	*Anomaloglossus* sp. BPN0850	575.389923216
357	*Anomaloglossus mitaraka* AF2732	575.389923216
358	*Anomaloglossus stepheni* AF2045	575.389923216
359	*Anomaloglossus stepheni* MJH3928	575.389923216
360	*Anomaloglossus surinamensis* 1 AF585	575.389923216
361	*Anomaloglossus surinamensis* 2 AF2456	575.389923216
362	*Anomaloglossus surinamensis* 5 AF3340	575.389923216
363	*Anomaloglossus tamacuarensis* MNRJ38049	575.389923216
364	*Anomaloglossus tepuyensis* MHNLS15613	575.389923216
365	*Anomaloglossus tepuyensis* VUB3734	575.389923216
366	"*Colostethus*" *ruthveni* MAR558	575.389923216
367	*Dendrobates tinctorius* TNHC64416	575.389923216
368	*Ectopoglossus saxatilis* IAvH14617	575.389923216
369	*Epipedobates tricolor* QCAZ21977	575.389923216
370	*Exidobates captivus* QCAZ27442	575.389923216
371	*Hyloxalus cepedai* MAA574	575.389923216
372	*Leucostethus brachistriatus* MHNUC360	575.389923216
373	*Leucostethus fugax* QCAZ16513	575.389923216
374	*Mannophryne* sp. (aff. *vulcano*) TNHC5666	575.389923216
375	*Mannophryne caquetio* MHNLS21219	575.389923216
376	*Mannophryne caquetio* MHNLS21220	575.389923216
377	*Mannophryne caquetio* MIZA323	575.389923216
378	*Mannophryne caquetio* MIZA333	575.389923216
379	*Mannophryne caquetio* MIZA337	575.389923216
380	*Mannophryne caquetio* MIZA338	575.389923216
381	*Mannophryne* aff. *herminae* ULABG4506	575.389923216
382	*Mannophryne leonardoi* MHNLS22336	575.389923216
383	*Mannophryne leonardoi* WES1035	575.389923216
384	*Mannophryne neblina* MHNLS22362	575.389923216
385	*Mannophryne trinitatis* ZSM1619	575.389923216
386	*Mannophryne trinitatis* ZSM1620	575.389923216
387	*Mannophryne trinitatis* ZSM1621	575.389923216
388	*Mannophryne* sp. (cf. *vulcano*) MHNLS21825	575.389923216
389	*Mannophryne* sp. (cf. *vulcano*) MHNLS21826	575.389923216
390	*Minyobates steyermarki* (Roberts *et. al*. 2006)	575.389923216
391	*Oophaga pumilio* TNHC4814	575.389923216

Position	Teminal name	Average distances
392	*Paruwrobates erythromos* QCAZ37750	575.389923216
393	*Phyllobates bicolor* 1233	575.389923216
394	*Prostherapis dunni*	575.389923216
395	*Ranitomeya toraro* OMNH36666	575.389923216
396	*Rheobates palmatus* MUJ3829	575.389923216
397	*Rheobates palmatus* TNHC4955	575.389923216
398	*Rheobates pseudopalmatus* MHUA5162	575.389923216
399	*Silverstoneia nubicola* SIUC7652	575.389923216
400	*Thoropa miliaris* AF1434	575.389923216

Appendix 6. Uncorrected pairwise distances (values in %) among 73 terminals of *Aromobates*, based on a similarity alignment of a 451 bp fragment of 16S without gaps and missing data. Values are presented as: minimum–maximum.

		1	2	3	4	5	6	7	8	9	10	11	12	13	14	15	16	17	18	19	20
1	*A*. sp. 1 (n= 5)	0.0																			
2	*A*. cf. sp. 1 (n= 5)	0.0	0.0																		
3	*A. ornatissimus* (n= 3)	7.1	7.1	0.0-0.4																	
4	*A*. sp. 2 (n= 4)	5.8	5.8	6.0	0.0																
5	*A. nocturnus* (n= 2)	5.1	5.1	6.0	4.2	0.0															
6	*A. molinarii* (n= 4)	6.7-6.9	6.7-6.9	7.1-7.3	3.3-3.5	4.7-4.9	0.0-0.2														
7	*A. zippeli* (n= 8)	6.7	6.7	7.1	3.3	4.7	0.9-1.1	0.0													
8	*A. meridensis* (n= 5)	7.8	7.8	7.8	4.9	5.3	5.1-5.3	5.1	0.0												
9	*A. ericksonae* (n= 4)	7.5	7.5	9.5	7.3	7.3	7.3-7.5	7.3	6.2	0.0											
10	*A. mayorgai* (n = 11)	7.5	7.5	9.5	7.3	7.3	7.3-7.5	7.3	6.2	0.0	0.0										
11	*A. cannatellai* (n= 5)	7.5	7.5	8.2	4.9	6.2	5.3-5.5	5.3	5.8	5.3	5.3	0.0									
12	*A*. sp. (aff. *cannatellai*) MUJ3726	8.2	8.2	8.0	5.3	6.9	6.0-6.2	6.0	5.5	5.3	5.3	1.8	-								
13	*A*. sp. (aff. *cannatellai*) Tama14	8.4	8.4	8.6	5.5	7.1	6.2-6.4	5.8	5.8	5.5	5.5	2.0	1.1	-							
14	*A*. sp. (aff. *cannatellai*) Asa4	7.1	7.1	8.2	4.9	6.2	5.3-5.5	4.9	5.8	4.9	4.9	1.3	2.2	2.0	-						
15	*A. tokuko* (n = 4)	7.1	7.1	7.3	5.1	5.8	5.5-5.8	5.5	5.3	4.7	4.7	2.0	2.4	2.7	2.4	0.0					
16	*A. saltuensis* (n = 4)	8.2	8.2	8.6	6.0	6.7	6.7-6.9	6.7	6.7	5.5	5.5	2.0	2.0	2.2	2.4	1.8	0.0				
17	*A*. sp. (aff. *saltuensis* 1) (n = 2)	8.4	8.4	8.4	5.3	6.4	6.2-6.4	6.2	6.0	5.8	5.8	1.8	1.8	2.0	2.2	1.6	0.7	0.0			
18	*A*. sp. (aff. *saltuensis* 2) LOA124	7.5	7.5	8.2	4.9	6.2	5.8-6.0	5.8	5.8	5.1	5.1	1.6	2.0	2.2	2.0	0.9	1.3	1.1	-		
19	*A*. sp. (aff. *saltuensis* 3) AOH	8.0	8.0	8.4	5.3	6.4	6.0-6.2	6.0	6.0	5.3	5.3	1.3	1.3	2.0	1.8	1.1	0.7	0.4	0.7	-	
20	*A*. sp. (aff. *saltuensis* 4) (n = 2)	8.0-8.2	8.0-8.2	8.4-8.6	5.3-5.5	6.4-6.7	6.0-6.4	6.0-6.2	6.0-6.2	5.3-5.5	5.3-5.5	1.3-1.6	1.3-1.6	2.0-2.2	1.8-2.0	1.1-1.3	0.7-0.9	0.4-0.7	0.7-0.9	0.0-0.2	0.2

Appendix 7. Uncorrected pairwise distances (values in %) among 16 terminals of *Aromobates*, based on a similarity alignment of a 291 bp fragment of Cyt-b without gaps and missing data. Values are presented as: minimum–maximum.

	Taxon	1	2	3	4	5	6	7	8	9	10	11	12	13	14	15	16
1	*A*. sp. 1 MHNLS21506	-															
2	*A*. cf. sp. 1 MHNLS21358	0.3	-														
3	*A. ornatissimus* WES626	18.9	18.6	-													
4	*A*. sp. 2 MHNLS22093b	16.2	15.8	14.4	-												
5	*A. nocturnus* AMNHA130041	16.2	15.8	17.5	13.1	-											
6	*A. nocturnus* AMNHA130042	16.2	15.8	17.5	13.1	0.0	-										
7	*A. meridensis* MHNLS22016	17.9	17.5	16.2	14.4	14.4	14.4	-									
8	*A. ericksonae* TNHC5540	17.9	17.5	19.9	15.8	16.8	16.8	14.4	-								
9	*A. mayorgai* MHNLS22003	17.9	17.5	19.9	15.8	16.8	16.8	14.4	0.0	-							
10	*A*. sp. (aff. *cannatellai*) MUJ3726	16.8	17.2	18.2	17.5	16.2	16.2	14.4	11.3	11.3	-						
11	*A. tokuko* MHNLS18478	18.2	17.9	18.9	15.8	15.1	15.1	14.4	11.3	11.3	4.5	-					
12	*A. saltuensis* TNHC5541	18.6	18.2	16.8	16.2	17.2	17.2	15.1	12.0	12.0	6.5	3.4	-				
13	*A. saltuensis* MHNLS17233	18.6	18.2	16.8	16.2	17.2	17.2	15.1	12.0	12.0	6.5	3.4	0.0	-			
14	*A*. sp. (aff. *saltuensis* 1) MHNLS22498	17.5	17.2	17.2	15.8	15.5	15.5	14.8	12.7	12.7	6.2	3.8	1.7	1.7	-		
15	*A*. sp. (aff. saltuensis 2) LOA124	19.6	19.2	20.3	16.2	15.5	15.5	15.1	13.4	13.4	7.6	3.8	5.2	5.2	4.8	-	
16	*A*. sp. (cf. saltuensis 3) AOH	18.9	18.6	18.2	16.2	15.8	15.8	15.1	12.7	12.7	5.8	2.1	3.4	3.4	3.8	3.8	-

Appendix 8. Uncorrected pairwise distances (values in %) among 205 terminals of *Mannophryne*, based on a similarity alignment of a 420 bp fragment of 16S without gaps and missing data. Values are presented as: minimum–maximum.

Continued (Part 2)...

	Taxon	1	2	3	4	5	6	7	8	9	10	11	12	13	14	15	16	17
1	*M. olmonae* (n = 3)	0.0																
2	*M. riveroi* (n = 4)	3.8	0.0															
3	*M. leonardoi* (n = 10)	5.5-6.0	5.0-5.7	0.0-1.2														
4	*M. trinitatis* (n = 6)	5.2	6.0	3.6-4.3	0.0-0.5													
5	*M. venezuelensis* (n = 7)	5.7-6.0	6.0-6.2	3.6-4.3	1.0-1.7	0.0-0.2												
6	*M.* sp. 1 (n = 6)	5.0-5.2	5.2-5.5	3.1-4.0	2.9-3.1	2.9-3.3	0.0-0.2											
7	*M.* aff. *vulcano* TNHC5666	5.7	5.2	3.8-4.5	3.1-3.6	3.8-4.0	1.4-1.7	-										
8	*M.* sp. (aff. *vulcano*) Araira (n =2)	6.2	5.0	4.3-5.0	3.6	3.6	1.7-1.9	1.7	0.0									
9	*M.* sp. 2 (n = 8)	5.7-6.2	5.0-5.2	3.8-4.8	3.1-3.6	3.1-3.8	1.2-1.9	1.2-1.7	0.2-0.5	0.0-0.5								
10	*M. vulcano* (n = 21)	6.2-6.7	5.0-5.2	4.0-5.2	3.6-4.0	3.6-4.3	1.7-2.4	1.7-2.1	0.0-0.5	0.2-1.0	0.0-0.7							
11	*M. neblina* MHNLS22362	5.7	6.0	5.0-5.7	6.7	6.2-6.4	6.0-6.2	6.9	6.9	6.4-6.9	6.7-7.4	-						
12	*M. oblitterata* (n = 6)	5.0	4.8	4.3-4.8	4.8	4.0-4.3	4.8-5.0	5.5	5.5	5.0-5.5	5.5-6.0	4.3	0.0					
13	*M. caquetio* (n = 6)	5.7-6.2	5.2-5.5	6.0-7.1	5.7-7.4	5.5-7.4	6.9-8.1	6.4-7.6	7.4-8.1	6.9-8.1	7.4-8.3	6.0-6.7	5.2-6.0	0.0-1.9				
14	*M.* sp. 3 (n = 8)	6.2	6.0	6.2-6.7	6.7	6.4-6.7	6.2-6.4	6.4	7.4	6.9-7.4	7.4-7.6	7.1	4.8	3.6-4.5	0.0			
15	*M.* aff. *herminae* ULABG4506	5.7	6.9	6.9-7.4	7.6	6.4-6.7	7.1-7.4	7.6	8.3	7.9-8.3	8.1-8.3	5.5	5.0	5.5-6.4	5.7	-		
16	*M.* sp. 4 (n = 7)	4.8	6.7	5.7-6.2	6.4	6.0-6.2	6.0-6.2	6.4	7.1	6.7-7.1	6.9-7.4	4.3	4.8	4.3-5.7	5.5	2.1	0.0	
17	*M. molinai* (n = 4)	4.8	6.7	5.7-6.2	6.4	6.0-6.2	6.0-6.2	6.4	7.1	6.7-7.1	6.9-7.4	4.3	4.8	4.3-5.7	5.5	2.1	0.5	0.0
18	*M.* cf. *molinai* Guayabito (n = 2)	5.0	6.4	6.4-6.9	6.7	6.0-6.2	6.7-6.9	7.1	6.9	6.4-6.9	6.7-7.1	4.5	4.5	4.5-5.5	5.7	2.4	1.2	0.7
19	*M.* cf. *molinai* Mayorica (n = 2)	4.8	6.7	5.7-6.2	6.4	6.0-6.2	6.0-6.2	6.4	7.1	6.7-7.1	6.9-7.4	4.3	4.8	4.3-5.7	5.5	2.1	0.5	0.0
20	*M.* cf. *molinai* Guáquira (n = 2)	4.8	6.7	5.7-6.2	6.4	6.0-6.2	6.0-6.2	6.4	7.1	6.7-7.1	6.9-7.4	4.3	4.8	4.3-5.7	5.5	2.1	0.5	0.0
21	*M.* cf. *molinai* Abrigo (n = 2)	5.2-5.7	6.7	6.7-7.1	6.9	6.4-6.7	6.7-6.9	6.9-7.4	6.7-7.1	6.2-7.1	6.7-7.4	4.3	4.8-5.2	4.8-5.7	6.0-6.4	2.6-3.1	1.4	1.0
22	*M.* sp. La Sierra (n = 4)	4.5	6.4-6.7	5.7-6.4	6.2-6.4	5.7-6.2	5.7-6.2	6.2-6.4	6.9-7.1	6.4-7.1	6.9-7.4	4.3-4.5	4.5-4.8	4.3-6.0	5.2-5.5	2.4	0.5-0.7	0.0-0.2
23	*M. herminae* (n = 9)	4.5	6.4	6.0-6.4	6.7	6.0-6.2	6.2-6.4	6.7	7.4	6.9-7.4	7.1-7.6	4.5	4.5	4.0-5.5	5.2	1.9	0.7	0.2
24	*M. orellana* (n = 6)	6.2-6.7	6.2-6.7	6.2-7.1	6.4-6.9	6.0-6.7	5.7-6.4	6.0-6.4	7.1-7.6	6.9-7.6	6.9-7.9	6.0-6.2	6.0-6.2	4.3-5.2	6.0-6.4	5.0-5.2	3.8-4.0	3.8-4.0
25	*M. cordilleriana* (n = 18)	5.5-5.7	6.0-6.2	5.7-6.4	6.0-6.7	5.5-6.0	5.7-6.2	6.4-6.7	7.1-7.4	6.7-7.1	6.9-7.6	5.5-5.7	5.5-5.7	4.0-4.8	5.7-6.0	4.3-4.5	3.1-3.3	3.1-3.3
26	*M. collaris* (n = 14)	6.7-6.9	6.7-7.1	6.2-6.9	6.0-6.2	5.5-6.0	6.2-6.7	6.4-6.7	7.1-7.4	6.7-7.4	6.9-7.9	6.2-6.4	5.2-5.5	5.2-6.0	6.2-6.4	6.0-6.2	5.0-5.2	5.0-5.2
27	*M. urticans* (n = 6)	6.9-7.4	7.6-7.9	6.4-7.4	6.2-6.7	5.7-6.4	6.4-7.1	6.7-7.1	7.4-7.9	6.9-7.6	7.1-8.3	6.4-6.9	5.5-6.0	5.5-6.7	6.4-6.7	6.0-6.4	5.0-5.5	5.0-5.5
28	*M. lamarcai* (n = 7)	6.4-6.9	7.1-7.6	6.2-6.9	5.5-5.7	5.0-5.5	6.0-6.7	6.2-6.7	7.1-7.4	6.7-7.1	6.9-7.9	6.0-6.4	4.8-5.0	5.0-6.4	6.0-6.4	5.5-6.0	4.5-5.0	4.5-5.0
29	*M. trujillensis* (n = 6)	7.1	7.1	6.2-6.7	6.4	6.0-6.2	6.7-6.9	6.9	7.6	7.1-7.6	7.4-8.1	6.2	5.2	5.2	6.2	6.7	5.7	5.7
30	*M. larandina* (n = 7)	6.7	6.9	6.2-6.7	6.0	5.5-5.7	6.2-6.4	6.4	7.1	6.7-7.1	6.9-7.6	6.2	5.2	5.2-5.7	6.2	6.2	5.2	5.2
31	*M. yustizi* (n = 4)	6.7	6.9	6.2-6.7	6.0	5.5-5.7	6.2-6.4	6.4	7.1	6.7-7.1	6.9-7.6	6.2	5.2	5.2-5.7	6.2	6.2	5.2	5.2
32	*M. speeri* MHNLS22606	6.9	7.1	6.4-6.9	6.2	5.7	6.4-6.7	6.7	7.4	6.9-7.4	7.1-7.9	6.4	5.0	5.5-6.0	6.4	6.4	5.5	5.5
33	*M. yustizi* complex (n = 10)	6.7	6.9	6.4-6.9	6.0-6.2	5.5-5.7	6.2-6.7	6.7	7.1-7.4	6.7-7.4	6.9-7.9	6.2-6.4	5.2	5.2-5.7	6.2	6.2	5.2-5.5	5.2-5.5
34	*M.* cf. *yustizi* Niquitao (n = 4)	6.7	6.9	6.2-6.7	6.0	5.5-5.7	6.2-6.4	6.4	7.1	6.7-7.1	6.9-7.6	6.2	5.2	5.2-5.7	6.2	6.2	5.2	5.2

Part two...

	Taxon	18	19	20	21	22	23	24	25	26	27	28	29	30	31	32	33	34
1	*M. olmonae* (n = 3)																	
2	*M. riveroi* (n = 4)																	
3	*M. leonardoi* (n = 10)																	
4	*M. trinitatis* (n = 6)																	
5	*M. venezuelensis* (n = 7)																	
6	*M.* sp. 1 (n = 6)																	
7	*M.* aff. *vulcano* TNHC5666																	
8	*M.* sp. (aff. *vulcano*) Araira (n =2)																	
9	*M.* sp. 2 (n = 8)																	
10	*M. vulcano* (n = 21)																	
11	*M. neblina* MHNLS22362																	
12	*M. oblitterata* (n = 6)																	
13	*M. caquetio* (n = 6)																	
14	*M.* sp. 3 (n = 8)																	
15	*M.* aff. *herminae* ULABG4506																	
16	*M.* sp. 4 (n = 7)																	
17	*M. molinai* (n = 4)																	
18	*M.* cf. *molinai* Guayabito (n = 2)	0.0																
19	*M.* cf. *molinai* Mayorica (n = 2)	0.7	0.0															
20	*M.* cf. *molinai* Guáquira (n = 2)	0.7	0.0	0.0														
21	*M.* cf. *molinai* Abrigo (n = 2)	0.2	1.0	1.0	0.5													
22	*M.* sp. (aff. *molinai*) (n = 4)	0.7-1.0	0.0-0.2	0.0-0.2	1.0-1.2	0.0-0.2												
23	*M. herminae* (n = 9)	0.5	0.2	0.2	0.7-1.2	0.2-0.5	0.0											
24	*M. orellana* (n = 6)	4.5-4.8	3.8-4.0	3.8-4.0	4.8-5.0	3.8-4.3	4.0-4.3	0.0-0.7										
25	*M. cordilleriana* (n = 18)	3.8-4.0	3.1-3.3	3.1-3.3	4.0-4.3	3.1-3.6	3.3-3.6	1.0-1.7	0.0-0.2									
26	*M. collaris* (n = 14)	5.2-5.5	5.0-5.2	5.0-5.2	5.5-5.7	5.0-5.5	5.2-5.5	1.9-2.6	2.4-2.9	0.0-0.2								
27	*M. urticans* (n = 6)	5.2-5.7	5.0-5.5	5.0-5.5	5.5-6.0	5.0-5.7	5.2-5.7	2.9-3.8	3.3-4.0	1.2-1.9	0.0-0.7							
28	*M. lamarcai* (n = 7)	5.0-5.2	4.5-5.0	4.8-5.0	5.2-5.5	4.5-5.2	4.8-5.2	2.4-3.3	2.9-3.6	1.0-1.4	0.7-1.4	0.0-0.2						
29	*M. trujillensis* (n = 6)	6.0	5.7	5.7	6.2	5.7-6.0	6.0	2.1-2.6	2.6-2.9	1.0-1.2	1.4-2.1	1.4-1.7	0.0					
30	*M. larandina* (n = 7)	5.5	5.2	5.2	5.7	5.2-5.5	5.5	2.1-2.6	2.6-2.9	0.5-0.7	1.0-1.7	1.0-1.2	0.5	0.0				
31	*M. yustizi* (n = 4)	5.5	5.2	5.2	5.7	5.2-5.5	5.5	2.1-2.6	2.6-2.9	0.5-0.7	1.0-1.7	1.0-1.2	0.5	0.0	0.0			
32	*M. speeri* MHNLS22606	5.7	5.5	5.5	6.0	5.5-5.7	5.7	2.4-2.9	2.9-3.1	0.7-1.0	1.2-1.9	1.2-1.4	0.7	0.2	0.2	-		
33	*M. yustizi* complex (n = 10)	5.5	5.2-5.5	5.2-5.5	5.7-6.0	5.2-5.7	5.5	2.1-2.9	2.6-3.1	0.5-1.0	1.0-1.9	1.0-1.4	0.5-0.7	0.0-0.2	0.0-0.2	0.2-0.5	0.0-0.2	
34	*M.* cf. *yustizi* Niquitao (n = 4)	5.5	5.2	5.2	5.7	5.2-5.5	5.5	2.1-2.6	2.6-2.9	0.5-0.7	1.0-1.7	1.0-1.2	0.5	0.0	0.0	0.2	0.0-0.2	0.0

Appendix 9. Uncorrected pairwise distances (values in %) among 73 terminals of *Mannophryne*, based on a similarity alignment of a 451 bp fragment of Cyt-b without gaps and missing data. Values are presented as: minimum–maximum.

Continued (Part 2)...

	Taxon	1	2	3	4	5	6	7	8	9	10	11	12	13	14
1	*M. olmonae* UWIZM2732	-													
2	*M. riveroi* MHNLS16433	9.3	-												
3	*M. leonardoi* (n = 3)	14.4-15.1	14.1-14.4	0.3-1.4											
4	*M. trinitatis* (n = 2)	14.8-15.1	18.9-19.2	14.4-15.1	0.3										
5	*M.* sp. 1 MHNLS16772	13.7	14.8	12.7-13.1	14.1-14.4	-									
6	*M.* sp. 2 (n = 2)	13.4	16.2	13.7-14.1	13.1-13.4	8.2	0.0								
7	*M. vulcano* MHNLS21140	12.4	15.8	13.1-13.4	12.4-12.7	7.2	3.4	-							
8	*M. neblina* MHNLS22362	14.8	17.5	18.2-18.6	15.5-15.8	18.6	20.3	19.9	-						
9	*M. oblitterata* MHNLS21818	11.7	15.1	16.2-16.8	15.5-15.8	17.2	15.8	14.8	18.9	-					
10	*M. caquetio* MHNLS21219	16.8	14.4	13.7-14.1	14.8-15.1	17.2	16.5	17.2	18.9	17.5	-				
11	*M.* sp. 3 MHNLS22360	15.5	14.8	16.8-17.5	17.9-18.2	14.8	16.5	16.2	17.9	17.5	12.0	-			
12	*M.* sp. 4 MHNLS22204	14.4	15.8	16.5-16.8	15.8-16.2	15.8	16.2	17.2	17.2	16.8	12.7	12.0	-		
13	*M. molinai* (n = 2)	14.1	16.2	15.8-16.2	14.8-15.1	15.8	16.5	16.8	16.2	17.5	13.4	12.7	2.1	0.0	
14	*M.* cf. *molinai* Guayabito (n = 2)	14.1	15.5	15.8-16.2	14.8-15.1	15.8	16.5	16.8	16.2	17.5	14.1	13.4	2.7	1.4	0.0
15	*M.* cf. *molinai* Abrigo (n = 2)	14.1	15.5	15.8-16.2	14.8-15.1	15.8	16.5	16.8	16.2	17.5	14.1	13.4	2.7	1.4	0.0
16	*M.* cf. *molinai* Guaquira MHNLS21205	14.4	16.5	16.2-16.5	14.4-14.8	16.2	16.8	17.2	15.8	17.5	13.7	13.1	2.4	0.3	1.7
17	*M.* sp. (aff. *molinai*) MHNLS17157	13.7	15.8	15.5-15.8	14.8-15.1	15.8	16.5	16.5	15.8	17.5	13.7	12.4	2.4	1.0	1.7
18	*M. herminae* MHNLS22106	14.4	16.5	16.2-16.5	15.1-15.5	16.2	16.5	17.2	16.5	17.9	13.7	13.1	2.4	1.0	1.7
19	*M. orellana* ULABG7469	14.1	13.7	17.2-17.9	16.5-16.8	14.8	16.2	16.5	15.8	15.8	14.1	14.8	13.7	13.4	13.4
20	*M. cordilleriana* ULABG5352	15.8	16.5	16.8-17.2	15.5-15.8	16.2	16.2	15.1	17.2	16.2	14.1	16.5	15.5	16.2	15.5
21	*M. collaris* TNHC5507	16.2	16.2	17.2-17.5	15.1-15.5	18.9	17.5	17.2	17.2	17.2	11.3	13.4	13.4	14.1	13.4
22	*M. urticans* MHNLS21555	17.9	16.5	17.5-17.9	16.5-16.8	19.9	19.2	18.9	17.9	15.8	12.0	12.4	14.8	15.5	14.8
23	*M. lamarcai* (n = 2)	17.2-17.5	15.8-16.2	16.8-17.5	16.5-17.2	19.2-19.6	18.9-19.2	18.2-18.6	18.6-18.9	15.8-16.2	11.7-12.0	12.0-12.4	14.4-14.8	14.8-15.1	14.1-14.4
24	*M. trujillensis* MHNLS22064	16.8	15.5	15.8-16.2	15.1-15.5	18.2	17.2	17.5	17.9	16.2	11.0	13.1	13.1	13.7	13.1
25	*M. larandina* (n = 2)	15.8	15.1	16.2-16.5	15.8-16.2	18.9	17.5	17.9	17.2	14.8	12.4	13.4	13.7	14.4	13.7
26	*M. speeri* MHNLS22606	16.8	15.1	16.2-16.5	14.8-15.1	17.9	16.5	16.8	17.9	15.8	11.3	12.4	14.1	14.8	14.1
27	*M. yustizi* complex (n = 4)	16.2-16.5	14.8-15.1	15.1-16.2	14.1-14.8	16.8-17.5	15.8-16.8	16.2-16.5	16.8-17.9	15.1-15.5	10.7-11.7	11.7-12.0	13.4-13.7	13.7-14.4	13.7-14.1
28	*M.* sp. (aff. *yustizi*) La Olla (n = 2)	17.2	15.8	15.8-16.2	15.5-15.8	17.9	17.2	17.5	17.5	15.8	12.0	12.4	13.4	14.1	13.4
29	*M.* cf. *yustizi* Niquitao MHNLS21169	16.5	14.8	15.8-16.2	14.4-14.8	17.5	16.2	16.5	17.5	15.5	11.3	11.7	14.1	14.8	14.1

Part two...

	Taxon	15	16	17	18	19	20	21	22	23	24	25	26	27	28	29
1	*M. olmonae* UWIZM2732															
2	*M. riveroi* MHNLS16433															
3	*M. leonardoi* (n = 3)															
4	*M. trinitatis* (n = 2)															
5	*M*. sp. 1 MHNLS16772															
6	*M*. sp. 2 (n = 2)															
7	*M. vulcano* MHNLS21140															
8	*M. neblina* MHNLS22362															
9	*M. oblitterata* MHNLS21818															
10	*M. caquetio* MHNLS21219															
11	*M*. sp. 3 MHNLS22360															
12	*M*. sp. 4 MHNLS22204															
13	*M. molinai* (n = 2)															
14	*M*. cf. *molinai* Guayabito (n = 2)															
15	*M*. cf. *molinai* Abrigo (n = 2)	0.0														
16	*M*. cf. *molinai* Guaquira MHNLS21205	1.7	-													
17	*M*. sp. La Sierra MHNLS17157	1.7	1.4	-												
18	*M. herminae* MHNLS22106	1.7	1.4	1.4	-											
19	*M. orellana* ULABG7469	13.4	13.7	13.7	13.7	-										
20	*M. cordilleriana* ULABG5352	15.5	16.5	16.2	16.5	8.2	-									
21	*M. collaris* TNHC5507	13.4	14.4	14.1	14.4	12.7	10.7	-								
22	*M. urticans* MHNLS21555	14.8	15.8	15.5	15.8	12.0	11.3	4.1	-							
23	*M. lamarcai* (n = 2)	14.1-14.4	15.1-15.5	14.8-15.1	15.1-15.5	12.0-12.4	11.7-12.0	3.8-4.1	1.0-1.4	1.0						
24	*M. trujillensis* MHNLS22064	13.1	14.1	13.7	14.0	12.4	12.4	3.1	3.8	3.4-3.8	-					
25	*M. larandina* (n = 2)	13.7	14.8	14.4	14.8	12.0	10.7	3.8	3.8	3.4-3.8	2.7	0.0				
26	*M. speeri* MHNLS22606	14.1	15.1	14.8	15.1	12.0	10.3	2.7	3.4	3.1-3.4	3.1	2.4	-			
27	*M. yustizi* complex (n = 4)	13.1-14.1	14.1-14.8	13.7-14.4	14.1-14.8	11.3-11.7	9.6-10.7	3.1-3.8	3.1-3.8	2.7-3.4	2.7-3.4	2.1-2.7	0.3-1.0	0.0-1.0		
28	*M*. sp. (aff. *yustizi*) La Olla (n = 2)	13.4	14.4	14.1	14.4	12.7	11.0	3.4	3.4	3.1-3.4	2.4	1.7	1.7	1.4-1.7	0.0	
29	*M*. cf. *yustizi* Niquitao MHNLS21169	14.1	15.1	14.8	15.1	11.3	10.3	3.4	3.4	3.1-3.4	3.1	2.4	0.7	0.3-1.0	1.7	-

Capítulo 2

Unveiling species diversity in collared frogs through morphological and bioacoustic evidence: a new *Mannophryne* (Amphibia, Aromobatidae) from Sierra de Aroa, northwestern Venezuela, and an amended definition and call description of *M. herminae* (Boettger, 1893)

FERNANDO J.M. ROJAS-RUNJAIC, MIGUEL E. MATTA-PEREIRA & ENRIQUE LA MARCA

Zootaxa 4461 (4): 451–476
http://www.mapress.com/j/zt/

Article

ISSN 1175-5326 (print edition)
ZOOTAXA
ISSN 1175-5334 (online edition)

https://doi.org/10.11646/zootaxa.4461.4.1
http://zoobank.org/urn:lsid:zoobank.org:pub:78CCF5EE-CE8A-42DF-8905-CBBC3B0DA763

Unveiling species diversity in collared frogs through morphological and bioacoustic evidence: a new *Mannophryne* (Amphibia, Aromobatidae) from Sierra de Aroa, northwestern Venezuela, and an amended definition and call description of *M. herminae* (Boettger, 1893)

FERNANDO J.M. ROJAS-RUNJAIC[1,2,6], MIGUEL E. MATTA-PEREIRA[3,4] & ENRIQUE LA MARCA[5]

[1]*Pontifícia Universidade Católica do Rio Grande do Sul (PUCRS), Laboratório de Sistemática de Vertebrados. Av. Ipiranga 6681, Porto Alegre, RS 90619-900, Brazil. E-mail: rojas_runjaic@yahoo.com*
[2]*Fundación La Salle de Ciencias Naturales, Museo de Historia Natural La Salle. Apartado Postal 1930, Caracas 1010-A, Venezuela.*
[3]*Asociación Civil Grupo Guardaparques Universitarios, Barquisimeto, Lara state, Venezuela. E-mail: miguelmatta357@gmail.com*
[4]*Universidad Central de Venezuela, Facultad de Ciencias, Escuela de Biología. Caracas, Venezuela*
[5]*Universidad de Los Andes, Laboratorio de Biogeografía, Colección de Anfibios y Reptiles, Mérida 5101, Venezuela. E-mail: enrique.lamarca@gmail.com*
[6]*Corresponding author*

Abstract

Species diversity in collared frogs of the genus *Mannophryne* is presumed to be underestimated due to the paucity of external morphology characters, but combining morphology with bioacoustics and other lines of evidence has shown to be useful in delimiting species of this group. Herein we describe a new species of *Mannophryne* from Sierra de Aroa in northwestern Venezuela. The new species is morphologically similar to *M. herminae* but is readily recognized by its strikingly different advertisement call. It also can be distinguished from all its congeners by the unique combination of its small body size, general color pattern, basal toe webbing, and advertisement call consisting of long trills of single tonal notes emitted at a rate of 2–3 notes/s. Additionally, to facilitate future diagnosis of undescribed species related to *M. herminae*, we amend the definition of the latter, describe in detail its advertisement call, and redefine its known distribution range. The new species increases the number of described species of *Mannophryne* to 20.

Key words: Anura, Aromobatinae, Coastal Range, Cordillera de la Costa, Dendrobatoidea, Integrative taxonomy

Resumen

Se presume que la diversidad de especies en sapitos acollarados del género *Mannophryne* está subestimada debido a la escasez de caracteres de morfología externa; no obstante, la combinación de morfología, bioacústica y otras líneas de evidencia ha demostrado ser eficiente para la delimitación de especies en este grupo. Aquí se describe una nueva especie de *Mannophryne* procedente de la sierra de Aroa en el noroccidente de Venezuela. La nueva especie se asemeja en su morfología a *M. herminae*, no obstante, se distingue fácilmente de esta por su vocalización de advertencia notablemente diferente. También se distingue de todos sus congéneres por la combinación única de su tamaño corporal pequeño, su patrón de coloración, la palmeadura basal entre los dedos pediales, y su llamado de advertencia consistente en series extensas de notas tonales individuales emitidas a una tasa de 2–3 notas/s. Adicionalmente, con la finalidad de facilitar el diagnóstico futuro de otras especies aún no descritas y relacionadas con *M. herminae*, se enmienda la definición de esta, se describe en detalle su vocalización de advertencia y se redefine su distribución conocida. Con esta nueva especie, el número de especies descritas de *Mannophryne* asciende a 20.

Accepted by E. Twomey: 28 Jun. 2018; published: 23 Aug. 2018

Introduction

Mannophryne La Marca, 1992 is a genus of cryptic colored aromobatid frogs, which are diurnal, terrestrial, and associated with small mountain creeks (La Marca 1994). Their distribution is mostly restricted to the mountain systems of north Venezuela, from the Táchira depression to the southwest of the Venezuelan Andes, and through Cordillera de Mérida and Cordillera de la Costa, to the Paria peninsula in the east, with only two species from Trinidad and Tobago, respectively (La Marca 1994; Barrio-Amorós *et al*. 2010a).

This genus was described to accommodate the species previously assigned to the *Colostethus collaris* group (*sensu* Rivero 1990) and is defined by three phenotypic synapomorphies: 1) a dark throat collar on both sexes (particularly conspicuous in females), 2) yellow throat in adult females, and 3) complex behaviors in females (agonistic displays associated to territoriality) and males (courtship displays) (La Marca 1992; 1994). Subsequent phylogenetic studies including additional species, and based on molecular and morphological evidence, have corroborated the monophyly of the genus and its sister relationship with *Aromobates* (La Marca *et al*. 2002; Vences *et al*. 2003, Grant *et al*. 2006, Manzanilla *et al*. 2009; Barrio-Amorós & Santos 2012; Grant *et al*. 2017).

Manzanilla *et al*. (2009) defined three phylogenetic species groups: *M. trinitatis* (clade A), *M. collaris* (clade B), and *M. oblitterata* (clade C). These clades are geographically restricted to central and oriental sections of Cordillera de la Costa plus Trinidad and Tobago (*M. trinitatis* species Group), Cordillera de Mérida and western of Cordillera de la Costa (*M. collaris* species Group), and central portion of Cordillera de la Costa (*M. oblitterata* species Group). Recently, Grant *et al*. (2017) corroborated the monophyly and expanded the species content of these groups.

Mannophryne currently comprises 19 species (Barrio-Amorós *et al*. 2010a; Frost 2017), but its diversity is suspected to be underestimated due to the paucity of clear diagnostic characters of external morphology (Manzanilla *et al*. 2009) which are the bulk of the evidence traditionally used in the taxonomy of the genus. In fact, recent descriptions of new species have relied on integrative approaches, combining several lines of evidence beyond the external morphology of adults such as larval morphology, bioacoustics, biogeography, and DNA sequences (Manzanilla *et al*. 2007a; Barrio-Amorós *et al*. 2010a).

Sierra de Aroa is located at the western end of the Cordillera de la Costa, in northwestern Venezuela (between Yaracuy and Lara states) and is isolated from this mountain system by the Yaracuy depression. Part of its extension is protected by the Yurubí National Park (MARNR 1992) and several studies have highlighted its high levels of biodiversity and endemism in vertebrates (Roze & Solano 1963; Mijares-Urrutia & Rivero 2000; Rodríguez-Olarte *et al.* 2006; García *et al.* 2012a, b; Quiroga-Carmona & Molinari 2012). Yústiz (1991) reported the presence of a population of *Mannophyrne* from Sierra de Aroa and referred it as belonging to a species related to *M. trinitatis*. Later, Barrio-Amorós (1999) reported a population from "Parque Yurubí (Yurubí National Park), San Felipe", also in the Sierra de Aroa, as *M. trinitatis*. However, Barrio-Amorós *et al*. (2006) and Manzanilla *et al*. (2007a) stated that *M. trinitatis* is restricted to Trinidad. Consequently, this population from Sierra de Aroa was left unassigned to a species name and was not mentioned in subsequent studies.

To further complicate matters, most populations of *Mannophryne* from the western portion of Cordillera de la Costa have been considered *M. herminae*. This perception is rooted in several studies stating that *M. herminae* is widely distributed in northern Venezuela (Rivero 1984a; La Marca 1992, 1994), which in turn probably derives from the limited morphological definition of this species (Boettger 1893; La Marca 1994), and the lack of new taxonomic revisions including additional lines of evidence (*e.g.* bioacoustics, DNA).

During several herpetological surveys in Sierra de Aroa between 2012 and 2014, we collected a series of collared frogs. A detailed study of their morphology combined with bioacoustic analysis and comparisons with specimens of *M. herminae* from the type locality and vicinities, revealed that the specimens from Sierra de Aroa belong to a new species that we describe herein. Additionally, we describe the advertisement call of *M. herminae* and amend its definition.

Material and methods

Morphology. All specimens of the type series are housed at the Museo de Historia Natural La Salle, Caracas, Venezuela (MHNLS), the Amphibian and Reptilian Collection of the Laboratorio de Biogeografía at the

Universidad de Los Andes, Mérida, Venezuela (ULABG), and the Amphibian Collection of Museu de Ciências e Tecnologia of Pontifícia Universidade Católica do Rio Grande do Sul, Porto Alegre, Brazil (MCP). Additional congeneric specimens examined (Appendix 1) are housed at MHNLS, Museo de Biología de la Universidad Central de Venezuela, Caracas, Venezuela (MBUCV), Colección de Vertebrados, Universidad de los Andes, Mérida, Venezuela (CVULA), Colección de Anfibios y Reptiles del Laboratorio de Biogeografía, Universidad de Los Andes, Mérida, Venezuela (ULABG), and Senckenberg Forschungsinstitut und Naturmuseum, Frankfurt, Germany (SMF). Taxonomy and terminology for morphological characters follow Grant *et al*. (2006). Webbing formula follows Savage & Heyer (1967), with modifications by Myers & Duellman (1982). Comparative morphological data of congeners was complemented with descriptions from Test (1956), Donoso-Barros (1965), Rivero (1984b), Dixon & Rivero-Blanco (1985), La Marca (1989, 1994, 2009), Yústiz (1991), Mijares-Urrutia & Arends (1999a, b), Manzanilla *et al*. (2007a, b), Vargas & La Marca (2007), Barrio-Amorós *et al*. (2010a, b). Sex and maturity were determined by inspection of secondary sexual characters (*i.e.*, presence or absence of vocal slits and vocal sac), and when necessary, by dissection (*i.e.*, presence and development of testes, or ovaries and convolute oviducts). Fingers (F) and toes (T) are numbered preaxially to postaxially from I–IV and I–V respectively. Measurements reported are only from adult frogs and follow Duellman (1970), Kaplan (1997), and Kok & Kalamandeen (2005), with some modifications from Rojas-Runjaic *et al*. (2011): Snout-Vent Length (SVL): straight length measured from tip of snout to vent; Thigh Length (ThL): from vent opening to flexed knee; Shank Length (SL): from outer edge of flexed knee to flexed heel; Foot Length (FL): from proximal edge of outer metatarsal tubercle to tip of Toe IV (TIV); Hand Length (HaL): from proximal edge of palmar tubercle to tip of Finger III (FIII); Head Length (HeL): from tip of snout to posterior edge of prootic, noted through the skin; Head Width (HW): measured across the skull at angle of jaws; Interorbital Distance (IoD): measured transversely at the narrowest point between the inner borders of the upper eyelids; Internarial Distance (InD): measured between centers of nares; Eye-to-Nostril Distance (EN): measured from the anterior edge of eye to nostril; Eye Diameter (ED): measured horizontally across eye; Eye-to-Snout Distance (ETS): distance between the anterior corner of the eye to the tip of snout; Tympanum Diameter (TD): measured horizontally across tympanum; Disc Width of Finger III (F3D): measured across widest part of disc; Disc Width of Toe IV (T4D): measured across widest part of disc; Length of Finger I (F1L): measured from outer edge of palmar tubercle to tip of disc; Length of Finger II (F2L): measured from outer edge of palmar tubercle to tip of disc. Disc expansion of all fingers and toes is expressed as a relation between the maximum disc width and the width of its adjacent phalanx (measured at the midpoint and excluding lateral keels and fringes) and categorized following the character states defined by Grant *et al*. (2006) as follows: unexpanded to very weakly expanded (up to 1.4), weakly expanded (≥1.5), moderately expanded (≥2.0), and greatly expanded (≥3.0). All measurements were taken with calipers to the nearest 0.1 mm.

Bioacoustics. Advertisement calls were obtained with an Olympus LS-10 digital recorder at a sampling rate of 44.1 kHz and 16 bits/sample, and using a Senheiser K6-ME66 directional microphone. The microphone was positioned about 1.5–2 m away from each calling male. We recorded three males from the type locality of the new species. These recordings were done during the day, between 11:45–18:30 h; air temperature at time of recordings ranged between 21–22.6 ºC. For *Mannophryne herminae* two specimens from San Esteban River, Carabobo state (near its type locality) were recorded. Calls were recorded in the morning, between 8:20–8:35 h, and air temperature was 24.9 ºC. Call recordings could not be associated to collected individuals, but voucher specimens are listed as type series of the new species, and in the Appendix 1 for *M. herminae*. Calls were analyzed using Raven Pro 1.3 (Bioacoustics Research Program 2008) and spectral analyses were conducted with frequency resolution of 82 Hz and 2,048 points, using Blackman window type. Advertisement calls of the two species consist of trills of short notes (see Results). For the description of spectral and temporal parameters, we selected 1–5 calls (n = 8) and 20 notes uniformly distributed along the length of calls of each male of the new species (n = 60 notes), and 5–10 calls (n = 15) and 20–30 duplets also uniformly distributed along the length of calls of each male of *M. herminae* (n = 50 duplets). The duration of calls, notes, silent intervals between notes (also between duplets for *M. herminae*), and the number of notes in each call, were measured from oscillograms. Fundamental frequency, peak frequency (and its bandwidth, upper and lower frequencies), and additional harmonics of notes (when detectable) were measured from power spectrum graphs. Additionally, we calculated the rate of note emission in each call (notes/s). Upper and lower values of peak frequency of each note were measured 20 dB below peak frequency intensity, avoiding overlap with background noise.

Results

The new species is assigned to *Mannophryne* based on the presence of a dark dermal throat collar in both sexes (La Marca 1992, 1994; Grant *et al*. 2006, 2017), and additionally on the following set of characters: dorsal cryptic coloration, yellow colored throat in adult females, presence of pale oblique lateral stripe and dorsolateral stripe, dorsal skin texture posteriorly granular, FIII of adult males not swollen, FI and FII equal to subequal in length, distal subarticular tubercle on FIV present, median lingual process absent, large intestine and adult testes unpigmented.

Mannophryne molinai sp. nov.

(Figs. 1–2, 4–5)

Suggested common name in English: Sierra de Aroa Collared Frog

Suggested common name in Spanish: sapito acollarado de la Sierra de Aroa

Holotype. Adult male, MHNLS 21355 (field number FR 588; Figs. 1–2), from Quebrada La Rondona, Sierra de Aroa, Sucre municipality, Yaracuy state, Venezuela (10°19'20.8"N, 68°52'24.0"W; 1180 m asl; Fig. 3), collected on April 05, 2014, by F.J.M. Rojas-Runjaic, E. Camargo, and J.L. Vieira.

Paratypes. Nine specimens (six adult males and three adult females) all collected at the type locality: three males (MHNLS 21536–21537, 21540; field numbers MEM 4, 7, 2, respectively) and two females (MHNLS 21535; field number MEM 6, and ULABG 7821 [field number MEM 11]), collected on December 19, 2012, by M. Matta-Pereira and J. Piñero; three males (MCP 13924 [ex-MHNLS 21336; Fig. 4c–d], MHNLS 21338–21339; field numbers FR 569, 571–572) and one female (MHNLS 21337; field number FR 570; Fig. 4a–b), collected on April 04–05, 2014, by F.J.M. Rojas-Runjaic, E. Camargo, and J.L. Vieira.

Referred specimens. Four juveniles, and two lots of tadpoles, all collected at the type locality: one juvenile (MHNLS 21356; field number FR 589) collected on April 05, 2014, by F.J.M. Rojas-Runjaic, E. Camargo and J.L. Vieira; two juveniles (MHNLS 21543–21544; field numbers MEM 3 and 5, respectively) collected on December 12, 2012, and one juvenile (MHNLS 21542; field number MEM 8) collected on February 27, 2014, by M. Matta-Pereira and J. Piñero; two lots of tadpoles (MHNLS 21546–21547; field numbers MEM 10 and 12; collected from the backs of the males MHNLS 21536 and 21537 respectively) collected on December 19, 2012, by M. Matta-Pereira and J. Piñero.

Definition. The new species is defined by the unique combination of the following characters: (1) Small body size, with adult males smaller than females (SVL = 20.5–23.4 mm in males *vs*. 25.2–25.5 mm in females); (2) dorsal skin of body and hind limbs shagreen, moderately granular on flanks; small tubercles present on posterior third of dorsum, body flanks, and dorsal surfaces of thighs and shanks; ventral skin smooth; (3) snout rounded in dorsal view, protruding in profile; (4) nares visible ventrally; (5) tympanum small (~1/2 of ED), defined, about 1/3 concealed posterodorsally by a low supratympanic fold; tympanic annulus present below skin; tympanic membrane not differentiated; (6) short teeth present on maxillary arch; (7) median lingual process absent; (8) vocal sac in males single, subgular; (9) carpal pad absent; (10) metacarpal ridge low; (11) thenar tubercle conspicuous; (12) nuptial excrescences on thumb absent; (13) FIII not swollen; (14) tip of FIV surpassing distal subarticular tubercle of FIII; (15) FI and FII equal in size; (16) thin lateral fringes present on preaxial side of FII–FIII; (17) low and poorly defined lateral keels on pre- and postaxial sides of FI and FIV, and postaxial side of FII–FIII; (18) tarsal keel well-defined in all its extension, nearly straight, extending from the base of TI, where is continuous with the preaxial fringe, to the mid-tarsus, not merged with the inner metatarsal tubercle nor reduced at the level of this tubercle; (19) tarsal fringe absent; (20) middle metatarsal tubercle present, larger than inner one, non-protuberant, weakly defined; (21) metatarsal fold present, strongly developed distally; (22) wide lateral (pre- and postaxial) fringes in all toes; (23) toes basally webbed, webbing formula: **I**(1½–2^{-})–(2½–2¾)**II**(1⅔–2^{-})–(3^{+}–3⅓)**III**(2½–3^{+})–(4^{-}–4^{+})**IV**(4^{-}–4^{+})–(2½–3^{-})**V**; (24) discs weakly to moderately expanded on FI–FIV; moderately expanded on TI–TIV, and weakly to moderately expanded on TV; (25) paired dorsal digital scutes present on fingers and toes; (26) cloacal sheath short and slender; (27) supracloacal dermal flap present, conspicuous; (28) cloacal tubercles present; (29) iridescent golden to cream spot at dorsal forelimb and hind limb insertions present, diffuse; (30) pale paracloacal mark present, diffuse; (31) diffuse yellowish spots on hidden parts of hind limbs absent; (32) thigh

dorsally pale brown with four to five transverse dark brown bands; (33) pale dorsolateral stripe diffuse, straight, reaching the level of the arm insertion or slightly surpassing midbody; (34) lateral dark band solid or formed by anastomosed spots, wider at the groin level; (35) oblique lateral stripe partial (not reaching the posterior border of the eye), solid, white or subtly tinged with yellow at the groin; (36) ventrolateral stripe white, cream or yellowish, poorly defined, formed by a wavy series of solid white spots; (37) dark dermal collar narrow, diffuse to solid, and complete in males; narrow (7.5–9.1% of SVL), reticulated, and complete in females; (38) dark lower labial stripe present, diffuse; (39) throat color in life: extensively colored with yellow in females, gray in males; (40) abdomen color white or spotted with yellow, and free or almost free of melanophores in females, dirty white in males; (41) iris golden, finely reticulated with black, with a dark copper horizontal band, pupil ring golden, complete; (42) tongue mustard yellow; (43) large intestine unpigmented; (44) adult testis unpigmented; (45) mature oocytes with the animal pole pigmented with dark brown; (46) skin blackening in males during call activity; (47) mercaptan-like odor present; (48) diurnal activity; (49) tadpole transport by males; (50) riparian habitat; (51) advertisement call composed of long trills of single tonal notes; (52) peak frequency of calls: 3.60–4.26 (3.96 ± 0.19) kHz; (53) fundamental frequency: 1.74–1.91 (1.87 ± 0.04) kHz; (54) rate of note emission: 2.08–3.36 notes/s (2.76 ± 0.52); (55) note duration: 0.04–0.13 (0.08 ± 0.03) s; (56) duration of silent intervals between notes: 0.14–0.57 (0.31 ± 0.10) s.

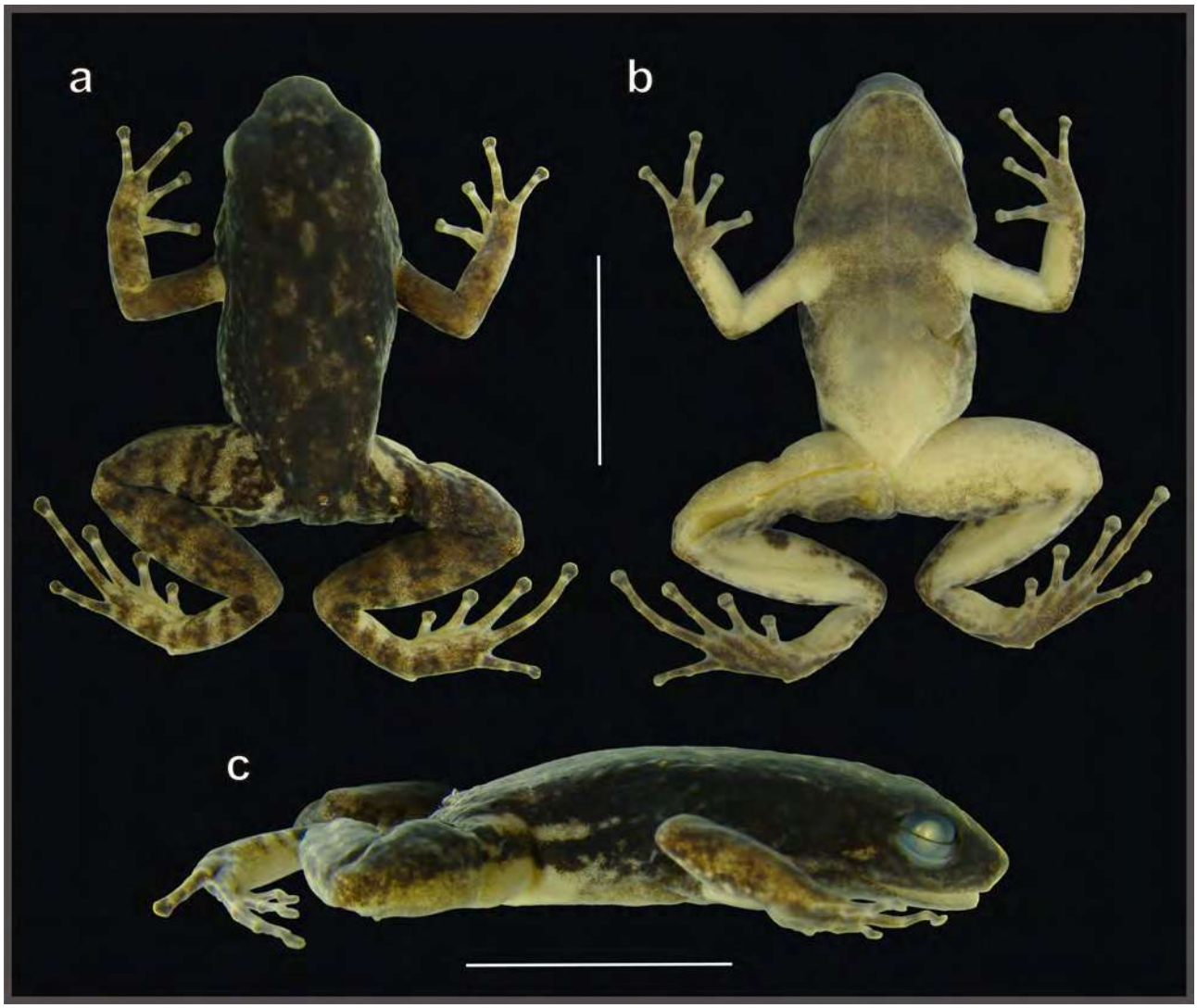

FIGURE 1. Male holotype (MHNLS 21355) of *Mannophryne molinai* **sp. nov.** in dorsal (a), ventral (b), and lateral (c) views. Scale bar represents 10 mm. Photos: F.J.M. Rojas-Runjaic

Diagnosis. Based on the geographic distribution, we only compare *Mannophryne molinai* with the species of the *M. collaris* species Group (*sensu* Manzanilla *et al*. 2007; Grant *et al*. 2017): *M. caquetio* Mijares-Urrutia &

Arends, 1999, *M. collaris* (Boulenger, 1912), *M. cordilleriana* La Marca, 1994, *M. herminae* (Boettger, 1893), *M. lamarcai* Mijares-Urrutia & Arends, 1999, *M. larandina* (Yústiz, 1991), *M. orellana* Barrio-Amorós, Santos & Molina, 2010, *M. urticans* Barrio-Amorós, Santos & Molina, 2010, and *M. yustizi* (La Marca, 1989). We also include in the diagnosis *M. trujillensis* Vargas & La Marca, 2007, and *M. speeri* La Marca, 2009 (not assigned to any species group) due to their geographic distribution (both from the Venezuelan Andes) and phenotypic affinities with this species group. Character states of *M. molinai* are presented in parentheses throughout the diagnosis.

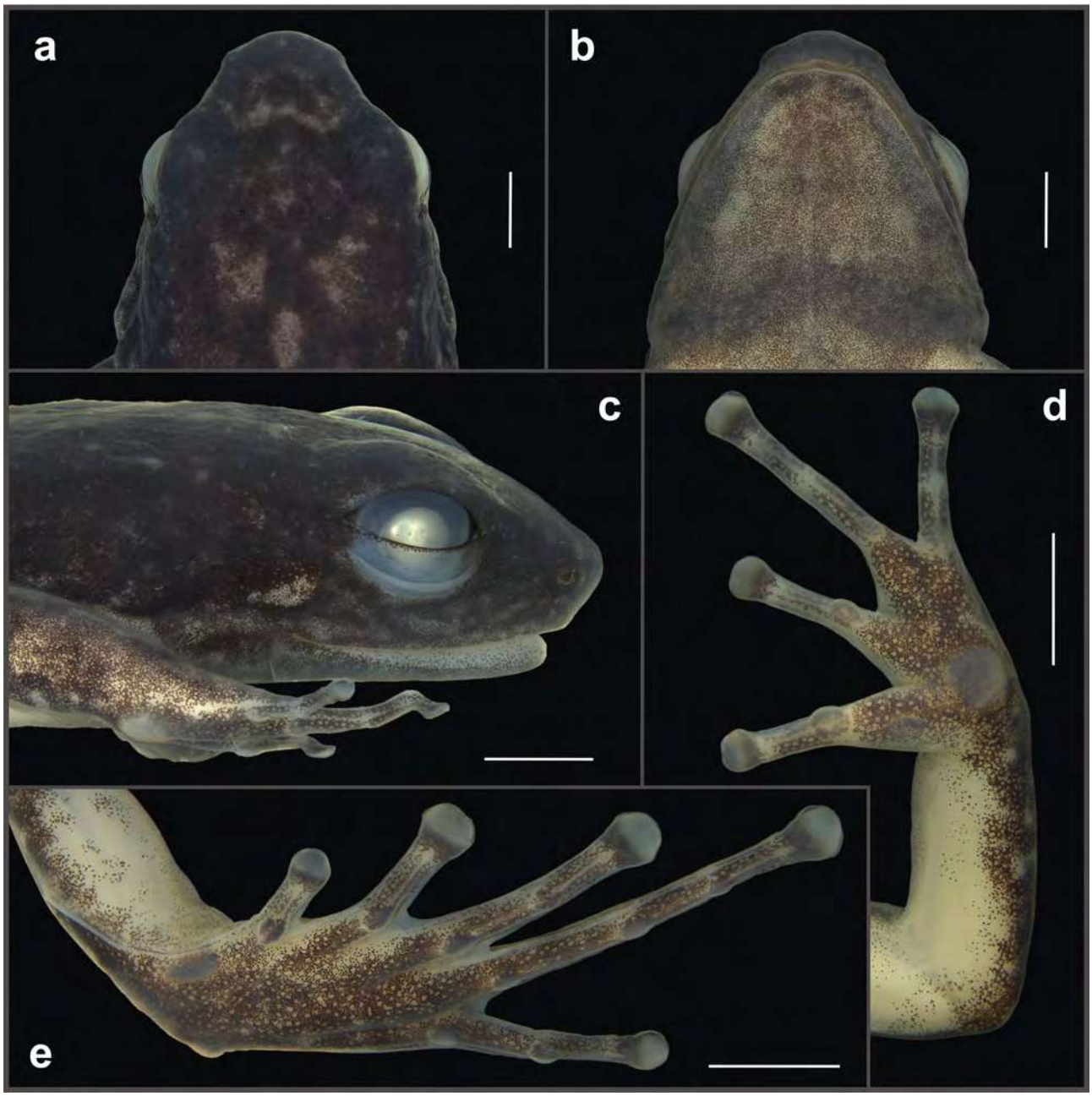

FIGURE 2. Detailed photos of the head (a, b, c), left hand (d) and foot (e) of the holotype (MHNLS 21355) of *Mannophryne molinai* **sp. nov.** Scale bars represent 2 mm. Photos: A. Jaramillo.

Mannophryne caquetio is only known from Sierra de Churuguara in the Sistema Coriano (or Falcón-Lara mountain system; Vivas 2012), northwesternmost portion of the Cordillera de la Costa. Its tympanum diameter is ~1/3 of ED (~1/2 of ED); the disc on FIII is moderately expanded, being 2.5–2.8 times wider than adjacent phalanx (1.9–2.4 times wider); a slightly less extensive toe webbing is present between preaxial side of TIV and preaxial side of TV: (4–4½)**IV**(4^{+}–4½)–3^{-}**V** (basally webbed, [4^{-}–4^{+}]**IV**[4^{-}–4^{+}]– [2½–3^{-}]**V**); its metatarsal fold is strong and almost reaching the outer metatarsal tubercle (also strong, but only extending on the distal third or distal half of the

metatarsus); lacks dark lower labial stripe (present, diffuse); and the pupil ring lacks peripheral lobes (with a ventral peripheral lobe).

Mannophryne collaris is restricted to the valley of the Chama river in the western versant of the Cordillera de Mérida in the Venezuelan Andes. Its adult size is larger and ranges between 24–26 mm SVL in males and 27–33 mm SVL in females (males: 20.5–23.4 mm; females: 25.2–25.5 mm SVL); it has more extensive toe webbing between postaxial side of TII and postaxial side of TIV: **II**(1–1½)–(2½–3)**III**2–(3–3½)**IV**(3–4) (basally webbed, **II**[1⅔–2⁻]–[3⁺–3⅓]**III**[2½–3⁺]–[4⁻–4⁺]**IV**[4⁻–4⁺]); it lacks dark lower labial stripe (present, diffuse); abdomen is light gray in adult males, profusely stippled with melanophores when seen under magnification (ivory white, less stippled); only the posterior two-thirds of throat on adult females are yellow in life, and pale free or almost free of melanophores in preservative (throat extensively yellow colored in life and free or almost free of melanophores in preservative); pupil ring lacks peripheral lobes (with a ventral peripheral lobe); the rate of note emission of calls is higher and ranges from 8–9 notes/s (2–3 notes/s); the duration of silent interval between notes is 0.06–0.08 s (0.14–0.57 s); and the peak frequency of calls is 3.55 kHz (3.60–4.26 kHz).

Mannophryne cordilleriana is restricted to the basins of the Santo Domingo and Calderas rivers in the eastern versant of the Cordillera de Mérida in the Venezuelan Andes. Body size in females is larger and ranges between 30–35 mm SVL (25.2–25.5 mm SVL); it has weakly expanded discs on TI–TII, being TI: 1.7–2.0, and TII: 1.8–2.4 times wider than adjacent phalanx (moderately expanded; TI: 2.0–2.3, TII: 2.5–2.7 times wider); more extensive toe webbing between postaxial side of TII and postaxial side of TIV: **II**(1–1½)–(2½–3)**III**(2–2½)– (3–3½)**IV**(3½–4) (basally webbed, **II**[1⅔–2⁻]–[3⁺–3⅓]**III**[2½–3⁺]–[4⁻–4⁺]**IV**[4⁻–4⁺]); only the posterior two-thirds of throat in adult females are yellow in life, and pale, free or almost free of melanophores in preservative (all throat yellow in life, and free or almost free of melanophores in preservative); abdomen may be evenly or irregularly stippled with melanophores in adult males, and irregularly stippled in adult females (evenly stippled in males, and free or almost free of melanophores in adult females); pupil ring without peripheral lobes (with a ventral peripheral lobe).

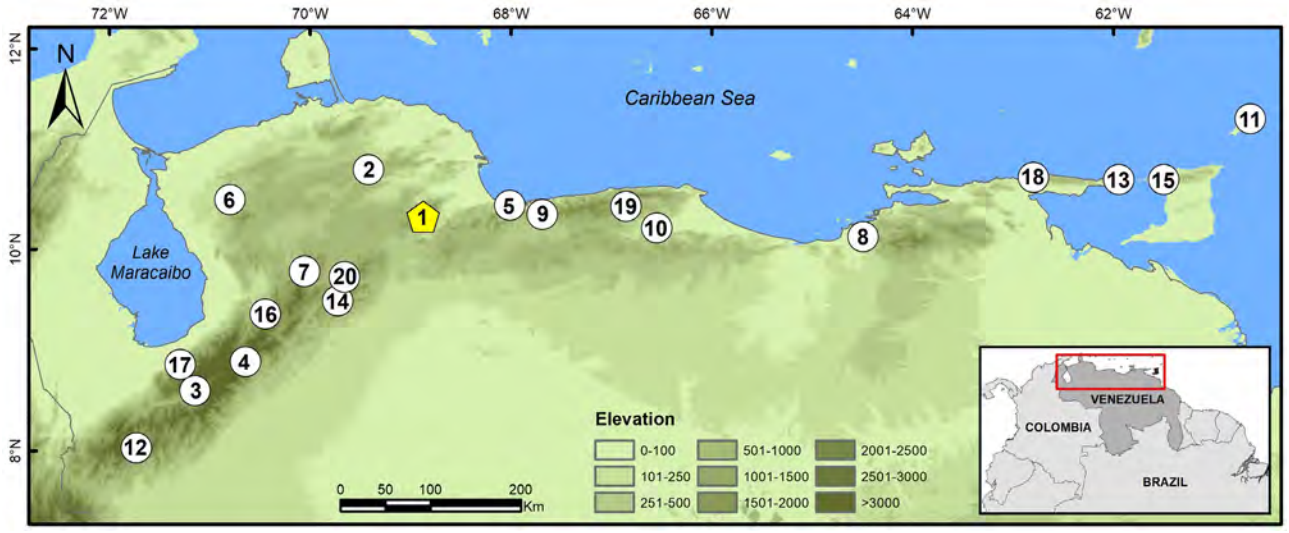

FIGURE 3. Map of northern Venezuela, and Trinidad and Tobago, indicating the type localities of the 20 known species of *Mannophryne*: 1. *M. molinai* **sp. nov.**; 2. *M. caquetio*; 3. *M. collaris*; 4. *M. cordilleriana*; 5. *M. herminae*; 6. *M. lamarcai*; 7. *M. larandina*; 8. *M. leonardoi*; 9. *M. neblina*; 10. *M. oblitterata*; 11. *M. olmonae*; 12. *M. orellana*; 13. *M. riveroi*; 14. *M. speeri*; 15. *M. trinitatis*; 16. *M. trujillensis*; 17. *M. urticans*; 18. *M. venezuelensis*; 19. *M. vulcano*; 20. *M. yustizi*.

Mannophryne herminae is known from the central portion of the northern slope of Cordillera de la Costa. It is very similar to *M. molinai* in body size, general color pattern and toe webbing, but can be easily distinguished by its markedly different advertisement call, which is composed by notes arranged in duplets emitted in long trills (trills of single notes, not arranged in duplets); its rate of note emission is higher, with 10–11 notes/s (2–3 notes/s), and up to 546 notes per trill (up to 89 notes per trill); the notes are shorter, ranging between 0.02–0.04 s (note duration: 0.04–0.13 s), and are less spaced, being 0.02–0.04 s the range of duration of the silent intervals between notes of each duplet, and 0.09–0.14 s between duplets (silent intervals between notes: 0.14–0.57); spectrally, its call differs only in the fundamental frequency, which ranges between 1.98–2.15 kHz (1.74–1.92 kHz).

Additionally, its metatarsal fold is strong and almost reaching the outer metatarsal tubercle (also strong, but only extending from the base of TV to the distal third or distal half of the metatarsus); dark dermal collar is solid or with some small white spots in females (reticulated); the width of the collar in females ranges between 10.9–15.9% of SVL (7.5–9.1% of SVL); pupil ring lacks peripheral lobes (with a ventral peripheral lobe).

Mannophryne lamarcai is restricted to the Serranía de Ziruma, between the northern limit of the Venezuelan Andes and the western limit of Cordillera de La Costa. Its snout is nearly truncate in dorsal view (rounded); it has more extensive toe webbing on preaxial side of TII, ranging between 2–2½ (toe webbing formula on preaxial side of TII is 2½–2¾), and also between postaxial side of TIII and preaxial side of TIV: **III**(2–2½)–(3½–4$^-$)**IV** (webbing less extensive between TIII–TIV: **III**[2½–3$^+$]–[4$^-$–4$^+$]**IV**); its metatarsal fold is strong and almost reaching the outer metatarsal tubercle (also strong, but only extending on the distal third or distal half of the metatarsus); dorsolateral stripe is solid or diffuse (always diffuse) and extensive, reaching midbody or up to the level of the groin (reaching the level of the arm insertion or the midbody); only the posterior half to posterior two-thirds of throat in adult females are yellow colored in life, and pale free or almost free of melanophores in preservative (all the throat yellow in life and free or almost free of melanophores in preservative); the dark dermal collar is solid in adult females (reticulated); pupil ring lacks peripheral lobes (with a ventral peripheral lobe).

Mannophryne larandina is known from Sierra de Barbacoas, northeastern limit of the Cordillera de Mérida in the Venezuelan Andes. Adult females of this species are larger, reaching up to 31.0 mm of SVL (up to 25.5 mm of SVL); the nares are laterodorsally oriented and barely visible in dorsal view (lateroventrally oriented and only visible in ventral view); the basal subarticular tubercles of toes are elongated (rounded to slightly elliptical); it has more extensive toe webbing: **I**(0$^+$–1$^-$)–(2$^-$–2$^+$)**II**(1$^-$–1$^+$)–(2⅔–3$^-$)**III**(2$^-$–2$^+$)–(3⅓–3½)**IV**(3⅔–4$^-$)–(2$^-$–2$^+$)**V** (basally webbed; **I**[1½–2$^-$]–[2½–2¾]**II**[1⅔–2$^-$]–[3$^+$–3⅓]**III**[2½–3$^+$]–[4$^-$–4$^+$]**IV**[4$^-$–4$^+$]–[2½–3$^-$]**V**); the posterior half of throat in adult females is yellow in life, and pale, free or almost free of melanophores in preservative (all the throat yellow in life and free or almost free of melanophores in preservative); dark dermal collar in adult males is diffuse and speckled with white (diffuse or solid but without white spots); abdomen in adult males is pale gray with discrete white spots (dirty ivory); pupil ring without peripheral lobes (with a ventral peripheral lobe).

Mannophryne orellana is restricted to the southern part of the eastern versant of the Cordillera de Mérida in the Venezuelan Andes. This is a larger species with adult males and females ranging between 25.4–27.3 mm, and 29.5–32.9 mm of SVL, respectively (males: 20.5–23.4 mm SVL; females: 25.2–25.5 mm SVL); basal subarticular tubercles of toes are elongated (rounded to slightly elliptical); has a much more extensive toe webbing: **I**(0$^+$–1$^-$)–(2–2$^+$)**II**(1$^+$–1⅓)–(2⅔–3$^-$)**III**(1⅔–2)–(2⅔–3$^+$)**IV**(3$^+$–3⅔)–(2$^-$–2$^+$)**V** (basally webbed; **I**[1½–2$^-$]–[2½–2¾] **II**[1⅔–2$^-$]–[3$^+$–3⅓]**III**[2½–3$^+$]–[4$^-$–4$^+$]**IV**[4$^-$–4$^+$]–[2½–3$^-$]**V**); lacks pale dorsolateral and ventrolateral stripes (both present); the dark dermal collar in females is narrow (wide), solid and without white spots (reticulated); posterior half of throat in adult females is yellow in life, and pale free or almost free of melanophores in preservative (all the throat yellow in life and free or almost free of melanophores in preservative). The calls of *Mannophryne orellana* are trills of pulsed notes (trills of tonal notes), emitted at a rate of 10–13 notes/s (2–3 notes/s); the note duration ranges between 0.03–0.04 s (0.04–0.13 s), and the silent interval between notes is 0.04–0.05 s (0.14–0.57 s); its peak frequency is about 3.42 kHz (3.60–4.26 kHz).

Mannophryne speeri is known from Sierra de Portuguesa, at the northern part of the eastern versant of the Cordillera de Mérida, in the Venezuelan Andes. Adult females of this species are smaller, ranging between 23.0–24.1 mm of SVL (females: 25.2–25.5 mm SVL); the discs on FI–FII are weakly expanded, being respectively 1.6–1.9, and 1.7–1.9 times wider than their adjacent phalanges (1.8–2.1, and 1.8–2.3 times wider); it has slightly more extensive toe webbing: **I**(1$^+$–1½)–(2$^+$–2⅓)**II**(1½–1⅔)–(3$^-$–3$^+$)**III**(2½–3$^-$)–(3⅔–4$^-$)**IV**(4$^-$–4$^+$)–(2⅓–2½)**V** (basally webbed; **I**[1½–2$^-$]–[2½–2¾]**II**[1⅔–2$^-$]–[3$^+$–3⅓]**III**[2½–3$^+$]–[4$^-$–4$^+$]**IV**[4$^-$–4$^+$]–[2½–3$^-$]**V**); nares are laterodorsally oriented and barely visible in dorsal view (lateroventrally oriented and only visible in ventral view); only the posterior half of throat in adult females is yellow in life, and pale free or almost free of melanophores in preservative (all the throat yellow in life and free or almost free of melanophores in preservative); pupil ring lacks peripheral lobes (with a ventral peripheral lobe).

Mannophryne trujillensis is endemic from the valley of the Castán river, in the eastern versant of the Cordillera de Mérida in the Venezuelan Andes. The adult females of this species are larger, reaching up to 27.5 mm of SVL (up to 25.5 mm of SVL); it has more extensive toe webbing: **I**(1$^+$–1½)–(2–2⅓)**II**(1$^+$–1½)–(2¾–3$^+$)**III**(2$^+$–2½)–(3½–3⅔)**IV**(4$^-$–4$^+$)–(2$^+$–2⅔)**V** (basally webbed; **I**[1½–2$^-$]–[2½–2¾]**II**[1⅔–2$^-$]–[3$^+$–3⅓]**III**[2½–3$^+$]–[4$^-$–4$^+$]**IV**[4$^-$–4$^+$]–

[2½–3⁻]**V**); its metatarsal fold is strong and almost reaching the outer metatarsal tubercle (also strong, but only extending on the distal third or distal half of the metatarsus); only the posterior two-thirds of throat in adult females are yellow in life, and pale free or almost free of melanophores in preservative (all throat yellow in life and free or almost free of melanophores in preservative); dark dermal collar is finely speckled with small white spots in adult females (reticulated); the abdomen typically is evenly stippled with melanophores in adult females (free or almost free of melanophores in adult females); pupil ring lacks peripheral lobes (with a ventral peripheral lobe).

Mannophryne urticans is restricted to the western piedmont of Cordillera de Mérida in the Venezuelan Andes. This is a larger species with adult males and females ranging between 23.8–27.5 mm, and 25.9–30.8 mm of SVL, respectively (males: 20.5–23.4 mm SVL; females: 25.2–25.5 mm SVL); has a slightly more extensive toe webbing: **I**(1⁺–1⁻)–(2–2¼)**II**(1⁺–1⅓)–(2⅔–3⁻)**III**(2⁻–2¼)–(3⅓–3½)**IV**(3⅔–4⁺)–(2⁻–2⁺)**V** (basally webbed; **I**[1½–2⁻]–[2½–2¾]**II**[1⅔–2⁻]–[3⁺–3⅓]**III**[2½–3⁺]–[4⁻–4⁺]**IV**[4⁻–4⁺]–[2½–3⁻]**V**); lacks pale dorsolateral and ventrolateral stripes (both present); dark dermal collar in females is narrower, ranging between 4.7–6.6% of SVL (wider, 7.5–9.1% of SVL), solid (reticulated) and medially broken or almost broken (always complete); only the posterior two-thirds of throat of adult females are yellow in life, and pale free or almost free of melanophores in preservative (all the throat yellow in life and free or almost free of melanophores in preservative). The calls of *Mannophryne urticans* are trills of pulsed notes (trills of tonal notes), emitted at a rate of 5–6 notes/s (2–3 notes/s); the notes have a duration of 0.02 s (0.04–0.13 s), and the silent interval between notes is 0.07–0.08 s (0.14–0.57 s); its peak frequency is about 3.56 kHz (3.60–4.26 kHz).

FIGURE 4. Female and male paratype specimens of *Mannophryne molinai* **sp. nov.** in life. (a) Dorsolateral and (b) ventral views of the paratype female MHNLS 21337; (c) dorsolateral and (d) ventral views of the paratype male MCP 13924 (ex-MHNLS 21336). Photos: F.J.M. Rojas-Runjaic

Finally, *Mannophryne yustizi* is known only from Sierra de Portuguesa, in the northernmost portion of the eastern versant of the Cordillera de Mérida in the Venezuelan Andes. Adult females of this species are larger, reaching 26.8–30.6 mm of SVL (25.2–25.5 mm of SVL); the basal subarticular tubercles of toes are elongated (rounded to slightly elliptical); has a slightly more extensive toe webbing between preaxial sides of TI and TIII: **I**(1^{+}–1½)–(2^{+}–2⅓)**II**(1⅓–1⅔)–(3^{-}–3^{+})**III** (basally webbed; **I**[1½–2^{-}]–[2½–2¾]**II**[1⅔–2^{-}]–[3^{+}–3⅓]**III**); the dorsolateral stripe is solid to diffuse (always diffuse) and more extensive, reaching the midbody or up to the level of the groin (reaching the level of the arm insertion or up to the midbody); only the posterior half of throat in adult females is yellow in life, and pale free or almost free of melanophores in preservative (all the throat yellow in life and free or almost free of melanophores in preservative); dark dermal collar in females is wider, ranging between 9.0–13.5% SVL (narrower, 7.5–9.1% SVL); in males the dark dermal collar is diffuse, speckled with small white spots to reticulated, and complete or medially broken (diffuse to solid, without white spots, and complete); the abdomen in males is pale gray, densely stippled with melanophores evenly distributed or clumped (dirty ivory, less stippled, non-clumped melanophores), and occasionally speckled with small white dots (without small white dots).

Description of the holotype. An adult male (Figs. 1–2) of 21.2 mm SVL. Body robust, short and slightly wider than head (Fig. 1a). Head as long as wide (HeL: 37.3% of SVL; HW: 37.7% of SVL; HeL/HW: 1.0). Snout short, rounded in dorsal view (Fig. 2a), protruding in profile (Fig. 2c). Eye-naris distance shorter than eye diameter (EN/ED: 0.6). Nares small, elliptical, lateroventrally oriented, situated laterally to the tip of the snout, visible from the front and barely visible ventrally, not visible dorsally; nares with a thin dermal flap on the posterior half which is posterodorsally lobulated. *Canthus rostralis* distinct, almost straight in dorsal view, slightly rounded in cross section; loreal region flat, vertical. Interorbital region wider than upper eyelid; interorbital distance slightly shorter than internarial distance (IoD/InD: 0.8). Eye prominent (ED: 13.2% of SVL). Tympanum small (DT/ED: 0.5), defined; tympanic annulus present concealed below skin but forming a weak relief in it; tympanic membrane not differentiated; about 1/3 of the tympanum concealed posterodorsally by a low supratympanic fold formed by superficial slip of *musculus depressor mandibulae*; tympanum posteroventral to the eye, almost touching the angle of jaws (Fig. 2c). Short teeth present on maxillary arch, concealed by inner surface of upper lip. Choanae small, rounded, anterolaterally positioned on the roof of the mouth, anterior to eye bulge. Tongue cordiform, 1/3 free posteriorly, without median lingual process.

Forelimb (Fig. 2d) slender, with three small ulnar tubercles longitudinally aligned on the ventroexternal surface of the forearm. Hand length 29.7% of SVL. Carpal pad absent. Palmar tubercle large, swollen, well-defined, rounded. Thenar tubercle elliptical (about two times longer than wide), small (larger diameter about 2/3 of palmar tubercle diameter), swelling, and evident in both palmar view and profile. One slightly elliptical subarticular tubercle each on FI and FII, similar in size to thenar tubercle, and two small, circular tubercles each on FIII and FIV; all subarticular tubercles conspicuous and swollen. Palmar supernumerary tubercles absent. Metacarpal ridge present, low. Nuptial excrescences on thumb absent. FIII not swollen. Relative length of adpressed fingers: III>IV>II>I; tip of FIV surpassing distal subarticular tubercle of FIII when fingers are juxtaposed. FI and FII equal in size. Thin lateral fringes present on preaxial side of FII–FIII, weak and poorly defined lateral keels on pre- and postaxial sides of FI and FIV, and on postaxial side of FII–FIII. Finger discs present, moderately expanded; width of discs corresponding (from FI to FIV, on both hands) to 2.0–2.1, 2.2–2.3, 2.2–2.4 and 2.0–2.2 times the width of their respective adjacent phalanges. Disc width of FIII 1/2 of tympanum diameter (F3D/TD: 0.5). Tip of discs slightly rounded to nearly truncated; disc pad transversely elliptical. Paired dorsal digital scutes conspicuous and protuberant in all fingers.

Hind limbs (Fig. 2e) robust; thigh, shank and foot similar in size (ThL: 48.1% SVL; SL: 49.5% SVL; FL: 49.1% SVL). Tarsal keel well-defined in all its extension, nearly straight, its proximal end reaching the mid-tarsus; distally extends along the preaxial side of inner metatarsal tubercle (without merging with it nor reduced to this level) to reach the base of TI, were it merges with the preaxial fringe of this toe. Tarsal fringe absent. Inner metatarsal tubercle large, slightly swollen, well-defined, elliptical, 1.7–2.0 times longer than wide. Outer metatarsal tubercle, rounded, swollen, smaller than inner metatarsal tubercle (about 1/2 of its size). A large middle metatarsal tubercle is present between the inner and outer ones; slightly greater than inner metatarsal tubercle, elliptical, flat, weakly defined, its distal border reaching the level of proximal borders of the other two metatarsal tubercles. Metatarsal fold present, strong at the base of TV but weak at its proximal portion; distally, this fold is continuous with the postaxial fringe of TV. Plantar supernumerary tubercles absent. Toes slender, all with wide lateral (pre- and postaxial) fringes and basally webbed; webbing formula: **I**1½–2½**II**1⅔–3^{+}**III**(2½–2⅔)–4^{-}**IV**4^{+}–

2½**V**. Subarticular tubercles small (about 1/2–1/3 size of the inner metatarsal tubercle), rounded to near elliptical (longitudinally) and swollen; one on TI–TII, two on TIII and TV, three on TIV. Relative lengths of adpressed toes: IV>III>V>II>I; tip of TIII reaching the mid-level between distal and median subarticular tubercles of TIV; tip of TV reaching the distal half of the median subarticular tubercle of TIV. Toe discs present, moderately expanded on TI–TIV, weakly expanded on TV; width of discs corresponding (from TI to TV, on both feet) to 2.0–2.3, 2.5–2.7, 2.2–2.5, 2.2–2.4 and 1.7 times the width of their respective adjacent phalanges. Disc width of TIV about 1/2 of tympanum diameter (T4D/TD: 0.6). Tip of discs slightly rounded to nearly truncated; disc pad transversely elliptical. Paired dorsal digital scutes conspicuous and slightly protuberant in all toes.

Dorsal skin of body and hind limbs shagreen; moderately granular on upper eyelids and body flanks, smooth on forelimbs; with scattered small tubercles on the posterior third of dorsum, body flanks, and dorsal surfaces of thighs and shanks; head flank with one to two large and horizontally enlongated postcommisural tubercles (Fig. 2c). Ventral skin smooth on throat, chest, belly, forelimbs, and thighs. Several large tubercles are present at the base of the retrolateral surface of thighs, flanking the cloaca. Dermal flap above cloaca present, conspicuous (Figs. 1a, c). Cloacal sheath short and slender; cloacal opening ventrally oriented, above midlevel of thighs.

Measurements of the holotype (in mm). SVL: 26.7; SL: 14.0; ThL: 14.2; FL: 13.0; HaL: 7.4; HeL: 9.5; HW: 9.4; IoD: 3.3.; InD: 3.6; EN: 2.3; ED: 3.7; TD: 1.7; ETS: 4.1; F3D: 0.7; T4D: 0.9; F1L: 5.0: F2L: 5.2.

Color in life of the holotype (based on field notes and photos). Dorsal background color grayish brown, with abundant small dark brown dots and some scattered irregular pale greenish gray spots; these pale spots are iridescent when seen under magnification. Pale dorsolateral stripe diffuse, ill-defined, straight, extending dorsolaterally from external edge of upper eyelid to the mid-level of dorsum.

Sides of body with a well-defined blackish brown lateral band, finely stippled with greenish gray dots; lateral band extending from tip of snout to upper level of groin, covering the naris, and the two superior thirds of the eye and tympanum; the upper border of this band is almost straight and in contact with the dorsolateral pale stripe; posterior to the tympanum its lower border becomes broader and irregular, reaching the upper insertion of the arm and continues to the groin delimited ventrally by the ventrolateral stripe. Oblique lateral stripe (OLS) solid white in almost all its extension, subtly tinged with yellow at the groin, anteriorly broken in small spots, reaching mid-way between groin and eye (about the level of the forearm). The trace of OLS is coincident with a series of small non-keratinized tubercles. Ventrolateral stripe (VLS) formed by a wavy series of solid white spots; with those close to the groin subtly tinged of yellow; VLS extending from the postcommisural area to the mid-level of the groin. Upper lip variegated with small cream and blackish brown spots.

Background color of throat cream translucent, dense and evenly stippled with melanophores; dark lower labial stripe present; dark dermal collar narrow, diffuse, with small scattered whitish dots (inconspicuous to eye naked but visible under magnification); its posterior border reaches the anterior level of arm insertion. Background color of the remaining ventral surfaces translucent grayish, densely stippled with melanophores on chest and decreasing in density toward posterior part of abdomen, undersurface of hind limbs. Parietal peritoneum on belly nacreous white, visible through skin. Ventral periphery of groin faintly tinged with yellow.

Dorsal surface of upper and forearm and hand pale brown, with small scattered greenish gray dots; a faint iridescent pale spot present at dorsal insertion of upper arm. A blackish brown stripe on the mid-level of both, pre- and postaxial sides of upper arm, extending from arm insertion to the articulation with the forearm. Two transverse blackish brown bands on dorsal surface of forearm; the three small ulnar tubercles longitudinally aligned on the ventroexternal surface of the forearm, white-colored. Dorsal surface of hand with one or two transverse blackish brown stripes. Fingers dorsally blackish brown, with small white spots coincident with the knuckles, more conspicuous on the distal ones of each finger. Dorsal digital scute coloration varies from almost completely white to stippled with white and blackish brown in a salt-and-pepper pattern. Palm and ventral surface of digits blackish gray, tubercles (palmar, thenar, subarticulars) and disc pads, pale gray.

Dorsal surface of hind limbs pale brown in brackground, speckled with white dots (coincident with small tubercles), and cross-banded with four to five transverse dark brown bands on thighs, three on shanks and tarsi, and two to three on the feet. A faint iridescent pale yellow spot present at dorsal insertion of thigh. Pale paracloacal marks short, diffuse, each merging with the background color of dorsal surface of thigh. A blackish brown stripe on the mid-level of both, pre- and postaxial sides of thigh, formed by a series of anastomosed irregular blotches; the preaxial stripe well-defined, extending from groin to knee, and fused with the transverse bands; the postaxial one less defined and only partially in contact with the transverse bands. Toes dorsally blackish brown, with small white

spots coincident with the knuckles, more conspicuous on the distal ones of each toe. Dorsal digital scutes from almost totally white to stippled with white and blackish brown in a salt-and-pepper pattern. Ventral surface of hind limbs translucent pale gray; undersurface of thighs evenly stippled with melanophores (when seen under magnification); soles and undersurface of toes blackish brown; tubercles (metatarsals, subarticulars) and disc pads pale gray.

Iris golden, with fine black reticulation, and a wide transversal dark copper band; pupil ring not broken and with a ventral lobe, golden on inferior and superior portions, copper on anterior and posterior portions. Tongue mustard yellow.

Color of the holotype in preservative (after three years, September 2017). Dorsal background color of body dark brown with irregular pale brown spots; dorsolateral stripe faded (Fig. 1a). Lateral blackish band slightly paler and barely contrasting with dorsal background (Fig. 1c); oblique lateral and ventrolateral stripes ivory white, the latter inconspicuous, poorly differentiated from ventral coloration (Fig. 1c). Yellowish tones on posterior part of the oblique lateral stripe, ventrolateral portion of groin, and faint iridescent pale yellow spots at dorsal insertion of thighs and arms vanished.

Ventral background color (including ventral surface of forelimbs and hind limbs) ivory white (Fig. 1b); dark lower labial stripe and dark dermal collar dark brown, diffuse, formed by a profusion of melanophores (noted under magnification; Fig. 2b); Throat, chest and anterior portion of belly densely stippled with melanophores, less dense and evenly stippled on posterior portion of belly (Figs. 1a, 2b).

Dorsal background color of forelimbs pale brown; the longitudinal blackish brown stripes on pre- and postaxial sides of upper arm, and transverse blackish brown bands on dorsal surface of forearm turned dark brown; ulnar tubercles and knuckles of fingers, ivory white; dorsal digital scutes of fingers grayish white; undersurface of upper arms evenly stippled with melanophores, almost free of melanophores on ventrointernal side of forearms; palms and ventral surfaces of fingers dark brown; tubercles and disc pads pale gray.

Dorsal background color of hind limbs pale brown, cream towards insertion of thigh and feet; paracloacal marks ivory white, fused with background color of thigh; cross-bands on thighs, shanks, tarsi and feet, and longitudinal pre- and postaxial stripes on thigh, dark brown; knuckles of toes ivory white; dorsal digital scutes of toes grayish white; undersurface of thighs evenly stippled with melanophores, undersurface of shanks almost free of melanophores; webbing translucent; soles and ventral surfaces of toes dark brown; tubercles and disc pads pale gray. Iris blackish brown; pupil ring not visible. Tongue creamy yellow.

Morphometric and color variation in the type series. As in all other species of the genus, *Mannophryne molinai* exhibits striking sexual dichromatism on the ventral surface of the body (in life), with a vivid yellow throat and a marked dark dermal collar in adult females, and grayish throat with poorly defined dark collar in adult males. Vocal slits and vocal sac are secondary sexual characters only present in males.

Sexual dimorphism is also seen in adult size, with males being smaller than females (SVL: 20.5–23.4 mm [21.6 ± 1.0; *n* = 7] in males *vs*. 25.2–25.5 mm [25.4 ± 0.2; *n* = 2] in females). The relative size of the tympanum varies between sexes, being larger in females (7.5–7.5% of SVL [7.5 ± 0.1; *n* = 2]) than in males (6.3–7.0% of SVL [6.7 ± 0.2; *n* = 7]). The relative size of the hands is larger in males (26.3–30.7% of SVL [28.4 ± 1.7; *n* = 7]) than in females (25.8–26.3% of SVL [26.0 ± 0.3; *n* = 2]). Hind limbs are also larger in males than in females: ThL: 48.1–54.7% of SVL (50.6 ± 2.7; *n* = 7) in males *vs*. 44.7–46.0% of SVL (45.4 ± 0.9; *n* = 2) in females; SL: 49.5–53.7% of SVL (51.3 ± 1.8; *n* = 7) in males *vs*. 47.1–47.6% of SVL (47.3 ± 0.4; *n* = 2) in females; FL: 47.4–52.8% of SVL (49.6 ± 1.9; *n* = 7) in males *vs*. 43.3–45.1% of SVL (44.2 ± 1.3; *n* = 2) in females. The discs on fingers are slightly wider in males than in females (from FI–FIV, males: 2.0–2.1, 2.1–2.3, 2.1–2.4, 2.0–2.2 *vs*. females: 1.8, 1.8–1.9, 1.9–2.3, 1.6–1.9 x width of the adjacent phalanges).

Variation in general morphometric characters of the type series is shown in Table 1. The proportions of the head (slightly longer than wide to as wide as long) are very similar in the type series (HeL/HW: 1.0–1.1 [0.1 ± 0.0; *n* = 9]), and its relative size is slightly variable (HeL: 35.0–37.7% of SVL [36.3 ± 0.8; n = 9]; HW: 33.3–37.7% of SVL (35.7 ± 1.6; *n* = 9]). Interobital distance varies from slightly shorter to as longer as internarial distance (IoD/InD: 0.8–1.0 [0.9 ± 0.1; *n* = 9]). The ratio of the tympanum diameter with respect to the eye diameter also varies slightly (TD/ED: 0.5–0.6 (0.5 ± 0.0; *n* = 9). The eye is prominent and its relative diameter shows similar variation in males and females (ED: 12.7–14.6% of SVL [13.8 ± 0.6; *n* = 9]). F3D/TD and T4D/TD ratios also show slight variation (F3D/TD: 0.4–0.5 [0.4 ± 0.0; *n* = 9]; T4D/TD: 0.5–0.6 [0.6 ± 0.1; *n* = 9]). The width of toe discs varies from weakly to moderately expanded but does not differ between sexes (from TI–TV: 2.0–2.3, 2.4–2.7, 2.2–2.8,

2.2–2.9, 1.7–2.2 x width of the adjacent phalanges). Foot webbing variation: **I**(1½–2⁻)–(2½–2¾)**II**(1⅔–2⁻)–(3⁺–3⅓)**III**(2½–3⁺)–(4⁻–4⁺)**IV**(4⁻–4⁺)–(2½–3⁻)**V** (*n* = 15); modal foot webbing formula: **I**1½–2½**II**2⁻–3⅓**III**2⅔–4**IV** 4⁺–2⅔**V** (*n* = 15).

TABLE 1. Morphometric variation (in mm) in the type series of *Mannophryne molinai* **sp. nov. Min–Max:** minimum–maximum; **X ± SD:** mean ± standard deviation.

Morphometric Characters	Males (n = 7)		Females (n = 2)	
	Min–Max	X ± SD	Min–Max	X ± SD
SVL	20.5–23.4	21.6 ± 1.0	25.2–25.5	25.4 ± 0.2
Thl	10.2–11.4	10.9 ± 0.4	11.4–11.6	11.5 ± 0.1
SL	10.5–11.6	11.0 ± 0.4	12.0–12.0	12.0 ± 0.0
FL	10.2–11.1	10.7 ± 0.3	10.9–11.5	11.2 ± 0.4
HaL	5.4–6.6	6.1 ± 0.4	6.5–6.7	6.6 ± 0.1
HeL	7.4–8.2	7.8 ± 0.3	9.4–9.5	9.5 ± 0.1
HW	7.3–8.0	7.6 ± 03	9.4–9.4	9.4 ± 0.0
IoD	2.5–2.8	2.6 ± 0.1	3.0–3.3	3.2 ± 0.2
InD	2.7–3.2	2.9 ± 0.2	3.8–3.8	3.8 ± 0.0
EN	1.8–2.0	1.9 ± 0.1	2.3–2.3	2.3 ± 0.0
ED	2.8–3.2	3.0 ± 0.2	3.4–3.6	3.5 ± 0.1
TD	1.4–1.6	1.4 ± 0.1	1.9–1.9	1.9 ± 0.0
ETS	3.1–3.3	3.2 ± 0.1	3.7–4.1	3.9 ± 0.3
F3D	0.6–0.7	0.6 ± 0.1	0.8–0.9	0.9 ± 0.1
T4D	0.7–0.9	0.8 ± 0.1	1.0–1.1	1.1 ± 0.1
F1L	4.0–4.8	4.3 ± 0.3	4.6–4.9	4.8 ± 0.2
F2L	4.0–4.9	4.4 ± 0.3	4.7–5.0	4.9 ± 0.2

The dorsal color pattern of dark brown spots is very variable and differs among all specimens; in some preserved males dorsal color turns almost uniformly dark brown (MHNLS 21339, 21536). Dorsolateral stripe varies in intensity in living specimens (Figs. 4a, c), but is always diffuse (almost imperceptible in most preserved specimens); also shows variation in extension, reaching the level of the arm insertion (*e.g.* MHNLS 21337; Fig. 4a) or extending to midbody, well past the arm insertion (*e.g.* MCP 13924; Fig. 4c). The lateral dark band varies from solid with small pale dots (*e.g.* MHNLS 21337; Fig. 4a), to solid on top and formed by a profusion of irregular spots anastomosed below the oblique lateral stripe (*e.g.* MHNLS 21535). The dark dermal collar is well defined, complete, narrow and reticulated in females (Fig. 5a–b), whereas in males is less conspicuous, complete, and solid (MCP 13924 [Fig. 4d], MHNLS 21338–21339, 21538 [Fig. 5d]) or diffuse (21355, 21537–21540; Fig. 5c). In life, the extension of the yellow coloration on the throat, chest and belly of adult females is also variable; the throat is yellow in all or almost all its extension, and some specimens have yellow coloration only on the posterior portion or the periphery of the belly, while others show most of belly and chest yellow (MHNLS 21337; Fig.4b).

Call description. Advertisement calls of *Mannophryne molinai* are composed of short tonal notes arranged in trills (Fig. 6a). The duration of call trills among the three males recorded was 13.58 ± 12.09 (1.93–39.55) s. The rate of note emission was 2.76 ± 0.52 (2.08–3.36) notes/s (Fig. 6c), and each call contained 36.43 ± 26.48 (4–89) notes. Note duration was 0.08 ± 0.03 (0.04–0.13) s, and the duration of silent intervals between notes 0.31 ± 0.10 (0.14–0.57) s. Notes have a slight ascending frequency modulation (Figs. 6b, d). Peak frequency was 3.96 ± 0.19 (3.60–4.26) kHz; with its lower and upper frequencies of 3.71 ± 0.23 (3.26–4.05) kHz and 4.20 ± 0.14 (3.82–4.43) kHz, respectively, and a bandwidth of 0.49 ± 0.13 (0.30–0.79) kHz. The fundamental frequency was 1.87 ± 0.04 (1.74–1.92) kHz. Four additional harmonics (3rd–6th; Figs. 6b, d) were observed above peak frequency, at 5.43–5.99, 6.80–7.47, 8.96–9.73, and 10.51–11.65 kHz, respectively. Fundamental frequency and the other four additional harmonics were not detected due to background noise in the spectrograms of calls emitted by two of the three specimens recorded.

Habitat and natural history. *Mannophryne molinai* inhabits narrow rapid mountain creeks surrounded by forest (Fig. 7) in Sierra de Aroa. The phytocoenoses of the type locality corresponds to Coastal cloud forest (Huber & Alarcón 1988), which ranges in this mountain system from 1,000 to 1,940 m asl (highest elevation for the Sierra de Aroa). Other populations of *Mannophryne* have been reported from lower altitudinal belts of this range (Barrio-Amorós 1999) whereas none are known from higher elevations (F.J.M. Rojas-Runjaic, pers. obs.) by which, we presume that the type locality is in the higher limit of the altitudinal distribution of this species, and probably it is more common at lower belts occupied by Premontane humid and very humid forests (Ewel *et al*. 1976).

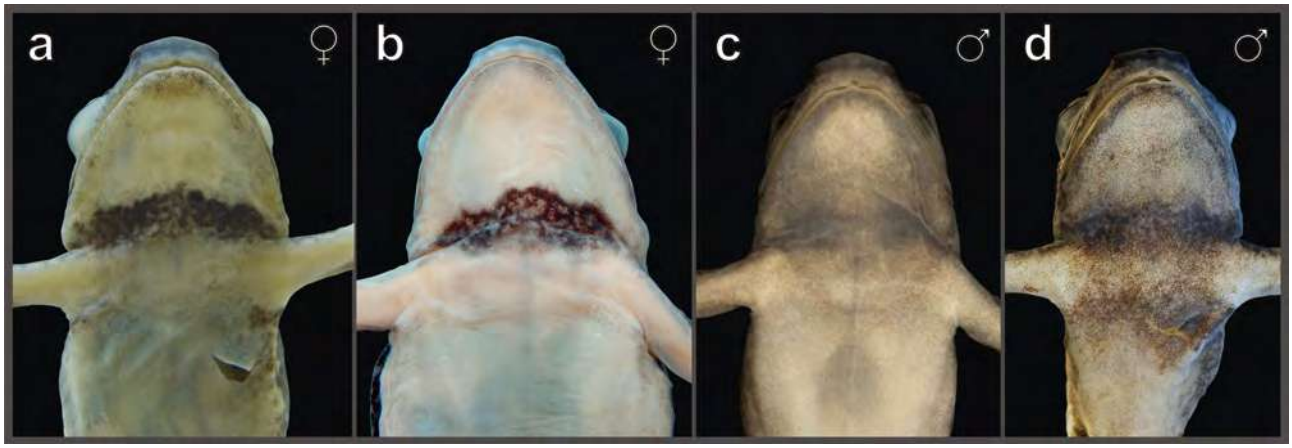

FIGURE 5. Ventral view of four preserved paratypes of *Mannophryne molinai* **sp. nov.** showing variation in the dark dermal collar. Paratype females MHNLS 21337 (a), and MHNLS 21535 (b); paratype males MHNLS 21537 (c), and MHNLS 21538 (d). Fotos: F.J.M. Rojas-Runjaic

The region has a seasonal climatic regime, with a dry period from October–March, and a rainy period from April–September, with a maximum rain peak in July. Annual precipitation ranges between 800–1,500 mm, and annual temperature varies from 10–26.55 ºC (Lentino & Bruni 1994).

Mannophryne molinai is a diurnal and riparian frog. Adult males, adult females and juveniles were all detected from the watercourse (above rocks) to about three meters from the edge of the water; no specimen was detected inside the forest beyond the limits of the creek. Adult males call actively during the day, either hidden in crevices near small waterfalls, under rocks and fallen trunks, or exposed above rocks or trunks, but always very close to the watercourse. Calling males found on April, 04–05, 2014 were recorded at different moments during the morning and evening (between 11:45–18:30 h) but call activity was detected almost uninterruptedly from around 9:00 h (when we arrived) until near nightfall (ca. 19:00 h). Peaks of call activity (*i.e.* more males calling, and individual males calling more actively) were apparently related to periods of higher solar intensity throughout the day. All males observed during call activity were uniformly black colored, but several minutes after collection they became brighter and a more complex color pattern emerged, consisting of a grayish brown background with blackish brown spots, bands, and pale stripes. During nocturnal surveys several specimens were found, apparently active on rocks and trunks, but there was no call activity.

Specimens located one to three meters away from the watercourse tended to escape when noticing our presence, executing a series of rapid jumps to take refuge under rocks, trunks or leaf litter, but when located near the edge of the creek they jumped into the water, either to stay static at the bottom (typically in pools), or to get carried away by the current and quickly reach the shore about one meter downstream.

As in other species of *Mannophryne*, tadpole transport is done by males. The specimens MHNLS 21536 and 21537, collected on December 19, 2012, were carrying 10 and 16 tadpoles on their backs (lots MHNLS 21546 and 21547, respectively). Tadpoles already released by the parents were found in small ponds of the creek. All the specimens collected released a mild mercaptan-like odor when handled.

Distribution. *Mannophryne molinai* is only known from its type locality (La Rondona), at the southeastern slope of Sierra de Aroa, in the western portion of the Cordillera de la Costa (Fig. 3). Other populations known from the northeastern and western foothills of Sierra de Aroa should be evaluated in order to determine if they correspond to the new species.

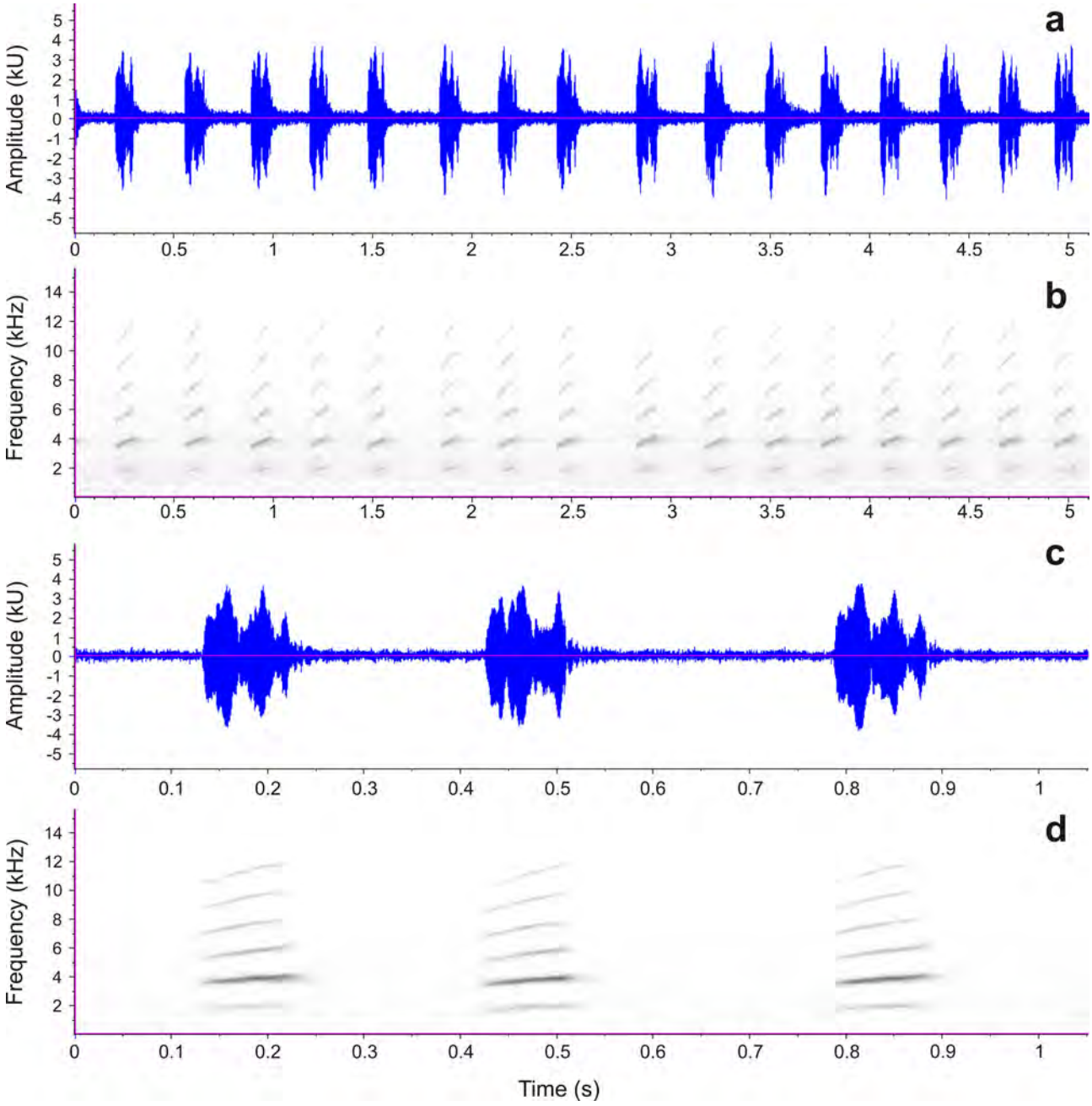

FIGURE 6. Advertisement call of *Mannophryne molinai* **sp. nov.** Oscillogram (a) and spectrogram (b) of a 5 s fragment of the call. Detailed view of the oscillogram (c) and spectrogram (d) of a 1 s section of the same recording.

Conservation status. The Sierra de Aroa has an extension of ca. 1,141 ha and is protected at its northern portion by the Yurubí national park. However, the original forests on the slopes (Premontane humid and very humid forests, and part of the cloud forest) of this mountain system were almost entirely replaced by crops, and only the highest areas still maintain intact their cloud forest (Hubber & Oliveira-Miranda 2010). Recently, the cloud forest of the Sierra de Aroa was classified as Vulnerable (Criterion A4) due that a reduction ≥ 30% of its extension is projected in the next 50 years (Oliveira-Miranda *et al*. 2010). *Mannophryne molinai* is known only from the type locality, at a creek in the cloud forest, and is locally abundant. As commented above, it is likely that its distribution is more extensive into the Sierra de Aroa toward the lower belts occupied by relicts of premontane forest, but restricted to this mountain system. Therefore, based on its presumed restricted area of occupancy, with a plausible future threat that could drive the species to Critically Endangered or even Extinct in a short time, we propose to classify *M. molinai* as Vulnerable under the criterion VU D2 of the IUCN (2012).

FIGURE 7. La Rondona creek, Sierra de Aroa, northwestern Venezuela, type locality of *Mannophryne molinai* **sp. nov.** (a) View of a small pool and (b) crevices below a waterfall were several specimens of the type series were found. Photos: F.J.M. Rojas-Runjaic.

FIGURE 8. César Ramón Molina Rodriguez (1960–2015) with an amplectant couple of the critically endangered Rancho Grande Harlequin Frog *Atelopus cruciger* in January 2010. We named *Mannophryne molinai* **sp. nov.** after him in a posthumous recognition of his friendship and contributions to the knowledge of the diversity and conservation of Venezuelan amphibians and reptiles. Photo: F.J.M. Rojas-Runjaic.

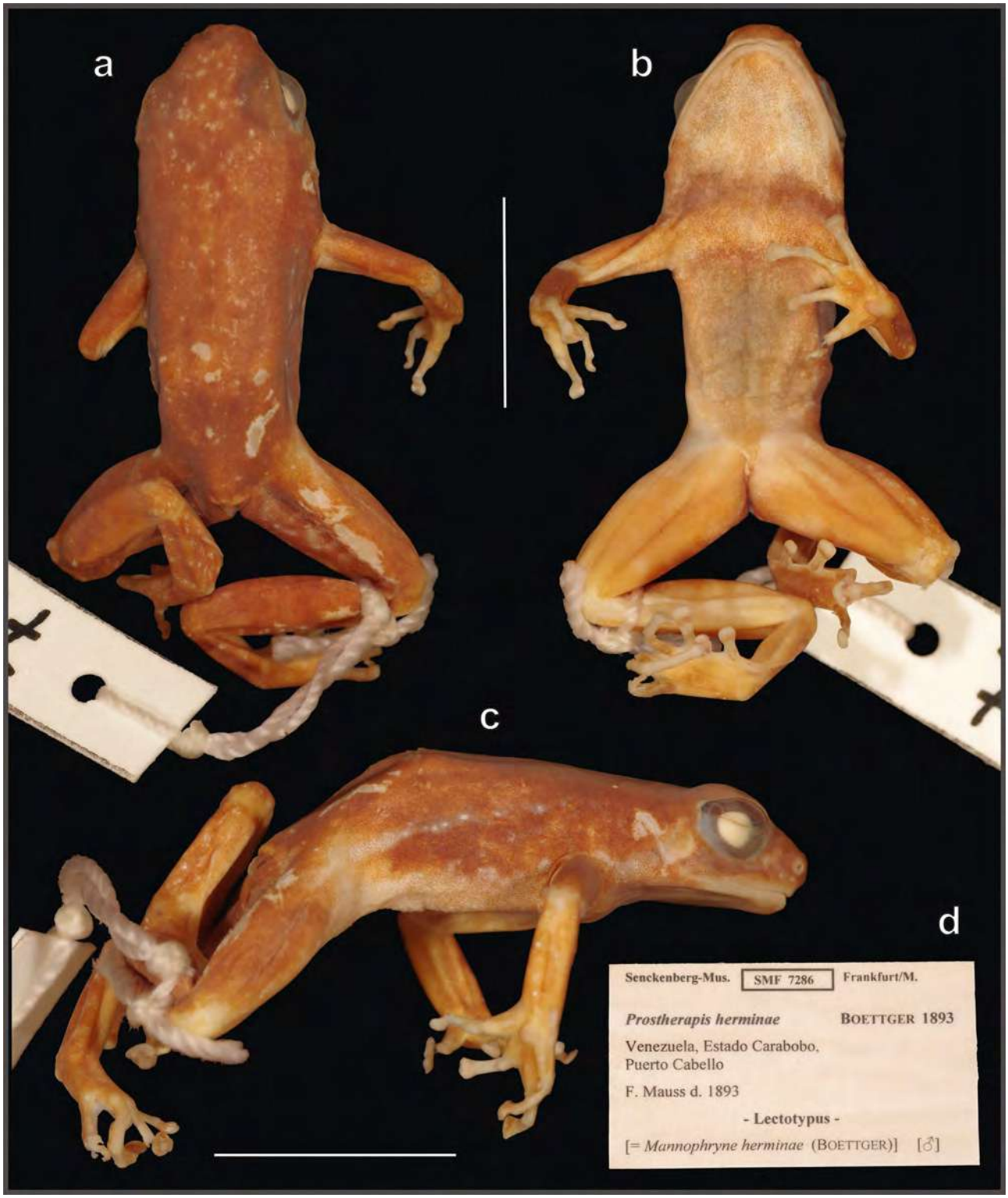

FIGURE 9. Lectotype male (SMF 7286) of *Mannophryne herminae*. Dorsal (a), ventral (b), and lateral (c) views; (d) label with catalog information of the lectotype. Scale bars represent 10 mm. Photos: S. Lotzkat.

Etymology. The specific epithet "*molinai*" is a patronymic honoring the late César Ramón Molina Rodríguez (1960–2015) (Fig. 8), a prominent Venezuelan herpetologist, colleague, and friend. César made great contributions to the knowledge of the diversity and conservation of Venezuelan amphibians and reptiles, materialized in nearly a hundred scientific papers, and several conservation strategies, action plans and projects. His dedication to the training of numerous students through the teaching of herpetology in classrooms, field courses, and mentoring of theses, evidenced his passion for the amphibians and reptiles, and his commitment with the development of the

study of the Venezuelan herpetofauna (Hernández 2015). César also had particular interest by the collared frogs; his PhD thesis was about the ecology of a population of *Mannophryne* from the valley of Caracas in Venezuela, and he co-authored the description of *M. orellana*, *M. urticans* and *M. vulcano* (Barrio-Amorós *et al*. 2010a). We make a posthumous recognition to his admirable work and friendship, naming this new species in his memory. The name "*molinai*" is used as a masculine singular noun, in the genitive case.

Mannophryne herminae **(Boettger, 1893)**
(Figs. 9–11)

Prostherapis herminae—Boettger, 1893: 37; Barbour & Noble, 1920: 401; Test, 1956: 2.
Phyllobates trinitatis—Brauer, 1899: 89; Stejneger, 1901: 179; Barbour & Noble, 1920: 401; Lutz, 1927: 40; Shreve, 1947: 537; Test, 1954: 140; Mertens, 1957: 340.
Hyloxalus collaris—Hellmich, 1940: 113.
Prostherapis trinitatis—Ginés, 1959: 91; Rivero, 1963: 96 (in part); Sexton, 1960: 108-115; Test, 1963: 125; Test, Sexton & Heatwole, 1966: 38.
Prostherapis trinitatus—Stebbins & Hendrickson, 1959: 506; Duellman, 1966: 217 (in part).
Prostherapis trinitatis trinitatis—Rivero, 1961: 158 (in part); Rivero, 1964: 310 (in part).
Colostethus trinitatis—Durant & Dole, 1975 (in part): 23; Wells, 1977: 248 (in part); Wells, 1980: 189 (in part).
Colostethus trinitatus—Edwards, 1971: 148; Rivero, 1976: 330 (in part); Rivero, 1979: 173 (in part).
Colostethus trinitatus herminae—Rivero, 1984 "1982": 14.
Colostethus herminae—Edwards, 1971: 148; Edwards, 1974: 2; Harding, 1983: 80; La Marca, 1992: 26 (in part).
Colostethus hermani (sic)—Lynch, 1979: 214 (*lapsus calami*).
Mannophryne herminae—La Marca, 1994: 21 (in part); Barrio, 1999: 21 (in part).

Remarks: Previously considered a species widely distributed in northern Venezuela (Rivero 1984b; La Marca 1992, 1994). In the last two decades it has been demonstrated that in fact as formerly defined geographically and morphologically, *Mannophryne herminae* constitutes a conglomerate of different species-level taxa, and until today five species (*M. caquetio*, *M. lamarcai*, *M. leonardoi*, *M. venezuelensis* and *M. vulcano*) have been described from populations originally considered as corresponding to *M. herminae* (Mijares-Urrutia & Arends 1999a,b; Manzanilla *et al*. 2007a,b; Barrio-Amorós *et al*. 2010a). However, after the above mentioned species delimitations, the geographic distribution of *M. herminae* is yet wide and probably there are still several different species under this name. In order to facilitate the future recognition of undescribed taxa related to *M. herminae*, we only consider as pertaining to this species the populations from the northern slope of Cordillera de la Costa that fit with the amended definition provided below, which is based on the type series (Figs. 9–10) and on additional specimens (Fig. 11) from the lower basins of San Esteban (near Puerto Cabello, the type locality), Patanemo, Cata, and Cuyagua rivers, and from Rancho Grande.

Regarding the type locality, as previously commented by La Marca (1994) Puerto Cabello probably only was the port of shipping of the type series and not the place where it was collected. Puerto Cabello is located within a Tropical dry forest area, an unlikely habitat for a collared frog. The type series most likely comes from the vicinities of Puerto Cabello (*e.g.* San Esteban valley), where small rivers surrounded by Premontane very humid forests and inhabited by *Mannophryne herminae* populations still occur.

Amended definition: (1) Small body size, with adult males smaller than females (males: 20.5–23.1 mm of SVL *vs*. females: 24.6–29.0 mm); (2) dorsal skin of body and hind limbs shagreen, moderately granular on flanks; small tubercles present on posterior third of dorsum, body flanks, and dorsal surface of thighs and shanks; ventrally smooth; (3) snout rounded to nearly truncate in dorsal view, rounded to protruding in profile; (4) nares visible ventrally; (5) tympanum small (~1/3–2/5 of ED), defined, about 1/4–1/3 concealed posterodorsally; (6) short teeth present on maxillary arch; (7) median lingual process absent; (8) vocal sac single subgular in males; (9) carpal pad absent; (10) metacarpal ridge low; (11) thenar tubercle conspicuous; (12) nuptial excrescences on thumb absent; (13) FIII not swollen; (14) tip of FIV surpassing distal subarticular tubercle of FIII; (15) FI and FII equal in size; (16) thin lateral fringes present on preaxial side of FII–FIII; (17) weak and poorly defined lateral keels on pre- and postaxial sides of FI and FIV, and postaxial side of FII–FIII; (18) tarsal keel well-defined in all its extension, nearly straight, extending from the base of TI where is continuous with the preaxial fringe, to the mid-tarsus, not merged with the inner metatarsal tubercle nor reduced at the level of this tubercle; (19) tarsal fringe absent; (20) middle

metatarsal tubercle present, similar in size to the inner one, non-protuberant, weakly defined; (21) metatarsal fold present, strong, almost reaching the outer metatarsal tubercle; (22) wide lateral (pre- and postaxial) fringes in all toes; (23) toes basally webbed, webbing formula: I(1^{+}–2^{-})–(2^{+}–2¾)**II**(1½–2^{-})–(3^{-}–3⅓)**III**(2⅓–3^{-})–(3⅔–4^{+})**IV**(4^{+}–4½)–(2½–3^{-})**V**; (24) disc weakly expanded on FI, moderately expanded on FIII–FIV; moderately expanded TI–TIV, and weakly to moderately expanded on TV; (25) paired dorsal digital scutes present on fingers and toes; (26) cloacal sheath short; (27) supracloacal dermal flap present, conspicuous; (28) cloacal tubercles present; (29) iridescent golden to cream spot at dorsal forelimb and hind limb insertions present, diffuse; (30) pale paracloacal mark present, diffuse; (31) diffuse yellowish spots on hidden parts of hind limbs absent; (32) thigh dorsally pale brown with three to four transverse dark brown bands; (33) pale dorsolateral stripe solid to diffuse, straight, reaching the level of the arm insertion or up to the level of the groin; (34) lateral dark band solid, wider at the middle of the flank; (35) oblique lateral stripe partial (not reaching the posterior border of the eye), solid, cream or subtly tinged with yellow at the groin; (36) ventrolateral stripe cream or yellowish, poorly defined, formed by a wavy series of spots; (37) dark dermal collar wide, diffuse to solid, non-speckled with small white dots and complete in males; broad (10.9–15.9% SVL), solid, with or without some small whitish dots, and complete in females; (38) dark lower labial stripe present, diffuse; throat color in life: extensively colored with yellow in females, gray in males; (39) abdomen color white to spotted with yellow (in life), and almost free to irregularly stippled with melanophores in females; pale gray, evenly stippled with melanophores in males; (40) iris bronze, finely reticulated of black, with a dark horizontal band, pupil ring bronze, complete; (41) tongue ocher yellow; (42) large intestine unpigmented; (43) adult testis unpigmented; (44) mature oocytes with the animal pole pigmented with dark brown; (45) skin blackening in males during call activity; (46) mercaptanlike odor present; (47) diurnal activity; (48) tadpole transport by males; (49) riparian habitat; (50) advertisement call composed of long trills of tonal notes arranged in duplets (51) peak frequency of calls: 3.79–4.24 (4.04 ± 0.09) kHz; (52) fundamental frequency: 1.98–2.15 (2.05 ± 0.04); (53) rate of note emission: 10.60–11.29 notes/s (11.02 ± 0.17); (54) note duration: 0.02–0.04 (0.03 ± 0.00) s; (55) duration of silent intervals between notes of a duplet: 0.14–0.57 (0.31 ± 0.10) s; (56) duration of silent intervals between duplets: 0.09–0.14 (0.10 ± 0.01) s.

TABLE 2. Temporal and spectral parameter values for the first and second notes of each duplet of the advertisement call of *Mannophryne herminae* from San Esteban river, Carabobo state, Venezuela. **Min–Max:** minimum–maximum; **X ± SD:** mean ± standard deviation; **s:** seconds; **kHz:** Kilohertz; *n* = 50 pairs of notes.

Parameter	1st note		2nd note	
	Min–Max	X ± SD	Min–Max	X ± SD
Note duration (s)	0.02–0.04	0.03 ± 0.00	0.02–0.04	0.03 ± 0.00
Fundamental frequency (kHz)	1.98–2.07	2.03 ± 0.03	2.02–2.15	2.07 ± 0.03
Peak frequency (kHz)	3.79–4.16	3.98 ± 0.07	3.85–4.24	4.09 ± 0.08
Lower frequency (kHz)	3.65–4.03	3.84 ± 0.08	3.71–4.11	3.94 ± 0.08
Upper frequency (kHz)	3.94–4.28	4.12 ± 0.08	4.01–4.39	4.22 ± 0.09
Bandwidth (kHz)	0.21–0.39	0.29 ± 0.04	0.22–0.42	0.28 ± 0.05
3rd harmonic (kHz)	5.69–6.27	5.97 ± 0.11	5.79–6.29	6.12 ± 0.11
4th harmonic (kHz)	7.60–8.27	7.94 ± 0.13	7.67–8.44	8.15 ± 0.17
5th harmonic (kHz)	9.52–10.27	9.96 ± 0.18	9.76–10.51	10.19 ± 0.18

Call description. Advertisement calls of *Mannophryne herminae* are composed of long trills of short tonal notes arranged in duplets (Fig. 12a, c). The notes show amplitude modulation and the number of amplitude peaks typically varies between 2–3 (Fig 12c). The duration of calls between the two males recorded was 30.16 ± 15.27 (7.00–49.49) s. The rate of note emission was 11.02 ± 0.17 (10.60–11.29) notes/s, and each call contained 331.73 ± 166.98 (78–546) notes. Note duration was 0.03 ± 0.00 (0.02–0.04) s, and the duration of silent interval between notes of each duplet was 0.03 ± 0.00 (0.02–0.04) s; the duration of duplets was 0.08 ± 0.00 (0.08–0.10) s, and duration of silent intervals between duplets 0.10 ± 0.01 (0.09–0.14) s. Notes have a very slight ascending frequency modulation (Figs. 12b, d). Fundamental frequency was 2.05 ± 0.04 (1.98–2.15) kHz. Peak frequency was 4.04 ± 0.09 (3.79–4.24) kHz, and its lower and upper frequencies were 3.89 ± 0.10 (3.65–4.11) kHz and 4.17 ± 0.10

(3.93–4.39) kHz, respectively; the bandwidth was 0.28 ± 0.04 (0.21–0.42) kHz. Three additional harmonics (3rd–5th; Fig. 12d) were observed above peak frequency, at 5.68–6.29, 7.60–8.44, and 9.52–10.51 kHz. Some small differences were observed in the spectral parameter values between the first and second note of each duplet, being the second note the one that shows the higher values. Discriminated temporal and spectral values for the first and second note of each duplet are listed in Table 2.

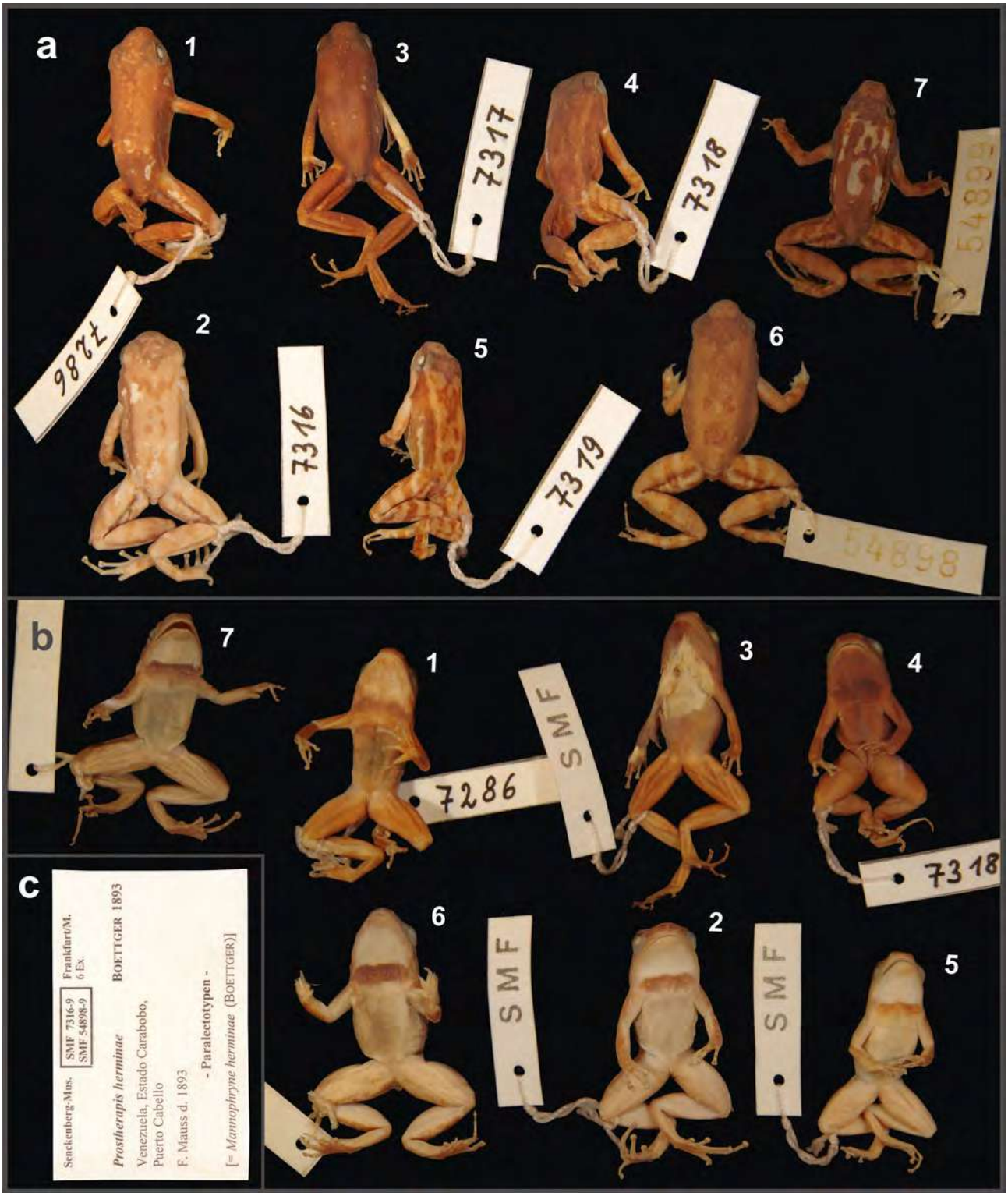

FIGURE 10. Dorsal (a) and ventral (b) views of the type series of *Mannophryne herminae*. 1. Lectotype male SMF 7286; Paralectotypes SMF 7316 (2, female), SMF 7317 (3, male); SMF 7318 (4, male); SMF 7319 (5, female); SMF 54898 (6, female); SMF 54899 (7, female). (c) Label with catalog information of the paralectotypes. Photos: S. Lotzkat.

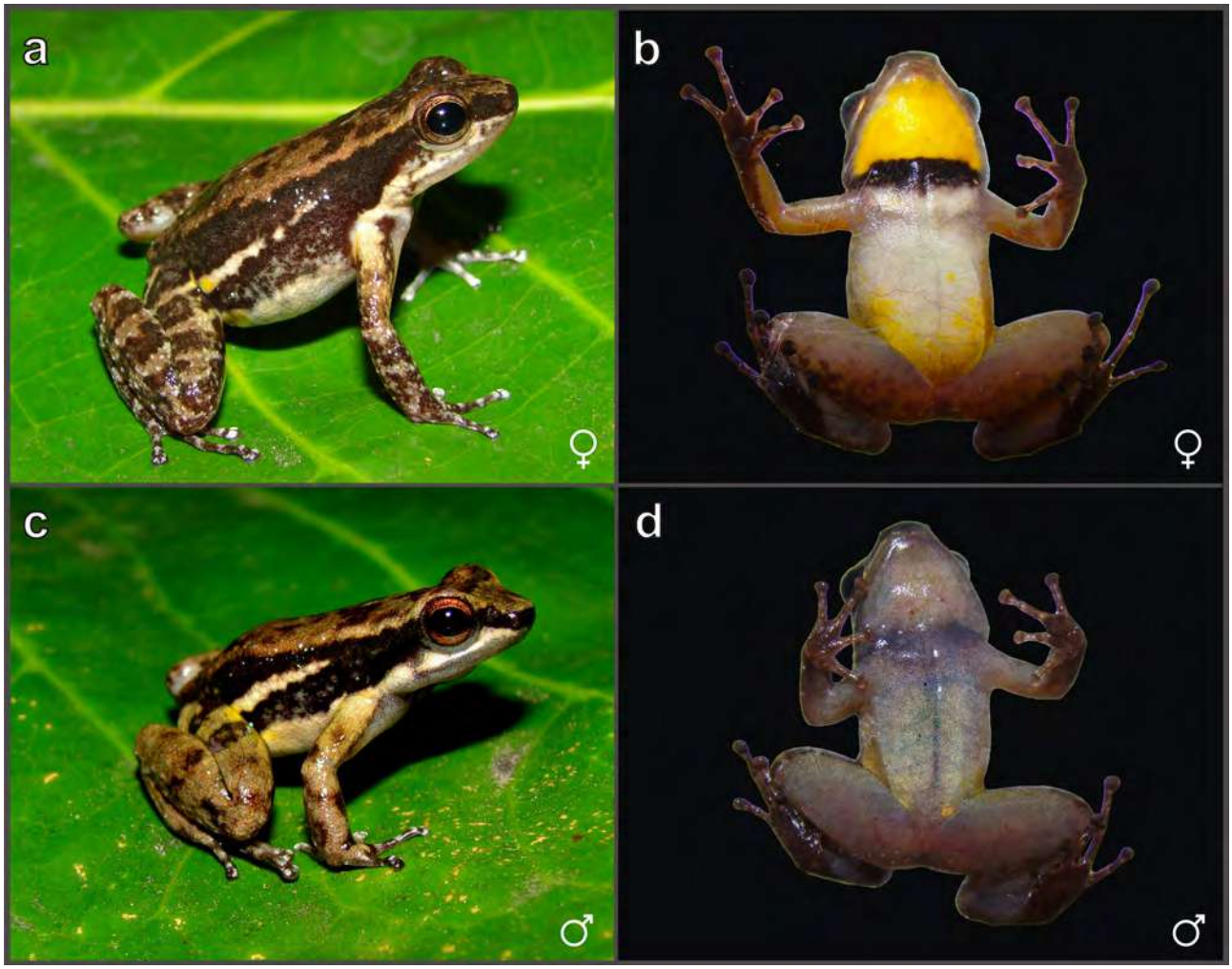

FIGURE 11. Live specimens of *Mannophryne herminae* from San Esteban River, Carabobo state, Venezuela (near the type locality). Adult female, dorsolateral (a) and ventral (b) views; adult male, dorsolateral (c) and ventral (d) views. Photos: F.J.M. Rojas-Runjaic.

Discussion

As mentioned in the diagnosis, *Mannophryne molinai* is similar in external morphology to *M. herminae*. These two species cannot be clearly distinguished from each other by size, general color pattern of dorsum and flanks, or by the extension of the toe webbing. However, the two species noticeably differ in the structure of their metatarsal fold (more extensive in *M. herminae*) and in the color pattern of the dark dermal collar in adult females (wider and non-reticulate in *M. herminae*). The last character apparently is related to species recognition and social interactions (Text 1954; Sexton 1960; Dole & Durant 1974; Durant & Dole 1975; Wells 1980), and it has proven to be useful in delimiting species (*e.g.* La Marca 1992; Manzanilla *et al*. 2007a, Barrio-Amorós *et al*. 2010a).

But, the most striking differences between these two species are the note arrangement and the temporal attributes of their advertisement calls, given that *M. molinai* emits trills of single, longer notes, spaced by longer silent intervals, whereas the call of *M. herminae* is composed of trills of shorter and less spaced notes, arranged in duplets (Figs. 6 and 12, respectively). Acoustic signals play a critical role in mate recognition and mate choice (Wells 2007) and are species-specific; hence, advertisement call differentiation between populations, even in absence of, or with little morphological variation, constitutes strong evidence of speciation (*e.g.* Angulo & Reichle 2008; Padial *et al*. 2008).

A similar situation to the one exhibited by *Mannophryne molinai* and *M. herminae* was found in two other species of *Mannophryne*: Formerly, populations of Trinidad and the Venezuelan Península de Paria were

considered as belonging to *M. trinitatis* due to their morphological similarities; but based on bioacoustic and molecular evidence, Manzanilla *et al*. (2007a) determined that continental populations (from Paria) were in fact, a different (and sister) species of *M. trinitatis* which they named as *M. venezuelensis*. These two species also differ strikingly in the note arrangement of their advertisement calls, which consist of trills of single notes in *M. venezuelensis* and trills of note duplets in *M. trinitatis*.

Traditionally, advertisement calls have received little attention as evidence in species delimitation among collared frogs of the genus *Mannophryne*, and at present the calls of 50% of the described species remain unknown. Moreover, in most cases where the advertisement call is known, the description of the vocalization was based on a single specimen or (in the best of cases) restricted to several specimens from a single population. Based on the two mentioned cases (*i.e. M. herminae-M. molinai*, and *M. trinitatis-M. venezuelensis*), it is to be expected that, as other populations would be acoustically characterized, additional morphologically similar or cryptic species of *Mannophryne* will be discovered.

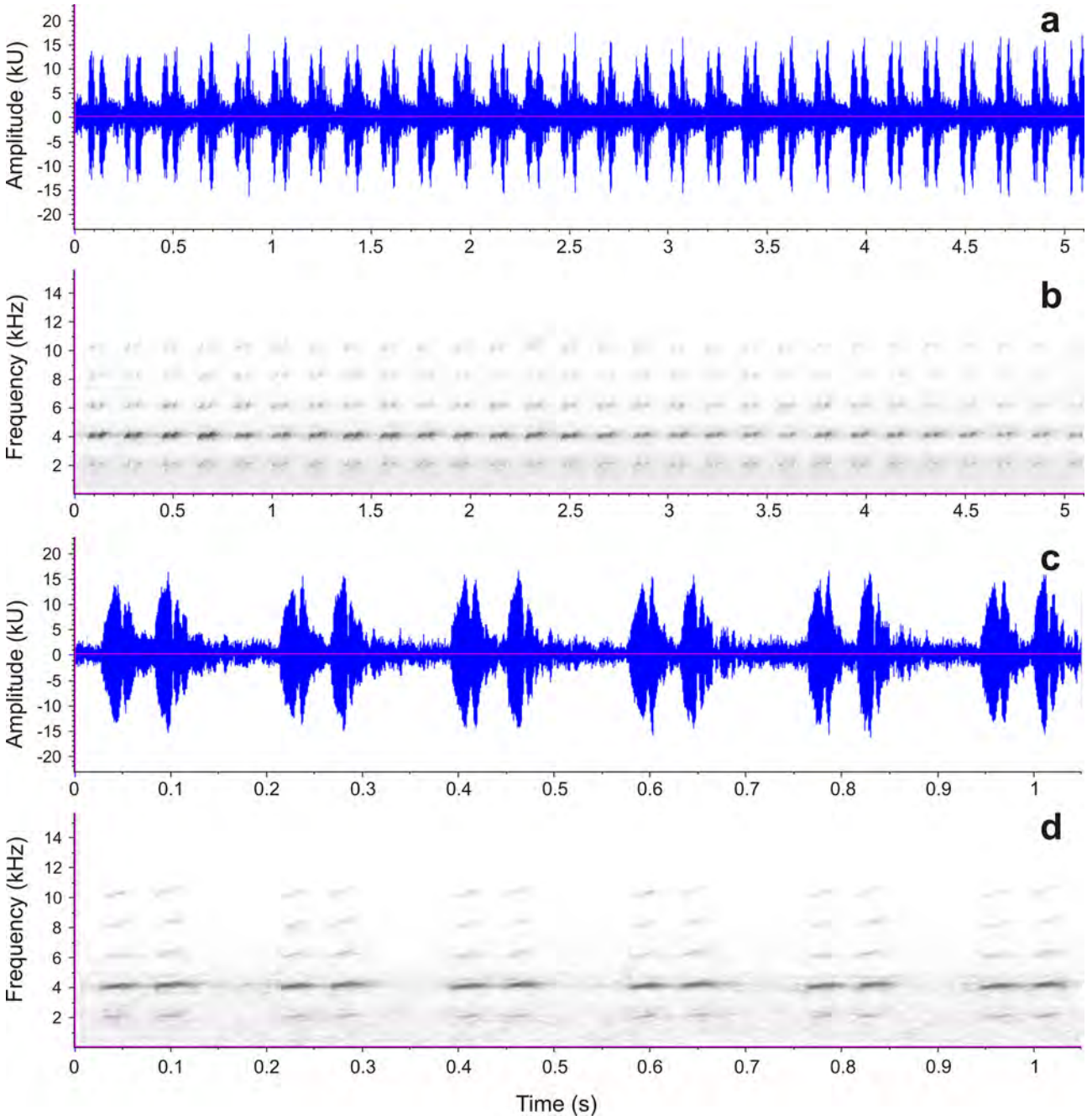

FIGURE 12. Advertisement call of *Mannophryne herminae*. Oscillogram (a) and spectrogram (b) of a 5 s fragment of the call. Detailed view of the oscillogram (c) and spectrogram (d) of a 1 s section of the same recording.

Acknowledgements

We thank Edward Camargo, Helga Terzenbach, José L. Vieira, Jhorman Piñero, Jesús Aguiar, and Nelson Castro for field assistance. We are also thankful to Pedro Cabello and Andrés Jaramillo for taking additional photos of the type series of the new species, to Sebastian Lotzkat for the photos of the type series of *Mannophryne herminae*, and to Amelia Díaz de Pascual for allowing access to specimens housed at herpetological collection of CVULA. Santiago Castroviejo-Fisher, Pedro Ivo Simões, and Lourdes Echevarría made valuable suggestions and helped with the English of the manuscript. Venezuelan permit for collecting (#361) was issued to FRR by the Ministerio del Poder Popular para el Ambiente. Currently, FRR is supported by a PhD scholarship from Brazilian Conselho Nacional de Desenvolvimento Científico e Tecnológico (CNPq, process 142444/2014-6).

References

Angulo, A. & Reichle, S. (2008) Acoustic signals, species diagnosis, and species concepts: the case of a new cryptic species of *Leptodactylus* (Amphibia, Anura, Leptodactylidae) from the Chapare region, Bolivia. *Zoological Journal of the Linnean Society*, 152, 59–77.
https://doi.org/10.1111/j.1096-3642.2007.00338.x

Barbour, T. & Noble, G.K. (1920) Some amphibians from northwestern Peru, with a revision of the genera *Phyllobates* and *Telmatobius*. *Bulletin of the Museum of Comparative Zoology*, 63, 395–427.
http://biodiversitylibrary.org/page/2817193

Barrio-Amorós, C.L. (1999 "1998") Sistemática y biogeografía de los anfibios (Amphibia) de Venezuela. *Acta Biologica Venezuelica*, 18, 1–93.

Barrio-Amorós, C.L. & Santos, J.C. (2012) A phylogeny for *Aromobates* (Anura: Dendrobatidae) with description of three new species from the Andes of Venezuela, taxonomic comments on *Aromobates saltuensis*, *A. inflexus*, and notes on the conservation status of the genus. *Zootaxa*, 3422, 1–31.

Barrio-Amorós, C.L., Rivas, G., Molina, C. & Kaiser, H. (2006) *Mannophryne trinitatis* (Anura: Dendrobatidae) is a Trinidadian single-island endemic. *Herpetological Review*, 37, 298–299.

Barrio-Amorós, C.L., Santos, J.C. & Molina, C.R. (2010a) An addition to the diversity of dendrobatid frogs in Venezuela: description of three new collared frogs (Anura: Dendrobatidae: *Mannophryne*). *Phyllomedusa*, 9, 3–35.
https://doi.org/10.11606/issn.2316-9079.v9i1p03-35

Barrio-Amorós, C.L., Rivas, G.A., Molina, C., Santos, J.C. & Kaiser, H. (2010b) Intraspecific variation in the endangered frog *Mannophryne riveroi* (Anura, Dendrobatidae, Aromobatinae), with comments on coloration and natural history. *Herpetology Notes*, 3, 151–160.

Boettger, O. (1893) Reptilien und Batrachier aus Venezuela. *Bericht der Senckenbergischen Naturforschenden Gesellschaft in Frankfurt am Main*, 1893, 35–42.

Brauer, A. (1899) Ein neuer Fall von Brutpflege bei Fröschen. *Zoologische Jahrbücher. Abteilung für Systematik, Geographie und Biologie der Tiere*, 12, 89–94.
http://direct.biostor.org/reference/181238

Dixon, J.R. & Rivero-Blanco, C. (1985) A new dendrobatid frog (*Colostethus*) from Venezuela with notes on its natural history and that of related species. *Journal of Herpetology*, 19, 177–184.
https://doi.org/10.2307/1564170

Dole, J.W. & Durant, P. (1974) Courtship behavior in *Colostethus collaris* (Dendrobatidae). *Copeia*, 1974, 988–990.
https://doi.org/10.2307/1442607

Donoso-Barros, R. (1965) Nuevos reptiles y anfibios de Venezuela. *Noticiario Mensual. Museo Nacional de Historia Natural, Santiago, Chile*, 102, 2–3.

Duellman, W.E. (1966) Aggressive behavior in dendrobatid frogs. *Herpetologica*, 22, 217–221. Available from: http://www.jstor.org/stable/3890687 (Accessed 22 Aug. 2018)

Duellman, W.E. (1970) The hylid frogs of Middle America. Vol. 1. *Monograph of the Museum of Natural History, University of Kansas*, 1, 1–427.
https://doi.org/10.5962/bhl.title.2835

Durant, P. & Dole, J.W. (1975) Aggressive behavior in *Colostethus* (=*Prostherapis*) *collaris* (Anura: Dendrobatidae). *Herpetologica*, 31, 23–26. Available from: http://www.jstor.org/stable/3891981 (Accessed 22 Aug. 2018)

Edwards, S.R. (1971) Taxonomic notes on South American *Colostethus* with descriptions of two new species (Amphibia, Dendrobatidae). *Proceedings of the Biological Society of Washington*, 84, 147–162. Available from: http://direct.biostor.org/reference/65699 (Accessed 22 Aug. 2018)

Edwards, S.R. (1974) Taxonomic notes on South American dendrobatid frogs of the genus *Colostethus*. *Occasional Papers of the Museum of Natural History, University of Kansas*, 30, 1–14.
https://doi.org/10.5962/bhl.part.22165

Ewel, J.J., Madriz, A. & Tosi, J.A. (1976) *Zonas de vida de Venezuela. Memoria explicativa sobre el mapa ecológico*. M.A.C. and FONAIAP, Caracas, 270 pp.
Frost, D.R. (2017) Amphibian Species of the World: an Online Reference. Version 6.0. Electronic Database. American Museum of Natural History, New York, USA. Accessible from: http://research.amnh.org/herpetology/amphibia/index.html. (accessed 28 December 2017)
García, F., Aular, L., Camargo, E. & Mújica, Y. (2012a "2010") Murciélagos de la sierra de Aroa, estado Yaracuy, Venezuela. *Memoria de la Fundación La Salle de Ciencias Naturales*, 173–174, 135–154.
García, F.J., Delgado-Jaramillo, M.I., Machado, M. & Aular, L. (2012b) Preliminary inventory of mammals from Yurubí National Park, Yaracuy, Venezuela with some comments on their natural history. *Revista de Biología Tropical*, 60, 459–472.
https://doi.org/10.15517/rbt.v60i1.2781
Ginés, H. (1959) Familias y géneros de anfibios -Amphibia- de Venezuela. *Memoria de la Sociedad de Ciencias Naturales La Salle*, 19, 84–146.
Grant, T., Frost, D.R., Caldwell, J.P., Gagliardo, R., Haddad, C.F.B., Kok, P.J.R., Means, B.D., Noonan, B.P., Schargel, W.E. & Wheeler, W.C. (2006) Phylogenetic systematics of dart-poison frogs and their relatives (Amphibia: Athesphatanura: Dendrobatidae). *Bulletin of American Museum of Natural History*, 299, 1–262.
https://doi.org/10.1206/0003-0090(2006)299[1:PSODFA]2.0.CO;2
Grant, T., Rada, M., Anganoy-Criollo, M., Batista, A., Dias, P.H., Jeckel, A.M., Machado, D.J. & Rueda-Almonacid, J.V. (2017) Phylogenetic systematics of dart-poison frogs and their relatives revisited (Anura: Dendrobatoidea). *South American Journal of Herpetology*, 12 (Special Issue 1), 1–90.
https://doi.org/10.2994/SAJH-D-17-00017.1
Harding, K.A. (1983) *Catalogue of New World Amphibians*. Pergamon Press, Oxford and New York, 406 pp.
Hellmich, W. (1940) Beiträge zur Kenntnis der Gattung Hyloxalus (Brachycephalidae, Amphibia). *Zoologischer Anzeiger*, 131, 113–128.
Hernández, O. (2015) In Memoriam: César Ramón Molina Rodriguez. *FrogLog*, 23, 26–28.
Huber, O. & Alarcón, C. (1988) *Mapa de vegetación de Venezuela*. 1:2.000.000. (map).
Huber, O. & Oliveira-Miranda, M.A. (2010). Ambientes terrestres. *In*: Rodríguez, J.P., Rojas-Suárez, F. & Giraldo H., D. (Eds.), *Libro Rojo de los Ecosistemas Terrestres de Venezuela*. Provita, Shell Venezuela, Lenovo, Caracas, pp. 29–89.
IUCN (2012) *IUCN Red List Categories and Criteria. Version 3.1*. 2nd Edition. Gland and Cambridge, 32 pp.
Kaplan, M. (1997) A new species of *Colostethus* from the Sierra Nevada de Santa Marta (Colombia) with comments on intergeneric relationships within the Dendrobatidae. *Journal of Herpetology*, 31, 369–375.
https://doi.org/10.2307/1565665
Kok, P.J.R. & Kalamandeen, M. (2008) Introduction to the taxonomy of the amphibians of Kaieteur National Park, Guyana. *Abc Taxa*, 5, 1–278.
La Marca, E. (1989) A new species of collared frog (Anura: Dendrobatidae: *Colostethus*) from Serrania de Portuguesa, Andes of Estado Lara, Venezuela. *Amphibia-Reptilia*, 10, 175–183.
https://doi.org/10.1163/156853889X00197
La Marca, E. (1992) Catálogo taxonómico, biogeográfico y bibliográfico de las ranas de Venezuela. *Cuadernos Geográficos*, 9, 1–297.
La Marca, E. (1994) Taxonomy of the frogs of the genus *Mannophryne* (Amphibia: Anura: Dendrobatidae). *Publicaciones de la Asociación Amigos de Doñana*, 4, 1–75.
La Marca, E., Vences, M. & Lötters, S. (2002) Rediscovery and mitochondrial relationships of the dendrobatid frog *Colostethus humilis* suggest parallel colonization of the Venezuelan Andes by poison frogs. *Studies of Neotropical Fauna and Environment*, 37, 233–240.
https://doi.org/10.1076/snfe.37.3.233.8566
Lentino, M. & Bruni, A.R. (1994) *Humedales costeros de Venezuela: situación ambiental*. Sociedad Conservacionista Audubon de Venezuela, Caracas, 188 pp.
Lutz, A. (1927) Notas sobre batrachios da Venezuela e da ihla de Trinidad. *Memórias do Instituto Oswaldo Cruz*, 20, 35–65.
https://doi.org/10.1590/S0074-02761927000100003
Lynch, J.D. (1979) The amphibians of the lowland tropical forests. *In*: Duellman, W.E. (Ed), *The South American Herpetofauna: its origin, evolution, and dispersal*. *Monograph 7*. Museum of Natural History, University of Kansas, Lawrence, Kansas, pp. 189–215.
Manzanilla, J., Jowers, M.J., La Marca, E. & García-París, M. (2007a) Taxonomic reassessment of *Mannophryne trinitatis* (Anura: Dendrobatidae) with a description of a new species from Venezuela. *Herpetological Journal*, 17, 31–42.
Manzanilla, J., La Marca, E. Jowers, M., Sánchez, D. & García-París, M. (2007b "2005") Un nuevo *Mannophryne* (Amphibia: Anura: Dendrobatidae) del macizo del Turimiquire, noreste de Venezuela. *Herpetotropicos*, 2, 105–113.
Manzanilla, J., La Marca, E. & García-París, M. (2009) Phylogenetic patterns of diversification in a clade of Neotropical frogs (Anura: Aromobatidae: *Mannophryne*). *Biological Journal of the Linnean Society*, 97, 185–199.
https://doi.org/10.1111/j.1095-8312.2009.01074.x
MARNR (Ministerio del Ambiente y los Recursos Naturales Renovables) (1992) *Áreas naturales protegidas de Venezuela. Serie Aspectos Conceptuales y Metodológicos. DGPOA/ACM/01*. Ministerio del Ambiente y de los Recursos Naturales

Renovables, Caracas, 150 pp.
Mertens, R. (1957) Zoologische Beobachtungen im Nebelwalde von Rancho Grande, Venezuela. *Natur und Volk*, 87, 337–344.
Mijares-Urrutia, A. & Arends, R.A. (1999a) Un nuevo *Mannophryne* (Anura: Dendrobatidae) del Estado Falcón, con comentarios sobre la conservación del género en el noroeste de Venezuela. *Caribbean Journal of Science*, 35, 231–327.
Mijares-Urrutia, A. & Arends, R.A. (1999b) A new *Mannophryne* (Anura: Dendrobatidae) from western Venezuela, with comments on the generic allocation of *Colostethus larandinus*. *Herpetologica*, 55, 106–114.
http://www.jstor.org/stable/3893069
Mijares-Urrutia, A.M. & Rivero, R.A. (2000) A new treefrog from the Sierra de Aroa, northern Venezuela. *Journal of Herpetology*, 34, 80–84.
https://doi.org/10.2307/1565242
Oliveira-Miranda, M.A., Huber, O., Rodríguez, J.P., Rojas-Suárez, F., De Oliveira-Miranda, R., Hernández-Montilla, M. & Zambrano-Martínez, S. (2010) Riesgo de eliminación de los ecosistemas terrestres de Venezuela. *In*: Rodríguez, J.P., Rojas-Suárez, F. & Giraldo, H.D. (Eds.), *Libro Rojo de los Ecosistemas Terrestres de Venezuela*. Provita, Shell Venezuela, Lenovo, Caracas, pp. 29–89.
Padial, J.M, Köhler, J., Muñoz, A. & De La Riva, I. (2008) Assessing the taxonomic status of tropical frogs through bioacoustics: geographical variation in the advertisement calls in the *Eleutherodactylus discoidalis* species group (Anura). *Zoological Journal of the Linnean Society*, 152, 353–365.
https://doi.org/10.1111/j.1096-3642.2007.00341.x
Quiroga-Carmona, M. & Molinari, J. (2012) Description of a new shrew of the genus *Cryptotis* (Mammalia: Soricomorpha: Soricidae) from the Sierra de Aroa, an isolated mountain range in northwestern Venezuela, with remarks on biogeography and conservation. *Zootaxa*, 3441, 1–20.
Rivero, J.A. (1961) Salientia of Venezuela. *Bulletin of the Museum of Comparative Zoology*, 126, 1–207.
https://biodiversitylibrary.org/page/2811325
Rivero, J.A. (1963) The distribution of Venezuelan frogs. II. The Venezuelan Andes. *Caribbean Journal of Science*, 3, 87–102.
Rivero, J.A. (1964) The distribution of Venezuelan frogs. IV. The Coastal Range. *Caribbean Journal of Science*, 4, 307–319.
Rivero, J.A. (1976) Notas sobre los anfibios de Venezuela II. Sobre los *Colostethus* de los Andes venezolanos. *Memoria de la Sociedad de Ciencias Naturales La Salle*, 35, 327–344.
Rivero, J.A. (1979) Sobre el origen de la fauna paramera de anfibios venezolanos. *In*: Salgado-Labouriau, M.L. (Ed.), *El Medio Ambiente Páramo*. Ediciones Centro de Estudios Avanzados, Mérida, pp. 165–179.
Rivero, J.A. (1984a) Una nueva especie de *Colostethus* (Amphibia, Dendrobatidae) de la Cordillera de la Costa, con anotaciones sobre otros *Colostethus*, de Venezuela. *Brenesia*, 22, 51–56.
Rivero, J.A. (1984b "1982") Sobre el *Colostethus mandelorum* (Schmidt) y el *Colostethus inflexus* Rivero (Amphibia, Dendrobatidae). *Memoria de la Sociedad de Ciencias Naturales La Salle*, 188, 9–16.
Rivero, J.A. (1990 "1988") Sobre las relaciones de las especies del género *Colostethus* (Amphibia: Dendrobatidae). *Memoria de la Sociedad de Ciencias Naturales La Salle*, 48, 3–32.
Rodríguez-Olarte, D., Amaro, A., Coronel, J. & Taphorn, D. (2006 "2005") Los peces del río Aroa, cuenca del Caribe, Venezuela. *Memoria de la Fundación La Salle de Ciencias Naturales*, 164, 101–127.
Rojas-Runjaic, F.J.M., Infante-Rivero, E.E. & Barrio-Amorós, C.L. (2011) A new frog of the genus *Aromobates* (Anura, Dendrobatidae) from Sierra de Perijá, Venezuela. *Zootaxa*, 2919, 37–50.
Roze, J.A. & Solano, H. (1963) Resumen de la familia Caeciliidae (Amphibia: Gymnophiona) de Venezuela. *Acta Biologica Venezuelica*, 3, 287–300.
Sexton, O.J. (1960) Some aspects of the behavior and of the territory of a Dendrobatid frog, *Prostherapis trinitatis*. *Ecology*, 41, 107–115.
https://doi.org/10.2307/1931944
Shreve, B. (1947) On Venezuelan reptiles and amphibians collected by Dr. H. G. Kugler. *Bulletin of the Museum of Comparative Zoology*, 99, 517–537.
https://biodiversitylibrary.org/page/4322504
Stebbins, R.C. & Hendrickson, J.R. (1959) Field studies of amphibians in Colombia, South America. *University of California Publications in Zoo*logy, 56, 497–540.
Stejneger, L. (1901) An annotated list of batrachians and reptiles collected in the vicinity of La Guaira, Venezuela, with descriptions of two new species of snakes. *Proceedings United States National Mus*eum, 24, 179–192.
https://doi.org/10.5479/si.00963801.24-1248.179
Test, F.H. (1954) Social aggressiveness in an amphibian. *Science*, 120, 140–141.
https://doi.org/10.1126/science.120.3108.140
Test, F.H. (1956) Two new dendrobatid frogs from northern Venezuela. *Occasional Papers of the Museum of Zoology, University of Michigan*, 577, 1–9.
Test, F.H. (1963) A protective behavior pattern in a Venezuelan frog of mountain streams. *Caribbean Journal of Science*, 3, 125–128.
Test, F.H., Sexton, O.J. & Heatwole, H. (1966) Reptiles of Rancho Grande and vicinity, Estado Aragua, Venezuela. *Miscellaneous Publications of the Museum of Zoology, University of Michigan*, 128, 1–63.
http://hdl.handle.net/2027.42/56372

Vargas, J.Y.G. & La Marca, E. (2007 "2006") A new species of collared frog (Amphibia: Anura: Aromobatidae: *Mannophryne*) from the Andes of Trujillo state, Venezuela. *Herpetotropicos*, 3, 51–57.
Vences, M., Kosuch, J., Boistel, R., Haddad, C.F.B., La Marca, E., Lötters, S. & Veith, M. (2003) Convergent evolution of aposematic coloration in Neotropical poison frogs: a molecular phylogenetic perspective. *Organisms Diversity and Evolution*, 3, 215–226.
https://doi.org/10.1078/1439-6092-00076
Vivas, L. (2012) *GeotemasVenezuela 2012*. Fondo Editorial Simón Rodríguez de la Lotería del Táchira, Gráficas El Portatítulo, Mérida, 278 pp.
Wells, K.D. (1977) The courtship of frogs. *In*: Taylor, D.H. & Guttman, S.I. (Eds.), *The Reproductive Biology of the Amphibians*. Plenum Publishing Corp, New York, pp. 233–262.
https://doi.org/10.1007/978-1-4757-6781-0_7
Wells, K.D. (1980) Social behavior and communication of a Dendrobatid frog (*Colostethus trinitatis*). *Herpetologica*, 36, 189–199.
http://www.jstor.org/stable/3891485
Wells, K.D. (2007) *The Ecology and Behavior of Amphibians*. The University of Chicago Press, Chicago, 1148 pp.
https://doi.org/10.7208/chicago/9780226893334.001.0001
Yústiz, E. (1991) Un nuevo *Colostethus* (Amphibia: Dendrobatidae) de la Sierra de Barbacoas, estado Lara, Venezuela. *Bioagro*, 3, 145–150.

APPENDIX 1. Additional specimens examined. All the listed specimens are from Venezuela except those of *Mannophryne trinitatis* that are from Trinidad (Trinidad and Tobago). Asterisks indicate specimens examined by photos.

Mannophryne caquetio (3): Falcón state: Sierra de San Luis, Curimagua, MHNLS 1521; Sierra de San Luis, El Chorro, road to La Chapa, MHNLS 21219–21220.
Mannophryne collaris (5): Mérida state: Santa María urbanization, Mérida, CVULA 1464, 1468; Libertador municipality, creek at Los Malabares street, 2.6 km WSW from Chamita sector, MHNLS 21591, 21593, 21595.
Mannophryne cordilleriana (4): Barinas state: Bolívar municipality, Potrerito, MHNLS 21601–21604.
Mannophryne herminae (33): Aragua state: Rancho Grande, Henri Pittier National Park, MHNLS 4023, 4027, 5750, 5754–5755; Lower basin of Cata river, Henri Pittier National Park, MHNLS 17078, 17477, 17651–17652; Carabobo state: Puerto Cabello, SMF 7286* (lectotype), 7316–19*, 54898–54899* (paralectotypes), Las Quiguas, San Esteban, MHNLS 1974, 1979; San Esteban, MHNLS 4071–4074; Los Campamentos, Patanemo, MHNLS 6639, 6643, 6647, 6651, 6664, 6670–6671; creek affluent of San Esteban river, ± 300 m upstream of the dam, P.N. San Esteban, MHNLS 22104–22105, 22110–22111.
Mannophryne larandina (4): Lara state: near Hato Arriba, road El Tocuyo-Barbacoas, MHNLS 22597–22600.
Mannophryne leonardoi (4): Monagas state: Cueva del Guácharo, Caripe, MHNLS 1387a–1387d.
Mannophryne neblina (2): Aragua state: Portachuelo pass, Rancho Grande, MBUCV 2091 (paratypes; ex-UMMZ 113021–113022; field numbers AB 4336 and 4376 respectively).
Mannophryne oblitterata (4): Miranda state: Araira river, MHNLS 21799, 21818–21819.
Mannophryne orellana (1): Táchira state: Pregonero-La Trampa road, CVULA 7161 (paratype).
Mannophryne riveroi (4): Sucre state: Paria peninsula, trail from park rangers station at Las Melenas to Cerro Humo, MHNLS 15740, 16433; trail from Macuro to Los Chorros, road to Uquire, MHNLS 16458; Las Melenas, first creek in the trail to Cerro Humo, MHNLS 17456.
Mannophryne speeri (4): Portuguesa state: La Fila, road Chabasquen-Villanueva, MHNLS 22607–22607, 22609–22610.
Mannoprhyne trinitatis (1): Trinidad, Arima-Blanchisseuse road, near Asa Wright Nature Center, Arima valley, MHNLS 17461.
Mannophryne trujillensis (8): Trujillo state: El Corozal farm, km 5 of the road Flor de Patria-Boconó, Santa Elena sector, MHNLS 17965–17966, 17969–17970, 17973; 3.2 km NE of Sabaneta, Trujillo municipality, MHNLS 22063, 22065, 22067.
Mannophryne urticans (11): Mérida state: Río Frío, CVULA 7227 (paratype); El Vigía, CVULA 5967; Las Maricelas, Panamerican's road, Carracciolo Parra Olmedo municipality, MHNLS 21556–21561, 21563; La Olinda II, 5km NNW from La Azulita, Andrés Bello municipality, MHNLS 21993–21994.
Mannophryne venezuelensis (3): Sucre state: trail from Macuro to Los Chorros, road to Uquire, MHNLS 16454; Macuro, Paria peninsula, MHNLS 20832–20833.
Mannophryne yustizi (8): Lara state: Yacambú National Park, CVULA 7928; La Pastora, 11 km SSW of Sanare, MHNLS 8508–8509, 9520–8521; El Blanquito, Yacambú National Park, MHNLS 21280–21282.
Mannophryne vulcano (4): VENEZUELA: Miranda state: Cerro El Ávila, Chacaito creek, Chacao municipality, MHNLS 20694–20695, 20698–20699.

Conclusões gerais

- *Aromobates* e *Mannophryne* são clados irmãos e reciprocamente monofiléticos.
- Nossos resultados também corroboram a monofilia de Aromobatinae, assim como a da família Aromobatidae, das outras duas subfamílias (Anomaloglossinae) e dos outros três gêneros (*Allobates*, *Anomaloglossus* e *Rheobates*).
- Corrobora-se a posição filogenética de todas as espécies de *Aromobates* reconhecidas até agora, como pertencentes a este gênero.
- "*Colostethus*" *caribe* é considerado como pertencente a um novo gênero, irmão de todos os demais Aromobatidae menos *Allobates*.
- "*Prostherapis*" *dunni* é considerado como pertencente um novo gênero de Anomaloglossinae, irmão de *Rheobates*.
- "*Phyllobates*" *mandelorum* é parte de Aromobatinae (irmão de *Aromobates* e *Mannophryne*), mas provisoriamente tratado como *insertae sedis*.
- Pelo menos oito espécies novas (quatro *Mannophryne* e quatro *Aromobates*) foram identificadas.
- Nossos resultados suportam o reconhecimento de quatro grupos de espécies dentro de *Mannophryne* em lugar de três como foi reconhecido até agora.
- Numerosas sinapomorfias fenotípicas não ambíguas foram identificadas para todos os táxons supraespecíficos em Aromobatidae, assim como também para os quatro grupos de espécies de *Mannophryne*.
- Os cantos de anúncio constituem uma valiosa fonte de evidência na delimitação de espécies morfologicamente crípticas em *Mannophryne*.

Pontifícia Universidade Católica do Rio Grande do Sul
Pró-Reitoria de Graduação
Av. Ipiranga, 6681 - Prédio 1 - 3º. andar
Porto Alegre - RS - Brasil
Fone: (51) 3320-3500 - Fax: (51) 3339-1564
E-mail: prograd@pucrs.br
Site: www.pucrs.br